

Origine et conséquences fonctionnelles des variant structuraux dans la tumorigénèse hépatique

Quentin Bayard

▶ To cite this version:

Quentin Bayard. Origine et conséquences fonctionnelles des variant structuraux dans la tumorigénèse hépatique. Human health and pathology. Université Paris Cité, 2021. English. NNT: 2021 UNIP7302. tel-04083183

HAL Id: tel-04083183 https://theses.hal.science/tel-04083183v1

Submitted on 27 Apr 2023

HAL is a multi-disciplinary open access archive for the deposit and dissemination of scientific research documents, whether they are published or not. The documents may come from teaching and research institutions in France or abroad, or from public or private research centers. L'archive ouverte pluridisciplinaire **HAL**, est destinée au dépôt et à la diffusion de documents scientifiques de niveau recherche, publiés ou non, émanant des établissements d'enseignement et de recherche français ou étrangers, des laboratoires publics ou privés.



Université de Paris

Ecole doctorale Hématologie Oncogenèse et Biothérapies (ED561)

INSERM UMRS-1138, Centre de Recherche des Cordeliers (CRC) Équipe 28 : Functional Genomics of Solid Tumors (FunGeST)

Origin and functional consequences of structural variations in liver tumorigenesis

Quentin Bayard

Thèse de doctorat d'Oncogenèse

Dirigée par Éric Letouzé

Présentée et soutenue publiquement le 15 Mars 2021

Devant un jury composé de :

Dr. Chunlong Chen, Chargé de recherche, Institut Curie

Dr. Pascal Pineau, Directeur de recherche, Institut Pasteur

Dr. Sabine Colnot, Directeur de recherche, CRC

Dr. Tatiana Popova, Chargé de recherche, Institut Curie

Dr. Olivier Delattre, Directeur de recherche, Institut Curie

Rapporteur Rapporteur Examinateur Examinateur Examinateur









Titre: Origine et conséquences fonctionnelles des variant structuraux dans la tumorigénèse hépatique.

Résumé:

Le cancer du foie est très hétérogène, avec un large spectre d'étiologies, de caractéristiques histologiques et de voies biologiques dérégulées. Les projets de séquençage à grande échelle réalisés durant la dernière décennie ont révélé de nombreuses mutations *driver* et des changements du nombre de copies. Cependant, le rôle des variant structuraux (VS) dans la tumorigénèse du foie est encore mal compris.

Au cours de mon projet de doctorat, j'ai développé des approches informatiques innovantes intégrant des données de séquençage du génome entier et de l'ARN pour identifier de nouveaux variant structuraux dans les cancers du foie. J'ai mis au jour des fusions récurrentes impliquant des oncogènes *ROS1* et *FRK*, conduisant à une activation constitutive de la voie JAK/STAT et au développement d'adénomes hépatocellulaires inflammatoires (AHC). J'ai également décrit un mécanisme oncogène original impliquant la perte d'éléments régulateurs post-transcriptionnels, conduisant à une surexpression massive d'*IL6* dans un cas clinique d'AHC inflammatoire associé à l'amylose. Enfin, j'ai identifié les VS *driver* affectant les éléments régulateurs dans les carcinomes hépatocellulaires (CHC), y compris les événements d'enhancer hijacking activant les oncogènes *CCNE1* ou *TERT*.

Afin de mieux comprendre l'origine des VS, j'ai mis en place un cadre d'analyse de signature prenant en compte la nature et la taille des variation structuraux identifiées dans chaque tumeur. Cette approche m'a permis de mettre en évidence les sous-groupes de HCC présentant des signatures de VS particulières. En particulier, j'ai découvert un nouveau sous-groupe de CHC clinique-moléculaire qui est caractérisé par l'activation de *CCNA2* ou *CCNE1* par des mécanismes *drivers*. Ces tumeurs (CCN-HCC) représentent 7% des carcinomes hépatocellulaire et présentent une signature spécifique de réarrangements (signature RS1) liés au stress réplicatif, avec des centaines de duplications focales et des « Template Insertion Cycles ». Les CCN-HCC sont des tumeurs agressives mais peuvent être ciblées par des inhibiteurs de la réponse ATR au stress réplicatif.

Dans l'ensemble, ces travaux contribuent à affiner la caractérisation moléculaire des tumeurs hépatiques bénignes et malignes en révélant de nouveaux gènes *drivers* et mécanismes moléculaires. Ces résultats ont des implications cliniques, car la définition de sous-groupes homogènes de cancers est essentielle pour développer des thérapies efficaces et adaptées.

Mots clefs:

Adénome hépatocellulaire, Carcinome hépatocellulaire, Séquençage génome complet, Variant Structuraux, Gènes drivers, Signature de réarrangements

Title: Origin and functional consequences of structural variations in liver tumorigenesis.

Abstract:

Liver cancers are extremely heterogeneous, with a wide spectrum of etiologies, histological characteristics and deregulated biological pathways. Large-scale sequencing projects in the last decade revealed numerous driver mutations and copy-number changes. However, the role of structural variations (SVs) in liver tumorigenesis is still poorly understood.

During my PhD project, I developed innovative computational approaches integrating whole genome and RNA sequencing data to identify new driver SVs in liver cancers. I unraveled recurrent fusions involving *ROS1* and *FRK* oncogenes, leading to a constitutive activation of the JAK/STAT pathway and to the development of inflammatory hepatocellular adenomas (HCA). I also described an original oncogenic mechanism involving the loss of post-transcriptional regulatory elements leading to a massive overexpression of *IL6* in a clinical case of inflammatory HCA associated with amyloidosis. Finally, I identified driver SVs affecting regulatory elements in hepatocellular carcinomas (HCC), including enhancer hijacking events activating *CCNE1* or *TERT* oncogenes.

To better understand the origin of SVs, I implemented a signature analysis framework considering the nature and size of SVs identified in each tumor. This approach allowed me to highlight HCC subgroups with particular SV signatures. In particular, I discovered a new clinicomolecular HCC subgroup driven by the activation of *CCNA2* or *CCNE1* by various mechanisms. These tumors (CCN-HCC) represent 7% of HCC and display a specific pattern of rearrangements (signature RS1) related to replication stress, with hundreds of focal duplications and templated insertion cycles. CCN-HCC are aggressive tumors but may be targetable by inhibitors of ATR response to replication stress.

Altogether, this work helps to refine the molecular characterization of both benign and malignant liver tumor by revealing new driver genes and molecular mechanisms. Those findings have clinical implications, as the definition of homogeneous cancer subgroups is essential to develop efficient tailored therapies.

Keywords:

Hepatocellular Adenoma, Hepatocellular Carcinoma, WGS, Structural Variations, Driver genes, Rearrangement Signature

Remerciements

Avant tout, je tiens à remercier mon jury de thèse pour avoir accepté d'examiner mes travaux de doctorat. C'est un honneur pour moi d'avoir l'opportunité de présenter l'aboutissement de mes travaux de thèse à des scientifiques experts dans leurs domaines. L'apport de votre expertise fera de ma soutenance de thèse une expérience des plus enrichissantes pour moi sur le plan scientifique.

Quatre années se sont écoulées depuis mon arrivée dans le laboratoire FunGeST, et j'en garderai un excellent souvenir, que ce soit sur le plan professionnel mais aussi personnel.

Pour cela, je remercie Jessica Zucman-Rossi, pour m'avoir accueilli dans son laboratoire et offert la possibilité de travailler sur la collection de données de séquençage NGS de HCC, tout à fait impressionnante. Par ailleurs, la richesse des raisonnements scientifique que tu apportes en labmeeting m'a grandement aidé dans mes propres réflexions.

Je tiens à remercier aussi Éric Letouzé, mon directeur de thèse. J'ai appris énormément pendant ces quelque année et en grande partie grâce à ta pédagogie et ton pragmatisme. Tes conseils pertinents et les discussions qu'on a pu avoir m'ont permis de clarifier à de nombreuses reprises mes objectifs et ouvrir le chemin à de nouvelles réflexions prometteuses. Tu es un directeur de thèse bienveillant, de bonne humeur et toujours pertinent dans les raisonnements scientifiques. Et puis ce n'est pas n'importe quel directeur de thèse qui accompagne ses étudiants à l'Oktoberfest! Batman approuve!

Je remercie chaleureusement tous mes collègues qui ont rendu si agréable cette expérience. Que ce soit en meetings, en congrès, mais aussi en pause déjeuner, pause-café ou after-work, j'ai passé des moments vraiment agréables avec vous tous et j'ose espérer retrouver une ambiance similaire dans mes prochaines aventures professionnelles.

Je remercie particulièrement les gens avec qui j'ai travaillé étroitement : Merci Sandrine pour toute les questions auxquelles tu m'as aidé à répondre ainsi que les pauses café du matin, merci Stefano pour ta 'jeunesse' éternelle et tes connaissances en stat, merci Théo pour ton énergie débordante et ta curiosité scientifique, merci Léa pour ton humour et le soutien mutuel inhérent à deux thésards contemporains. Merci à Eric T., Jayendra, Benedict, Raphaël, Amélie, Laura, Lisa, Camille, Anna-Line, Ana, Hélène, Clément, Jie, Jill, Massih, JC, JB, Guillaume, Julie, Maya, Elvire, Michalina, Alix, Pan Long, Gabrielle, Barkha, Samantha, Sandra, Didier et François.... Vous êtes nombreux et pourtant chacun d'entre vous a rendu ce 'voyage' exceptionnel.

Merci à ma famille, je regrette que je vous ne puissiez pas venir à ma soutenance à cause de la situation sanitaire. J'ai hâte de vous retrouver !

Merci à mes amis les plus proches, la compote complète (Tanguy, Kelbeu et Palmito) ainsi qu'Alexandre et Mika avec qui j'ai partagé des moments d'exception depuis 4 années et qui m'ont beaucoup apporté sur le plan personnel.

Enfin je remercie Tiziana, qui m'a grandement soutenu pendant cette dernière ligne droite et sans qui la dernière année covidesque aurait été bien déprimante...

ABBREVIATIONS

AA	Amyloid A		
AAV2	Adeno-associated Virus Type 2		
ATR	Ataxia Telangiectasia and Rad3-related		
BCLC	Barcelona Clinic Liver Cancer		
bex3HCA	Betacatenin exon 3 HCA		
bex7,8HCA	Betacatenin exon 7/8 HCA		
BFB	Breakage-Fusion-Bridge		
BIR	Break-Induced Replication		
BWA	Burrow-Wheeler Aligner		
CCN	Cyclin		
cDNA	Complementary DNA		
CFS	Common Fragile Sites		
CGC	Cancer Gene Census		
ChIP-Seq	Chromatin Immunoprecipitation sequencing		
CNA	Copy-number alterations		
COSMIC	Catalogue Of Somatic Mutations In Cancer		
CRP	C-Reactive Protein		
CTCF	CCCTC-binding factor		
DNA	DesoxyriboNucleic Acide		
DNase	DeoxyriboNuclease		
DRR	DNA Damage Response		
DSBs	Double Strand Breaks		
ENCODE	Encyclopedia of DNA Elements		
FDA	Food and Drug Administration		
FGFR	Fibroblast Growth Factor Receptors		
FLC	Fibrolamellar Carcinoma		
HBV	Hepatitis B virus		
НСС	HépatoCellular Carcinoma		
HCV	Hepatitis C virus		
ННСА	HNF1A activated HCA		
HI-C	HIgh-throughput Chromatin conformation capture		
HPV	Human Papilloma Virus		
HR	Homologous recombination		
ICGC	International Cancer Genome Consortium		
ID	small Insertions and Deletions signature		
IHCA	Inflammatory HCA		
LICA-CN	Liver Cancer - CN		
LICA-FR	Liver Cancer - FR		
LIHC-US	Liver Hepatocellular carcinoma - TCGA, US		
LINC-JP	Liver Cancer - NCC, JP		
LIRI-JP	Liver Cancer - RIKEN, JP		
MCC	Merkel Cell Carcinoma		
MCPyV	Merkel Cell Polyomavirus		
MODY	maturity-onset diabetes of the young		
mRNA	messenger RNA		

NAFLD	Non-Alcoholic Fatty Liver Disease
NASH	Non-Alcoholic SteatoHepatitis
NER	Nucleotide Excision Repair
NGS	Next Generation Sequencing
NHEJ	Non-Homologous End Joining
NK-cells	Natural Killer Cells
NMF	Non-negative Matrix Factorization
OC	Oral Contraception
pancan	pan-cancer
PARP	poly ADP ribose polymerase
PCAWG	Pan-cancer Analysis of Whole Genomes
PD-1	Programmed cell death-1
PDGFR	Platelet-derived growth factor receptor
PEI	Percutaneous Ethanol Injection
qPCR	quantitative Polymerase Chain Reaction
RFA	Percutaneous radiofrequency ablation
RNA	RiboNucleic Acide
RNA-Seq	RNA Sequencing
ROS	Reactive Oxygen Species
RS	Rearrangement Signature
SAA	Serum Amyloid A
SBS	Single Base Substitution signature
SH2	Src Homology 2
SH3	Src Homology 3
shHCA	sonic hedgehog HCA
SMC	Structural Maintenance of Chromosomes
SNVs	Single Nucleotide Variations
SVs	Structural Variations
TACE	Trans-Arterial ChemoEmbolization
TADs	Topologically Associated Domains
TCGA	The Cancer Genome Atlas
TC-NER	transcription-coupled nucleotide excision repair
TERTp	TERT promoter
TIC	Template Insertion Cycle
TSG	Tumor Suppressor Gene
UHCA	Unclassified HCA
UTRs	UnTranslated Regions
UV	Ultra-Violet
VEGFR	vascular endothelial growth factors receptors
WES	Whole Exome Sequencing
WGS	Whole Genome Sequencing
WNT	Wingless/Integrated

INDEX

I	INTRODUCTION	1
1. Ca	ncer is a disease of the genome	1
1.1.	Hallmarks of cancer	2
1.2.	Next-generation sequencing of cancer genomes	5
1.3.	Unraveling driver events	8
1.4.	The Pan Cancer Atlas of driver alterations	14
2. Fu	nctional consequences and molecular origin of SVs	16
2.1.	Functional impact of structural variants	16
2.2.	Mechanisms at the origin of structural variants	23
2.3.	Signatures of processes generating somatic alterations	28
3. Liv	ver cancer	34
3.1.	Hepatocellular adenomas	34
3.2.	Hepatocellular carcinoma	38
4. Ob	jectives of the PhD	45
II	MATERIAL AND METHODS	47
	ta used in the project	
1.1.	Tissue samples	
1.2.	Sequencing methods	
	pinformatics Pipelines	
2.1.	RNAseq alignement and expression matrix generation:	
2.2.	RNAseq Gene Set Enrichment Analysis (GSEA):	
2.3.	RNAseq fusion calling	
2.4.	WES / WGS alignment and mutation calling	
2.5.	WES / WGS copy number analysis and SV calling	
2.6.	Signature analysis and statistical tools	
2.7.	Table of pipeline used by project	51

III		RESULTS	53
1.	Ide	entification of oncogenic SVs in HCA	53
Arti	cle 1: S	Systemic AA Amyloidosis Caused by Inflammatory Hepatocellular Adenoma	55
Artio	cle 2:	Recurrent chromosomal rearrangements of ROS1, FRK and IL6 activating JAk	K/STAT
path	ıway iı	n inflammatory hepatocellular adenomas	73
2.	Stri	ructural rearrangement signatures reveal a new molecular entity of HCC	83
Artio	cle 3:	Palimpsest: an R package for studying mutational and structural variant sign	natures
alon	g clon	nal evolution in cancer	85
Artio	cle 4:	: Cyclin A2/E1 activation defines a hepatocellular carcinoma subclass	with a
		ment signature of replication stress	
IV		DISCUSSION	101
1.	Ide	entification of new driver structural rearrangements	101
	1.1.	Gene fusions altering protein structure	
	1.2.	Gene fusions inducing the overexpression of oncogenes	
	1.3.	Structural rearrangements altering regulatory sequences	103
2.	Rea	arrangement signatures in HCC	104
3.	In-c	depth characterization of the RS1 signature	109
	3.1.	RS1 as a replication stress signature in HCC	109
	3.2.	In-depth characterization of RS1 rearrangements by long-read optical mappin	g 111
4.	Clir	nical implications of the results	114
	4.1.	Liver cancer therapeutic options	
	4.2.	Identification of biomarkers of IHCA or CCN-HCC	
	4.3.	Tailored therapy for CCN-HCC and IHCA tumors	115
V		REFERENCES	118
VI		ANNEXES	1
1.	Anr	nex 1: Supplementary data Article 2	1
2.		nex 2: Supplementary data Article 4	
3.	Anr	nex 3: Article 5	58

I INTRODUCTION

1. Cancer is a disease of the genome

Cancer is the second leading cause of death worldwide after cardiovascular diseases and correspond to a major public health concern, with 9.6 million deaths from cancer worldwide in 2018 (Ferlay et al., 2019). First description of cancer was written approximately 2600BC, found in the Edwin Smith Papyrus, where Egyptian physician Imhotep describes breast cancer as a "bulging mass in the breast" that was resistant to any known treatment available at that time (Mukherjee, 2010). Medicine development during modern era led in the 17th and 18th centuries to various observations that directed strong links between chemical exposures and cancer development. Of note, in 1777, Percival Pott from London described an enrichment of scrotal cancers in chimney sweeps, which was caused by soot that was collected in the skin folds of the scrotum (Brown and Thornton, 1957). However, our understanding of cancer at the cellular and molecular level was initiated by its first scientific description using modern microscopes (Lin, 1983). Then, in the early 20th century, David Von Hansemann and Theodor Boveri's work led suggested that all cancers arise from a single cell undergoing genetic alterations that lead to abnormal behavior and uncontrolled cell division (Boveri, 1914). In the 1950's, Watson and Crick's findings on the double helix structure of DNA drastically accelerated genome comprehension (Watson and Crick, 1953). Three key studies paved the way for modern cancer genomics, as they described for the first time that cancers originate from somatic alterations in the human genome:

- In 1973, the Philadelphia chromosome (translocation between chromosomes 9 and 22) in chronic myeloid leukemia was the first identified genomic alteration related to cancer (Rowley, 1973).
- Ten years later, a single nucleotide base substitution (G>T) in the *HRAS* gene was shown to induce neoplastic cell transformation (Reddy *et al.*, 1982).
- Another study showed the requirement of src gene in Rous sarcoma virus to form neoplasm into chicken cells (Bishop, 1983).

Cancer cases dramatically increased in recent decades; in 2018 there were 18.1 million cases and 9.6 million deaths reported worldwide (Ferlay *et al.*, 2019), justifying the global research effort invested every year. The identification of molecular alterations at the origin of cancer has led to the development of effective targeted treatments in some specific tumor types. However, molecular studies revealed tremendous inter- and intraorgan heterogeneity. An exhaustive characterization of cancer subtypes and the molecular mechanisms driving them is essential for the development of effective treatments and diagnosis tools.

1.1. Hallmarks of cancer

The year 2000 marked the first sketch of important cellular capabilities fostering cancer development (Hanahan and Weinberg, 2000). This study highlighted six essential alterations in cell physiology that collectively dictate malignant growth (Figure 1):

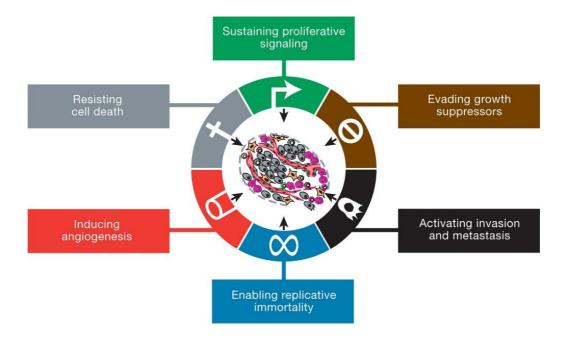


Figure 1: Representation of six functional capabilities acquired by most if not all cancers during their development. Those biological features can be acquired through various mechanisms (Hanahan and Weinberg, 2000).

- self-sufficiency in proliferative signaling;
- insensitivity to growth suppressors (antigrowth) signals;
- evasion of programmed cell death (i.e.: apoptosis);
- limitless replicative potential;
- sustained angiogenesis;
- tissue invasion and metastasis.

Some capabilities are required from the first steps of tumor growth, including self-sufficiency in proliferative signaling, insensitivity to growth suppressor signals, evading apoptosis and a limitless replicative potential. Other, like angiogenesis and metastasis potential, become necessary as the tumor develops. Additional knowledge gained from genomic and functional studies led Hanahan and Weinberg to update their landscape of tumor cell capabilities with two additional hallmarks (Hanahan and Weinberg, 2011). Firstly, tumor cells have the capability to modify or reprogram cell metabolism to accelerate neoplastic proliferation. Secondly, cancer cells are able to evade immunological destruction, in particular from T and B-lymphocytes, macrophages and NK-cells. In this update, authors also described two additional "enabling characteristics" of cancer cells that facilitate the acquisition of the hallmarks: genomic instability that accelerates the acquisition of driver events, and inflammation that contributes multiple hallmarks by supplying growth factors, pro-angiogenic factors, and extracellular matrix-modifying enzymes to the tumor microenvironment, sustaining proliferation, angiogenesis, invasion, and metastasis (Hanahan and Weinberg, 2011).

The alteration of functional capabilities mentioned above results from genomic alterations that can be inherited from parent genetic material or accumulated along cell divisions due to intrinsic mutational processes or environmental exposures. However, not all genomic alterations contribute to malignant transformation or cancer progression. Genomic alterations that provide a selective growth advantage and contribute to cancer development are called "driver" mutations; those that do not are termed "passenger" mutations (Stratton, Campbell and Futreal, 2009). Thus, the accumulation of driver events leads to more and more aggressive tumor cells. In some cases, disruption of DNA repair pathways can induce mutator phenotypes, accelerating the acquisition of additional drivers (Figure 2).

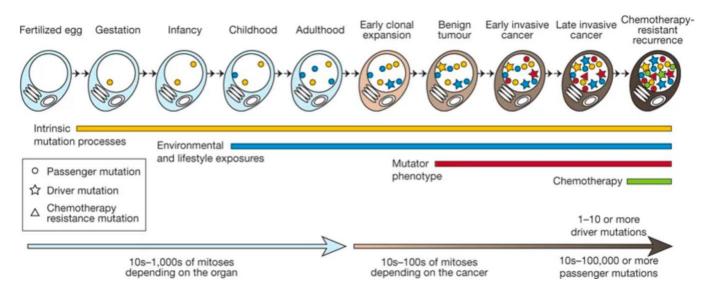


Figure 2: Model of somatic mutation accumulation in a cell lineage, contributing to cancer progression, through intrinsic mutational processed and environmental exposures. Those alterations are selected by giving cell a selective advantage, leading to clonal expansion cancer development. (Stratton, Campbell and Futreal, 2009)

The age distribution of cancer mortality rates let the statisticians Armitage and Doll to predict that 5 to 8 driver events were necessary for cancer development (Armitage and Doll, 1954). In agreement with this prediction, the Pan-Cancer Whole Genome (PCAWG) analysis from the International Cancer Genome Consortium (ICGC) recently demonstrated that cancer genomes harbor on average 4-5 driver mutations (Campbell et al., 2020). Finding these drivers is like looking for a needle in a haystack as thousands of passenger mutation accumulate from the zygote to the final tumor cell. Genes that have been identified as drivers in at least one cancer type are described as cancer genes and are categorized as oncogenes or tumor suppressor genes (TSG). Oncogenes are activated by mechanisms increasing their expression (e.g. chromosome amplifications) or missense mutations at specific hotspot regions increasing the activity of the protein. Tumor suppressors are inactivated by chromosome rearrangements (e.g. deletions), inactivating missense mutations or nonsense/frameshift mutations dispersed across the gene (Kern et al., 2006; Winter, Brody and Kern, 2006). Thus, cancer is a disease rooted in our genes, triggered by specific alterations in DNA, changing the biological equilibrium of a single cell and leading to clonal expansion. Recent evolution in sequencing technology lead to a discipline known as cancer genomics, aiming at unraveling genomic alterations to better understand cancer and develop more efficient treatments.

1.2. Next-generation sequencing of cancer genomes

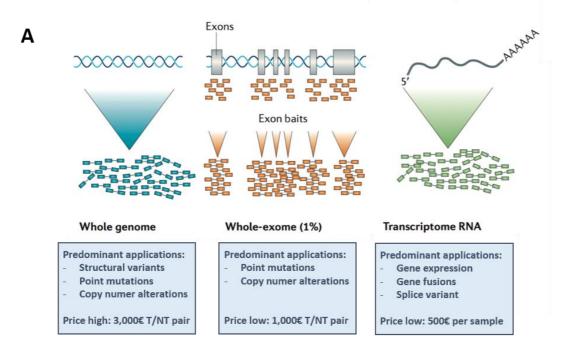
Pioneer works by Frederik Sanger on the development of the first generation of automated DNA sequencers (Sanger sequencing) and further technological improvements allowed the Human Genome Project to produce the first draft of the human genome in early 21th century (Craig Venter *et al.*, 2001; Lander *et al.*, 2001). This project paved the way for modern high throughput sequencing method, termed Next Generation Sequencing (NGS). Three methods are extensively used in cancer genomics: whole exome, whole genome and RNA sequencing (Figure 3).

Whole exome sequencing (WES) involves the capture and sequencing of the coding regions (around 1%) of the genome and is massively used to identify coding cancer driver mutations. Two main protocols can be used for the capture step:

- In amplicon-based capture, hybridization probes are designed based on sequences of annotated exons available in transcriptome libraries, such as Ensembl (Cunningham *et al.*, 2019), and fixed to a microarray. After extracting and fragmenting the hybridized DNA, sequencing adapters are attached to the double-stranded DNA fragment in order to produce short sequences, which correspond to both ends of the fragment.
- In-solution hybridization capture methods involve fragmenting double-stranded DNA and ligating adapters to those fragments. Then, target sequences are labeled using a pool of custom oligonucleotides designed to capture annotated exons, as in previous method. Those oligonucleotides are labeled with beads, allowing the separation of sequences of interest.

Finally sequencing step will produce short-read reads covering the exons of the genome.

Exponential decrease of sequencing costs allowed the democratization of *whole genome sequencing (WGS)* in cancer genomics. The protocol consists in extracting and fragmenting DNA of a tissue. Then, adapters are added to each end of the fragments and the DNA library is sequenced. Contrary to WES, that only allows the analysis of exonic mutations and copy-number alterations, WGS reveals mutations and structural variations in non-coding RNA genes and regulatory regions (enhancers, transcription-factor binding sites, insulators) that can profoundly alter the expression of cancer genes.



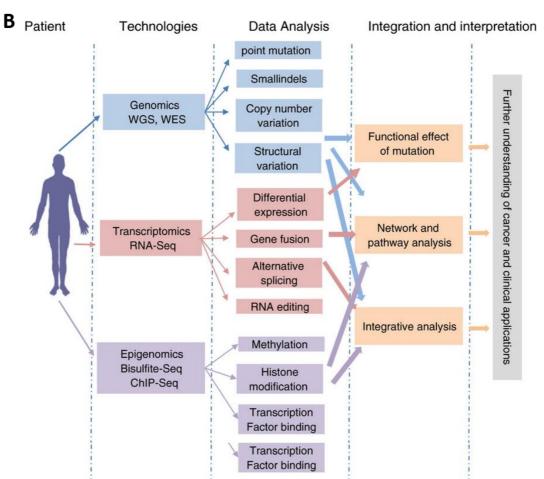


Figure 3: Next Generation Sequencing in cancer genomics. A: Scheme representing the material sequenced in WGS, WES and RNAseq. WGS gives access to the whole genome but is the most expensive technique. WES is a cheaper alternative, but only targets the coding part of the genome. Finally, RNAseq purpose is to sequence the transcriptome, giving a different information that can be integrated with genomic data to identify functional alterations. B: The 3 above-mentioned methods, additionally with innovative implementation of epigenetics sequencing (ChIP-Seq, HI-C, Bisulfite-Seq) must be integrated to identify genomic/epigenetic alterations and their functional consequences to better characterize cancer deregulations and foster the development of tailored therapies. (Liu et al, 2013).

The 3rd method, *RNA sequencing (RNAseq)*, gives access to the transcriptome. Two protocols exist for RNAseq. The first protocol involves isolating RNA using a deoxyriboluclease (DNase) and sequencing the whole RNA material in a sample. The second method consists in capturing messenger RNAs with 3'polyadeylated (poly(A)) tail by mixing RNA with polyT oligomers covalently attached to magnetic beads. Then, RNA material from both methods can be converted into double-stranded cDNA fragments and sequenced using classical NGS workflow. This method is complementary with WGS and WES as it gives access to gene expression changes and abnormal transcripts such as fusion genes and alternative splicing events.

Besides the information provided by each NGS technology, integration of WGS with RNAseq is a powerful way to reveal driver events affecting the expression of genes or transcript structure. For example, mutations in gene promoters can both increase or decrease the expression level of genes, by changing the affinity of cis regulatory elements (Nault and Zucman-Rossi, 2016). Splice site mutations can alter the splicing process of the pre mRNA and modify the structure of the mRNA.

Finally, recent development of alternative sequencing approaches expands the possibilities of cancer genomics. These sequencing technologies allow identifying epigenetic alterations, corresponding to modifications in the genome structure or regulation, without direct alteration of the sequence. Recent studies have exploited those types of data to better understand the causes and consequences of cancer driver alterations:

- ChipSeq (chromatin immunoprecipitation coupled with sequencing) consists in sequencing the DNA regions bound by a specific protein. This method allows identification of transcription factor binding sites, histone modifications and more (Raha, Hong and Snyder, 2010). This method is largely used to understand epigenetic deregulations, at the origin of driver gene expression changes that could cause tumorigenesis (Bender *et al.*, 2013)
- Hi-C (chromatin conformation capture) data provide contact probabilities between genomic regions at high resolution. This information is fundamental to understand some alterations activating distant region of the genome by changing genome 3D conformation (Lieberman-Aiden *et al.*, 2009).

RepliSeq data give a high resolution view of replication timing along the genome, using a differential marking of nascent DNA during replication (Hansen *et al.*, 2010). Replication timing is indeed known to influence spatial organization of the genome, and thus shape the mutational landscapes of cancer genomes (De and Michor, 2011).

1.3. Unraveling driver events

Computational analysis of NGS data involves two main steps to unravel the driver events leading to tumorigenesis:

- First, the identification of somatic alterations in each tumor by comparing sequencing data of tumors versus its paired healthy tissue or a pool of non-tumor data.
- Second, the identification of functional events, supported by either a significant recurrence or a functional proof that the alteration of a gene favors tumor development.

1.3.1. Identifying somatic alterations

Once the raw sequencing data has been aligned to a human genome reference with algorithms like BWA mem (Li *et al.*, 2009), various tools are applied to unravel different types of somatic alterations:

between aligned reads and the reference genome and compare the distribution of variant reads between the tumor and matched normal sample. The main challenge is to distinguish real variants from sequencing errors. Tumor heterogeneity and contamination of clinical samples with normal cells makes this task challenging. MuTect2, developed by the Broad Institute, is one of the most popular algorithm to identify somatic point mutations and small insertions and deletions (indels) (Benjamin *et al.*, 2019). It uses two Bayesian classifiers: the first one detects whether the tumor is non-reference at a given genomic position and, for those sites that are found as non-reference, the second classifier makes sure the non-tumor sample does not carry this specific variant. Post-filtering steps are also included to

remove recurrent artifact mutations like variants found in a panel of non-tumor samples or occurring in a region with many clustered variants (Figure 4).

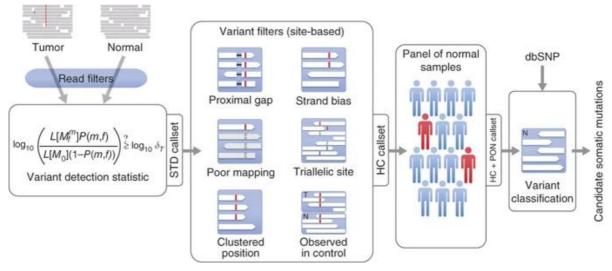


Figure 4: Reads of sequencing generated from tumor and non-tumor sample are differentially aligned to the reference genome. After initial calling of variant by the Bayesian classifier, post filtering is used to remove first recurrent artefactual results, but also putative somatic mutations that are compared to a panel of normal samples to remove residual false-positives, caused by rare errors (Cibulskis et al., 2013).

Copy-number alterations (CNA) analysis is based on the depth of sequencing. The genome is split in equal-size regions, and the median coverage in the tumor and non-tumor sample (WGS or WES) is calculated in each window. The log-ratio of tumor versus non-tumor depth is calculated for each bin i:

$$LRR_{i} = log_{2} \left(\frac{Depth_{T_{i}}}{Depth_{NT_{i}}} \right)$$

LRR can then be processed by simple segmentation algorithm, that compare the LRR points distribution along the chromosomes and extract segments with a similar LRR distribution. Then amplifications, gains, deletions and homozygous deletions can be estimated genome wide. Additionally some methods, such as the Genome Alteration Print (Popova *et al.*, 2009), were developed to exploit both LRR changes and allelic imbalance at germline polymorphisms (B Allele Frequency, BAF). In other words, BAF is the normalized proportion of arbitrary established allele B in a two allele mixture (Figure 5). This information can be very useful in case of copy-neutral loss of heterozygosity (cn-LOH), where a parental allele is lost and the other duplicated, that can foster tumorigenesis for example by deregulating imprinted regions (O'Keefe, McDevitt and Maciejewski, 2010).

Results

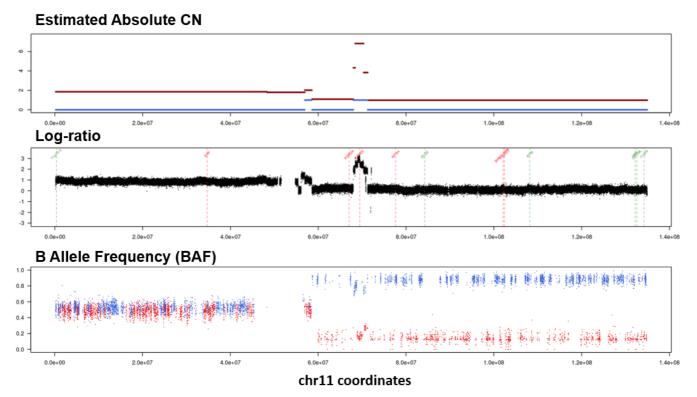


Figure 5: CCND1 amplification identified in an HCC sample by WGS. Top: estimated absolute copy number. Red line corresponds to the total number of copy at each position, while the blue correspond to the minority allele. Middle, log-ratio estimated from tumor and non-tumor sequencing coverage. Bottom: B Allele Frequency (BAF). Blue dots represent the fraction of major allele while red dots represent the minor allele fraction. This track allows to identify copy neutral LOH, when a parental allele is removed and replaced by the other parental allele. This can lead to deregulation of parentally imprinted loci.

Finally, Structural Variations (SVs) are more and more described to be involved in cancer development. Manta (Chen *et al.*, 2016) is a tool developed by Illumina for SV calling, that operates in two phases: first a graph of all distant junction of the genome is built where edges represent putative somatic abnormal junction between 2 distant genomic regions. In this step, the entire reads mapped on the genome are scanned to fine evidence of i) multi-mapped individual reads, ii) matereads aligned on two distant regions, supporting a long range association or iii) reads whose mate is not mapped at all (Figure 6A-B). In the second step, Manta analyses these individual graph edges and groups highly connected edges to unravel and score SVs of high confidence (Figure 6C). Robust identification of SV somatic events can be more challenging than detection of SNVs. Indeed, recent benchmark of somatic variant callers by the ICGC consortium showed that the sensitivity of identification is way lower for SVs than for SNVs on simulated data (Alioto *et al.*, 2015). This results in an under-representation of SVs among driver alterations in cancer (Huddleston and Eichler, 2016; Audano *et al.*, 2019).

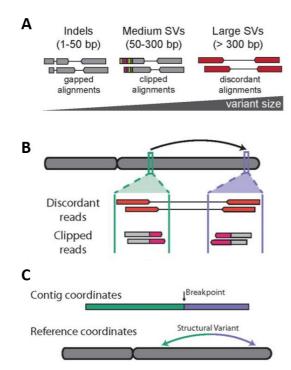


Figure 6: Calling of SV from short-read WGS. A: Representation of the different read pairs that can be informative to find evidences of SV. On the left, gapped alignment are the consequence of small indels, whose size is of the same order of magnitude than read length. For medium sized SV, most informative reads are soft-clipped alignment, where one of the two mate pair is half aligned on both distant contig corresponding to the abnormal junction. Also this kind of mapping is used to obtain the precise coordinate of the breakpoint. Finally, for large SVs, mate-pair reads, aligning on very distant regions of the genome are informative of abnormal junction. B: Chromosomal representation of a distant abnormal junction between green and purple loci. Different supporting reads are schematized below. Reconstruction of the rearranged molecule from supportive reads. Modified from Jeremiah Wala et al 2018.

1.3.2. Recurrence and genomic covariates

Using the abovementioned methods, we can obtain the catalogue of somatic alterations in a series of tumors. The next step is to discriminate driver from passenger alterations. The most widely used approach is to look for significantly recurrent events, as drivers should be selected in multiple tumors whereas passengers occur by chance and should be different across tumors. Several studies, from the lab and others, have used this approach to define the landscape of driver genes in liver cancers from recurrent mutations and focal CNAs (Schulze, Imbeaud, Letouzé, *et al.*, 2015; Fujimoto *et al.*, 2016).

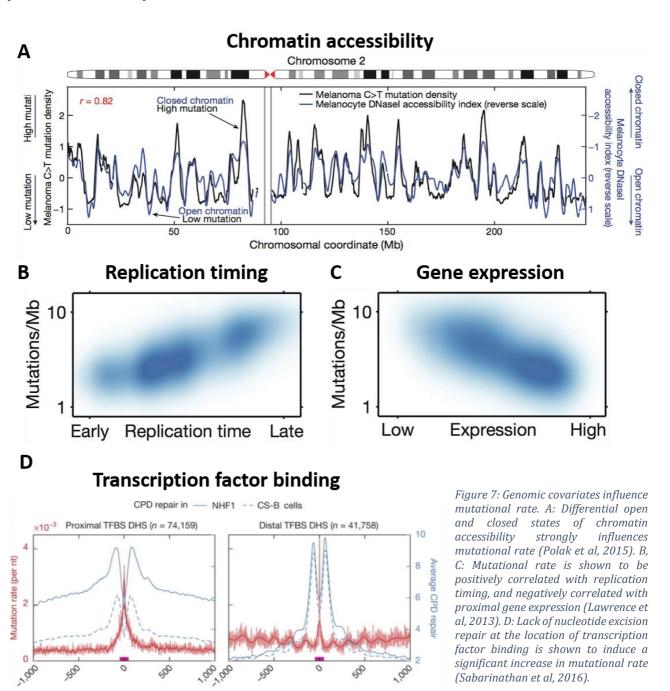
Importantly, several genomic covariates impact the mutation rate along the genome such as chromatin organization, DNA accessibility, local base composition, gene expression and DNA replication timing (Lawrence *et al.*, 2013; Polak *et al.*, 2014; Morganella *et al.*, 2016; Glodzik *et al.*, 2017). Key genomics covariates are detailed below:

- **Chromatin accessibility.** Chromatin is the complex of DNA and proteins corresponding to chromosomes. Nucleosomes are the protein complexes that regulate the 3D architecture of chromatin, in order to maintain cell phenotype (Woodcock and Ghosh, 2010; Gibcus and Dekker, 2013). Nucleosomes are involved in differential DNA packaging, by maintaining two different chromatin

states: relaxed (euchromatin) and condensed (heterochromatin). These differential 3D states have a key role in gene regulation, as open chromatin is required for active gene expression. Besides regulation, 3D conformation also has an impact on mutation rate. Indeed, heterochromatin and repressive histone marks like H3K9me3 are associated with elevated mutation rates, whereas euchromatin and active marks like H3K27ac have lower mutation rates (Schuster-Böckler and Lehner, 2012; Polak *et al.*, 2014, 2015) (Figure 7A). This may be due to restricted activity of DNA repair enzymes to dense chromatin regions.

- Replication. DNA replication processes segments of ~400-800kb in a specific order during the S phase of the cell cycle. Thus, the genome of a specific cell type can be divided into early and late replication domains. Late-replicating regions are known to have higher mutation rates (Lawrence *et al.*, 2013; Sima and Gilbert, 2014) (Figure 7B). This change in mutation rate was shown to be a consequence of mutations occurring after the inactivation of the DNA mismatch repair (MMR) mechanism in late replicated regions (Chen *et al.*, 2010; Supek and Lehner, 2015). Moreover, some SVs tends to be enriched in late replicated regions, congaing Common Fragile Sites (CFS) (Glover, Wilson and Arlt, 2017; Gómez-González and Aguilera, 2019), while some SVs such as duplications are shown to be enriched in early replicated regions (Li *et al.*, 2020).
- (Lawrence *et al.*, 2013) (Figure 7C). The transcription-coupled nucleotide excision repair (TC-NER) can efficiently remove mutations occurring on the transcribed strand. This mechanism reduces the overall mutation burden in expressed genes and results in a mutational asymmetry between the two DNA strands aptly known as transcriptional strand bias (Haradhvala *et al.*, 2016). Finally, a strong enrichment of mutations at transcription factor binding sites was demonstrated in cell lines, as a consequence of decreased nucleotide excision repair (NER) activity (Sabarinathan *et al.*, 2016) (Figure 7D).

Interestingly, recent studies have shown that different mutational processes can have different interactions with genomic covariates (Morganella *et al.*, 2016). For example, mutational processes related to bulky DNA adducts (tobacco, aflatoxin B1) are strongly repressed in highly expressed genes due to the removal of adducts by TC-NER, whereas a mutational signature related to alcohol consumption is activated in the same regions (Letouzé *et al.*, 2017).



Those genomic covariates can bias the analysis of mutation recurrence by generating hotspots due to high local mutability rather than functional selection of alterations. Tools like MutSigSV (Lawrence *et al.*, 2013), developed by the Broad institute, take into account

the abovementioned parameters and the background distribution of mutations in the tumor series to identify significantly recurrent mutations while controlling for genomic covariates. Similarly, a regression approach taking into account various (epi)genomic features was recently proposed to identify significantly recurrent SVs not explained by local genomic context in breast cancer genomes (Glodzik *et al.*, 2017). Other methods have been developed to identify recurrent CNAs, like GISTIC2.0 (Mermel *et al.*, 2011) that takes into account both the frequency and amplitude of CNAs to define hotspots of gains and deletions.

1.4. The Pan Cancer Atlas of driver alterations

In the last decade, many sequencing projects were conducted by individual laboratories or international consortia like TCGA (The Cancer Genome Atlas; https://www.cancer.gov/tcga) and ICGC (International Cancer Genome Consortium; https://icgc.org/), producing WES, WGS and/or RNAseq data from thousands of tumors spanning most cancer types. This scientific effort allowed to establish the landscape of driver genes involved in each cancer.

1.4.1. Cancer Gene Census

The Cancer Gene Census (CGC) is an ongoing effort to catalogue those genes, which contain mutations causally implicated in cancer. Regularly updated by the COSMIC (Sondka *et al.*, 2018) literature curation team, 719 cancer-driving genes are now described with a variety of alteration mechanisms across all human cancer types. This pan-cancer list of driver genes is a useful resource to annotate new data with known drivers. However, it is important to keep in mind that rare alterations remain to be identified, especially in rare tumor entities.

1.4.2. PCAWG (Pan Cancer Analysis of Whole Genomes)

The most comprehensive pan-cancer genome analysis to date is probably the ICGC-PCAWG (https://dcc.icgc.org/pcawg) published in Nature in early 2020. The PCAWG consortium analyzed whole genome sequences from 2,600 primary cancers and their matching normal tissues across 38 distinct tumor types (Campbell *et al.*, 2020), to define an exhaustive landscape of driver genes and reconstruct the natural history of cancers.

Across the PCAWG tumors, 43,778,859 somatic SNVs, 2,418,247 somatic indels and 288,416 somatic SVs were identified and used to define an integrated set of driver events.

91% of tumors had at least one identified driver mutation, with an average of 4.6 drivers per tumor and 2.6 coding driver mutations per tumor, consistent with previous TCGA publication (Martincorena *et al.*, 2017). 25% of PCAWG tumors harbored at least one putative non-coding driver mutation, with 1/3 of them affecting *TERT* promoter (9% of PCAWG tumors). This underlines the benefit of WGS over WES to define the exhaustive set of driver events in a tumor genome (Figure 8A). This work also confirmed that many driver mutations affecting TSG are two-hit inactivation events: on the 954 tumors in the cohort with driver mutations in *TP53*, 736 (77%) had both alleles mutated, 96% of which (707 out of 736) combined a somatic point mutation that affected one allele with somatic deletion of the other allele (Figure 8C).

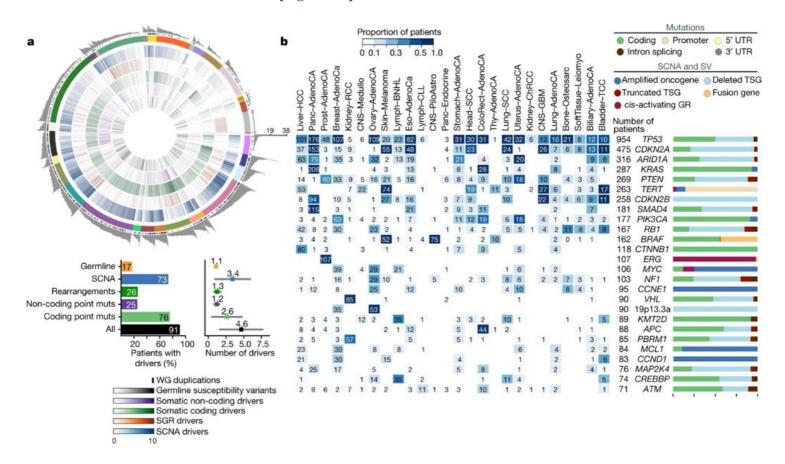


Figure 8: Landscape of PCAWG pan-cancer driver analysis (Campbell et al, 2020). A: The circos plot represents putative driver mutations identified in the PCAWG project. Each colored sector represents a tumor type. From the periphery to the center of the plot the concentric rings represent: (1) the total number of driver alterations; (2) the presence of whole-genome (WG) duplication; (3) the tumor type; (4) the number of driver CNAs (SCNA); (5) the number of driver genomic rearrangements (SGR); (6) driver coding point mutations; (7) driver non-coding point mutations; and (8) pathogenic germline variants. On the bottom, bar plot (left) represents the proportion of patients with different types of drivers. The dot plot (right) represents the mean number of each type of driver mutation across tumor cohort with at least one event (the square dot) and the standard deviation (grey whiskers), based on n = 2,583 patients.

B, Driver genes targeted by different types of mutations in the cohort. Both germline and somatic variants are included. Left, the heatmap shows the recurrence of alterations across cancer types. The color indicates the proportion of mutated tumors and the number indicates the absolute count of mutated tumors. Right, the proportion of each type of alteration that affects each gene. C:

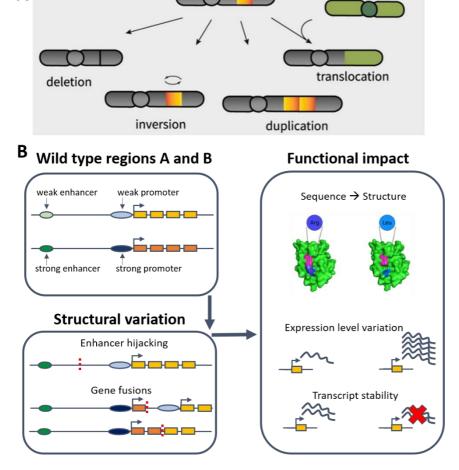
Tumor-suppressor genes with biallelic inactivation in 10 or more patients. The values included under the gene labels represent the proportions of patients who have biallelic mutations in the gene out of all patients with a somatic mutation in that gene.

PCAWG efforts led to a complete landscape of driver alteration associated to each cancer type, with more than 90% of PCAWG cases with at least one identified driver. However, in 181 tumors no driver alteration was identified. This can be due to either low quality or contaminated samples but also statistical power limitation associated with cohort size, leading to failures in the bioinformatic algorithms to identify new driver genes (Campbell *et al.*, 2020). Notably, structural variations in non-coding regions are more and more shown to be involved in tumorigenesis and there is evidences that this type of alteration is under-represented among driver alteration of cancer (Huddleston and Eichler, 2016; Audano *et al.*, 2019).

2. Functional consequences and molecular origin of SVs

2.1. Functional impact of structural variants

Structural Variations (SV) represent all the rearrangements of chromosome structure and include 4 fundamental types: deletions, duplications, inversions and translocations (Figure 9).



Α

Figure 9: A: The 4 fundamental types of structural variation of the genome. Deletions, inversions, duplications and translocations are known to be recurrent molecular mechanisms at the origin of cancer development (Yi & Ju 2018). B: Functional consequences of abnormal junctions (red dotted line) induced by structural variations. breakpoint can modulate gene expression by altering regulatory regions such as promoters enhancer. transcriptional regulatory domains. Moreover, protein structure can be impaired following intragenic alteration (chimeric protein following gene fusion, truncated protein, post-translational regulatory domains alteration)

SVs can induce copy-number changes that alter the expression of target genes. Besides, they induce abnormal junctions between distant regions of the genome. Those junctions can have functional consequences by i) joining exons of two different genes, producing a chimeric transcript with a tumorigenic potential (Hutchinson *et al.*, 2013), ii) altering the gene structure and induce loss of negative regulatory regions (Mudduluru *et al.*, 2011), iii) placing the gene under the influence of a strong enhancer, called enhancer hijacking (Northcott *et al.*, 2014), and iv) placing the gene in a region of open chromatin and more accessible to transcription factors (Weischenfeldt *et al.*, 2017).

2.1.1. Copy-number alterations

CNAs include gains, amplifications (focal regions with a high number of extra copies), heterozygous and homozygous deletions of chromosome regions. Last decade, WES was extensively used to identify driver CNAs and revealed deletion hotspots involving many tumor suppressor genes (*CDKN2A*, *PTEN* or *RB1*...). In contrast, hotspots of genomic amplification contribute to the overexpression of oncogenes (*CCND1*/*FGF19*, *MYC*, *CCNE1*...). A recent pan-cancer study established that 70 genes are recurrently amplified and 70 genes are recurrently deleted across all their pan-cancer cohort including almost 5,000 tumors from 11 cancer-types (Zhang *et al.*, 2018). However, WES does not allow to define the mechanisms at the origin of CNAs, as the abnormal junction are usually located outside coding regions covered by this approach. Thus, WGS and RNAseq are necessary to identify other types of driver SVs.

2.1.2. Gene fusions

Gene fusions occur when a structural rearrangement brings together the 5' and 3' ends of two different genes. Philadelphia chromosome, discovered in 1960, induces the *BCR-ABL1* fusion in myeloid leukemia. This fusion leads to a constitutively active tyrosine kinase domain, inducing downstream activation of PI3K and MAPK pathways (Cilloni and Saglio, 2012; Hantschel, 2012; Sinclair, Latif and Holyoake, 2013). Since this early discovery, many oncogenic fusions have been identified. For example, a frequent translocation between chromosomes 11 and 22 creates the *EWSR1-FLI1* fusion, characteristic of Ewing sarcoma. This fusion combines the 5' transcriptional activation domain of *EWSR1* with the 3' ETS DNA-binding domain of *FLI1* to yield a potent oncogene through transcription factor activation (Delattre *et al.*, 1992, 1994). Some fusions are cancer specific, like the *PRKACA-DNAJB1* fusion specific of fibrolamellar carcinomas that is used to differentiate this specific cancer type from other liver tumors (Honeyman *et al.*,

2014; Dinh *et al.*, 2017). On the contrary some fusions are seen in a large variety of cancers, like the *FGFR3-TACC3* in-frame activating kinase fusion found in glioblastomas, lung adenocacrinomas and gliomas (Singh *et al.*, 2012; Collisson *et al.*, 2014; Lasorella, Sanson and Iavarone, 2017). Some studies used public RNAseq data from thousands of tumor samples to perform pan-cancer analyses of fusions and develop comprehensive databases such as ChimerDB (Lee *et al.*, 2017; Jang *et al.*, 2020). The TCGA consortium analyzed gene fusions in almost 10,000 tumors from 33 cancer types. They concluded that fusions frequently involve a kinase domain and drive tumorigenesis in 16.5% of cancer cases. Importantly, 1% of cancer cases are characterized by a single gene fusion as driver event fueling tumorigenesis (Gao *et al.*, 2018) (Figure 10). Gene fusions are thus interesting targets for precision medicine, exemplified by the success of inhibitors targeting the kinase activity of *RET*, *ROS1* and *ALK* fusions in lung cancer (Takeuchi *et al.*, 2012; Kohno *et al.*, 2015).

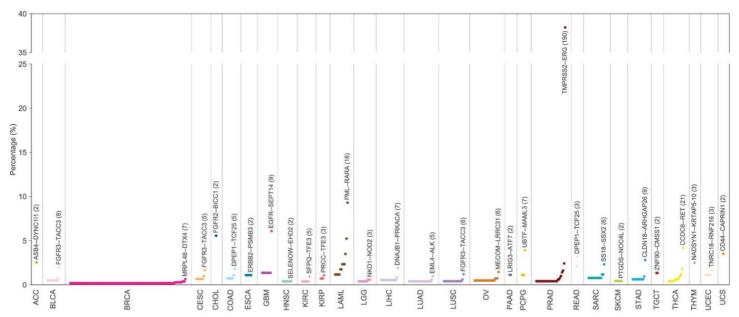


Figure 10: Frequency of gene fusions in 29 cancer types. The dot plot shows the frequency of recurrent fusions found in each cancer type. The most recurrent fusion in each cancer type is labeled. Cancer types without recurrent fusions are not shown. (Gao et al, 2018).

2.1.3. Enhancer Hijacking

Structural variations can also alter the regulatory regions and thus the transcription of cancer genes. Direct alteration of cis-regulatory regions was extensively studied. In hepatocellular carcinomas (HCC), *TERT* promoter mutation is required as an early event to trigger *TERT* expression and activate the telomere maintenance pathway (Nault *et al.*, 2013). Apart from *TERT* promoter, WGS studies revealed few non-coding driver mutations, but more frequent examples of SVs altering the regulatory regions of

driver genes (Fredriksson *et al.*, 2014; Weinhold *et al.*, 2014; Rheinbay *et al.*, 2020). A well-known mechanism named "*enhancer hijacking*" corresponds to the displacement of a strong enhancer upstream an oncogene. Enhancer hijacking was first described in medulloblastma (Northcott *et al.*, 2014). In this work, the authors identified a cluster of SVs leading to the juxtaposition of *GFI1B* and *GFI1* to local or distal DNA elements. Using ChIPseq, they confirmed the presence of enhancer chromatin marks in this region, with peaks of H3K27ac and H3K9ac immediately adjacent to the SV breakpoints, leading to the activation of *GFI1B* or *GFI1* (Figure 11).

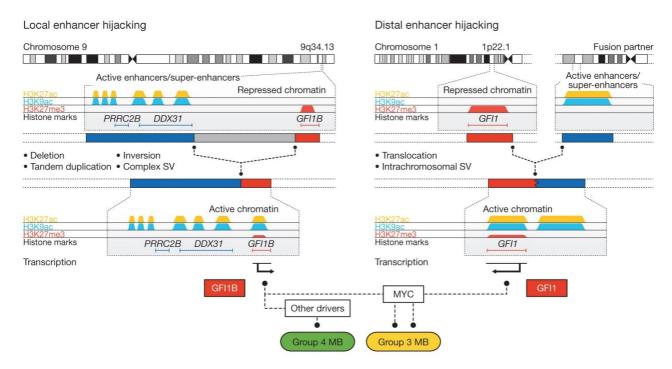


Figure 11: Mechanisms of SV leading to enhancer hijacking observed in GFI1/GFI1B-activated medulloblastomas. Activation of GFI1 and GFI1B are respectively induced by intra (left) and inter-chromosomal (right) rearrangements. Both oncogenes can cooperate with MYC to promote medulloblastoma pathogenesis. (Northcott et al., 2014)

A related mechanism, called promoter hijacking, was recently descried in the lab in a subgroup of hepatocellular adenomas. In these tumors, a focal deletion juxtaposes the promoter and exon 1 of the highly expressed *INHBE* gene upstream the *GLI1* oncogene. This promoter hijacking induces a massive over-expression of *GLI1* and the development of adenomas activating sonic hedgehog pathway (shHCA)(Nault *et al.*, 2017).

2.1.4. Local alteration of the 3D architecture

Eukaryotic genome has a highly organized three-dimensional (3D) structure, with an important role in gene regulation. Different levels of organization were described, using methods like HI-C (Lieberman-Aiden *et al.*, 2009) (Figure 12):

- **Nuclear center versus periphery**. This first level of organization involves two distinct nuclear compartments. Expressed genes tend to be located in euchromatin, in the nuclear center, while repressed genes are located in heterochromatic regions, at the periphery of the nucleus (Bickmore, 2013).
- **Chromosomes territories**. Chromosomes occupy distinct sub-nuclear territories, with transcriptionally active loci located at the surface of those structures (Cremer and Cremer, 2001, 2010) (Figure 12A).
- Compartments A and B. Chromosomes segregate into regions corresponding to long-range interactions, forming two distinct compartments names "A" and "B". The A compartments are characterized by active chromatin, enriched in highly expressed genes, whereas "B" compartment correspond to inactive chromatin, enriched in repressed genes (Lieberman-Aiden *et al.*, 2009). Thus A and B compartments are tens to hundreds of kilo-bases regions, characterized by intradomain interactions but a lack of inter-domain interaction. These intra-domains contacts are commonly named Topologically Associated Domains (Nora *et al.*, 2012) (Figure 12A).
- **Topologically Associated Domains (TADs)**. In mammals, TADs are strongly conserved features bordered by protein complexes composed of the CCCTC-binding factor (CTCF) and the structural maintenance of chromosomes (SMC) cohesin complex (Dixon *et al.*, 2012). CTCF and cohesion protein complexes also define intra-TAD chromatin loops. These shorter length structures enable more subtle regulatory control of enhancer-promoter interactions (Matthews and Waxman, 2018).

Genomic alterations disrupting 3D chromatin conformation can trigger tumorigenesis by altering gene regulation. For example, a pan-cancer study revealed recurrent overexpression of *TERT*, *IRS4* and *IGF2* oncogenes in different cancers due to SVs disrupting TADs boundaries (Weischenfeldt *et al.*, 2017) (Figure 12B).

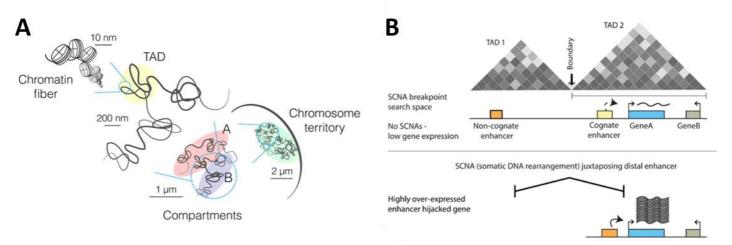


Figure 12: A: Representation of chromatin structure, from chromosome territories to Topologically Associated Domains (TADs) (Szabo et al., 2019). B: Model of enhancer hijacking following TAD boundaries disrupting. Heatmap shade of greys indicate contact probability between pair of genomic regions. In this scheme, the orange enhancer, associated to TAD1, will activate blue gene transcription following a TAD disrupting through somatic structural rearrangement. (Weischenfeldt et al. 2017)

2.1.5. Alteration of post-transcriptional regulatory regions

After transcription, untranslated regions (UTRs) and polyA tails control the stability of the transcripts. Alterations of those post-transcriptional regulatory regions can activate oncogenes or inactivate TSG. For example, recurrent *CSF1* fusions have been described in tenosynovial giant cell tumors (upstream *COL6A3* in 33% of cases), with a junction always downstream exon 5 of *CFS1*. This fusion leads to an overexpression of the transcript and the first interpretation was that *COL6A3* or other partner genes may bring active regulatory domains leading to increased transcription (Möller *et al.*, 2008). However, recent work showed that deletion of *CSF1* 3' UTR triggers tumorigenesis even in absence of gene fusion, suggesting that the loss of regulatory elements in 3'UTR explains the increased expression (Ho *et al.*, 2020).

2.1.6. Viral insertions

Viral DNA can integrate into the human genome and induce trigger tumorigenesis by placing a potent viral enhancer upstream an oncogene a mechanism called "insertional mutagenesis" (Bishop, 1987). Only 4 viruses are known to be able to induce insertional mutagenesis:

- **Human Papilloma Virus (HPV).** HPV is frequently integrated in the host cell genome and associated with the partial or complete loss of the E1 and E2 viral

genes, which regulate the activity of viral oncoproteins E6 and E7. However, hotspots of HPV integrations in the human genome have been described, including *MYC*, *POU5F1B*, *FHIT*, *KLF12*, *KLF5*, *LRP1B* and *LEPREL1* (Gudlevičiene *et al.*, 2015; Hu *et al.*, 2015). As those genes are involved in modulating cell proliferation, development and carcinogenesis both oncoproteins and insertional mutagenesis may have a tumorigenic effect

- Merkel Cell Polyomavirus (MCPyV). MCPyV DNA is detected in around 80% of biopsies of Merkel Cell Carcinoma (MCC), a rare and aggressive skin cancer. Polyomaviruses depend on the host cell to replicate and use two DNA-binding proteins to trigger replication: the large T antigen physically interacts with and inhibits tumor suppressors pRB and p53, allowing the cell to progress through the G1-to-S checkpoint, and small T antigen induces transcription of E2F, necessary for turning on essential S phase genes. In MCCs, the MCPyV genome random integrations contain the large T antigen gene, but systematically mutated in helicase and DNA binding domains, inducing an inhibition of viral replication and preventing lytic viral replication that could be lethal for cancer cells. However, the produced chimeric protein is still able to interfere with pRB and drive cell proliferation, leading to a pro-oncogenic state that may lead to carcinomas (Erstad and Cusack, 2014).
- Hepatitis B Virus (HBV). This virus has a tropism for liver and is a major cause of hepatocellular carcinomas (HCC). Most frequently the virus acts through indirect mechanism by the role of its oncoproteins or by inducing liver cirrhosis, an inflammatory environment prone to HCC development. Conversely, HBV can directly activate driver genes following HBV insertional mutagenesis. TERT, CCNE1, KMT2B, SENP5 and ROCK1 are well-known oncogenes whose expression is recurrently activated by HBV in liver cancer (Sung et al., 2012).
- Adeno-associated Virus Type 2(AAV2). AAV2 was identified in the lab as a new virus able to generate insertional mutagenesis. In 2015, recurrent AAV2 integrations were described in HCC affecting the well-known oncogenes *TERT*, *CCNA2*, *CCNE1* and *TNFSF10* (Nault *et al.*, 2015). In 2019, another oncogene, *GLI1*, was identified to be activated through AAV2 insertions in HCC developed from benign hepatocellular adenomas (HCA) (La Bella *et al.*, 2020). The insertional mutagenesis of both HBV and AAV2 in *TERT* promoter suggests that viral

insertions are early events in the tumorigenesis process, as *TERT* promoter mutations were recurrently found in pre-neoplastic lesions (Nault *et al.*, 2013) (Figure 2).

2.2. Mechanisms at the origin of structural variants

Whole genome sequencing of thousands of tumors, notably by the ICGC-PCAWG consortium (Li *et al.*, 2020), revealed considerable variability in the number and types of structural variations both across and within cancer types (Figure 13). Some tumors display large numbers of SVs belonging to a same category, defining deletor or duplicator phenotypes that can be further subdivided by the size of rearrangements (Degasperi *et al.*, 2020). Other tumors are dominated by clustered or non-clustered inter-chromosomal translocations. These distinct phenotypes suggest the existence of various mechanisms of genomic instability operative with different strength across tumors.

In addition to the 4 simple SV categories (deletions, duplications, inversions and translocations), complex rearrangements involving many abnormal junctions and copynumber changes acquired through a single event have been identified:

Breakage-fusion-bridge (BFB) cycle is a complex pattern of rearrangement that was first described almost a century ago (McClintock, 1939) and later shown to be associated with the amplification of *RUNX1* driving acute lymphoblastic leukemia, (Papaemmanuil *et al.*, 2014). In a situation of telomere crisis, at the anaphase step of mitosis, telomeres of sister chromatids can fuse together before being pulled apart in opposite directions. This will lead to a dicentric chromosome and the formation of an anaphase bridge, visible in microscopy (Figure 14A bottom). Eventually the two fused chromatids will break, but not necessarily at the fusion point, resulting in a daughter cell with an arm loss when the other harbors a fold-back inversion and gain of genomic material (Murnane, 2012). Since resulting chimeric chromosomes still lack telomeres, this process can repeat and produce recognizable patterns fold-back inversion junctions and stair-like copy-number increase at the extremity of the altered chromosome arm (Figure 14A top).

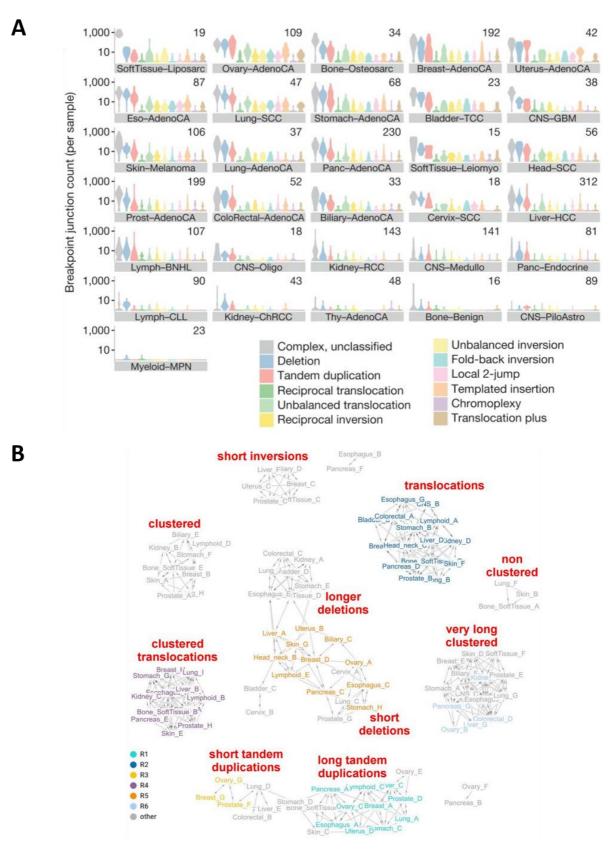


Figure 13: A: Violin plots of types of SVs across different cancer types. In each panel, the number of patients is indicated at the top right. AdenoCA, adenocarcinoma; BNHL, B-cell non-Hodgkin lymphoma; ChRCC, chromophobe renal cell carcinoma; CLL, chronic lymphocytic leukaemia; CNS, central nervous system; GBM, glioblastoma; HCC, hepatocellular carcinoma; leiomyo, leiomyosarcoma; medullo, medulloblastoma; MPN, myeloproliferative neoplasm; eso, oesophageal; oligo, oligodendrocytic; panc, pancreatic; piloastro, pilocytic astrocytoma; prost, prostate; RCC, renal cell carcinoma; sarc, sarcoma; SCC, squamous cell carcinoma; TCC, transitional cell carcinoma; thy, thyroid. (Li et al., 2020) B: Network connecting highly similar rearrangement signatures across different organs. Each circle represents a signature and particular phenotypes of deletions, duplications, etc. are annotated (Degasperi et al. 2020).

- **Chromothripsis** (from the greek *thripsis* which means "shattering into pieces") is a complex rearrangement first described in 2011 (Stephens et al., 2011). Chromothripsis induces hundreds of DNA breaks simultaneously on one or a few chromosomes. The chromosome fragments are then randomly stitched together or lost, presumably by the non-homologous end-joining (NHEJ) repair mechanism (Stephens et al., 2011). Chromotripsis results in chimeric chromosomes with numerous copy-number changes (oscillations between normal and deleted states) and abnormal junctions (Figure 14B top), both of which can induce gene expression changes. For example, chromothripsis has been shown to induce recurrent loss of SMAD4, APC, PTEN or CDKN2A. On the contrary, abnormal junctions can activate oncogenes like CCND1, CDK4 or MDM2 (Cortes-Ciriano et al., 2014). The most frequent chromothripsis-associated driver gene is *TP53*, probably because inactivation of genes maintaining the genome stability favors chromothripsis occurrence and selection. Two main mechanisms linked to missegregated chromosomes have been proposed to be at the origin of chromothripsis (Ly and Cleveland, 2017). The first one is a telomere crisis leading to chromosome or sister chromatids end-to-end fusions, followed by formation of chromatin bridges (Garsed et al., 2014). The second proposed mechanism is a micronuclei formation during mitosis (Kato and Sandberg, 1968; Johnson and Rao, 1970). Molecular processes in micronuclei are known to be error prone, and it was proposed that isolated genomic materials can be massively broken into pieces and reassembled.
- chromoplexy (from the greek *pleko*, meaning to weave) is another complex rearrangement pattern. It was first described in prostate cancers harboring *ETS* gene fusions, then in other solid tumors like non-small cell lung, head and neck and melanomas cancers (Baca *et al.*, 2013). In contrast to chromothripsis, this phenomenon is mostly characterized by inter-chromosomal translocations, involving up to 8 chromosomes, whereas chromothripsis is restricted to 1 or 2 chromosomes. In addition, the altered regions are focal on each chromosome, whereas chromothripsis alterations can be chromosome wide. Finally, Baca and collaborators defined chromoplexy as a closed chain of rearrangements, occasionally combined with focal "deletion bridges" in the vicinity of abnormal

junction. Except those deletions bridges, there is no loss of genomic regions characteristic of the 2 levels of copy number seen in chromothripsis. Recent pancancer studies (Agrawal *et al.*, 2014; Cortés-Ciriano *et al.*, 2020) described recurrent oncogenic events induced by chromoplexy, such as *RET*, *BRAF* and *NTRK3* fusions, or *IGF2BP3* enhancer hijacking. The genome-wide distribution of DSBs in chromoplexy is enriched in actively transcribed and open chromatin regions (Marnef, Cohen and Legube, 2017), suggesting that these catastrophic events may occur in nuclear transcription hubs where many co-regulated genomic regions from different chromosomes are spatially aggregated (Baca *et al.*, 2013) (Figure 14C). Thus, the proposed mechanism is a multiple breakage of DNA in a restricted transcription hub, followed by the mis-reparation of the different bluntend (Figure 14D).

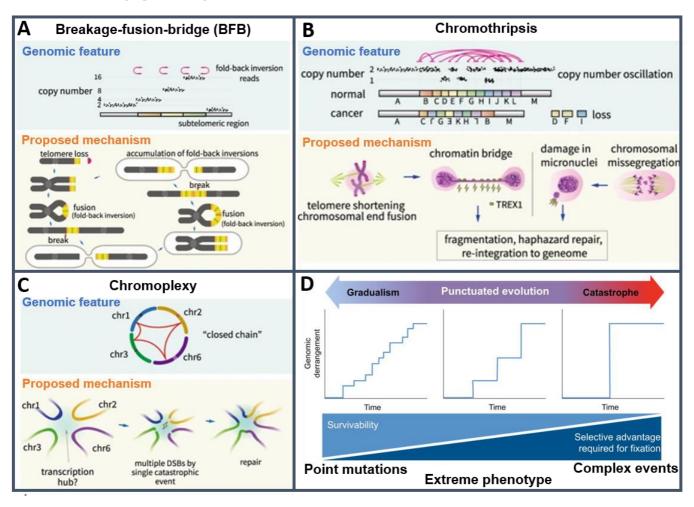


Figure 14: A-C: Complex genomic alteration recurrently seen in cancer, and their associated proposed mechanisms. (modified from Yi et al., 2018). D: Proposed model of punctuated evolution of cancer, where tumorigenesis can progressively be triggered by i) gradual accumulation of simple mutations, giving progressively cell survivability, ii) Rapid accumulation of alteration induced by a particular biological defect of environmental exposure, or iii) a single catastrophic event, giving a significant selective advantage to become a clonal feature. (modified from Baca et al., 2013)

In addition to these 3 well-documented events, Li *et al.* recently described new categories of complex SVs (Li *et al.*, 2020) . Thus, we are only beginning to understand the diversity of structural rearrangements in cancers.

Chromothripsis and chromoplexy are complex events occurring at a single time of cell life (Stephens *et al.*, 2011; Baca *et al.*, 2013). Thus, there is a heterogeneous dynamic in cancer development that can be discretized in three states (Figure 14D).

- First cancer can slowly develop, by progressively accumulating mutations such as stochastic "clock-like" mutations described by L. Alexandrov and collaborators, induced by stochastic error and repair mechanisms (Alexandrov *et al.*, 2015).
- Secondly, rapid accumulation of alteration in a short period can be the result of particular biological defect, as the extreme phenotypes described by Degasperi and collaborators, triggered by homologous recombination deficiency (Degasperi et al., 2020). Accelerated evolution of cancer can also be induced by specific exposures such as Aflatoxin B1 mycotoxin produced by Aspergillus flavus and Aspergillus parasiticus which grow in soil or decaying vegetation. Exposure to this mycotoxin was shown to be associated with specific pattern of mutations in hepatocellular carcinoma inducing an increase of mutational burden (Letouzé et al., 2017).
- Finally, singe catastrophic events are probably lethal for the cell and may tend to require co-occurring oncogenic lesions to become fixed in a tumor by giving a strong selective advantage (Baca *et al.*, 2013) (Figure 14D).

In summary, different patterns of SVs were described in cancer, reflecting the diverse mechanisms at their origin, more or less active in different tumors. SVs may be due to i) stochastic biological errors such as mis-segregation of chromosomes, ii) abnormal cell state such as telomere crisis leading to inherent errors of NHEJ, triggered by an abnormal biological context, or iii) a specific gene defect leading to inhibition of a repair mechanism, such as *BRCA1*-mutated breast cancer harboring a HR defect. However, the molecular cause of most SV phenotypes remains to be unraveled. Defining signatures of SVs related to specific processes is important for basic research, but also to develop efficient personalized therapies. For example, breast cancers patients harboring a *BRCA1* or *BRCA2*

mutations and the associated signature of duplications are good responders to PARP inhibitors (Sikov *et al.*, 2015).

2.3. Signatures of processes generating somatic alterations

Cancer cells accumulate somatic alterations through various intrinsic and extrinsic processes. Those processes leave characteristic imprints on the genome, termed mutational signatures (Alexandrov, Nik-Zainal, Wedge, Campbell, et al., 2013). Mutational signatures are more or less active in each tumor depending on intrinsic biological processes (e.g. DNA repair) or environmental factors, and the contribution of each process to the tumor mutation burden is called its *exposure*. Mutational processes can also evolve between the early and late steps of tumorigenesis. The combination of processes a cancer cell has been exposed to results in its final mutational portrait (Figure 15). For example, one of the first mutational patterns related to a cancer risk factor was the abundance of C>T / G>A substitutions and CC>TT / GG>AA dinucleotide substitutions associated to UV (Ultra-Violet) *exposure*. This observation soon led to the first description of mutational processes signatures (Howard and Tessman, 1964; Witkin, 1969).

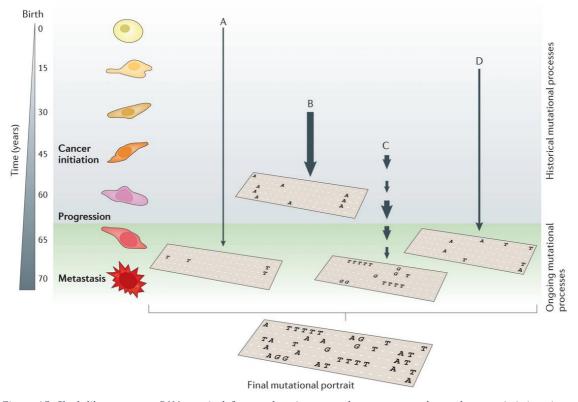


Figure 15: Clock-like processes, DNA repair defects and environmental exposures can leave characteristic imprints, termed signatures, in cancer genome. Arrows indicate both duration and intensity of mutational process exposure. In this model, the final mutational portrait is the sum of the 4 mutational processed involved (A, B, C and D) and their identification is useful to understand tumor biology and develop targeted therapies. (Helleday et al., 2014)

2.3.1. NMF implementation for mutational signatures

With the advent of NGS, and in particular whole genome sequencing, the characterization of mutational signatures has greatly improved in the last decade. Ludmil Alexandrov, at the Wellcome Trust Sanger Institute, developed the first mathematical method to extract signatures of single nucleotide variations (SNVs) (Alexandrov, Nik-Zainal, Wedge, Campbell, *et al.*, 2013). First, SNVs are classified into 96 categories based on the type of substitution and the 3' and 5' bases around the mutation. Using the pyrimidine (C or A) of base pair as reference, 6 substitutions can be defined: C:G > A:T; C:G > G:C; C:G > T:A; T:A > A:T; T:A > C:G, and T:A > G:C. The 3' and 5' bases around the mutation define 16 different trinucleotide contexts, resulting in 96 (6x16) SNV categories that can be used to describe the mutation catalogue of a tumor (Figure 16, left).

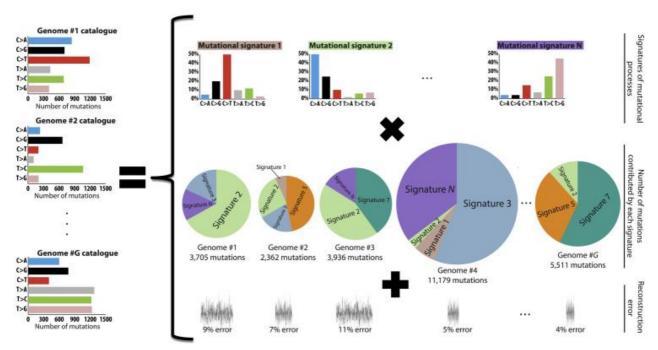


Figure 16: Scheme illustrating mutational processes operative in a set of G cancer genomes catalogues of mutations. This data can be used to deconvolute the signatures of N mutational processes as well as the number of mutations caused by each of the processes in each of the genomes. As the inverse process corresponding to reconstruction of the original from signatures and respective exposure lead to slight variations with the original catalogue. This is the result of genome-specific reconstruction error. (Alexandrov et al., 2013a).

Alexandrov *et al.* also introduced a statistical framework to extract, from the mutation catalogues of a series of tumors, the number of operative mutational processes, their signatures and their *exposure* in each tumor (Figure 16, right). This is a classic case of "cocktail party" problem (Alexandrov, Nik-Zainal, Wedge, Campbell, *et al.*, 2013). Imagine a cocktail party room with tens of guest groups speaking about various subjects, resulting in an incomprehensible mixture of sounds. This room is equipped with several record devices, located at different spots in the room, recording the mixture of conversations,

whose respective intensities depend on the distance of guest groups from each microphone. By integrating the different records, their location in the room and the differential intensity of conversations, it can be possible to decompose each distinct conversation from the mixture of sounds and locate them in the room. In this analogy, distinct conversations are mutational signatures, individual records are the catalogue of mutational signature in one tumor and the intensity of a recorded conversation is the *exposure*. By integrating the series of mutations catalogues, it is possible to decipher the set of mutational signatures at the origin of alterations and their respective exposure in each cancer. From a mathematical point of view, the mutational catalogue of a cancer genome is the linear combination of a set of signatures whose exposures can be very heterogeneous among the different cancers of the cohort. Moreover, in the case of NGS data, catalogues of alterations are expected to contain noise due to stochastic sequencing/analysis errors. We can express the mutational catalogues over the tumor series as a matrix M, with M_{ij} enumerating over mutation categories i and cancer samples j. The mutation matrix *M* can be decomposed into 2 matrices of smaller size (Alexandrov, Nik-Zainal, Wedge, Campbell, et al., 2013):

$$M_{ij} = \sum_{k=1}^{N} S_{ik} E_{kj} + \mathcal{E}_{ij},$$

where N represents the number of active signatures in the cohort, and E the minimized residual matrix. The columns of matrix S describe the composition of the signature in terms of mutation categories, with S_{ik} the frequency of mutation category i in signature k. The second matrix E is the exposure matrix of each signature k in row, associated to each sample j in column.

In a more generalized definition, the mutational catalogue is approximately the sum of mutational signatures multiplied by their respective exposures:

$$M \approx SE$$
 (Eq.1)

In order to deconvolute signal and extract S and E matrices, the mutational signature extraction computational workflow is based on the Non-Negative Matrix Factorization (NMF). This core step corresponds to the Brunet et al. implementation of the multiplicative update algorithm, shown to extract biologically meaningful components from complex biological data (Lee and Seung, 1999; Brunet *et al.*, 2004). Formally, the NMF extracts N signatures, approximately solve the Equation 1, by finding non-negative matrices S and E that minimize the Frobenius norm:

$$\min_{S \ge 0, E \ge 0} ||M - SE||_F^2$$

This framework paved the way to the association of etiologies and specific mutational patterns at the origin of tumorigenesis. Ludmil Alexandrov et al. applied this innovative framework to analyze 4,938,362 mutations from 7,042 cancers, subdivided in 30 cancer types and extracted more than 20 distinct mutational signatures (Alexandrov, Nik-Zainal, Wedge, Aparicio, et al., 2013). More recently, pan-cancer analysis of 4,645 cancer genomes and 19,184 cancer exomes by the PCAWG group revealed an extended set of 49 mutational signatures (Alexandrov et al., 2020). These signatures can be consulted in the COSMIC c.3 database [https://cancer.sanger.ac.uk/cosmic/signatures]. Single Base Substitution (SBS) signatures identified so far include (Figure 17):

- Clock-like signatures SBS1 (deamination of methylated cytosines) and SBS5 (unexplained) that accumulate with age in all cell types.
- Signatures related to specific environmental exposures like SBS4 (tobacco), SBS7 (UV light) or SBS24 (aflatoxin B1 exposure)
- Signatures of DNA repair defects like SBS3 (BRCA1/2 mutations inducing homologous recombination deficiency) or SBS6 (mismatch repair deficiency).
- Finally, some signatures are induced by genotoxic treatments. For example, SBS11 and SBS31/35 are respectively associated with temozolomide and cisplatin treatment.

The repertoire of mutational signature (Figure 17) is heterogeneous in terms of etiologies, but also in term of organs, some signatures being ubiquitous (SBS1), or on the contrary restricted to a few cancer types (SBS24). Finally, the mutational burden induce by each signature is extremely variable.

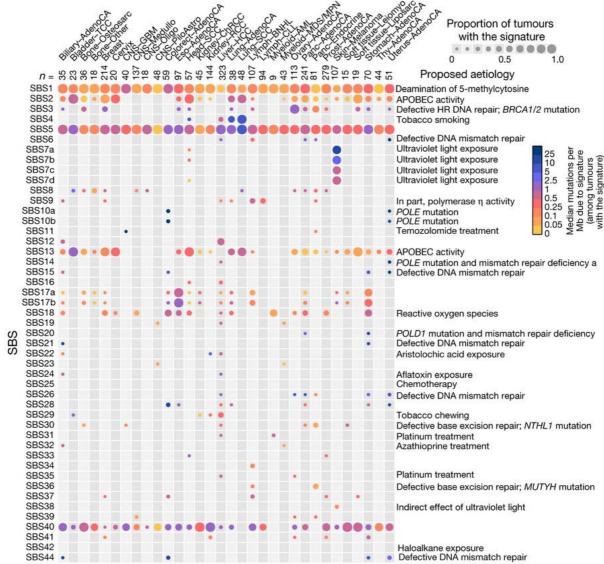


Figure 17: Number of mutations associated to each SBS mutational signature in PCAWG tumors.. Dot size represents the proportion of samples of each tumor type that harbor the mutational signature. The color of each dot represents the median mutation burden of the signature in exposed samples. There is a large heterogeneity in signature exposure across the different tissue types. Moreover, the mutational burden induced by signature is also heterogeneous with some signature inducing large number of mutations compared to others. (Alexandrov et al., 2020).

2.3.2. Extension of signatures to structural rearrangements

The signature analysis framework, based on NMF algorithm, was first developed for point mutations but it can be extended to any type of alteration. For example, the recent work by the PCAWG group identified, in addition to the 49 single-base-substitution signatures, 11 doublet-base-substitution and 17 small insertions and deletions (indel) signatures (Alexandrov *et al.*, 2020). The definition of categories needs to be adapted to each type of alteration, but the core step of signature deconvolution remains unchanged. This approach has also been applied to structural variations (SVs) to identify tumor phenotypes characterized by an enrichment of specific types of rearrangements. Nik-Zainal and collaborators described the first SV signature analysis framework to unravel

rearrangement signatures in 560 breast cancer genomes. In this framework, SVs were divided in 32 categories based on 3 criteria:

- **The type of alteration**, within the 4 fundamental types of SVs: inversions, duplications, deletions and translocations.
- **The size of the event** (for inversions, deletions and duplications only), i.e. the distance between the two breakpoints: 1-10kb; 10kb-100kb; 100kb-1Mb; 1Mb-10Mb and more than 10Mb.
- **Rearrangement clusters**. Clustered rearrangements and non-clustered rearrangements are considered separately.

This classification allowed the authors to extract 6 distinct rearrangement signatures operative in breast cancers (Nik-Zainal *et al.*, 2016) (Figure 18) including a signature of focal tandem duplications (<10 kb) related to *BRCA1* inactivation, a signature of large tandem duplications (>100 kb), and a signature of focal deletions associated with *BRCA2* deficiency.

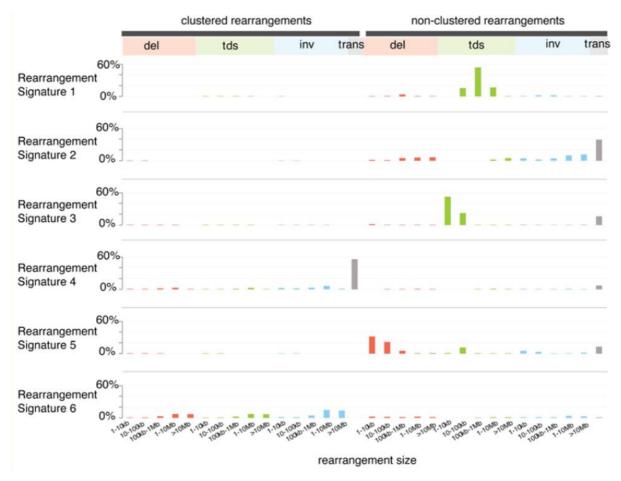


Figure 18: Six rearrangement signatures extracted using Non-Negative Matrix Factorization. Probability of rearrangement element on y-axis. Rearrangement size on x-axis. Del= deletion, $tds = tandem\ duplication$, inv = inversion, trans = translocation. (Nik-Zainal et al., 2016a)

3. Liver cancer

Liver cancer is the second leading cause of cancer-related deaths worldwide. With an incidence of approximately 850,000 new cases and 810,000 deaths per year (overall ratio of incidence to mortality of 0.95) this cancer has a very poor prognosis (Llovet *et al.*, 2016; Bray *et al.*, 2018). Liver neoplasms include benign and malignant lesions. Hepatocellular adenoma (HCA) is the most studied benign tumor because of its clinical management associated with tumor bleeding and malignant transformation into hepatocellular carcinoma (HCC). HCC is a very aggressive malignant tumor representing approximately 90% of all cases of primary liver cancer. Both HCA and HCC are developed from hepatocytes, the main liver cell type managing metabolic and detoxification processes.

3.1. Hepatocellular adenomas

3.1.1. Epidemiology and risk factors for HCA

HCA are rare benign tumors, with an overall prevalence around one case per million. Various associated risk factors have been identified:

- **Hormonal exposure.** Oral contraception (OC) administration and in general androgen and estrogens are the major risk factor for HCA development. Indeed, this cancer mostly arises in young women, with a 30-fold increased incidence associated to the use of oral contraceptives (OC), and a significantly increased risk after 5 years of treatment (Rooks *et al.*, 1977). This results in an higher incidence of HCA in western countries where the use of oral contraception is more common compared to Asia or Africa (Matsumoto *et al.*, 2011). Moreover, androgen administration for therapeutic use (ie: Fanconi anemia) is associated with HCA development (Touraine *et al.*, 1993). Similarly, anabolic androgenic steroids abuse for bodybuilding purpose is also a risk factor of HCA (Sánchez-Osorio *et al.*, 2008).
- **Alcohol and obesity.** Alcohol consumption and obesity were shown to be risk factors for HCA development (Bedossa *et al.*, 2007; Guichard *et al.*, 2012). This results presumably from the direct toxic role of alcohol or the production of cytokines during both long-term alcohol consumption and chronic liver inflammation associated with obesity. Interestingly those two risk factor are restricted to an inflammatory subgroup of HCA (Nault *et al.*, 2017).
- **Genetic background**. Finally, several rare genetic syndromes are strongly associated with HCA occurrence. MODY (maturity-onset diabetes of the young)

type 3 is a type of non-insulin dependent diabetes mellitus with autosomal dominant inheritance, occurring usually before the age of 25. This pathology is associated with a germline monoallelic HNF1A mutation leading to the development of liver adenomatosis, characterized by more than ten hepatic adenomas (Bacq et al., 2003; Reznik et al., 2004). In MODY3 patients, HCA development follows a "2-hit" alteration model of TSG where the germline alteration is followed by a somatic inactivation of the second wild type allele of HNF1A (Nault et al., 2017). Another rare genetic disease associated with HCA development is glycogenosis type 1a. This is a rare recessive metabolic syndrome occurring in very young patients and characterized by a germline mutation inactivating G6PC (glucose-6-phosphatase). G6PC inactivation leads to the accumulation of glycogen and fat in the liver and to a 25 to 75% risk of HCA development depending on the studies (Labrune et al., 1997; Froissart et al., 2011). Finally, McCune-Albright syndrome, characterized by "café au lait" skin macula and fibrous dysplasia of bones, is also strongly associates with HCA development. This syndrome is caused by a somatic mosaic mutation of *GNAS* gene, located on an imprinted locus, that leads to aberrant activation of adelylate cyclase (Weinstein and Shenker, 1993). Interestingly, GNAS gene is recurrently mutated in the inflammatory subgroup of HCAs (Nault et al., 2017).

Risk factors associated to HCA are various, resulting in multiple subgroups of HCA, characterized by specific molecular alterations and clinical presentation, such as the inflammatory adenomas above-mentioned.

3.1.2. Molecular diversity of HCA

Before NGS studies, targeted sequencing of candidate loci had revealed 4 HCA driver genes (*HNF1A*, *CTNNB1*, *IL6ST* and *GNAS*) but a large part of tumors remained without a molecular driver alteration (Calderaro *et al.*, 2013). Next generation sequencing allowed non supervised multi-omics analysis that helped refine the heterogeneous landscape of HCA sub-groups. The current classification, based on molecular and transcriptomic features is constituted of 6 HCA subgroups, associated with specific risks factors, clinical behavior and tumor histology (Nault *et al.*, 2017) (Figure 19):

- Inflammatory HCA (**IHCA**) is the most frequent HCA subgroup, accounting for 34 to 44% of all HCAs. IHCA is characterized by constitutive activation of the

IL6/JAK/STAT signaling pathway due to activating mutations of various members of the pathway. IHCA driver genes include *IL6ST* encoding gp130 receptor (77%), *FRK* encoding a src kinase (9%), *STAT3* encoding a transcription factor of JAK/STAT pathway (4%), *GNAS* encoding stimulatory G-protein alpha subunit (3%) and *JAK1* encoding a tyrosine kinase protein of the JAK/STAT pathway (1%). 6% of IHCAs remain without identified molecular alteration (Nault *et al.*, 2017). Those different alterations lead to the translocation of STAT3 in the nucleus, triggering the uncontrolled activation of the inflammatory pathway, characterized by an over-expression of acute phase inflammatory proteins CRP (C-Reactive Protein) and SAA (Serum Amyloid A).

- HCAs harboring a *CTNNB1* exon 3 or exon 7,8 represent respectively 13% and 7% of all HCAs. **b**^{ex3}**HCA** harbor mutations or deletions in *CTNNB1* exon 3 that inhibit β-catenin protein phosphorylation by APC/GSK3B/AXIN complex, preventing proteasome degradation. This unregulated β-catenin will be translocated to the nucleus, inducing the strong activation of WNT/β-catenin target genes, such as *GLUL*, *ZNRF3* or *LGR5* (Rebouissou *et al.*, 2016). The smaller **b**^{ex7,8}**HCA** subgroup is defined by *CTNNB1* mutations in two hotspots in exon 7 or 8, leading to a weaker activation of the WNT/β-catenin pathway (Pilati *et al.*, 2014). Interestingly, half of *CTNNB1*-mutated HCAs (either bex3HCA and bex7,8HCA) also display an inflammatory phenotype through CRP and SAA protein over-expression following *JAK/STAT* pathway activation. This leads to two mixed subtypes of HCA: **b**^{ex3}**IHCA** and **b**^{ex7,8}**IHCA**. (Nault *et al.*, 2017) (Figure 19).
- *HNF1A* inactivated HCAs (**HHCA**) are the second most frequent subtype of HCA. This sub-group is defined by a bi-allelic inactivation of *HNF1A*, a key transcription factor involved in hepatocyte differentiation (Bluteau *et al.*, 2002). Its inactivation leads to glycolysis and aberrant fatty acid production that can induce tumor steatosis, lipogenesis and mammalian target of rapamycin (mTOR) activation (Merle *et al.*, 2019).
- The last identified subgroup is characterized by the activation of sonic hedgehog pathway (**shHCA**) and represents 4% of HCAs. The molecular mechanism at their origin is a small deletion leading to the *INHBE-GLI1* gene fusion. *INHBE* is highly expressed in the liver. *GLI1* is the key transcription factor of sonic hedgehog pathway and is normally barely expressed in the liver. The fusion leads to a

- chimeric transcript, producing an over-expressed functional *GLI1* protein. shHCA are associated with a high risk of bleeding (Nault *et al.*, 2017).
- Finally, around 7% of HCAs (**UHCAs**) tumors are still unclassified. These tumors do not harbor any mutation in known driver genes nor particular transcriptomic signature (Nault *et al.*, 2017).

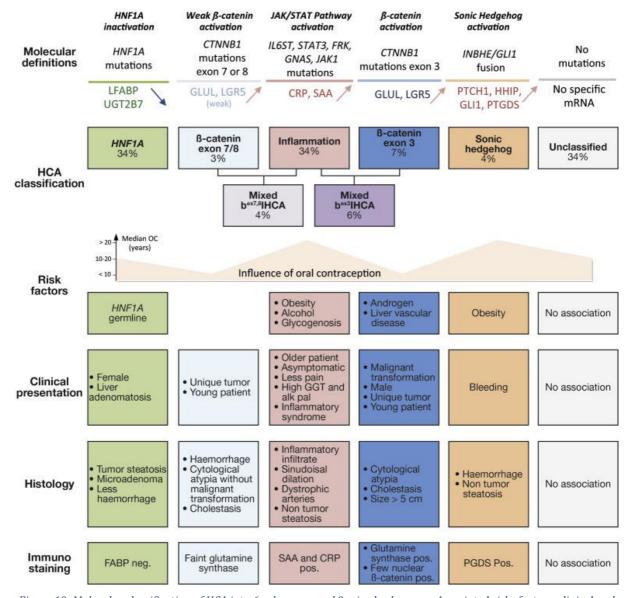


Figure 19: Molecular classification of HCA into 6 subgroups and 2 mixed subgroups. Associated risks factors, clinical and histological features of tumors are detailed above each subgroup (Nault et al., 2017).

3.1.3. Clinical features

Hepatocellular adenomas require clinical management to avoid the main complications that are tumor bleeding (in shHCA) and malignant transformation to hepatocellular carcinoma (HCC) (Nault *et al.*, 2017). Mutations in *CTNNB1* exon 3 are

known to be associated with a high risk of malignant transformation, making $b^{ex3}HCA$ and $b^{ex3}IHCA$ subgroups the most at risk of progression into HCC. By contrast, $bex^{7,8}HCA$ and $bex^{7,8}IHCA$ subgroups are not associated with HCC development, suggesting that a strong WNT/ β -catenin activation is necessary to trigger malignant transformation. (Zucman-Rossi *et al.*, 2006; Pilati *et al.*, 2014; Rebouissou *et al.*, 2016; Nault *et al.*, 2017). *TERT* promoter mutations activating telomerase maintenance pathway were shown to be a recurrent second hit in adenoma to carcinoma transition, following *CTNNB1* exon 3 mutation (Pilati *et al.*, 2014).

3.2. Hepatocellular carcinoma

3.2.1. Epidemiology and risks factors for HCC

Hepatocellular carcinoma is the most frequent primary liver cancer (Yang and Roberts, 2010) and is responsible for more than 500,000 deaths yearly, making it the 3rd deadliest cancer worldwide (Bray *et al.*, 2018). HCC incidence depends on the geographical location, with around 80% of cases occurring in southeast Asia and sub-Saharan Africa (McGlynn *et al.*, 2001). Interestingly, etiology is also highly associated with geography (Figure 20A).

In Africa and Asia, HCC are most of the time associated with Hepatitis B Virus (HBV) chronic infection, whereas Hepatitis C Virus (HCV) is the main cause of HCC in some countries like Japan or Egypt (Wansbrough-Jones *et al.*, 1998; Lok *et al.*, 2009). HBV and HCV viruses induce acute of chronic hepatitis and ultimately cirrhosis, favoring HCC development (Baron, 1996). Indeed, chronic liver damage leads to a cycle of cell death, regeneration and fibrosis during which HCC precursor cells undergo malignant transformation. Moreover, insertional mutagenesis of HBV but also AAV2 are shown to drive tumorigenesis by activating oncogenes (Nault *et al.*, 2015; La Bella *et al.*, 2020). Aflatoxin B1 exposure is another major risk factor for HCC in those countries. Aflatoxin B1 is produced by *Aspergillus flavus*, a fungus that infects maize kernels in hot and wet countries, inducing subsequent accumulation of this toxin, one of the most potent carcinogens produced in nature (McGregor *et al.*, 1998), in growing food. Moreover, individuals exposed to both high levels of aflatoxin B1 and chronic hepatitis B virus infection have an increased risk of liver cancer (Liu and Wu, 2010). Another example of toxin as risk factor of HCC is aristolochic acid, a toxin produced plants from the genus

Aristolochia. This compound largely affects Southeast Asia region due to its use in traditional herbal medicine. Metabolites of aristolochic acid form DNA adducts on adenine residues leading to a specific mutational signature of T>A substitutions (Nault and Letouzé, 2019).

In western countries, the main risk factors are completely different. In France, HCC development is related to alcohol abuse in 50% of the cases (Rosa *et al.*, 2010). In the United States, obesity is the major risk factor of HCC as accumulation of fat in the liver induces chronic liver inflammation (Ascha *et al.*, 2010). Some rare diseases such as hemochromatosis that lead to iron deposit in liver can lead to cirrhosis (Kew, 2014). Finally, Nonalcoholic steatohepatitis (NASH), corresponding to liver steatosis and strong necro-inflammation, is the most common cause of chronic liver disease in developed countries and its incidence is rapidly increasing worldwide. As schematized on figure 20B, Nonalcoholic fatty liver diseases (NAFLD) are associated to risks factor such as obesity and diabetes and eventually lead to cirrhosis and NASH, that are both highly predisposing factor for HCC development (Fujii *et al.*, 2013; Anstee *et al.*, 2019) (Figure 20B).

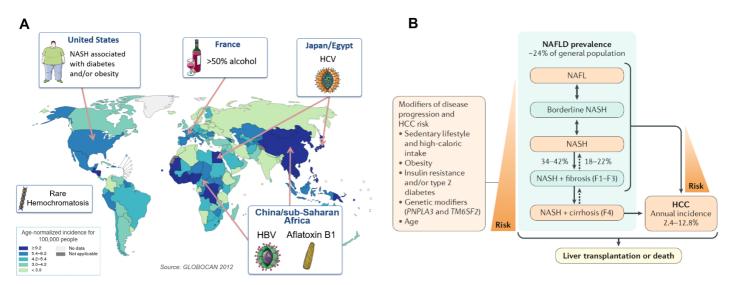


Figure 20: A: Estimated incidence rate of liver cancer worldwide. Major risk factor associated with specific regions are also represented. Data from GLOBOCAN 2012. B: Relation between nonalcoholic fatty liver disease (NAFLD) and HCC development initiated by various risks factors such as obesity or diabetes types I/II. NAFLD can lead to and further to NASH (steatosis and strong necro-inflammation), fibrosis, cirrhosis and eventually hepatocellular carcinoma (HCC). The HCC incidence vary from 2.4 to 12.8% depending on the disease state. (Anstee et al., 2019)

HCC develops most of the time on a diseased liver, with underlying cirrhosis in 80-90% of cases (Figure 21). Liver cirrhosis occurs after years of chronic liver inflammation induced by abovementioned exposures or diseases. Chronic inflammation induces a stress leading to excess of extracellular matrix and permanent fibrotic scars in the liver

(Wynn, 2004). The Metavir score indicates different stages of fibrosis, from F0 (normal liver) to F4 (cirrhosis). This liver background induces architecture changes leading to the formation of structurally abnormal nodules. Cells in these lesions accumulate somatic alterations such as mutations associated to high risk of developing HCC and hepatic function alteration (Ginès *et al.*, 2016; Brunner *et al.*, 2019). For example, *TERT* promoter mutation is a well-known early-acquired genetic alteration in the transformation of premalignant nodules in hepatocellular carcinoma on cirrhosis, with more than 60% of early HCC harboring such alteration. (Nault *et al.*, 2013) (Figure 21).

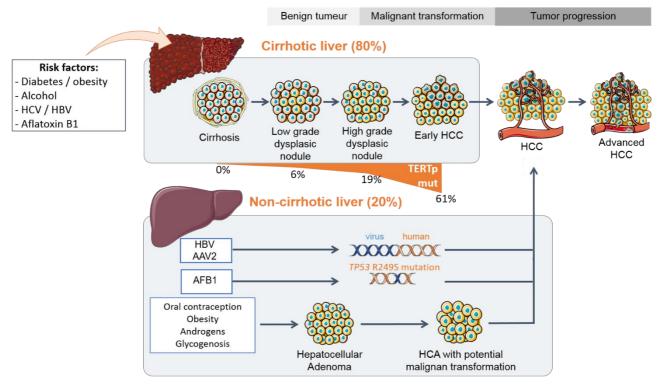


Figure 21: HCC develops most of the time on a cirrhosis liver background associated to specific risks factors. The transition from cirrhotic liver to early HCC is characterized by a recurrent early alteration of TERT promoter, leading to tumor progress. However, HCC can also be developed from HCA malignant transformation of specific tumorigenic process such as insertional mutagenesis of HBV and AAV2 or exposure of Aflatoxin B1, known to induce R249S TP53 hotspot mutation. Modified from Zucman-Rossi J et al. 2015; Nault et al. 2015.

HCC also develops in a healthy liver in around 10-20% of cases (Figure 21). Except HCA transformation already discussed in the previous chapter, insertional mutagenesis by HBV or AAV2 viruses, or specific mutagenic exposures can trigger HCC tumorigenesis without long term damage induced by cirrhosis (Figure 21).

3.2.2. Major biological pathways altered in HCC

Since the advent of NGS, large cohorts of HCC were analyzed using WES, RNAseq and WGS (Schulze, Imbeaud, Letouzé, *et al.*, 2015; Fujimoto *et al.*, 2016), allowing to elucidate the landscape of driver genes and biological pathways recurrently altered in HCC (Zucman-Rossi *et al.*, 2015) (Figure 22).

- harboring an increased telomerase expression (Farazi *et al.*, 2003; Plentz *et al.*, 2007). *TERT* gene encodes the catalytic sub-unit of the telomerase complex that is crucial to maintain telomere length and genome stability. This gene is not expressed in normal liver but activated in the early stages of hepatocarcinogenesis. Molecular mechanisms at the origin of *TERT* activation are i) TERT promoter mutation in 54 to 60% of cases (Nault *et al.*, 2013), ii) gene amplification or other structural rearrangements in 5 to 6% of cases (Totoki *et al.*, 2014) and iii) insertional mutagenesis in *TERT* promoter by HBV and AAV2 in 10 to 15% of cases (Nault *et al.*, 2015).
- WNT/β-catenin pathway is altered in 17 to 44% of HCCs (depending of geographical and etiological background) characterized by the transcriptional activation of *CTNNB1* target genes, such as *GLUL* and *LGR5* (Boyault *et al.*, 2007). This pathway activation is frequently associated with *TERT* promoter, suggesting a cooperation between the two pathways (Nault *et al.*, 2013; Totoki *et al.*, 2014; Schulze, Imbeaud, Letouzé *et al.*, 2015). This pathway is crucial for liver function, controlling important mechanisms such as cell differentiation in hepatocytes (Touboul *et al.*, 2016). The most common driver events in this pathway are *CTNNB1* mutations in exon 3 or in frame deletions in the exon 3. In addition, mutations in *AXIN1*, *ZNRF3* or *APC* tumor suppressor genes are found in respectively 10%, 3% and 1-2% of HCCs, also triggering WNT/β-catenin pathway activation (Yanai *et al.*, 2000; Basham *et al.*, 2019).
- Cell cycle pathway is altered in at least half of HCC, with TP53 mutations in 12 to 48% of cases (Bressac et al., 1991; Hsu et al., 1991; Guichard et al., 2012; Schulze, Imbeaud, Letouzé et al., 2015; Fujimoto et al., 2016). As already described for TSG, TP53 mutations are spread along all the gene, except for the R249S hotspot characteristic of aflatoxin B1 exposure (Guichard et al., 2012; Fujimoto et al., 2016). TP53 is the most frequently altered gene in cancer, and is involved in

multiple biological processes such as G1/S cell cycle transition, DNA repair and apoptosis (Aubrey *et al.*, 2018). The retinoblastoma pathway, that controls the G1/S phase transition, is also recurrently altered in HCC, following homozygous deletions of *CDKN2A* (2-12%) or *RB1* (3-8%) (Guichard *et al.*, 2012; Ahn *et al.*, 2014; Totoki *et al.*, 2014). Finally, *CCNE1* gene and *CCND1/FGF19* locus, both involved in cell cycle progression, are recurrently altered by insertional mutagenesis or amplifications in 5% and 5-14% of cases, respectively (Sawey *et al.*, 2011; Sung *et al.*, 2012; Kan *et al.*, 2013). Interestingly, *TP53* and *CTNNB1* mutations are exclusive (Friemel *et al.*, 2019).

- Oxidative stress pathway alterations are seen in 5-15% of HCCs and are recurrent in a context of chronic liver inflammation or long term exposure to toxic compounds such as alcohol (Llovet *et al.*, 2016). These liver insults lead to the accumulation of Reactive Oxygen Species (ROS) and subsequent selection of drivers events activating the detoxification program controlled by NRF2 (Denicola *et al.*, 2011; Bryan *et al.*, 2013). These driver events include activating mutations of *NFE2L2* (nuclear factor erythroid 2-related factor 2) encoding NRF2, or inactivating *KEAP1* (Kelch-like ECH-associated protein 1) mutations preventing NRF2 from proteasome degradation (Guichard *et al.*, 2012; Sporn and Liby, 2012; Cleary *et al.*, 2013).
- PI3K/AKT/MTOR and RAS/RAF/mitogen-activated protein kinase pathways are also frequently altered in HCC. PI3K/AKT/MTOR is involved in metabolism and cell proliferation (Laplante and Sabatini, 2012) while RAS/RAF/MAPK is involved in cell proliferation, differentiation and survival (Schubbert, Shannon and Bollag, 2007). PI3K/AKT/MTOR is altered by homozygous deletions or mutations of *PTEN* (1-3%), inactivating mutation of *TSC1*, *TSC2* (2-8%) (Totoki *et al.*, 2014) and *FGF3*, *FGF4*, *FGF19* amplifications (5%) that could induce FGFR receptor over-expression (Babina and Turner, 2017). RAS/RAF/MAPK is altered through *RPS6KA3* inactivating mutation in 2-9% of cases, leading to a constitutive activation of the pathway (Zucman-Rossi *et al.*, 2015).
- **Epigenetic modifiers** are the last identified pathway recurrently altered in HCC through chromatin remodeling complexes or histone methyl-transferase alterations (Schulze, Imbeaud, Letouzé *et al.*, 2015) (Figure 13). Recurrent inactivating mutations affect *ARID1A/B* (4-17% of HCC) and *ARID2* (3-18%),

involved in the SWI/SNF chromatin remodeling complexes BAF and PBAF. Histone methyl transferase complexes alterations include inactivating mutations in *KMT2A* (3-4%), *KMT2B* (3-4%), KMT2C (3-6%) and *KMT2D* (2-3%), or HBV insertional mutagenesis in *KMT2B* (10%) (Sung *et al.*, 2012; Cleary *et al.*, 2013; Schulze, Imbeaud, Letouzé, Ludmil B. Alexandrov, *et al.*, 2015).

3.2.3. Treatments

The BCLC (Barcelona Clinic Liver Cancer) stage of HCC development is the major metric to guide the management of patients with HCC. This stage depends on various physio-pathological parameters, the number and size of tumor nodules (Figure 23).

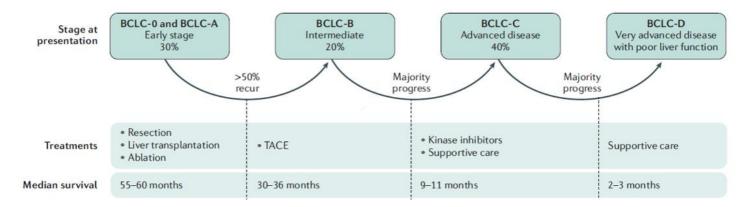


Figure 22: Percentage of patients with HCC within the different BCLC stages. Within the first 2 years after liver resection, around 50% of patients relapse with liver cancer. Modified from (Anstee et al. 2019).

For BCLC-0 and BCLC-A stages, transplantation is the best therapeutic option as it resolves both tumor and cirrhosis. However, the number of donors is obviously limited. Resection and percutaneous ablation through Percutaneous Ethanol Injection (PEI) or Percutaneous radiofrequency ablation (RFA) are alternative curative treatments, but require a preserved hepatic function of the patient, that is altered by both cancer developments and cirrhosis. Unfortunately, patients are frequently diagnosed at advances stages of HCC development, limiting curative treatments. Altogether, only 15% of all hepatocellular carcinomas are amenable to operative treatment (Bruix and Llovet, 2002; Chedid, 2017).

For patients not eligible to curative treatment, two categories of non-curative treatments are used according to the BCLC stage. For BCLC-B (intermediate HCC), intra-arterial chemoembolization preventing blood supplying to the tumor and intra-arterial

chemotherapy are the two options. Those types of treatment increase patient survival but can have important side effects (Galuppo *et al.*, 2014).

For patients with BCLC-C (advanced HCC), 4 multi-kinase inhibitors targeting PI3K/AKT/MTOR or RAS/RAF/MAPK pathways are approved. Sorafenib was for a long time the only therapeutic option. This is an inhibitor of VEGFR-1/2/3 (vascular endothelial growth factors receptors), BRaR/CRaF (serine threonine kinase) and PDGFR- α/β (platelet-derived growth factor receptors). This treatment was shown to increase the median survival by 3 months (Llovet *et al.*, 2008). Regorafenib is a multi-kinase inhibitor more efficient against VEFGR kinases, with a wider activity than sorafenib, also targeting TIE2, KIT and RET kinases involved in ontogenesis. This treatment showed positive results in a cohort of patients progressing under sorafenib (Bruix *et al.*, 2017). Recently, new compounds were approved for the treatment of advanced HCC such as lenvatinib (multi-kinase inhibitor of VEGFR 1-3, FGFR 1-4, PDGFR α and RET), Cabozantinib in second line, an inhibitor of the tyrosine kinases c-Met and VEGFR2, and the tyrosine kinase receptors AXL and RET (Abou-Alfa *et al.*, 2018). Moreover, Ramucirumab, a monoclonal anti-body targeting VEGFR-2 shown promising result in clinical phase III (Zhu *et al.*, 2019).

Immune checkpoint inhibitors are emerging in HCC because of their considerable efficacy in other cancers, particularly in patients with melanoma, lung, renal, and bladder cancer (Smyth *et al.*, 2016). Nivolumab and pembrolizumab, two monoclonal antibodies against PD-1 (Programmed cell death-1), have just received accelerated approval by the FDA based on promising results from two Phase 2 studies showing a reduction in tumor mass in 20% and 17% of patients previously treated with sorafenib, respectively (El-Khoueiry *et al.*, 2017; Guo, Zhang and Chen, 2017; Zhu *et al.*, 2018). Thus, immunotherapy is promising in HCC treatment, and phase III studies are ongoing, including a phase III trial comparing sorafenib to nivolumab in first line (CheckMate 459; NCT02576509). However, treatment response is heterogeneous and, in a small proportion of patients, these treatments can cause severe and possibly permanent auto-immune adverse effect such as diarrhea, skin reactions, fatigue and hypertension (Weber *et al.*, 2015). Thus, there is a huge need to identify candidate bio-markers to target patients who are likely to benefit from immunotherapies. So far only PD-L1 expression has been approved as biomarker but does not seems to be associated with nivolumab response in HCC (El-Khoueiry

et al., 2017). A recent study defined an "immune exclusion phenotype" subgroup of HCC, characterized by *CTNNB1* mutations, lower immune infiltration (based on immune-specific gene signature) and overexpression of *PTK2*, an oncogenic pathway associated with low T-cell infiltrate in the tumor (Luke *et al.*, 2019).

Despite the recent increase in available therapies, the prognosis of HCC patients is still very bad, with a median survival of less than 1 year. Furthermore, patient response to available therapies is heterogeneous, making the discovering of new therapeutic options crucial. The recent advances in cancer genomics lead to a new era in cancer research consisting in identifying molecular and transcriptomic subgroups of tumors harboring similar molecular features, likely to respond well to the same targeted therapy. Unraveling the diversity of molecular alterations and transcriptomic deregulation is thus crucial to i) understand the tumor biology and deregulated pathways in order to develop efficient patient tailored therapy and ii) identify biomarkers of homogeneous molecular subgroups. For example, MEK inhibitors already used in breast cancer, melanoma and lung cancer displayed efficacy in HCC patients characterized by RAS pathway activation (Das *et al.*, 2018).

4. Objectives of the PhD

Liver cancers are extremely heterogeneous, with a wide spectrum of etiologies, tumor histological characteristics, deregulated biological pathways and molecular alterations. Our understanding of the mechanisms driving tumor initiation and development increased a lot in the last decade, both in terms or biological pathways and altered oncogenes or TSG. However, some tumors remain poorly understood, and even if the majority of them are well characterized in terms of biological phenotype, the underlying driver alterations are sometimes missing. The aim of my PhD project was to better understand the molecular mechanisms at the origin of HCAs and HCCs. More precisely, I focused on structural variations (SVs) that had not been analyzed extensively in liver cancers. Indeed, when I arrived in the laboratory, the only known driver SV was the INHBE-GL11 fusion, characteristic of the shHCA cancer subgroup. Additionally, SV

signature analysis helped to better understand biological mechanisms at the origin of specific genomic rearrangement.

In this project, I developed innovative computational strategies applied to WGS and RNA-seq data of HCA and HCC tumor collections of the UMRS 1138 INSERM laboratory, obtained from collaborations with various French hospitals. I also used public data sets to increase statistical power and/or validate results, including TCGA (334 HCC samples with multi-omic data) and ICGC series (257 HCC samples with WGS). Finally, I used epigenetic data generated by the ENCODE and ROADMAP consortia, such as replication timing, chromatin opening and histone marks to better understand both the origin and functional consequences of structural rearrangements.

Overall, during my PhD, I contributed to shape the landscape of both HCA and HCC cancers subgroups:

- First, by integrating WGS and RNAseq data, I characterized 3 new driver alterations in inflammatory HCA. These include recurrent fusions activating *FRK* and *ROS1* genes, and an original mechanism leading to *IL6* gene overexpression following the loss of regulatory 3'UTR regions. All these alterations lead to a constitutive activation of the JAK/STAT pathway characteristic of inflammatory HCA.
- Secondly, by analyzing SV signatures in HCC, I discovered a unique rearrangement signature of tandem duplications and templated insertion cycles, induced by replication stress. This signature allowed me to define a new HCC subgroup driven by various oncogenic mechanisms activating CCNA2 or CCNE1.

II MATERIAL AND METHODS

1. Data used in the project

1.1. Tissue samples

Tumor samples from both hepatocellular carcinoma (HCC) or hepatocellular adenoma (HCA) samples and their non-tumor counterparts were collected from patients surgically treated in four French hospitals located in Bordeaux and Paris region. Institutional review board committees (CCPRB Paris Saint-Louis, 1997, 2004, and 2010, approval number 01–037; Bordeaux, 2010-A00498–31) approved the studies. Written informed consent was obtained in accordance with French legislation. All samples were immediately frozen in liquid nitrogen and stored at –80 °C. HCC were enriched in cases developed on a non-cirrhotic liver with an over-representation of tumors developed in non-fibrotic (METAVIR F0-F1) compared to tumors developed in chronic hepatitis (F2–F3) and in cirrhotic liver (F4). Clinicopathological data were available for all cases (detailed tables can be found in respective articles). A diversity of risk factors were represented in the cohorts mentioned in this manuscript, including alcohol, metabolic syndrome, HBV, HCV infections, hemochromatosis and without particular etiologies.

1.2. Sequencing methods

1.2.1. Target sequencing

Target sequencing was performed on panels of genes including *HNF1A* (exon 1–10), *IL6ST* (exons 6 and 10), *CTNNB1* (exons 2, 3, 4, 7 and 8), *FRK* (exon 6), *STAT3* (exons 3, 6, 17 and 21), *GNAS* (exons 7, 8 and 9) and *JAK1* (all exons). Those genes were sequenced by either Sanger sequencing or Miseq Illumina PCR-based sequencing. Somatic mutations were confirmed by sequencing of the tumor and non-tumor counterpart.

1.2.2. Whole Exome Sequencing (WES)

Whole Exome Sequencing data was performed by IntegraGen (Evry, France). Agilent insolution enrichment was used with the manufacturer's biotinylated oligonucleotide probe library SureSelect Human All-Exon kit V.4 70Mb, or SureSelect Human All-Exon kit V.5 +UTRs, or Twist Human Core Exome Enrichment System. Genomic DNA was sonicated and purified to yield fragments of 150–200bp. Adaptor oligo-nucleotides were ligated on A-tailed fragments and enriched by four to six PCR cycles. Purified libraries (500ng) were hybridized to the library for 24 hours. The eluted enriched DNA sample was sequenced

on an Illumina HiSeq 2000 or HiSeq 4000 as paired-end 75bp reads.

1.2.3. RNA-seq

RNA samples were enriched for polyadenylated RNA from $5\mu g$ of total RNA, and the enriched samples were used to generate sequencing libraries with the NEBNext Ultra II Directional RNA or Illumina TruSeq Stranded mRNA kits and associated protocol as provided by the manufacturer. Libraries were sequenced by IntegraGen (Evry, France) on an Illumina HiSeq 2000 or 4000 as paired-end 75 or 100 bp reads.

1.2.4. Whole Genome Sequencing (WGS)

Whole Genome Sequencing of samples was realized by the Centre National de Génotypage (Evry, France) or were sequenced at Integragen (Evry, France). Samples were sequenced on an Illumina HiSeq X Five as paired-end 75, or 101 base pair (bp) reads.

1.2.5.	Table of sequ	encing data	hy project
1.4.3.	Table of sequ	chicing uata	Dy project

Project	Sample type	Gene panel sequencing	WGS	WES	RNA-seq	Other Public Data
Article1: Systemic AA amyloidosis	HCA / NT	NA	N=1	NA	N=2	
Article2: Inflammatory HCA alterations Article3:	НСА	N=657 (533 already published)	NA	N=19 (4 already published)	N=22 (1 already published)	
Palimpsest	Method paper, not using any specific data set					
Article4: Cyclin A2/E1 activated HCC	нсс	NA	N=45 (35 already published)	N=156 (96 already published)	N=160	- TCGA series of HCC (n=334 RNAseq; n=334 WES; n=48WGS) -ICGC-JP series of HCCs (n=257 WGS/RNAseq) -PCAWG SVs from 2606 tumors WGS -Encode and Roadmap annotations

2. Bioinformatics Pipelines

2.1. RNAseq alignement and expression matrix generation:

Full Fastq files were aligned to the reference human genome GRCh38 using TopHat2 V.2.0.14. Read mapping from multiple locations was removed and HTSeq was used to obtain the number of reads associated with each gene in the Gencode V.27 database, restricting to protein-coding genes, pseudogenes, antisense and lincRNAs. Bioconductor

DESeq2 package was used to import raw HTSeq counts for each sample into R statistical software and apply variance stabilising transformation to the raw count matrix. FPKM scores (number of fragments per kilobase of exon model and millions of mapped reads) were calculated by normalizing the count matrix for the library size estimated with DESeq2 package and the coding length of each gene. In order to handle batch effect, we used an in-house method. Briefly, area under the ROC curve (AUC) was used to identify and remove genes with a significant batch effect (AUC >0.95 between one sequencing project and others).

2.2. RNAseq Gene Set Enrichment Analysis (GSEA):

To perform gene set enrichment analysis (GSEA) analysis, genes expression from previous pipeline were sorted according to fold-change from Limma analysis (genes with positive fold-changes first, then negative fold-changes) using an input of 16387 genes (Hallmarks gene set; MSigDB V.6 database used). This gene list was obtained from Genecode database; then genes with a variance equal 0 or with a total number of reads from samples inferior of 50 were removed.

2.3. RNAseq fusion calling

Fusions detected by TopHat2 (--fusion-search; --fusion-min-dist 2000; --fusion-anchorlength 13; --fusion-ignore-chromosomes chrM) were filtered using the TopHatFusion pipeline. Fusions validated by BLAST and with at least 10 split-reads or pairs of reads spanning the fusion event were retained, whereas any fusion identified at least twice in a cohort of normal liver samples was removed.

2.4. WES / WGS alignment and mutation calling

Sequences were aligned to the hg19 version of the human genome using BWA version 0.7.12. and variant calling was processed using Mutect2 by comparing each tumor sample with its matched non-tumor counterpart and a panel of normal (PON) file, following the genome analysis toolkit (GATK) best practices.

Mutations belonging to the ENCODE Data Analysis Consortium blacklisted regions (http://hgdownload.cse.ucsc.edu/goldenPath/hg19/encodeDCC/wgEncodeMapability/wgEncodeDacMapabilityConsensusExcludable.bed.gz) were excluded and regions covered by < 6reads in the tumor or normal sample. We then selected only single nucleotide variants (SNVs) with a MuTect2 flag among "PASS", "clustered_events", "t_lod_fstar", "alt_allele_in_normal" or "homologous_mapping_event" and small insertions

and deletions (indels) with a MuTect2 flag among "PASS", "cluster-ed_events" or "str_contraction". To improve specificity in the calling of mutations with low variant allele frequency (VAF), we quantified the number of high quality variant reads in the tumor (mapping quality ≥ 20 , base quality ≥ 20) and the number of variant reads in the non-tumor sample with no quality threshold using bamreadcount (https://github.com/genome/bam-readcount). Only variants matching the following criteria were finally retained: VAF $\geq 2\%$ in the tumor with ≥ 3 variant reads, VAF $\leq 5\%$ in the non-tumor samples with ≤ 2 variant reads, and a VAF ratio ≥ 5 between the tumor and non-tumor sample.

2.5. WES / WGS copy number analysis and SV calling

The copy number profiles were defined using an in-house pipeline. Briefly, the logR ratio was processed using the coverage of each tumor and its non-tumor counterpart in each 1kb genomic windows; then a segmentation was done in order to identify copy number alterations.

MANTA software was used to identify somatic structural rearrangements in WGS data. To keep only the most reliable events, we selected only rearrangements supported by ≥ 10 reads and with a variant allele fraction $\geq 5\%$.

2.6. Signature analysis and statistical tools

Some biological processes linked to cancer development was shown to be at the origin of particular pattern of alterations, as explain in Introduction section. Those patterns of alterations associated to cancer are called mutational signatures and the combination of those processes in a cancer cell result in a complex mutational portrait. This portrait can be deconvoluted in order to extract the different biological sources of alteration in each tumor. Non-negative Matrix Factorization (NMF) mathematical method was shown to be very effective in the deconvolution of complex biological signal. This method implemented the Palimpsest R is in package (https://github.com/FunGeST/Palimpsest), corresponding to the 3rd Article of this manuscript. All function related to signature analysis was realized using this package.

Concerning in house developed methods, both R (version from 3.4.4 to 4.0.2) and Python (versions 2.7 and 3.6) were used in the bioinformatics analysis, including graphical representation and statistical analysis through hypothesis testing.

2.7. Table of pipeline used by project

Project	Target sequencing	RNAseq	WGS	WES	
Article1: Systemic AA amyloidosis	NA	-Gene expression	-Structural variant calling	NA	
Article2: Inflammatory HCA alterations	-Mutation calling -Expression of gene panel	-Gene expression -Gene fusions -GSEA	-Structural variant calling	-Mutation calling -Copy number alterations	
Article3: Palimpsest	Method paper, not using any processed data from specific dataset				
Article4: Cyclin A2/E1 activated HCC	NA	-Gene expression -Gene fusions -GSEA	-Structural variation calling -Mutation calling -Viral insertion calling	-Mutation calling -Copy number alterations	

III RESULTS

1. Identification of oncogenic SVs in HCA

The first goal of my thesis was to identify new SVs driving hepatocellular adenoma development. As explained in the introduction, when I started my PhD, the molecular landscape of HCA was divided in 6 groups (Figure 10) associated with specific molecular alterations: HHCA with *HNF1A* inactivation, bex3HCA and bex7,8HCA with *CTNNB1* activation, shHCA with *GLI1* activation and IHCA with *IL6ST*, *FRK*, *STAT1*, *GNAS*, *JAK1* mutations and UHCA without known driver. However, this landscape was still incomplete. Firstly, because the driver genes of UHCA are still missing. Secondly because a large part of IHCA samples, characterized by SAA and CRP protein over-production, had no identified molecular driver mechanism. Except for the recently described *INHBE-GLI1* fusion characteristic of shHCA, all driver alterations in HCA were point mutations. The aim of this project was to unravel new alterations such as gene fusions or regulatory region alterations that could trigger tumorigenesis of HCA.

To that aim, we leveraged the large HCA tumor collection from the lab, including extensive clinical and molecular features:

- Clinical data and history of patients
- Histological images of tumor tissue
- Gene panel sequencing (from Illumina's MiSeq technology)
- Gene panel expression (from Fluidigm technology)

This large cohort was explored to select samples belonging to IHCA subgroup (based on gene expression) without identified point mutations in known driver genes. Selected samples were sequenced using RNA-seq and/or WGS, and analyzed to identify the missing drivers. This project lead to two original articles describing new alterations in IHCA subgroup.

Article 1 describes a rare clinical case associating inflammatory HCA with amyloid A (AA) systemic amyloidosis, a complication of chronic inflammatory diseases induced by deposits of insoluble SAA deposits. The patient, a 49-years-old woman, was admitted to emergency for diarrhea, rectal bleeding and lower limbs edema. Her clinical history was also characterized by an unexplained chronic inflammation for at least 10 years. Medical analysis revealed inflammation, renal failure, and SAA amyloid deposits were found in

kidneys, intestines and rectum. Liver biopsy led to HCA diagnosis that was further explored using both RNA-seq and WGS. WGS data revealed an inversion in chromosome 7 leading to the loss of *IL6* gene 3'UTR that contains post-transcriptional regulatory sequences involved in the degradation of this unstable transcript. RNAseq data indicated a massive over-expression of the *IL6* transcript. This mechanism of IHCA development is very different from those already known, where *STAT3* is activated through activation of a major actor of signal transduction of the IL6 axis, such as *IL6ST*, *JAK1*, *GNAS*, *FRK* or *STAT3* itself. In addition to IHCA development, the autocrine interleukine-6 secretion by the tumor triggers SAA production not only in the IHCA nodule but also in the surrounding liver tissue. Interestingly, amyloidosis symptoms improved following HCA resection. Thus, this single genomic alteration allowed us to make a link between IHCA and AA-amyloidosis, recurrently associated in literature regarding the very low prevalence of both diseases.

Article 2 describes the identification of new driver gene fusions leading to JAK/STAT pathway activation in previously unexplained IHCAs. The first recurrent fusions involve *FRK*, already known to be mutated in 8% of IHCA (Nault *et al.*, 2017). *FRK* fusions downstream different partner genes were identified in 5 patients (2% of the IHCA cohort), leading to chimeric transcripts only including exons 3 to 8 of FRK. The resulting proteins have lost the SH2 and SH3 auto-inhibitor elements of FRK, leading to constitutive activation of the tyrosine protein kinase domain. In addition, we identified recurrent gene fusions involving *ROS1* in 10 patients (3% of the IHCA cohort). The chimeric transcripts only retain exons 33 to 43, 34 to 43 or 35 to 43 of *ROS1*. In these samples, the upstream partner gene induces a massive overexpression of the truncated *ROS1* that contains kinase domain. *FRK* and *ROS1* fusions constitute new driver events activating the JAK/STAT pathway and leading to the development of IHCA.

Article 1: Systemic AA Amyloidosis Caused by Inflammatory Hepatocellular Adenoma

Systemic AA Amyloidosis Caused by Inflammatory Hepatocellular Adenoma

TO THE EDITOR: Amyloid A (AA) systemic amyloidosis is a complication of chronic inflammatory diseases that is caused by the deposition of insoluble aggregates of cleaved N-terminal fragments of serum amyloid A (SAA) protein in tissues and organs throughout the body. Under physiologic conditions, SAA protein is produced by hepatocytes during the acute inflammatory phase in response to various cytokines such as interleukin-6. SAA is also overexpressed by neoplastic hepatocytes in inflammatory hepatocellular adenomas, a specific molecular subtype of benign liver tumors. 2,3

Here, we describe a 49-year-old female patient who presented with diarrhea, rectal bleeding, and leg edema and received a diagnosis of systemic AA amyloidosis. Clinical characteristics of the patient are provided in Table S1 in the Supplementary Appendix, available with the full text of this letter at NEJM.org. An inflammatory hepatocellular adenoma was identified and resected, resulting in the improvement of amyloidosis-related symptoms, with progressive normalization of the serum C-reactive protein (Fig. 1A) and SAA levels. Unfortunately, the patient's kidney function did not improve, and she died 18 months after surgery from fulminant septic shock.

Whole-genome sequencing of the inflammatory hepatocellular adenoma revealed a complex structural rearrangement on chromosome 7 with an inversion leading to the truncation of the *IL6* 3′ untranslated region (3′UTR), which comprises key sequences involved in the degradation of this unstable transcript (Fig. 1, and Tables S2 and S3

Figure 1 (facing page). Biologic, Imaging, Pathological, and Molecular Findings in Our Patient.

As shown in Panel A, liver resection was followed by a clinically significant decrease in serum levels of C-reactive protein (CRP) (top), and magnetic resonance imaging showed a heterogeneous, 5-cm liver mass at the tip of segment VI on T₂-weighted sequences (bottom, arrow). As shown in Panel B, microscopic examination of the resected specimen revealed a well-differentiated tumor with massive amyloid deposits (arrows) (subpanel a, Congo red staining, low magnification) and typical yellow-green birefringence under polarized light (subpanel b, low magnification). Immunohistochemical tests showed positive staining for serum amyloid A (SAA) protein in neoplastic hepatocytes (black arrows) and amyloid deposits (red arrows) in the tumor (T) sample (subpanel c, high magnification); SAA expression was also observed in the adjacent nontumorous (NT) parenchyma (subpanel d, high magnification). CRP was expressed in the tumor (T) (subpanel e, low magnification) (neoplastic hepatocytes, black arrows) and the adjacent NT liver tissue (subpanel f, high magnification) (non-neoplastic hepatocytes, black arrows) As shown in Panel C, whole-genome sequencing of the tumor sample obtained from the patient revealed a cluster of somatic structural rearrangements at the IL6 locus on chromosome 7. The blue line in the outer circle indicates copy number, and structural rearrangements are indicated in the inner circle. Red indicates deletion, blue inversion, gray interchromosomal translocation, and black classic chromatin staining of the cytobands. As shown in Panel D, although overexpression of IL6 was specific to the tumor sample, the genes SAA1 and CRP were also massively overexpressed in the adjacent liver tissue, as compared with normal liver tissue. FPKM denotes fragments per kilobase of exon per 1 million reads in the RNA sequencing experiment. As shown in Panel E, chromosomal inversion with one breakpoint located in the 3' untranslated region (UTR) of the gene IL6 and the other breakpoint in an intergenic region at 7p14.1 led to the massive overexpression of an interleukin-6 transcript lacking regulatory 3'UTR elements in the patient's tumor (top, structural rearrangement identified by means of whole-genome sequencing; bottom, gene expression and transcript structure identified by means of RNA sequencing). AU denotes adenylate-uridylate.

N ENGL J MED 379;12 NEJ M.ORG SEPTEMBER 20, 2018

The New England Journal of Medicine

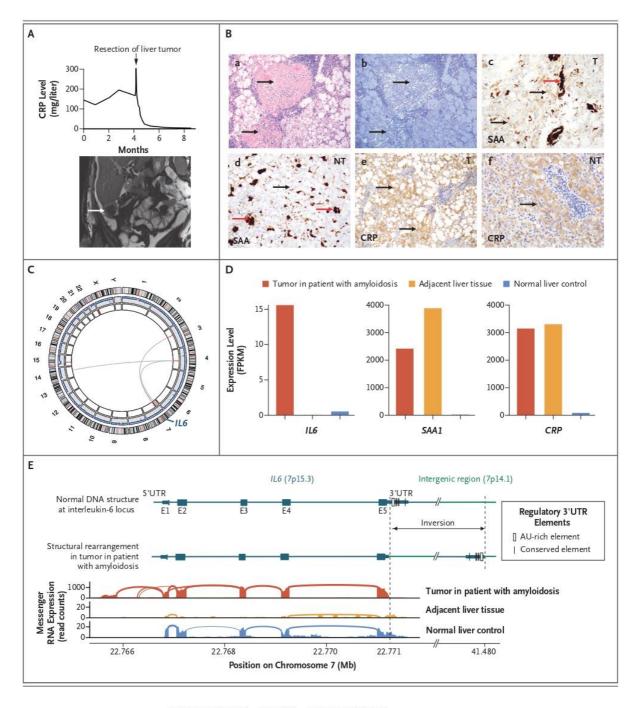
Downloaded from nejm org at INSERM DISC DOC on May 6, 2020. For personal use only. No other uses without permission.

Copyright © 2018 Massachusetts Medical Society. All rights reserved.

CORRESPONDENCE

in the Supplementary Appendix). RNA sequenctumor and nontumorous liver. Amyloid deposits ing consistently showed a massive overexpression of an interleukin-6 transcript lacking all 3' regulatory elements; this overexpression was limited to the tumor area. However, in contrast by the inflammatory hepatocellular adenoma to classic inflammatory hepatocellular adenoma, with activation of a paracrine Janus kinase-signal we observed overexpression of SAA in both the transducers and activators of transcription 3

were also identified in the adenoma and the adjacent parenchyma (Fig. 1). These results support an autonomous production of interleukin-6



N ENGL J MED 379;12 NEJM.ORG SEPTEMBER 20, 2018

The New England Journal of Medicine Downloaded from nejm.org at INSERM DISC DOC on May 6, 2020. For personal use only. No other uses without permission. Copyright © 2018 Massachusetts Medical Society. All rights reserved.

The NEW ENGLAND JOURNAL of MEDICINE

(JAK-STAT3) pathway in the liver (Fig. S1 in the Dominique Franco, M.D., Ph.D. Supplementary Appendix).

In the literature, we identified eight additional patients with both AA amyloidosis and hepatocellular adenomas. In at least six of these patients, amyloid-related symptoms also improved after surgical resection of the liver tumor (Table S4 in the Supplementary Appendix). We reviewed the liver histologic findings of two patients from the literature and identified features that were similar to those of our patient; inflammatory hepatocellular adenoma with SAA expression by the tumor and the adjacent parenchyma was indeed identified in both cases from the literature (Fig. S2 in the Supplementary Appendix).^{4,5} Birefringent, SAA-positive amyloid deposits were also identified in the adenomas and adjacent liver tissue.

In conclusion, rare cases of inflammatory hepatocellular adenoma can induce massive SAA production by the tumor and nontumorous liver, leading to systemic AA amyloidosis. Molecular analyses identified a somatic rearrangement of the IL6 3'UTR leading to an autocrine interleukin-6 secretion by the tumor. We speculate that this subset of AA amyloidosis may be treatable by surgical resection of the liver tumor.

Julien Calderaro, M.D., Ph.D. Henri Mondor University Hospital Créteil, France

Eric Letouzé, Ph.D. Quentin Bayard, Ph.D. Anais Boulai INSERM Unité 1162 Paris France

Victor Renault Jean-François Deleuze, Ph.D.

Centre National de Recherche en Génomique Humaine Évry, France

Oriol Bestard, M.D., Ph.D. Bellvitge University Hospital Barcelona, Spain

Antoine Béclère University Hospital Clamart, France

Elie-Serge Zafrani, M.D. Henri Mondor University Hospital Créteil, France

Jean-Charles Nault, M.D., Ph.D. INSERM Unité 1162 Paris, France

Michel Moutschen, M.D., Ph.D. Liege University Hospital

Liege, Belgium Jessica Zucman-Rossi, M.D., Ph.D.

INSERM Unité 1162

Paris, France

jessica.zucman-rossi@inserm.fr

Drs. Calderaro, Letouzé, and Bayard contributed equally to this letter.

Supported by the Institut National du Cancer with the International Cancer Genome Consortium (ICGC Liver Cancer-France project), INSERM with the "Cancer et Environnement" (plan Cancer) and Heterogeneity of Colorectal and Liver Cancer (HETCOLI) projects (Tumor Heterogeneity and Ecosystem program), the Ligue Nationale contre le Cancer (Equipe Labellisée), Labex OncoImmunology Investissement d'Avenir, Coup d'Elan de la Fondation Bettencourt-Schueller, the Site de Recherche Intégrée sur le Cancer-Cancer Research and Personalized Medicine (SIRIC CARPEM), Fondation Mérieux, Cancéropôle Ile de France (exhauTrans project), and Instituto de Salud Carlos III (Spanish competitive grants FIS PI16/01321 and INT15/00112, to Dr. Bestard) through the European Regional Development Fund for research.

Disclosure forms provided by the authors are available with the full text of this letter at NEJM.org.

- 1. Wechalekar AD, Gillmore JD, Hawkins PN. Systemic amyloidosis. Lancet 2016;387:2641-54.
- 2. Nault JC, Couchy G, Balabaud C, et al. Molecular classification of hepatocellular adenoma associates with risk factors, bleeding, and malignant transformation. Gastroenterology 2017; 152(4):880-894.e6.
- 3. Rebouissou S, Amessou M, Couchy G, et al. Frequent inframe somatic deletions activate gp130 in inflammatory hepatocellular tumours. Nature 2009;457:200-4.
- 4. Bestard Matamoros O, Poveda Monje R, Ibernon Vilaró M, Carrera Plans M, Grinyó Boira JM. Systemic AA amyloidosis induced by benign neoplasms. Nefrologia 2008;28:93-8. (In Spanish.)
- Fievet P, Sevestre H, Boudjelal M, et al. Systemic AA amyloidosis induced by liver cell adenoma. Gut 1990;31:361-3.

DOI: 10.1056/NEJMc1805673

Supplementary Appendix

Table of contents

Additional clinical, biological and molecular data	2
Author contributions	4
Supplementary material and methods	5
Table S1	7
Table S2	8
Table S3.	9
Table S4	11
Figure S1	12
Figure S2	13
References	14

Additional clinical, biological and molecular data

Additional clinical and biological data

The 49-year-old female patient was admitted to the emergency department at CHU de Liège (Belgium) for diarrhea, rectal bleeding and lower limbs edema. She had been suffering from chronic inflammation for at least 10 years, a condition that remained unexplained despite multiple explorations performed in another hospital. Her medical history revealed pregnancy-associated thyrotoxicosis treated with propylthiouracil, she was chronically treated with bisoprolol and had no particular familial history.

Physical examination showed a body mass index of 32, a blood pressure of 175/110 mm Hg, a heart rate of 120 bpm and a body temperature of 36.7 °C. Severe pitting edema was present at the lower limbs level. Blood and urine analyses revealed major inflammation, renal failure, and nephrotic syndrome with normal procalcitonin (Table S1). Colonoscopy showed diffuse erythema and petechiae. Abdominal Computerized Tomography scan demonstrated a 5 cm hypodense lesion of segment VI of the liver, that was further confirmed by magnetic resonance imaging. Kidney biopsy showed nodular mesangial thickening with strong positivity for SAA protein in the mesangium, interstitium and vessel walls. Typical SAA amyloid deposits were also present on rectal and colic biopsies. A biopsy of the liver nodule concluded to a diagnosis of HCA, and the tumor was further surgically resected. Pathological examination of the liver tumor revealed hallmark features of IHCA: neoplastic hepatocytes without cytological atypia and arranged in thin trabeculae, inflammatory infiltrates, dystrophic vessels, sinusoidal dilatation. IHCA are benign monoclonal proliferations of hepatocytes and are characterized in 80% of the cases by an activating somatic mutation of one of the genes of the IL6 axis (IL6ST, GNAS, FRK, JAK1 or STAT3) that lead to constitutive STAT3 signaling pathway activation. These genetic alterations are responsible for the production by neoplastic cells of acute phase proteins such as SAA and C-reactive protein (CRP), regardless of the presence of ligands such as IL6.

Partial hepatectomy allowed rapid improvement of general condition and diarrhea. Serum CRP and SAA progressively normalized. Unfortunately, kidney function did not improve and the patient had to remain under dialysis. Eighteen months after her initial admission, she developed a methicillin-resistant Staphylococcus aureus bacteremia (presumably originating from the dialysis catheter) and died from a fulminant septic shock. Besides observations related to the shock, necropsy revealed multiple SAA deposits in the liver, spleen, kidneys, adrenal glands, thyroid and ovaries.

Molecular data

Whole-genome sequencing of tumor showed a relatively low mutation burden, with 3,132 somatic mutations (1.1 mutations/Mb) including 22 protein-coding mutations (Table S2), 5 copy-number alterations, and 31 structural rearrangements (Table S3). The tumor did not harbor any mutation in known IHCA driver genes involved in the IL6 signaling pathway (IL6ST, JAK1, STAT3, FRK, GNAS), but we identified a complex cluster of structural rearrangements on chromosome 7, including an inversion leading to the truncation of IL6 3'UTR sequence. IL6 mRNA is unstable and degraded with a half-life of 30 minutes. Key regions for the post-transcriptional degradation of IL6 are located in its 3'UTR region and include 6 AU-rich elements and a conserved region predicted to form a stem-loop structure recognized by the RNase Zc3h12a. The inversion breakpoint was located in the 5' of all these features

and we confirmed by RNA-sequencing the massive overexpression (184-fold) of an IL6 transcript lacking all 3' regulatory elements. Interestingly, the acute inflammatory response genes including SAA and CRP were overexpressed in the tumor and non-tumor liver whereas IL6 overexpression was restrained to the tumor area (Figure 1). Expression of SAA and CRP by non-neoplastic hepatocytes are usually not observed in classical IHCA except in the context of tumor hemorrhage and/or chronic inflammatory syndromes of other origin.³ Altogether, these findings support a paracrine JAK/STAT pathway activation in the liver caused by an autonomous production of IL6 produced by the IHCA (Figure S1).

Discussion

In the present study, we showed a recurrent association between two rare diseases, inflammatory hepatocellular adenoma (prevalence lower than 1/100,000 female) and AA-amyloidosis (incidence around 1/1,000,000 person/y in Europe). This association together with improved amyloidosis related symptoms after tumor resection supports a causal relationship between the two diseases (Figure S1). The role of IHCA in AA-amyloidosis was further elucidated by the identification of a unique somatic chromosome rearrangement at the IL-6 3'UTR leading to an autocrine IL-6 secretion by the tumor. In the liver, IL-6 acts as a ligand to activate STAT3 signaling in normal hepatocytes and the synthesis of the inflammatory acute phase proteins.⁴ In the index patient we identified an IL-6 production by the adenoma hepatocytes that induced paracrine effects on the surrounding non-neoplastic hepatocytes in the entire liver. We further showed the massive production of SAA by the tumor and the non-tumor liver tissues in the 2 additional cases of IHCA associated with amyloidosis analyzed by immunohistochemistry. This mechanism is different from the classical IHCAs in which STAT3 is activated in the absence of IL6 expression by a somatic mutation activating one of the major actors of signal transduction: IL6ST, JAK1, GNAS1, FRK or STAT3 itself.

In the patients with IHCA and amyloidosis, the total amount of SAA proteins produced by the whole liver is probably higher than SAA produced by a classical IHCA. The amount and duration of chronic SAA production by the tumor and non-tumor liver tissues are probably major sources of amyloidosis deposits in the body. This hypothesis is strongly supported by the clinical stabilization or resolution of the amyloidosis symptoms observed in the majority of the patients after IHCA resection. However, in our index patient, the kidneys were already severely injured at the time of surgery and renal function did not improve, underscoring the importance of an early diagnosis and a complete resection of the tumor.

In conclusion, rare cases of IHCA characterized by an autonomous IL-6 expression are able to induce massive SAA production by the liver, leading to systemic AA amyloidosis. This subset of AA-amyloidosis may be treatable by the resection of the liver tumor. Antibodies blocking IL-6, which have been approved in other conditions characterized by IL6 overproduction such as Castleman disease, may also be of interest in unresectable IHCA associated with amyloidosis.⁵

Author contributions

Study concept and design: JC, EL, JCN, MM and J.Z.R.

Acquisition of data: JC, EL, QB, AB, VR, JFD, OB, DF, ESZ, JCN, MM, and J.Z.R.

Analysis and interpretation of data: JC, EL, QB, AB, VR, JFD, ESZ, JCN, MM, and J.Z.R.

Drafting the manuscript: JC, EL, JCN and J.Z.R.

Critical revision of the manuscript: JC, EL, QB, AB, VR, JFD, OB, DF, ESZ, JCN, MM, and J.Z.R.

Statistical analysis: E.L. and QB

Obtained funding: J.Z.R.

Supplementary material and methods

Patients

The index patient has signed an inform consent for molecular and genetic research investigations. Frozen liver tumor and non-tumor tissues were analyzed at the Inserm U1162 laboratory (Paris, France), as part of a research project approved by Paris Saint-Louis and Inserm Institutional Review Board committees (Paris Saint-Louis, 2004; INSERM IRB 2010).

Histological and immunohistochemical analyses

Slides stained with Hematein-Eosin-Saffron and Congo Red were reviewed by two expert pathologists (JC and ESZ), using an Olympus BX51 microscope. Amyloid deposits were identified using Congo Red staining and examination under polarized light.

For immunohistochemistry, 4 μ m thick sections were cut from paraffin embedded blocks. Slides were processed on an automated autostainer (Leica Bondmax). After deparaffinisation and rehydratation, sections were placed into a boiling target retrieval solution (Leica Epitope Retrieval Solution 1 for CRP and Leica Epitope Retrieval Solution 2 for SAA). Endogenous peroxidase was blocked with Peroxide Block (Leica). Sections were further incubated with primary anti-bodies against CRP (Abcam, Clone Y284, AB32412, dilution 1/4000) or SAA (Dako, Clone MC1, M0759, dilution 1/2000).

After incubation with a polymer system (Leica Polymer Refine Detection), and staining with 3,3' diaminobenzidine (Dako) as chromogen, slides were counterstained with Mayer's haematoxylin, dehydrated and coverslipped.

Sequencing and bioinformatic analyses

Whole genome sequencing

Whole-genome-sequencing was performed by the Centre National de Recherche en Génomique Humaine (Evry, France) on an Illumina HiSeqX5 platform as paired-end 150 bp reads. RNA-sequencing was performed by Integragen (Evry, France) on an Illumina HiSeq2000 as paired-end 100bp reads. WGS and RNAseq were analyzed as previously described. More details on sequencing and bioinformatics analyses are provided in the Supplementary Appendix. Raw WGS and RNA-seq data have been deposited in the EGA (European genome-phenome archive, http://www.ebi.ac.uk/ ega/) database, accessions numbers are pending).

We extracted DNA using a salting-out procedure. Genomic DNA was loaded on a 0.8% agarose gel for quality control; only DNA >10 kb in size was selected. DNA quantification was performed using Hoechst 33258 from Sigma Chemical. Whole genome sequencing (WGS) was performed by the Centre National de Recherche en Génomique Humaine (Institut de biologie François Jacob, CEA). WGS libraries were prepared using the Illumina TruSeq DNA PCR-Free Library Preparation Kit according to the manufacturer's instructions, and the tumor and matched normal liver were sequenced on an Illumina HiSeqX5 platform as paired-end 150 bp reads. Sequences were aligned to the hg19 version of the human genome using BWA version 0.7.12. We used Picard tools version 1.108 (http://broadinstitute.github.io/picard/) to remove PCR duplicates and GATK version v3.5 for local indel realignment and base quality recalibration, as recommended in GATK best practices. Pilo We obtained an average depth of 90-fold for the tumor and 60-fold for the normal sample. We used MuTect2 to call somatic mutations (single nucleotide variants and small insertions and deletions) the tumor sample with its matched non-tumor counterpart and a panel of normal samples from the lab 11.

We selected only mutations with a "PASS" MuTect2 filter and we excluded mutations belonging to the ENCODE Data Analysis Consortium blacklisted regions (http://hgdownload.cse.u csc.edu/goldenPath/hg19/encodeDCC/wgEncodeMapability/wgEncodeDacMapabilityConsensusExclu dable.bed.gz).

We used cgpBattenberg algorithm for copy-number analysis and MANTA software to identify somatic structural variations from the tumor and normal bam files. ^{12,13} To keep only the most reliable events, we selected only structural variants (SVs) supported by ≥15 reads (for all SV types), representing ≥10% of reads (for inversions and interchromosomal translocations). Raw sequences have been deposited in the EGA (European genome-phenome archive - http://www.ebi.ac.uk/ega/) database (EGAS00001003025) and variant calls are available on the International Cancer Genome Consortium (ICGC) data portal (http://dcc.icgc.org/).

RNA-sequencing

Index tumor (#2615T) sample and control normal and IHCA mutated for IL6ST were analyzed by RNA-sequencing. Libraries were prepared by Integragen (Evry, France) using Illumina TruSeq Stranded mRNA kit according to the manufacturer's instructions, and sequenced as paired-end 100bp reads on an Illumina HiSeq2000. Fastq files were aligned to the reference human genome hg19/GRCh37 with TopHat2 (-p 24 -r 150 -g 2 --library-type fr-firststrand). After removing reads mapping to multiple locations, we used HTSeq to obtain the number of reads associated to each gene in the GENCODE v24lift37 database (restricted to protein-coding genes, antisense and lincRNAs). We used the Bioconductor DESeq package to import raw HTSeq counts for each sample into R statistical software and extract the count matrix. After normalizing for library size, we normalized the count matrix by the coding length of genes to compute FPKM scores (number of fragments per kilobase of exon model and millions of mapped reads). We used Integrative Genomics Viewer (IGV) to visualize the IL6 transcripts and generate Sashimi plots. Raw sequences have been deposited in the EGA (European genome-phenome archive - http://www.ebi.ac.uk/ega/) database (accessions numebrs are pending).

Table S1. Blood and urine biological analyses of the patient.

	Patient values at diagnosis	Normal values
Hemoglobin	10 g/dL	11.7-15.0
Mean corpuscular volume	69.8 fL	83.7-100.8
Platelet count	533,000/mm ³	150,000-353,000
Leukocytes (total)	12,900/ mm ³	4,600-10,100
Neutrophils	10,060/ mm ³	2,200-6,100
Lymphocytes	1,650/ mm ³	1,100-3,700
Fibrinogen	8.02 g/L	2.30-4.30
CRP	145.3 mg/L	0.0-6.0
SAA	153.0 mg/L	0.0-6.4
Procalcitonin	0.43 mg/L	0.00-0.50
Urea	0.97 g/L	0.15-0.53
Creatinine	41.7 mg/L	5.5-10.2
Alkaline phophatase	493 U/L	34-117
GGT	265 U/L	05-50
ASAT	29 U/L	14-40
ALAT	41 U/L	06-40
LDH	190 U/L	<250
Protein (total)	62 g/L	66-83
Albumin	26 g/L	38-49
Protein (urine)	7,481 mg/L	0-150
Alpha-1-microglobulin (urine)	298.0 mg/L	<12
IL-2	8.96 pg/mL	0.79-21.7
IL-6	186.64 pg/mL	0.62-8.0
IL-7	1.74 pg/mL	0.40-3.2
IL-10	33.65 pg/mL	0.0-4.3
IL-17A	5.46 pg/mL	0.0-15.1
sCD154	16.39 pg/mL	10.9-286.4
IFN gamma	0 pg/mL	0.0-2.7

Table S2: Coding somatic mutations identified in the tumor of the index patient (#2615T)

Chromosome	Position	Reference base	Variant base	Hugo Symbol	Variant Classification	Genome Change	cDNA Change	Protein Change
chr1	180022207	G	Т	CEP350	Missense_Mutation	g.chr1:180022207G>T	c.4895G>T	p.S1632I
chr1	236979804	Α	Т	MTR	Missense_Mutation	g.chr1:236979804A>T	c.725A>T	p.E242V
chr10	134659633	С	Α	TTC40	Missense_Mutation	g.chr10:134659633C>A	c.6366G>T	p.Q2122H
chr11	113103452	T	С	NCAM1	Missense_Mutation	g.chr11:113103452T>C	c.1054T>C	p.S352P
chr14	77605915	Α	Т	ZDHHC22	Missense_Mutation	g.chr14:77605915A>T	c.167T>A	p.F56Y
chr17	5462679	Т	G	NLRP1	Missense_Mutation	g.chr17:5462679T>G	c.1337A>C	p.K446T
chr17	38572320	Α	G	TOP2A	Splice_Site	g.chr17:38572320A>G	c.269T>C	p.V90A
chr19	55954202	Α	Т	SHISA7	Missense_Mutation	g.chr19:55954202A>T	c.29T>A	p.L10Q
chr20	37174999	Α	G	RALGAPB	Missense_Mutation	g.chr20:37174999A>G	c.2816A>G	p.H939R
chr3	123167254	С	CG	ADCY5	Frame_Shift_Ins	g.chr3:123167254_12316 7254insCG	c.139_139ins CG	p46fs
chr4	90872904	Т	Α	MMRN1	Splice_Site	g.chr4:90872904T>A		
chr4	94690579	G	Т	GRID2	Missense_Mutation	g.chr4:94690579G>T	c.2579G>T	p.G860V
chr6	3123976	С	Α	BPHL	Missense_Mutation	g.chr6:3123976C>A	c.142C>A	p.L481
chr6	30673359	T	G	MDC1	Missense_Mutation	g.chr6:30673359T>G	c.3601A>C	p.T1201P
chr6	32007362	G	С	CYP21A2	Missense_Mutation	g.chr6:32007362G>C	c.589G>C	p.E197Q
chr6	56472969	Α	Т	DST	Missense_Mutation	g.chr6:56472969A>T	c.5824T>A	p.L1942I
chr7	29918696	G	T	WIPF3	Nonsense_Mutation	g.chr7:29918696G>T	c.295G>T	p.G99*
chr7	73254374	AT	Α	WBSCR27	Frame_Shift_Del	g.chr7:73254374delAT	c.465delAT	p.Q155fs
chr8	26722021	С	Т	ADRA1A	Missense_Mutation	g.chr8:26722021C>T	c.466G>A	p.V156I
chr8	38205493	Α	С	WHSC1L1	Missense_Mutation	g.chr8:38205493A>C	c.197T>G	p.L66R
chrX	99596960	G	Α	PCDH19	Missense_Mutation	g.chrX:99596960G>A	c.2789C>T	p.A930V
chrX	142716743	C	T	SLITRK4	Missense_Mutation	g.chrX:142716743C>T	c.2182G>A	p.E728K

Table S3. Somatic structural rearrangements identified in the tumor of the index patient (#2615)

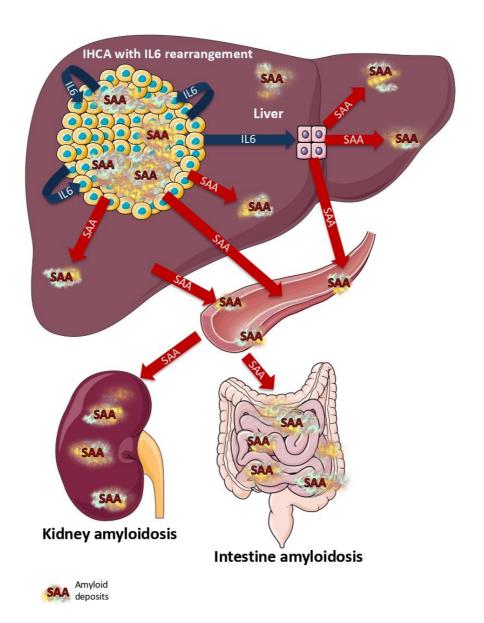
Rearrangement Type	Breakpoint 1 Chromosome	Breakpoint 1 Position	Breakpoint 1 Category	Breakpoint 1 Gene	Breakpoint 2 Chromosome	Breakpoint 2 Position	Breakpoint 2 Category	Breakpoint 2 Gene
Interchromosomal Translocation	chr1	243119768	Intergenic Region	NA	chrY	13977276	Intergenic Region	NA
Inversion	chr11	44572105	Intergenic Region	NA	chr11	116683145	RNA	AP006216.5
Interchromosomal Translocation	chr12	116911744	Intergenic Region	NA	chr18	39532046	Intergenic Region	NA
Inversion	chr15	100338220	RNA	DNM1P46	chr15	102306887	RNA	DNM1P47
Deletion	chr15	26879870	Intron	GABRB3	chr15	48647047	Intergenic Region	NA
Interchromosomal Translocation	chr16	88439347	Intergenic Region	NA	chr17	43059782	lincRNA	CTD-2534I21.9
Interchromosomal Translocation	chr17	70083524	RNA	AC005152.2	chrX	8451963	Intergenic Region	NA
Interchromosomal Translocation	chr2	18817184	Intergenic Region	NA	chr20	22308518	Intergenic Region	NA
Deletion	chr3	69767360	Intergenic Region	NA	chr3	69768630	Intergenic Region	NA
Interchromosomal Translocation	chr3	69767777	Intergenic Region	NA	chr7	36903921	Intron	ELMO1
Interchromosomal Translocation	chr3	69768559	Intergenic Region	NA	chr7	41484105	Intergenic Region	NA
Inversion	chr4	109747252	Intron	COL25A1	chr4	110927627	Intron	EGF
Interchromosomal Translocation	chr4	109747817	Intron	COL25A1	chr14	69289448	Intergenic Region	NA
Inversion	chr4	109749159	Intron	COL25A1	chr4	109749299	Intron	COL25A1
Deletion	chr4	109749231	Intron	COL25A1	chr4	110921447	Intron	EGF
Deletion	chr4	109749327	Intron	COL25A1	chr4	110960547	Intergenic Region	NA
Interchromosomal Translocation	chr4	110921542	Intron	EGF	chr14	69289392	Intergenic Region	NA
Inversion	chr4	110982418	Intron	ELOVL6	chr4	111017388	Intron	ELOVL6
Interchromosomal Translocation	chr4	110984500	Intron	ELOVL6	chr7	21930994	Intron	DNAH11
Interchromosomal Translocation	chr4	111018301	Intron	ELOVL6	chr7	22662350	RNA	AC002480.5
Deletion	chr4	111226035	Intergenic Region	NA	chr4	111226721	Intergenic Region	NA
Interchromosomal Translocation	chr4	185597507	Intron	PRIMPOL	chr22	36449794	Intergenic Region	NA
Deletion	chr4	91931666	Intron	CCSER1	chr4	91933525	Intron	CCSER1
Interchromosomal Translocation	chr6	154638263	Intron	IPCEF1	chr10	53209375	Intron	PRKG1
Deletion	chr6	32458343	Intergenic Region	NA	chr6	32504751	Intergenic Region	NA
Interchromosomal Translocation	chr7	128151688	Intergenic Region	NA	chr17	60535882	5'Flank	TLK2

Deletion	chr7	16599884	Intron	LRRC72	chr7	16600278	Intron	LRRC72
Deletion	chr7	16626595	Intergenic Region	NA	chr7	16627762	Intergenic Region	NA
Deletion	chr7	21019896	lincRNA	AC006481.1	chr7	39390092	Intron	POU6F2
Tandem Duplication	chr7	22666192	RNA	AC002480.5	chr7	36894098	3'UTR	ELMO1
Inversion	chr7	22771257	3'UTR	IL6	chr7	41479923	Intergenic Region	NA
Tandem Duplication	chr7	22979435	Intergenic Region	FAM126A	chr7	37030083	Intron	ELMO1
Inversion	chr7	36901703	Intron	ELMO1	chr7	38573324	Intron	AMPH
Inversion	chr7	36903099	Intron	ELMO1	chr7	38573032	Intron	AMPH
Inversion	chr7	37031598	Intron	ELMO1	chr7	41480304	Intergenic Region	NA
Deletion	chr7	39389384	Intron	POU6F2	chr7	41484626	Intergenic Region	NA
Deletion	chrX	6355883	Intergenic Region	NA	chrX	6396739	Intergenic Region	NA

Table S4. Clinical and biological features of patients with AA amyloidosis and hepatocellular adenoma. $^{18-25}$

Patient ID	Clinical features of the patient	Symptoms at diagnosis	Clinical follow-up	Tumor characteristics/ Pathology	Reference
Index case #2615	49 year-old female, thyrotoxicosis, hypertension	Renal insufficiency, proteinuria, biological inflammatory syndrome, renal and digestive amyloidosis	Regression of digestive symptoms and decrease of the peripheral inflammatory syndrome after resection	5cm IHCA, Amyloid deposits and SAA expression in both the tumor and non-tumor liver tissues	Index
1	56 year-old male, hypertension, hyper- cholesterolemia, alcohol abuse	Renal insufficiency, proteinuria, biological inflammatory syndrome, hepatic, renal and digestive amyloidosis	Renal function stabilization and decrease of the peripheral inflammatory syndrome after resection	11cm IHCA, Amyloid deposits and SAA expression in both the tumor and non-tumor liver tissues	Fievet et al., Gut 1990
2	34 year-old female, oral contraception, hyperlipidemia	Nephrotic syndrome; hepatic, renal and rectal amyloidosis	Acute renal failure, favorable evolution after kidney transplantation and resection	IHCA, Amyloid deposits and SAA expression in both the tumor and non-tumor liver tissues	Bestard Matamoros et al., Nefrologia 2008
3	37 year old female, oral contraception, Spain	Nephrotic syndrome, intra-tumor bleeding	Regression of nephrotic syndrome and HCA after oral contraception withdrawal	8cm HCA, amyloid deposits in the non-tumor liver and the kidney	Cosme et al. Liver, 1995
4	32 year old male, Japan	Renal, heart and digestive amyloidosis	Regression of nephrotic syndrome and faborable outcome after surgical resection	SAA negative HCA with SAA expression in the non tumor liver, amyloid deposits in the tumor	Shibasaki et al., 1997
5	39 year old female, oral contraception, Sweden	Nephrotic syndrome	Regression of nephrotic syndrome	15cm HCA with histological features consistent with IHCA, lack of SAA expression by immunofluorescence, amyloid deposits in the tumor and non- tumor liver tissues, and kidney	Thysell et al. J Hepatol, 1986
6	28 year old female, oral contraception, France	Proteinuria and biological inflammatory syndrome	Regression of nephrotic and inflammatory syndrome after surgical resection	HCA, amyloid deposits in the HCA, non-tumor liver and the kidney.	Melin et al., Nephron, 1993
7	49 year old male	Non-resectable HCA at 32 years. Transformation in HCC associated with amyloidosis and nephrotic syndrome at 49 years	Death from HCC	HCA transformed in HCC, amyloid deposits in the liver and kidney.	Delgado et al. J LA State Med Soc, 1999
8	40 year old male, Glycogen storage disease type 1b, hypertension	Severe renal dysfunction	15	Multiple adenomas (no biopsy or resection), Amyloidosis in the liver, kidney and spleen	Dick et al., Clin Kidney J, 2012

Figure S1. Schematic representation of the biological mechanisms leading to systemic AA amyloidosis in the index patient.



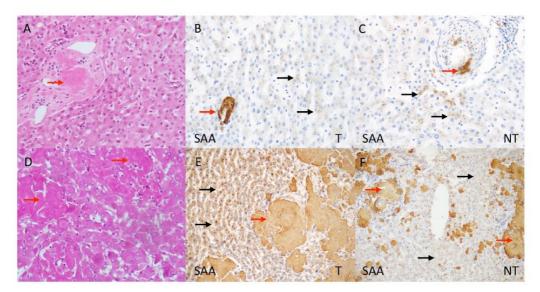


Figure S2. Histological findings of two additional cases of IHCA associated with amyloidosis.

Microscopic examination of case n°2 (Bestard Matamoros et al., Nefrologia, 2008) showed a well-differentiated tumor with amyloid deposits (Panel A, red arrows, Hematein-Eosin-Saffron, X400). Immunohistochemical experiments demonstrated SAA expression in both neoplastic and non neoplastic hepatocytes, along with stained amyloid deposits (Panel B: tumor, Panel C: adjacent parenchyma, black arrows: hepatocytes, red arrows: amyloid deposits, X400). Case n°3 (Fievet et al., Gut 1990) displayed massive amyloid deposits (Panel D, red arrows, Hematein-Eosin-Saffron, X400). As observed for case n°2, SAA was expressed in the tumor and the non-tumoral liver (Panel E: tumor, Panel F: adjacent parenchyma, black arrows: hepatocytes, red arrows: amyloid deposits, X200). A strong staining was observed in the deposits (Panel E and F, red arrows, X200). T: tumor; NT: non-tumor liver.

References

- 1. Paschoud S, Dogar AM, Kuntz C, Grisoni-Neupert B, Richman L, Kuhn LC. Destabilization of interleukin-6 mRNA requires a putative RNA stem-loop structure, an AU-rich element, and the RNA-binding protein AUF1. Molecular and cellular biology 2006;26:8228-41.
- 2. Matsushita K, Takeuchi O, Standley DM, et al. Zc3h12a is an RNase essential for controlling immune responses by regulating mRNA decay. Nature 2009;458:1185-90.
- 3. Sa Cunha A, Blanc JF, Lazaro E, et al. Inflammatory syndrome with liver adenomatosis: the beneficial effects of surgical management. Gut 2007;56:307-9.
- 4. Heinrich PC, Castell JV, Andus T. Interleukin-6 and the acute phase response. The Biochemical journal 1990;265:621-36.
- 5. Garbers C, Heink S, Korn T, Rose-John S. Interleukin-6: designing specific therapeutics for a complex cytokine. Nat Rev Drug Discov 2018.
- 6. Letouze E, Shinde J, Renault V, et al. Mutational signatures reveal the dynamic interplay of risk factors and cellular processes during liver tumorigenesis. Nature communications 2017;8:1315.
- 7. Miller SA, Dykes DD, Polesky HF. A simple salting out procedure for extracting DNA from human nucleated cells. Nucleic acids research 1988;16:1215.
- 8. Li H, Durbin R. Fast and accurate short read alignment with Burrows-Wheeler transform. Bioinformatics 2009;25:1754-60.
- 9. McKenna A, Hanna M, Banks E, et al. The Genome Analysis Toolkit: a MapReduce framework for analyzing next-generation DNA sequencing data. Genome research 2010;20:1297-303.
- 10. DePristo MA, Banks E, Poplin R, et al. A framework for variation discovery and genotyping using next-generation DNA sequencing data. Nature genetics 2011;43:491-8.
- 11. Cibulskis K, Lawrence MS, Carter SL, et al. Sensitive detection of somatic point mutations in impure and heterogeneous cancer samples. Nature biotechnology 2013;31:213-9.
- 12. Nik-Zainal S, Van Loo P, Wedge DC, et al. The life history of 21 breast cancers. Cell 2012;149:994-1007.
- 13. Chen X, Schulz-Trieglaff O, Shaw R, et al. Manta: rapid detection of structural variants and indels for germline and cancer sequencing applications. Bioinformatics 2016;32:1220-2.
- 14. Kim D, Pertea G, Trapnell C, Pimentel H, Kelley R, Salzberg SL. TopHat2: accurate alignment of transcriptomes in the presence of insertions, deletions and gene fusions. Genome biology 2013:14:R36.
- 15. Anders S, Pyl PT, Huber W. HTSeq--a Python framework to work with high-throughput sequencing data. Bioinformatics 2015;31:166-9.
- 16. Anders S, Huber W. Differential expression analysis for sequence count data. Genome biology 2010;11:R106.
- 17. Robinson JT, Thorvaldsdottir H, Winckler W, et al. Integrative genomics viewer. Nature biotechnology 2011;29:24-6.
- 18. Fievet P, Sevestre H, Boudjelal M, et al. Systemic AA amyloidosis induced by liver cell adenoma. Gut 1990;31:361-3.
- 19. Bestard Matamoros O, Poveda Monje R, Ibernon Vilaro M, Carrera Plans M, Grinyo Boira JM. [Systemic AA amyloidosis induced by benign neoplasms]. Nefrologia 2008;28:93-8.
- 20. Cosme A, Horcajada JP, Vidaur F, Ojeda E, Torrado J, Arenas JI. Systemic AA amyloidosis induced by oral contraceptive-associated hepatocellular adenoma: a 13-year follow up. Liver 1995;15:164-7.
- 21. Shibasaki T, Matsumoto H, Watabe K, et al. A case of renal amyloidosis associated with hepatic adenoma: the pathogenetic role of tumor necrosis factor-alpha. Nephron 1997;75:350-3.
- 22. Thysell H, Ingvar C, Gustafson T, Holmin T. Systemic reactive amyloidosis caused by hepatocellular adenoma. A case report. Journal of hepatology 1986;2:450-7.
- 23. Delgado MA, Liu JY, Meleg-Smith S. Systemic amyloidosis associated with hepatocellular carcinoma. Case report and literature review. J La State Med Soc 1999;151:474-8.

- 24. Dick J, Kumar N, Horsfield C, Jayawardene S. AA Amyloidosis in a patient with glycogen storage disorder and progressive chronic kidney disease. Clinical kidney journal 2012;5:559-61.
- 25. Melin JP, Lecrique T, Wynckel A, et al. Remission of nephrotic syndrome related to AA amyloidosis after hepatic adenomectomy. Nephron 1993;64:157-8.

Article 2: Recurrent chromosomal rearrangements of ROS1, FRK and IL6 activating JAK/STAT pathway in inflammatory hepatocellular adenomas.

Hepatology

ORIGINAL RESEARCH

Recurrent chromosomal rearrangements of *ROS1*, *FRK* and *IL6* activating JAK/STAT pathway in inflammatory hepatocellular adenomas

Quentin Bayard, ¹ Stefano Caruso, ¹ Gabrielle Couchy, ¹ Sandra Rebouissou, ¹ Paulette Bioulac Sage, ^{2,3} Charles Balabaud, ³ Valerie Paradis, ^{4,5} Nathalie Sturm, ⁶ Anne de Muret, ⁷ Catherine Guettier, ⁸ Benjamin Bonsang, ⁹ Christiane Copie, ⁹ Eric Letouzé, ¹ Julien Calderaro, ⁹ Sandrine Imbeaud ¹ Jean-Charles Nault ¹ Jessica Zucman-Rossi ^{1,12}

► Additional material is published online only. To view please visit the journal online (http://dx.doi.org/10.1136/ gutjnl-2019-319790).

For numbered affiliations see end of article.

Correspondence to

Dr Jean-Charles Nault, INSERM UMR 1338, INSERM, Paris 93140, France; naultjc@gmail.com Professor Jessica Zucman-Rossi; jessica.zucman-rossi@inserm.fr

J-CN and JZ-R are joint senior

Received 4 September 2019 Revised 27 November 2019 Accepted 14 December 2019

Check for updates

© Author(s) (or their employer(s)) 2020. No commercial re-use. See rights and permissions. Published by BMJ.

To cite: Bayard Q, Caruso S, Couchy G, et al. Gut Epub ahead of print: [please include Day Month Year]. doi:10.1136/ gutjnl-2019-319790

ABSTRACT

Background Inflammatory hepatocellular adenomas (IHCAs) are benign liver tumours characterised by an activation of the janus kinase (JAK)/signal transducers and activators of transcription (STAT) pathway caused by oncogenic activating mutations. However, a subset of IHCA lacks of identified mutation explaining the inflammatory phenotype.

Methods 657 hepatocellular adenomas developed in 504 patients were analysed for gene expression of 17 genes and for mutations in seven genes by sequencing. 22 non-mutated IHCAs were analysed by whole-exome and/or RNA sequencing.

Results We identified 296 IHCA (45%), 81% of them were mutated in either IL6ST (61%), FRK (8%), STAT3 (5%), GNAS (3%) or JAK1 (2%). Among non-mutated IHCA, RNA sequencing identified recurrent chromosome rearrangement involving ROS1, FRK or IL6 genes. ROS1 fusions were identified in 8 IHCA, involving C-terminal part of genes highly expressed in the liver (PLG, RBP4, APOB) fused with exon 33-35 to 43 of ROS1 including the tyrosine kinase domain. In two cases a truncated ROS1 transcript from exon 36 to 43 was identified. ROS1 rearrangements were validated by fluorescence in situ hybridisation (FISH) and led to ROS1 overexpression. Among the 5 IHCA with FRK rearrangements, 5 different partners were identified (MIA3, MIA2, LMO7, PLEKHA5, SEC16B) fused to a common region in FRK that included exon 3-8. No overexpression of FRK transcript was detected but the predicted chimeric proteins lacked the auto-inhibitory SH2-SH3 domains. In two IHCA, we identified truncated 3'UTR of IL6 associated with overexpression of the transcript.

Conclusion Recurrent chromosomal alterations involving *ROS1*, *FRK* or *IL6* genes lead to activation of the JAK/STAT pathway in IHCAs.

INTRODUCTION

Hepatocellular adenomas (HCAs) are rare benign tumours mainly fostered by exposure to oestrogen, particularly in women taking oral contraceptives. Management of hepatocellular adenoma requires assessment of the risk of complications mainly related to tumour bleeding and malignant

Significance of this study

What is already known on this subject?

- Inflammatory hepatocellular adenomas (IHCAs) are benign liver tumours characterised by an activation of the JAK/STAT pathway caused by oncogenic activating mutations.
- A subset of IHCA lacks of identified mutation explaining the inflammatory phenotype.

What are the new findings?

- ► We identified recurrent chromosomal alterations involving ROS1, FRK or IL6 in IHCAs.
- ROS1 activation is a novel mechanism of JAK/ STAT pathway activation in human benign liver tumours.

How might it impact on clinical practice in the foreseeable future?

- These new genetic alterations could be potential diagnostic biomarkers of a subtype of hepatocellular adenoma.
- Targeted therapies adapted to genetic alterations could be tested in selected patients with multiple or unresectable IHCAs.

transformation to hepatocellular carcinoma (HCC).²

Genotype/phenotype classification of HCA has dissected adenomas in homogeneous subgroups characterised by somatic genetic alterations dysregulating signalling pathways and linked with specific risk factors, clinical behaviours, histological and imaging features.3 The first subgroups of HCA (HHCA, 30%-40%) are defined by bi-allelic inactivating mutations of HNF1A and are associated with tumour steatosis, lipogenesis and mammalian target of rapamycin (mTOR) activation. 45 Another group of HCA is defined by mutations in CTNNB1, coding for ß-catenin, either in exon 3 (bex3HCA, around 15% of HCA) or in exon 7 or 8 (bex7,8HCA, around 10% of HCA).3 6 Mutations in CTNNB1 exon 3 are associated with a high risk of malignant transformation in HCC.3 A new subgroup associated





Hepatology

with a high risk of tumour bleeding was recently described in 4%–5% of the patients (sonic hedgegog hepatocellular adenoma (shHCA)); it is defined by an activation of the sonic hedgehog pathway due to a *GLI1* overexpression caused by a somatic fusion with *INHBE*, its neighbouring gene.⁷

The most prevalent subgroup of HCA are inflammatory tumours (inflammatory hepatocellular adenomas (IHCAs), around 50% of HCA), characterised by the constitutive and uncontrolled activation of interleukin 6 (IL-6)/JAK/STAT pathway easily detectable by the overexpression of serum amyloid A (SAA) and C-reactive protein (CRP) at the transcriptomic level, associated with inflammatory infiltrate, sinusoidal dilatation and dystrophic arteries at histological level.8 Overexpression of SAA and CRP in the tumour on immunohistochemistry helps to identify this subtype in routine. Interestingly, a subset of IHCA is mixed, harbouring mutation of CTNNB1 either in exon 3 or exon 7/8 (bex3IHCA, bex7,8IHCA). Risk factors for development of IHCA are high alcohol consumption and obesity.9 Several genetic alterations are responsible for the constitutive activation of JAK/STAT pathway in IHCA. The most frequent mutation are in IL6ST (coding for the gp130 receptor), STAT3 (coding for a transcription factor of the JAK/ STAT pathway), FRK (coding for a src kinase), JAK1 (coding for one of the protein tyrosine kinase of the JAK/STAT pathway) and GNAS (coding stimulatory G-protein alpha subunit). 6 10 11 Inflammatory syndrome, anaemia or fever could be observed in patients with IHCA; these symptoms regress after tumour resection. Recently, we described an IHCA with a rearrangement of the 3'UTR of the IL6 gene leading to a secondary amyloidosis through an autocrine/paracrine mechanism of activation of JAK/ STAT pathway by IL-6 in the whole liver. 12 However, a subset of IHCA has currently no known genetic alterations explaining the constitutive activation of JAK/STAT pathway.

The aim of our study was to unravel new mechanisms of activation of inflammatory pathway in inflammatory adenomas without any mutation in known driver genes to better understand the mechanism of regulation of IL-6/JAK/STAT pathway in hepatocytes and its role in benign liver tumourigenesis.

MATERIAL AND METHODS

Selection of tumours and patients

Frozen samples from 657 HCA developed in 504 patients were analysed. This series included 124 new HCA cases apart from previously analysed HCA cases by Nault *et al*⁷. Samples were collected in 28 centres in France from 2000 to 2017. All patients gave their informed consent according to French law. All samples were frozen in nitrogen immediately after resection or biopsy and conserved at -80° C.

DNA sequencing

HNF1A (exon 1–10), IL6ST (exons 6 and 10), CTNNB1 (exons 2, 3, 4, 7 and 8), FRK (exon 6), STAT3 (exons 3, 6, 17 and 21), GNAS (exons 7, 8 and 9) and JAK1 (all exons) were sequenced by either Sanger sequencing or Miseq Illumina PCR-based sequencing (for detailed protocol see ^{6 13 14}). Somatic mutations were confirmed by sequencing of the tumour and non-tumour counterpart.

Quantitative RT-PCR

Gene expression of a selection of 17 genes was assessed by quantitative reverse transcriptase PCR (RT-PCR) using Fluidigm technology with Taqman probes detailed in online supplementary table 1, as previously described.⁷ ¹³ Data were normalised using

RNA ribosomal 18S as calibrator. We used the 2 delta delta CT method with the level of the corresponding gene expression in tumour tissues expressed as an n-fold ratio compared with the mean level of expression in five normal livers.

As previously described, HHCAs were defined by HNF1A bi-allelic mutations and/or downregulation of LFABP and UGT2B7 (T/N<0.2); IHCAs were defined by SAA and/or CRP overexpression T/N>5 and/or activating mutations in IL6ST, FRK, JAK1, STAT3, GNAS. bex3 HCAs were defined by mutations or in frame deletion of CTNNB1 exon 3, bex7,8 HCAs were defined by mutations of CTNNB1 in exon 7 or 8, bHCAs were defined by overexpression of Wnt/catenin pathway target genes GLUL or LGR5 (T/N>5) without identified gene mutation. bex3 IHCAs were identified by the combination of bex3 HCA and IHCA criteria, bIHCA by the combination of bHCA and IHCA criteria shHCA was defined by overexpression of the following target genes of sonic hedgehog pathway: GLI1, TNNC1, FCRLA, GPR97, HHIP, PTCH1 and PTGDS.

Whole exome sequencing

Whole exome data were analysed in 19 HCA cases which included 4 previously published and 15 new cases. Sequence capture, enrichment and elution of genomic DNA samples from the tumour/normal pairs were performed by IntegraGen (Evry). Agilent in-solution enrichment was used with the manufacturer's biotinylated oligonucleotide probe library SureSelect Human All-Exon kit V.4 70Mb (n=4), SureSelect Human All-Exon kit V.5 +UTRs (n=8), or Twist Human Core Exome Enrichment System (n=7). Briefly, 3 µg of each genomic DNA was sonicated and purified to yield fragments of 150-200 bp. Adaptor oligonucleotides were ligated on A-tailed fragments and enriched by four to six PCR cycles. Purified libraries (500 ng) were hybridised to the SureSelect library for 24 hours. The eluted enriched DNA sample was sequenced on an Illumina HiSeq 2000 (n=12) or HiSeq 4000 (n=7) as paired-end 75 bp reads. Sequencing details for each sample are indicated in online supplementary table 2. Variant calling was processed using Mutect2 by comparing each tumour sample with its matched non-tumour counterpart, following the genone analysis toolkit (GATK) best practices. 15 16 The copy number profiles were defined using an in-house pipeline. Briefly, the logR ratio was processed using the coverage of each tumour and its non-tumour counterpart in each 1kb genomic windows; then a segmentation was done in order to identify copy number alterations.

RNA sequencing

RNA samples from the 22 HCA tumours were sequenced comprising 1 previously published 12 and 21 new cases. RNA samples were enriched for polyadenylated RNA from 5 µg of total RNA, and the enriched samples were used to generate sequencing libraries with the NEBNext Ultra II Directional RNA (n=13) or Illumina TruSeq Stranded messenger RNA (mRNA) (n=9) kits and associated protocol as provided by the manufacturer. Libraries were sequenced by IntegraGen on an Illumina HiSeq 2000 or 4000 as paired-end 101 bp or 75 bp reads (n=8 and n=14, respectively). Full Fastq files were aligned to the reference human genome GRCh38 using TopHat2 V.2.0.14. TopHat2 are indicated in online supplementary table 2. Read mapping from multiple locations was removed and HTSeq 18 was used to obtain the number of reads associated with each gene in the Gencode V.27 database, restricting to protein-coding genes,

Hepatology

pseudogenes, antisense and lincRNAs (n=39947). Bioconductor DESeq2 package¹⁹ was used to import raw HTSeq counts for each sample into R statistical software and apply variance stabilising transformation to the raw count matrix. FPKM scores (number of fragments per kilobase of exon model and millions of mapped reads) were calculated by normalising the count matrix for the library size estimated with DESeq2 package and the coding length of each gene. In order to handle batch effect, we used an in-house method, according to our previous published method.²⁰ Briefly, area under the ROC curve (AUC) was used to identify and remove 2696 genes with a significant batch effect (AUC >0.95 between one sequencing project and others).

To perform gene set enrichment analysis (GSEA) analysis, genes from RNA-seq data were sorted according to fold-change from Limma analysis (genes with positive fold-changes first, then negative fold-changes) using an input of 16387 genes (Hallmarks gene set; MSigDB V.6 database used). This gene list was obtained from Genecode database; then genes with a variance equal 0 or with a total number of reads from samples inferior of 50 were removed.

Gene fusion detection

Fusions detected by TopHat2 (--fusion-search --fusion-min-dist 2000 --fusion-anchor-length 13 --fusion-ignore-chromosomes chrM) were filtered using the TopHatFusion²⁰ pipeline. Fusions validated by BLAST and with at least 10 split-reads or pairs of reads spanning the fusion event were retained, whereas any fusion identified at least twice in a cohort of 36 normal liver samples was removed. For each fusions of interest, the sequence corresponding to chimaera was generated and used as a reference to realign RNAseq reads. Visual inspection of chimaera alignments on Integrative Genome Viewer (broad institute) was used to refine junction positions and determine in phase chimeric transcripts. Oncofuse V.1.0.9b2 was finally used to annotate fusions of interest.²¹

FISH experiment

Whole-tissue sections from formalin-fixed, paraffin-embeded surgical samples of HCA were deparaffinised in xylene and washed in ethanol. After rehydratation, they were subjected to heat pre-treatment (Pre-Treatment Solution, DakoCytomation, 10 min, 75°C). After digestion with pepsin (10 min, DakoCytomation) and airdrying, the SPEC ROS1 dual colour break apart probe (Zytovision Z-2144) was applied to the tissue sections. Probe mixture and tissue sections were further codenatured and hybridised overnight (Dako Hybridizer). After washing, dehydration and drying, tissue sections were finally counterstained using fluorescence mounting media containing de-amidino-phenyl-indole.

Statistical analysis

Statistical analysis was performed using the GraphPad Prism and the R V.3.4.2 software. Comparison between qualitative data was performed using Fisher's exact test. Quantitative data in two different group were compared using the non-parametric Mann-Whitney test. All tests were two-tailed and a p value < 0.05 was considered as significant.

Data availability

The aligned sequencing data reported in this paper have been deposited to the EGA (European Genome-phenome Archive) database (RNA-seq accession EGAS00001003025 and

	Number (percentage			
Variables	n=657			
HCA	605 (92%)			
Borderline lesions (HCA/HCC)	39 (6%)			
HCC on HCA	13 (2%)			
H HCA	226 (34%)			
IHCA	222 (34%)			
bex ^{7,8} IHCA	21 (3%)			
bex³ IHCA	44 (7%)			
b IHCA	9 (1%)			
bex ^{7,8} HCA	19 (3%)			
bex ³ HCA	52 (8%)			
b HCA	4 (1%)			
Sh HCA	34 (5%)			
U HCA	26 (4%)			

b IHCA, IHCA with activation of B-catenin pathway without mutations. b HCA, HCA with activation of B-catenin pathway without mutations; bex³ IHCA, IHCA with mutations of CTNNB1 in exon 3; bex³.8 IHCA, IHCA with mutations of CTNNB1 in exon 7 or 8; bex³ HCA, HCA with mutations of CTNNB1 in exon 3; bex².8 HCA, HCA with mutations of CTNNB1 in exon 7 or 8; H HCA, HNF1A inactivated HCA; HCA, when the mutation of CTNNB1 in exon 7 or 8; H HCA, HNF1A inactivated HCA; HCA, hepatocellular adenoma; HCC on HCA, hepatocellular carcinoma developed on hepatocellular adenoma; HCC, hepatocellular carcinoma; IHCA, inflammatory hepatocellular adenoma; Sh HCA, sonic hedgehog HCA; U HCA, unclassified HCA;

EGAS00001003685; WES accessions EGAS00001000679 and EGAS00001003686).

RESULTS

Clinical features of the cohort of patients

657 HCA developed in 504 patients with a median age of 38 years and comprising of 85% of women with 87% intake of oral contraceptive pills were included in the study (see flow chart, online supplementary figure 1).

Forty-four patients harboured liver adenomatosis (features of the series are described in table 1). 296 HCA (45%) were IHCA with an overexpression of SAA and CRP at the transcriptomic level and/or a mutation in the JAK/STAT signalling pathway (see material and methods). 76% of patients with IHCA showed an increase in serum CRP. Patients with IHCA were older (median age 40 years old vs 36 years old, p value=0.039, Mann-Whitney test), with a longer cumulative uses of oral contraception (median 19 years vs 11 years, p value<0.0001, Mann-Whitney test), a higher body mass index (median 25 kg/m² vs 22 kg/m², p value=0.003, Mann-Whitney test) and more frequent chronic alcohol intake (24% vs 9%, value=0.002, Fisher's exact test) compared with patients harbouring other subgroups of HCA.

Spectrum of mutations in known oncogenes in IHCA

Among the 296 IHCA, 74 were mixed tumours with 21 bex7,8 IHCA (3% of the whole series, defined by mutations of CTNNB1 in exon 7 or 8) and 53 bex3 IHCA/bIHCA (8% of the whole series) including 44 bex3 IHCA (defined by a mutation of CTNNB1 in exon 3, 7%) and 9 bIHCA (defined by an overexpression of Wnt/catenin pathway target genes without mutation of CTNNB1, 1%). Borderlines lesions between HCA and HCC or HCC developed on HCA were identified in 6% of all IHCA (n=18). Nine borderlines lesions between HCA and HCC or HCC developed on HCA were identified among 53 bex3 IHCA/bIHCA (17%) versus 9 among 243 IHCA without activation of β-catenin pathway (4%, p value Fisher's exact=0.0013) confirming that activation of β-catenin pathway is associated

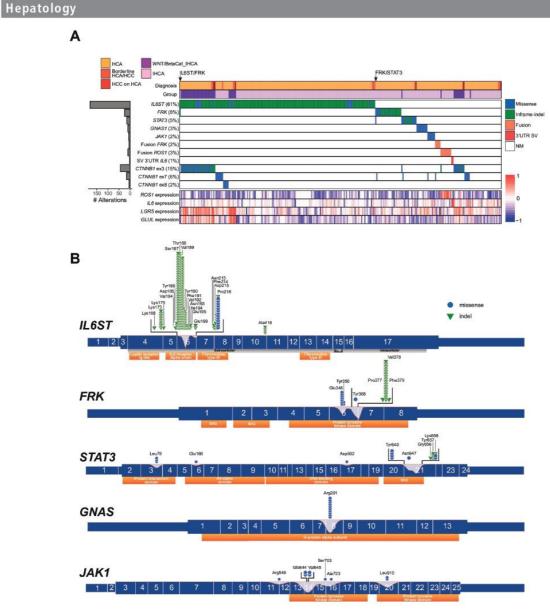


Figure 1 Distribution of mutations in inflammatory hepatocellular adenomas (IHCAs). (A) We represented a heatmap of the somatic mutations and chromosomal rearrangements in driver genes (IL6ST, FRK, STAT3, GNAS, JAK1, ROS1, IL6 in line) in 296 IHCA (in column) (top). We included the expression level in log2 of ROS1, IL6, GLUL, LGR5, assessed by quantitative RT-PCR (bottom). (B) Mutational spectrum of IL6ST, FRK, STAT3, GNAS and JAK1. Red curves represent the density of mutation among genes. Orange boxes are protein domains annotations from the pfam database. HCA, hepatocellular adenoma; IHCA, inflammatoryhepatocellular adenoma; HCC on HCA, hepatocellular carcinoma developed on hepatocellular adenoma; indel, inframe deletion.

with malignant transformation even in IHCA. In contrast, *HNF1A* inactivation (n=226) and sonic hedgehog activation (n=34) were almost exclusive from the inflammatory phenotype since only one mixed IHCA with bi-allelic inactivating mutations of *HNF1A* (#1355) was identified in our series.

Among the 296 IHCA, we identified an activating mutation of a gene belonging to the *JAK/STAT* pathway in 81% of the cases (figure 1A and B, online supplementary table 3):

Mutations in IL6ST, identified in 180 cases, were almost all located in exon 6 in the IL-6 receptor alpha-chain domain and were mostly small in-frame deletions and rarely point mutations. Nevertheless, the remaining four in-frame

- deletions clustered in exon 10 corresponding to the D4 domain of gp130 delineating this second hotspot of mutations in *IL6ST*.
- ► FRK mutations, identified in 25 cases, clustered in the protein tyrosine kinase domain (exon 6) and were mainly small in-frame deletions. Interestingly, three samples displayed two FRK mutations on the same allele in exon 6 including two samples with p.Glu346Gly/p.Tyr350Cys mutations and one sample with p.Glu346Gly/p.Tyr368Cys mutations.
- ➤ STAT3 mutations, identified in 15 cases, were either small in frame deletion or single nucleotide variation located in exons 3, 6, 17 and 21. Most of the mutations clustered in exons 3

Bayard Q, et al. Gut 2020;0:1-10. doi:10.1136/gutjnl-2019-319790

Hepatology

and 21 coding for the protein interaction and SH2 domains, respectively. Interestingly, one sample with a mutation in STAT3 exon 21 was also mutated in exon 17 (p.Lys658Tyr/p. Asp502Tyr) and another was mutated both in exons 21 and 3 (p.Tyr640Phe/p.Leu78Arg). Finally, one IHCA harboured a single mutation in exon 6 (p.Glu166Gln).

- All mutations in GNAS, identified in 10 cases, were missense identified at the Arginine 201, the known exon 8 hotspot activating the protein Gs-alpha subunit.
- ► JAK1 mutations were identified in seven cases (2% of IHCA) in exons 11, 14, 15, 16 and 20 all leading to amino acid substitution activating JAK1. Interestingly, two samples were double mutated in JAK1 exon 14 on the same allele at residues 644 and 645.

All oncogenic mutations identified in IHCA were mutually exclusive except for two cases: an IHCA harboured both STAT3 (p.Leu78Arg) and FRK (p.Glu346Gly) mutations, another tumour showed an IL6ST in-frame deletion (p.Tyr186_Tyr190del) together with a FRK mutation (p.Val378_Lys380delinsGlu) (figure 1A). As previously described, 11 the expression level of SAA2 and CRP was lower in GNAS activating mutated IHCA compared with IHCA with other genetic alterations (online supplementary figure 2)

Overall, 61 IHCA (21%) harboured no mutations in driver genes known to activate the JAK/STAT pathway.

Identification of recurrent ROS1 fusion genes in IHCA

In order to search for new oncogenes in IHCA, we performed whole exome sequencing (WES) in 19 IHCA without known mutations. Comparing tumours and matched non-tumour liver samples, a median number of 2 synonymous mutations and 14 non-synonymous mutations per tumour were identified (online supplementary table 4). None of these samples harboured recurrent genetic alterations or recurrent copy number variation and no genes belonging to the *JAK/STAT* pathway was altered (online supplementary tables 4,5).

In contrast, using RNA sequencing in 22 IHCA without a known driver gene mutation, recurrent ROS1 transcript alterations were identified in 10 cases (figure 2, online supplementary table 6); among these, 8 IHCA showed a chimeric transcript between the 3' part of ROS1 and the 5' part of three different partner genes which are highly expressed in normal hepatocytes. PLG-ROS1 fusions were identified in five cases as the result of a chromosome translocation t(6,10) (q22.1;q23.33). RBP4-ROS1 fusions were identified in two cases as the result from a chromosome inversion at chromosome 6, Inv6 (q22.1-q25.3). Finally, APOB-ROS1 fusion was identified in one case resulting from a chromosome translocation t(2,6) (q22.1;q24.1). Breakpoints in ROS1 and the partner genes were variable leading in each case to at least one in phase transcript . However, all fusions included at least the last 9 exons of ROS1 (exon 33-43 in one case, exon 34-43 in six cases and exon 35-43 in one case) fused in frame with the 5' of the various partner genes. One tumour with a ROS1 fusion was also mutated for CTNNB1 in exon 3 (figure 1A, online supplementary table 2).

Finally, in the last two cases, we identified a truncated mRNA of ROS1 with an overexpression of exons 36–43 (#4089T) or 37–43 (#1896T) and, in these cases, we did not identify any fusion partner in RNA sequencing data; however, RNA-seq quality of sample #1896T was poor, due to a degraded RNA. In three cases, we performed a FISH experiment that confirmed the ROS1 break in each tumour, including the two samples with only a truncated transcript identified (#4089T and #1896T)

(figure 2D). GSEA analyse of the transcriptome of HCA with ROS1 fusions confirmed an enrichment in JAK/STAT pathway (HALLMARK IL6 JAK STAT3 SIGNALING; online supplementary figure 3).

In all the cases, the tyrosine kinase domain of ROS1 (located in exons 36–42) was retained in the rearranged genes and the ROS1 transcript was highly overexpressed (figure 2B, median FPKM=20.4) compared with HCA without ROS1 fusion (median FPKM= 7.5×10^{-3} , p value= 8.6×10^{-5}) and compared with non-tumour liver (n=4, median FPKM= 5.1×10^{-2} , p value= 7.0×10^{-3}).

Identification of recurrent FRK fusion genes in IHCA

By analysing the 22 IHCA with RNAseq, five tumours with a chimeric transcript involving FRK were identified (figure 3A, online supplementary table 6), with one of them also mutated for CTNNB1 in exon 7 (online supplementary table 2). All of them harboured an enrichment in genes belonging to JAK/STAT signalling at the transcriptomic level using GSEA analysis (online supplementary figure 3). FRK fusions resulted from various translocations linking exons 1-25 of MIA3 (chromosome 1q41), or exons 1-20 of MIA2 (chromosome 14q21.1) or exons 1-25 of LMO7 (chromosome 13q22.2) or exons 1-19 of PLEKHA5 (chromosome 12p12.3) with exons 3-8 of FRK (chromosome 6q21.1). The last FRK fusion linked exons 1-20 of SEC16B (chromosome 1q25.2) to exon 1-8 of FRK resulting in both a chimeric transcript including all exons of FRK and a truncated transcript starting with an alternative TSS in the intron 2 (figure 3C). All the fusions were in phase at the nucleotide level. In all the chimeric transcript, the tyrosine kinase domain of FRK (exons 4-8) was retained whereas the auto-inhibitory SH2 and SH3 domains were absent in the predicted aberrant protein. The expression level of FRK was not increased in IHCA with FRK fusions compared with other HCA (figure 3B).

Recurrent IL6 gene rearrangements in IHCA

Finally, we identified two IHCA with abnormal 3' untranslated region (UTR) of *IL6* on RNA sequencing (figure 4A) and characterised by activation of JAK/STAT pathway (GSEA analysis, online supplementary figure 3). One case was previously published (#2615T with inflammatory SAA amyloidosis); the tumour showed a deletion of 3'UTR of *IL6* due to an inversion of 18.7 megabases validated by whole genome sequencing. We identified a second IHCA, #1215T, with a truncation of the 3'UTR regulatory region of *IL6* due to a eight megabases deletion identified using RNA sequencing. In contrast to the first case, #1215T was not associated with SAA amyloidosis symptoms. In these two IHCA, *IL6* was strongly overexpressed (figure 4B, median FPKM=56.4) compared with others IHCA (median FPKM=2.01×10⁻¹, p value=2.6×10⁻²).

Finally, six IHCAs analysed by WES and/or RNA sequencing remained without identifiable driver genetic alterations. Interestingly, on pathological reviewing, 5 among these 6 IHCA (83%) showed haemorrhage on histology (vs 58% in the whole series of IHCA) with a minimal expression of CRP and SAA at the transcriptomic level.

DISCUSSION

IHCA serves as a unique model to study the inflammatory pathways in mature hepatocytes and to identify new drivers of oncogene-induced inflammation in benign liver tumourigenesis. Based on the analysis of a large number of IHCA (see flow chart,

Hepatology n22.1:6n25.3 anslocation(6;16 (q22.1;q23.33) RBP4 RQS1 APOB #375T #744T C 10kb Coverage 200 #533T ROS1 FISH: Coverage ROS1 FISH: #2729T N.D. Coverage #4110T ROS1 FISH: mon Coverage #375T ROS1 FISH: N.D. 1-13 14 - 1 ROS1 FISH: N.D. Coverage ROS1 FISH: N.D. Coverage #1343T ROS1 FISH: N.D. FRA10AC1 Coverage #477T ROS1 FISH: N.D. Coverage ROS1 FISH: #40897 Dissociated signa 27-30 31 32 - 34 35 - 38 Coverage ROS1 FISH: 27-30 31 32 - 34 35 - 38 7-11 12-15 16 17 18-21 22-25 26 39.41 D #4089T Control

Figure 2 Recurrent *ROS1* fusions in inflammatory hepatocellular adenomas (IHCAs). (A) Representation of the *ROS1* fusion in 8 IHCAs whereas 2 IHCAs with *ROS1* truncated transcript were not represented. IHCA, inflammatory hepatocellular adenoma. (B) Expression level of *ROS1* in FPKM (log 10) in 22 hepatocellular adenoma analysed by RNA sequencing (10 IHCA with *ROS1* fusion/truncated transcripts and 12 IHCA with other genetic alterations). The p value compare the level of expression of *ROS1* between IHCA with *ROS1* alterations versus other IHCA using the Mann-Whitney non-parametric test. (C) Sashimi plots showing RNA-seq alignments for the wild-type *ROS1* in a normal liver (#933N) (top) and 10 cases of IHCA with *ROS1* fusion (bottom). Splice junction reads are represented as arcs connecting a pair of exons. Arc width is proportional to the number of reads aligning to the junction. Grey exon number shows exons not involved in chimeric transcripts and bold exon number represents the *ROS1* exons involved in the in-frame junction of the chimeric transcript. Black arrow indicates stop of transcription following abnormal junction. (D) FISH using *ROS1* dual-colour break-apart probe in 1 IHCA with known *ROS1* fusion and one control. White arrows indicate wild-type *ROS1* with combined red and green signals. Red arrows indicate dissociated signals validating *ROS1* rearrangement.

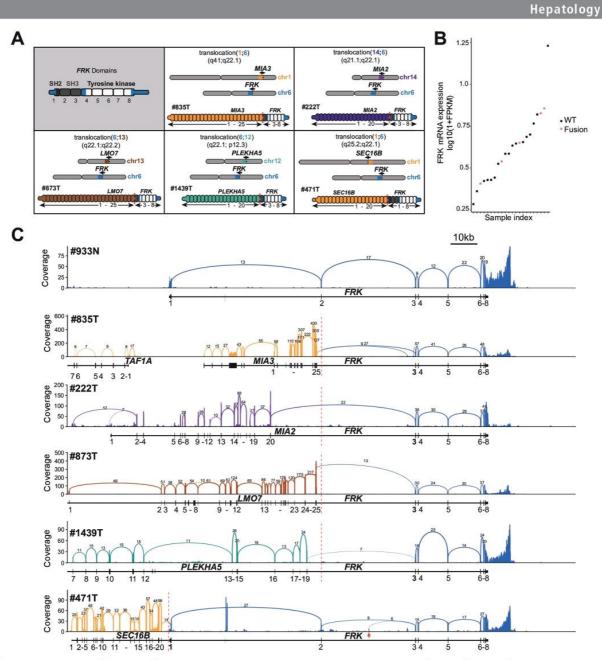


Figure 3 Recurrent FRK fusions in inflammatory hepatocellular adenomas (IHCAs). (A) Representation of the FRK fusions in five IHCAs. (B) Expression level of FRK in FPKM (log 10) in 22 HCA analysed by RNA sequencing. (C) Sashimi plots showing RNA-seq alignments for the wild-type FRK in a normal liver (#933N) (top) and five cases of IHCA with FRK fusion (bottom). Splice junction reads are represented as arcs connecting a pair of exons. Arc width is proportional to the number of reads aligning to the junction. Bold exon number represents the ROS1 exons involved in the inframe junction of the chimeric transcript. Red arrow indicates alternative transcription start site in the FRK-SEC16B fusion.

online supplementary figure 1), we identified novel recurrent somatic chromosomal rearrangements of ROS1, FRK and IL6.

In our study, IHCA is the most frequent molecular subgroup with 45% of HCA harbouring an inflammatory phenotype. Overall, we now described in IHCA a total of seven genes that are able to activate the JAK/STAT pathway in hepatocytes when mutated and therefore are associated with benign liver tumourigenesis. ²² Some of these oncogenes belong directly to the JAK/STAT pathway such as *IL6ST* (61% of mutations), *STAT3* (5%

of mutations), JAK1 (2% of mutations) or IL6 (1% of alterations). ⁶ ¹⁰ However, the remaining three genes, FRK (8% of mutations, 2% of fusions, mutually exclusive), GNAS (3% of mutations) and ROS1 (3% of fusions), belong to other signalling pathways but are also known to activate the IL-6/JAK/STAT pathway in cellulo (figures 1A and 5). ⁶ ¹¹ ²³ Though in most of the IHCA, gene mutations were exclusive, in two cases, we observed a concomitant mutation of STAT3 L78R with either a classical FRK or STAT3 mutations. We had previously shown,

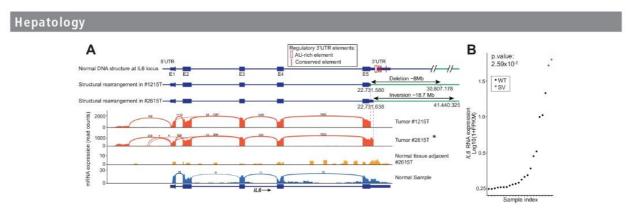


Figure 4 //L6 rearrangements in inflammatory hepatocellular adenomas (IHCAs). (A) Sashimi plots showing RNA-seq alignments for the wild-type //L6 in a normal liver and a corresponding non-tumour liver (bottom) and two cases of IHCA with truncation of 3'UTR (top). Splice junction reads are represented as arcs connecting a pair of exons. Arc width is proportional to the number of reads aligning to the junction. *already published¹². (B) Expression level of //L6 in FPKM (log 10) in 22 HCA analysed by RNA sequencing. The p value compared the level of expression of //L6 between IHCA with //L6 alterations versus other IHCA using the Mann-Whitney non-parametric test. Coordinates in GRCh38. FPKM, fragments per kilobase of exon model per million reads mapped; IHCA, inflammatory hepatocellular adenoma; WT, wild type; SV, structural variants.

in cellulo, that *STAT3* L78R mutations alone can only weakly activate the JAK/STAT pathway.²⁴ Another study suggested that the L78R mutation, located in the N-terminal domain, could prolong the activation of *STAT3*.²⁵ We could hypothesise that

STAT3 L78R mutation could cooperate with additional mutation in the JAK/STAT pathway to induce an inflammatory response in mature hepatocytes.

Driver genetic alterations in inflammatory hepatocellular adenomas

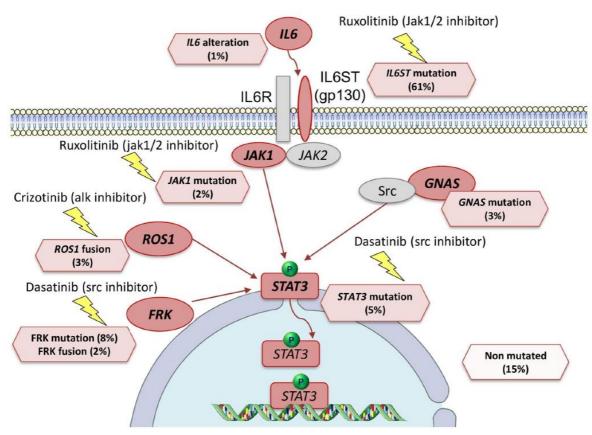


Figure 5 Mutations in oncogenes in inflammatory hepatocellular adenomas (IHCAs). Frequencies of somatic genetic alterations in driver genes observed in IHCA are indicated. Targeted therapies potentially active against each genetic alteration are indicated by a yellow flag. IHCA, inflammatory hepatocellular adenoma.

Hepatology

In this work, we identified recurrent ROS1 rearrangements in 10 IHCA without other mutations in driver genes. ROS1 is a tyrosine kinase receptor composed of a N-terminal extracellular domain, a transmembrane domain and a C-terminal intracellular tyrosine kinase domain, known to activate several downstream pathways such as the MAP kinase and AKT/mTOR pathways. 26 27 Recurrent ROS1 rearrangements are identified in 2% of nonsmall cell lung carcinoma and in other cancer types including cholangiocarcinoma, lymphoma, glioblastoma, colorectal and gastric carcinoma.²⁶ In anaplastic lymphoma and in inflammatory myofibroblastic tumours, ROS1 fusions induce a strong activation of the JAK/STAT pathway.^{23 28} To our knowledge IHCA is the second type of benign tumour showing ROS1 fusion after Spitz nevi.²⁹ This observation reinforces the hypothesis that ROS1 fusion is an early event during the mechanism of carcinogenesis in solid tumours but it is not sufficient alone to promote a full malignant transformation of hepatocyte or melanocyte.

In IHCA, exons 33-35 of ROS1 are fused in-phase with different partners including PLG, APOB and RBP4. All these partners are highly expressed in adult liver whereas ROS1 is almost not expressed in normal hepatocytes. Resulting from the gene fusion, ROS1 is under the control of the promoter of the different partner genes and consequently overexpressed specifically in all IHCA harbouring the ROS1 rearrangement. Interestingly, all ROS1 fusions retained the intracellular tyrosine kinase domain (exon 36-42) and lost the transmembrane domain. These findings are similar to all the ROS1 fusion proteins already identified in lung cancer, lymphoma or cholangiocarcinoma that all retained the tyrosine kinase domain, essential for its oncogenic activity. 23 30 31 In cellulo model we have also demonstrated that ROS1 fusions were able to activate STAT3 in haematological cancer.²³ Moreover, most of ROS1 fusions described in cancer lack their transmembrane domain leading to the relocalsation of the fusion proteins in the cytoplasm that could interact with different proteins and modified downstream signalling pathway. $^{27\ 32}$ In two of the IHCA cases, though we identified a truncated overexpressed ROS1 mRNA, its partner genes could not be identified owing to the poor quality of RNA. However, ROS1 breaks were confirmed by FISH in both the cases.

We previously identified in IHCA recurrent mutations of FRK able to activate JAK/STAT pathway in cellulo.6 In this study, recurrent FRK fusions were identified in five cases of IHCA, all showed an in-frame fusion gene. The fusion transcript was predicted to code for a chimeric protein retaining the tyrosine kinase domain, encoded by exons 4-8, but lacking the SH2 and SH3 auto-inhibitory domains, encoded by exons 1-3.33 Interestingly, FRK fusions have been described in acute myeloid leukaemia with ETV6-FRK and in anaplastic large cell lymphoma with CAPRIN-FRK, all with a similar junctions at exon 3 of FRK34.35 In cellulo model showed that ETV6-FRK fusion protein has a constitutive autophosphorylation on its tyrosine residues with an elevated kinase activity.35 All these data suggested that in hepatocyte like in haematological diseases, the deletion of the SH2/SH3 domain together with an intact tyrosine kinase domain is critical for the oncogenic mechanism of FRK fusions.

We also described two cases of somatic alterations of *IL6* with truncation of the 3'UTR due to large chromosome inversion or deletion at the genomic level. These two IHCA harboured a strong overexpression of *IL6* suggesting that the lacks of the 3'UTR regulatory elements induced an overexpression of the transcript. Interestingly, the IL-6 mRNA has a short half-life of around 30 min that is regulated by the 3'UTR. ³⁶ Consequently, the truncation of the 3'UTR in these two IHCA could lead to an increased stability and accumulation of the transcript. We

previously described one of the cases that was associated with occurrence of inflammatory amyloidosis, ¹² but the second case did not.

In our series, we identified *IL6* alterations, *ROS1* and *FRK* fusions in 3%, 2% and 1% of all HCA, respectively. In all these HCA, no other driver mutations were identified except one *CTNNB1* mutation exon 3 in one case and one *CTNNB1* mutation exon 7 in another case. As *ROS1* and *IL6* rearrangements induced an mRNA overexpression, we did not identify an additional candidate IHCA for these genetic alterations after screening of the whole series of IHCA by quantitative RT-PCR. In contrast, the exact frequency of *FRK* rearrangement could be under-estimated.

In six IHCAs, no functional genetic alterations were identified using next generation sequencing. However, in 5 of these 6 cases, we observed haemorrhage at histological level which is known to induce inflammation and thus a slight increase in SAA and CRP expression in these adenomas without a genomic driven activation of the *IL6/JAK/STAT3* pathway.

Finally, IHCA harboured several driver genes that could be used as a target for drug therapy in the future in clinical practice. ROS1 fusion could be targeted by crizotinib, a small molecule currently approved by Food and Drug Administration (FDA) for the treatment of lung cancer with ROS1 fusion. The Moreover, we previously showed that dasatinib, a src inhibitor, shutdown JAK/STAT activation due to FRK mutations in cellulo. We can predict that the same results could be obtained in IHCA with FRK fusions. These data suggested that targeted therapies adapted to genetic alterations (ruxolitinib in IL6ST mutation, dasatinib for FRK mutations/fusions and crizotinib for ROS1 fusion) could be tested in selected patients with multiple or unresectable IHCA (figure 5). We can predict the selected patients with multiple or unresectable IHCA (figure 5).

In conclusion, we described recurrent chromosomal alterations of ROS1, FRK and IL6 as new mechanisms of JAK/STAT pathway activation driving benign tumourigenesis in IHCAs that could be tested as therapeutic targets in future clinical trials.

Short summary

We identified recurrent chromosomal alterations involving ROS1, FRK or IL6 in IHCAs. ROS1 activation is a novel mechanism of JAK/STAT pathway activation in human benign liver tumours.

Author affiliations

¹Centre de Recherche des Cordeliers, Sorbonne Université, Inserm, Université de Paris, Université Paris 13, Functional Genomics of Solid Tumors laboratory, F-75006 Paris, France

²Service de Pathologie, Hôpital Pellegrin, CHU de Bordeaux, F 33076 Bordeaux, France

³Université Bordeaux, UMR1053 Bordeaux Research in Translational Oncology, BaRITOn, F-33076 Bordeaux, France

⁴Service d'anatomopathologie, Hôpital Beaujon, Assistance-Publique Hôpitaux de Paris, Clichy, France

INSERM U1149, Clichy, France

⁶Service d'anatomopathologie, CHU, Grenoble, France

Service d'anatomopathologie, CHU, Tours, France

⁸Service d'anatomopathologie, CHU Bicètre, Assistance-Publique Hôpitaux de Paris, Bicètre, France, Bicètre, France

 Service d'anatomopathologie, Hôpital Henri Mondor; Université Paris Est, Inserm U955, Team 18, Institut Mondor de Recherche Biomédicale, France, Créteil, France
 Service d'hépatologie, Hôpital Jean Verdier, Hôpitaux Universitaires Paris-Seine-Saint-Denis, Assistance-Publique Hôpitaux de Paris, Bondy, France

¹¹Unité de Formation et de Recherche Santé Médecine et Biologie Humaine, Université Paris 13, Communauté d'Universités et Etablissements Sorbonne Paris Cité, Paris, France, Paris, France

¹²Hôpital Européen Georges Pompidou, F-75015, Assistance Publique-Hôpitaux de Paris, Paris, France

Hepatology

Twitter Jean-Charles Nault @naultjc and Jessica Zucman-Rossi @Zucmanrossi

Acknowledgements This study was previously presented as an abstract at the American Association for the Study of Liver Diseases liver meeting 2019

Contributors Author contributions to manuscript—study design: J-CN, JZ-R; generation of experimental data: QB, GC, SC, J-CN, BB, CB, JZ-R; analysis and interpretation of data: QB, GC, SC, J-CN, SI, EL, SR, JZ-R; collection of samples and related histological and clinical data: PBS, CB, VP, NS, AdM, CG, J-CN; drafting of the manuscript; OB, SC, EL, J-CN, JZ-R; revision of the manuscript and approval of the final version of the manuscript: all the authors. J-CN, JZ-R: these authors shared the

Funding This work was supported by Institut National du Cancer (INCa) with the International Cancer Genome Consortium (ICGC LICA-FR project), INSERM with the 'Cancer et Environnement' (plan Cancer) and MUTHEC projects (INCa). The group is supported by the Ligue Nationale contre le Cancer (Equipe Labellisée), Labex Oncolmmunology (investissement d'avenir), grant IREB, Coup d'Elan de la Fondation Bettencourt-Schueller, the SIRIC CARPEM, Raymond Rosen Award from the Fondation pour le Recherche Médicale, Prix René and Andrée Duquesne Comité de Paris Ligue Contre le Cancer and Fondation Mérieux.

Competing interests None declared

Patient consent for publication Not required.

Ethics approval Paris Saint-Louis Institutional Review Board committee approved this study (Paris Saint-Louis, 2004; INSERM IRB 2010; the French Liver Biobanks network—AFAQ NF S96-900 and Hepatobio bank)

Provenance and peer review Not commissioned; externally peer reviewed.

Data availability statement Data are available in a public, open access

Sandrine Imbeaud http://orcid.org/0000-0001-8439-6732 Jean-Charles Nault http://orcid.org/0000-0002-4875-9353

- European Association for the Study of the Liver (EASL). EASL clinical practice guidelines on the management of benign liver tumours. J Hepatol 2016;65:386-98.
- Nault J-C, Paradis V, Cherqui D, et al. Molecular classification of hepatocellular adenoma in clinical practice. J Hepatol 2017;67:1074-83.
- 3 Zucman-Rossi J, Jeannot E, Nhieu JTV, et al. Genotype-Phenotype correlation in hepatocellular adenoma: new classification and relationship with HCC. Hepatology 2006:43:515-24
- 4 Bluteau O, Jeannot E, Bioulac-Sage P, et al. Bi-Allelic inactivation of TCF1 in hepatic adenomas. Nat Genet 2002;32:312-5
- Pelletier L, Rebouissou S, Paris A, et al. Loss of hepatocyte nuclear factor 1alpha function in human hepatocellular adenomas leads to aberrant activation of signaling pathways involved in tumorigenesis. Hepatology 2010;51:557-66.
- 6 Pilati C, Letouzé E, Nault J-C, et al. Genomic profiling of hepatocellular adenomas reveals recurrent FRK-activating mutations and the mechanisms of malignant transformation, Cancer Cell 2014;25:428-41.
- 7 Nault J-C, Couchy G, Balabaud C, et al. Molecular Classification of Hepatocellular Adenoma Associates With Risk Factors, Bleeding, and Malignant Transformation. Gastroenterology 2017;152:880-94.
- 8 Bioulac-Sage P, Rebouissou S, Thomas C, et al. Hepatocellular adenoma subtype classification using molecular markers and immunohistochemistry. Hepatology 2007:46:740-8
- 9 Paradis V, Champault A, Ronot M, et al. Telangiectatic adenoma: an entity associated with increased body mass index and inflammation. Hepatology 2007;46:140–6.
- 10 Rebouissou S, Amessou M, Couchy G, et al. Frequent in-frame somatic deletions activate gp130 in inflammatory hepatocellular tumours. Nature 2009;457:200-4
- 11 Nault JC, Fabre M, Couchy G, et al. GNAS-activating mutations define a rare subgroup of inflammatory liver tumors characterized by STAT3 activation. J Hepatol 2012:56:184-91.

- 12 Calderaro J. Letouzé E. Bayard O. et al. Systemic AA amyloidosis caused by inflammatory hepatocellular adenoma. N Engl J Med 2018;379:1178-80. 20.
- Rebouissou S, Franconi A, Calderaro J, et al. Genotype-Phenotype correlation of CTNNB1 mutations reveals different B-catenin activity associated with liver tumor progression. Hepatology 2016;64:2047-2061.
- 14 Nault JC, Mallet M, Pilati C, et al. High frequency of telomerase reverse-transcriptase promoter somatic mutations in hepatocellular carcinoma and preneoplastic lesions. Nat Commun 2013;4:2218.
- 15 DePristo MA, Banks E, Poplin R, et al. A framework for variation discovery and genotyping using next-generation DNA sequencing data. Nat Genet 2011;43:491–8.
- Van der Auwera GA, Carneiro MO, Hartl C, et al. From FastQ data to high confidence variant calls: the genome analysis toolkit best practices pipeline. Curr Protoc Bioinformatics 2013;43.
- Kim D, Pertea G, Trapnell C, et al. TopHat2: accurate alignment of transcriptomes in
- the presence of insertions, deletions and gene fusions. *Genome Biol* 2013;14:R36. Anders S, Pyl PT, Huber W. HTSeq--a Python framework to work with high-throughput sequencing data. *Bioinformatics* 2015;31:166–9.
- Love MI, Huber W, Anders S. Moderated estimation of fold change and dispersion for RNA-Seg data with DESeg2. Genome Biol 2014;15:550.
- 20 Bayard Q, Meunier L, Peneau C, et al. Cyclin A2/E1 activation defines a hepatocellular carcinoma subclass with a rearrangement signature of replication stress. Nat Commun
- Shugay M, Ortiz de Mendíbil I, Vizmanos JL, et al. Oncofuse: a computational framework for the prediction of the oncogenic potential of gene fusions. Bioinformatics 2013;29:2539-46
- 22 Bromberg JF, Wrzeszczynska MH, Devgan G, et al. Stat3 as an oncogene. Cell 1999:98:295-303.
- Crescenzo R, Abate F, Lasorsa E, et al. Convergent mutations and kinase fusions lead to oncogenic STAT3 activation in anaplastic large cell lymphoma. Cancer Cell 2015:27:516-32
- Pilati C, Amessou M, Bihl MP, et al. Somatic mutations activating STAT3 in human inflammatory hepatocellular adenomas. J Exp Med 2011;208:1359–66.
- Domoszlai T, Martincuks A, Fahrenkamp D, et al. Consequences of the diseaserelated L78R mutation for dimerization and activity of STAT3. J Cell Sci 2014;127:1899-910.
- Davies KD, Doebele RC. Molecular pathways: ROS1 fusion proteins in cancer. Clin Cancer Res 2013;19:4040-5
- Uguen A, De Braekeleer M. Ros1 fusions in cancer: a review. Future Oncol 2016;12:1911-28.
- Lovly CM, Gupta A, Lipson D, et al. Inflammatory myofibroblastic tumors harbor multiple potentially actionable kinase fusions. Cancer Discov 2014;4:889-95.
- Wiesner T, He J, Yelensky R, et al. Kinase fusions are frequent in spitz tumours and spitzoid melanomas. Nat Commun 2014;5:3116.
- Takeuchi K, Soda M, Togashi Y, et al. Ret, ROS1 and ALK fusions in lung cancer. Nat Med 2012:18:378-81.
- Gu T-L, Deng X, Huang F, et al. Survey of tyrosine kinase signaling reveals ROS kinase fusions in human cholangiocarcinoma. PLoS One 2011;6:e15640.
- 32 Pal P, Khan Z. ROS1 [corrected]. J Clin Pathol 2017;70:1001-9.
- Goel RK, Lukong KE. Understanding the cellular roles of fyn-related kinase (FRK): implications in cancer biology. Cancer Metastasis Rev 2016;35:179-99.
- Hu G, Dasari S, Asmann YW, et al. Targetable fusions of the FRK tyrosine kinase in ALK-negative anaplastic large cell lymphoma. Leukemia 2018;32:565-9.
- Hosoya N, Qiao Y, Hangaishi A, et al. Identification of a SRC-like tyrosine kinase gene, FRK, fused with ETV6 in a patient with acute myelogenous leukemia carrying a t(6;12) (q21;p13) translocation. Genes Chromosomes Cancer 2005;42:269-79.
- 36 Paschoud S, Dogar AM, Kuntz C, et al. Destabilization of interleukin-6 mRNA requires a putative RNA stem-loop structure, an AU-rich element, and the RNA-binding protein AUF1. Mol Cell Biol 2006;26:8228-41.
- Shaw AT, Kim D-W, Nakagawa K, et al. Crizotinib versus chemotherapy in advanced ALK-positive lung cancer. N Engl J Med 2013;368:2385–94.
- 38 Poussin K, Pilati C, Couchy G, et al. Biochemical and functional analyses of gp130 mutants unveil JAK1 as a novel therapeutic target in human inflammatory hepatocellular adenoma. Oncoimmunology 2013;2:e27090.

2. Structural rearrangement signatures reveal a new molecular entity of HCC

The second objective of my PhD was to explore the causes and consequences of structural variations in hepatocellular carcinomas. As for HCA, I exploited RNAseq data but I also implemented an innovative approach to explore SV signatures from WGS data. This approach allowed me to extract subgroups of tumors sharing similar patterns of structural variations, induced by a shared biological defect.

During my first year of PhD, I participated to the development of Palimpsest (https://github.com/FunGeST/Palimpsest), an R package dedicated to the analysis of mutational signatures from NGS data. **Article 3** presents Palimpsest's functionalities, including *de novo* or supervised analysis of mutation and SV signatures, but also clonality reconstruction to unravel the mutational history of each tumor. I contributed to this work by implementing the SV signature analysis workflow.

Article 4 presents the application of Palimpsest's rearrangement signature framework to a large cohort of HCC samples. In this work, I identified six rearrangement signatures, characterized by preferential types and sizes of SVs, operative with different intensities in each tumor. In particular, rearrangement signature 1 (RS1), characterized by focal duplications (10s to 100s of kb) and complex rearrangements called Template Insertion Cycles (T.I.C.), revealed a homogenous HCC subgroup with a widespread duplicator phenotype. All tumors of this subgroup (named CCN-HCC) displayed an activation of *CCNA2* or *CCNE1* gene by various mechanisms. *CCNA2* activating events included new gene fusions and insertional mutagenesis by HBV or AAV2 virus, all leading to the production of a truncated cyclin A2 protein lacking regulatory domains while keeping functional domains. *CCNE1* activation resulted from insertional mutagenesis by HBV and AAV2, but also SVs leading to enhancer hijacking or gene amplifications.

Cyclins E1 and A2 are involved in S phase entry and progression, and cyclin E1 activation is known to induce replicative stress and genomic instability in various models. Consistently, CCN-HCC displayed an overexpression of ATR pathway implicated in the response to replication stress. These data, and the fact that duplications and TIC can be induced when collapsed replication forks are processed by the break-induced replication

(BIR) mechanism, suggest that RS1 is a signature of replication stress. Integrative analysis of HCC genomes with epigenetic data from Encode and ROADMAP consortia revealed an enrichment of RS1 breakpoints in early replicated, highly expressed active chromatin domains. Besides, RS1 events frequently associate active chromatin with quiescent regions, which may induce secondary oncogenic events like *TERT* promoter activation by enhancer hijacking, recurrent in CCN-HCC.

Overall, SV signature analysis allowed us to identify a new HCC entity (CCN-HCC), with homogenous molecular and clinical features. These tumors usually develop in non-cirrhotic liver tissue, in absence of classical risk factors. They have a very poor prognosis but may benefit from targeted treatment against replication stress response.

Article 3: Palimpsest: an R package for studying mutational and structural variant signatures along clonal evolution in cancer

Bioinformatics, 34(19), 2018, 3380–3381 doi: 10.1093/bioinformatics/bty388 Advance Access Publication Date: 16 May 2018 Applications Note



Genome analysis

Palimpsest: an R package for studying mutational and structural variant signatures along clonal evolution in cancer

Jayendra Shinde^{1,*}, Quentin Bayard¹, Sandrine Imbeaud¹, Théo Z. Hirsch¹, Feng Liu², Victor Renault², Jessica Zucman-Rossi^{1,3} and Eric Letouzé^{1,*}

¹INSERM, UMR-1162, Génomique Fonctionnelle des Tumeurs Solides, Equipe Labellisée Ligue Contre le Cancer, Institut Universitaire d'Hématologie; Faculté de Médecine, Université Paris Descartes, Labex Immuno-Oncology, Sorbonne Paris Cité; Unité de Formation et de Recherche Santé, Médecine, Biologie Humaine, Université Paris 13, Sorbonne Paris Cité, Bobigny, France; Université Paris Diderot, Paris, France, ²Laboratory for Bioinformatics, Fondation Jean Dausset – CEPH, Paris F-75010, France and ³Assistance Publique-Hôpitaux de Paris, Hopital Europeen Georges Pompidou, Paris F-75015, France

*To whom correspondence should be addressed.

Associate Editor: Russell Schwartz

Received on March 26, 2018; revised on May 2, 2018; editorial decision on May 3, 2018; accepted on May 12, 2018

Abstract

Summary: Cancer genomes are altered by various mutational processes and, like palimpsests, bear the signatures of these different processes. The *Palimpsest* R package provides a complete workflow for the characterization and visualization of mutational signatures and their evolution along tumor development. The package covers a wide range of functions for extracting both base substitution and structural variant signatures, inferring the clonality of each alteration and analyzing the evolution of mutational processes between early clonal and late subclonal events. *Palimpsest* also estimates the probability of each mutation being due to each process to predict the mechanisms at the origin of driver events. *Palimpsest* is an easy-to-use toolset for reconstructing the natural history of a tumor using whole exome or whole genome sequencing data.

Availability and implementation: *Palimpsest* is freely available at www.github.com/FunGEST/ Palimpsest.

Contact: jayendra.shinde91@gmail.com and eric.letouze@inserm.fr

Supplementary information: Supplementary data are available at Bioinformatics online.

1 Introduction

Mutational signature analysis is a powerful approach to understand the origin of somatic mutations in cancer (Alexandrov *et al.*, 2013). This approach can be extended to any kind of genomic alteration including structural variants (Helleday *et al.*, 2014). Mutational processes may evolve over time, giving different mutational signatures in early clonal and late subclonal mutations (Nik-Zainal *et al.*, 2012; Rubanova *et al.*, 2018). Next-generation sequencing data also allow to reconstruct the timing of copy-number alterations (CNAs)

by distinguishing clonal/subclonal events and using the proportion of duplicated mutations to time chromosome duplications (Greenman et al., 2012). Finally, different mutational processes have different propensities to target specific loci depending on the local chromatin state (Polak et al., 2015; Sabarinathan et al., 2016) and sequence context (Letouzé et al., 2017). Understanding how mutational processes evolve during tumorigenesis and alter specific driver genes is critical to better understand the natural history of cancers and eventually predict and influence their clinical behavior.

© The Author(s) 2018. Published by Oxford University Press. All rights reserved. For permissions, please e-mail: journals.permissions@oup.com

A Input files: Somatic mutations (VCF) alterations Structural variants

Copy-number alterations Variants

Clonality analysis

Clonality analysis

Clonality analysis

Assigning the causal process of each individual alteration

Palimpsest 3381

Fig. 1. (A) Workflow of a typical analysis with *Palimpsest*. (B) Oncogenic timeline of a tumor representing the number of clonal/subclonal mutations, the contribution of mutational processes to each step and the timing of driver mutations (colored according to their most likely causal mutational process) and CNAs

To the best of our knowledge, no comprehensive workflow integrates mutational signature and clonality analyses to reconstruct the natural history of a tumor. In addition, no automated tools for extracting structural variant signatures, timing chromosome duplications and estimating the process at the origin of each mutation are currently available. The *Palimpsest* R package provides an extensive toolset to explore and visualize the diverse processes generating somatic alterations in a tumor, their evolution along tumorigenesis and their interaction with driver genes.

2 Features of palimpsest

B

Palimpsest takes as input somatic mutations and structural variants (optional), copy-number data and a minimal sample annotation file indicating gender and tumor purity. Figure 1A and Supplementary Figure S1 illustrate a typical Palimpsest analysis, as described step by step below.

Mutational signature analysis. Palimpsest allows both de novo extraction of novel mutational signatures or quantification of previously described signatures using non-negative matrix factorization (NMF), as implemented in the NMF R package (Gaujoux and Seoighe, 2010). Utilities are provided to visualize signatures, transcriptional strand biases and inter-mutation distance, and to compare signatures using cosine similarity.

Structural variant signature analysis. Palimpsest implements an adaptation of the mutational signature analysis framework for structural variants (SVs). SVs are first classified into 38 categories according to the type (deletion, tandem duplication, inversion and interchromosomal translocation) and size of rearrangements (Nik-Zainal et al., 2016). NMF then allows extracting new or known structural variant signatures and their contribution to each tumor genome.

Predicting the process at the origin of each individual mutation. Once the mutation catalogue of a tumor has been deconvoluted as the addition of several mutational processes, *Palimpsest* estimates the probability of each individual mutation being due to each process using simple Bayesian statistics (Letouzé *et al.*, 2017). This key feature, available for both point mutations and structural variants, allows predicting the processes most likely at the origin of driver events in each tumor.

Clonality analysis and evolution of mutational signatures. Palimpsest integrates variant allele fraction, tumor purity and local copy number to estimate the proportion of tumor cells harboring each mutation and classify them as clonal or subclonal. Then, the package extracts and compares mutational signatures operative in clonal and subclonal mutations to explore the evolution of mutational processes along tumorigenesis.

Timing CNAs. Several tools have been described to differentiate clonal from subclonal CNAs, which can be directly specified in the CNA input file. In addition, *Palimpsest* will estimate the molecular timing of duplications using the proportion of duplicated/non-duplicated somatic mutations.

Oncogenic timelines. Finally, *Palimpsest* integrates the results of clonality and mutational signature analyses to generate a comprehensive representation of the natural history of the tumor (Fig. 1B).

3 Conclusions

Unraveling what mutational processes generate driver mutations and fuel the initiation and progression of tumor clones is crucial to better understand the natural history of cancers and optimize personalized patient care. *Palimpsest* integrates a broad range of functions within a single convenient workflow to provide a complete picture of tumorigenesis. The minimum basic input data make the package easy-to-use in any cancer genomic study downstream classical variant calling and copy number analyses.

Acknowledgements

We thank the CIT program from the French Ligue Nationale Contre le Cancer for providing useful R codes (cit.x functions).

Funding

This work was supported by INSERM ("Cancer et environnement" & HTE program), cancéropôle Ile-de-France (exhauTrans project), Région Ile-de-France, BPI France (ICE project), CARPEM and ICGC. The group is supported by the Ligue Nationale contre le Cancer (Equipe Labellisée), Labex OncoImmunology Investissement d'Avenir and Fondation Mérieux.

Conflict of Interest: none declared.

References

Alexandrov, L.B. et al. (2013) Signatures of mutational processes in human cancer. Nature, 500, 415–421.

Gaujoux,R. and Seoighe,C. (2010) A flexible R package for nonnegative matrix factorization. BMC Bioinformatics, 11, 367.

Greenman, C.D. et al. (2012) Estimation of rearrangement phylogeny for cancer genomes. Genome Res., 22, 346–361.

Helleday, T. et al. (2014) Mechanisms underlying mutational signatures in human cancers. Nat. Rev. Genet., 15, 585–598.

Letouzé, E. et al. (2017) Mutational signatures reveal the dynamic interplay of risk factors and cellular processes during liver tumorigenesis. Nat. Commun., 8, 1315.

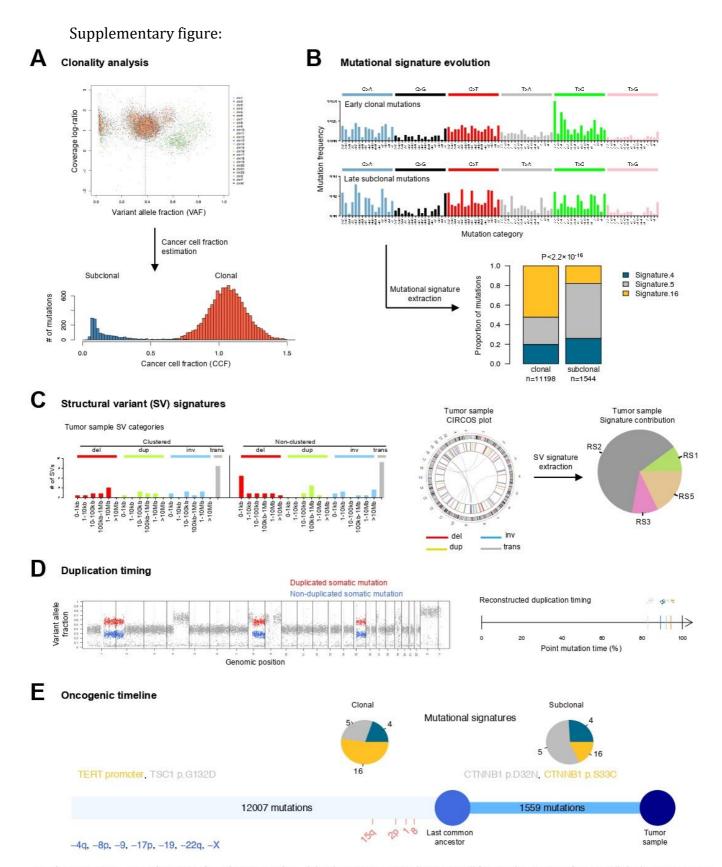
Nik-Zainal, S. et al. (2012) The life history of 21 breast cancers. Cell, 149, 994–1007.

Nik-Zainal, S. et al. (2016) Landscape of somatic mutations in 560 breast cancer whole-genome sequences. Nature, 534, 47–54.

Polak, P. et al. (2015) Cell-of-origin chromatin organization shapes the mutational landscape of cancer. Nature, 518, 360–364.

Rubanova, Y. et al. (2018) TrackSig: reconstructing evolutionary trajectories of mutation signature exposure. bioRxiv, 260471.

Sabarinathan, R. et al. (2016) Nucleotide excision repair is impaired by binding of transcription factors to DNA. Nature, 532, 264–267.



Supplementary Fig. 1. Typical outputs of a *Palimpsest* analysis. (A) *Palimpsest* estimates the cancer cell fraction (proportion of tumor cells harboring a somatic variant) and classifies each variant as clonal or subclonal. (B) Mutational signatures analyzed separately in early clonal and late subclonal mutations highlight the evolution of mutational processes along tumorigenesis. (C) *Palimpsest* can also extract structural variant (SV) signatures considering the type and size of SVs identified in the tumor. Del: deletion; dup: duplication; inv: inversion; trans: translocation. (D) The ratio of duplicated/non-duplicated somatic mutations allows estimating the timing of each chromosome duplication in molecular time. (E) Finally, an oncogenic timeline of the tumor is generated, with the number of clonal and subclonal mutations, their distribution per mutation signature, the driver alterations (colored according to the most likely causal mutational process) and CNA timing. This example comes from a previously analyzed tumor (Letouzé *et al.*, 2017).

Supplementary note:

Palimpsest: an R package for studying mutational and structural variant signatures along clonal evolution in cancer.

Jayendra Shinde, Quentin Bayard, Sandrine Imbeaud, Théo Z Hirsch, Feng Liu, Victor Renault, Jessica Zucman-Rossi and Eric Letouzé*

*Corresponding author. E-mail: eric.letouze@inserm.fr

In this supplementary note, we describe in more details the methodological details underlying the main functions of the *Palimpsest* package.

S1. Mutational signature analysis

Palimpsest allows both de novo analysis of mutational signatures and quantification of previously described signatures. In both cases, a set of base substitutions from a tumor series is first imported from a VCF file and each mutation is assigned to one of 96 mutation categories, defined by the 6 substitution types multiplied by 16 possible trinucleotide contexts (Alexandrov et al., 2013). We can then represent the mutational catalog of the n tumors as a mutation

The goal of mutational signature analysis is to deconvolute this matrix M as the product of a

matrix of mutational processes
$$P = \begin{pmatrix} p_1^1 & \dots & p_K^1 \\ \vdots & \ddots & \vdots \\ p_1^{96} & \dots & p_K^{96} \end{pmatrix}$$
 where p_i^j is the probability of the process

$$i$$
 to cause a mutation of category j , and a matrix of exposures $E = \begin{pmatrix} e_1^1 & \dots & e_n^1 \\ \vdots & \ddots & \vdots \\ e_1^K & \dots & e_n^K \end{pmatrix}$ where e_i^j is

the number of mutations attributed to process i in tumor j. To solve this problem, we use nonnegative matrix factorization, as implemented in the *NMF* package (Gaujoux and Seoighe, 2010). For a *de novo* analysis, the number of processes K can be manually defined by the user or estimated automatically considering the cophenetic correlation coefficients and residual sum of squares (RSS) for each number of signatures. NMF then identifies the matrices P and E that verifies $M \approx P \times E$ and minimizes a Frobenius norm while maintaining non-negativity. For an analysis of previously described signatures, the user provides the matrix of processes P, and NMF is used only to reconstruct the exposure matrix E. The P matrix for the 30 signatures currently referenced in the COSMIC database is provided with the Palimpsest package.

S2. Association of mutational signatures with driver genes

Once a cancer genome has been deconvoluted as a combination of several mutational processes, we can estimate the probability of each somatic mutation being generated by each

mutational process using simple Bayes statistics (Letouzé et al., 2017). This key feature has been introduced in Palimpsest as follows:

Consider a mutation category c out of the 96 mutation categories, the number of mutations of category *c* in a tumor *t* can be expressed as:

$$m_t^c = \sum_{s=1}^{10} p_s^c \times e_t^s$$

where the product $p_s^c \times e_t^s$ represents the number of mutations of category c attributed to signature s in tumor t. The probability P(m,s) of a mutation m of category c in tumor t being due to signature s can then be estimated as:

$$P(m,s) = \frac{p_s^c \times e_t^s}{\sum_{s=1}^{10} p_s^c \times e_t^s}$$

This important feature of Palimpsest can be used to predict the mutational processes (point mutations or structural variants) at the origin of driver alterations in a cancer genome.

S3. Structural rearrangement signature analysis

Palimpsest performs structural rearrangement signature analysis by applying the same statistical framework used for mutational signature analysis. Somatic structural rearrangements from a series of tumors are first classified into 38 categories considering the type (deletion, tandem duplication, inversion, interchromosomal translocation) and size (<1kb, 1-10kb, 10-100kb, 100kb-1Mb, 1-10Mb, >10Mb) of rearrangements, as previously described (Nik-Zainal et al., 2016). Clustered events, defined by the presence of ≥10 breakpoints within a 1Mb window, are identified using the bedr package (Haider et al., 2016) and considered separately from non-clustered events. We then used non-negative matrix factorization, as implemented in the NMF package, to extract rearrangement signatures and their exposure in each tumor. Like mutational signature analysis, structural rearrangement signature analysis can be performed de novo or using a pre-defined set of known signatures to estimate the exposure matrix.

S4. Estimating the cancer cell fraction and clonality

Using the variant allele fraction (VAF), tumor cell content and absolute copy-number estimates, *Palimpsest* estimates the cancer cell fraction (CCF), i.e. the proportion of tumor cells harboring each mutation:

$$CCF = VAF \times \frac{\rho N_t + (1 - \rho)N_n}{\rho n_{chr}}$$

where ρ is the tumor cell content, N_t and N_n the copy-number at the locus in tumor and normal cells, and n_{chr} the number of chromosomal copies harboring the mutation in tumor cells (also

called multiplicity of the mutation). ρ and N_t can be estimated from copy-number data using various algorithms. The multiplicity of each mutation (n_{chr}) is set to the integer value closest to:

$$max\left(1, VAF \times \frac{\rho N_t + (1-\rho)N_n}{\rho}\right)$$

Finally, Palimpsest determines the 95% confidence of VAF using a binomial test and converts this interval to obtain the 95% confidence interval of CCF using the above formula. A mutation is then classified subclonal if the upper boundary of the 95% confidence interval is below a threshold set by the user (default 0.95), and clonal otherwise.

S5. Timing chromosomal duplications

When a chromosome is duplicated, mutations harbored by the chromosome are also duplicated and their VAF is increased as compared to mutations present on the other chromosome copy, or acquired after the duplication. The ratio of duplicated/non-duplicated mutations can thus be used to time the chromosome duplication event, early events having a low amount of duplicated mutations as compared to late events (Nik-Zainal *et al.*, 2012). *Palimpsest* uses previously described formulas (Letouzé *et al.*, 2017) to estimate the point mutation time of each chromosome duplication with a minimum of 30 mutations located on the duplicated segment.

Let us consider the simple case of a chromosome with absolute copy-number N_t =3. The molecular time at which the extra copy of the chromosome was gained can be estimated as:

$$T = \frac{N_{dup}}{N_{dup} + \frac{N_{ndup} - N_{dup}}{3}} \times 100$$

where N_{dup} and N_{ndup} are the number of duplicated and non-duplicated mutations, respectively.

We extrapolated this formula to chromosomes with $N_t \ge 4$. In this case, we timed the first duplication event using:

$$T = \frac{N_{dup}}{N_{dup} + \frac{N_{ndup} - N_{dup}}{(3 + N_t)/2}} \times 100$$

where N_{dup} is the number of mutations at the maximal level of multiplicity and N_{ndup} the number of mutations at intermediate levels of multiplicity or non-duplicated.

For cases where the two parental chromosome copies were duplicated, e.g. N_t =4 with 2 copies of each chromosome copy, we adapted the formula as follows:

$$T = \frac{N_{dup}/2}{N_{dup}/2 + \frac{N_{ndup}}{(3 + N_t)/2}} \times 100$$

S6. Limitations of the package – number of mutations needed

Palimpsest can be applied to both whole genome and whole exome sequencing data. However, whole genome data are preferable for structural rearrangement signature analysis and timing chromosome duplications. Factors influencing extraction of mutational signatures have been extensively analyzed elsewhere (Alexandrov et al., Cell Rep 2013) using simulated data with varying numbers of signatures, similarities between signatures, numbers of tumors and numbers of mutations per tumor. The authors concluded that, although both whole genome and whole exome sequencing data are suitable to accurately extract mutational signatures, the number of required mutations/samples increases with the number of signatures, and it is preferable to have more mutations/sample (e.g. whole genome sequences) than more samples with less mutations (e.g. large whole exome series). However, giving precise limitations regarding a required number of mutations per sample is delicate as it also depends on the type of mutational signatures analyzed. In our experience, very specific signatures caracterized by only a few mutation categories mutated at high frequency will be easily identified with relatively few mutations, whereas signatures with widespread mutation spectra will by harder to quantify.

References

- Alexandrov, L.B. et al. (2013) Deciphering signatures of mutational processes operative in human cancer. Cell Rep., 3, 246–259.
- Gaujoux,R. and Seoighe,C. (2010) A flexible R package for nonnegative matrix factorization. *BMC Bioinformatics*, **11**, 367.
- Haider, S. et al. (2016) A bedr way of genomic interval processing. Source Code Biol. Med., 11, 14.
- Letouzé, E. et al. (2017) Mutational signatures reveal the dynamic interplay of risk factors and cellular processes during liver tumorigenesis. *Nat. Commun.*, **8**, 1315.
- Nik-Zainal,S. *et al.* (2016) Landscape of somatic mutations in 560 breast cancer whole-genome sequences. *Nature*, **534**, 47–54.
- Nik-Zainal,S. et al. (2012) The life history of 21 breast cancers. Cell, 149, 994–1007.

Article 4: Cyclin A2/E1 activation defines a hepatocellular carcinoma subclass with a rearrangement signature of replication stress.



ARTICLE

DOI: 10.1038/s41467-018-07552-9

OPEN

Cyclin A2/E1 activation defines a hepatocellular carcinoma subclass with a rearrangement signature of replication stress

Quentin Bayard 1,2,3,4, Léa Meunier^{1,2,3,4}, Camille Peneau^{1,2,3,4}, Victor Renault 5, Jayendra Shinde^{1,2,3,4}, Jean-Charles Nault^{1,2,3,4,6,7}, Iadh Mami^{1,2,3,4}, Gabrielle Couchy^{1,2,3,4}, Giuliana Amaddeo^{8,9}, Emmanuel Tubacher⁵, Delphine Bacq¹⁰, Vincent Meyer¹⁰, Tiziana La Bella^{1,2,3,4}, Audrey Debaillon-Vesque¹¹, Paulette Bioulac-Sage^{12,13}, Olivier Seror^{1,14}, Jean-Frédéric Blanc^{11,12}, Julien Calderaro^{8,15}, Jean-François Deleuze^{5,10}, Sandrine Imbeaud 1,2,3,4</sup>, Jessica Zucman-Rossi 1,2,3,4,16

Cyclins A2 and E1 regulate the cell cycle by promoting S phase entry and progression. Here, we identify a hepatocellular carcinoma (HCC) subgroup exhibiting cyclin activation through various mechanisms including hepatitis B virus (HBV) and adeno-associated virus type 2 (AAV2) insertions, enhancer hijacking and recurrent *CCNA2* fusions. Cyclin A2 or E1 alterations define a homogenous entity of aggressive HCC, mostly developed in non-cirrhotic patients, characterized by a transcriptional activation of E2F and ATR pathways and a high frequency of *RB1* and *PTEN* inactivation. Cyclin-driven HCC display a unique signature of structural rearrangements with hundreds of tandem duplications and templated insertions frequently activating *TERT* promoter. These rearrangements, strongly enriched in early-replicated active chromatin regions, are consistent with a break-induced replication mechanism. Pan-cancer analysis reveals a similar signature in *BRCA1*-mutated breast and ovarian cancers. Together, this analysis reveals a new poor prognosis HCC entity and a rearrangement signature related to replication stress.

¹INSERM, UMR-1162, Génomique Fonctionnelle des Tumeurs Solides, Equipe Labellisée Ligue Contre le Cancer, Institut Universitaire d'Hématologie, Paris 75010, France. ² Université Paris Descartes, Labex Immuno-Oncology, Sorbonne Paris Cité, Faculté de Médecine, Paris 75006, France. ³ Université Paris 13, Sorbonne Paris Cité, Unité de Formation et de Recherche Santé, Médecine, Biologie Humaine, Bobigny 93017, France. ⁴ Université Paris Diderot, Sorbonne Paris Cité, Paris 75013, France. ⁵ Laboratory for Bioinformatics, Fondation Jean Dausset – CEPH, Paris 75010, France. ⁶ Liver unit, Hôpital Jean Verdier, Hôpitaux Universitaires Paris-Seine-Saint-Denis, Assistance-Publique Hôpitaux de Paris, APHP, Bondy 93140, France. ⁷ Unité de Formation et de Recherche Santé Médecine et Biologie Humaine, Université Paris 13, Communauté d'Universités et Etablissements Sorbonne Paris Cité, Bobigny 93017, France. ⁸ Inserm, U955, Team 18, Université Paris-Est Créteil, Faculté de Médecine, Créteil 94010, France. ⁹ Assistance Publique-Hôpitaux de Paris, Service d'Hépatologie, CHU Henri Mondor, Créteil 94010, France. ¹⁰ Centre National de Recherche en Génomique Humaine, CEA, Evry 91000, France. ¹¹ Service Hépato-Gastroentérologie et Oncologie Digestive, Hôpital Haut-Lévêque, Centre Hospitalier Universitaire de Bordeaux, Bordeaux 33076, France. ¹² Université Bordeaux, Bordeaux Research in Translational Oncology, Bordeaux 33076, France. ¹³ Service de Pathologie, Hôpital Pellegrin, Centre Hospitalier Universitaire de Bordeaux, Bordeaux 33000, France. ¹⁴ Radiology Department, Jean Verdier Hospital, Hôpitaux Universitaires Paris-Seine-Saint-Denis, APHP, Bondy 93140, France. ¹⁵ Assistance Publique-Hôpitaux de Paris, Département de Pathologie, Hôpital Henri Mondor, Créteil 94010, France. ¹⁶ Assistance Publique-Hôpitaux de Paris, Département de Pathologie, Hôpital Henri Mondor, Créteil 94010, France. ¹⁶ Assistance Publique-Hôpitaux de Paris, Département de Pathologie, Hôpital Henri Mondor, Créteil 94010, France

epatocellular carcinoma (HCC) is the third leading cause of cancer death worldwide. Only 30% of cases are diagnosed at an early stage and are amenable to curative treatment by tumor resection or liver transplantation¹. The multikinase inhibitors sorafenib² and regorafenib³ are currently the only drugs approved for advanced HCC cases, but the median life expectancy of patients with HCC on sorafenib is only 1 year. All phase III clinical trials involving targeted molecular therapies have failed so far for various reasons including liver toxicity, lack of antitumoral potency, and the molecular heterogeneity of the disease⁴. Identifying homogeneous HCC subgroups sharing similar driving mechanisms and vulnerabilities is thus crucial to design successful patient-tailored clinical trials.

Most HCC develop in a cirrhotic liver, associated with various etiologies including hepatitis B virus (HBV) and hepatitis C virus (HCV) infections, alcohol abuse, metabolic disease, and exposure to carcinogenic compounds like aflatoxin B1⁵. The natural history of HCC in cirrhosis follows a well-established sequence with the successive development of dysplastic nodules that can transform into early stage and advanced HCC. TERT promoter mutations are the initial oncogenic events already detected in dysplastic nodules⁶ whereas alterations in other HCC drivers^{7–11} involved in cell cycle control (TP53, RB1, CCND1, CDKN2A), Wnt/ß-catenin signaling (CTNNB1, AXIN1), oxidative stress response (NFE2L2, KEAP1) epigenetic regulation (ARID1A, ARID2) and the AKT/mTOR and MAP kinase pathway (RPS6KA3, TSC1, TSC2, PTEN) only occur in progressed HCC¹².

In 20% of the cases, HCC develops in absence of cirrhosis. These patients usually maintain adequate liver functions and, being less subject to liver toxicity, may be eligible for more treatment options. The etiology of HCC in absence of cirrhosis is largely unknown, but one mechanism of transformation involves insertional mutagenesis by the HBV virus. The first oncogenic HBV insertion was identified in cyclin A2 gene (CCNA2)¹³. Since then, recurrent HBV insertions were mapped in several oncogenes including CCNE1, KMT2B and TERT^{14,15}. Recently, we identified adeno-associated virus type 2 (AAV2) insertions as a new etiology for HCC developed in absence of cirrhosis, with recurrent insertions in CCNA2 and CCNE1 genes¹⁶. However, the molecular consequences of viral insertions in cyclin genes and their precise role in HCC development remain poorly understood.

Here, we report the systematic screening of *CCNA2* and *CCNE1* alterations in 751 HCC. We identify new mechanisms of cyclin A2/E1 activation, and we explore the clinical and molecular characteristics of this tumor subgroup.

Results

Viral insertions and gene fusions activate cyclin A2. To identify the exhaustive landscape of *CCNA2* and *CCNE1* alterations in HCC, we analyzed 751 HCC comprising an in-house series of 160 tumors (LICA-FR) analyzed by RNA sequencing (RNAseq, n = 160), whole exome (WES, n = 156) and whole genome sequencing (WGS, n = 45) (Supplementary Data 1), the TCGA¹⁷ series (334 HCC with RNA-seq and WES, 48 or which also analyzed by WGS) and the ICGC-JP¹¹ series (257 HCC with WGS data, Supplementary Data 2).

We first screened the LICA-FR series of 160 tumors to characterize the exhaustive mechanisms activating CCNA2 and CCNE1 in HCC. We identified one HBV and 5 AAV2 insertions (four previously described in the ref. ¹⁶) in CCNA2 gene (Supplementary Data 3), all but one located within CCNA2 intron 2 (Fig. 1a). Viral insertions were associated with CCNA2 mRNA over-expression ($P = 8.2 \times 10^{-9}$, fold-change = 5.6, Fig. 1b), but also altered the transcript and protein structure.

AAV2 and HBV insertions induced the expression of various abnormal transcripts (Supplementary Fig. 1), predicted to generate a truncated cyclin A2 protein starting at methionine 148 or 158 with occasionally a few amino acids translated from the viral genome (Fig. 1c).

In addition we identified novel gene fusions in 4 tumors (Supplementary Data 4), all involving the C-terminal part of CCNA2 (exons 3-8) at chromosome 4q27 downstream 3 different partner genes: GSTCD at 4q24, SNX29 at 16p13.13 and TET2 (×2) at 4q24 (Fig. 1a, d). In the TET2-CCNA2 and GSTCD-CCNA2 fusion transcripts, the first untranslated exons of TET2 and GSTCD were linked with CCNA2 exons 3-8. The SNX29-CCNA2 fusion revealed an alternative transcription start site (TSS) in SNX29 intron 14 generating a 448-nucleotide sequence spliced with CCNA2 exon 3. In all fusions, the predicted translation initiation site of the fused RNA was located at methionine 158 in CCNA2 exon 3, predicted to generate a truncated cyclin A2 protein of 275 amino acids (32 Kda), lacking the destruction box¹⁸ and ubiquitination targeting sequences¹⁹ but retaining the functional cyclin box, without any protein fragment from the partner genes (Fig. 1e).

Western blot analysis of 9 tumors with viral insertion or gene fusion confirmed the over-expression, as predicted, of a truncated 32 KDa protein (Fig. 1f). Thus, gene fusions and viral insertions in *CCNA2* both lead to the production of a stable protein lacking the N-terminal regulatory domains.

In the TCGA series, we identified 7 CCNA2 fusions with 5 different partner genes (FAM160A1, KIAA1109 × 3, LIPC, UBA6 and TDO2, Fig. 1a, d), all of which involved the first untranslated exon(s) of the partner gene linked with exons 3-8 of CCNA2. WGS revealed in another tumor a focal deletion starting in the 5' UTR region and ending in CCNA2 intron 2 (Supplementary Fig. 2). All these events were predicted to generate the same 32 KDa truncated cyclin A2 protein lacking N-terminal regulatory domains. We also identified one tumor with HBV insertion and 3 tumors with AAV2 insertions in CCNA2. Finally, 6 tumors strongly overexpressed CCNA2 (FPKM > 15), 3 of which displayed 23-48 Mb intra-chromosomal deletions linking the intergenic region downstream CCNA2 with the highly expressed ALB, AFP, and ADH6 genes (Supplementary Fig. 2). The ICGC-JP cohort comprised one HBV insertion in CCNA2 intron 2 and one fusion between the first untranslated exon of ANXA5 and exons 3-8 of CCNA2 (Fig. 1a, d).

In total, we identified 10 HCC with CCNA2 activation events in the LICA-FR series (6.2%), 2 in the ICGC-JP series (0.8%) and 18 in the TCGA series (5.4%), associated with a significant increase of CCNA2 mRNA expression, but also generating a truncated cyclin A2 protein lacking the N-terminal destruction box and the ubiquitination site.

Viral insertions and enhancer hijacking activate cyclin E1. In our series of 160 HCC, we identified 5 AAV2 insertions (three previously described in the ref. ¹⁶) and one HBV insertion in the 5' region or upstream the transcription start site (TSS) of *CCNE1* (Fig. 2a, Supplementary Data 3). These viral insertions induced a massive overexpression of the full-length *CCNE1* gene (Fig. 2b), confirmed by western-blot analysis (Supplementary Fig. 3). Interestingly, one case with AAV2 insertion (FR2141T) also displayed an amplification of *CCNE1* locus including the viral sequence (Supplementary Fig. 3), suggesting a two-step selection of *CCNE1* activation in the natural history of this tumor. Four other tumors overexpressed *CCNE1* (FPKM > 6), explained by high-level amplification in one case. In the 3 remaining cases, whole genome sequencing revealed interchromosomal translocation breakpoints in the regulatory region of *CCNE1* (Fig. 2a). Tumor FR2048T

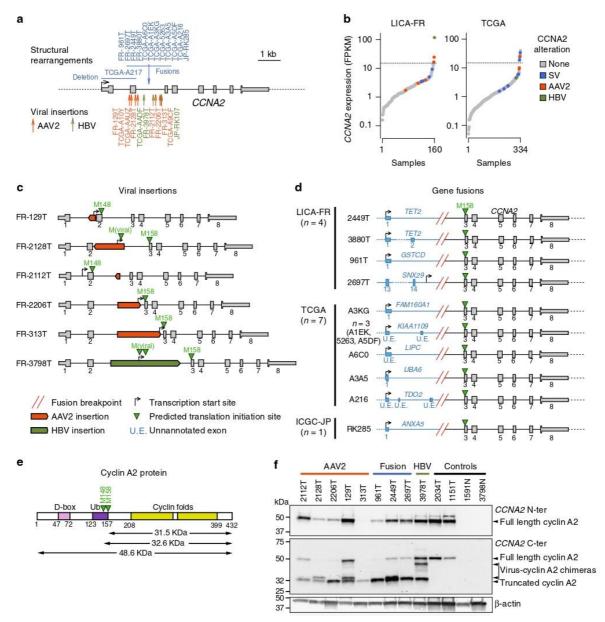


Fig. 1 Diverse mechanisms leading to CCNA2 activation in HCC. a Summary of structural rearrangements (top) and viral insertions (bottom) affecting CCNA2 gene identified in 751 HCC from the LICA-FR, TCGA and ICGC-JP cohorts. b Sorted CCNA2 expression (log scale) in the LICA-FR and TCGA cohorts. Gene expression was obtained from RNA-seq data and is given in fragments per kilobase of exons per million reads (FPKM). Samples harboring structural variants (SV) or viral insertions are indicated with a color code. c Functional consequences of AAV2 and HBV insertions in CCNA2. Viral insertions identified in the LICA-FR cohort were precisely mapped using WGS or viral capture data, and RNA-seq reads were aligned on the reconstructed chimeric DNA to identify the transcription start sites and predicted translation initiation sites of abnormal transcripts. d CCNA2 fusions identified in the LICA-FR, TCGA and ICGC-JP cohorts. The transcription start site of the fusion transcript is represented together with the predicted translation initiation site. Fusions with KIAA1109, LIPC and TDO2 involve 5' exons not annotated in transcript databases but expressed in normal liver. e Schematic representation of cyclin A2 protein with functional domains. D-box Destruction box; Ub, Ubiquitination targeting sequences. f Western blot analysis of cyclin A2 using antibodies targeting the N-terminal (top) or C-terminal (middle) domains. Tumors with viral insertions or gene fusions are compared with tumors without CCNA2 alteration and non-tumoral liver controls

displayed a translocation placing *CCNE1* downstream the first untranslated exon of the highly expressed *ERRFI1* gene, leading to a highly expressed *ERRFI1-CCNE1* fusion. The two other translocations lead to juxtapose *CCNE1* promoter with enhancer-rich chromatin areas located close to the highly expressed genes *RAPH1*

and CYB5A (Fig. 2c). Thus, both viral insertions and structural rearrangements can activate CCNE1 expression by bringing viral or distal human enhancers in the regulatory region of the gene.

In the TCGA series, 10 tumors overexpressed *CCNEI* (Fig. 2b), including 2 cases with HBV insertion, one with HBV insertion

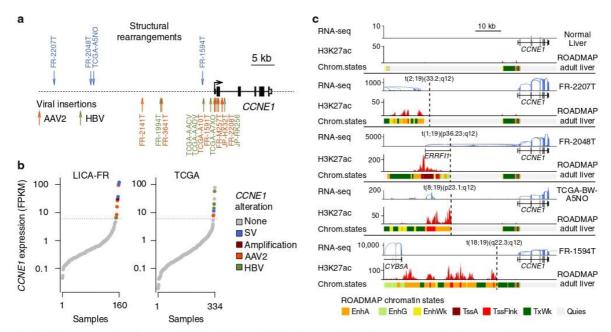


Fig. 2 Viral and non-viral mechanisms of CCNE1 activation in HCC. a Summary of structural rearrangements (top) and viral insertions (bottom) affecting CCNE1 gene identified in 751 HCC from the LICA-FR, TCGA and ICGC-JP cohorts. b Sorted CCNE1 expression (log scale) in the LICA-FR and TCGA cohorts. Gene expression was obtained from RNA-seq data and is given in fragments per kilobase of exons per million reads (FPKM). Samples harboring structural variants (SV), focal amplifications and viral insertions are indicated with a color code. c Functional consequences of structural rearrangements affecting CCNE1 regulatory region. RNA-seq read counts along CCNE1 locus are represented in normal liver (top) and in 4 tumors harboring structural rearrangements upstream CCNE1 trancription start site (TSS). H3K27Ac chromatin immunoprecipitation sequencing (ChIP-seq) signal and chromatin states in adult liver were obtained from the ROADMAP consortium and are depicted below each reconstruted DNA sequence. EnhA: active enhancer; EngG: genic enhancer; EnhWk: weak enhancer; TssA: active TSS; TssFInk: flanking TSS; TxWk: weak transcription; Quies: quiescent chromatin

plus high-level amplification, one with AAV2 insertion and one with a translocation between *CCNE1* regulatory region and an enhancer-rich region on chromosome 5 (Fig. 2c). In the 5 remaining cases, the mechanism leading to *CCNE1* overexpression remained unexplained in absence of WGS data. In the ICGC-JP cohort, we identified one AAV2 and one HBV insertion associated with *CCNE1* overexpression. In total, we identified 10 HCC with *CCNE1* activation events in the LICA-FR cohort (6.2%), two in the ICGC series (0.8%) and 10 in the TCGA series (3.0%)

Across the three data sets, 52/751 tumors (6.9%) displayed an activation of cyclin A2 (n=30) or E1 (n=22) due to viral insertions or structural rearrangements. These are later referred to as CCN-HCC. The proportion of CCN-HCC varied between the cohorts (12.5% in our series, 8.4% in TCGA and 1.6% in ICGC-JP) due to differences in etiological backgrounds (Supplementary Data 2). It was particularly high in our series enriched in cancers developed in a non-fibrotic liver, and low in the IGGC-Japan series dominated by HCV-related cases.

Cyclin A2 or E1 activation defines a homogenous HCC subgroup. We next explored the molecular and clinical characteristics of CCN-HCC. Gene expression analysis of the LICA-FR and TCGA showed that CCN-HCC defined homogeneous transcriptional clusters (Fig. 3a). They were characterized by an overexpression of cell cycle genes, in particular E2F targets, and an activation of the ATR pathway in response to replication stress (Fig. 3b, Supplementary Data 5). The most significant downregulated pathways were oxidative phosphorylation, suggesting a metabolic switch to aerobic glycolysis (Warburg effect), and MYC targets. We also compared the alteration frequencies of known

liver cancer driver genes¹⁰ between CCN-HCC and others. CCNA2 and CCNE1 activation events were remarkably exclusive from CTNNB1 and TERT promoter mutations, but frequently associated with PTEN and RB1 inactivation in both the LICA-FR and TCGA series (Fig. 3b, Supplementary Data 6). RB1 inactivation may allow cells to overcome oncogene-induced senescence²⁰ in these tumors, whereas PTEN inactivation might favor the oncogenic metabolic switch that we observed at the transcriptional level²¹. Compared to the other tumors in the LICA-FR series, CCN-HCC were enriched in large tumors (median largest nodule diameter = 115 vs. 60 mm, P = 0.0033), of poor prognosis (median overall survival = 21 vs. 69 months, P = 0.0072, Fig. 3c), developed in younger patients (median age = 57 vs. 67 years old, P = 0.050) with a non-fibrotic liver (fibrosis stage F0-F1 80 vs. 42%, P = 0.0011). Thus, CCN-HCC define a homogenous HCC entity with characteristic clinical and molecular features.

CCN-HCC display a unique structural rearrangement signature. To identify mutational signatures associated with CCN-HCC, we analyzed the whole genome sequences of 45 of our 160 HCC (35 were previously published 22 , 10 new), including 13 CCN-HCC. With a median of 12,463 mutations, CCN-HCC were rather less mutated than others (median = 16,397 mutations, P = 0.065). Mutational signatures 4, 5, and 16 (COSMIC nomenclature), ubiquitous in liver cancers 22 , accounted for most mutations in CCN-HCC, with a slight increase of signature 5 (53 vs. 33%, P = 0.036) and decrease of signature 16 (23 vs. 32%, P = 0.05) as compared with other HCC (Supplementary Fig. 4).

In contrast, CCN-HCC displayed > 3 times more structural variants (median = 415 vs. 126, $P = 1.1 \times 10^{-4}$). We identified 6 rearrangement signatures, termed RS1 to RS6, characterized by

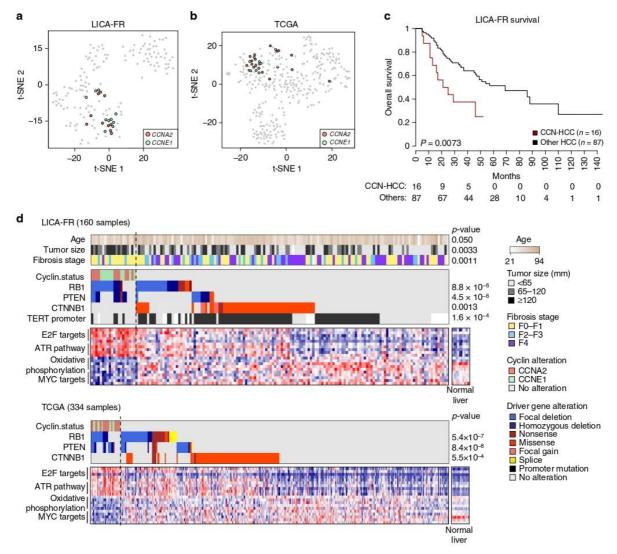


Fig. 3 Clinical and molecular features of cyclin-activated HCC. a t-SNE plots depicting the classification of HCC from the LICA-FR and TCGA cohorts based on their transcriptional profiles. Tumors harboring CCNA2 or CCNE1 activating alterations are indicated with a color code. b Clinical characteristics, driver genes and deregulated pathways associated with CCN-HCC in the LICA-FR (top) and TCGA (bottom) cohorts. c Overall survival in CCN-HCC as compared with other HCC in the LICA-FR cohort. Only HCC with curative resection (RO) were included

different combinations of rearrangement categories defined according to the type, size, and clustered nature of rearrangements (Fig. 4a). Strikingly, a high number of rearrangements attributed to signature RS1 (≥50 events) was specifically encountered in a cluster of 13 tumors corresponding exactly to CCN-HCC ($P = 1.4 \times 10^{-11}$, Fig. 4b). We validated this association using WGS data from the ICGC-JP series and a subset of 48 samples from the TCGA series (Fig. 4c, Supplementary Data 7). In absence of WGS data for the rest of the TCGA series, we used SNP array data to estimate the number of focal gains (<200 kb) in each tumor as a surrogate marker of the RS1 signature. With a median of 120 events, CCN-HCC displayed a significant increase of focal gains as compared with other HCC in the TCGA series (median = 6, $P < 2.2 \times 10^{-16}$, Supplementary Fig. 5). Thus, CCN-HCC have a relatively low mutation burden but a large number of structural rearrangements with a specific

RS1, characterized by a combination of small tandem duplications (<100 kb) and inter-chromosomal translocations (Fig. 4d). CCN-HCC also displayed a typical copy-number profile showing hundreds of focal gains, usually one copy above surrounding chromosome segments (Supplementary Fig. 6). Surprisingly, overlaying structural rearrangement breakpoints with copy-number profiles revealed that only 68% of these gains were due to tandem duplications, other gains being frequently surrounded by translocation or inversion breakpoints (Fig. 4e, Supplementary Fig. 6). A recurrent feature consisted of several chromosome segments, usually between 10 and 100 kb, stung together and with the same duplication level relative to their

source chromosomes. Most of these events involved segments

from two (Fig. 4f) or more (Supplementary Fig. 7) different chromosomes, a feature recently described as templated

RS1 features suggest a replication stress-induced mechanism.

Almost all rearrangements in CCN-HCC belonged to signature

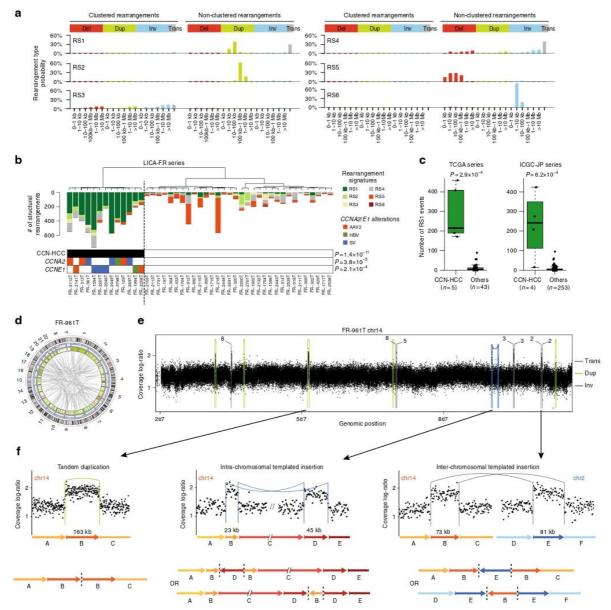


Fig. 4 Cyclin-activated HCC display a specific signature or structural rearrangements. **a** Six rearrangement signatures identified across 350 HCC genomes by non-negative matrix factorization. Structural rearrangements were classified in 38 categories considering their type (del: deletion, dup: tandem duplication, inv: inversion, trans: inter-chromosomal translocation) and size, and distinguishing clustered from non-clustered events. The probability of each rearrangement category in each signature is represented, with rearrangement types indicated above and rearrangement sizes below. **b** Unsupervised classification of 45 HCC from the LICA-FR cohort based on the contribution of rearrangement signatures in each tumor. Significant molecular alterations associated with the cluster of tumors having a high contribution of signature RS1 are represented below. *P*-values were obtained using Fisher's exact tests. **c** Validation of the association between the RS1 signature and CCN-HCC in the TCGA and ICGC-JP series. The middle bar, median; box, interquartile range; bars extend to 1.5 times the interquartile range. **d** CIRCOS plot representing the structural rearrangement profile of a representative CCN-HCC (FR-961T, harboring a *GSTCD-CCNA2* fusion). **e** Copy-number profile showing the accumulation of focal gains along chromosome 14 in tumor FR-961T. Structural rearrangements are overlaid on the copy-number profile with a color code indicating the type of event. trans: inter-chromosomal translocation; dup: tandem duplication; inv: inversion. **f** Three types of rearrangements leading to focal chromosome gains in CCN-HCC. A representative example of each type of event is shown with a copy-number plot above and a schematic representation of the rearranged chromosome below. Structural rearrangements were represented with the same color code as in **e**. Dashed lines on schematic chromosome reconstructions represent the abnormal junctions detected in WGS data

insertion cycle²³. Inter-chromosomal templated insertions accounted for 11% of focal gains in CCN-HCC. Other events, which we call intra-chromosomal templated insertions, involved distal segments of a same chromosome and appeared as couples of inversions (Fig. 4f) or duplication and deletion (Supplementary Fig. 7), depending on the orientation of thejunctions. Intra-chromosomal templated insertions accounted for 7% of focal gains in CCN-HCC. All these events are consistent with a replication-based mechanism in which a DNA polymerase at a stalled replication fork would switch template, replicate one or more other DNA regions and switch back to the original template strand behind the point of departure, generating a duplication on the host chromosome^{23–26}. Such mechanism could be particularly active in CCN-HCC due to replication stress induced by premature S phase entry.

Structural rearrangements activate TERT promoter in CCN-HCC. To better understand the functional consequences of the rearrangement phenotype observed in CCN-HCC, we examined the location of 8466 breakpoints attributed to the RS1 signature among the 350 liver cancer genomes from the LICA-FR, TCGA and ICGC cohorts. RS1 breakpoints were not distributed evenly along the genome but formed clusters located almost exclusively within active topologically associated domains (TADs, Fig. 5a) characterized by early replication, high gene expression and active chromatin states in normal liver (Fig. 5b). In particular, RS1 breakpoint hotspots were frequently observed at loci encoding very highly expressed liver enzymes exemplified by the albumin (ALB), alcohol dehydrogenase (ADH) and hydroxysteroid 17-Beta dehydrogenases (HSD17B) loci on chromosome 4 (Fig. 5a, Supplementary Fig. 8). Among the 18 chromatin states defined by the ROADMAP consortium in normal adult liver, active transcription start sites (TSS) and enhancer regions were the most strongly enriched in RS1 breakpoints (fold-change > 3), whereas quiescent and heterochromatin domains were the most depleted (Fig. 5c). TSS and enhancer regions were also enriched, to a lesser extent, in breakpoints related to signature RS2 characterized by large tandem duplications. By contrast, breakpoints related to signature RS6, dominated by inversions < 10 kb, were predominantly observed in heterochromatin and ZNF repeats.

We then used binomial regression²⁷ to model the density of rearrangement breakpoints along the genome considering an extensive set of genomic features (Supplementary Fig. 9) and to identify hotspots harboring more breakpoints than expected by chance from the background model, which may indicate positive selection in CCN-HCC. We identified a single significant locus corresponding to TERT promoter region (q=0.0029, Fig. 5d). Although TERT promoter mutations were rare in CCN-HCC (9 vs. 55% in others, $P = 2.4 \times 10^{-5}$), TERT promoter rearrangements were highly enriched (82 vs. 7%, $P = 1.8 \times 10^{-15}$, Fig. 5e) and involved regions of active chromatin in normal liver, in the vicinity of highly expressed liver enzymes (ALB, FGG, SEP15, SLC12A7 and BAAT) or transcription factors (HNF4A, CEBPA, and CEBPB) (Supplementary Data 8, Supplementary Fig. 10). TERT promoter rearrangements induced an overexpression of TERT, stronger than promoter mutations but lower than HBV insertions (Supplementary Fig. 11). Of the 18 TERT promoter rearrangements identified in CCN-HCC, 16 could be associated with signature RS1 with a probability ≥ 0.5 (Fig. 5f). By contrast, most TERT promoter rearrangements in other HCC were related to signature RS4. Thus, structural rearrangements induced by replication stress are enriched at active chromatin regions and can promote CCN-HCC development by activating oncogenes like TERT.

CCN-HCC share a similar signature with BRCA1-altered cancers. To investigate the prevalence of the RS1 signature in other cancer types, we applied our method to 2606 tumors from the ICGC PanCancer Analysis of Whole Genomes (PCAWG) dataset^{23,28,29}. In this pan-cancer series, we identified 9 rearrangement signatures (Supplementary Fig. 12), including one signature (RS1-pancan) highly similar to the RS1 signature that we identified in liver cancers (cosine similarity = 0.91). The RS1pancan signature was detected at low frequency in several cancer types (e.g. bladder, lung, esophageal and gastric cancers), and was highly active in breast (18% of samples with ≥ 50 RS1 events) and ovarian (33%) cancers. However, this signature was associated with CCNA2/E1 rearrangements only in liver cancer (Fig. 6a, Supplementary Data 9). Thus, the relationship between cyclin A2/ E1 activation and signature RS1 is specific to liver cancer, and the molecular cause of this signature in other cancer types remains to be elucidated. In ovarian and breast cancer, RS1 signature was not associated with CCNE1 amplifications but with BRCA1 inactivation (Fig. 6b, c), consistent with previous reports 30,31. Despite sharing a common signature of short tandem duplications and templated insertions, CCNA2, CCNE1 and BRCA1-altered tumors displayed slightly different characteristics. First, the number of RS1 rearrangements was higher in CCNA2-activated HCC (median = 269) than in CCNE1-activated HCC (137) and BRCA1-altered breast (132) and ovarian (159) cancers (Fig. 6d). Second, tandem duplications were larger in CCNE1-activated HCC (median = 39 kb) than in CCNA2-activated HCC (22 kb), and smaller in BRCA1-altered breast (9 kb) and ovarian (10 kb) cancers (Fig. 6e). Finally, duplication and translocation breakpoints were strongly enriched in early-replicated regions in CCN-HCC as compared with other HCC, but not in BRCA1-altered as compared with other breast and ovarian cancers (Fig. 6f). Cyclin E1 activation was recently shown to induce replication stress by firing novel replication origins located within highly transcribed genes and prone to collapse³². BRCA1 is implicated in the response to replication stress^{33,34} and its inactivation leads to tandem duplication formation at stalled forks by a replication restart-bypass mechanism35. Cyclin A2/E1 activation in HCC and BRCA1 inactivation in breast and ovarian cancers may thus converge towards a similar rearrangement signature, with specificities reflecting the different ways by which these genetic alterations induce replication stress or modulate response to it (Fig. 6g).

Discussion

Here, we report the characterization of a homogeneous HCC subgroup driven by the activation of CCNA2 or CCNE1 gene. CCN-HCC represent 7% of HCC across the 3 data sets analyzed here, but up to 14% of HCC developed in a non-fibrotic liver. These patients often have atypical clinical presentation, without any history of primary risk factors, and can be remarkably young, exemplified by tumor FR-3880T developed in a 32 year-old woman without any risk factor, due to a TET2-CCNA2 fusion. CCN-HCC are usually large tumors of poor prognosis but share molecular characteristics, in particular high proliferation and replication stress, that could provide therapeutic opportunities³⁶. First, conventional chemotherapies mainly affect actively dividing cells by generating DNA damage or blocking DNA replication, and the tandem duplicator phenotype was identified as a marker for chemotherapeutic response in breast cancer cell lines and patient-derived xenografts³⁷. Transarterial chemoembolization (TACE) with doxorubicin, cisplatin or epirubicin, usually recommended for patients with intermediate HCC not eligible for surgery, may thus be an interesting option for CCN-HCC. Poly (ADP-ribose) polymerase (PARP) inhibitors, the first clinically

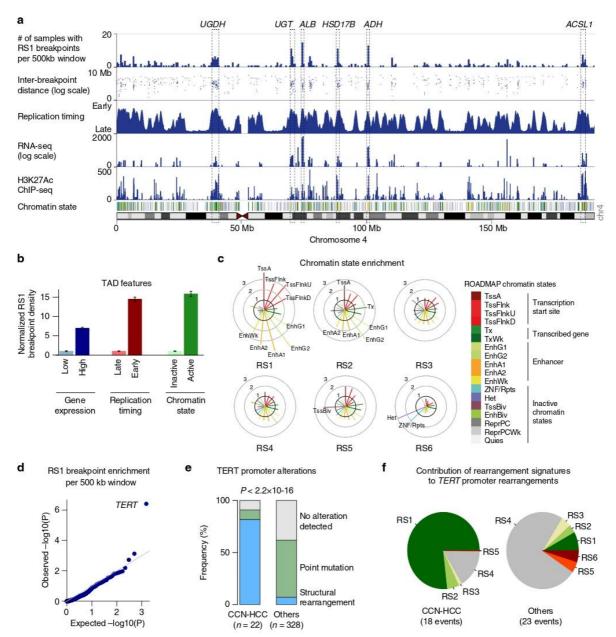
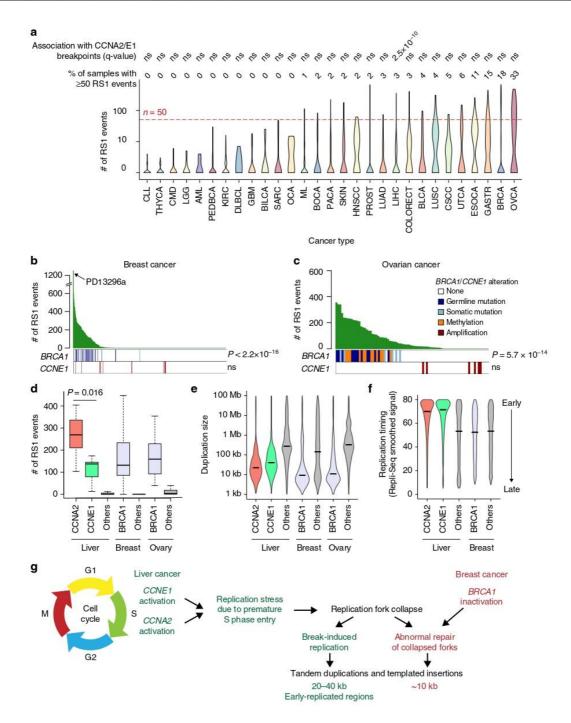


Fig. 5 Hotspot analysis of rearrangement signature 1 (RS1) breakpoints. a The density of RS1 breakpoints along chromosome 4 is displayed above replication timing, RNA-seq expression, H3K27Ac ChIP-seq profile and chromatin state. Replication timing was determined using Repli-Seq data from the liver cancer cell line HepG2. RNA-seq profile was generated from a normal liver sample. H3K27Ac and chromatin states in normal adult liver were obtained from the ROADMAP consortium. The legend for chromatin state color codes is displayed in c. Hotspots corresponding to highly expressed liver enzymes are annotated (UGDH, UDP-glucose 6-dehydrogenase; UGT, UDP glucuronosyltransferase family cluster; ALB, albumin; HSD17B, hydroxysteroid 17-Beta dehydrogenases 11 and 13, ADH, alcohol dehydrogenase cluster; ACSL1, acyl-CoA synthetase long chain family member 1). b RS1 breakpoint density in topologically associated domains (TADs). TADs were defined in human embryonic stem cells (H1) and classified based on gene expression in normal liver, replication timing and chromatin state. For each comparison, breakpoint density was normalized to be 1 in the group with the lowest density. Error bars indicate the 95% confidence interval. c Enrichment of rearrangement breakpoints in ROADMAP chromatin states for the 6 rearrangement signatures identified in HCC. For each signature, the fold-change between the observed and expected number of breakpoints falling within each chromatin state is represented, and chromatin states with a >2-fold enrichment are annotated. d Quantile-quantile plot of RS1 breakpoint enrichment p-values across 500 kb windows. e Proportion of TERT promoter alterations in CCN-HCC and other HCC analyzed by WGS. f Contribution of the 6 rearrangement signatures to TERT promoter rearrangements in CCN-HCC and other HCC



approved drugs designed to exploit synthetic lethality, have demonstrated benefit for patients carrying *BRCA1* mutations³⁸. CCN-HCC do not harbor a DNA repair defect but share with *BRCA1*-altered tumors a signature of genomic instability that could conceivably confer these tumors sensitivity to PARP inhibitors. Finally, there are currently several compounds in phase I and II trials targeting the replication stress response pathway members *ATR*, *CHK1* and *WEE1*³⁹. If brought to the clinic, such compounds would be promising for CCN-HCC treatment, given that the ATR pathway is strongly upregulated in CCN-HCC and

overexpression of *CCNE1* has been shown to confer increased sensitivity to ATR inhibition ⁴⁰.

We describe for the first time recurrent fusions involving *CCNA2* gene and recurrent rearrangements of *CCNE1* promoter region. *CCNA2* fusions are only the second recurrent fusion event identified in hepatocellular carcinoma, after the *PRKACA-DNAJB1* fusion characteristic of the rare fibrolamellar carcinoma subtype ⁴¹. These fusions always involve the untranslated 5' region of different partner genes upstream exons 3–8 of *CCNA2*, which constitutes an original mechanism leading to oncogene activation

Fig. 6 Pan-cancer analysis of the RS1 signature a Violin plots representing the number of rearrangements attributed to signature RS1 across patients within each cancer type in the ICGC PCAWG data set. For each cancer type, we assessed the association between tumors with ≥ 50 RS1 events and tumors with a rearrangement breakpoint < 80 kb from CCNA2 or CCNE1 gene using Fisher's exact tests. ns: not significant. The definition of cancer codes and number of samples per cancer type are available in Supplementary Data 9. b Number of RS1 events across 524 breast cancer genomes³⁰ and association with BRCA1 alterations and CCNE1 amplifications. PD13296a, the only tumor with both BRCA1 mutation and CCNE1 amplification, has the highest number of RS1 events in the series. c Number of RS1 events across 80 ovarian cancer genomes⁷⁵ and association with BRCA1 alterations and CCNE1 amplifications. P-values were obtained using one-sided Wilcoxon rank-sum tests. d Number of RS1 events in liver, breast and ovarian cancers with or without CCNA2, CCNE1 and BRCA1 alterations. The middle bar, median; box, interquartile range; bars extend to 1.5 times the interquartile range. e, Violin plots representing the distribution of tandem duplication sizes across liver, breast and ovarian cancers with or without CCNA2, CCNE1 and BRCA1 alterations. f Violin plots representing the replication timing of duplication and inter-chromosomal translocation breakpoint loci in liver and breast cancers with or without CCNA2, CCNE1 and BRCA1 alterations. Replication timing was determined using Repli-Seq data from the HepG2 cell line for liver cancer and from the MCF-7 cell line for breast cancer. g Proposed connexion beween rearrangement signatures in CCN-HCC and in BRCA1-inactivated breast and ovarian cancers

by truncating a regulatory N-terminal domain. Apart from liver cancers, none of the 2606 tumor genomes from the ICGC PCAWG dataset displayed a rearrangement breakpoint in CCNA2 intron 2. Consistently, a recent RNA-seq analysis of 9,624 TCGA samples from 33 cancer types⁴² did not reveal any CCNA2 fusion in other cancer types. CCNA2 fusions thus appear to be specific of liver cancers. Rearrangements affecting CCNE1 promoter region result in the overexpression of cyclin E1 by bringing active enhancer regions upstream the transcription start site, mirroring the effect of viral enhancers. This mechanism was more frequent than CCNE1 amplification in the liver cancer series we analyzed. Although HBV and AAV2 insertions were previously identified in CCNA2 and CCNE114,16, the functional consequences of these insertions were unknown. By integrating WGS and RNA-seq data, we demonstrate here that viral insertions in CCNA2, like gene fusions, induce abnormal transcripts leading to truncated proteins lacking N-terminal regulatory domains. By contrast, viral insertions in CCNE1 region lead to the overexpression of a full-length transcript and protein.

CCN-HCC display a characteristic transcriptional program, with a strong overexpression of E2F targets. Activation of the E2F pathway is expected in RB1-altered tumors and was already described in HCC⁴³. However, E2F pathway is also activated in CCN-HCC without RB1 inactivation event and may be partly explained by the ability of cyclin E/Cdk2 complexes to phosphorylate Rb. Interestingly, E2F-1 overexpression in the liver causes dysplasia and tumors in mice⁴³, and E2F1 was shown to inhibit c-Myc-driven apoptosis by activating PIK3CA/Akt/mTOR and c-Myb/COX-2 pathways⁴⁴.

A striking feature of CCN-HCC is the accumulation of hundreds of tandem duplications and templated insertion cycles. A recent study showed that CCNE1 activation in U2OS cell lines leads to shortened G1 phase, early S phase entry and firing of normally silenced replication origins in highly expressed genes, prone to collapse and associated with DNA double-strand breaks formation³². Double-strand breaks formed following replication fork breakdown are primarily repaired by break-induced replication (BIR)45. In a cyclin E overexpression model of DNA replication stress, BIR was shown to be required for cell cycle progression and to induce duplications < 200 kb⁴⁶. In addition, template switching may occur during BIR and generate complex chromosome rearrangements^{24,25,47}. Thus, the nature of rearrangements identified in CCN-HCC and the enrichment of breakpoints in early-replicated, actively transcribed regions are consistent with a BIR mechanism induced by replication stress. However, future studies addressing the precise molecular mechanism generating templated insertions will be crucial to fully understand the relationship between replication stress and the RS1 rearrangement signature. The mechanism of tandem duplication formation in BRCA1-mutant cells was recently identified 35. It involves abnormal repair of collapsed replication forks by a

"replication restart bypass" mechanism with extension of the stalled leading strand by a migration bubble mechanism similar to BIR⁴⁸, terminated by end joining or by microhomology-mediated template switching. Thus, structural rearrangements induced by cyclin activation and BRCA1 deficiency are initiated by replication fork collapse and processed by different repair mechanisms leading to a similar rearrangement signature with subtle differences regarding the size of rearrangements and breakpoint location. Interestingly, BRCA1 inactivation and CCNE1 amplification are mutually exclusive in ovarian cancers⁴⁹, and have been shown to be synthetically lethal⁵⁰. The single breast tumor that we identified with both BRCA1 mutation and CCNE1 amplification (PD13296a) had the highest number of rearrangements related to the RS1 signature (n=1221) across all the tumors we analyzed.

Contrary to CCNA2 alterations that seem to be specific of liver cancers, CCNE1 activation by high-level amplification is frequent across human cancers, in particular in gynecologic cancers⁵¹. Yet, CCNE1 amplification in breast and ovarian cancers does not lead to the rearrangement phenotype that we observed in CCN-HCC. Several reasons may explain this discrepancy. First, adult hepatocytes are quiescent, rarely divide, and may thus be particularly sensitive to replication stress. Second, CCNE1 is mostly activated by viral insertions and structural rearrangements of regulatory regions in HCC, rather than chromosome amplifications. These alterations may not have exactly the same functional consequence. Finally, we believe that viral insertions and structural rearrangements activating CCNA2 or CCNE1 are early events triggering hepatocarcinogenesis because they occur in patients without cirrhosis and in absence of other oncogenic event like CTNNB1 mutations. CCNE1 amplifications may occur later in breast and ovarian tumors, not leaving enough time for rearrangements to accumulate. Fujimoto et al. reported a positive correlation between the number of structural rearrangements and HBV insertion sites, suggesting that double-strand breaks generated by structural rearrangements may provide opportunities for HBV integration¹¹. Here we describe the reciprocal relationship where viral insertions in cyclin genes lead to structural rearrangement formation due to replication stress.

The propensity of signature RS1 breakpoints to occur in enhancer-rich regions makes these rearrangements likely to activate oncogenes in trans. In this limited series of 22 CCN-HCC analyzed by WGS, we identified a single significantly recurrent hotspot at *TERT* promoter. However, the power to identify recurrent somatic rearrangement hotspots increases sharply with sample size²⁷, and future studies of larger CCN-HCC series may uncover additional sites under positive selection in CCN-HCC.

In conclusion, viral insertions and structural rearrangements activating *CCNA2* and *CCNE1* define a homogeneous subgroup of aggressive HCC developed in non-cirrhotic liver, sharing similar transcriptional profiles and frequent inactivation of *RB1*

and *PTEN*. These tumors display a specific rearrangement signature induced by replication stress that sustains tumor growth by activating *TERT* but may constitute a targetable vulnerability.

Methods

Description of the LICA-FR cohort. A series of 160 hepatocellular carcinoma (HCC) samples and their non-tumor counterparts were collected from patients surgically treated in four French hospitals located in Bordeaux and Paris region. The study was approved by institutional review board committees (CCPRB Paris Saint-Louis, 1997, 2004, and 2010, approval number 01–037; Bordeaux, 2010–A00498–31). Written informed consent was obtained in accordance with French legislation. All samples were immediately frozen in liquid nitrogen and stored at $-80~^{\circ}\mathrm{C}$. HCC were enriched in cases developed on a non-cirrhotic liver (107/160, 67%): 75 tumors developed in non-fibrotic (METAVIR F0-F1), 32 in chronic hepatitis (F2–F3) and 53 in cirrhotic liver (F4). Clinicopathological data were available for all cases. A diversity of risk factors were represented in our series, including alcohol (n=63), metabolic syndrome (n=37), HBV (n=30), and HCV infection (n=30). Twenty-nine patients had none of the above risk factors. These 160 samples were analyzed by RNA sequencing, 156 were analyzed by whole exome sequencing (including 96 were previously published 10) and 45 by whole genome sequencing (35 were previously published 22). Detailed clinical characteristics and sequencing details for each sample are provided in Supplementary Data 1.

Whole genome sequencing. Whole genome data from 45 tumors of the LICA-FR series were analyzed in this study, comprising 35 previously published²² and 10 new cases. The whole genomes of 10 new tumor/normal pairs were sequenced for this project at the Center National de Recherche en Génomique Humaine (CNRGH, Evry, France) on an Illumina HiSeq X Five as paired-end 151 bp reads. Sequences were aligned to the hg19 version of the human genome using BWA⁵² version 0.7.12. We used Picard tools version 1.108 (http://broadinstitute.github.io/picard/) to remove PCR duplicates and GATK⁵³ version v3.5 for local indel realignment and base quality recalibration, as recommended in GATK best practices⁵⁴. We obtained an average depth of 119-fold for tumors (range 104–126) and 41-fold for matched non-tumor liver samples (range 38–43).

Whole exome sequencing. Whole exome data from 156 tumors of the LICA-FR series were analyzed in this study, comprising 96 previously published 10 and 60 new cases. Sequence capture, enrichment and elution of genomic DNA samples from the 60 new tumor/normal pairs was performed by IntegraGen (Evry, France). Agilent in-solution enrichment was used with the manufacturer's biotinylated oligonucleotide probe library SureSelect Human All-Exon kit v5 + UTRs (n=39) or SureSelect Clinical Research Exome V2 (n=21) according to the manufacturer's instructions. The eluted enriched DNA sample was sequenced on an Illumina HiSeq 2000 (n=39) or HiSeq 4000 (n=21) as paired-end 75 bp reads. Sequencing details for each sample are indicated in Supplementary Data 1.

Somatic mutation calling. We used MuTect2 to call somatic mutations from WES and WGS data by comparing each tumor sample with its matched non-tumor counterpart and a panel of normals (PON) file. We excluded mutations belonging to the ENCODE Data Analysis Consortium blacklisted regions (http://hgdownload.cse.ucsc.edu/goldenPath/hg19/encodeDCC/wgEncodeMapability/ wgEncodeDacMapability/ConsensusExcludable.bed.gz) and regions covered by < 6 reads in the tumor or normal sample. We then selected only single nucleotide variants (SNVs) with a MuTect2 flag among "PASS", "clustered_events", "t_lod_fstar", "alt_allele_in_normal" or "homologous_mapping_event" and small insertions and deletions (indels) with a MuTect2 flag among "PASS", "clustered_events" or "str_contraction". To improve specificity in the calling of mutations with low variant allele frequency (VAF), we quantified the number of high quality variant reads in the tumor (mapping quality ≥ 20, base quality ≥ 20) and the number of variant reads in the non-tumor sample with no quality threshold using bamreadcount (https://github.com/genome/bam-readcount). Only variants matching the following criteria were finally retained: VAF ≥ 2% in the tumor with ≥ 3 variant reads, VAF ≤ 5% in the non-tumor samples with ≤ 2 variant reads, and a VAF ratio ≥ 5 between the tumor and non-tumor sample:

Copy-number and structural rearrangement analysis. We used MANTA⁵⁵ software to identify somatic structural rearrangements in WGS data. To keep only the most reliable events, we selected only rearrangements supported by ≥ 10 reads and with a variant allele fraction ≥ 5%. We used cgpBattenberg⁵⁶ algorithm to reconstruct copy-number profiles from WGS data. We used the circular binary segmentation algorithm implemented in the Bioconductor package DNAcopy⁵⁷ to reconstruct copy-number profiles from WES data.

RNA sequencing. RNA samples from the 160 tumors of the LICA-FR series were sequenced in several batches with slightly different protocols. RNA samples were enriched for polyadenylated RNA from 5 µg of total RNA, and the enriched samples were used to generate sequencing libraries with the Illumina TruSeq or

Illumina TruSeq Stranded mRNA kit and associated protocol as provided by the manufacturer. Libraries were sequenced by IntegraGen (Evry, France) on an Illumina HiSeq 2000 or 4000 as paired-end 75 or 100 bp reads. Full Fastq files were aligned to the reference human genome hgl9 using TopHat2 58 . Sequencing details for each sample and the parameters used for TopHat2 are indicated in Supplementary Data 1. We removed reads mapping to multiple locations, and we used HTSeq 59 to obtain the number of reads associated to each gene in the Gencode v19 database, restricting to protein-coding genes, pseudogenes, antisense and lincRNAs (n=42540). We used the Bioconductor DESeq2 package 60 to import raw HTSeq counts for each sample into R statistical software and apply variance stabilizing transformation (VST) to the raw count matrix. FPKM scores (number of fragments per kilobase of exon model and millions of mapped reads) were calculated by normalizing the count matrix for the library size and the coding length of each gene. We used the area under the ROC curve (AUC) to identify and remove 2724 genes with a significant batch effect (AUC>0.95 between one sequencing project and others).

Gene fusion detection. Fusions detected by TopHat2 (--fusion-search --fusion-min-dist 2000 --fusion-anchor-length 13 --fusion-ignore-chromosomes chrM) were filtered using the TopHatFusion-post algorithm. We kept only fusions validated by BLAST and with at least 10 split-reads or pairs of reads spanning the fusion event, and we removed fusions identified at least twice in a cohort of 36 normal liver samples.

Gene expression analysis. We used t-distributed stochastic neighbor embedding (t-SNE) to classify HCC based on their gene expression profiles. We selected the 1000 most variably expressed genes, and we used 1 minus the weighted Pearson correlation coefficient as the distance measure. Pairwise Pearson correlation was calculated using the wtd.cors function of the *weights* R package. We used standard deviation substracted by 0.2 as the weight, giving more variable genes greater influence. The resulting distance matrix was used to perform the t-SNE analysis using the R package $Rtsne^{61}$ with default parameters except the following: theta = 0, is_distance = T, pca = F, max_iter = 2000. We used the Bioconductor limma package 62 to test for differential expression between CCN-HCC and other HCC of all genes expressed in at least five samples (FPKM > 0). We applied a q-value threshold of \leq 0.05 to define differentially expressed genes. We used an in-house adaptation of the GSEA method 63 to identify gene sets from the MSigDB v6 database overrepresented among upregulated and downregulated genes.

Viral insertion screening. AAV2 insertions had previously been screened by viral capture and whole exome sequencing in 83 tumors from the LICA-FR cohort¹6. We extended this screen to AAV2 and HBV insertions in all HCC from the LICA-FR cohort using RNA-seq and WES data. In the ICGC-JP cohort, AAV2 and HBV insertions had already been screened using WGS data and were provided by Fujimoto et al.¹¹ In the TCGA cohort, we screened AAV2 and HBV insertions using RNA-seq data from all tumors and WES data from 37 tumors showing viral reads or overexpression of CCNA2 or CCNE1 in RNA-seq data. For each tumor and matched normal sample, the sequence reads were mapped to the AAV2 (AF043303.1) and HBV (X02763, renumbered using the EcoR1 restriction site as the +1) reference genomes using BWA⁵². Read pairs with at least one read aligned on the virus were extracted using samtools⁶⁴, and aligned to a custom reference genome including human chromosomes and virus fasta sequences as pseudo-chromosomes. Tumors with ≥ 6 chimeric reads or read pairs aligned on both the human and viral genomes were further analyzed. All viral insertions were validated by visual inspection on IGV⁶⁵. We used chimeric reads to identify insertion breakpoints at base resolution by mapping sequences on both sides of the junctions. Of the 12 LICA-FR tumors with viral insertions detected in CCNA2 or CCNE1, 7 were previously analyzed by viral capture sequencing¹⁶ and 3 were analyzed by whole genome sequencing. For these 10 tumors, we were able to extract reads covering the full length of the inserted viral genome and to reconstruct the complete human-virus-human chimeric sequence.

Consequences of cyclin A2 alterations on protein structure. All tumors from the LICA-FR series harboring AAV2 or HBV insertions in CCNA2 were analyzed by WGS or viral capture¹⁶ to determine the precise boundaries of viral insertion breakpoints. RNA-seq reads were then aligned on the reconstructed chimeric sequence with TopHat2⁵⁸, and we used Cufflinks v2.2.1⁶⁶ to identify and quantify the different transcripts. We used ElemeNT⁶⁷ to predict transcription initiation sites and Alamut Visual software (Interactive Biosoftware) to identify splicing signals on the chimeric DNA sequence. We used ATGpr⁶⁸ to identify translation initiation sites on abnormal transcripts resulting from viral insertion or gene fusions.

Western blot analysis of cyclin A2 and cyclin E1 proteins. Cell protein extracts were prepared using hot Laemmli buffer (50 mM Tris, pH = 6.8, 2% SDS, 5% glycerol, 2 mM DTT, 2.5 mM EDTA, 2.5 mM EGTA, Protease inhibitor cocktail complete MINI EDTA-free (Roche Applied Science), 1× HALT Phosphatase inhibitor (Perbio), 2 mM Na3VO4 and 10 mM NaF). Protein concentration was assessed using the BCA Protein Assay Kit (Pierce). Western blot analyses were

conducted using the following primary antibodies: CCNA2 N-ter (#211735, Abcam); CCNA2 C-ter (#32386, Abcam), CCNE1 (#33911, Abcam), and β -actin (#4967, Cell Signaling Technology) used as loading control. Proteins of interest were detected using an anti-rabbit IgG horseradish peroxidase–linked secondary antibody (#7074, Cell Signaling Technology) and the ECL Chemiluminescence Western Blotting Detection Kit (GE Healthcare), according to the provided protocol. Signal detection was performed using the ChemiDoc XRS system and the Image Lab software (Bio-Rad). All antibodies were used at 1:1000 dilution except secondary antibody, which was used at 1:2000.

Mutational and rearrangement signature analysis. We used the *Palimpsest* R package⁶⁹ to extract mutational and rearrangement signatures from WGS data. For point mutations, we quantified the contribution of the 10 mutational signatures referenced on the COSMIC website (https://cancer.sanger.ac.uk/cosmic/signatures) and described as operative in liver cancers (signatures 1, 4, 5, 6, 12, 16, 17, 22, 23, 24)²² to each tumor genome. For structural rearrangements, we performed a de novo signature analysis across the 350 HCC genomes from the LICA-FR, TCGA and ICGC-JP datasets. We identified 6 rearrangement signatures that were very similar to the 6 signatures we previously obtained on a smaller dataset²², except that the two initially described deletion signatures were now merged into signature RS5, and that a new signature emerged (RS6, dominated by inversions <10 kb). We used *Palimpsest* to quantify the contribution of each signature to each tumor genome and to estimate the probability of each structural rearrangement being due to each process.

Identification of rearrangement hotspots. We identified 8466 breakpoints attributed to signature RS1 (probability > 0.5) across the 350 HCC genomes from the LICA-FR, TCGA and ICGC-JP datasets. To account for the uneven distribution of rearrangements in the genome, we then modeled the background distribution of breakpoints considering various genomic features as described by Glodzik et al.²7, with some modifications. In short, we divided the genome into 500 kb bins, and we characterized for each bin 17 genomic features likely to influence the density of rearrangements: replication timing in HepG2 cell line (ENCODE²0), highly expressed (top 25%) and low-expressed (remaining 75%) genes in normal liver, average copy-number in the cohort, repetitive sequences (segmental duplications, ALU elements and other repeats), number of N bases in the reference genome, known fragile sites²¹¹, chromatin staining, DNAse hyper-sensitive sites and 6 histone marks (H3K4me1, H3K4me3, H3K9me3, H3K27me3, H3K36me3, H3K27ac) in adult liver (ROADMAP²²). All features were normalized to a mean of 0 and standard deviation of 1 across the bins. The total number of RS1 breakpoints were counted for each bin, and we used negative binomial regression to model the distribution of breakpoints according to the 17 normalized features. The model was trained across 4993 bins after removing bins containing validated cancer genes from the Cancer Gene Census²³ (https://cancer.sanger.ac.uk/census). For signature RS1, the most predictive features of a high breakpoint density were DNAse accessibility, H3K27 acetylation and early replication timing. We then used this model to estimate the expected number of observed breakpoints to the number of expected breakpoints using a one-sided binomial test. Finally, p-values were corrected for multiple testing using Benjamini-Hochberg procedure.

Chromatin state analysis. We used various genomic features to correlate with structural rearrangement density and to better understand the functional consequences of rearrangements. We used replication sequencing (Repli-seq) wavelet-smoothed signals downloaded generated by the ENCODE⁷⁰ consortium for the liver cancer cell line HepG2 to define early and late-replicating regions. We used ChIP-seq data for various histone modifications (H3K4me1, H3K4me3, H3K9me3, H3K27me3, H3K27ac) and chromatin states derived from these modifications in normal adult liver by the ROADMAP consortium⁷². Topologically associated domain (TAD) boundaries in human embryonic stem cells (H1) were provided by Tsirigos et al.⁷⁴

Pan-cancer analysis of structural rearrangement signatures. Somatic structural rearrangements called by a uniform pipeline over 2,606 tumor genomes were downloaded from the ICGC PanCancer Analysis of Whole Genomes (PCAWG) project 23,28,29 . Using *Palimpsest of Pancancer analysis of Whole Genomes (PCAWG) project Pancancer analysis of Whole Genomes (PCAWG) project Pancancer and Weight Pancancer and Weight Pancancer and Weight Pancancer in this data set, including one (RS1-pancan) very similar to the RS1 signature identified in CCN-HCC, and we quantified the contribution of each signature to each tumor genome. In each cancer type, we tested if the presence of \geq 50 rearrangements attributed to signature RS1-pancan was associated with the presence of rearrangement breakpoints < 80 kb from CCNA2 or CCNE1 gene using Fisher's exact test. We analyzed two additional series of breast (n=524)^{30} and ovarian (n=80)^{75} cancer genomes to correlate the amount of RS1-pancan events with CCNE1 amplifications and BRCA1 alterations.*

Clinical associations. We tested the association of CCN-HCC in the LICA-FR cohort with gender, age, etiology, liver fibrosis, Edmonson grade, and vascular invasion using Wilcoxon rank sum test for continuous variables, Fisher's exact test for binary variables and Chi square test for trend for categorical variables. We used

log-rank test and Kaplan–Meier method to compare overall survival between CCN-HCC and others, considering only HCC with curative resection (R0) and excluding patients who died within 3 months after surgery.

Computing codes. The functions used to perform the signatures analysis and associated figures are available as an open-source R package, Palimpsest, available on Github: https://github.com/FunGeST/Palimpsest.

URLs. ICGC data portal, https://dcc.icgc.org/; COSMIC database, https://cancer.sanger.ac.uk/cosmic; ENCODE project, https://www.encodeproject.org; GENCODE v19, http://www.gencodegenes.org/releases/19.html; ROADMAP project, http://www.roadmapepigenomics.org; NCI GDC data portal, https://portal.gdc.cancer.gov.

Data availability

The sequencing data reported in this paper have been deposited to the EGA (European Genome-phenome Archive) database (RNA-seq accession [EGAS00001002879]; WES accessions [EGAS00001000217], [EGAS00001001002] and [EGAS00001003063]; WGS accessions [EGAS00001002408], [EGAS00001000706] and [EGAS00001002888]) and the Inter- national Cancer Genome Consortium (ICGC) data portal (http://dcc.icgc.org/; release 27, April 2018)

Received: 23 July 2018 Accepted: 8 November 2018 Published online: 07 December 2018

References

- European Association for the Study of the Liver & European Organisation for Research and Treatment of Cancer EASL-EORTC clinical practice guidelines: management of hepatocellular carcinoma. J. Hepatol. 56, 908–943 (2012)
- Llovet, J. M. et al. Sorafenib in advanced hepatocellular carcinoma. New Engl. J. Med. 359, 378–390 (2008).
- Bruix, J. et al. Regorafenib for patients with hepatocellular carcinoma who progressed on sorafenib treatment (RESORCE): a randomised, double-blind, placebo-controlled, phase 3 trial. *Lancet* 389, 56–66 (2017).
 Llovet, J. M. & Hernandez-Gea, V. Hepatocellular carcinoma: reasons for
- Llovet, J. M. & Hernandez-Gea, V. Hepatocellular carcinoma: reasons for phase III failure and novel perspectives on trial design. *Clin. Cancer Res.* 20, 2072–2079 (2014).
- Llovet, J. M. et al. Hepatocellular carcinoma. Nat. Rev. Dis. Prim. 2, 16018 (2016).
- Nault, J. C. et al. Telomerase reverse transcriptase promoter mutation is an early somatic genetic alteration in the transformation of premalignant nodules in hepatocellular carcinoma on cirrhosis. *Hepatology* 60, 1983–1992 (2014).
- Guichard, C. et al. Integrated analysis of somatic mutations and focal copynumber changes identifies key genes and pathways in hepatocellular carcinoma. Nat. Genet. 44, 694–698 (2012).
- Fujimoto, A. et al. Whole-genome sequencing of liver cancers identifies etiological influences on mutation patterns and recurrent mutations in chromatin regulators. *Nat. Genet.* 44, 760–764 (2012).
- Ahn, S.-M. et al. Genomic portrait of resectable hepatocellular carcinomas: Implications of RB1 and FGF19 aberrations for patient stratification. Hepatology 60, 1972–1982 (2014).
- Hepatology 60, 1972–1982 (2014).
 Schulze, K. et al. Exome sequencing of hepatocellular carcinomas identifies new mutational signatures and potential therapeutic targets. Nat. Genet. 47, 505–511 (2015).
- Fujimoto, A. et al. Whole-genome mutational landscape and characterization of noncoding and structural mutations in liver cancer. *Nat. Genet.* 48, 500–509 (2016).
- Zucman-Rossi, J., Villanueva, A., Nault, J.-C. & Llovet, J. M. Genetic landscape and biomarkers of hepatocellular carcinoma. *Gastroenterology* 149, 1226–1239.e4 (2015).
- Wang, J., Chenivesse, X., Henglein, B. & Bréchot, C. Hepatitis B virus integration in a cyclin A gene in a hepatocellular carcinoma. *Nature* 343, 555–557 (1990).
- Sung, W.-K. et al. Genome-wide survey of recurrent HBV integration in hepatocellular carcinoma. Nat. Genet. 44, 765–769 (2012).
- Ding, D. et al. Recurrent targeted genes of hepatitis B virus in the liver cancer genomes identified by a next-generation sequencing-based approach. PLoS Genet. 8, e1003065 (2012).
- Nault, J.-C. et al. Recurrent AAV2-related insertional mutagenesis in human hepatocellular carcinomas. Nat. Genet. 47, 1187–1193 (2015).
- Cancer Genome Atlas Research Network. Electronic address: wheeler@bcm. edu & Cancer Genome Atlas Research Network. Comprehensive and

- integrative genomic characterization of hepatocellular carcinoma. Cell 169, 1327-1341.e23 (2017).
- 18. Geley, S. et al. Anaphase-promoting complex/cyclosome-dependent proteolysis of human cyclin A starts at the beginning of mitosis and is not subject to the spindle assembly checkpoint. J. Cell. Biol. 153, 137-148 (2001).
- 19. Fung, T. K., Yam, C. H. & Poon, R. Y. C. The N-terminal regulatory domain of cyclin A contains redundant ubiquitination targeting sequences and acceptor sites. Cell Cycle 4, 1411-1420 (2005).
- 20. Sage, J., Miller, A. L., Pérez-Mancera, P. A., Wysocki, J. M. & Jacks, T. Acute mutation of retinoblastoma gene function is sufficient for cell cycle re-entry. Nature 424, 223-228 (2003).
- Garcia-Cao, I. et al. Systemic elevation of PTEN induces a tumor suppressive metabolic state. *Cell* **149**, 49–62 (2012). Letouzé, E. et al. Mutational signatures reveal the dynamic interplay of risk
- factors and cellular processes during liver tumorigenesis. Nat. Commun. 8,
- Li, Y. et al. Patterns of structural variation in human cancer. Preprint at https://www.biorxiv.org/content/early/2017/08/27/181339, https://doi.org/ 10.1101/181339 (2017).
- Lee, J. A., Carvalho, C. M. B. & Lupski, J. R. A. DNA replication mechanism for generating nonrecurrent rearrangements associated with genomic disorders. Cell 131, 1235-1247 (2007)
- 25. Hastings, P. J., Ira, G. & Lupski, J. R. A microhomology-mediated breakinduced replication model for the origin of human copy number variation. PLoS Genet. 5, e1000327 (2009).
- 26. Carvalho, C. M. B. et al. Inverted genomic segments and complex triplication rearrangements are mediated by inverted repeats in the human genome. Nat. Genet. 43, 1074-1081 (2011).
- 27. Glodzik, D. et al. A somatic-mutational process recurrently duplicates germline susceptibility loci and tissue-specific super-enhancers in breast cancers. Nat. Genet. 49, 341-348 (2017).
- Campbell, P. J., Getz, G., Stuart, J. M., Korbel, J. O. & Stein, L. D. Pan-cancer analysis of whole genomes. Preprint at https://www.biorxiv.org/content/early/ 2017/07/12/162784, https://doi.org/10.1101/162784 (2017).
- Wala, J. A. et al. Selective and mechanistic sources of recurrent rearrangements across the cancer genome. Preprint at https://www.biorxiv. org/content/early/2017/09/14/187609, https://doi.org/10.1101/187609 (2017).
- Nik-Zainal, S. et al. Landscape of somatic mutations in 560 breast cancer whole-genome sequences. Nature 534, 47-54 (2016).
- Waszak, S. M. et al. Germline determinants of the somatic mutation landscape in 2,642 cancer genomes. Preprint at https://www.biorxiv.org/content/early/2017/11/01/208330, https://doi.org/10.1101/208330 (2017).
- 32. Macheret, M. & Halazonetis, T. D. Intragenic origins due to short G1 phases underlie oncogene-induced DNA replication stress. Nature 555, 112-116
- 33. Schlacher, K., Wu, H. & Jasin, M. A distinct replication fork protection pathway connects Fanconi anemia tumor suppressors to RAD51-BRCA1/2. Cancer Cell 22, 106-116 (2012).
- Pathania, S. et al. BRCA1 haploinsufficiency for replication stress suppression
- in primary cells. *Nat. Commun.* 5, 5496 (2014). Willis, N. A. et al. Mechanism of tandem duplication formation in BRCA1mutant cells. Nature 551, 590-595 (2017).
- Forment, J. V. & O'Connor, M. J. Targeting the replication stress response in cancer. Pharmacol. Ther. https://doi.org/10.1016/j.pharmthera.2018.03.005 (2018)
- Menghi, F. et al. The tandem duplicator phenotype as a distinct genomic configuration in cancer. Proc. Natl Acad. Sci. USA 113, E2373–E2382 (2016).
- Lord, C. J. & Ashworth, A. PARP inhibitors: synthetic lethality in the clinic. Science 355, 1152-1158 (2017)
- 39. O'Connor, M. J. Targeting the DNA damage response in cancer. Mol. Cell 60, 547-560 (2015).
- Toledo, L. I. et al. A cell-based screen identifies ATR inhibitors with synthetic lethal properties for cancer-associated mutations. Nat. Struct. Mol. Biol. 18, 721-727 (2011)
- 41. Honeyman, J. N. et al. Detection of a recurrent DNAJB1-PRKACA chimeric transcript in fibrolamellar hepatocellular carcinoma. Science 343, 1010-1014 (2014).
- Gao, Q. et al. Driver fusions and their implications in the development and treatment of human cancers. Cell Rep. 23, 227-238.e3 (2018).
- Conner, E. A. et al. Dual functions of E2F-1 in a transgenic mouse model of liver carcinogenesis. Oncogene 19, 5054-5062 (2000).
- Ladu, S. et al. E2F1 inhibits c-Myc-driven apoptosis via PIK3CA/Akt/mTOR and COX-2 in a mouse model of human liver cancer. *Gastroenterology* 135, 1322-1332 (2008).
- Kramara, J., Osia, B. & Malkova, A. Break-induced replication: the where, the why, and the how. Trends Genet. 34, 518-531 (2018).
- 46. Costantino, L. et al. Break-induced replication repair of damaged forks induces genomic duplications in human cells. Science 343, 88-91 (2014).

- 47. Smith, C. E., Llorente, B. & Symington, L. S. Template switching during breakinduced replication. Nature 447, 102-105 (2007)
- Saini, N. et al. Migrating bubble during break-induced replication drives conservative DNA synthesis. *Nature* **502**, 389–392 (2013).
- Cancer Genome Atlas Research Network. Integrated genomic analyses of ovarian carcinoma. Nature 474, 609-615 (2011).
- Etemadmoghadam, D. et al. Synthetic lethality between CCNE1 amplification and loss of BRCA1. Proc. Natl Acad. Sci. USA 110, 19489-19494 (2013).
- Sanchez-Vega, F. et al. Oncogenic signaling pathways in The Cancer Genome Atlas. Cell 173, 321-337.e10 (2018).
- Li, H. & Durbin, R. Fast and accurate short read alignment with Burrows-Wheeler transform. Bioinformatics 25, 1754-1760 (2009).
- McKenna, A. et al. The Genome Analysis Toolkit: A MapReduce framework for analyzing next-generation DNA sequencing data. Genome Res. 20, 1297-1303 (2010).
- 54. DePristo, M. A. et al. A framework for variation discovery and genotyping using next-generation DNA sequencing data. Nat. Genet. 43, 491-498 (2011).
- Chen, X. et al. Manta: rapid detection of structural variants and indels for germline and cancer sequencing applications. Bioinformatics 32, 1220-1222
- Nik-Zainal, S. et al. The life history of 21 breast cancers. Cell 149, 994-1007
- Olshen, A. B., Venkatraman, E. S., Lucito, R. & Wigler, M. Circular binary segmentation for the analysis of array-based DNA copy number data Biostatistics 5, 557-572 (2004).
- Kim, D. et al. TopHat2: accurate alignment of transcriptomes in the presence of insertions, deletions and gene fusions. Genome Biol. 14, R36 (2013).
- Anders, S., Pyl, P. T. & Huber, W. HTSeq-a Python framework to work with high-throughput sequencing data. *Bioinformatics* 31, 166–169 (2015). Love, M. I., Huber, W. & Anders, S. Moderated estimation of fold change and
- dispersion for RNA-seq data with DESeq2. Genome Biol. 15, 550 (2014).
- van der Maaten, L. & Hinton, G. Visualizing data using t-SNE. J. Mach. Learn. Res. 9, 2579-2605 (2008).
- Ritchie, M. E. et al. limma powers differential expression analyses for RNA-
- sequencing and microarray studies. *Nucleic Acids Res.* **43**, e47 (2015). Subramanian, A. et al. Gene set enrichment analysis: a knowledge-based approach for interpreting genome-wide expression profiles. Proc. Natl Acad. Sci. USA 102, 15545-15550 (2005).
- Li, H. et al. The sequence alignment/Map format and SAMtools. *Bioinformatics* **25**, 2078–2079 (2009).
- Robinson, J. T. et al. Integrative genomics viewer. Nat. Biotechnol. 29, 24-26
- Trapnell, C. et al. Differential gene and transcript expression analysis of RNAseq experiments with TopHat and Cufflinks. Nat. Protoc. 7, 562-578 (2012).
- Sloutskin, A. et al. ElemeNT: a computational tool for detecting core promoter elements. Transcription 6, 41-50 (2015).
- Nishikawa, T., Ota, T. & Isogai, T. Prediction whether a human cDNA sequence contains initiation codon by combining statistical information and similarity with protein sequences. Bioinformatics 16, 960-967 (2000).
- Shinde, J. et al. Palimpsest: an R package for studying mutational and structural variant signatures along clonal evolution in cancer. *Bioinformatics*. https://doi.org/10.1093/bioinformatics/bty388 (2018).
- ENCODE Project Consortium. An integrated encyclopedia of DNA elements in the human genome. Nature 489, 57-74 (2012).
- Bignell, G. R. et al. Signatures of mutation and selection in the cancer genome. Nature 463, 893-898 (2010).
- Roadmap Epigenomics Consortium. et al. Integrative analysis of 111 reference human epigenomes. Nature 518, 317-330 (2015).
- Futreal, P. A. et al. A census of human cancer genes. Nat. Rev. Cancer 4, 177-183 (2004).
- 74. Gong, Y. et al. Stratification of TAD boundaries reveals preferential insulation of super-enhancers by strong boundaries. Nat. Commun. 9, 542 (2018).
- 75. Patch, A.-M. et al. Whole-genome characterization of chemoresistant ovarian cancer. Nature 521, 489-494 (2015).

Acknowledgements

We thank Hidewaki Nakagawa for fruitful discussions and providing TERT promoter mutation data for the ICGC-JP series. We thank Rameen Beroukhim and Joachim Weischenfeldt for helping us access ICGC structural variant tables, and Aristotelis Tsirigos for providing topologically associated domain boundaries. We thank Tatiana Popova and Céline Vallot for critical discussion of the results. We thank the principal investigators of the liver cancer TCGA (Lewis Roberts, David Wheeler) and ICGC-JP (Tatsuhiro Shibata, Hidewaki Nakagawa) projects, and the ICGC consortium as a whole for providing the high quality data sets used in this study. We thank all the clinician surgeons and pathologists who have participated to this work: Jean Saric, Christophe Laurent, Laurence Chiche, Brigitte Le Bail, Claire Castain (CHU Bor deaux), Alexis Laurent, Daniel Cherqui, Daniel Azoulay (CHU Henri Mondor, Créteil,

APHP), Marianne Ziol, Nathalie Ganne-Carrié and Pierre Nahon (Jean Verdier Hospital, Bondy, APHP). We also thank the Réseau national CRB Foie (BB-0033-0085), the tumor banks of CHU Bordeaux (BB-0033-00036), Jean Verdier Hospital (APHP) and CHU Henri Mondor (APHP) for contributing to the tissue collection. This work was supported by INCa within the ICGC project, MUTHEC project (INCa translationnel PRTK2014), France Génomique, Cancéropole Ile de France (ExhauTrans project), ITMO Cancer AVIESAN (Alliance Nationale pour les Sciences de la Vie et de la Santé, National Alliance for Life Sciences & Health) within the framework of the Cancer Plan ("HTE program-HetColi network" and "Cancer et environnement program"), BPI France (ICE project), ANRS and the French Liver Biobanks network – INCa, BB-0033-00085, Hepatobio bank. The group is supported by the Ligue Nationale Contre le Cancer (Equipe Labellisée), Labex OncoImmunology (investissement d'avenir), Coup d'Elan de la Fondation Bettencourt-Shueller, the SIRIC CARPEM and Fondation Mérieux. QB and LM are supported by a fellowship from the HOB doctoral school and the ministry of Education and Research, TLB is supported by an "Attractivite IDEX" fellowship from IUH and CP is supported by a doctoral fellowship funded by ANRS.

Author contributions

J.Z-R. and E.L. conceived and directed the research. Q.B., L.M., C.P., S.I., J.Z-R., and E.L. designed the study and wrote the manuscript. C.P., L.M., G.C., and T.L-B. performed the experiments. Q.B., L.M., C.P., I.M., T.L-B., S.I., J.Z-R., and E.L. analyzed and interpreted the data. D.B., V.M., and J-E.D. generated whole-genome sequencing data. Q.B., L.M., C. P., V.R., J.S., E.T., D.B., V.M. S.I., and E.L. performed bioinformatics and statistical analysis. J-C.N., G.A., A.D-V, P.B-S., O.S., J-E.B., and J.C. provided essential biological resources and collected clinical data. All authors approved the final manuscript and contributed to critical revisions to its intellectual context.

Additional information

Supplementary Information accompanies this paper at https://doi.org/10.1038/s41467-018-07552-9.

Competing interests: The authors declare no competing interests.

Reprints and permission information is available online at http://npg.nature.com/ reprintsandpermissions/

Publisher's note: Springer Nature remains neutral with regard to jurisdictional claims in published maps and institutional affiliations.



Open Access This article is licensed under a Creative Commons Attribution 4.0 International License, which permits use, sharing,

adaptation, distribution and reproduction in any medium or format, as long as you give appropriate credit to the original author(s) and the source, provide a link to the Creative Commons license, and indicate if changes were made. The images or other third party material in this article are included in the article's Creative Commons license, unless indicated otherwise in a credit line to the material. If material is not included in the article's Creative Commons license and your intended use is not permitted by statutory regulation or exceeds the permitted use, you will need to obtain permission directly from the copyright holder. To view a copy of this license, visit http://creativecommons.org/licenses/by/4.0/.

© The Author(s) 2018

IV DISCUSSION

1. Identification of new driver structural rearrangements

Using innovative approaches integrating WGS and RNAseq data, I was able to unravel several new driver alterations, both in HCA and HCC. These alterations are the result of genomic rearrangements and can be separated in two categories. First, I identified gene fusions that alter the protein structure of specific driver genes. Second, I was able to highlight "regulatory rearrangements" events, whose alteration involve a change in transcription level or a change in post-transcriptional regulation.

1.1. Gene fusions altering protein structure

During my masters 2 internship, I set up a pipeline to identify gene fusions from the large RNAseq collection of HCC and HCA tumor samples available in the lab. This work allowed me to characterize new recurrent fusions in HCA and HCC during my PhD.

First I found recurrent fusions involving CCNA2 or FRK oncogenes downstream various partner genes, respectively at the origin of CCN-HCC and inflammatory HCA development. The particularity of these fusions is that they involve the loss of regulatory protein domains, leading to more stable or constitutively active proteins. In the case of CCNA2 fusions, chimeric transcripts only include untranslated regions of partner genes upstream the exons 3 to 8 of CCNA2. In silico identification of translation starting sites indicated an alternative Kozak sequence at Methionine 158 of CCNA2, leading to the accumulation of a truncated CCNA2 protein lacking negative regulatory domains, which was confirmed by Western blot. CCNA2 protein accumulation leads to premature S phase entry and replicative stress characteristic of CCN-HCC tumors. In IHCAs, FRK fusions also involve different partner genes in 5'. Chimeric transcripts contain translated regions from the partner genes but lack FRK's SH2 and SH3 regulatory domains that auto-inhibit the protein kinase domain of FRK. The oncogenic effect of those fusions is thus induced by the lack of regulatory domains of FRK resulting in a constitutively activated protein able to trigger JAK/STAT pathway. Consequently, expression data showed that in both CCNA2 and FRK fusions, the level of the transcript is not significantly altered in tumors harboring respective gene fusions.

Gene fusions can also reveal inactivating SVs leading to the disruption of tumor suppressors. Recently, I contributed to the characterization of a new HCC subgroup harboring mixed features with fibrolamellar carcinomas (FLC), a rare histological subtype

of HCC (Hirsch *et al.*, 2020) (Article 5: Annex 3). This subgroup is similar to FLC, enriched in fibrotic tumors without underlying liver disease. However, whereas FLC tumors are triggered by the specific *PRKACA-DNAJB1* fusions, this subgroup was characterized by biallelic *BAP1* (BRCA1-associated protein 1) inactivation. Most *BAP1* alterations were mutations, but I also identified two tumors with gene fusions involving *BAP1*. The first tumor harbored an inversion leading to an out of frame fusion between *DAG1* (exons 1-2) and *BAP1* (exons 13-17). The second tumor harbored a complex balanced translocation involving 3 regions of chromosomes 2 and 3, resulting in i) a frame-shift fusion of *RAB3GAP1* (exons 1-23) with *BAP1* (exons 5-17) and ii) a truncated exons 1 to 3 of *BAP1*, placed upstream *LINC01460* gene (Article 5: Annex 3 Sup.Fig.6). Thus, both rearrangements lead to the inactivation of *BAP1*. Importantly, BAP1-HCC are older and with a poorer prognosis than FLC tumors, so the identification of this subgroup has clinical implications.

1.2. Gene fusions inducing the overexpression of oncogenes

In addition to protein structure, gene fusions can alter the expression of partner genes, in particular when their baseline expression is very different. During my PhD, I identified recurrent fusions involving highly expressed genes upstream oncogenes, leading to their massive overexpression.

In IHCA, *ROS1* gene is recurrently activated by this mechanism. *ROS1*, encoding a receptor tyrosine kinase activating several signaling pathways related to cell proliferation, is normally poorly expressed in hepatocytes. I identified recurrent fusions involving various highly expressed liver genes (*APOB* n=1; *PLG* n=5, *RBP4* n=2), upstream exons 33-35 of *ROS1*. These events induce the high expression of a chimera containing exons of both genes. However, as the predicted transcript is in phase, the kinase domain of ROS1 protein is still functional. In addition to the increased expression, *ROS1* is a transmembrane protein, and the relocation of the protein from the membrane to the cytoplasm could also be involved in the constitutive activation of the JAK/STAT pathway in these tumors.

I also identified one case of CCN-HCC resulting from a gene fusion between the highly expressed *ERRFI1* gene and *CCNE1*. Because the chimeric transcript only includes untranslated exon 1 of *ERRFI1*, it will be translated using the same Kozak starting site as the wild-type *CCNE1* transcript, leading to an overexpression of the normal cyclin E1

protein. This fusion is an example of *promoter hijacking*, like the recurrent *INHBE-GLI1* fusions identified earlier in the lab (Nault *et al.*, 2017), where only the promoter and 5'UTR of a highly expressed genes is fused to an oncogene, leading to the overexpression of the full length oncogenic protein, without any part of the 5' partner gene.

1.3. Structural rearrangements altering regulatory sequences

Although gene fusions identification from RNAseq is a powerful tool in cancer genomics, some structural variations affect only the regulatory sequences of cancer genes, without the existence of a chimeric transcript. By integrating WGS and RNAseq data, as well as epigenetic features from public databases, I could identify new driver events involving regulatory sequences in liver cancers.

In CCN-HCC, I identified recurrent enhancer hijacking events leading to the activation of *CCNE1*. Translocations lead to juxtapose *CCNE1* promoter with enhancer-rich chromatin areas located close to highly expressed liver genes (*RAPH1*, *CYB5A* and *ERGIC1*), leading to massive over-expression of *CCNE1* transcript. In addition, replication stress-induced structural rearrangements, in particular templated insertion cycles (T.I.C.), lead to frequent enhancer hijacking of *TERT* as secondary events in CCN-HCC. *TERT* enhancer hijacking was demonstrated using an integrated analysis of SV breakpoints from WGS, with the annotation of chromatin features such as H3K27ac chromatin immunoprecipitation sequencing (ChIP-Seq) signal and chromatin states in adult liver (Roadmap Epigenomics Consortium *et al.*, 2015) (Article 4: Sup.Fig.10). All tumors with *TERT* enhancer hijacking display a massive overexpression of the transcript (Article 4: Sup.Fig.11).

The last level of transcript expression regulation is post-transcriptional. In inflammatory adenomas, I identified a new mechanism of JAK/STAT pathway activation. In two IHCA characterized by a massive overexpression of *IL6* transcript, WGS revealed structural rearrangements (one inversion, one deletion) leading to the loss of regulatory sequences in the 3'UTR region of *IL6*. The lost 3'UTR part in the 2 tumors contain multiple mRNA-destabilizing elements, highly conserved and responsible for the short half-life of *IL6* transcripts (Paschoud *et al.*, 2006). Moreover, in murine models, those regions were shown to be targeted by Zc3h12a, an RNase responsible of immune response modulation by regulating mRNA decay (Matsushita *et al.*, 2009). Disruption of *IL6* 3'UTR region

induces a tremendous overexpression that is the consequence of impaired degradation of the transcript rather than increased transcription.

To conclude, this work allowed us to update the landscape of driver alterations in liver cancer with various new driver genes and mechanisms of activation. However, the complexity and diversity of cancer genomics is becoming evident as increasingly sophisticated sequencing technologies are developed. Consequently, others mechanisms of liver tumorigenesis remain to be explored, such as alterations impacting the 3D conformation of the chromatin.

2. Rearrangement signatures in HCC

The development of a computational tool for structural rearrangement signature analysis (Palimpsest, Article 3) allowed me to identify 6 rearrangement signatures in HCC (RS1 to RS6, Article 4). We unraveled the molecular cause of signature RS1: replication stress induced by CCNA2/E1 activation. However, the molecular cause of the remaining signatures remains to be established. Besides, these signatures can be operative in a small proportion of the tumors (e.g. 7% for CCN-HCC displaying high RS1 contribution). Thus, it is important to continue exploring rearrangement signatures in larger HCC cohorts. Recently, I integrated SV data from 616 liver tumor samples, from my laboratory (French cohort, n=190), TCGA (North-American cohort, n=53) and ICGC (Japanese cohorts LIRI-JP, n=258; LINC-JP, n=28 and Chinese cohort LICA-CN, n=87) series. Using Palimpsest package, I was able to extract an extended set of 8 rearrangement signatures (RS) operating with different intensities in each tumor and leading to extreme SV phenotypes in subsets of HCC (Figure 25) This larger cohort revealed 2 new signatures compared to the 6 RS described in Article 4. The RS1 (short-duplications), RS2 (long-duplications), RS4 (mixed, non-clustered events) and RS6 (inversions) from Article 4 remained unchanged; however, RS3 and RS5 were subdivided into two signatures, respectively. I then examined correlations between each signature and various driver alterations.

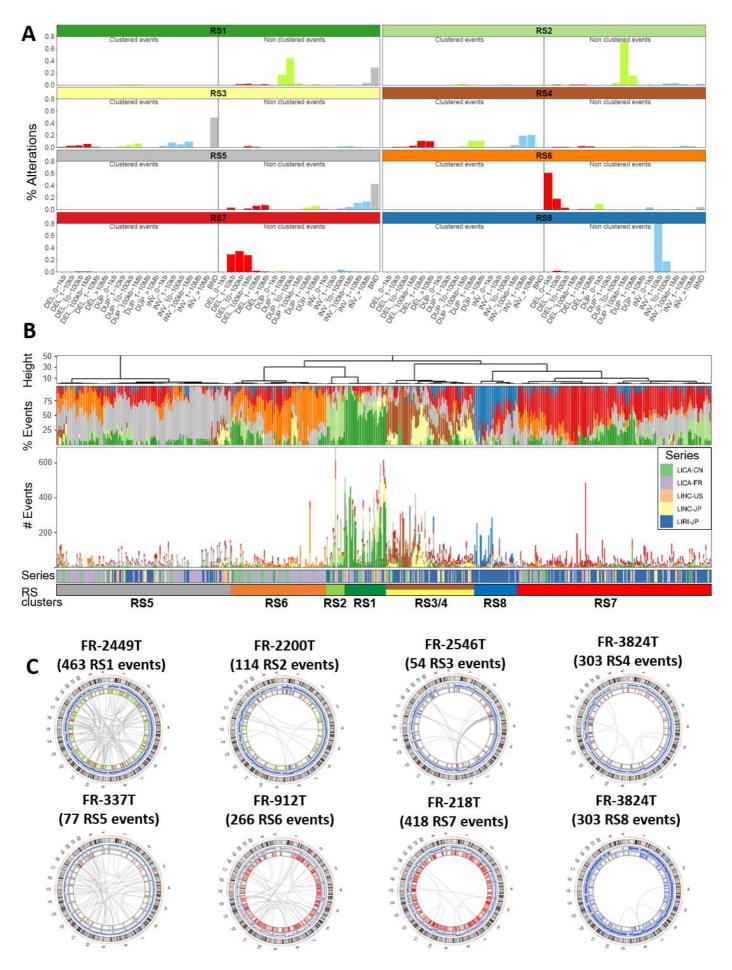


Figure 25: Summary of rearrangement signature results in 616 HCC samples. A: Barplots representing the 8 rearrangement signatures extracted by NMF and characterized by specific category of rearrangements seen in subgroups of tumors. B: From top to bottom: Hierarchical clustering using cosine distance from number of SV associated to each tumor; Proportion of SV related to each RS per sample; Number of SV related to each RS per sample; Series of the sample (PCAWG project IDs are given); Manually defined cluster of signature, based on the hierarchical clustering. Signatures are operating at different intensities in each tumor with some signatures characterized by a higher number of generated rearrangements (ie: RS1). C: Circos plots of representative tumors of each RS. Circle heatmap represent duplications, deletions and inversions, respectively in green, red and blue. Grey arcs represent inter-chromosomal translocations. Blue line track represents LRR. In those examples, the corresponding signature mainly represents the global exposure of those tumors.

Signatures RS1 and RS2 are dominated by tandem duplications of respectively short (1-100Kb) and large size (100Kb-1Mb), RS1 is the signature of replication stress driven by CCNA2/E1 activation that we described in Article 4. We validated the association with CCNA2/E1 activating events in each cohort of our meta-series, including the Chinese cohort that had not been studied before. In addition to tandem duplications, RS1 displays frequent inter-chromosomal translocations corresponding to template insertion cycles, that will be described in more details in the next section. By contrast, signature RS2 is only characterized by tandem duplications. Like signature RS1, this signature is highly active in a small subset of HCC (4.4% tumors with ≥40 RS2 events). However, we have not found any significant molecular association that could indicate the molecular cause for this signature. Interestingly, phenotypes of large duplication have been seen in prostate and ovary tumors harboring a CDK12 inactivating mutation, respectively named the tandem duplicator phenotype in prostate cancer (duplication median size = 1.3Mb) (Viswanathan et al., 2018) and the tandem duplicator-plus phenotype in ovary cancer (duplication median size = 3Mb) (Popova et al., 2016). However, RS2 median duplication size (around 270Kb) is not consistent with these phenotypes, additionally, *CDK12* mutation was not associated with RS2 signature in HCC.

Signatures RS3 and RS4 are characterized by clustered rearrangements. RS3 inter-chromosomal translocations involves clustered and intra-chromosomal rearrangements smaller than 1Mb. RS4 involves large (>1Mb) intra-chromosomal rearrangements without inter-chromosomal translocations (Figure 25A). Visualization of SV clusters together with CNA profiles at the chromosome level revealed that RS3 and RS4 are representative of chromoplexy and chromothripsis, respectively (Figure 26). Indeed, RS3-altered tumors displayed clusters of structural variations on various chromosomes, interconnected by inter-chromosomal translocations and associated with copy number fluctuations (Figure 26A top). RS4-exposed tumors displayed clusters of intrachromosomal rearrangements inducing a characteristic 2 copy-number state, consistent with chromothripsis description (Figure 26A middle). Interestingly, RS3 and RS4 frequently co-occur in the same tumors (Figure 26A bottom), consistent with recent work from the PCAWG showing that half of chromothripsis events are co-localized with other complex genomic alterations (Cortés-Ciriano *et al.*, 2020). Many evidence suggest that chromothripsis might occur before or after additional events of complex rearrangements, such as BFB cycles that have been identified as a predisposing factor for chromothripsis (Rausch *et al.*, 2012; Li *et al.*, 2014; Nones *et al.*, 2014; Maciejowski *et al.*, 2015). Both RS3 and RS4 activities were enriched in *TP53*-mutated HCC (Wilcoxon p-value: 1.0x10⁻³ and 1.6x10⁻¹², respectively) (Figure 26B), suggesting that those complex alterations are the consequences of genome instability induced by *TP53* inactivation, as already described for chromothripsis in medulloblastoma (Rausch *et al.*, 2012).

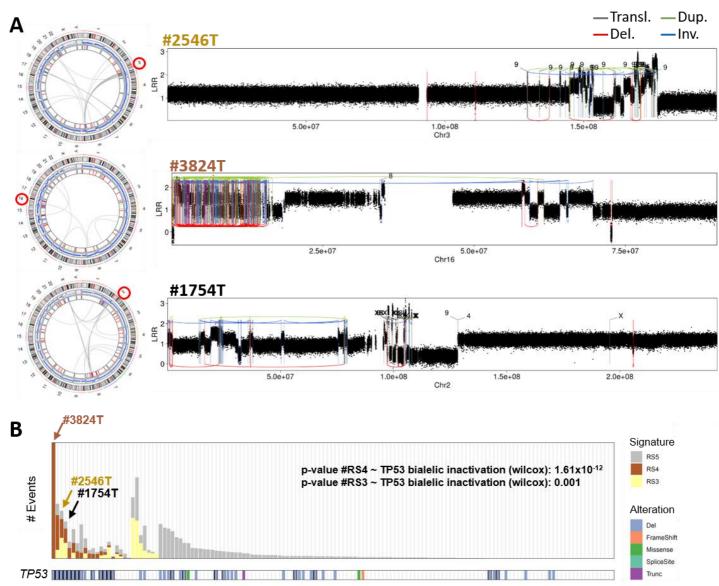


Figure 26: A: From top to bottom, circos plot and a representative chromosome (indicated with a red circle on the circos plot) are display for three tumors. The first one is characterized by lots of RS3 SV, associated to chromoplexy, which is altering chromosomes 3 and 9 of this tumor. The second tumor is highly enriched in RS4 events, and harbor an event of chromothripsis localized at the chr16p region. Finally, on the bottom is exemplified a tumor harboring, on a single chromosome, both chromothripsis and chromoplexy, inducing this presence of RS3 and RS4 in some tumors. B: Barplot representing the number of SV associated to RS3, RS4 and RS5 in each tumor of the French HCC cohort, the heatmap on the bottom indicate TP53 alterations. Black squared indicated bi-allelic inactivation of TP53. Association p-value between the number of RS3 and RS4 alterations is respectively indicated (Wilcoxon test)

In particular, tumors from African patients exposed to aflatoxin B1 displayed high contributions of RS3 and RS4. Aflatoxin B1 exposure induces a particular mutational signature (COSMIC signature 24) leading to a specific hotpot of *TP53* mutations (R249S) (Schulze, Imbeaud, Letouzé *et al.*, 2015). These tumors illustrate a complex relationship between risk factors, mutational signatures and driver genes: aflatoxin B1 exposure induces *TP53* mutations by mutational signature 24, favoring the occurrence of chromothripsis and chromoplexy events.

RS5 signature is dominated by non-clustered translocations and intrachromosomal rearrangements of various lengths. This signature is operative at low intensity in a large proportion of the tumors and does not contribute to a particular extreme phenotype (Figure 25B, 26B). Visual inspection of characteristic rearrangements of this signature revealed either isolated structural variations or complex rearrangements not clustered enough to be associated to RS3 or RS4. Thus, RS5 may correspond to the inherent rearrangements accumulating stochastically during cell divisions.

Signatures RS6 and RS7 were associated to deletions of respectively focal (<1Kb) and large size (1Kb to 1Mb) and were highly active in a small subset of HCC (1.0% of tumors with \geq 40 RS6 events, 5.8% of tumors with \geq 40 RS7 events). Unfortunately, even if those signatures were extremely active in some tumors, no significant association with etiological or molecular features was identified. However, RS6 is very similar to a breast cancer signature of short deletion (Figure 18, RS5) that was found to be associated with bi-allelic *BRCA2* inactivation (Nik-Zainal *et al.*, 2016). Interestingly, the tumor FR912T harboring the most RS6 alterations (Figure 25C) has a rare *BRCA2* germline frame-shift mutation, coupled with a somatic loss of second wild-type allele. This tumor is also characterized by a high mutational burden of COSMIC SBS3 (Single Base Substitution signature 3) and ID8 (small Insertions and Deletions signature 8) signature, consistent with homologous recombination deficiency (Nik-Zainal *et al.*, 2016). Thus, RS6 may highlight rare HCC with homologous recombination deficiencies, which needs to be confirmed in larger cohorts.

Signature RS8 is new to this analysis and is characterized by a large number of focal inversions distributed all along the genome of some tumors (Figure 25C). Surprisingly, this signature was only detected in the LIRI-JP cohort from the Riken research center in Japan. Further investigations are needed to determine if it corresponds

to a true biological phenotype, e.g. related to a specific exposure to local mutagens, or to a technical artifact in this series.

Overall, driver alterations have been identified associated with signatures RS1 (*CCNA2/E1*), RS3 (*TP53*), RS4 (*TP53*) and possibly RS6 (*BRCA2*). The molecular cause of other signatures remains to be found.

3. In-depth characterization of the RS1 signature

3.1. RS1 as a replication stress signature in HCC

RS1 signature is characteristic of CCN-HCC, driven by *CCNA2/E1* activation (Figure 25B, 25C top-left), that display an accumulation of hundreds of tandem duplications and template insertion cycles. We interpreted RS1 as a signature of replication stress in HCC because i) cyclins A2 and E1 promote S phase entry and progression, and cyclin E1 activation was shown to induce replication stress, ii) CCN-HCC display a transcriptional activation of ATR response to replication stress pathway and iii) RS1 breakpoints are strongly enriched in early-replicated regions. In addition, recent works suggest that RS1 alterations may result from replication machinery defects, and more precisely break induced replication mechanism:

- First, a recent study showed that *CCNE1* activation in U2OS cells leads to a shortened G1 phase, early S phase entry and firing of normally silenced replication origins in regions containing highly expressed genes, prone to collapse and associated with DNA double-strand break (DSB) formation (Macheret and Halazonetis, 2018).
- Secondly, DSB occurring when replication fork collapses are handled and repaired by the break-induced replication (BIR) repair mechanism (Malkova, 2018).
- In a budding yeast model of replication stress induced by cyclin E overexpression, BIR was shown to be required for progression through cell cycle while inducing focal duplications (<200Kb) (Costantino *et al.*, 2014).
- Additionally, template switching of the replication machinery may occur following BIR involvement in DSB, inducing complexes chromosome rearrangements (Lee,

Carvalho and Lupski, 2007; Smith, Llorente and Symington, 2007; Hastings, Ira and Lupski, 2009).

Thus, RS1 enrichment in early-replicated, highly expressed regions is consistent with a BIR mechanism. In addition, the nature of RS1 rearrangements (tandem duplications and templated insertion cycles) is consistent with a replication-based mechanism in which the DNA polymerase at a stalled replication fork would switch template, replicate one or more other regions and move back to the original template were the replication machinery stalled in the first place, generating a duplication of the involved regions (Lee, Carvalho and Lupski, 2007; Hastings, Ira and Lupski, 2009; Carvalho *et al.*, 2011; Li *et al.*, 2020).

We also investigated the prevalence of RS1 signature in other cancers. To do so, we applied our rearrangement signature framework to the PCAWG pan-cancer cohort of WGS. This analysis revealed a signature RS1-pancan (similar to RS1), that was highly active in some liver, breast and ovarian cancers. However, the association with *CCNA2/E1* activation was specific to the liver. By contrast, RS1 was significantly associated with *BRCA1* inactivation in breast and ovarian cancers. Despite sharing this RS1-pancan signature of short tandem duplication and T.I.C., *CCNA2/E1*-altered liver tumors and *BRCA1*-altered breast and ovary tumors display slightly different features (Article 4: Fig 6b-f):

- The number of RS1-pancan rearrangements is higher in *CCNA2*-activated HCC (median = 269) than in *CCNE1*-activated HCC (137) and *BRCA1*-altered breast (132) and ovarian (159) cancers.
- Tandem duplications are larger in *CCNE1*-activated HCC (median = 39 kb) than in *CCNA2*-activated HCC (22 kb), and smaller in *BRCA1*-altered breast (9 kb) and ovarian (10 kb) cancers.
- Duplication and translocation breakpoints are strongly enriched in early-replicated regions in CCN-HCC as compared with other HCC, but not in *BRCA1*-altered as compared with other breast and ovarian cancers.

BRCA1 is known to be involved in the response to replication stress (Schlacher, Wu and Jasin, 2012; Pathania *et al.*, 2014). Its inactivation leads to tandem duplication formation at stalled forks by a replication restart-bypass mechanism, terminated by end joining or

by microhomology-mediated template switching, with extension of the stalled leading strand by a migration bubble mechanism similar to BIR (Willis *et al.*, 2017). Cyclin A2/E1 activation in HCC and *BRCA1* inactivation in breast and ovarian cancers may thus converge towards a similar rearrangement signature, with specificities reflecting the different ways by which these genetic alterations induce replication stress or modulate response to it (Article 4: Fig 6g). Indeed, rearrangements induced by cyclin activation in liver or *BRCA1* inactivation in breast and ovary cancers are initiated by replication fork collapse that will be processed by different repair mechanism, leading to similar signature of rearrangements.

Interestingly, *CCNE1* amplifications are seen in various cancer types, particularly breast and ovary cancers (Sanchez-Vega *et al.*, 2018). However, those alterations do not induce RS1 phenotype in those tumors (Article 4: Fig 6b-c). This fact could be explained by different reasons:

- First, cell types are very different, as adult hepatocytes are quiescent, rarely divide and may thus be particularly sensitive to replication stress.
- Second, CCNE1 activation in HCC is the consequence of insertional mutagenesis or enhancer hijacking, rather than amplification as it's the case in other cancers.
 Those mechanism of activation could have different functional consequences.
- Finally, viral insertions and SV activating *CCNA2/E1* genes in HCC are early events triggering hepato-carcinogenesis as they occur in patients without underlying liver disease and in absence of other oncogenic early events such as *CTNNB1* or *TERTp* mutations. On the other hand, *CCNE1* amplification may occur later in breast and ovary, not leaving enough time for RS1-pancan rearrangements to accumulate.

3.2. In-depth characterization of RS1 rearrangements by longread optical mapping

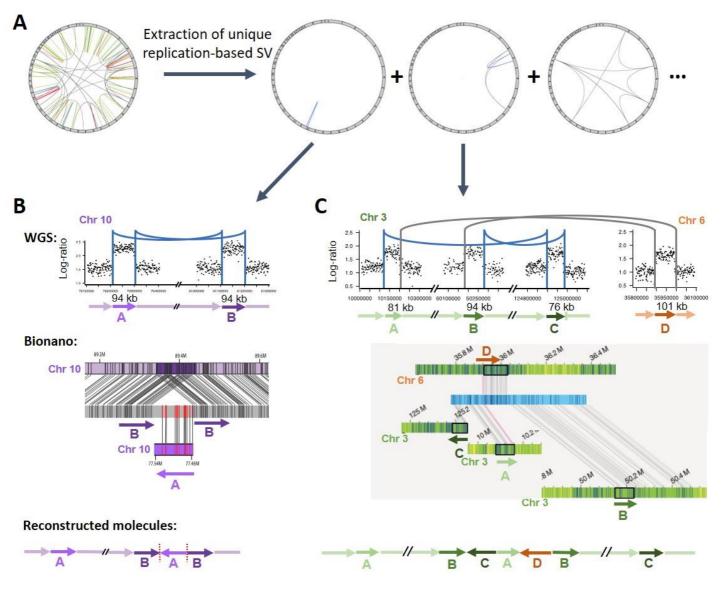
Replication-based mechanisms are more and more described as a major source of complex rearrangements in cancers (Lee, Carvalho and Lupski, 2007; Hastings, Ira and Lupski, 2009; Carvalho *et al.*, 2011; Li *et al.*, 2020). These rearrangements, like templated

insertion cycles, have been proposed based on the abnormal junctions and copy-number changes identified in WGS data, but their existence cannot be formally demonstrated with short-read sequencing. Besides, short read data do not allow to reconstruct the precise molecule resulting from complex rearrangements, as several scenarios are often equally possible [Article 4: Fig.5]. Thus, new approaches allowing the analysis of long sequences are necessary to formally demonstrate the existence of such events and their role in cancer development.

To elucidate in detail the replication stress signature RS1, we analyzed 4 tumors (2 CCN-HCC and 2 other HCC) with Bionano's optical mapping. This approach involves labeling high-molecular-weight DNA with fluorescent agents targeting specific sequences distributed on the human genome with an average inter-marker distance of 5 kb. Images of these long molecules are then captured in nanochannels by Saphyr Chip's technology, allowing simultaneous analysis of hundreds of thousands of DNA molecules. These images are processed by dedicated algorithms that recognize the "barcodes" of fluorescent markers, map each molecule to the human genome reference and identify structural variants in comparison with matched normal samples (Chan, 2018). With this approach, we obtained a genome coverage between 275X and 325X from molecules longer than 150 kb. This data allowed us to demonstrate, for the first time, the existence of T.I.C. that we had predicted from short-read data (Figure 27).

First, I developed a computational framework to extract templated insertion cycles from WGS data, by integrating abnormal junctions and copy-number gains (Figure 27A). Then, optical mapping data corresponding to T.I.C. regions was analyzed using both SV called from optical mapping technology and visual inspection of molecules of interest. Different patterns of T.I.C. were defined depending on the genomic location where the complex rearrangement is hosted (acceptor region) and the orientation of the fragments (donor regions). Intra-chromosomal T.I.C. may appear as pairs of inversions (Figure 27B) or deletion+duplication depending on fragment orientation. Inter-chromosomal T.I.C. may involve two or more (Figure 27C) regions from different chromosomes stitched together within an acceptor locus. Finally, complex events often involve a combination of

intra- and inter-chromosomal T.I.C. We are now characterizing in detail the proportion of each type of T.I.C. in our CCN-HCC series.



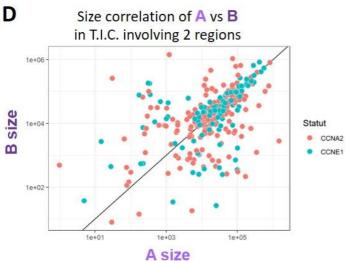


Figure 27: A: Abnormal junction from short-read WGS SV calling was integrated with focal copy-number gains to extract individual events of replication-based rearrangements. B: Log-ratio profiles with inversion in blue and schematized involved fragments A and B corresponding to an intra-chromosomal T.I.C. (top). Optical mapping representation supporting the presence of a molecule where A region is inserted between two copies of B region (middle). Reconstructed molecule corresponding to the rearrangement, where B locus is the host of the T.I.C. C. Same representation for a T.I.C. involving 4 regions located on chromosomes 3 and 6. In this case, the B region on the chromosome 3 is demonstrated to host the complex alteration that occurred in a single catastrophic event triggered by replication stress. D: Scatterplot of size between region A and region B (in panel B example) for each individual T.I.C. involving 2 regions in the 2 CCN-HCC analyzed with Bionano technology. The with x=y curve is represented in black.

Strikingly, the size of segments involved in a same intra- or inter-chromosomal T.I.C. is highly correlated (Figure 27D). Functional studies are required to explain this association, which may be due to the precise replication timing at which rearrangements occur, the speed of the replication machinery at the first breakpoint location, or the BIR mechanism itself.

In addition to the demonstration and characterization of T.I.C., optical mapping data, will allow me to automatically detect for each T.I.C. the host genomic region in which initial stalling occurred, and the inserted segment(s) to which template switching occurred during BIR. I will analyze these regions to better understand the properties favoring replication fork blockade as well as the properties of regions to which the replication machinery is switched in order to resolve this blockade. For example, a recent paper shows that double-strand breaks associated with replication stress tend to occur next to long A-T tracts (Tubbs et al., 2018). It has also been shown, in cellular models, that activation of Cyclin E1 induces early initiation of replication at ectopic origins in the vicinity of highly expressed genes (Macheret and Halazonetis, 2018). Thus, the perspectives for this project are to analyze in detail the location of hundreds of rearrangements induced by replicative stress in CCN-HCC to identify (epi)genomic parameters (A-T sequences, ectopic initiation sites, gene expression, chromatin opening...) favoring the occurrence of RS1 breakpoints. Moreover, the analysis and comparison of sequences on each side of abnormal junctions will allow me to better understand the affinity properties (ie: micro-homologies) leading to the association of distant regions of the genome with each other following the "jumps" of the replication machinery.

4. Clinical implications of the results

4.1. Liver cancer therapeutic options

Past decade improvement of sequencing technologies made consequent contribution to the understanding of liver cancer biology landscape. However this knowledge has not been translated into clinical practices (Sia and Llovet, 2017). Indeed, the current algorithm for management of HCC only take in account the BCLC including only clinical features (Figure 23). Furthermore, only 2 drugs are used in first line and 3 in

second line, a very limited panel of therapeutic options regarding the complexity of liver cancer genomics. In order to improve HCC and HCA patient management, two axes need to be explored. Firstly, precision medicine requires predictive biomarkers to identify specific molecular subgroups of cancer. Secondly, novel targeted therapy development is required to fit each tumor subgroup biology (De Gramont *et al.*, 2015).

4.2. Identification of biomarkers of IHCA or CCN-HCC

In this project, I identified recurrent rearrangements triggering inflammatory adenomas (Articles 1 & 2) and cyclin-driven hepatocellular carcinomas (Article 4). Different biomarkers can be proposed to identify patients with IHCA or CCN-HCC. First, some alterations induce massive overexpression of driver genes. For example, *CCNE1* activation in CCN-HCC, *ROS1* and *IL6* activation in IHCA may be detected at diagnosis using RNAseq or low cost high throughput technology such as Fluidigm real-time qPCR system. RNAseq is also an interesting clinical tool in addition to WES to detect recurrent fusions in liver tumors (*FRK*, *ROS1* and *INHBE-GLI1* fusions in HCA, *CCNE1* and *CCNA2* in HCC, *PRKACA-DNAJB1* in fibrolamellar carcinoma). However, it may be difficult to obtain biological samples from advanced stage HCC. Analysis of DNA and mRNA from circulating tumor cells or cell-free plasma in liquid biopsies is thus a promising option to guide therapeutic decision in the future (Mullard, 2016; Xu *et al.*, 2017).

Finally, rearrangement signatures are emerging as useful biomarkers in cancer. For example, defective HR in *BRCA1*-mutated breast cancers induces specific signature of mutations and SVs (Nik-Zainal *et al.*, 2012; Alexandrov, Nik-Zainal, Wedge, Aparicio, *et al.*, 2013). These tumors respond well to Poly(ADP-ribose) polymerase (PARP) inhibitors (olaparib), the first clinically approved drugs designed to exploit synthetic lethality by decreasing the DNA Damage Response (DRR) in cancer cells (Crown, O'Shaughnessy and Gullo, 2012; Kanjanapan, Lheureux and Oza, 2017; Lord and Ashworth, 2017). Thus, HR deficiency mutational signatures are useful biomarkers to identify patients eligible to PARP inhibitors (Chopra *et al.*, 2020). Similarly, RS1 signature is an excellent biomarker of CCN-HCC that may be exploited for therapy.

4.3. Tailored therapy for CCN-HCC and IHCA tumors

Concerning hepatocellular carcinomas, this work allowed me to characterize a homogeneous subgroup of HCC driven by the activation of *CCNA2* or *CCNE1* genes,

representing 7% of HCCs. CCN-HCC are usually large tumors of poor prognosis. However, they share molecular characteristics, in particular high proliferation and replication stress, that could be used as therapeutic opportunities for these patients (Forment and O'Connor, 2018).

- First, chemotherapies affecting actively dividing cells may be a good option for these highly proliferative tumors with strong overexpression of E2F targets. Duplicator phenotype in breast cancer cell lines or xenografts was identified as a marker of positive chemotherapy response (Menghi *et al.*, 2018). Thus, trans-arterial chemoembolization (TACE) with doxorubicin, cisplatin or epirubisin, normally recommended with intermediate HCC nor eligible for surgery, may be an interesting therapeutic option for CCN-HCC.
- Secondly, as previously introduced, PARP inhibitors have demonstrated benefits in tumors carrying *BRCA1* mutations (Kanjanapan, Lheureux and Oza, 2017). Although CCN-HCC do nots harbor a DNA repair defect, these tumors share with *BRCA1* altered breast and ovarian tumors a similar rearrangement signature (RS1-pancan), hence PARP inhibitors may be an interesting therapeutic option for CCN-HCC.
- Finally, several compounds targeting replication stress response genes such as ATR,
 CHK1 and WEE1 are currently tested in phase I and II trials (Forment and O'Connor,
 2018). Furthermore, CCNE1 overexpression was shown be associated with increased sensitivity to ATR inhibition (Toledo et al., 2011).

To evaluate at large scale, the clinical behavior of CCN-HCC, Barkha Gupta (anatomopathologist in the lab) is testing immunostaining of cyclin A2 and E1, which would allow CCN-HCC screening in the clinic from histological slides, and give us access to large retrospective series. We also started a collaboration with Amaia Lujambio (from Icahn School of Medicine at Mount Sinai, New-York) to set up a murine model of CCN-HCC. Amaia and her team have developed a mouse model of *CCNE1*-activated HCC by hydrodynamic tail injection. We have sequenced the whole genome of a few tumors and I am currently analyzing their profiles to determine if they reproduce the CCN-HCC phenotype. Indeed, accurate pre-clinical models will be crucial to test the different treatment options mentioned above and develop tailored therapy for patients with aggressive CCN-HCC.

Concerning hepatocellular adenomas, this work revealed 3 new driver alterations in the inflammatory HCA subgroup. Even if HCA is a benign tumor, it can be associated with clinical complication such as chronic inflammation or tumor bleeding. Moreover, malignant HCC can develop from a benign HCA tumor. Consequently, molecular characterization is also important for this cancer type and could be used to design drug therapy in future clinical practice. Indeed, *ROS1* fusions can be targeted by crizotinib, a small molecule currently approved by the Food and Drug Administration (FDA) for the treatment of lung cancers (Shaw *et al.*, 2013). Additionally, previous work from my laboratory showed *in cellulo* that dasatinib, a src inhibitor, inhibits JAK/STAT pathway activation due to *FRK* mutations (Pilati *et al.*, 2014). We can then predict that this compound will also be effective in IHCA harboring *FRK* gene fusion. Further analyses must be done to test the proposed targeted therapies associated to driver alteration (Article 2: Fig.5).

V REFERENCES

Abou-Alfa, G. K. *et al.* (2018) 'Cabozantinib in patients with advanced and progressing hepatocellular carcinoma', *New England Journal of Medicine*. doi: 10.1056/NEJMoa1717002.

Agrawal, N. *et al.* (2014) 'Integrated Genomic Characterization of Papillary Thyroid Carcinoma', *Cell.* doi: 10.1016/j.cell.2014.09.050.

Ahn, S. M. *et al.* (2014) 'Genomic portrait of resectable hepatocellular carcinomas: Implications of RB1 and FGF19 aberrations for patient stratification', *Hepatology*. doi: 10.1002/hep.27198.

Alexandrov, L. B., Nik-Zainal, S., Wedge, D. C., Campbell, P. J., *et al.* (2013) 'Deciphering Signatures of Mutational Processes Operative in Human Cancer', *Cell Reports*. doi: 10.1016/j.celrep.2012.12.008.

Alexandrov, L. B., Nik-Zainal, S., Wedge, D. C., Aparicio, S. A. J. R., *et al.* (2013) 'Signatures of mutational processes in human cancer', *Nature*. doi: 10.1038/nature12477.

Alexandrov, L. B. *et al.* (2015) 'Clock-like mutational processes in human somatic cells', *Nature Genetics*. doi: 10.1038/ng.3441.

Alexandrov, L. B. *et al.* (2020) 'The repertoire of mutational signatures in human cancer', *Nature*. doi: 10.1038/s41586-020-1943-3.

Alioto, T. S. *et al.* (2015) 'A comprehensive assessment of somatic mutation detection in cancer using wholegenome sequencing', *Nature Communications*. doi: 10.1038/ncomms10001.

Anstee, Q. M. et al. (2019) 'From NASH to HCC: current concepts and future challenges', *Nature Reviews Gastroenterology and Hepatology*. doi: 10.1038/s41575-019-0145-7.

Armitage, P. and Doll, R. (1954) 'The age distribution of cancer and a multi-stage theory of carcinogenesis', *British Journal of Cancer*. doi: 10.1038/bjc.1954.1.

Ascha, M. S. *et al.* (2010) 'The incidence and risk factors of hepatocellular carcinoma in patients with nonalcoholic steatohepatitis', *Hepatology*. doi: 10.1002/hep.23527.

Aubrey, B. J. *et al.* (2018) 'How does p53 induce apoptosis and how does this relate to p53-mediated tumour suppression?', *Cell Death and Differentiation*. doi: 10.1038/cdd.2017.169.

Audano, P. A. *et al.* (2019) 'Characterizing the Major Structural Variant Alleles of the Human Genome', *Cell.* doi: 10.1016/j.cell.2018.12.019.

Babina, I. S. and Turner, N. C. (2017) 'Advances and challenges in targeting FGFR signalling in cancer', *Nature Reviews Cancer*. doi: 10.1038/nrc.2017.8.

Baca, S. C. *et al.* (2013) 'Punctuated evolution of prostate cancer genomes', *Cell.* Elsevier Inc., 153(3), pp. 666–677. doi: 10.1016/j.cell.2013.03.021.

Bacq, Y. et al. (2003) 'Familial Liver Adenomatosis Associated with Hepatocyte Nuclear Factor 1α Inactivation', Gastroenterology. doi: 10.1016/j.gastro.2003.07.012.

Baron, S. (1996) *Medical Microbiology. 4th edition, University of Texas Medical Branch at Galveston*. doi: NBK8035 [bookaccession].

Basham, K. J. *et al.* (2019) 'A ZNRF3-dependent Wnt/β-catenin signaling gradient is required for adrenal homeostasis', *Genes and Development*. doi: 10.1101/gad.317412.118.

Bedossa, P. *et al.* (2007) 'Evidence for a role of nonalcoholic steatohepatitis in hepatitis C: A prospective study', *Hepatology*. doi: 10.1002/hep.21711.

La Bella, T. *et al.* (2020) 'Adeno-associated virus in the liver: Natural history and consequences in tumour development', *Gut.* doi: 10.1136/gutjnl-2019-318281.

Bender, S. *et al.* (2013) 'Reduced H3K27me3 and DNA Hypomethylation Are Major Drivers of Gene Expression in K27M Mutant Pediatric High-Grade Gliomas', *Cancer Cell.* doi: 10.1016/j.ccr.2013.10.006.

Benjamin, D. et al. (2019) 'Calling Somatic SNVs and Indels with Mutect2', bioRxiv. doi: 10.1101/861054.

Bickmore, W. A. (2013) 'The Spatial Organization of the Human Genome', *Annual Review of Genomics and Human Genetics*. doi: 10.1146/annurev-genom-091212-153515.

Bishop, J. M. (1983) 'Cellular Oncogenes and Retroviruses', *Annual Review of Biochemistry*. doi: 10.1146/annurev.bi.52.070183.001505.

Bishop, J. M. (1987) 'The molecular genetics of cancer', Science. doi: 10.1126/science.3541204.

Bluteau, O. et al. (2002) 'Bi-allelic inactivation of TCF1 in hepatic adenomas', *Nature Genetics*. doi: 10.1038/ng1001.

Boveri, T. (1914) 'Zur Frage der Entstehung Maligner Tumoren [Origin of malignant tumors]', *Gustav Fisher, Jena*. doi: 10.1016/j.yexcr.2012.02.003.

Boyault, S. *et al.* (2007) 'Transcriptome classification of HCC is related to gene alterations and to new therapeutic targets', *Hepatology*. doi: 10.1002/hep.21467.

Bray, F. *et al.* (2018) 'Global cancer statistics 2018: GLOBOCAN estimates of incidence and mortality worldwide for 36 cancers in 185 countries', *CA: A Cancer Journal for Clinicians*. doi: 10.3322/caac.21492.

Bressac, B. *et al.* (1991) 'Selective G to T mutations of p53 gene in hepatocellular carcinoma from southern Africa', *Nature*. doi: 10.1038/350429a0.

BROWN, J. R. and THORNTON, J. L. (1957) 'Percivall Pott (1714-1788) and chimney sweepers' cancer of the scrotum', *British journal of industrial medicine*. doi: 10.1136/oem.14.1.68.

Bruix, J. *et al.* (2017) 'Regorafenib for patients with hepatocellular carcinoma who progressed on sorafenib treatment (RESORCE): a randomised, double-blind, placebo-controlled, phase 3 trial', *The Lancet*. doi: 10.1016/S0140-6736(16)32453-9.

Bruix, J. and Llovet, J. M. (2002) 'Prognostic prediction and treatment strategy in hepatocellular carcinoma', *Hepatology*. doi: 10.1053/jhep.2002.32089.

Brunet, J. P. et al. (2004) 'Metagenes and molecular pattern discovery using matrix factorization', *Proceedings of the National Academy of Sciences of the United States of America*. doi: 10.1073/pnas.0308531101.

Brunner, T. B. *et al.* (2019) 'The Role of Stereotactic Body Radiotherapy (SBRT) in Locally Advanced Hepatocellular Carcinoma Versus Transarterial Chemoembolization (TACE): A Prospective, Non-Randomized Observational Trial (HERACLES)', *International Journal of Radiation Oncology*Biology*Physics*. doi: 10.1016/j.ijrobp.2019.06.2058.

Bryan, H. K. *et al.* (2013) 'The Nrf2 cell defence pathway: Keap1-dependent and -independent mechanisms of regulation', *Biochemical Pharmacology*. doi: 10.1016/j.bcp.2012.11.016.

Calderaro, J. *et al.* (2013) 'Molecular characterization of hepatocellular adenomas developed in patients with glycogen storage disease type i', *Journal of Hepatology*. doi: 10.1016/j.jhep.2012.09.030.

Campbell, P. J. et al. (2020) 'Pan-cancer analysis of whole genomes', *Nature*. doi: 10.1038/s41586-020-1969-6.

Carvalho, C. M. B. *et al.* (2011) 'Inverted genomic segments and complex triplication rearrangements are mediated by inverted repeats in the human genome', *Nature Genetics*. doi: 10.1038/ng.944.

Chan, S. (2018) *Copy Number Variants Methods and Protocols Methods in Molecular Biology 1833*. Available at: http://www.springer.com/series/7651.

Chedid, M. F. (2017) 'Nonalcoholic Steatohepatitis: The Second Leading Indication for Liver Transplantation in the USA', *Digestive Diseases and Sciences*. doi: 10.1007/s10620-017-4724-6.

Chen, C. L. *et al.* (2010) 'Impact of replication timing on non-CpG and CpG substitution rates in mammalian genomes', *Genome Research*. doi: 10.1101/gr.098947.109.

Chen, X. *et al.* (2016) 'Manta: Rapid detection of structural variants and indels for germline and cancer sequencing applications', *Bioinformatics*, 32(8), pp. 1220–1222. doi: 10.1093/bioinformatics/btv710.

Chopra, N. *et al.* (2020) 'Homologous recombination DNA repair deficiency and PARP inhibition activity in primary triple negative breast cancer.', *Nature communications*. Springer US, 11(1), p. 2662. doi: 10.1038/s41467-020-16142-7.

Cilloni, D. and Saglio, G. (2012) 'Molecular pathways: BCR-ABL', *Clinical Cancer Research*. doi: 10.1158/1078-0432.CCR-10-1613.

Cleary, S. P. *et al.* (2013) 'Identification of driver genes in hepatocellular carcinoma by exome sequencing', *Hepatology*. doi: 10.1002/hep.26540.

Collisson, E. A. *et al.* (2014) 'Comprehensive molecular profiling of lung adenocarcinoma: The cancer genome atlas research network', *Nature*. doi: 10.1038/nature13385.

Cortes-Ciriano, I. *et al.* (2014) 'Proteochemometric modeling in a Bayesian framework', *Journal of Cheminformatics*, 6(1), pp. 1–16. doi: 10.1186/1758-2946-6-35.

Cortés-Ciriano, I. *et al.* (2020) 'Comprehensive analysis of chromothripsis in 2,658 human cancers using whole-genome sequencing', *Nature Genetics.* doi: 10.1038/s41588-019-0576-7.

Costantino, L. *et al.* (2014) 'Break-induced replication repair of damaged forks induces genomic duplications in human cells', *Science*. doi: 10.1126/science.1243211.

Craig Venter, J. et al. (2001) 'The sequence of the human genome', Science. doi: 10.1126/science.1058040.

Cremer, T. and Cremer, C. (2001) 'Chromosome territories, nuclear architecture and gene regulation in mammalian cells', *Nature Reviews Genetics*. doi: 10.1038/35066075.

Cremer, T. and Cremer, M. (2010) 'Chromosome territories.', *Cold Spring Harbor perspectives in biology*. doi: 10.1101/cshperspect.a003889.

Crown, J., O'Shaughnessy, J. and Gullo, G. (2012) 'Emerging targeted therapies in triple-negative breast cancer', *Annals of Oncology*. doi: 10.1093/annonc/mds196.

Cunningham, F. et al. (2019) 'Ensembl 2019', Nucleic Acids Research. doi: 10.1093/nar/gky1113.

Das, K. *et al.* (2018) 'Protease-activated receptor 2 promotes actomyosin dependent transforming microvesicles generation from human breast cancer', *Molecular Carcinogenesis*. doi: 10.1002/mc.22891.

De, S. and Michor, F. (2011) 'DNA replication timing and long-range DNA interactions predict mutational landscapes of cancer genomes', *Nature Biotechnology*. doi: 10.1038/nbt.2030.

Degasperi, A. *et al.* (2020) 'A practical framework and online tool for mutational signature analyses show intertissue variation and driver dependencies', *Nature Cancer*. doi: 10.1038/s43018-020-0027-5.

Delattre, O. et al. (1992) 'Gene fusion with an ETS DNA-binding domain caused by chromosome translocation in human tumours', *Nature*. doi: 10.1038/359162a0.

Delattre, O. *et al.* (1994) 'The ewing family of tumors — a subgroup of small-round-cell tumors defined by specific chimeric transcripts', *New England Journal of Medicine*. doi: 10.1056/NEJM199408043310503.

Denicola, G. M. *et al.* (2011) 'Oncogene-induced Nrf2 transcription promotes ROS detoxification and tumorigenesis', *Nature*. doi: 10.1038/nature10189.

Dinh, T. A. *et al.* (2017) 'Comprehensive analysis of the Cancer Genome Atlas reveals a unique gene and noncoding RNA signature of fibrolamellar carcinoma', *Scientific Reports*. doi: 10.1038/srep44653.

Dixon, J. R. *et al.* (2012) 'Topological domains in mammalian genomes identified by analysis of chromatin interactions', *Nature*. doi: 10.1038/nature11082.

El-Khoueiry, A. B. *et al.* (2017) 'Nivolumab in patients with advanced hepatocellular carcinoma (CheckMate 040): an open-label, non-comparative, phase 1/2 dose escalation and expansion trial', *The Lancet.* doi: 10.1016/S0140-6736(17)31046-2.

Erstad, D. J. and Cusack, J. C. (2014) 'Mutational analysis of merkel cell carcinoma', *Cancers*. doi: 10.3390/cancers6042116.

Farazi, P. A. *et al.* (2003) 'Differential impact of telomere dysfunction on initiation and progression of hepatocellular carcinoma', *Cancer Research*.

Ferlay, J. et al. (2019) 'Estimating the global cancer incidence and mortality in 2018: GLOBOCAN sources and methods', *International Journal of Cancer*. doi: 10.1002/ijc.31937.

Forment, J. V. and O'Connor, M. J. (2018) 'Targeting the replication stress response in cancer', *Pharmacology and Therapeutics*. doi: 10.1016/j.pharmthera.2018.03.005.

Fredriksson, N. J. *et al.* (2014) 'Systematic analysis of noncoding somatic mutations and gene expression alterations across 14 tumor types', *Nature Genetics*. doi: 10.1038/ng.3141.

Friemel, J. et al. (2019) 'Characterization of HCC mouse models: Towards an etiology-oriented subtyping approach', *Molecular Cancer Research*. doi: 10.1158/1541-7786.MCR-18-1045.

Froissart, R. *et al.* (2011) 'Glucose-6-phosphatase deficiency', *Orphanet Journal of Rare Diseases*. doi: 10.1186/1750-1172-6-27.

Fujii, M. *et al.* (2013) 'A murine model for non-alcoholic steatohepatitis showing evidence of association between diabetes and hepatocellular carcinoma', *Medical Molecular Morphology*. doi: 10.1007/s00795-013-0016-1.

Fujimoto, A. *et al.* (2016) 'Whole-genome mutational landscape and characterization of noncoding and structural mutations in liver cancer', *Nature Genetics*. Nature Publishing Group, 48(5), pp. 500–509. doi: 10.1038/ng.3547.

Galuppo, R. et al. (2014) 'Synergistic inhibition of HCC and liver cancer stem cell proliferation by targeting RAS/RAF/MAPK and WNT/ β -Catenin pathways', *Anticancer Research*.

Gao, Q. et al. (2018) 'Driver Fusions and Their Implications in the Development and Treatment of Human Cancers', *Cell Reports*. doi: 10.1016/j.celrep.2018.03.050.

Garsed, D. W. *et al.* (2014) 'The Architecture and Evolution of Cancer Neochromosomes', *Cancer Cell*, 26(5), pp. 653–667. doi: 10.1016/j.ccell.2014.09.010.

Gibcus, J. H. and Dekker, J. (2013) 'The Hierarchy of the 3D Genome', $Molecular\ Cell.$ doi: 10.1016/j.molcel.2013.02.011.

Ginès, P. *et al.* (2016) 'Screening for liver fibrosis in the general population: a call for action', *The Lancet Gastroenterology and Hepatology*. doi: 10.1016/S2468-1253(16)30081-4.

Glodzik, D. *et al.* (2017) 'A somatic-mutational process recurrently duplicates germline susceptibility loci and tissue-specific super-enhancers in breast cancers', *Nature Genetics*. Nature Publishing Group, 49(3), pp. 341–348. doi: 10.1038/ng.3771.

Glover, T. W., Wilson, T. E. and Arlt, M. F. (2017) 'Fragile sites in cancer: More than meets the eye', *Nature Reviews Cancer*. Nature Publishing Group, 17(8), pp. 489–501. doi: 10.1038/nrc.2017.52.

Gómez-González, B. and Aguilera, A. (2019) 'Transcription-mediated replication hindrance: A major driver of genome instability', *Genes and Development*. doi: 10.1101/gad.324517.119.

De Gramont, Armand *et al.* (2015) 'Pragmatic issues in biomarker evaluation for targeted therapies in cancer', *Nature Reviews Clinical Oncology*. doi: 10.1038/nrclinonc.2014.202.

Gudlevičiene, Ž. *et al.* (2015) 'Distribution of human papillomavirus type 16 variants in Lithuanian women with cervical cancer', *Medicina* (*Lithuania*). doi: 10.1016/j.medici.2015.11.005.

Guichard, C. *et al.* (2012) 'Integrated analysis of somatic mutations and focal copy-number changes identifies key genes and pathways in hepatocellular carcinoma', *Nature Genetics*. doi: 10.1038/ng.2256.

Guo, L., Zhang, H. and Chen, B. (2017) 'Nivolumab as Programmed Death-1 (PD-1) Inhibitor for Targeted Immunotherapy in Tumor', *Journal of Cancer*. doi: 10.7150/jca.17144.

Hanahan, D. and Weinberg, R. A. (2000) 'The hallmarks of cancer', *Cell*, 100, pp. 57–70. doi: 10.1007/s00262-010-0968-0.

Hanahan, D. and Weinberg, R. A. (2011) 'Hallmarks of cancer: The next generation', Cell. doi: 10.1016/j.cell.2011.02.013.

Hansen, R. S. *et al.* (2010) 'Sequencing newly replicated DNA reveals widespread plasticity in human replication timing', *Proceedings of the National Academy of Sciences of the United States of America*. doi: 10.1073/pnas.0912402107.

Hantschel, O. (2012) 'Structure, Regulation, Signaling, and Targeting of Abl Kinases in Cancer', *Genes and Cancer*. doi: 10.1177/1947601912458584.

Haradhvala, N. J. *et al.* (2016) 'Mutational Strand Asymmetries in Cancer Genomes Reveal Mechanisms of DNA Damage and Repair', *Cell.* doi: 10.1016/j.cell.2015.12.050.

Hastings, P. J., Ira, G. and Lupski, J. R. (2009) 'A microhomology-mediated break-induced replication model for the origin of human copy number variation', *PLoS Genetics*. doi: 10.1371/journal.pgen.1000327.

Hirsch, T. Z. *et al.* (2020) 'BAP1 mutations define a homogeneous subgroup of hepatocellular carcinoma with fibrolamellar-like features and activated PKA', *Journal of Hepatology*. doi: 10.1016/j.jhep.2019.12.006.

Ho, J. *et al.* (2020) 'Detection of CSF1 rearrangements deleting the 3' UTR in tenosynovial giant cell tumors', *Genes Chromosomes and Cancer*. doi: 10.1002/gcc.22807.

Honeyman, J. N. *et al.* (2014) 'Detection of a recurrent DNAJB1-PRKACA chimeric transcript in fibrolamellar hepatocellular carcinoma.', *Science (New York, N.Y.)*, 343(6174), pp. 1010–4. doi: 10.1126/science.1249484.

Howard, B. D. and Tessman, I. (1964) 'Identification of the altered bases in mutated single-stranded DNA', *Journal of Molecular Biology*. doi: 10.1016/s0022-2836(64)80214-x.

Hsu, I. C. *et al.* (1991) 'Mutational hot spot in the p53 gene in human hepatocellular carcinomas', *Nature*. doi: 10.1038/350427a0.

Hu, Z. *et al.* (2015) 'Genome-wide profiling of HPV integration in cervical cancer identifies clustered genomic hot spots and a potential microhomology-mediated integration mechanism', *Nature Genetics*. doi: 10.1038/ng.3178.

Huddleston, J. and Eichler, E. E. (2016) 'An incomplete understanding of human genetic variation', *Genetics*. doi: 10.1534/genetics.115.180539.

Hutchinson, K. E. *et al.* (2013) 'BRAF fusions define a distinct molecular subset of melanomas with potential sensitivity to MEK inhibition', *Clinical Cancer Research*. doi: 10.1158/1078-0432.CCR-13-1746.

Jang, Y. E. *et al.* (2020) 'ChimerDB 4.0: an updated and expanded database of fusion genes', *Nucleic acids research*. doi: 10.1093/nar/gkz1013.

Johnson, R. T. and Rao, P. N. (1970) 'Mammalian cell fusion: Induction of premature chromosome condensation in interphase nuclei', *Nature*. doi: 10.1038/226717a0.

Kan, Z. *et al.* (2013) 'Whole-genome sequencing identifies recurrent mutations in hepatocellular carcinoma', *Genome Research.* doi: 10.1101/gr.154492.113.

Kanjanapan, Y., Lheureux, S. and Oza, A. M. (2017) 'Niraparib for the treatment of ovarian cancer', *Expert Opinion on Pharmacotherapy*. doi: 10.1080/14656566.2017.1297423.

Kato, H. and Sandberg, A. A. (1968) 'Chromosome pulverization in human cells with micronuclei', *Journal of the National Cancer Institute*. doi: 10.1093/jnci/40.1.165.

Kern, J. S. *et al.* (2006) 'Expanding the COL7A1 mutation database: Novel and recurrent mutations and unusual genotype - Phenotype constellations in 41 patients with dystrophic epidermolysis bullosa', *Journal of Investigative Dermatology*. doi: 10.1038/sj.jid.5700219.

Kew, M. C. (2014) 'Hepatic iron overload and hepatocellular carcinoma', *Liver Cancer*. doi: 10.1159/000343856.

Kohno, T. *et al.* (2015) 'Beyond ALK-RET, ROS1 and other oncogene fusions in lung cancer', *Translational Lung Cancer Research*. doi: 10.3978/j.issn.2218-6751.2014.11.11.

Labrune, P. et al. (1997) 'Hepatocellular adenomas in glycogen storage disease type I and III: A series of 43 patients and review of the literature', *Journal of Pediatric Gastroenterology and Nutrition*. doi: 10.1097/00005176-199703000-00008.

Lander, E. S. *et al.* (2001) 'Initial sequencing and analysis of the human genome', *Nature*. doi: 10.1038/35057062.

Laplante, M. and Sabatini, D. M. (2012) 'MTOR signaling in growth control and disease', *Cell.* doi: 10.1016/j.cell.2012.03.017.

Lasorella, A., Sanson, M. and Iavarone, A. (2017) 'FGFR-TACC gene fusions in human glioma', *Neuro-Oncology*. doi: 10.1093/neuonc/now240.

Lawrence, M. S. *et al.* (2013) 'Mutational heterogeneity in cancer and the search for new cancer-associated genes', *Nature*. doi: 10.1038/nature12213.

Lee, D. D. and Seung, H. S. (1999) 'Learning the parts of objects by non-negative matrix factorization', Nature. doi: 10.1038/44565.

Lee, J. A., Carvalho, C. M. B. and Lupski, J. R. (2007) 'A DNA Replication Mechanism for Generating Nonrecurrent Rearrangements Associated with Genomic Disorders', *Cell.* doi: 10.1016/j.cell.2007.11.037.

Lee, M. *et al.* (2017) 'ChimerDB 3.0: An enhanced database for fusion genes from cancer transcriptome and literature data mining', *Nucleic Acids Research*, 45(D1), pp. D784–D789. doi: 10.1093/nar/gkw1083.

Letouzé, E. *et al.* (2017) 'Mutational signatures reveal the dynamic interplay of risk factors and cellular processes during liver tumorigenesis', *Nature Communications*. doi: 10.1038/s41467-017-01358-x.

Li, H. *et al.* (2009) 'The Sequence Alignment/Map format and SAMtools', *Bioinformatics*, 25(16), pp. 2078–2079. doi: 10.1093/bioinformatics/btp352.

Li, Y. *et al.* (2014) 'Constitutional and somatic rearrangement of chromosome 21 in acute lymphoblastic leukaemia', *Nature*. doi: 10.1038/nature13115.

Li, Y. *et al.* (2020) 'Patterns of somatic structural variation in human cancer genomes', *Nature*. doi: 10.1038/s41586-019-1913-9.

Lieberman-Aiden, E. *et al.* (2009) 'Comprehensive mapping of long-range interactions reveals folding principles of the human genome', *Science*. doi: 10.1126/science.1181369.

Lin, J. I. (1983) 'Rudolf Virchow: Creator of Cellular Pathology', *Laboratory Medicine*. doi: 10.1093/labmed/14.12.791.

Liu, Y. and Wu, F. (2010) 'Global burden of Aflatoxin-induced hepatocellular carcinoma: A risk assessment', *Environmental Health Perspectives*. doi: 10.1289/ehp.0901388.

Llovet, J. M. *et al.* (2008) 'Sorafenib in advanced hepatocellular carcinoma.', *The New England journal of medicine*, 359(4), pp. 378–90. doi: 10.1056/NEJMoa0708857.

Llovet, J. M. *et al.* (2016) 'Hepatocellular carcinoma', *Nature Reviews Disease Primers*. doi: 10.1038/nrdp.2016.18.

Lok, A. S. *et al.* (2009) 'Incidence of Hepatocellular Carcinoma and Associated Risk Factors in Hepatitis C-Related Advanced Liver Disease', *Gastroenterology*. doi: 10.1053/j.gastro.2008.09.014.

Lord, C. J. and Ashworth, A. (2017) 'PARP inhibitors: Synthetic lethality in the clinic', *Science*. doi: 10.1126/science.aam7344.

Luke, J. J. *et al.* (2019) 'WNT/b-catenin pathway activation correlates with immune exclusion across human cancers', *Clinical Cancer Research*. doi: 10.1158/1078-0432.CCR-18-1942.

Ly, P. and Cleveland, D. W. (2017) 'Rebuilding Chromosomes After Catastrophe: Emerging Mechanisms of Chromothripsis', *Trends in Cell Biology*. Elsevier Ltd, 27(12), pp. 917–930. doi: 10.1016/j.tcb.2017.08.005.

Macheret, M. and Halazonetis, T. D. (2018) 'Intragenic origins due to short G1 phases underlie oncogene-induced DNA replication stress', *Nature*. Nature Publishing Group. doi: 10.1038/nature25507.

Maciejowski, J. *et al.* (2015) 'Chromothripsis and Kataegis Induced by Telomere Crisis', *Cell.* doi: 10.1016/j.cell.2015.11.054.

Malkova, A. (2018) 'Break-Induced Replication: The Where, The Why, and The How', *Trends in Genetics*. doi: 10.1016/j.tig.2018.04.002.

Marnef, A., Cohen, S. and Legube, G. (2017) 'Transcription-Coupled DNA Double-Strand Break Repair: Active Genes Need Special Care', *Journal of Molecular Biology*. doi: 10.1016/j.jmb.2017.03.024.

Martincorena, I. *et al.* (2017) 'Universal Patterns of Selection in Cancer and Somatic Tissues', *Cell.* doi: 10.1016/j.cell.2017.09.042.

Matsumoto, Y. *et al.* (2011) 'Perception of oral contraceptives among women of reproductive age in Japan: A comparison with the USA and France', *Journal of Obstetrics and Gynaecology Research*. doi: 10.1111/j.1447-0756.2010.01461.x.

Matsushita, K. et al. (2009) 'Zc3h12a is an RNase essential for controlling immune responses by regulating

mRNA decay', Nature. doi: 10.1038/nature07924.

Matthews, B. J. and Waxman, D. J. (2018) 'Computational prediction of CTCF/ cohesin-based intra-TAD loops that insulate chromatin contacts and gene expression in mouse liver', *eLife*. doi: 10.7554/eLife.34077.001.

McClintock, B. (1939) 'The Behavior in Successive Nuclear Divisions of a Chromosome Broken at Meiosis', *Proceedings of the National Academy of Sciences*. doi: 10.1073/pnas.25.8.405.

McGlynn, K. A. *et al.* (2001) 'International trends and patterns of primary liver cancer', *International Journal of Cancer*. doi: 10.1002/ijc.1456.

McGregor, D. B. *et al.* (1998) 'An IARC evaluation of polychlorinated dibenzo-p-dioxins and polychlorinated dibenzofurans as risk factors in human carcinogenesis', in *Environmental Health Perspectives*. doi: 10.2307/3433830.

Menghi, F. *et al.* (2018) 'The Tandem Duplicator Phenotype Is a Prevalent Genome-Wide Cancer Configuration Driven by Distinct Gene Mutations', *Cancer Cell.* doi: 10.1016/j.ccell.2018.06.008.

Merle, P. et al. (2019) 'Doxorubicin-loaded nanoparticles for patients with advanced hepatocellular carcinoma after sorafenib treatment failure (RELIVE): a phase 3 randomised controlled trial', *The Lancet Gastroenterology and Hepatology*. doi: 10.1016/S2468-1253(19)30040-8.

Mermel, C. H. *et al.* (2011) 'GISTIC2.0 facilitates sensitive and confident localization of the targets of focal somatic copy-number alteration in human cancers', *Genome Biology*. doi: 10.1186/gb-2011-12-4-r41.

Möller, E. *et al.* (2008) 'Molecular identification of COL6A3-CSFI fusion transcripts in tenosynovial giant cell tumors', *Genes Chromosomes and Cancer*. doi: 10.1002/gcc.20501.

Morganella, S. *et al.* (2016) 'The topography of mutational processes in breast cancer genomes', *Nature Communications*. doi: 10.1038/ncomms11383.

Mudduluru, G. *et al.* (2011) 'Curcumin regulates miR-21 expression and inhibits invasion and metastasis in colorectal cancer', *Bioscience Reports*. doi: 10.1042/BSR20100065.

Mukherjee, S. (2010) *The emperor of all maladies : a biography of cancer*. Scribner.

Mullard, A. (2016) 'Reining in the supersized Phase I cancer trial', *Nature Reviews Drug Discovery*. doi: 10.1038/nrd.2016.110.

Murnane, J. P. (2012) 'Telomere dysfunction and chromosome instability', *Mutation Research - Fundamental and Molecular Mechanisms of Mutagenesis*. doi: 10.1016/j.mrfmmm.2011.04.008.

Nault, J.-C. *et al.* (2017) 'Molecular Classification of Hepatocellular Adenoma Associates With Risk Factors, Bleeding, and Malignant Transformation', *Gastroenterology*, 152(4), pp. 880-894.e6. doi: 10.1053/j.gastro.2016.11.042.

Nault, J. C. *et al.* (2013) 'High frequency of telomerase reverse-transcriptase promoter somatic mutations in hepatocellular carcinoma and preneoplastic lesions', *Nature Communications*. doi: 10.1038/ncomms3218.

Nault, J. C. *et al.* (2015) 'Recurrent AAV2-related insertional mutagenesis in human hepatocellular carcinomas', *Nature Genetics*. doi: 10.1038/ng.3389.

Nault, J. C. and Letouzé, E. (2019) 'Mutational Processes in Hepatocellular Carcinoma: The Story of Aristolochic Acid', *Seminars in Liver Disease*. doi: 10.1055/s-0039-1685516.

Nault, J. C. and Zucman-Rossi, J. (2016) 'TERT promoter mutations in primary liver tumors', *Clinics and Research in Hepatology and Gastroenterology*. doi: 10.1016/j.clinre.2015.07.006.

Nik-Zainal, S. et al. (2012) 'Mutational processes molding the genomes of 21 breast cancers', Cell. doi:

10.1016/j.cell.2012.04.024.

Nik-Zainal, S. *et al.* (2016) 'Landscape of somatic mutations in 560 breast cancer whole-genome sequences', *Nature*, 534(7605), pp. 47–54. doi: 10.1038/nature17676.

Nones, K. *et al.* (2014) 'Genomic catastrophes frequently arise in esophageal adenocarcinoma and drive tumorigenesis', *Nature Communications*. doi: 10.1038/ncomms6224.

Nora, E. P. *et al.* (2012) 'Spatial partitioning of the regulatory landscape of the X-inactivation centre', *Nature*. doi: 10.1038/nature11049.

Northcott, P. A. *et al.* (2014) 'Enhancer hijacking activates GFI1 family oncogenes in medulloblastoma', *Nature*. doi: 10.1038/nature13379.

O'Keefe, C., McDevitt, M. A. and Maciejewski, J. P. (2010) 'Copy neutral loss of heterozygosity: A novel chromosomal lesion in myeloid malignancies', *Blood*. doi: 10.1182/blood-2009-10-201848.

Papaemmanuil, E. *et al.* (2014) 'RAG-mediated recombination is the predominant driver of oncogenic rearrangement in ETV6-RUNX1 acute lymphoblastic leukemia', *Nature Genetics*. doi: 10.1038/ng.2874.

Paschoud, S. *et al.* (2006) 'Destabilization of Interleukin-6 mRNA Requires a Putative RNA Stem-Loop Structure, an AU-Rich Element, and the RNA-Binding Protein AUF1', *Molecular and Cellular Biology*. doi: 10.1128/mcb.01155-06.

Pathania, S. *et al.* (2014) 'BRCA1 haploinsufficiency for replication stress suppression in primary cells', *Nature Communications*. doi: 10.1038/ncomms6496.

Pilati, C. *et al.* (2014) 'Genomic profiling of hepatocellular adenomas reveals recurrent FRK-activating mutations and the mechanisms of malignant transformation', *Cancer Cell.* doi: 10.1016/j.ccr.2014.03.005.

Plentz, R. R. *et al.* (2007) 'Telomere shortening and inactivation of cell cycle checkpoints characterize human hepatocarcinogenesis', *Hepatology*. doi: 10.1002/hep.21552.

Polak, P. et al. (2014) 'Reduced local mutation density in regulatory DNA of cancer genomes is linked to DNA repair', *Nature Biotechnology*. doi: 10.1038/nbt.2778.

Polak, P. *et al.* (2015) 'Cell-of-origin chromatin organization shapes the mutational landscape of cancer', *Nature*. doi: 10.1038/nature14221.

Popova, T. *et al.* (2009) 'Genome Alteration Print (GAP): A tool to visualize and mine complex cancer genomic profiles obtained by SNP arrays', *Genome Biology*. doi: 10.1186/gb-2009-10-11-r128.

Popova, T. *et al.* (2016) 'Ovarian cancers harboring inactivating mutations in CDK12 display a distinct genomic instability pattern characterized by large tandem duplications', *Cancer Research*. doi: 10.1158/0008-5472.CAN-15-2128.

Raha, D., Hong, M. and Snyder, M. (2010) 'ChIP-Seq: A method for global identification of regulatory elements in the genome', *Current Protocols in Molecular Biology*. doi: 10.1002/0471142727.mb2119s91.

Rausch, T. *et al.* (2012) 'Genome sequencing of pediatric medulloblastoma links catastrophic DNA rearrangements with TP53 mutations', *Cell.* doi: 10.1016/j.cell.2011.12.013.

Rebouissou, S. *et al.* (2016) 'Genotype-phenotype correlation of CTNNB1 mutations reveals different ß-catenin activity associated with liver tumor progression', *Hepatology*. doi: 10.1002/hep.28638.

Reddy, E. P. *et al.* (1982) 'A point mutation is responsible for the acquisition of transforming properties by the T24 human bladder carcinoma oncogene', *Nature*. doi: 10.1038/300149a0.

Reznik, Y. et al. (2004) 'Hepatocyte nuclear factor-1α gene inactivation: Cosegregation between liver

adenomatosis and diabetes phenotypes in two maturity-onset diabetes of the young (MODY)3 families', *Journal of Clinical Endocrinology and Metabolism*. doi: 10.1210/jc.2003-031552.

Rheinbay, E. *et al.* (2020) 'Analyses of non-coding somatic drivers in 2,658 cancer whole genomes', *Nature*. doi: 10.1038/s41586-020-1965-x.

Roadmap Epigenomics Consortium *et al.* (2015) 'Integrative analysis of 111 reference human epigenomes', *Nature.* doi: 10.1038/nature14248.

Rooks, J. B. *et al.* (1977) 'The association between oral contraception and hepatocellular adenoma - a preliminary report', *International Journal of Gynecology and Obstetrics*. doi: 10.1002/j.1879-3479.1977.tb00664.x.

Rosa, I. *et al.* (2010) '585 A FRENCH MULTICENTRIC LONGITUDINAL DESCRIPTIVE STUDY OF HEPATOCELLULAR CARCINOMA MANAGEMENT (THE CHANGH COHORT): PRELIMINARY RESULTS', *Journal of Hepatology*. doi: 10.1016/s0168-8278(10)60587-9.

Rowley, J. D. (1973) 'A new consistent chromosomal abnormality in chronic myelogenous leukaemia identified by quinacrine fluorescence and Giemsa staining', *Nature*. doi: 10.1038/243290a0.

Sabarinathan, R. *et al.* (2016) 'Nucleotide excision repair is impaired by binding of transcription factors to DNA', *Nature*. doi: 10.1038/nature17661.

Sánchez-Osorio, M. et al. (2008) 'Anabolic-androgenic steroids and liver injury', Liver International. doi: 10.1111/j.1478-3231.2007.01579.x.

Sanchez-Vega, F. et al. (2018) 'Oncogenic Signaling Pathways in The Cancer Genome Atlas', Cell. doi: 10.1016/j.cell.2018.03.035.

Sawey, E. T. *et al.* (2011) 'Identification of a Therapeutic Strategy Targeting Amplified FGF19 in Liver Cancer by Oncogenomic Screening', *Cancer Cell.* doi: 10.1016/j.ccr.2011.01.040.

Schlacher, K., Wu, H. and Jasin, M. (2012) 'A Distinct Replication Fork Protection Pathway Connects Fanconi Anemia Tumor Suppressors to RAD51-BRCA1/2', *Cancer Cell*. doi: 10.1016/j.ccr.2012.05.015.

Schubbert, S., Shannon, K. and Bollag, G. (2007) 'Hyperactive Ras in developmental disorders and cancer', *Nature Reviews Cancer*. doi: 10.1038/nrc2109.

Schulze, K., Imbeaud, S., Letouzé, E., Alexandrov, Ludmil B, *et al.* (2015) 'Exome sequencing of hepatocellular carcinomas identifies new mutational signatures and potential therapeutic targets', *Nature Genetics*, 47(5), pp. 505–511. doi: 10.1038/ng.3252.

Schulze, K., Imbeaud, S., Letouzé, E., Alexandrov, Ludmil B., *et al.* (2015) 'Exome sequencing of hepatocellular carcinomas identifies new mutational signatures and potential therapeutic targets', *Nature Genetics*. doi: 10.1038/ng.3252.

Schuster-Böckler, B. and Lehner, B. (2012) 'Chromatin organization is a major influence on regional mutation rates in human cancer cells', *Nature*. doi: 10.1038/nature11273.

Shaw, A. T. *et al.* (2013) 'Crizotinib versus chemotherapy in advanced ALK-positive lung cancer', *New England Journal of Medicine*. doi: 10.1056/NEJMoa1214886.

Sia, D. and Llovet, J. M. (2017) 'Liver cancer: Translating "-omics" results into precision medicine for hepatocellular carcinoma', *Nature Reviews Gastroenterology and Hepatology*. doi: 10.1038/nrgastro.2017.103.

Sikov, W. M. *et al.* (2015) 'Impact of the addition of carboplatin and/or bevacizumab to neoadjuvant onceper-week paclitaxel followed by dose-dense doxorubicin and cyclophosphamide on pathologic complete response rates in stage II to III triple-negative breast cancer: CALGB 40603 (A', *Journal of Clinical Oncology*.

doi: 10.1200/JCO.2014.57.0572.

Sima, J. and Gilbert, D. M. (2014) 'Complex correlations: Replication timing and mutational landscapes during cancer and genome evolution', *Current Opinion in Genetics and Development*. doi: 10.1016/j.gde.2013.11.022.

Sinclair, A., Latif, A. L. and Holyoake, T. L. (2013) 'Targeting survival pathways in chronic myeloid leukaemia stem cells', *British Journal of Pharmacology*. doi: 10.1111/bph.12183.

Singh, D. *et al.* (2012) 'Transforming fusions of FGFR and TACC genes in human glioblastoma', *Science*. doi: 10.1126/science.1220834.

Smith, C. E., Llorente, B. and Symington, L. S. (2007) 'Template switching during break-induced replication', *Nature*. doi: 10.1038/nature05723.

Smyth, M. J. *et al.* (2016) 'Combination cancer immunotherapies tailored to the tumour microenvironment', *Nature Reviews Clinical Oncology*. doi: 10.1038/nrclinonc.2015.209.

Sondka, Z. *et al.* (2018) 'The COSMIC Cancer Gene Census: describing genetic dysfunction across all human cancers', *Nature Reviews Cancer*. doi: 10.1038/s41568-018-0060-1.

Sporn, M. B. and Liby, K. T. (2012) 'NRF2 and cancer: The Good, the bad and the importance of context', *Nature Reviews Cancer*. doi: 10.1038/nrc3278.

Stephens, P. J. *et al.* (2011) 'Massive genomic rearrangement acquired in a single catastrophic event during cancer development', *Cell.* Elsevier Inc., 144(1), pp. 27–40. doi: 10.1016/j.cell.2010.11.055.

Stratton, M. R., Campbell, P. J. and Futreal, P. A. (2009) 'The cancer genome', *Nature*. doi: 10.1038/nature07943.

Sung, W. K. *et al.* (2012) 'Genome-wide survey of recurrent HBV integration in hepatocellular carcinoma', *Nature Genetics*. doi: 10.1038/ng.2295.

Supek, F. and Lehner, B. (2015) 'Differential DNA mismatch repair underlies mutation rate variation across the human genome', *Nature*. doi: 10.1038/nature14173.

Takeuchi, K. *et al.* (2012) 'RET, ROS1 and ALK fusions in lung cancer', *Nature Medicine*. doi: 10.1038/nm.2658.

Toledo, L. I. *et al.* (2011) 'A cell-based screen identifies ATR inhibitors with synthetic lethal properties for cancer-associated mutations', *Nature Structural and Molecular Biology*. doi: 10.1038/nsmb.2076.

Totoki, Y. *et al.* (2014) 'Trans-ancestry mutational landscape of hepatocellular carcinoma genomes', *Nature Genetics*. doi: 10.1038/ng.3126.

Touboul, T. *et al.* (2016) 'Stage-specific regulation of the WNT/β-catenin pathway enhances differentiation of hESCs into hepatocytes', *Journal of Hepatology*. doi: 10.1016/j.jhep.2016.02.028.

Touraine, R. L. *et al.* (1993) 'Hepatic tumours during androgen therapy in Fanconi anaemia', *European Journal of Pediatrics*. doi: 10.1007/BF01955250.

Tubbs, A. *et al.* (2018) 'Dual Roles of Poly(dA:dT) Tracts in Replication Initiation and Fork Collapse', *Cell*, 174(5), pp. 1127-1142.e19. doi: 10.1016/j.cell.2018.07.011.

Viswanathan, S. R. *et al.* (2018) 'Structural Alterations Driving Castration-Resistant Prostate Cancer Revealed by Linked-Read Genome Sequencing', *Cell.* doi: 10.1016/j.cell.2018.05.036.

Wansbrough-Jones, M. H. et al. (1998) 'Prevalence and genotype of hepatitis C virus infection in pregnant women and blood donors in Ghana', *Transactions of the Royal Society of Tropical Medicine and Hygiene*. doi:

10.1016/S0035-9203(98)90887-2.

Watson, J. D. and Crick, F. H. C. (1953) 'Molecular structure of nucleic acids: A structure for deoxyribose nucleic acid', *Nature*. doi: 10.1038/171737a0.

Weber, J. S. *et al.* (2015) 'Toxicities of immunotherapy for the practitioner', *Journal of Clinical Oncology*. doi: 10.1200/JCO.2014.60.0379.

Weinhold, N. *et al.* (2014) 'Genome-wide analysis of noncoding regulatory mutations in cancer', *Nature Genetics*. doi: 10.1038/ng.3101.

Weinstein, L. S. and Shenker, A. (1993) 'G protein mutations in human disease', *Clinical Biochemistry*. doi: 10.1016/0009-9120(93)90109-J.

Weischenfeldt, J. *et al.* (2017) 'Pan-cancer analysis of somatic copy-number alterations implicates IRS4 and IGF2 in enhancer hijacking', *Nature Genetics*, 49(1), pp. 65–74. doi: 10.1038/ng.3722.

Willis, N. A. *et al.* (2017) 'Mechanism of tandem duplication formation in BRCA1-mutant cells', *Nature*. Nature Publishing Group, 551(7682), pp. 590–595. doi: 10.1038/nature24477.

Winter, J. M., Brody, J. R. and Kern, S. E. (2006) 'Multiple-criterion evaluation of reported mutations: A proposed scoring system for the intragenic somatic mutation literature', *Cancer Biology and Therapy*. doi: 10.4161/cbt.5.4.2552.

Witkin, E. M. (1969) 'Ultraviolet-Induced Mutation and DNA Repair', *Annual Review of Microbiology*. doi: 10.1146/annurev.mi.23.100169.002415.

Woodcock, C. L. and Ghosh, R. P. (2010) 'Chromatin higher-order structure and dynamics.', *Cold Spring Harbor perspectives in biology*. doi: 10.1101/cshperspect.a000596.

Wynn, T. A. (2004) 'Fibrotic disease and the TH1/TH2 paradigm', *Nature Reviews Immunology*. doi: 10.1038/nri1412.

Xu, R. H. *et al.* (2017) 'Circulating tumour DNA methylation markers for diagnosis and prognosis of hepatocellular carcinoma', *Nature Materials*. doi: 10.1038/NMAT4997.

Yanai, H. *et al.* (2000) 'The colorectal tumour suppressor APC is present in the NMDA-receptor-PSD-95 complex in the brain', *Genes to Cells.* doi: 10.1046/j.1365-2443.2000.00368.x.

Yang, J. D. and Roberts, L. R. (2010) 'Hepatocellular carcinoma: a global view', *Nature Reviews Gastroenterology & Hepatology*, 7(8), pp. 448–458. doi: 10.1038/nrgastro.2010.100.

Zhang, Y. *et al.* (2018) 'A Pan-Cancer Compendium of Genes Deregulated by Somatic Genomic Rearrangement across More Than 1,400 Cases', *Cell Reports*. ElsevierCompany., 24(2), pp. 515–527. doi: 10.1016/j.celrep.2018.06.025.

Zhu, A. X. *et al.* (2018) 'Pembrolizumab in patients with advanced hepatocellular carcinoma previously treated with sorafenib (KEYNOTE-224): a non-randomised, open-label phase 2 trial', *The Lancet Oncology*. doi: 10.1016/S1470-2045(18)30351-6.

Zhu, A. X. et al. (2019) 'Ramucirumab after sorafenib in patients with advanced hepatocellular carcinoma and increased α -fetoprotein concentrations (REACH-2): a randomised, double-blind, placebo-controlled, phase 3 trial', *The Lancet Oncology*. doi: 10.1016/S1470-2045(18)30937-9.

Zucman-Rossi, J. *et al.* (2006) 'Genotype-phenotype correlation in hepatocellular adenoma: New classification and relationship with HCC', *Hepatology*. doi: 10.1002/hep.21068.

Zucman-Rossi, J. *et al.* (2015) 'Genetic Landscape and Biomarkers of Hepatocellular Carcinoma', *Gastroenterology*, 149(5), pp. 1226–1239. doi: 10.1053/j.gastro.2015.05.061.

VI ANNEXES

1. Annex 1: Supplementary data Article 2

Supplementary material Gut

Supplementary Table 1: List of taqman probes

Gene	Unabbreviated gene name	Taqman probe
RNA18S5	RNA, 18S Ribosomal 5	Hs03928990_g1
FABP1	Fatty Acid Binding Protein 1	Hs00155026_m1
UGT2B7	UDP Glucuronosyltransferase Family 2 Member B7	Hs00426592_m1
CRP	C-Reactive Protein	Hs04183452_g1
SAA2	Serum Amyloid A2	Hs00754237_s1
GLUL	Glutamate-Ammonia Ligase	Hs00374213_m1
LGR5	Leucine Rich Repeat Containing G Protein-Coupled Receptor 5	Hs00173664 m1
PTCH1	Patched 1	Hs00181117_m1
GLI1	Glioma-Associated Oncogene Homolog 1	Hs00171790_m1
HHIP	Hedgehog Interacting Protein	Hs01011015_m1
TNNC1	Troponin C1, Slow Skeletal And Cardiac Type	Hs00896999 g1
FCRLA	Fc Receptor Like A	Hs00262071_m1
PTGDS	Prostaglandin D2 Synthase	Hs00168748_m1
ADGRG3	Adhesion G Protein-Coupled Receptor G3	Hs00416887_m1
ROS1	ROS Proto-Oncogene 1	Hs01090625_m1
FRK	Fyn Related Src Family Tyrosine Kinase	Hs00176619 m1
IL6	Interleukin 6	Hs00985639 m1

Sample #2363T	ption of the 296 IHCA hological_diagn G HCA	Gender Age IH	CA molecular classification	on /utation_CTNNB1_exM	lutation_CTNNB1	ex Mutation_CTNNB1	stype_mutation Cl
#477T	HCA HCA	NA NA F 23	ЫНСА ЫНСА	M	NM NM	NM NM	missense
#1129T #1131T	HCA HCA	F 41 F 31	biHCA biHCA	M	NM NM	NM NM	missense missense
#1275T #1287T	HCA HCA	F 40 NA NA	biHCA biHCA	M	NM NM	NM NM	missense
#2196T	HCA	F 40	biHCA	M	NM	NM	missense
#2809T #2823T	HCA HCA	F 39 F 30	biHCA biHCA	M	NM NM	NM NM	missense missense
#2849T #4058T	HCA HCA	F NA	biHCA biHCA	M	NM NM	NM NM	missense missense
#4098T #4117T	HCA HCA	NA NA F NA	biHCA biHCA	M	NM NM	NM NM	indel missense
#536T	HCA	F 46	biHCA	M	NM	NM	missense
#1343T #819T	HCA HCA	F 42 F 45	IHCA biHCA	NM M	NM NM	NM NM	missense
#823T #1250T	HCA	F 45	biHCA biHCA	M	NM NM	NM NM	missense indel
#2827T	HCA HCA	F 31 F 40	biHCA	M	NM	NM	missense
#372T #974T	HCA HCA	F 48 F 42	biHCA biHCA	M	NM NM	NM NM	missense missense
#979T #1896T	HCA HCA	M 58 F 45	biHCA IHCA	M	NM NM	NM NM	missense
#2729T	HCA	F 25	IHCA	NM	NM	NM	
#375T #4110T	HCA HCA	F 54 NA NA	IHCA IHCA	NM MM	NM NM	NM NM	-
#533T #755T	HCA HCA	M 32 F 39	IHCA biHCA	NM M	NM NM	NM NM	missense
#1851T	HCA	F 40	biHCA	M	NM	NM	indel
#711T #1940T	HCA HCA	F 26 F 40	biHCA biHCA	M	NM	NM	missense indel
#757T #222T	HCA HCA	F 48 M 29	IHCA biHCA	MM	NM M	NM NM	missense
#1234T	HCA	F 21 F 37	biHCA	M	NM	NM	missense
#2798T #3074T	HCA HCA	F 37	biHCA biHCA	M	NM NM	NM NM	missense missense
#3723T #4116T	HCA HCA	F 28 NA NA	biHCA biHCA	M	NM NM	NM NM	missense indel
#1355T	HCA	F 40	IHHCA	NM	NM	NM	WINGET
#1439T #760T	HCA HCA	F 49 F 30	IHCA biHCA	NM MM	NM NM	NM NM	
#471T #2561T	HCA HCA	F 30 M 41	IHCA biHCA	NM NM	NM NM	NM NM	
#1231T	HCA	F 36	bIHCA	NM	NM	NM	
#1496T #835T	HCA HCA	F 52 F 37	biHCA IHCA	NM NM	M NM	NM NM	missense
#554T #574T	HCA HCA	F 40 M 54	bIHCA bIHCA	NM NM	M M	NM NM	missense missense
#1342T	HCA	F 41	biHCA	NM	M	NM	missense
#1354T #364T	HCA HCA	F 56 F 35	biHCA biHCA	NM MM	M M	NM NM	missense missense
#377T #390T	HCA HCA	F 50 M 50	biHCA biHCA	NM NM	M M	NM NM	missense missense
#742T	HCA	M 18	bIHCA	NM	M	NM	missense
#1891T #378T	HCA HCA	F 21 F 56	biHCA biHCA	NM NM	M	NM NM	missense missense
#458T #506T	HCA HCA	F 25 F 56	biHCA biHCA	NM MM	M	NM NM	missense missense
#582T	HCA	F 35	biHCA	NM	M	NM	missense
#631T #680T	HCA HCA	F 36 F 42	ЫНСА	NM MN	NM NM	M M	missense missense
#684T #691T	HCA HCA	F 29 F 35	biHCA biHCA	NM NM	NM NM	M	missense missense
#955T	HCA	F 39	bIHCA	NM NM	NM	M	missense
#341T #2834T	HCA HCA	M 47 F 48	IHCA IHCA	NM	NM NM	NM NM	
#1130T #1239T	HCA HCA	F 31 F 41	IHCA IHCA	NM NM	NM NM	NM NM	
#1240T	HCA	F 41	IHCA	NM	NM	NM	
#1263T #1325T	HCA HCA	F 37 F 49	IHCA IHCA IHCA	NM MN	NM NM	NM NM	
#873T #2615T	HCA HCA	M 33 F 50	IHCA IHCA	MM MM	NM NM	NM NM	
#1508T #2193T	HCA HCA	F 26 F 43	IHCA IHCA	NM NM	NM NM	NM NM	
#2197T	HCA	F 35	IHCA	NM	NM	NM	
#2330T #2331T	HCA HCA	F 36	IHCA IHCA	NM NM	NM NM	NM NM	-
#2804T #2828T	HCA HCA	F 27 F 22	IHCA IHCA	NM NM	NM NM	NM NM	
#2836T	HCA	F 33	IHCA	NM	NM	NM	
#3049T #4106T	HCA HCA	F 22 NA NA	IHCA IHCA	NM NM	NM NM	NM NM	1
#544T #782T	HCA HCA	F 41 F 38	IHCA IHCA	NM NM	NM NM	NM NM	
#970T	HCA HCA	F 49	IHCA	NM	NM	NM	
#627T #1215T	HCA HCA	F 30 F 33	IHCA IHCA	NM NM	NM NM	NM NM	1
#1490T #756T	HCA HCA	F 34 F 48	IHCA	NM M	NM NM	NM NM	missense
#1424T	HCA	F 29	ЫНСА	M	NM	NM	missense
#2334T #480T	HCA HCA	F 50 F 34	IHCA IHCA	NM MM	NM NM	NM NM	
#1021T #1351T	HCA HCA	F 39	IHCA IHCA	NM NM	NM NM	NM NM	
#2369T	HCA	M 28	IHCA	NM	NM	NM	
#786T #2773T	HCA/HCC HCA	M 60 F 28	biHCA IHCA	M NM	NM NM	NM NM	indel
#2877T #2879T	HCA HCA	M NA F NA	IHCA IHCA	NM MM	NM NM	NM NM	
#379T	HCA	F 45	IHCA	NM	NM	NM	
#708T #966T	HCA HCA	M 54 F 40 M 37	IHCA IHCA	NM NM	NM NM	NM NM	
#1001T #1286T	HCA HCA	M 37 NA NA	IHCA IHCA IHCA	NM NM	NM NM	NM NM	
#1519T #2810T	HCA	F 24	IHCA IHCA	MM MM	NM NM	NM NM	
#2811T	HCA HCA	F 36 F 36	IHCA	NM	NM	NM	
#478T #854T	HCA HCA	F 33 F 46	IHCA IHCA	NM MN	NM NM	NM NM	
#958T #1002T	HCA HCA	F 51 F 43	IHCA IHCA	NM NM	NM NM	NM NM	
#1004T	HCA	F 42	IHCA	NM	NM	NM	
#1020T #343T	HCA HCA	F 39 F 47	IHCA biHCA	NM M	NM NM	NM NM	missense
#1121T #1216T	HCA HCA	F 25 F 43	IHCA IHCA	NM NM	NM NM	NM NM	
#1232T	HCA	F 36	IHCA	NM	NM	NM	
#1235T #1238T	HCA HCA	F 41 F 41	IHCA IHCA	NM NM	NM NM	NM NM	
#1243T #1251T	HCA HCA	F 26 F 26	IHCA	NM NM	NM NM	NM NM	
#1252T	HCA HCA	F 26	IHCA IHCA	NM	NM	NM	
#1285T	HCA HCA	M 34 F 54 F 47	IHCA IHCA	NM MN	NM NM	NM NM	
#1289T	HCA HCA	F 47 F 47	IHCA IHCA	NM NM	NM NM	NM NM	
#1289T #1290T #1291T	HCA	F 51	IHCA	NM	NM	NM	
#1290T #1291T #1296T	HCA	F 51 F 43	IHCA IHCA	NM NM	NM NM	NM NM	
#1290T #1291T	HCA		IHCA	NM NM	NM NM	NM NM	
#1290T #1291T #1296T #1297T #1301T #1302T	HCA HCA	F 43					L
#1290T #1291T #1296T #1297T #1301T #1302T #1304T #1305T	HCA HCA HCA	F 43 F 43 F 43	IHCA IHCA	NM	NM	NM	
#1290T #1291T #1296T #1296T #1301T #1302T #1304T #1305T #1306T #13131T	HCA HCA HCA HCA HCA	F 43 F 43 F 43 F 43 M 40	IHCA IHCA IHCA	NM NM	NM NM	NM NM NM	
#1290T #1291T #1296T #1296T #1301T #1301T #1304T #1305T #1306T #13131T #1319T	HCA HCA HCA HCA HCA HCA HCA	F 43 F 43 F 43 F 43 M 40 F 42	IHCA IHCA IHCA	MM MM MM	NM MM	NM NM NM	
#1290T #1291T #1291T #1297T #1301T #1302T #1304T #1305T #1306T #1313T #1319T #2874T #3759T	HCA HCA HCA HCA HCA HCA HCA HCA HCA	F 43 F 43 F 43 F 43 M 40 F 42 F NA F 47	IHCA IHCA IHCA IHCA biHCA biHCA	MM MM MM MM	NM NM NM NM	NM NM NM NM NM	
#1290T #1291T #1296T #1297T #1300T #1300T #1300T #1306T #1313T #1319T #2874T	HCA HCA HCA HCA HCA HCA HCA HCA HCA HCA	F 43 F 43 F 43 F 43 M 40 F 42 F NA F 47 F 40	IHCA IHCA IHCA IHCA IHCA IHCA IHCA IHCA	MM MM MM	NM NM NM	NIM NIM NIM NIM NIM NIM	
#1290T #1291T #1296T #1296T #1300T #1300T #1300F #1300F #1300F #1313F #2874T #2759F #1330T #1330T #1330T #1333T	HCA HCA HCA HCA HCA HCA HCA HCA HCA HCA	F 43 F 43 F 43 F 43 M 40 F 42 F NA F 47 F 40 F 40 F 40 F 40	IHCA IHCA IHCA IHCA IHCA IHCA IHCA IHCA	NM NM NM NM NM NM NM	NM NM NM NM NM NM	NM NM NM NM NM NM NM NM	
#1250T #1251T #1251T #1256T #1257T #1301T #1302T #1305T #1305T #1305T #1305T #1313T #1313T #1313T #1313T #1315T #1	HCA HCA HCA HCA HCA HCA HCA HCA HCA HCA	F 43 F 43 F 43 F 43 M 40 F 42 F NA F 47 F 40 F 40 F 43 F 43 F 43 F 43 F 43 F 39	IHCA IHCA IHCA IHCA IHCA IHCA IHCA IHCA	NAM	NM NM NM NM NM NM NM	NM NM NM NM NM NM NM NM NM	
#1290T #1291T #1296F #1297T #1300T #1300T #1300T #1300T #13130T #13130T #1330T #1330T #1330T #1330T #1330T #1330T #1330T #1330T #1330T #1330T #1330T #1330T #1330T #1330T #1330T #1330T	HCA	F 43 F 43 F 43 F 43 M 40 E 42 F NA F 47 F 40 F 40 F 43 F 43 F 43 F 39	IHCA IHCA IHCA IHCA IHCA IHCA IHCA IHCA	MM	NM NM NM NM NM NM NM NM	NM NM NM NM NM NM NM NM NM NM	
#1290T #1291T #129FF #1297T #1300T #1300T #1300T #1300F #1300F #1310F	HCA HCA HCA HCA HCA HCA HCA HCA HCA HCA	F 43 F 43 F 43 F 43 F 43 M 40 F 42 F NA F 47 F 40 F 40 F 43 F 43 F 43 F 43 F 43 F 43 F 43 F 43	HICA HICA HICA HICA BHICA BHICA HICA HICA HICA HICA HICA HICA HICA	NAM	NM N	NM NM NM NM NM NM NM NM NM NM NM NM NM	
#1290T #1291T #129FF #1297T #1300T #1300T #1300T #1300F #1300F #1313F #1	HICA HICA HICA HICA HICA HICA HICA HICA	F 43 F 43 F 43 F 43 F 43 F 42 F NA F 42 F NA F 47 F 40 F 40 F 43 F 43 F 43 F 43 F 43 F 43 F 43 F 43	IHCA IHCA IHCA IHCA IHCA IHCA IHCA IHCA	NAM	NIM	NM NM NM NM NM NM NM NM NM NM NM NM NM N	
#1290T #1291T #1296T #1297T #1390T #1390T #1390T #1390T #1319T #1319T #2274T #2374T #3759T #1319T	HICA HICA HICA HICA HICA HICA HICA HICA	F 43 F 43 F 43 F 43 F 43 F 43 F 42 F NA F 47 F 40 F 40 F 40 F 44 F 43 F 43 F 43 F 43 F 43 F 43 F 44 F 42 F 42 F 42 F 42 F 42 F 42 F 43 F 43 F 44 F 45 F 45 F 45 F 45 F 45 F 45 F 45	HICA HICA HICA HICA HICA HICA HICA HICA	NAM	NMM	NM N	

#1518T #1523T #1664T #669T	HCA	F 24		NM	NM	NM	1
M669T	HCA HCA	M 20 F 37	IHCA IHCA	NM NM	NM NM	NM NM	
	HCA	F 38	IHCA	NM	NM	NM	
#1676T #1677T	HCA HCA	F 45	IHCA IHCA	NM NM	NM NM	NM NM	
#2191T #2189T	HCA HCA	F 37 M 18	IHCA IHCA	NM NM	NM NM	NM NM	
#2370T #754T	HCA	M 28 M 29	IHCA biHCA	NM M	NM NM	NM NM	indel
#2371T	HCA/HCC HCA	M 28	IHCA	NM	NM	NM	indei
#2372T #2373T	HCA HCA	M 28 M 28 M 28	IHCA IHCA	NM NM	NM NM	NM NM	
#2375T #2376T	HCA	M 28 M 28 M 28	IHCA	NM NM	NM NM	NM NM	
#2377T	HCA HCA	M 28	IHCA IHCA	NM	NM	NM	
#2568T #2571T	HCA HCA	F 51 F 36	IHCA IHCA	NM NM	NM NM	NM NM	
#2585T #2590T	HCA HCA	F 47 F 51	IHCA	NM NM	NM NM	NM NM	
#2769T	HCA	F 48	IHCA IHCA	NM	NM	NM	
#2793T #2795T	HCA HCA	M 31 F 44	IHCA IHCA	NM NM	NM NM	NM NM	
#2802T #2803T	HCA HCA	F 53 F 50	IHCA IHCA	NM NM	NM NM	NM NM	
#2826T	HCA	NA NA	IHCA	NM	NM	NM	
#2829T #2830T	HCA HCA	F 44	IHCA IHCA	NM NM	NM NM	NM NM	
#2835T #2837T	HCA HCA	F 48 F 33	IHCA IHCA	NM NM	NM NM	NM NM	
#2856T	HCA	F NA	IHCA	NM	NM	NM	
#750T #2900T	HCA HCA	F 24 F NA	IHCA IHCA	NM NM	NM NM	NM NM	
#2901T #3104T	HCA HCA	F NA	IHCA	NM NM	NM NM	NM NM	
#3107T	HCA	F NA	IHCA IHCA	NM	NM	NM	
#344T #3781T	HCA HCA	F 40 F 28	IHCA IHCA	NM NM	NM NM	NM NM	
#382T	HCA	F 45	IHCA IHCA	NM NM	NM	NM	
#4108T #4109T	HCA HCA	NA NA NA NA	IHCA IHCA	NM	NM NM	NM NM	
#2217T #455T	HCA/HCC HCA	F 13 F 27	biHCA IHCA	M NM	NM NM	NM NM	missense
#456T	HCA	F 27	IHCA	NM	NM	NM	
#457T #466T	HCA HCA	F 27 F 50	IHCA IHCA	NM NM	NM NM	NM NM	
#473T	HCA	F 38	IHCA	NM	NM	NM	
#481T #490T	HCA HCA	F 31 F 50	biHCA IHCA	NM NM	NM NM	NM NM	
#503T	HCA	F 48	IHCA	NM	NM NM	NM	mir
#1023T #1124T	HCA HCA	M 34 M 50	bihca bihca	M M	NM	NM NM	missense missense
#552T #555T	HCA HCA	F 55	IHCA IHCA	NM NM	NM NM	NM NM	
#560T	HCA	F 49	IHCA	NM	NM	NM	
#581T #594T	HCA HCA	F 51 F 39	IHCA IHCA	NM NM	NM NM	NM NM	
#670T #698T	HCA HCA	F 38 F 31	IHCA	NM NM	NM NM	NM NM	
#745T	HCA	F 43	IHCA IHCA	NM	NM	NM	
#751T #769T	HCA HCA	F 39 F 34	IHCA IHCA	NM NM	NM NM	NM NM	
#771T #772T	HCA	F 34	IHCA IHCA	NM NM	NM NM	NM NM	
W821T	HCA HCA	F 34 F 45	IHCA IHCA	NM	NM	NM	
#844T #858T	HCA HCA	F 40	IHCA IHCA	NM NM	NM NM	NM NM	
#861T	HCA	F 51 F 33	IHCA	NM	NM	NM	
#864T #867T	HCA HCA	F 31	IHCA IHCA	NM NM	NM NM	NM NM	
#973T #975T	HCA HCA HCA	F 38 F 52 F 50	IHCA IHCA	NM NM	NM NM	NM NM	
#1666T	HCA	F 36	biHCA	M	NM	NM	missense
#2825T #2857T	HCA HCA	F 23 F NA	IHCA IHCA	NM NM	NM NM	NM NM	
#4094T	HCA	NA 46	IHCA	NM	NM	NM	
#468T #839T	HCA HCA	F 50 F 46	IHCA IHCA	NM NM	NM NM	NM NM	
#470T #1916T	HCA HCA	F 32	ынса	M	NM NM	NM NM	missense
#1328T	HCA HCA	M 43 F 40	biHCA IHCA	NM	NM	NM	indel
#1329T #1337T	HCA HCA	F 40 F 46	IHCA IHCA	NM NM	NM NM	NM NM	
#469T	HCConHCA	F 32	biHCA	M	NM	NM	missense
#1434T #1915T	HCA HCConHCA	F 38 M 43	IHCA biHCA	NM M	NM NM	NM NM	indel
#1488T	HCA	F 35	IHCA	NM	NM	NM	-7950
#1489T #624T	HCA HCA	F 35 F 30	IHCA IHCA	NM NM	NM NM	NM NM	
#1432T #1678T	HCA HCA	F 38	IHCA IHCA	NM NM	NM NM	NM	
#389T		F AS		NM	.4111		
	HCA HCA	F 45 F 30	IHCA		NM	NM NM	
#4089T #744T	HCA HCA	F 29 F 42	IHCA IHCA	NM NM	NM NM	NM NM	
#744T #623T	HCA HCA	F 29 F 42 F 30	IHCA IHCA IHCA IHCA	NM NM NM	NM NM NM	NM NM NM	
#744T #623T #1241T #1269T	HCA HCA HCA HCA	F 29 F 42 F 30 F 26 F 30	IHCA IHCA IHCA IHCA IHCA	NM NM NM NM	NM NM NM NM	NM NM NM NM	
#744T #623T #1241T #1269T #1430T	HCA HCA HCA HCA HCA	F 29 F 42 F 30 F 26 F 30 F 49	IHCA IHCA IHCA IHCA IHCA	MM NM NM NM NM	NM NM NM NM NM	NM NM NM NM NM	
#744T #623T #1241T #1269T #1430T #2192T #2192T	HCA HCA HCA HCA HCA HCA HCA	F 29 F 42 F 30 F 26 F 30 F 49 F 50 F 14	IHCA IHCA IHCA IHCA IHCA IHCA IHCA IHCA	MM MM MM MM MM MM MM	NM NM NM NM NM NM	NM NM NM NM NM NM NM	
#744Y #623Y #1241Y #1269T #1430T #2192Y #2219T #2378T #2589T	HCA HCA HCA HCA HCA HCA HCA HCA	F 29 F 42 F 30 F 26 F 30 F 49 F 50 F 14	IHCA IHCA IHCA IHCA IHCA IHCA IHCA IHCA	NIM NM	NMM	NM NM NM NM NM NM NM	
#744Y #623Y #1241Y #1269Y #1430V #2192Y #2219Y #2378Y #2589Y #2328Y	HCA	F 29 F 42 F 30 F 26 F 30 F 49 F 50 F 14 F 32 M 20	IHCA IHCA IHCA IHCA IHCA IHCA IHCA IHCA	NIM NM	NIM	NM NM NM NM NM NM NM NM NM	indel
#744Y #623Y #1241Y #1269T #1430F #2192Y #2192Y #2378F #2589F #2589F #2589F #2591F	HCA	F 29 F 42 F 30 F 26 F 30 F 49 F 50 F 14 F 48 F 32 M 20 F 51 M 29	НСА НСА НСА НСА НСА НСА НСА НСА НСА НСА	NM MM M	NIM	NM NM NM NM NM NM NM NM NM NM NM	indel
#744Y #623Y #1241T #1269T #1430T #2192T #2219T #2378T #2589T #2588T	HCA	F 29 F 42 F 30 F 26 F 30 F 49 F 50 F 14 F 48 F 32 M 20 F 51 M 29 F NA	HICA HICA HICA HICA HICA HICA HICA HICA	MIN	NIM NIM NIM NIM NIM NIM NIM NIM NIM NIM	NM NM NM NM NM NM NM NM NM NM	indel
97441 96231 #12417 #12697 #14307 #21921 #22197 #22197 #23197 #23197 #23287 #23287 #259917 #27967 #30731 #30731 #30731	HCA	F 29 F 42 F 30 F 26 F 30 F 49 F 50 F 14 F 48 F 32 M 20 F 51 M 29 F NA F 44 F 44 F 44 F 44	HI-CA	NM N	NIM	NM NM NM NM NM NM NM NM NM NM NM NM NM N	indel
#7441 #623T #12417 #1269T #1430T #2192T #2219T #2219T #231	HCA	F 29 F 42 F 30 F 26 F 30 F 30 F 49 F 50 F 14 F 48 F 32 M 20 F 51 M 29 F NA F 51 M 29 F NA F 51 F 14 F 48 F 32 F 32 F 51 F 51 F 51 F 51 F 51 F 51 F 51 F 51	HI-CA	NM N	NIM	NMM	indel
#744Y #623Y #1269Y #1269Y #1430Y #2192Y #2219Y #2378F #2593Y #2594Y #2594Y #30073Y #30173 #30173 #3766F	HCA	F 29 F 42 F 30 F 26 F 30 F 30 F 49 F 50 F 14 F 48 F 32 M 20 F 51 M 29 F NA F 51 M 29 F NA F 51 F 14 F 48 F 32 F 32 F 51 F 51 F 51 F 51 F 51 F 51 F 51 F 51	HIGA HIGA HIGA HIGA HIGA HIGA HIGA HIGA	NMM	MM	NIMM NIMM NIMM NIMM NIMM NIMM NIMM NIMM	indel
67-44Y 6623Y 81245Y 81245Y 81245Y 81245Y 81245Y 81245Y 81255Y 81255Y 81255Y 81255Y 81255Y 81259Y 812	HCA	F 29 F 42 F 30 F 26 F 30 F 30 F 48 F 50 F 14 F 50 F 14 F 32 M 20 F 51 M 20 F 51 F 48 F 52 F 51 F 52 F 51 F 52 F 52 F 53 F 54 F 54 F 54 F 54 F 54 F 54 F 54 F 54	HIGA HIGA HIGA HIGA HIGA HIGA HIGA HIGA	NAM. NAM. NAM. NAM. NAM. NAM. NAM. NAM.	NIM	NIMM NIMM NIMM NIMM NIMM NIMM NIMM NIMM	indel
#7-441 #0-237 #12417 #12597 #14307 #12197 #22197 #22197 #22387 #22591 #22591 #22591 #225917 #2318	HCA	F 29 F 42 F 30 F 26 F 30 F 26 F 30 F 49 F 50 F 14 F 32 M 20 F 51 M 29 F 14 F 32 M 20 F 14 F 51 F 48 F 32 M 20 F 51 F 7 F 7 F 8 F 7 F 7 F 7 F 7 F 7 F 7 F 7 F 7 F 7 F 7	HI-CA	NNM	NIM	NAM	indel
## 7.44T ##	HCA	F 29 F 42 F 30 F 26 F 30 F 26 F 30 F 49 F 50 F 14 F 32 M 20 F 51 M 29 F 14 F 32 M 20 F 14 F 51 F 48 F 32 M 20 F 51 F 7 F 7 F 8 F 7 F 7 F 7 F 7 F 7 F 7 F 7 F 7 F 7 F 7	HICA H	NNM	NIM	NAM	indel
87-441 8-221 81241T 81264T 81260T 81450T 81450T 81450T 81260T 81278T 812	HICA HICA HICA HICA HICA HICA HICA HICA	F 29 F 42 F 30 F 36 F 38 F 39 F 39 F 14 F 32 M 20 F 51 M 20 F 51 M 20 F 51 F 52 F 52 F 52 F 53 F 54 F 54 F 52 F 52 F 53 F 54 F 54 F 55 F 54 F 54 F 55 F 55 F 54 F 54	HICA H	NNM	MMM MMM MMM MMM MMM MMM MMM MMM MMM MM	NAM	indel
### ### #### #### ####################	HICA HICA HICA HICA HICA HICA HICA HICA	F 29 F 42 F 30 F 26 F 36 F 36 F 30 F 48 F 48 F 48 F 32 M 20 F 51 M 20 F 51 F 51 M 20 F 51 F 51 F 51 F 51 F 51 F 51 F 51 F 51	HICA H	NNM NMM NEW NEW NEW NNM NNM NNM NNM NNM NNM NNM NNM NNM NN	AMM NOTE NOTE NOTE NOTE NOTE NOTE NOTE NOTE	NAM	indel
87441 86231 18121	HCA HCA	F 29 F 42 F 30 F 50 F 50 F 50 F 14 F 50 F 14 F 14 F 12 M 29 F 14 F 14 F 14 F 14 F 15 F 14 F 14 F 15 F 15 F 16 F 51 M 29 F 14 F 15 F 16 F 17 M 29 F 18 F 18 F 18 F 18 F 18 F 18 F 18 F 18	HICA	NNM	MMM MMM MMM MMM MMM MMM MMM MMM MMM MM	NAM	indel
#7-441 #6231 #12411-07 #134307 #134307 #21297 #21297 #21297 #21297 #2229	HICA HICA HICA HICA HICA HICA HICA HICA	F 29 F 42 F 30 F 26 F 36 F 36 F 30 F 48 F 48 F 48 F 32 M 20 F 51 M 20 F 51 F 51 M 20 F 51 F 51 F 51 F 51 F 51 F 51 F 51 F 51	HICA H	NNM	MMM MMM MMM MMM MMM MMM MMM MMM MMM MM	NAM	indel
#7-441 #6231 T1 #12-607 #12-60	HIGA HIGA HIGA HIGA HIGA HIGA HIGA HIGA	F 29 F 43 F 38 F 38 F 39 F 49 F 50 F 32 M 20 F 51	HICA H	NOME. NO	MACH. MA	NAM	indel
#7-441 #6231 #12307 #12	HIGA HIGA HIGA HIGA HIGA HIGA HIGA HIGA	F 29 F 449 F 459 F 559 F	HICA	NAME	HMM	NAM	indel
#7-44T #7	HCA	F 29 F 44 1 19 19 19 19 19 19 19 19 19 19 19 19 1	HICA H	NOTAL STATE OF THE	MACH. MA	NIME NIME NIME NIME NIME NIME NIME NIME	indel
#7-441 #6231 #12307 #12	HCA	F 29 F 24 25 25 25 25 25 25 25	HICA H	NOTAL STATE OF THE	MACH. MA	NIME NIME NIME NIME NIME NIME NIME NIME	indel
#744T #745T	HCA	F 29 F 25 F 50 F 51 F 51 F 52 F 7 52 F 7 52 F 7 53	HICA H	NAME	HMM	NIME NIME NIME NIME NIME NIME NIME NIME	indel
#7-441 #6231 #6231 #6231 #6231 #6231 #6231 #6231 #6231 #6231 #6232	HCA	F 29 F 25 75 25 F 25 75 25 75 25 25 25 25	HICA H	NOTAL STATE OF THE	MACH MACH MACH MACH MACH MACH MACH MACH	NAME NAME NAME NAME NAME NAME NAME NAME	irdel
#244T #241T	HCA HCCA HCA HCCA HCA HC	F 29 F 240 F 25 7 25 F 25 7 25 7 25 25 25 25	HICA H	NAME	HMM	NAM	
#744T	HCA	F 29 F 42 F 19 F 1	HICA H	NAME	MACH MACH MACH MACH MACH MACH MACH MACH	NAME NAME NAME NAME NAME NAME NAME NAME	indel
#744T #745T	HCA	F 29 F 42 S F 53	HICA H	NAME	MMC MMC MMC MMC MMC MMC MMC MMC	NAME AND ADDRESS OF THE ADDRESS OF T	
#244T #241T	HCA	F 29 F 24 25 25 25 25 25 25 25	HICA H	NAME	HMM	NAM	
#7-441 #6231 #6331	HCA	F 29 F 29 F 29 F 29 F 29 F 29 F 20 F	HICA H	NOTAL STATE OF THE	MMC MMC MMC MMC MMC MMC MMC MMC	MAM	
#744T	HICA HICA HICA HICA HICA HICA HICA HICA	F 29 F 42 F 28 F 69 F 7	HICA H	NAME	MMC MMC MMC MMC MMC MMC MMC MMC	NAME AND ADDRESS OF THE ADDRESS OF T	
#744T #621T	HCA	F 29 F 25 F 50 F 51 F 20 F 52 F 52 F 53 F 53 F 53 F 53 F 54 F 54 F 54 F 54	HICA H	NOTAL STATE OF THE	HMM	MAM	missense
#7-44T #6-21T #6	HEA	F 29 F 29 F 29 F 29 F 25 F	HICA H	NOTAL STATE OF THE	MMC MMC MMC MMC MMC MMC MMC MMC	MAI	missense
#744T #745 #745 #745 #745 #745 #745 #745 #745	HICA HICA HICA HICA HICA HICA HICA HICA	F 29 P 44 P 51 P 51 P 51 P 52 P 52 P 53 P 7 P 53 P 7 P 53 P 7 P 54	HICA H	NOTAL STATE OF THE	MMC MMC MMC MMC MMC MMC MMC MMC	MAM	
#7-441 #62331 #62331	HEA	F 29 F 29 F 29 F 29 F 29 F 29 F 20 F	HICA H	NAM	MMC MMC MMC MMC MMC MMC MMC MMC	MAM	missense
#744T #744T #745T	HICA HICA HICA HICA HICA HICA HICA HICA	F 29 F 430 F 25 F 25 F 30	HICA H	NAME	MMC MMC MMC MMC MMC MMC MMC MMC	MAG	missense
#744T	HICA HICA HICA HICA HICA HICA HICA HICA	F 29 F 29 F 25 F	HICA H	NAME	MMC MMC MMC MMC MMC MMC MMC MMC	MAM	missense
#244T #245T #245T #255T	HICA HICA HICA HICA HICA HICA HICA HICA	F 29 F 24 25 7 25 7 25 7 25 7 25 7 25 7 25 7 25 7 25 7 25 7 25 7 25 25	HICA H	NAM	MMC MMC MMC MMC MMC MMC MMC MMC	MAI	missense
### #### #############################	HICA HICA HICA HICA HICA HICA HICA HICA	F 29 F 29 F 25 F	HICA H	NAME	MMC MMC MMC MMC MMC MMC MMC MMC	MAM	Missense

	#4058T	M	indel	NM		NM		NM	T .	NM	
1	#4098T #4117T	M	indel	NM NM		NM NM		NM NM		NM NM	
	#536T #1343T	M NM	indel	NM NM		NM NM		NM NM		NM NM	NM
	#819T	M	indel	NM		NM		NM		NM	Nin
	#823T #1250T	M M	missense			NM NM		NM NM		NM NM	
	#2827T #372T	M	missense missense	NM NM		NM NM		NM NM		NM NM	
	#974T #979T	M	missense	NM		NM NM		NM NM		NM NM	
	#1896T	NM	missense	NM.		NM		NM		NM	NM
	#2729T #375T	NM NM		NM NM		NM NM		NM NM		NM NM	NM NM
	#4110T #533T	NM NM		NM NM		NM NM		NM NM		NM NM	NM NM
	#75ST	NM		NM		NM		NM		NM	nie.
	#1851T #711T	M	indel indel	NM NM				NM NM		NM NM	
	#1940T #757T	M NM	indel	NM		NM		NM		NM	NM
	W222T	NM		NM		NM		NM		NM	NM
	#1234T #2798T	NM NM	-	NM NM		NM NM		NM NM		NM NM	
	#3074T #3723T	NM NM		NM NM		NM NM		NM NM		NM NM	0 8
	#4116T	NM		NM		NM		NM		NM	
	#1355T #1439T	NM NM		NM NM		M NM	missense	NM NM		NM NM	NM
	#760T #471T	M NM	missense	NM NM		NM NM		NM NM		NM NM	NM
	#2561T	M	missense			5570550		8		3 270000 3	No.
	#1231T #1496T	NM NM		NM NM		NM NM		NM NM		NM M	missense
	#835T #554T	NM NM		NM NM		NM MM		NM M	mirronro	NM NM	NM
	#574T	NM		NM		М	missense	NM	missense	NM	
-	#1342T #1354T	M	indel	NM NM		NM NM		NM NM	-	NM NM	
	#364T #377T	M	indel	NM NM		NM MM		NM NM		NM NM	
	#390T	M	indel	NM		NM		NM		NM	
	#742T #1891T	M	indel	NM NM		NM NM		NM NM		NM NM	
	#378T #458T	NM NM		NM NM		NM NM		NM NM		NM NM	
	#506T	NM		NM		NM		NM		NM	
	#582T #631T	NM M	indel	NM NM		NM NM		NM NM		NM NM	
	#680T #684T	M	indel	NM NM		NM NM		NM NM		NM NM	
	#691T	M	indel	NM		NM		NM		NM	
	#955T #341T	M NM	indel	NM NM		NM M	missense	NM NM	1	NM M	missense
	#2834T #1130T	M	indel	NM NM		NM MM		NM		M	indel
	#1239T	NM NM		NM		NM		NM NM		M	missense missense
	#1240T #1263T	NM NM		NM NM		NM NM		NM NM		M	indel indel
	#1325T #873T	NM NM		NM NM		NM NM		NM NM		M	missense
	#2615T	NM	_	NM	-	NM		NM		NM	NM NM
	#1508T #2193T	NM NM		NM NM		NM MM		NM NM		M	indel indel
	#2197T	NM		NM		NM		NM		M	indel
	#2330T #2331T	NM NM	-	NM NM		NM NM		NM NM		M	missense indel
	#2804T #2828T	NM		NM NM		NM NM		NM		M	indel
	#2836T	NM NM		NM		NM		NM NM		M	indel indel
	#3049T #4106T	NM NM	-	NM NM	-	NM MM		NM NM	-	M	indel missense
	#544T	NM		NM		NM		NM		M	indel
	#782T #970T	NM NM		NM NM		NM NM		NM NM		M	indel indel
	#627T #1215T	NM NM		NM NM		NM		NM NM		M	indel NM
	#1490T	NM		NM		NM NM		M	missense	NM	NM
	#756T #1424T	M NM	indel	NM NM		NM		NM NM		NM NM	NM NM
	#2334T #480T	NM NM		NM NM		NM NM		M	missense missense	NM NM	
	#1021T	NM		NM		M	indel	NM	mageroe	NM	
	#1351T #2369T	NM NM	-	NM NM		M	indel missense	NM NM		NM NM	
	#786T #2773T	M NM	indel	NM NM		NM M	indel	NM NM		NM NM	
	#2877T	NM		NM		м	missense	NM		NM	
	#2879T #379T	NM		NM NM	-	M	indel indel	NM NM NM		NM	
	#708T #966T	NM		NM		M M					
		NM NM					missense	NM		NM NM	_
	#1001T	NM NM		NM M	missense	M NM	missense	NM NM		NM NM	
	#1286T #1519T	NM NM NM		M M M	missense	NM MM		NM NM NM		NM	
	#1286T #1519T #2810T	NM NM NM NM		M M M M	missense missense missense	NM NM NM		NM NM NM NM		NM NM NM NM	
	#1286T #1519T #2810T #2811T #478T	NM NM NM NM NM NM		M M M M M	missense missense missense missense missense	MM MM MM MM MM		NM NM NM NM NM NM		NM NM NM NM NM NM	
	#1286T #1519T #2810T #2811T #478T #854T	NM NM NM NM NM NM NM NM		M M M M M M	missense missense missense missense	MM MM MM MM MM MM MM		NM NM NM NM NM NM NM		NM NM NM NM NM NM NM NM	
	#1286T #1519T #2810T #2810T #2811T #478T #854T #958T	NM NM NM NM NM NM NM NM	indel	M M M M M M M	missense missense missense missense missense missense	MM MM MM MM MM MM MM MM		NM NM NM NM NM NM NM		NM NM NM NM NM NM NM NM	
	#1286T #1519T #2810T #2810T #2811T #478T #854T #958T #1002T #1004T	NM NM NM NM NM NM NM NM NM NM	indel indel indel	M M M M M M M M M M M M M M M M M M M	missense missense missense missense missense missense	MIN MIN MIN MIN MIN MIN MIN MIN MIN MIN		NM NM NM NM NM NM NM NM NM NM NM		NM NM NM NM NM NM NM NM NM	
	#12867 #15197 #28107 #28117 #4787 #8547 #9587 #10027 #10007 #10007 #10007 #110207	NM NM NM NM NM NM NM NM NM NM NM NM NM M M	indel	MM MM MM MM NM NM NM	missense missense missense missense missense missense	MM		NM NM NM NM NM NM NM NM NM NM NM NM		NM NM NM NM NM NM NM NM NM NM NM	NM
	#1286T #1519T #2810T #2810T #2811Y #2811Y #354T #354T #3504T #1000T #1000Y #1000Y #11210T #11210T	NM NM NM NM NM NM NM NM NM NM NM M M M	indel indel indel	MM MM MM NM NM NM	missense missense missense missense missense missense	MM NMM NMM NMM NMM NMM NMM NMM NMM NMM		NM N		NM NM NM NM NM NM NM NM NM NM NM NM	NM
	#12867 #15197 #28107 #28117 #28117 #0547 #0547 #0547 #10007 #10007 #10007 #11217 #11217 #12217 #12237	NM NM NM NM NM NM NM NM NM M M M M M M	indel indel indel indel indel	MM MM MM NM NM NM NM NM	missense missense missense missense missense missense	MM		NM NM NM NM NM NM NM NM NM NM NM NM NM N		NM NM NM NM NM NM NM NM NM NM NM NM NM N	NM
	#12867 #15197 #28107 #28117 #28117 #28117 #35417 #30047 #30047 #30047 #30047 #30047 #31027 #34317 #34317 #34317 #34317 #34317 #34317 #34317 #34317 #34317 #34317 #34317 #34317	NM NM NM NM NM NM NM NM NM M M M M M M	indel indel indel indel indel indel indel	NM M M NM NM NM NM NM NM	missense missense missense missense missense missense	MM		NIM		NM N	NM
	#12861 #12861 #15197 #28107 #28107 #28107 #28107 #28107 #28107 #28111 #16107 #1610007 #161007 #161007 #161007 #161007 #161007 #161007 #161007	NM NM NM NM NM NM NM NM NM NM M M M M M	indel indel indel indel indel indel	MM MM MM NM NM NM NM NM NM	missense missense missense missense missense missense	MM NM N		NM N		NM N	NM
	#1256 #1256 #1256 #1256 #1256 #1256 #1256 #1256 #1256 #1256 #1256 #1256 #1256 #1256 #1256 #1257	NM NM NM NM NM NM NM NM NM NM M M M M M	indel indel indel indel indel indel indel indel indel indel	NM M M M M M M M M M M M M M M M M M M	missense missense missense missense missense missense	MAN AMN AMN AMN AMN AMN AMN AMN AMN AMN		NIM		NM N	NM
	#22667 #28107 #28107 #28107 #28107 #28111 #4781 #4781 #4781 #5581	NM NM NM NM NM NM NM NM NM NM M M M M M	indel indel indel indel indel indel indel indel indel indel indel	NM M M M M M M M M M M M M M M M M M M	missense missense missense missense missense missense	NM N		NIM		NIM	NM
	#2266 #25197 #28107 #28107 #28107 #28107 #28111 #28111 #28111 #28111 #28111 #28111 #28111 #28111 #28111 #28111 #2812 #28121 #281	NM NM NM NM NM NM NM NM NM NM M M M M M	indel	NM M M M M M M M M M M M M M M M M M M	missense missense missense missense missense missense	MM NAM NAM NAM NAM NAM NAM NAM NAM NAM N		NIM		NIM	NM
	#22567 #22607	NM NM NM NM NM NM NM NM NM NM M M M M M	indel	NM M M M M M M M M M M M M M M M M M M	missense missense missense missense missense missense	NM N		NIM		NIM	NM
	#22867 #25197	NM NM NM NM NM NM NM NM NM NM NM M M M	indel	NM M M M M M M M M M M M M M M M M M M	missense missense missense missense missense missense	NM N		NM N		NIM	NM
	#12867 #28107 #2	NM N	indel	NM M M M M M M M M M M M M M M M M M M	missense missense missense missense missense missense	MAN		NM N		NIM	NM
	#22867 #25197 #2	NM NM NM NM NM NM NM NM NM NM M M M M M	indel	NM M M M M M M M M M M M M M M M M M M	missense missense missense missense missense missense	MAN		NM NM NM NM NM NM NM NM		NIM	NM.
	#12867 #12877	NMM	indel	NM M M M M M M M M M M M M M M M M M M	missense missense missense missense missense missense	MAN		NM.		NIM	
	#1286F #2810F #2	NM N	indel	NM M M M M M M M M M M M M M M M M M M	missense missense missense missense missense missense	MAN		NM NM NM NM NM NM NM NM		NIM	NM NM NM NM
	#22867 #28107 #2	NM N	indel	NMM MM MM NMM NMM NMM NMM NMM NMM NMM N	missense missense missense missense missense missense	MAN		NM NM NM NM NM NM NM NM		NIM	NM NM
	#12861 #12877	NM	indel	NMM MM NMM NMM NMM NMM NMM NMM NMM NMM	missense missense missense missense missense missense	MAN		NM		NIM	NM NM
	#22867 #23807	NM	indel	NMM NM	missense missense missense missense missense missense	MAN		NM N		NMM	NM NM
	#12867 #12867	NMM	indel	NMM NM	missense missense missense missense missense missense	MAN		NM		NMS	NM NM NM
	#1286F	NMM	indel	NMM MM NMM NMM NMM NMM NMM NMM NMM NMM	missense missense missense missense missense missense	NIME STATE OF THE		NM		NO.5 NO.5 NO.5 NO.5 NO.5 NO.5 NO.5 NO.5	NM NM NM
	#1286F #15197 #1	NMM	indel	NMM M M M M M M M M M M M M M M M M M M	missense missense missense missense missense missense	NAM		NM N		NMS	NM NM NM
	#1286F	NMM	Indel	NMM MM NMM NMM NMM NMM NMM NMM NMM NMM	missense missense missense missense missense missense	NAME AND ADDRESS OF THE ADDRESS OF T		NM NM NM NM NM NM NM NM		No.65	NM NM NM
	#1286F #2810F #2	NM	Indel	NIM M M M M M M M M M M M M M M M M M M	missense missense missense missense missense missense	NIM NAM NAM NAM NAM NAM NAM NAM NAM NAM NA		NM N		No.60	NM NM NM
	#12861 #15197 #1	NMM	indel	NMM MM	missense missense missense missense missense missense	NIME STATE OF THE		NM		NO.50	NIM NIM NIM NIM NIM
	#1286F #1289F	NMM	Indel	NMM MM NMM NMM NMM NMM NMM NMM NMM NMM	missense missense missense missense missense missense	NIME NAME NAME NAME NAME NAME NAME NAME NA		No. No.		No.60	NIM NIM NIM NIM NIM
	#12861 #15197 #1	NMM	indel	NMM M M M M M M M M M M M M M M M M M M	missense missense missense missense missense missense	NIME NAME NAME NAME NAME NAME NAME NAME NA		NM		No.00 No.0	NIM NIM NIM NIM NIM NIM
	#12861 #12877 #1287	NMM	Indel	NMM M M M M M M M M M M M M M M M M M M	missense missense missense missense missense missense	NIME NAME NAME NAME NAME NAME NAME NAME NA		NM NM NM NM NM NM NM NM	missense	No.00	NIM NIM NIM NIM NIM
	#1286F #2380F #2	NMM	Indel	NMM M M M M M M M M M M M M M M M M M M	missense missense missense missense missense missense	NIME NAME NAME NAME NAME NAME NAME NAME NA		No.	missense	No.60 No.6	NIM NIM NIM NIM NIM NIM
	#12861 #15197 #1	NMM	Indel	NMM M M M M M M M M M M M M M M M M M M	missense missense missense missense missense missense	NIME NAME NAME NAME NAME NAME NAME NAME NA		NM NM NM NM NM NM NM NM	missense	No.61	NIM NIM NIM NIM NIM NIM
	#22867 #23807 #2	NMM	Indel	NMM MM NMM NMM NMM NMM NMM NMM NMM NMM	missense missense missense missense missense missense	NIME NAME NAME NAME NAME NAME NAME NAME NA		No.	missense	No.00 No.0	NIM NIM NIM NIM NIM NIM NIM
	#12861 #15197 #1	NMM	Indel	NIM M M M M M M M M M M M M M M M M M M	missense missense missense missense missense missense	NIME NAME NAME NAME NAME NAME NAME NAME NA		NM NM NM NM NM NM NM NM	missense	No.61	NIM NIM NIM NIM NIM NIM NIM

The color	#2373T					NM		NM		NM	-
April	#2375T	M	indel	NM NM		NM		NM		NM	
PAGES 10	#2376T	M	indel	NM		NM		NM		NM	
PAGES 10	#2568T	M	indel	NM		NM NM		NM NM		NM	
Property 10	#2571T	M		NM		NM		NM		NM	
PRODUCT 10	#2590T	M	indel	NM		NM		NM		NM	
PRODUCT 10	#2769T	M	indel	NM		NM		NM		NM	
PRODUCT 10	#2793T #2795T	M	indel	NM NM		NM NM		NM NM		NM NM	
PART	#2802T	M		NM		NM		NM		NM	
PART	#2803T #2826T	M	indel	NM NM		NM NM		NM NM		NM NM	
PART	#2829T	M	indel	NM		NM		NM		NM	
ADD	#2830T		indel	NM		NM NM		NM		NM	
ACCOUNTY TOTAL T	#2837T	M	indel	NM		NM		NM		NM	
A S S S S S S S S S	#2856T	M	indel	NM		NM		NM		NM	NA
A S S S S S S S S S	#2900T	M	indel	NM		NM		NM		NM	NIN
P. STOT	#2901T	M				NM		NM		NM	
P. STOT	#31041 #3107T	M	indel	NM		NA		NM		818.6	
P. STOT	#344T		indel	NM		NM		NM		NM	
#150F	#3821	M	indel	NM		NM		NM		NM NM	
RESCUE	#4108T	M	indel			NM		NM			
RECOT	#41091 #2217T		indel	NM NM		NM NM		NM NM		NM NM	1
RECOT	#455T	M	indel	NM		NM		NM		NM	
March Marc	MAC 7T	M	indel	NM		NM NM		NM NM		NM	
March Marc	#466T	M	indel	NM		NM		NM		NM	
POST	#473T #491Y	M		NM		NM NAA		NM NAA		NM	=
PROPER W. Color MA Co			indel	NM							
PROPER W. Color MA Co	#503T	M	indel	NM		NM		NM		NM	
PROPER W. Color MA Co	#1023T #1124T	M	indel	NM		MM MM		NM NM		NM NM	
PROPER W. Color MA Co	#552T	M	indel	NM		NM		NM		NM	
SHOP	#555T #560T	M	indel	NM		MM MM		NM NM		NM NM	
SHOP	#581T	M	indel	NM		NAA		NM		NM	
BOST	#594T #670T	M	indel	NM NM		NM NM		NM NM	_	NM NM	
F7777	#698T	M	indel	NM		NM		NM		NM	
F7777	#745T #751T	M	indel	NM NM		NM NAA		NM NM		NM	
F7777	#769T	M		NM		NM		NM		NM	
BEATT	#771T	M	indel	NM NM		NM		NM		NM NM	
BEATT	MODAT	M	indel	215.4		818.6		AIRA		242.4	
BEATT	#844T #850T	M	indel	NM		NM NAA		NM NA		NM	
## 1955 M	#861T	M	indel	NM		NM		NM		NM	
## 1955 M	#864T	M	indel	212.4	i i	313.6		NIRA		111.4	
# 1566FT M index MM MM NM	#973T		indel	NM		NM		NM		NM	
#2857T M Proserve NM	#975T		indel	NM		NM		NM		NM	
REPUBLIC M. Protection M. M. M. M. M. M. M. M	#2825T	M	missense	NM s		NM		NM		NM	
REPUBLIC M. Protection M. M. M. M. M. M. M. M	#2857T		missense	NM NM		NM		NM		NM	
REPUBLIC M. Protection M. M. M. M. M. M. M. M	#468T	M	missense	NAM		NW		INIM		14/41	
# \$12397						NM		NM		NM	
## # # # # # # # # # # # # # # # # # #	#8391	M	missense	NM		NM		NM NM		NM	
#1337T M by bodd NM NAC	#839T	M	missense	NM NM		NM		NM NM NM		NM	
154487	#839T #470T #1916T #1328T	M M M	missense indel indel	NM NM		MM MM MM		NM NM NM		NM NM NM	
154487	#339T #470T #1916T #1328T #1329T #1337T	M M M M M	missense indel indel	NM NM NM NM NM		MM MM MM MM MM		NM NM NM NM NM		NM NM NM NM NM	
# 1499F	#839T #470T #1916T #1328T #1329T #1337T #469T	M M M M M	missense indel indel	NM NM NM NM NM NM		MM MM MM MM MM		NM NM NM NM NM		NM NM NM NM NM	
##2-17	#839T #470T #1916T #1328T #1329T #1337T #469T #1434T #1915T	M M M M M M M	missense indel indel indel indel indel indel indel	NM NM NM NM NM NM		MM NM N		NM NM NM NM NM NM NM		NM NM NM NM NM NM NM NM	
## ## ## ## ## ## ## ## ## ## ## ## ##	#8391 #4707 #19167 #13287 #13297 #13377 #4697 #14347 #19157	M M M M M M M M M	missense indel indel indel indel indel indel indel	NM NM NM NM NM NM NM NM		MM		NM NM NM NM NM NM NM NM		NM NM NM NM NM NM NM NM	indel
## ## ## ## ## ## ## ## ## ## ## ## ##	#8391 #4707 #13187 #13287 #13297 #13397 #4697 #14347 #19157	M M M M M M M M M M M M M M M M M M M	missense indel indel indel indel indel indel indel	NM NM NM NM NM NM NM NM NM		MM		NM NM NM NM NM NM NM NM NM NM		NM NM NM NM NM NM NM NM	indel indel indel
## 6744T NM	#8391 #4707 #13187 #13287 #13297 #13397 #4697 #14347 #19157	M M M M M M M M M M M M M M M M M M M	missense indel indel indel indel indel indel indel	NM NM NM NM NM NM NM NM NM		MM		NM NM NM NM NM NM NM NM NM NM		NM NM NM NM NM NM NM NM	indel indel indel
## ## ## ## ## ## ## ## ## ## ## ## ##	#8391 #4701 #19167 #19267 #13297 #13297 #13297 #14847 #14847 #14847 #14847 #14847 #14847 #14847 #14847 #14847 #15787	M M M M M M M M M M M M M M M M M M M	missense indel indel indel indel indel indel indel	NM NM NM NM NM NM NM NM NM NM NM NM NM N		NM NM NM NM NM NM NM NM NM NM NM NM NM N		NM NM NM NM NM NM NM NM NM NM NM NM NM N		NM NM NM NM NM NM NM NM NM M M M	indel
# 2120FT NAM	#8391 #4301 #130101 #13101 #131377 #131377 #14317 #14317 #14887 #14887 #14887 #14887 #14887 #14887 #14887 #14887 #14887	M M M M M M M M M M M M M M M M M M M	missense indel indel indel indel indel indel indel	NM NM NM NM NM NM NM NM NM NM NM NM NM N		NMM		NM N		NIM NIM NIM NIM NIM NIM NIM NIM M M M NIM NI	NM NM
# 2120FT NAM	#8.991 #A.901 #A.901 #1.1281 #1.1287 #1.1287 #1.1287 #1.13.377 #1.4697 #1.14147 #1.1517 #1.14147 #1.14	M M M M M M M M M M M M M M M M M M M	missense indel indel indel indel indel indel indel	NM N		NIM		NM NM NM NM NM NM NM NM NM NM NM NM NM N		NM NM NM NM NM NM NM NM M M M NM NM NM N	NM NM
# 27597 NM	##507 ##507	M M M M M M M M M M M M M M M M M M M	missense indel indel indel indel indel indel indel	NM N		NM N		NM N		NIM	NM NM
# 25597 N.M. N.M. N.M. N.M. N.M. N.M. N.M. N.M	## 8007 # 12267 # 12267 # 12297 # 12397 # 12397 # 12397 # 12467 # 12467 # 12467 # 12467 # 12427 # 12427	M M M M M M M M M M M M M M M M M M M	missense indel indel indel indel indel indel indel	NM NM NM NM NM NM NM NM NM NM NM NM NM N		NM N		NM N		NM N	NM NM
# 25597 N.M. N.M. N.M. N.M. N.M. N.M. N.M. N.M	88.007 87.0161 87.0167 87.0167 87.0167 87.0167 87.0167 88.607 88.607 87.0167 88.607 87.0167 88.017	M M M M M M M M M M M M M M M M M M M	missense indel indel indel indel indel indel indel	NM NM NM NM NM NM NM NM NM NM NM NM NM N		NM.		NM N		NIM	NM NM
# 25931 NM	88.007 87.0161 87.0167 87.0167 87.0167 87.0167 87.0167 88.607 88.607 87.0167 88.607 87.0167 88.017	M M M M M M M M M M M M M M M M M M M	missense indel indel indel indel indel indel indel	NM NM NM NM NM NM NM NM NM NM NM NM NM N		NM.		NM N		NIM	NM NM
# 27967 NM	## ## ## ## ## ## ## ## ## ## ## ## ##	M M M M M M M M M M M M M M M M M M M	missense indel indel indel indel indel indel indel	NM		NM.		NIM. NIM. NIM. NIM. NIM. NIM. NIM. NIM.		NIM	NM NM
#2073T NM	## ## ## ## ## ## ## ## ## ## ## ## ##	M M M M M M M M M M M M M M M M M M M	missense indel indel indel indel indel indel indel	NM		NM.		NIM		NIM	NM NM
## ## ## ## ## ## ## ## ## ## ## ## ##	## ## ## ## ## ## ## ## ## ## ## ## ##	M M M M M M M M M M M M M M M M M M M	missense indel indel indel indel indel indel indel	NM		NM.		NIM		NIM	NM NM
# 27/00 NM	## 8007 # 101517 # 10	M M M M M M M M M M M M M M M M M M M	missense indel indel indel indel indel indel indel	NM		NMC		NM N		NIM	NM NM
# 27/00 NM	## 8007 # 101517 # 10	M M M M M M M M M M M M M M M M M M M	missense indel indel indel indel indel indel indel	NM		NMC		NM N		NIM	NM NM
BSOFF	## 8007 # 101517 # 10	M M M M M M M M M M M M M M M M M M M	missense indel indel indel indel indel indel indel	NM		NMC		NM N		NIM	NM NM
MR PA PA PA PA PA PA PA P	## 807 # 8251 # 8251 # 81287 # 81287 # 84607 # 86347 #	M M M M M M M M M M M M M M M M M M M	missense indel indel indel indel indel indel indel	2 NMM NMM NMM NMM NMM NMM NMM NMM NMM NM		NAME NAME NAME NAME NAME NAME NAME NAME		NM N		NIM	NM NM
## ## ## ## ## ## ## ## ## ## ## ## ##	## ## ## ## ## ## ## ## ## ## ## ## ##	M M M M M M M M M M M M M M M M M M M	missense indel indel indel indel indel indel indel	2 NMM		1966 19		NM		NIM	NM NM
## ## ## ## ## ## ## ## ## ## ## ## ##	## ## ## ## ## ## ## ## ## ## ## ## ##	M M M M M M M M M M M M M M M M M M M	missense indel indel indel indel indel indel indel	2 NMM		NM6		NM N		NIM	NM NM
## 1857 M 1046 NM 1046	## ## ## ## ## ## ## ## ## ## ## ## ##	M M M M M M M M M M M M M M M M M M M	missense indel ind	2 NMM		NAME OF THE STATE		NM N		NIM	NM NM
## 1857 M 1046 NM 1046	## ## ## ## ## ## ## ## ## ## ## ## ##	M M M M M M M M M M M M M M M M M M M	missense indel ind	2 NMM		NME NAME NAME NAME NAME NAME NAME NAME N		NM N		NIM	NM NM
## 1857 M 1046 NM 1046	## ## ## ## ## ## ## ## ## ## ## ## ##	M M M M M M M M M M M M M M M M M M M	missense indel ind	N		NAME OF STATE OF STAT		NM N		NIM	NM NM
## \$2507 M Fold NM NM NM NM NM NM NM N	## ## ## ## ## ## ## ## ## ## ## ## ##	M M M M M M M M M M M M M M M M M M M	missense in de la missense in della missense in	N		NAME OF STATE OF STAT		NM N		NIM	NM NM
## \$2507 M Fold NM NM NM NM NM NM NM N	## ## ## ## ## ## ## ## ## ## ## ## ##	M M M M M M M M M M M M M M M M M M M	missensnipen indel	2 NMM		NAME - NA		NM N		NAME	NM NM
#25507 M lodd NM	## ## ## ## ## ## ## ## ## ## ## ## ##	M M M M M M M M M M M M M M M M M M M	missensnipen indel	2 NMM		NAME OF THE STATE		NM N		NAME	NM NM
#2579T MM "misserie NM misserie NM misseri	## ## ## ## ## ## ## ## ## ## ## ## ##	M M M M M M M M M M M M M M M M M M M	missensnipen indel	NM N		NAME NAME NAME NAME NAME NAME NAME NAME		NMA NMA		No.	NM NM
# 2575T M b lodel	## ## ## ## ## ## ## ## ## ## ## ## ##	M M M M M M M M M M	indel	2 NMM NMM NMM NMM NMM NMM NMM NMM NMM NM		1946 1 19		NM N		NAME	NM NM
# 2575T M b lodel	## ## ## ## ## ## ## ## ## ## ## ## ##	M M M M M M M M M M M M M M M M M M M	missingel indel in	2 NMM NMM NMM NMM NMM NMM NMM NMM NMM NM		1946 1 19		NM N		No.	NM NM
# 346-5T NM N NM P356-7F NM India NM	## ## ## ## ## ## ## ## ## ## ## ## ##	M M M M M M M M M M M M M M M M M M M	missense indel	2 NMM NMM NMM NMM NMM NMM NMM NMM NMM NM		1946 1 19		NM N		No.	NM NM
# 346-5T NM N NM P356-7F NM India NM	## 8007 ## 81267 ## 81267 ## 81267 ## 81267 ## 81267 ## 84667 ## 8	M M M M M M M M M M M M M M M M M M M	indel	2 NMM NM		NAME		NM N		NO.50	NM NM
#21597 NM NM NM M misserue NM	## 1907 ## 13287 ## 1	M M M M M M M M M M	indel	2 NMM NMM NMM NMM NMM NMM NMM NMM NMM NM		1945 1945 1945 1945 1945 1945 1945 1945		No.		NAME	NM NM
#21597 NM NM NM M misserue NM	## 1907 ## 13287 ## 1	M M M M M M M M M M M M M M M M M M M	indel	2 NMM NMM NMM NMM NMM NMM NMM NMM NMM NM	missense	NAME		NM		300.00 100.00	NM NM
#5287 M indel NM NM NM NM NM 828057 M missions NM	## 1907 ## 13287 ## 13287 ## 13287 ## 13287 ## 13287 ## 13287 ## 13287 ## 14887 ## 1	M M M M M M M M M M M M M M M M M M M	missense indel ind	2 NIM	missense missense	NAME OF STATE OF STAT		NM		NAME	NM NM
WS4ST NM NM NM NM NM NM NM NM	## ## ## ## ## ## ## ## ## ## ## ## ##	M M M M M M M M M M	indel	2 NMM	missense misserise	Marco	missense	NM NM NM NM NM NM NM NM		300.00 100.00	NM NM
# # # # # # # # # # # # # # # # # # #	## ## ## ## ## ## ## ## ## ## ## ## ##	M M M M M M M M M M	missense indel ind	2 NMM	miserne miserne	Marco	missense	NM NM NM NM NM NM NM NM		300.00 100.00	NM NM
#2582T NM NM NM M missense NM NM NM #1314T NM NM NM	## ## ## ## ## ## ## ## ## ## ## ## ##	M M M M M M M M M M	missense indel ind	2 NMM	miseroe miseroe	NAME	nissenie	NM NM NM NM NM NM NM NM		No.001	Indel NM
	### ### #### #### ####################	M M M M M M M M M M	missense indel ind	2 NMM	missense missense	Marc	missense	NM		NAME	Indel NM
	## ## ## ## ## ## ## ## ## ## ## ## ##	M M M M M M M M M M	missense indel ind	2 NMM	misserise misserise	Made	missense	NM NM NM NM NM NM NM NM		300.00 100.00	Indel NM

Sample	Fusion_R0S1	usion_F	Ral_Var	RNAseq	Sequencer_RNAseq	Capture_Kit_RNAseq	Read_Size_RNAseq	brary_orientation_RNA	EGAS_RNA-	WES	Sequencer	Capture_Kit_Exome	Read_Size_	Library_orie	EGAS_WES
#2363T															
#477T	M	NM	NM	yes	HiSeq 4000	Next Ultra II Directional	75	Stranded, PE	EGAS000010	yes	HiSeq 4000	Twist Human Core Exome Enric	75	PE	EGAS00001003688
#1129T															
#1131T									2 2						
#1275T															
#1287T									8	0.00					
#2196T															
#2809T															
#2823T															
#2849T										0.00					
#4058T															
#4098T															
#4117T															
#536T															
#1343T	M	NM	NM	yes	HiSeq 2000	TruSeq Stranded mRNA	101	Stranded, PE	EGAS000010	yes	HiSeg 2000	SureSelect Human All-Exon kit v	7:	PE	EGAS0000100368
#819T															
#823T															
#1250T		-	-												
#2827T									8 8	5 5					
#372T															
#974T									1 1						

#979Y		L	I												
#1896T #2729T	M	NM	NM NM	yes yes	HiSeq 4000 HiSeq 4000	Next Ultra II Directional Next Ultra II Directional	75 75	Stranded, PE Stranded, PE	EGAS000010 EGAS000010	yes		Twist Human Core Exome Enric Twist Human Core Exome Enric	75 75	PE	EGAS00001003686 EGAS00001003686
W375T	M	NM NM	NM	yes yes	HiSeq 4000	Next Ultra II Directional	75 75	Stranded, PE	EGAS000010	yes	HiSeq 4000	Twist Human Core Exome Enric		PE	EGAS00001003686
#4110T #533T	M		NM NM	yes yes	HiSeq 4000 HiSeq 4000	Next Ultra II Directional Next Ultra II Directional	75	Stranded, PE Stranded, PE	EGAS000010 EGAS000010	yes	HiSeq 4000 HiSeq 4000	Twist Human Core Exome Enric Twist Human Core Exome Enric	75	PE	EGAS00001003686 EGAS00001003686
#755T #1851T									0 0		100				
#711T								8	8						
#1940T #757T	M	NA	NM	yes	HiSeq 4000	Next Ultra II Directional	75	Stranded, PE	EGAS000010	unio	HiSon 4000	Twist lauman Core Exome Foric	75	DE	EGAS00001003686
#222T	NM	M	NM	yes	HiSeq 4000	Next Ultra II Directional	75 75	Stranded, PE	EGAS000010	yes	HiSeq 2000	Twist Human Core Exome Enric SureSelect Human All-Exon kit v	75 75	PE	EGAS00001003686
#1234T #2798T															
#3074T							,								
#3723T #4116T															
#1355T								1.0							
#1439T #760T	NM	M	NM	yes	HiSeq 4000	Next Ultra II Directional	75	Stranded, PE	EGAS000010	yes	HiSeq 2000	SureSelect Human All-Exon kit v	75	PE	EGAS00001000679
#471T	NM	M	NM	yes	HiSeq 4000	Next Ultra II Directional	75	Stranded, PE	EGAS000010	yes	HiSeq 2000	SureSelect Human All-Exon kit v	75	PE	EGAS00001000679
#2561T #1231T															
#1496T	0.0000	1000			111.000.000.000.000		0.000.00							2222	
#835T #554T	NM	M	NM	yes	HiSeq 2000	TruSeq Stranded mRNA	101	Stranded, PE	EGAS000010	yes	HiSeq 2000	SureSelect Human All-Exon kit v	75	PE	EGAS00001003686
#574T															
#1342T #1354T		-	-						-						
#364T			=												
#377T #390T			-				16								
#742T							i i								
#1891T #378T							2		8 8						
#458T															
#506T #582T	_	-					10								-
#631T															
#680T #684T			-												-
#691T #955T			- 3												
#341T															
#2834T #1130T			=												
#1239T															
#1240T #1263T			-												
#1325T															
#873T #2615T	NM NM	M NM	NM M	yes yes	HiSeq 2000 HiSeq 2000	TruSeq Stranded mRNA TruSeq Stranded mRNA	101 101	Stranded, PE Stranded, PE	EGAS000010	yes	HiSeq 2000 HiSeq 2000	SureSelect Human All-Exon kit v SureSelect Human All-Exon kit v	75 75	PE	EGAS00001003686 EGAS00001003686
#1508T			-	,	1,000			3.00,10			, 2000	and the Capital Capita C			100000
#2193T #2197T		_	-												-
#2330T															
#2331T #2804T			-								_				
#2828T															
#2836T #3049T															
#4106T									8 7						
#544T #782T			-								_				
W970T															
#627T #1215T	NM	NM	М	yes	HiSeq 2000	TruSeq Stranded mRNA	101	Stranded, PE	EGAS0000100	3685					
#1490T				yes	Hiseq 2000	Trusey scranged mikrys	101	Stranded, PC	EGAGOGOTO	73003					
#756T	NM NM	NM	NM NM	yes	HiSeq 4000	Next Ultra II Directional	75	Stranded, PE	EGAS000010	1005	Hisaa 2000	SureSelect Human All-Exon kit v	76	PE	EGAS00001000679
#1424T #2334T	TOW	19091	NIM	yes	Hideq 4000	Next Olda ii Directional	- /3	Stranded, PE	20/000010	yes	riiseq 2000	Sureselect Human Air Exon Kit t	- "	r c	E0/0000100079
#480T #1021T	_	-	-												
#1351T							,								
#2369T															
#786T		_													
#786T #2773T															
#786T #2773T #2877T															
#786T #2773T #2877T #2879T #379T															
#786T #2773T #2877T #2879T #379T #708T							9								
#7861 #2773T #2877T #2879T #379T #708T #966T #1001T															
#786T #2773T #2877T #2879T #379T #708T #966T #1001T #1286T															
#786T #2773T #2877T #2879T #379T #708Y #366T #1001T #1286T #1519T #2810T															
#7807 #27731 #28777 #28797 #3791 #7087 #9607 #10017 #12867 #15197 #28107															
#7861 #27731 #28777 #28797 #3791 #7087 #9667 #10011 #12867 #28107 #28107 #4781															
#7801 #27731 #287771 #28797 #3797 #37057 #37067 #37067 #35137 #35137 #35137 #35137 #35137 #35137															
#7801 #22771 #22771 #23777 #23777 #23777 #23777 #2681 #258107 #258107 #278117 #278117 #278117 #278117															
#7801 #27731 #22771 #22777 #27797 #27797 #27797 #270017 #25107 #25107 #25117 #25117 #25117 #25117 #25117 #25117	NM	NAM	NM		HSer 2000	Trusan Stranded mRNA	101	Standed PE	FGAS000010	Wes .	HiSon 2000	Sorfelert Human All Evon Lit	75	DE	FEANOMORPHISE
#1905 #277917 #2277917 #2277917 #2277917 #2277917 #2277917 #237917 #230017 #23	NM	NM	NM	YIS .	Hi5eq 2000	TruSeg Stranded mRNA	101	Stranded, PE	EGAS000010	yes	HiSeq 2000	SureSelect Human All-Exon lot s	75	PE	EGAS50001003685
#1801 #27791 #27791 #27791 #27791 #17	NM	NM	NM	A22	HSeq 2000	Trusseg Stranded mRNA	101	Stranded, PE	EGAS000010	yes	HiSeq 2000	SureSelect Human All-Exon kit v	75	PE	EGA500001003685
# 1965 1757	NM	NM	NM	M2	HSeq 2000	TruSeg Stranded mRNA	101	Stranded, PE	EGAS000010	yes	HiSeq 2000	SureSelect Human All-Exon kit v	75	PE	EGAS00001003685
# 1905 # 22771	NM	NM	NM	745	HSeq 2000	TruSeg Stranded mRNA	101	Stranded, PE	EGA5000010	yes	HiSeq 2000	SureSelect Human All: Exon bit s	75	PE	EGA50001003685
# 17861 # 227791 # 237997 # 237997 # 27687 # 27687 # 236001 # 128607 # 236001 # 23600 # 236001 # 23600 # 236001 # 2360001 # 236001 # 236001 # 236001 # 236001 # 236001 # 236001 # 2360001 # 2360001 # 2360001 # 2360001 # 2360001 # 2360001 # 2360001	NM	NM	NM	W22	HSeq 2000	TruSeg Stranded mRNA	101	Stranded, PE	EGAS000010	yes	HiSeq 2000	SureSelect Human All-Exon Nit v	75	PE	EGA50001003686
# 1960 F 12231 F I2231	NM	NM	NM	YES	HSeq 2000	TruSeg Stranded mRNA	101	Stranded, PE	EGAS0000100	yes	HiSeq 2000	Sure-Select Human All-Exon let s	75	PE	EGA500011003686
# 1965 ### 1977 ##	NM	NM	NM	745	HSeq 2000	Yruśsię Stranded mRNA	101	Stranded, PE	EGA5000010	yes .	HiSeq 2000	SureSelect Human All-Exon Nit s	75	PE	EGA500001003686
# 1960 F 1225 F	NM	NM	NM	Mo	H5ng 2000	TruSeq Stranded mRNA	101	Stranded, PE	EGA5000010	yes	HiSeq 2000	SureSelect Human All-Exon kit v	75	PE	EGAS/00/10/3885
# 17861 # 2779	NM	NM	NM	Yes	H5rq 2000	Truseg Stranded mRNA	191	Stranded, PE	EGAS0000100	yes	HiSeq 2000	SureSelect Human All Exon lit s	75	PE	104500100386
# 17861 # 2777	NM	NM	NM	M2	H5eq 2000	TruSeq Stranded mRNA	191	Stranded, PE	EGAS0000100	yes	HiSeq 2000	SureSelect Human All-Exon kit v	25	PE	ECAGO003003666
# 1960 ### 1200 ##	NM	NM	NM	YES	H5sq 2000	TruSeg Stranded mRNA	161	Stranded, PE	EGA5000010	yes	HiSeq 2000	SureSelect Human All-Exon kit u	75	RE	EGAS0001003886
# 1960 ### 1977 #### 1977 #### 1977 #### 1977 #### 1977 #### 1977 ##### 1977 ##### 1977 ###################################	NM	NM	NM	745	MGre 2000	Trusseg Stranded mRNA	101	Stranded, PE	EGA5000016	yes	HiSeq 2000	SureSelect Human All-Exon kit s	75	PE .	(5450000000000
# 1780 # 1777 # 1777 # 1750 #	NM	NM	NM	M22	H5ng 2000	TruSeg Stranded mRNA	101	Stranded, PE	EGAS0000100	yes	HiSeq 2000	SureSelect Human All-Exon kit v	75	PE	EGAS/2001003885
# 17861 # 2777					Н5га 2000	Trusing Stranded miRNA	191	Stranded, PE	EGAS000010	1422	HiSeq 2000	SureSelect Human All-Exon bit v	755	PE	TGA60001003865
# 1786 # 1777 # 1	NM NM NM				H5ng 2000	TruSeq Stranded mRNA	191	Stranded, PE	EGAS000016	yes	HiSeq 2000	SureSelect Human All-Exon kit v	75	RE	CCASO001003685
# 1986 # 1977 # 1	NM	NM NM NM			H6sq 2000	Truseg Stranded mRNA	191	Stranded, PE	EGAS0000100	NG2	HiSeq 2000	SureSelect Human All-Exon Mr v	Ж	К	EGA5000100386
# 17801 # 2777	NM NM	NM NM	NM NM		HSrq 2000	Yruśsią Stranded mRNA	101	Stranded, PE	EGA5000016	No.	H5rq 2000	SureSelect Human All-Exon kit v	75	R	[6450001003885
# 1986 #### 1986 #### 1986 #### 1986 #### 1986 #### 1986 ###### 1986 ####################################	NM NM NM	NM NM	NM NM		H5ng 2000	TruSeg Stranded mRNA	163	Stranded, PE	EGAS000110	Yes	H5rq 2000	Sure-Select Human All-Exon let v	8	и	EGA50001003885
# 1960 127711 127	NM NM	NM NM	NM NM		H56q 2000	Yrušeig Stranded miRNA	301	Stranded, PE	(GAS000)10	No.	H5rq 2000	SureSelect Human All-Econ kit s	75	R	CGAG000000000088
# 1960 127711 127	NM NM NM	NM NM	NM NM		H5rq 2000	TruSeq Stranded mRNA	101	Stranded, PE	TGS50007D	yes	H6rq 2000	SureSelect Human All-Exon kit v	78	R	EGAS20001003885
# 1960 ### 1200 ##	NM NM NM	NM NM	NM NM		NGre 2000	Truskeg Stranded miRNA	101	Stranded, PE	(64000010	Nec	H5rq 2000	SureSelect Human All-Exon Nrt v	8	R	TGA50001003465
# 1760 # 1770 # 1	NM NM NM	NM NM	NM NM		H5ng 2000	Trusea Stranded mRNA	191	Stranded, PE	E6A500076	Yes	H6rq 2000	SoreSelect Human All-Exon kit v	75	R	CCASCOCIOCISSS
# 1986 # 1977 # 1	NM NM NM NM NM	NM NM NM NM	NM NM NM		H5rq 2000	Trusing Stranded miRNA	191	Stranded, PE	(GA500076	NO.	H5eq 2000	Sure-Select Human All-Exon Mr v	8	R	TGA50001003865
# 1760 # 1770 # 1	NM NM NM	NM NM	NM NM NM		H5eq 2000	TruSeg Stranded mRNA	101	Stranded, PE	(64000000)	Nes.	H6rq 2000	SureSelect Human All-Exon kit v	38	R	TGAS0001003685
# FIRST # FIRS	NM NM NM NM NM	NM NM NM NM	NM NM NM		H5rq 2000	Truses Stranded mRNA	191	Stranded, PE	[GA500076	Nea.	H6rq 2000	SureSelect Human All-Exon Mr v	75	K	
# FIRST # FIRS	NM NM NM NM NM	NM NM NM NM	NM NM NM		HSrq 2000	Yruśsią Stranded miRNA	301	Stranded, PE	[GA300016	Nez	H6mg 2000	SureSelect Human All-Econ kit v	75	R	CGAGGGGGGGGGGGGGGGGGGGGGGGGGGGGGGGGGGG
# 1960 12771	NM NM NM NM NM	NM NM NM NM NM	NM NM NM NM		H5rq 2000	Truseg Stranded mRNA	193	Stranded, PE	[GA500076	hez	H5rq 2000	Sure-Select Human All-Exon let v	8	ĸ	EGA60001003485
# 1780 # 1777 # 1	NM NM NM NM NM	NM NM NM NM	NM NM NM NM		HSeq 2000	YruSeig Stranded miRNA	301	Stranded, PE	(64800016	Mo	H66q 2000	SureSelect Human All Exon kit s	35	R	704000000000000000000000000000000000000
# 1780 # 1770 # 1	NM NM NM NM NM	NM NM NM NM NM	NM NM NM NM		H5nq 2000	Truses Stranded mRNA	191	Stranded, PE	[GA300010	No.	H5rq 2000	SureSelect Human All-Exon kit v	В	К	CCASCOCIOCISSS
# FIRST # FIRS	NIM NIM NIM NIM NIM NIM	NIM NIM NIM NIM NIM NIM	NM NM NM NM												
# 1786 # 1777 # 1	NM NM NM NM NM	NIM NIM NIM NIM NIM NIM	NM NM NM NM			Truseg Stranded mRNA	191		[CAX0000]0			SureSelect Human All-Exon kit v			ECASCO001003665
# 1700 # 1	NIM NIM NIM NIM NIM NIM	NIM NIM NIM NIM NIM NIM	NM NM NM NM												
# 1786 # 1777 # 1	NIM NIM NIM NIM NIM NIM	NIM NIM NIM NIM NIM NIM	NM NM NM NM												
# 1786 # 1777 # 1	NIM NIM NIM NIM NIM NIM	NIM NIM NIM NIM NIM NIM	NM NM NM NM												
# 1786 # 1770 # 1	NIM NIM NIM NIM NIM NIM	NIM NIM NIM NIM NIM NIM	NM NM NM NM												
# 1786 127711 12771 12771 127711 127711 12771 12771 12771 127711 127711 127711 127711 127711	NIM NIM NIM NIM NIM NIM	NIM NIM NIM NIM NIM NIM	NM NM NM NM												
# 1905 # 1907 #	NIM NIM NIM NIM NIM NIM	NIM NIM NIM NIM NIM NIM	NM NM NM NM												
# 1786 # 1787 # 1	NIM NIM NIM NIM NIM NIM	NIM NIM NIM NIM NIM NIM	NM NM NM NM												
# 1780 # 1777 # 1	NIM NIM NIM NIM NIM NIM	NIM NIM NIM NIM NIM NIM	NM NM NM NM												
# 1786 # 1787 # 1	NIM NIM NIM NIM NIM NIM	NIM NIM NIM NIM NIM NIM	NM NM NM NM												

#2802T															
#2802T #2803T #2826T															
#2826T #2929T									0 0					_	
#2829T #2830T										0 0					
#2837T #2856T		_	-												-
#750T #2900T	NM	NM	NM	yes	HiSeq 2000	TruSeq Stranded mRNA	101	Stranded, PE	EGAS000010	yes	HiSeq 2000	SureSelect Human All-Exon kit	75	PE	EGAS00001003686
#2900T															
#2901T #3104T		_	-							-	_			_	-
#3107T #344T										7					
#344T		_	-						-					_	
#3781T #382T											_			_	
#4108T #4109T															
#4109T #2217T			-											-	
MASST															
#456T															
#456T #457T #466T			-								-			_	_
#473T #481T															
#481T														-	
#490T #503T															
#1023T															
#1124T #552T		_												-	
DETENT.															
#560T #581T			=												
#5811 #594T #670T			_												
#670T #698T							2		9						
#698T #745T	_	-	-		_						_		_	-	\vdash
#745T #751T															
#7547 #7717 #7727 #8217 #8447															
#771T #772T			-							_				_	\vdash
#821T															
#844T #858T			-												
#861T														_	
#864T															
#867T #973T		_	-												
#973T #975T #1666T															
#1666T							,								
#2825T #2857T		_	-				2				_			-	
#468T #839T															
#470T #1916T			-				0							_	-
#1916T															
#1328T #1329T															
										_	_		_	_	
#469T															
#469T #1434T															
#469T #1434T #1915T #1488T															
#469T #1434T #1915T #1488T															
#469T #1434T #1915T #1488T #1489T #624T															
#469T #1434T #1915T #1488T #1489T #624T #1432T #1678T															
#469T #14324T #1915T #1488T #1489T #624T #1432T #1678T #189T	NM M	NM NM	NM NM	yes_ ves	HiSeq 4000	TruSeg Stranded mRNA	75 75	Stranded, PE Stranded PE	EGA5000010	03685					
#4697 #13347 #19157 #14887 #14897 #6247 #14327 #15787 #3897 #46897	NM M	NM NM NM	NM NM	Yes Yes Yes	HiSeq 4000 HiSeq 4000	TruSeq Stranded mRNA Next Ultra II Directional Next Ultra II Directional	75 75 75	Stranded, PE Stranded, PE Stranded, PE	EGAS000010 EGAS000010 EGAS000010	03685 03685					
#4697 #13347 #19157 #14887 #14897 #6247 #14327 #15787 #3897 #46897	NM M M	NM NM NM	NM NM	Nez Nez Nez	HiSeq 4000 HiSeq 4000 HiSeq 4000	TruSeq Stranded mRNA Next Ultra II Directional Next Ultra II Directional	75 75 75	Stranded, PE Stranded, PE Stranded, PE	EGAS000010 EGAS000010	03685 03685 03685 1yes	HiSeq 2000	SureSelect Human All-Exon kit	, 75	PE	EGAS00001000679
#4697 #1434T #1935T #1488T #1489T #624T #1432T #1528T #1890T #444T #623T #1244T	NM M M	NM NM NM	NM NM NM	Nez Nez Nez	HiSeq 4000 HiSeq 4000 HiSeq 4000	TruSeq Stranded mRN/N Vext Ultra II Directional	75 75 75 75	Stranded, PE Stranded, PE Stranded, PE	EGAS000010 EGAS000010	03685 03685	HiSeq 2000	SureSelect Human All-Exon ldt	, 75	PE	EGAS00001000679
#4697 #1434T #1935T #1488T #1489T #624T #1432T #1528T #1890T #444T #623T #1244T	NM M M	NM NM NM	NM NM NM	Ace Ace Ace	HiSeq 4000 HiSeq 4000 HiSeq 4000	Truseq Stranded mRNAN Next Ultra II Directional Vext Ultra II Directional	75 75 75 75	Stranded, PE Stranded, PE Stranded, PE	EGAS000010 EGAS000010	03685 03685	HiSeq 2000	SureSelect Human All-Exon kit	, 75	PE	EGAS00001000679
#469Y #1434Y #1515Y #1468Y #524Y #524Y #1578Y #1578Y #4696Y #6691Y #1574Y #1574Y #1597 #1597	NM M M	NM NM NM	NM NM NM	Nez Asz Asz	HiSeq 4000 HiSeq 4000 HiSeq 4000	TruSeq Stranded mRNANAN Next Ultra II Directional Next Ultra II Directional	75 75 75	Stranded, PE Stranded, PE Stranded, PE	EGAS000010 EGAS000010	03685 03685	HiSeq 2000	SureSelect Human All-Exon lot	75	PE	EGAS00001000679
#469Y #1434Y #1515Y #1468Y #524Y #524Y #1578Y #1578Y #4696Y #6691Y #1574Y #1574Y #1597 #1597	NM M M	NM NM NM	NM NM NM	7955 7965 7965	HiSeq 4000 HiSeq 4000 HiSeq 4000	TruSeg Stranded mRNA Next Ultra II Directional Next Ultra II Directional	75 75 75	Stranded, PE Stranded, PE Stranded, PE	EGAS000010 EGAS000010	03685 03685	HiSeq 2000	Sure-Select Human All-Exon Sitt	, 75	PE	EGAS00001000679
#469Y #1434Y #1595Y #1685Y #654Y #654Y #1678Y	NM M M	NM NM NM	NM NM NM	745 745 745	HiSeq 4000 HiSeq 4000 HiSeq 4000	Trusee Stranded miRNA Next Ultra II Directional Next Ultra II Directional	75 75 75 75	Stranded, PE Stranded, PE Stranded, PE	EGAS000010 EGAS000010	03685 03685	HiSeq 2000	SurdSelect Human All-Exon lot	755	PE	EGAS00001000679
#469Y #1434Y #1595Y #1685Y #654Y #654Y #1678Y	NM M M	NM NM NM	NM NM NM	795 795 795 795	HiSeq 4000 HiSeq 4000 HiSeq 4000	TruSeg Stranded miNNA Next Ultra II Directional Next Ultra II Directional	75 75 75	Stranded PE Stranded PE Stranded, PE	EGAS000010 EGAS000010	03685 03685	HiSeq 2000	SureSelect Human All-Exon Set	75	PE	EGAS00001000679
##607 #144417 #144417 #144697 #14697	NM M M	NM NM NM	NM NM NM	Yes	HiSeq 4000 HiSeq 4000 HiSeq 4000	TruSeg Stranded mRNA Next Ultra II Directional Vext Ultra II Directional	75 75 75	Stranded, PE Stranded, PE Stranded, PE	EGAS000110 EGAS000110	03685 03685	HiSeq 2000	Suréselect Human All-Exon let	75	PE	EGAS00001000579
##607 #144417 #144417 #144697 #14697	NM M M	NM NM NM	NM NM NM	795 795 795 795	HiSeq 4000 HiSeq 4000 HiSeq 4000	Truses stranded m8NNA Next Ultra II Directional Next Ultra II Directional	75 75 75 75	Stranded, PE Stranded, PE Stranded, PE	EGAS000010 EGAS000010	03685 03685	HiSeq 2000	SureSelect Human All-Cron Sct.	75	PE	EGAS00001000879
##607 #14441 #14441 #14487 #14887 #14887 #14887 #14887 #14887 #14887 #14441 #14	NM M M	NM NM NM	NM NM NM	YES YES YES	HiSeq 4000 HiSeq 4000 HiSeq 4000	Truseg Stranded milbland Sect Uttra II Directional Next Uttra II Directional	75 76 75 75	Stranded, PE Stranded, PE Stranded, PE	EGAS000010 EGAS000010 EGAS000010	03685 03685	HiSeq 2000	Surefellect Human All-Econ let	75	PE	EGAS00001000679
##607 #14441 #14441 #14487 #14887 #14887 #14887 #14887 #14887 #14887 #14441 #14	NM M M	NM NM NM	NM NM NM	Age	HiSeq 4000 HiSeq 4000 HiSeq 4000	Truseg Stranded mRNAN Next Ultra II Directional Next Ultra II Directional	75 75 75	Stranded PE Stranded PE Stranded, PE Stranded, PE	EGAS000010 EGAS000010	03685 03685	HiSeq 2000	SunSelect Human All-Exon lot	75	PE	EGASC0001000679
##697 ##607 ##607 ##607	NM M M	NM NM NM	NM NM NM	V65 V65 V65	H564 4500 H564 4500 H564 4500	Trudes Sounded miRNA Next Ultra III Directional Next Ultra III Directional	75 75 75	Stranded PE Stranded PE Stranded, PE	EGAS000011C EGAS00001C	03685 03685	HiSeq 2000	Surphilect Human Alli Lion let	75	PE	EGAS00001000679
##691 #14541 #14541 #14541 #14541 #14541 #14541 #14541 #14541 #14541 #14541 #14541 #14541 #14541 #14541 #14541 #14541 #14541 #14561 #14	NM M M	NM NM NM	NM NM NM	Age	HiSeq 4000 HiSeq 4000 HiSeq 4000	Trusing Stranded miRNA Next Ultra II Directional Next Ultra II Directional Next Ultra II Directional	75 75 75	Stranded PE Stranded PE Stranded, PE Stranded, PE	EGAS00001G EGAS00001G EGAS00001G	03685 03685	HiSeq 2000	SureSelect Human All-Exon lot	75	PE	EGASSO0010006 79
##607 ##607	NM M M	NM NM NM	NM NM NM	N62 N62	HSsq 4900 HSsq 4000 HSsq 4000	Truses Stranded miRNA Nest Ultra II Directional Nest Ultra II Directional Nest Ultra II Directional Nest Ultra II Directional	73 75 75	Stranded PE Stranded PE Stranded PE	EGAS000016 EGAS000016	03685 03685	HiSeq 2000	Sursishert Human Alli Com let	755	PE	EGASG0001000879
##691 #14541 #14541 #14541 #14541 #14541 #14541 #14541 #14541 #14541 #14541 #14541 #14541 #14541 #14541 #14541 #14541 #14541 #14561 #14	NM M M	NM NM NM	NM NM NM	YES YES YES	H56q 4500 H56q 4500 H56q 4500	Trubes Stranded mRNA files	5 5 5 7	Stranded, PE Stranded, PE Stranded, PE	EGAS000016 EGAS00016	03685 03685	HiSeq 2000	SurpSelect Human All Corn lot	75	PE	(6480000000)
##691 #14541 #14541 #14541 #14541 #14541 #14541 #14541 #14541 #14541 #14541 #14541 #14541 #14541 #14541 #14541 #14541 #14541 #14561 #14	NM M M	NM NM NM	NM NM NM	V65 V65	HSnc 4000 HSnc 4000 HSnc 4000 HSnc 4000	Trudes Stranded mRNA New Unit in Trudes Stranded mRNA New Unit in Trudestowal	73 75 75 75	Stranded PE Stranded PE Stranded PE	EGAS00010 EGAS00010	03685 03685	HiSeq 2000	Surskelect Human All-Exon ker	75	PE	EGA60001000879
##691 #14541 #14541 #14541 #14541 #14541 #14541 #14541 #14541 #14541 #14541 #14541 #14541 #14541 #14541 #14541 #14541 #14541 #14561 #14	NM M M	NM NM NM	NM NM NM	7755 7755 7755 7755	H56q 6500 H56q 6500 H56q 6000	Trudes Stranded mWHATE	5 5 7	Stranded PE Stranded PE Stranded, PE	EGAS000010 EGAS000010	03685 03685	HiSeq 2000	Sursilect Human All-Econ let	75	PE	EGAS0001000-79
### ##################################	NM M	NM NM NM	NM NM NM	V62 V65	HSca 4000 HSca 4000 HSca 4000 NSca 4000	Trudes Stranded mRNAM New Units II Decisional Management of the Committee	73 75 75 75	Stranded PE Stranded PE Stranded PE	EGAS000010 EGAS000010 EGAS000010	03685 03685	HiSeq 2000	Surskelect Human All-Exon ker	75	FE	E0A60001000F79
#### #################################	NMA M M	NM NM NM	NM NM NM	YES YES YES	H5sq 9500 H5sq 8000 H5sq 8000	Trudeg Stranded mRNA Meet UPI all Directional	5 5 7 7	Stranded PE Stranded PE Stranded, PE	EGAS000010 EGAS000010 EGAS000010	03685 03685	HiSeq 2000	Surselect Human All-Licon let	75	PE	[GA50001000/9]
#### #################################	NMA MA M	NM NM NM	NM NM NM	VES PRES	Hone 4000 Hone 4000 Hone 4000 None 4000	Trudee Stranded mRNAM view of the Court of the Cour	75 75 75 75	Stranded, PE Stranded, PE Stranded, PE	EGAS000110 EGAS000110 EGAS000110	03685 03685	HiSeq 2000	Surskelect Human Alf-Exon let	75	PE	608000100079
#### #################################	NM M M	NM NM NM	NM NM NM	YES YES YES	HSicq 9000 HSicq 8000 HSicq 8000	Trudeg Stranded mRNA Meet UP in 1 Directional Meet UP in 1 Direction	3 3 5 7	Stranded PE Stranded PE Stranded, PE	EGA0000011C	03685 03685	HiSeq 2000	Surdelect Human All-Escon let	75	PE PE	G04500010006/9
##607 ##607	NMA M M M	NM NM NM	NM NM NM	WES WEST	H5nc 4000 H6sc 4000 H6sc 4000	Trudes Stranded mRNA for the Country of the Country	75 75 75 75	Stranded, PE Stranded, PE Stranded, PE	[GAA0000116]	03685 03685	HiSeq 2000	Surphilect Human All-Exon let	75	PE	60450001000879
##607 #14441 #14	NSM M M	NM NM NM	NM NM NM	Yes Yes Yes	HScq 6000 HScq 6000 HScq 6000	Trudeg Stranded mRNA Meet UFIS I Directional Meet UFIS I DIRECTION MEET UFIS I DIREC	5 5 7 7	Stranded, PE Stranded, PE Stranded, PE	E6A40000116	03685 03685	H56q 2000	Surdelect Human All-Econ Int	75	R	[GAS00000007]
##607 ##607	NMA M M M	NM NM NM	NM NM NM	WS W	H5nc 4000 H6sc 4000 H6sc 4000	Trudes Stranded mRNAM in the Control of	75 75 75 75	Stranded, PE Stranded, PE Stranded, PE	[CA400001]	03685 03685	H56q 2000	Surdislect Human Affi Exon let	4 75	PE	608000100079
##007 #14447 #14	NM M	NM NM NM	NM NM NM	Yes Yes Yes	HScq 6000 HScq 6000 HScq 6000	Trudes Stranded mRNA Meet UFIS II Directional Meet UFIS II Direction	5 5 7 7	Stranded, PE Stranded, PE Stranded, PE	EGASO00011 EGASO00011 EGASO00011	03685 03685	History 2000	Sursiblect Human All-Econ let	75	PE	[GAS0000000679
##007 #14447 #14	NMM M M	NM NM NM	NM NM NM	V65 V65 V65	H5ne 4000 H6ne 4000 H6ne 4000	Trudes Stranded mRNAM in the Control of	75 75 75 75	Stranded, PE Stranded, PE Stranded, PE	ECASOSSITION CONTRACTOR CONTRACTO	03685 03685	H5rq 2000	Surfelect Human All-Econ let	75	PE	EGASG0001000879
##097 #14447 #14	NMA M M	NM NM NM	NM NM NM	YES YES YES YES	HSsq 4000 HSsq 4000 HSsq 4000 HSsq 4000	Truses Stranded mRNAME (Fig. 1) Trusted Stranded mRNAME (Fig. 1) Directional Meet Urins in Direc	5 5 7 8	Stranded, PE Stranded, PE Stranded, PE	(2A0000101 (2A20000101 (2A20000101 (2A20001010101010101010101010101010101010	03685 03685	History 2000	Surdalect Human All-Econ let	75	PE	[GAS0000000879
##007 ##000 ##000	NIM NM M M	NIM NAM NAM	NM NM NM	V65 V65 V65	H5nd 4000 H6nd 4000 H6nd 4000	Trubbeg Stranded mRNAM has been controlled to the controlled management of	75 75 75	Stranded, PE Stranded, PE Stranded, PE	EAACOODIG TO ACCOUNT OF THE PART OF THE PA	03685 03685	H649,2000	Surfsleet Human All-Econ let	73	R	CGASGOO1000879
##007 #14447	NMA M M	NIM NM NM	NM NM NM	V45 V45 V46	HSrq 4000 HSrq 4000 HSrq 4000 HSrq 4000	Trusses Stranded mRNA Med Urra II Drectional	5 5 5 7	Stranded, PE Stranded, PE Stranded, PE	[GAA000010] [GAA000010] [GAA000010]	03685 03685	H56q 2000	Sureleilet Human All-Exen let	75	Æ	E0450001008/9
##007 ##14417	NIM NI NI M	NMA NAM NMA	NM NM NM	yes yes	H5nd 4000 M5dd 4000 H6nd 4000	Trubbeg Stranded mRNAM has been controlled to the controlled mean to	75 75 75	Stranded, PE Stranded, PE Stranded, PE	[GAS00001C] [GAS00001C] [GAS00001C]	03685 03685	H6sq 2000	Surdelect Human All-Econ let	3	R	GGASGOO310008 79
##007 ##007	NMA M M	NM NM NM	NM NM NM	V65 V65 V65	HSrc 4000 HSrc 4000 HSrc 4000	Trusses Stranded miNNAM to the Current Strands of the Current Strand	5 5 5 3	Stranded, PE Stranded, PE Stranded, PE	EGA400001E	03685 03685	H56q 2000	Surchitect Human All-Exen let	4 73	K	[GAS0000000079
##607 #14441	NIM NI M M	NM NM NM	NM NM NM	WES WES WES WEST WAS A STATE OF THE PROPERTY O	H5nd 4000 H5nd 4000 H5nd 4000	Trubes Stranded mRNAM to the Country of the Country	35 35 35	Stranded, PE Stranded, PE Stranded, PE	EGAS00011 EGAS000011 CGAS000011	03685 03685	H56q 2000	Surpleiect Human All-Econ let	75	PE	GGASGOO1000879
##607 ##6007 ##6000 ##6000 ##6000 ##6000 ##6000 ##6000 ##6000 ##6000 ##6000 ##6000 ##6000 ##6000 ##6000 ##6000 ##6000 ##6	M	NM NM	NM	V65	H5sc 4000 H5sc 4000 H5sc 4000 H5sc 4000	Trusses Stranded miRNAM in the CHITAIN TO STREET MAN	5 5 5 3	Stranded, PE Stranded, PE Stranded, PE	EGASO0001E	03685 03685	H56q 2000	Surdelect Human All-Loon let	4 75	PE .	[GJS00000000279
##607 ##607	NM M M	NM N	NM	WES WES WEST WAS A STATE OF THE	H5nd 4000 H5nd 4000 H5nd 4000	Trubes Stranded mRNAM to the Country of the Country	35 35 35	Stranded, PE Stranded, PE Stranded, PE	EGASOOGIE (GASOOGIE)	03685 03685	H56e 2000	Surpleiect Human All-Econ let	75	PE	[GASG0001000879
##007 ##007	M	NM NM	NM	V62 V65	H5sc 4000 H5sc 4000 H5sc 4000 H5sc 4000	Trusses Stranded miRNAM in the CUPTS II Deschool with the CUPTS II Deschool well Ulina II Deschool well Ulina II Deschool with II Deschool wit	75 75 75 75	Stranded, PE Stranded, PE Stranded, PE	EGA400001E	03685 03685	H56q 2000	Sursishert Human All-Loon let	4 75	PE .	E0450001000 79
##007 #15557 #15667	M M	NM NM	NM	WES WES WEST	H5nd 4000 H5nd 4000 H5nd 4000	Trubes Stranded mRNAM better that the control of th	35 35 36	Stranded, PE Stranded, PE Stranded, PE	EGASOOGIE (GASOOGIE)	03685 03685	H56q 2000	Surpleiect Human All-Econ let	75	PE	[GASG0001000879

MEC-Indistruction

MEC-Indistruc

Supplementary Figure 1

Flow chart

657 HCA samples

Analysis of:

- Somatic Mutation (7 genes)

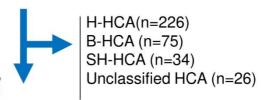
 HNF1A IL6ST CTNNB1 FRK STAT3

 GNAS JAK1
- Expression (17 genes)

 RNA18S FABP1 UGT2B7 CRP SAA2

 GLUL LGR5 PTCH1 GLI1 HHIP TNNC1

 FCRLA PTGDS ADGRG3 ROS1 FRK IL6



296 Inflammatory HCA

IL6ST mutation (n=180; 61%)

FRK mutation (n=25; 8%)

STAT3 mutation (n=15; 5%)

GNAS mutation (n=10; 3%)

JAK1 mutation (n=7; 2%)

Non Mutated (n=61, 21%)

Deep sequencing:

- RNAseq (n=22;

1 already published*, 21 new)

- WES (n=19;

4 already published*, 15 new)

22 non mutated IHCA analyzed by deep sequencing

ROS1 fusion	FRK fusion	<i>IL6</i> rearrangements	Non Mutated
(n=10)	(n=5)	(n=2)	(n=5)

upplementa	ry Table 3: Somatic mutations in JAK/STAT path	4			-					
Sample	IL6ST_Mutation(NM_002184.3)	type_mutatio n_IL6ST	GNAS1_Mutation(NM_000516. 4)	type_mutation_ GNAS1	STAT3_Mutation(NM_139276.2)	type_mutation_ STAT3	JAK1_Mutation(NM_002227.2)	type_mutation _JAK1	FRK_Mutation(NM_002031.2)	type_mutation _FRK
#480T							c.1932G>T; p.Gln644His / c.1933G>T; p.Val645Phe	missense		
#1678T #2334T							c.1932G>T; p.Gin644His / c.1933G>T; p.Val645Phe c.1646G>A / c.1647A>T; p.Arg549His	missense		
#222T							C.1040G-M./ C.1047A-71, p.Aig543His	missense		
#331T										
#341T					c.233T>G;p.Leu78Arg	missense			c.1037A>G;p.Glu346Gly	missense
#343T #344T	c.560_571del;p.Ser187_Tyr190del	indel								
#362T	c.560_571del;p.Ser187_Tyr190del	indel								
#552T	c.563_574del;p.Thr188_Val192delinslle	indel								
#364T #372T	c.565_576del;p.Val189_Val192del c.647C>A;p.Pro216His	indel								
#375T										
#377T	c.565_576del;p.Val189_Val192del	indel								
#378T #379T				c 1504G	>T;p.Asp502Tyr / c.1972_1974delinsTAT;p.L	missenserindel				
#382T	c.560_571del;p.Ser187_Tyr190del	indel		0.23010	1,000,000,000,000,000,000,000,000,000	maserocimoci				
#389T										
#390T #455T	c.557_574del;p.Tyr186_Val192delinsPhe	indel								
#456T	c.565_576del;p.Val189_Val192del c.565_576del;p.Val189_Val192del	indel								
N457T	c.565_576del;p.Val189_Val192del	indel								
#458T		1000000								
#466T #467T	c.560_571del;p.Ser187_Tyr190del	indel								
#468T	c.647C>A;p.Pro216His	missense								
#469T	c.557_571del;p.Tyr186_Tyr190del	indel								
#470T #471T	c.557_571del;p.Tyr186_Tyr190del	indel								
#4711 #473T	c.564_575del;p.Val189_Val192del	indel								
#477T										
#478T	00000000000000000000000000000000000000		c.602G>A;p.Arg201His	missense						
#481T #485T	c.615_644dup;p.Phe214_Asp215dup c.647C>A; p.Pro216His	indel								
#490T	c.557_571del;p.Tyr186_Tyr190del	indel								
#503T	.566_580delinsATG;p.Val189_lle194delinsAspVa	indel								
#504T										
#506T #528T	c.557_571del;p.Tyr186_Tyr190del	indel								
#533T	4337_31444[KIN440_IN43444									
#536T	c.566_577del;p.Val189_Asn193delinsAsp	indel								
#544T #545T								c	.1132_1137del;p.Val378_Phe379d	indel
#554T							c.2729T>C; p.Leu910Pro	missense		
#555T	c.503_580del;p.Lys168_Asn193del	indel								
#560T	c.557_571del;p.Tyr186_Tyr190del	indel			Village of the second	No. agreement of the				
#574T #581T	c.560_571del;p.Ser187_Tyr190del	indel			c.496G>C;p.Glu166Gln	missense				
#582T										
#594T	c.563_574del;p.Thr188_Val192delinslle	indel								
#623T #624T								c.11	33_1138del;p.Val378_Lys380delin	indel
#627T									1140delinsA;p.Phe379_Lys380de	
#631T	c.636_644del;p.Asn213_Asp215del	indel								
#669T	s 560 571dalin Sas197 Tur190dal	Indal					c.2729T>C; p.Leu910Pro	missense		
#670T #672T	c.560_571del;p.Ser187_Tyr190del	indel								
#680T	c.563_577del.p.Thr188_Val192del	indel								
#684T	c.565_576del;p.Val189_Val192del	indel								
#691T #698T	c.518_532del;p.Lys173_Asp177del c.568_579del;p.Tyr190_Asn193del	indel								
#706T										
#708T	Mary Company of the C	T myganen			c.1919A>T;p.Tyr640Phe	missense				
#711T #742T	c.643_645del;p.Asp215del c.518_532del;p.Lys173_Asp177del	indel								
#7421 #744T		indei								
#745T	c.562_573del;p.Thr188_Phe191del	indel								
#748T										
#750T #751T	c.560_571del;p.Ser187_Tyr190del	indel								
W754T	c.647C>A;p.Pro216His	missense								
#755T										
#756T	c.552_566del;p.Asp185_Val189del	indel								
#757T #760T	c.647C>A;p.Pro216His	missense								
	c.557_571del;p.Tyr186_Tyr190del	indel								
#769T		1 10000000								
#769T #771T	c.564_575del;p.Val189_Val192del	indel								
#771T #772T	c.564_575del;p.Val189_Val192del c.562_573del;p.Thr188_Phe191del	indel							1132 1137dalia Voltaza al	ledel
#779T #771T #772T #782T	c.562_573del;p.Thr188_Phe191del	indel						c	.1132_1137del;p.Val378_Phe379d	indel
#771T #772T								c	.1132_1137del;p.Val378_Phe379d	indel
#779T #771T #772T #782T #786T	c.562_573del;p.Thr188_Phe191del	indel						c	1132_1137del;p.Val378_Phe379d	indel

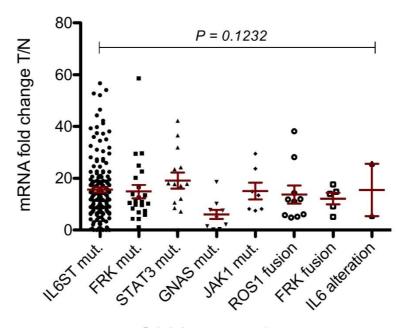
		92		5-	yl-		0.			
#839T	c.647C>A;p.Pro216His	missense								
#844T	c.562_573del;p.Thr188_Phe191del	indel								
#854T			c.602G>A;p.Arg201His	missense						
#857T	c.560_571del;p.Ser187_Tyr190del	indel	V=0.000.000.000.000.000.000.000.000.000.							
#858T	c.563_574del;p.Thr188_Val192delinsile	indel								
W861T	c.560_571del;p.Ser187_Tyr190del	indel								
#864T	c.1252_1263del;p.Ala418_Phe421del	indel								
#867T	c.583_588del;p.Glu195_Val196del	indel								
#873T	9.000.00									
#955T	c.556_571delinsA;p.Tyr186_Phe191delinslle	indel								
#958T			c.602G>A;p.Arg201His	missense						
#966T			W 4299		c.1919A>T;p.Tyr640Phe	missense				
#969T										
#970T								c	.1132_1137del;p.Val378_Phe379de	indel
#973T	c.569_578delinsC;p.Tyr190_Asn193delinsSer	indel								
#974T	c.647C>A;p.Pro216His	missense								
#975T	c.560_571del;p.Ser187_Tyr190del	indel								
#976T	c.570_578del;p.Phe191_Asn193del	indel								
W979T	c.646_648del;p.Pro216del	indel								
#1001T			c.601C>T;p.Arg201Cys	missense						
#1002T	c.592_618del;p.Glu199_Val207del	indel								
#1004T	c.592_618del;p.Glu199_Val207del	indel								
#1021T					c.1969_1980dup;p.Tyr657_Met660dup	indel				
#1020T	p.Tyr186_Tyr190del	indel								
#1023T	c.646_647ins33;p.Asp215_Pro216ins11	indel								
#1121T	c.557_571del;p.Tyr186_Tyr190del	indel								
#1124T	c.571_579del;p.Phe191_Asn193del	indel								
#1129T	c.560_571del;p.Ser187_Tyr190del	indel								
#1131T	c.564_576delinsA;p.Val189_Val192del	indel								
#1130T								c.1037	N>G;p.Glu346Gly/c.1049A>G;p.Tyr	missense
#1215T									W. 141	
#1216T	c.1252_1263del;p.Ala418_Phe421del	indel								
#1231T										
#1232T	c.563_574del;p.Thr188_Val192delinsile	indel								
#1234T										
#1238T	c.573_582delinsG;p.Phe191_lle194delinsLeu	indel								
#1239T	c.575_Sozdelinso,p.rne252_ne254delinsted	moer							c.1037A>G;p.Glu346Gly	missense
#1240T									.1132_1137del;p.Val378_Phe379d	
#1235T	c.565_574delinsT;p.Val189_Val192delinsPhe	indel								
#1250T	c.647C>A;p.Pro216His	missense								
#1241T										
#1243T	c.557_574del;p.Tyr186_Val192delinsPhe	indel								
#1251T	c.560_571del;p.Ser187_Tyr190del	indel								
#1252T	c.560_571del;p.Ser187_Tyr190del	indel								
#1263T	C.500_5/10C/,p.5C/10/_T//12/00C/	mour						c.1132_113	33delinsAAACTAAA;p.Val378delins	indel
#1269T										
#1275T	c.643_645del;p.Asp215del	indel								
#1285T	c.568_579del;p.Tyr190_Asn193del	indel								
#1286T	and a second of the second of		c.602G>A;p.Arg201His	missense						
#1287T	c.557_571del;p.Tyr186_Tyr190del	indel	a control of the cont							
	518_535delinsCCG;p.Lys173_Pro179delinsThrAl	indel								
#1290T	c.577_580delinsT;p.Asn193_lle194delinsPhe	indel								
#1291T	c.564_575del;p.Val189_Val192del	indel								
#1296T	c.567_578del;p.Tyr190_Asn193del	indel								
#1297T	c.562_573del;p.Thr188_Phe191del	indel								
#1301T	c.643_645del;p.Asp215del	indel								
#1302T	c.560_571del;p.Ser187_Tyr190del	indel								
#1302T	c.565_576del;p.Val189_Val192del	indel								
#1305T	c.518_532del;p.Lys173_Asp177del	indel								
#1306T	c.557_571del;p.Tyr186_Tyr190del	indel								
#1313T	c.560_571del;p.Ser187_Tyr190del	indel								
#1313T										
#13141 #1319T	c.560_571del;p.Ser187_Tyr190del	indel								
#1321T	c.573_582delinsG;p.Phe191_lle194delinsLeu	indel								
#13211 #1325T		mdei						c 1027	AbG in Glu346Gly/r 10494 bg in Time	missenra
#1325T	c.567_578del;p.Tyr190_Asn193del	indel						C.1037/	4>G;p.Glu346Gly/c.1049A>G;p.Tyr	masense
#13281 #1329T	c.560_571del;p.Ser187_Tyr190del	indel								
#13291 #1331T	mind Same at Charles and Charl	indel								
#1331T #1330T	c.567_578del;p.Tyr190_Asn193del									
	c E19 E23dolin I 123 A 123d-1			-						
-	c.518_532del.p.Lys173_Asp177del	indel								
#1440T	c.557_571del;p.Tyr186_Tyr190del	indel								
#1440T #1335T	c.557_571del;p.Tyr186_Tyr190del c.557_571del;p.Tyr186_Tyr190del	indel								
#1440T #1335T #1336T	c.557_571del;p.Tyr186_Tyr190del c.557_571del;p.Tyr186_Tyr190del c.560_571del;p.Ser187_Tyr190del	indel indel indel								
#1440T #1335T #1336T #1337T	c.557_571del.p.Tyr186_Tyr190del c.557_571del.p.Tyr186_Tyr190del c.560_571del.p.Ser187_Tyr190del c.1252_1263del.p.Ala418_Phe421del	indel indel indel indel								
#1440T #1335T #1336T #1337T #1339T	c.557_571del:p.Tyr186_Tyr190del c.557_571del:p.Tyr186_Tyr190del c.560_571del:p.Ser187_Tyr190del c.1252_1263del:p.Ala418_Phe421del c.564_576delinsA:p.Val189_Val192del	indel indel indel indel								
#1440T #1335T #1336T #1337T #1339T #1342T	c.557_571del.p.Tyr186_Tyr190del c.557_571del.p.Tyr186_Tyr190del c.560_571del.p.Ser187_Tyr190del c.1252_1263del.p.Ala418_Phe421del	indel indel indel indel								
#1440T #1335T #1336T #1337T #1339T #1342T	c.557_571del:p.Tyr186_Tyr190del c.557_571del:p.Tyr186_Tyr190del c.560_571del:p.Ser187_Tyr190del c.1252_1263del:p.Ala418_Phe421del c.564_576delinsA:p.Val189_Val192del	indel indel indel indel								
#1440T #1335T #1336T #1337T #1339T #1342T #1343T	c557_571delp_Tyr186_Tyr190del c557_571delp_Tyr186_Tyr190del c560_571delp_Ser187_Tyr190del c1252_1266delp_Ala418_Phe212del c.564_576delimAp_Val189_Val1924el c.518_532delp_Lys173_App177del	indel indel indel indel indel indel			c.1968_1969insTTT:p.Gly656_Tyr657insPhe	indel				
#1440T #1335T #1336T #1337T #1339T #1342T #1343T #1351T	c.557_571delp_Tyr186_Tyr190del c.557_571delp_Tyr186_Tyr190del c.560_571delp_Ser187_Tyr190del c.122_1286delp_Alex18_Phe21del c.564_576delinnAp_Val189_Val192del c.518_532delp_Lys179_App177del c.518_532delp_Lys179_App177del	indel indel indel indel indel indel			c.1968_1969insTTT;p.Gly656_Tvr657insPhe	indel				
#1440T #1335T #1336T #1337T #1339T #1342T #1343T #1351T #1350T	c557_571delp_Tyr186_Tyr190del c557_571delp_Tyr186_Tyr190del c560_571delp_Ser187_Tyr190del c1252_1266delp_Ala418_Phe212del c.564_576delimAp_Val189_Val1924el c.518_532delp_Lys173_App177del	indel indel indel indel indel indel								
#1440T #1335T #1336T #1337T #1339T #1342T #1343T #1351T #1350T #1354T #1355T	c.557_571delp_Tyr186_Tyr190del c.557_571delp_Tyr186_Tyr190del c.550_571delp_Ser187_Tyr190del c.122_1206delp_Als18_Phe421del c.564_576delimAp_Vs189_Vs182del c.518_532delp_Lys173_App177del c.518_532delp_Tyr186_Tyr190del c.556_573delp_Tyr186_Tyr190del	indel indel indel indel indel indel indel indel indel			c.1968_1969/ns/TTI_p GN/556_TVr657/msPhe c.1940A-T_p Aun647/le	indel				
#1440T #1335T #1336T #1337T #1339T #1342T #1343T #1351T #1350T #1355T #1356T	c557_571delp_Tyr186_Tyr190del c557_571delp_Tyr186_Tyr190del c550_571delp_Tyr186_Tyr190del c150_571delp_per187_Tyr190del c1252_1263delp_Alas18_Phe421del c564_57fdelmAp_val189_Val189_Val192del c518_532delp_Lys179_Asp177del c518_532delp_Lys179_Asp177del c556_573delp_Tyr186_Tyr190del c556_573delp_Tyr186_Tyr190del c556_573delp_Tyr186_Tyr190del	indel								
#1440T #1335T #1336T #1337T #1339T #1342T #1343T #1351T #1350T #1354T #1355T #1356T	c557_571delp_Tyr186_Tyr190del c557_571delp_Tyr186_Tyr190del c559_571delp_Ser187_Tyr190del c1552_1263delp_Ala118_Phe321del c564_576delmAp_Val189_Val192del c518_532delp_Lys173_App177del c518_532delp_Lys173_App177del c556_575delp_Tyr186_Tyr190del c566_573delp_Tyr186_Tyr190del c566_573delp_Tyr186_Tyr190del	indel								
#1440T #1335T #1336T #1337T #1339T #1342T #1343T #1351T #1350T #1354T #1355T #1356T #1356T	c.557_571delp_Tyr186_Tyr390del c.557_571delp_Tyr186_Tyr390del c.550_571delp_SperitS_Tyr390del c.1252_1163delp_Ala418_Phe421del c.564_576delimAp_Val189_Val182del c.518_512delp_Lys173_Aup177del c.518_512delp_Tyr186_Tyr390del c.556_5751delp_Tyr186_Tyr390del c.556_573delp_Tyr186_Tyr390del c.556_573delp_Tyr186_Tyr390del c.557_571delp_Tyr186_Tyr390del c.557_571delp_Tyr186_Tyr390del c.557_571delp_Tyr186_Tyr390del	indel								
#1440T #1335T #1336T #1337T #1339T #1342T #1343T #1350T #1350T #1355T #1356T #1356T #1386T #1388T #1388T	c557_571delp_Tyr186_Tyr190del c557_571delp_Tyr186_Tyr190del c550_571delp_Tyr186_Tyr190del c1252_1263delp_Alas18_Phe212del c564_576delm_Alas18_Phe212del c564_576delm_Alas18_Phe212del c564_576delm_Alas18_Tyr197del c518_532delp_Lyr173_Apj177del c556_573delp_Tyr186_Tyr190del c556_573delp_Tyr186_Tyr190del c556_573delp_Tyr186_Tyr190del c557_571delp_Tyr186_Tyr190del c557_571delp_Tyr186_Tyr190del	indel								
#1440T #1335T #1336T #1337T #1339T #1342T #1343T #1351T #1350T #1354T #1355T #1356T #1356T	c.557_571delp_Tyr186_Tyr390del c.557_571delp_Tyr186_Tyr390del c.550_571delp_SperitS_Tyr390del c.1252_1163delp_Ala418_Phe421del c.564_576delimAp_Val189_Val182del c.518_512delp_Lys173_Aup177del c.518_512delp_Tyr186_Tyr390del c.556_5751delp_Tyr186_Tyr390del c.556_573delp_Tyr186_Tyr390del c.556_573delp_Tyr186_Tyr390del c.557_571delp_Tyr186_Tyr390del c.557_571delp_Tyr186_Tyr390del c.557_571delp_Tyr186_Tyr390del	indel								

							-			
#1413T	c.564_575del;p.Val189_Val192del	indel								
#1399T	c.575_577del;p.Val192_Asn193delinsAsp	indel								
#1421T	c.565_577delinsT;p.Val189_Asn193delinsTyr	indel								
#1424T										
#1430T		-								
#1432T	c.1841-2A>T;p.Ala614_splice	splice					c.2108G>T;p.Ser703lle	missense		
#1434T	c.560_571del;p.Ser187_Tyr190del	indel								
#1433T	c.618_641dup;p.Asn213_Phe214dup	indel								
#1435T #1439T	c.557_571del;p.Tyr186_Tyr190del	indel								
#1455T			c.601C>T;p.Arg201Cys	missense						
#1469T			c.602G>A;p.Arg201His	missense						
#1488T								c	.1132_1137del;p.Val378_Phe379de	indel
#1489T									33_1138del;p.Val378_Lys380delin	indel
#1490T							c.2168C>A;p.Ala723Asp	missense		
#1496T									c.1037A>G;p.Glu346Gly	missense
#1508T								c	1132_1137del;p.Val378_Phe379de	indel
#1518T	c.556_571delinsA;p.Tyr186_Phe191delinsIle	indel								
#1519T			c.602G>A;p.Arg201His	missense						
#1521T	c.563_574del;p.Thr188_Val192delinslle	indel								
#1523T	c.518_532del; p.Lys173_Asp177del	indel								
#1664T	c.643_645del;p.Asp215del	indel								
#1666T	c.564_576delinsA;p.Val189_Val192del	indel								
#1676T	c.557_571del;p.Tyr186_Tyr190del	indel								
#1677T #1768T	c.560_571del;p.Ser187_Tyr190del	indel								
#1768T #1851T	c.560_571del;p.Ser187_Tyr190del c.563_574del;p.Thr188_Val192delinslle	indel								
#1880T	c.560_571del;p.Ser187_Tyr190del	indel								
#1891T										
#1896T										
#1915T	c.560_571del;p.Ser187_Tyr190del	indel								
#1916T	c.560_571del;p.Ser187_Tyr190del	indel								
#1918T	c.553_567del; p.Asp185_Val189del	indel								
#1940T	c.563_574del;p.Thr188_Val192delinsile	indel								
#2187T				c	1919A>T; p.Tyr640Phe / c.233T>G;p.Leu78Ar	missense				
#2189T										
#2191T	c.557_571del;p.Tyr186_Tyr190del	indel								
#2192T										
#2193T	5 000 M (4 4 4 10 0 0 0 0 0 0 0 0 0 0 0 0 0 0 0 0	0.00000						c.11	33_1138del;p.Val378_Lys380delin	indel
#2196T	c.522_536del;p.Lys175_Pro179del	indel						70.000		N CHINA
#2197T								c.11	.31_1137delinsG;p.Val378_Phe379	indel
#2217T #2219T										
#2328T										
#2329T	c.580_585del;p.lle194_Glu195del	indel								
#2330T								c.1037A	>G; p.Glu346Gly / c.1103A>G; p.Ty	missense
#2331T									3_1134insAAA; p.Val378_Phe379ir	indel
#2363T					c.1972 A>T; p.Lys658Tyr	missense				
#2369T					c.1972_1974delinsTAT; p.Lys658Tyr	missense				
#2370T	c.565_579del; p.Val189_Asn193del	indel								
#2371T	c.556_573del;p.Tyr186_Phe191del	indel								
#2372T	c.565_579del;p.Val189_Asn193del	indel								
#2373T	c.569_577del;p.Phe191_Asn193del	indel				_				
#2375T	c.574_582del;p.Val192_lle194del	indel								
#2376T	c.569_578delinsC;p.Tyr190_Asn193delinsSer	indel								
#2377T	c.565_579del;p.Val189_Asn193del	indel								
#2378T		-1								
#2561T #2568T	c.647C>A;p.Pro216His	missense								
#2568T #2571T	c.560_571del;p.Ser187_Tyr190del c.570_578del;p.Phe191_Asn193del	indel								
#2573T										
#2574T	c.564_575del;p.Val189_Val192del	indel								
#2575T	c.557_571del;p.Tyr186_Tyr190del	indel								
#2576T	c.560_571del;p.Ser187_Tyr190del	indel								
#2582T					c.1919A>T;pTyr640Phe	missense				
#2585T	c.579_584del;p.Asn193_Glu195delinsLys	indel								
#2589T										
#2590T	c.582_587del; p.Glu195_Val196del	indel								
#2591T										
#2615T	No transporter habita o Ale Alexandria de la casa de la	1000000								
#2620T	c.557_571del;p.Tyr186_Tyr190del	indel								
#2729T		0,000						_		
#2769T	c.643_645del; p.Asp215del	indel				1000				
#2773T #2793T		indal			c.1969_1980dup; p.Tyr6S7_Met660dup	indel				
#Z/93T		indel								
#270EY	c.568_579del;p.Tyr190_Asn193del									
#2795T #2796T	c.570_578del; p.Phe191_Asn193del	indel					1	_		
#2796T		indel								
#2796T #2798T	c.570_578del; p.Phe191_Asn193del									
#2796T #2798T #2802T	c.570_578del; p.Phe191_Asn193del c.560_571del; p.Ser187_Tyr190del	indel								
#2796T #2798T #2802T #2803T	c.570_578del; p.Phe191_Asn193del								1132 1137del ; p.Val378 Phe=270d	indel
#2796T #2798T #2802T	c.570_578del; p.Phe191_Asn193del c.560_573del; p.Fhe191_Tyr190del c.562_573del;p.Thr188_Phe191del	indel						с.	1132_1137del ; p Val378_Phe379d	indel
#2796T #2798T #2802T #2803T #2804T	c.570_578del; p.Phe191_Asn193del c.560_571del; p.Ser187_Tyr190del	indel indel						с.	1132_1137del ; p Val378_Phe379d	indel
#2796T #2798T #2802T #2803T #2804T #2805T	c.570_578dei; p.Phc191_Asn193dei c.560_571dei; p.Ser187_Tvr190dei c.562_573dei; p.Thr188_Phc191dei c.647CAp.Pro218His	indel indel missense	c.601C>T;p.Arg201Cys	missense				с.	1132_1137del ; p.Val378_Phe379d	indel
#2796T #2798T #2802T #2803T #2804T #2805T #2809T	c.570_578dei; p.Phc191_Asn193dei c.560_571dei; p.Ser187_Tvr190dei c.562_573dei; p.Thr188_Phc191dei c.647CAp.Pro218His	indel indel missense	c.601C>T;p.Arg201Cys	missense missense				c.	1132_1137del ; p.Val378_Fhe379d	indel

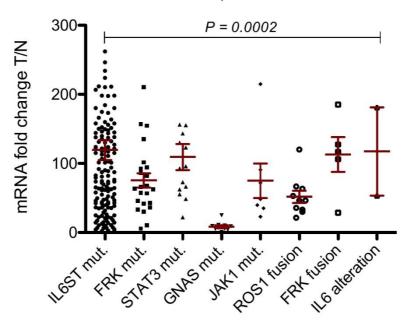
#2825T	c.647C>A;p.Pro216His	missense						
#2826T	c.557_571del;p.Tyr186_Tyr190del	indel						
#2827T	c.647C>A;p.Pro216His	missense						
#2828T	The artists of the second of t						c.1129insAGA; p.insPro377	indel
#2829T	c.560_571del; p.Ser187_Tyr190del	indel						
#2830T	c.562_573del;p.Thr188_Phe191del	indel						
#2834T	c.557_571del;p.Tyr186_Tyr190del	indel				c.11	33_1138del;p.Val378_Lys380delin	indel
#2835T	c.565_576del;p.Val189_Val192del	indel						
#2836T						c.11	33_1139del;p.Val378_Lys380delin	indel
#2837T	c.557_571del;p.Tyr186_Tyr190del	indel						
#2849T	c.565_576del;p.Val189_Val192del	indel						
#2856T	c.565_576del;p.Val189_Val192del	indel						
#2857T	c.563_574del;p.Thr188_Val192delinslie	indel						
#2874T	c.1252_1263del; p.Ala418_Phe421del	indel						
#2877T				c.233T>G;p.Leu78Arg	missense			
#2879T				c.1969_1980dup; p.Tyr6S7_Met660dup	indel			
#2900T	c.565_576del;p.Val189_Val192del	indel						
#2901T	c.565_576del;p.Val189_Val192del	indel						
#2902T								
#3049T							1132_1137del;p.Val378_Phe379de	indel
#3073T								
#3074T								
#3104T	c.518_532del; p.Lys173_Asp177del	indel						
#3107T	c.563_580del; p.Thr188_Asn193del	indel						
#3410T								
#3723T								
#3759T	c.555_566del; p.Asp185_Val189delinsGlu	indel						
#3766T								
#3780T								
#3781T	c.571_579del; p.Phe191_Asn193del	indel						
#4058T	c.565_576del;p.Val189_Val192del	indel						
#4089T								
#4094T	c.647C>A; p.Pro216His	missense						
#4098T	c.565_576del; p.Val189_Val192del	indel						
#4106T							1037A>G; p.Glu346Gly	missense
#4108T	c.556_573del; p.Tyr186_Phe191del	indel						
#4109T	c.560_571del; p.Ser187_Tyr190del	indel						
#4110T								
#4116T								
#4117T	c.565_576del; p.Val189_Val192del	indel						

Supplementary Figure 2

CRP expression



SAA2 expression



500000000000000000000000000000000000000		0.0000000000000000000000000000000000000	300000000000000000000000000000000000000	200000000000000000000000000000000000000	900000	150000	500000000000000000000000000000000000000	100000000000000000000000000000000000000		303500330000000000000000000000000000000	10,000	555******
Sample	Histological.Tumor.Initia	CHROM	POS_hg19	POS_hg38	REF	ALT	Hugo_Symbol	Protein_Change	Variant_Classification	Variant_Type	VAF	FILTER
#471T	HCA HCA	chr8	144391654 144990757	143309484 143916589	A G	c	TOP1MT PLEC	p.F588C p.A4548G	Missense_Mutation	SNV	0,231788079	PASS
#471T	HCA	chr17	78223022	80249223	G	C T	SLC26A11	p.G531V	Missense_Mutation Missense Mutation	SNV	0,27173913	PASS
#471T	HCA	chr1	114354555	113811933	G	A	RSBN1	p.A160A	Silent	SNV	0,157894737	PASS
#471T	HCA	chr2	179635319	178770592	T	c	TTN	p.N2734D	Missense_Mutation	SNV	0,2875	PASS
#471T	HCA	chr6	27861316	27893538	G	c	HIST1H2BO	p.D26H	Missense_Mutation	SNV	0,343137255	PASS
#471T	HCA	chr6	109787264	109466061	c	T	ZBTB24	p.G628G	Silent	SNV	0,11111111	PASS
#471T	HCA	chr6	165723063	165309574	G	c ·	C6orf118	p.R5G	Missense_Mutation	SNV	0,154761905	PASS
#471T #471T	HCA HCA	chr22 chr16	21384369 84449104	21030080 84415498	G A	A C	SLC7A4 ATP2C2	p.54185 p.K177N	Silent Missense Mutation	SNV	0,36	PASS
8471T	HCA	chr19	40828162	40322255	c	A	C19orf47	p.G299V	Missense_Mutation	SNV	0,251101322	PASS
#471T	HCA	chr3	45677668	45636176	G	т	LIMD1	p.V479L	Missense_Mutation	SNV	0,255813953	PASS
#471T	HCA	chr5	31299738	31299631	A	G	CDH6	p.S271G	Splice_Site	SNV	0,304347826	PASS
#471T	HCA	chr5	120021947	120686252	T	G	PRR16	p.L153R	Missense_Mutation	SNV	0,121212121	PASS
#471T	HCA	chr7	98506371	98908748	T	A	TRRAP	p.L379Q	Missense_Mutation	SNV	0,285714286	PASS
#471T	HCA	chr7	98609721 100681483	99012098 101038202	C A	T G	TRRAP MUC17	p.R3775W	Missense_Mutation Silent	SNV	0,272727273	PASS
#471T	HCA HCA	chr14	21831003	21362844	T	C	SUPT16H	p.T2262T p.I539V	Missense_Mutation	SNV	0,108108108	PASS
#471T	HCA	chr12	21459836	21306902	TTAAAATCTGGGTTCCAT	C	SLCO1A2	p.NGTQILR135fs	Frame_Shift_Del	DEL	0.107142857	PASS
#471T	HCA	chr12	31249835	31096901	G	A	DDX11	p.R558Q	Missense_Mutation	SNV	0,173913043	PASS
#471T	HCA	chr10	6557001	6515039	С	T	PRKCQ	p.V33I	Missense_Mutation	SNV	0,1875	PASS
#1343T	HCA	chr20	48140657	49524120	С	A	PTGIS	p.E265*	Nonsense_Mutation	SNV	0,234234234	PASS
#1343T	HCA	chr20	62863566	64232213	G	A	MYT1	p.A909T	Missense_Mutation	SNV	0,224489796	PASS
#1343T #1343T	HCA	chr5	115837936 147820738	116502240	A G	G	SEMA6A FBXO38	p.163T	Missense_Mutation	SNV	0,242424242	PASS
#1343T	HCA HCA	chr5	174938514	148441175 175511511	C	A T	SFXN1	p.R1109K p.L165L	Missense_Mutation Silent	SNV	0,262773723	PASS
#1343T	HCA	chr1	23111399	22784906	c	т	EPHB2	p.A214V	Missense_Mutation	SNV	0,207253886	PASS
#1343T	HCA	chr1	25072111	24745620	G	A	CLIC4	p.V23I	Missense_Mutation	SNV	0,142857143	t_lod_fstar
#1343T	HCA	chr1	63788807	63323136	T	c	FOXD3	p.D26D	Silent	SNV	0,304347826	PASS
#1343T	HCA	chr1	153905222	153932746	c	G	DENND48	p.G1219R	Missense_Mutation	SNV	0,212121212	PASS
#1343T	HCA	chr1	216465689	216292347	A	G	USH2A	p.Y556Y	Silent	SNV	0,286956522	PASS
#1343T	HCA	chrX	153927694	154699419	c	T	GAB3	p.G406E	Missense_Mutation	SNV	0,193548387	PASS
#1343T #1343T	HCA HCA	chr19 chr19	9084834 13059076	8974158 12948262	G C	T A	MUC16 RAD23A	p.S23275 p.P107H	Silent Missense_Mutation	SNV	0,252873563	PASS t_lod_fstar
#1343T	HCA	chr4	77231007	76309854	A	G	FAM47E-STBD1	p.1311V	Missense_Mutation Missense_Mutation	SNV	0,237837838	PASS
#1343T	HCA	chr16	70884418	70850515	c	A	HYDIN	p.C4195F	Missense_Mutation	SNV	0,209302326	PASS
#1343T	HCA	chr16	70884419	70850516	A	С	HYDIN	p.C4195G	Missense_Mutation	SNV	0,209302326	PASS
#1343T	HCA	chr14	68221790	67755073	Т	С	ZFYVE26	p.M2322V	Missense_Mutation	SNV	0,260869565	PASS
#1343T	HCA	chr14	99925461	99459124	T	c	SETD3	p.N136S	Missense_Mutation	SNV	0,303797468	PASS
#1343T #1343T	HCA HCA	chr14 chr2	102461583 106746217	101995246 106129761	C G	T	DYNC1H1 UXS1	p.l1170l p.l159M	Silent Missense Mutation	SNV	0,247191011	PASS
#1343T #1343T	HCA HCA	chr2 chr18	106746217 56202862	106129761 58535630	C	G	ALPK2	p.C159M p.G1519G	Missense_Mutation Silent	SNV	0,241176471	PASS
#1343T	HCA	chr11	56143847	56376371	A	G	OR8U1	p.1250V	Missense_Mutation	SNV	0,234042553	events;homologous_r
#1343T	HCA	chr3	108076930	108358083	С	Т	HHLA2	p.L309F	Missense_Mutation	SNV	0,156862745	PASS
#1343T	HCA	chr3	186386829	186669040	С	Т	HRG	p.P97S	Missense_Mutation	SNV	0,224137931	PASS
#1343T	HCA	chr3	197505276	197778405	G	т	PYTTD1	p.V267F	Missense_Mutation	SNV	0,301886792	PASS
#1343T	HCA	chr17	1373763	1470469	c	Т	MYO1C	p.A743T	Missense_Mutation	SNV	0,142857143	t_lod_fstar
#1343T #1343T	HCA HCA	chr17	77769355 79914528	79795556 81956652	C C	T G	CBX8 NOTUM	p.A83A p.R329P	Silent	SNV	0,279069767	PASS PASS
#1343T	HCA	chr12	124941695	124457149	G	A	NCOR2	p.A240V	Missense_Mutation Missense_Mutation	SNV	0,284722222	PASS
#1343T	HCA	chr15	31355405	31063202	G	c	TRPM1	p.P294R	Missense_Mutation	SNV	0,206896552	PASS
#1343T	HCA	chr15	44951472	44659274	A	т	SPG11	p.5158T	Missense_Mutation	SNV	0,310344828	PASS
#1343T	HCA	chr9	117071558	114309278	С	т	COL27A1	p.R1746W	Missense_Mutation	SNV	0,207207207	PASS
#1343T	HCA	chr9	135117267	132241880	С	A	NTNG2	p.N454K	Missense_Mutation	SNV	0,130434783	t_lod_fstar
#1343T	HCA	chr7	21609806	21570188	A	G	DNAH11	p.R438R	Silent	SNV	0,191176471	PASS
#1343T	HCA	chr7	83034788	83405472	A	G	SEMA3E	p.F326L	Missense_Mutation	SNV	0,235294118	PASS
#1343T #1424T	HCA HCA	chr7	100086942 70443636	100489319 71223786	C G	A GTCATCT	NYAP1 GJB1	p.5533Y p.31_32insIF	Missense_Mutation In_Frame_Ins	SNV	0,136363636 0,186567164	t_lod_fstar PASS
#1424T	HCA	chr16	21712217	21700896	G	T	OTOA	p.51_52Hsir p.1283L	Silent	SNV	0,204301075	PASS
W1424T	HCA	chr8	21856713	21999202	AC	A	XPO7	p.Y847fs	Frame_Shift_Del	DEL	0,275862069	PASS
W1424T	HCA	chr12	21013980	20861046	A	G	SLCO1B3	p.N1305	Missense_Mutation	SNV	0,285714286	PASS
#1424T	HCA	chr2	196548462	195683738	G	T	SLC39A10	p.G350C	Missense_Mutation	SNV	0,294117647	PASS
#1424T	HCA	chr2	198571711	197706987	A	G	mars-02	p.T528A	Missense_Mutation	SNV	0,321888412	PASS
#1424T	HCA	chr3	41266136	41224645	T	c	CTNNB1	p.S45P	Missense_Mutation	SNV	0,27607362	PASS
#1424T	HCA HCA	chr3	112718267 41004292	112999420 42852275	C C	A T	GTPBP8 AOC3	p.A223del p.A311V	Splice_Site Missense Mutation	DEL	0,270833333	PASS
#1424T	HCA	chr17	80049332	82091456	G	A	FASN	p.1420L	Silent	SNV	0,33333333	PASS
#1424T	нса	chr9	140250762	137356310	T	G	EXD3	p.R239R	Silent	SNV	0,322580645	PASS
#1424T	HCA	chr9	140392635	137498183	G	A	PNPLA7	p.5582L	Missense_Mutation	SNV	0,211538462	PASS
#1424T	HCA	chr1	186287894	186318762	G	A	TPR	p.P2212L	Missense_Mutation	SNV	0,181818182	PASS
#1424T	HCA	chr10	48388031	47351329	Α	Т	RBP3	p.A949A	Silent	SNV	0,248648649	PASS
#1424T	HCA	chr10	101557010	99797253	G T	T	ABCC2	p.K263N	Missense_Mutation	SNV	0,254237288	PASS
#1424T #1439T	HCA HCA	chr19 chr1	8966741 16577371	8856065 16250876	T C	C A	MUC16 FBXO42	p.R14404R p.D650Y	Silent Missense_Mutation	SNV	0,395833333	PASS
#1439T	HCA HCA	chr1	27105955	26779464	c	T	ARID1A	p.D6507 p.Q1856*	Missense_Mutation Nonsense Mutation	SNV	0,263157895	PASS
#1439T	HCA	chr1	33235860	32770259	G	т	KIAA1522	p.L301L	Silent	SNV	0,218543046	PASS
#1439T	HCA	chr1	36029439	35563838	G	T	NCDN	p.G561V	Missense_Mutation	SNV	0,261363636	PASS
#1439T	HCA	chr1	153742249	153769773	A	G	INTS3	p.Q773R	Missense_Mutation	SNV	0,257425743	PASS
#1439T	HCA	chr1	161136956	161167166	G	T	PPOX	p. A52S	Missense_Mutation	SNV	0,272727273	PASS
#1439T	HCA	chr12	15103534	14950600	A T	G	ARHGDIB	p.M38T	Missense_Mutation	SNV	0,225	PASS
#1439T	HCA	chr12	25702459	25549525		C	IFLTD1	p.V16V	Silent Microsco Mutation	SNV	0,234042553	PASS
#1439T #1439T	HCA HCA	chr18 chr7	65180925 6189847	67513688 6150216	c c	A T	DSEL USP42	p.W317C p.L674L	Missense_Mutation Silent	SNV	0,228813559	PASS
#1439T	HCA	chr7	47876601	47837003	G	A	PKD1L1	p.T1954M	Missense_Mutation	SNV	0,214285714	PASS
#1439T	нса	chr7	123119855	123479801	С	A	IQUB	p.L468F	Missense_Mutation	SNV	0,33333333	PASS
#1439T	HCA	chr7	139762530	140062730	С	т	PARP12	p. E40K	Missense_Mutation	SNV	0,25	PASS
#1439T	HCA	chr7	151842334	152145249	С	Т	KMT2C	p.R4693Q	Missense_Mutation	SNV	0,211764706	PASS
#1439T	HCA	chrX	53349824	53320626	c	Т	IQSEC2	p.l.166L	Silent	SNV	0,35	PASS
#1439T #1439T	HCA HCA	chrX	106845648 139586928	107602418 140504763	C G	A T	FRMPD3 SOX3	p.T1493N p.P100T	Missense_Mutation	SNV	0,135416667	PASS
#1439T #1439T	HCA HCA	chrX chr3	139586928 1394027	140504763 1352343	G	T	SOX3 CNTN6	p.P100T p.G462C	Missense_Mutation Missense_Mutation	SNV	0,142857143	PASS
#1439T	HCA	chr3	44683972	44642480	G	A	ZNF197	p.G450G	Silent	SNV	0,20754717	PASS
#1439T	HCA	chr3	45637381	45595889	T	A	UMD1	p.F337Y	Missense_Mutation	SNV	0,259259259	PASS
#1439T	HCA	chr3	171969171	172251381	Т	G	FNDC3B	p.P210P	Silent	SNV	0,293478261	PASS
#1439T	HCA	chr19	6312466	6312455	G	С	ACER1	p.L46L	Silent	SNV	0,236842105	PASS
#1439T	HCA	chr17	3919620	4016326	G	С	ZZEF1	p.F2714L	Missense_Mutation	SNV	0,208	PASS
#1439T	HCA	chr17	63010387	65014269	A	С	GNA13	p.L374L	Silent	SNV	0,283333333	PASS
#1439T #1439T	HCA HCA	chr5	149748277 150072470	150368714 150692908	A T	C A	TCOF1 RBM22	NA p.P373P	Splice_Site Silent	SNV	0,266666667	PASS
W1439T	HCA HCA	chr5	150072470	163459904	G	T T	NUDCD2	p.P373P p.S49R	Missense_Mutation	SNV	0,375	PASS
#14391 #1439T	HCA HCA	chr5	162886910 24222614	23999744	A A	G	UBXN2A	p.349K p.T219T	Missense_Mutation Silent	SNV	0,204081633	PASS
#1439T	HCA	chr2	27464238	27241370	A	G	CAD	p.K1890E	Missense_Mutation	SNV	0,191489362	PASS
#1439T	HCA	chr2	29416436	29193570	G	A	ALK	p.T1506M	Missense_Mutation	SNV	0,266666667	PASS
#1439T	HCA	chr2	102789219	102172759	A	Т	IL1R1	p.R304S	Missense_Mutation	SNV	0,264705882	PASS
#1439T	HCA	chr2	148683685	147926116	T	TA	ACVR2A	p.K435fs	Frame_Shift_Ins	INS	0,194805195	PASS
#1439T	HCA	chr2	179394748	178530021	A	G	TTN	p.Y33849Y	Silent	SNV	0,227272727	PASS
#1439T	HCA	chr10	101594208	99834451	c	A	ABCC2	p.l1110i	Silent	SNV	0,170731707	PASS
#1439T	HCA	chr10	115804707	114044948	G	A	ADRB1	p.P272P	Silent	SNV	0,181818182	PASS
#1439T	HCA HCA	chr11 chr21	94564658 30464877	94831492 29092556	A C	T G	AMOTL1 MAP3K7CL	p.E533D	Missense_Mutation Silent	SNV	0,357142857	PASS
WIAPOT		1/11/21	304098//	42035330	U U	9	IMPL SK/CL	p.P115P	sient	ar4V	V,17148930Z	PASS
#1439T #1439T	HCA	chr16	67418914	67385011	C	A	LRRC36	p.S7295	Silent	SNV	0,257142857	PASS

#1439T #1439T #1439T		The same of the sa		794 7 7 7 7 7 7 7 7 7 7 7 7 7 7 7 7 7 7	T .			11177 at an Tanana 1	1	900000		
	HCA HCA	chr20 chr6	5157350 71289193	5176704 70579490	C C	T	CDS2 C6orf57	p.V116V p.S47S	Silent	SNV	0,260869565	PASS PASS
	HCA	chr6	116938047	116616884	G	A	RSPH4A	p.5475 p.P87P	Silent	SNV	0,318518519	PASS
W1439T	HCA	chr8	22880498	23022985	c	G	TNFRSF10B	NA.	Splice_Site	SNV	0,293333333	PASS
W1439T	HCA	chr8	41504023	41646504	A	Т	NKX6-3	p.L118Q	Missense_Mutation	SNV	0,28888889	PASS
W1439T	HCA	chr8	125074230	124061989	С	G	FER1L6	p.P1095P	Silent	SNV	0,21875	PASS
W2189T	HCA	chr6	4049256	4049022	С	A	PRPF48	p.R648S	Missense_Mutation	SNV	0,130434783	t_lod_fstar
#2189T	HCA	chr7	97862808	98233496	G	Т	TECPR1	p.L533M	Missense_Mutation	SNV	0,130434783	t_lod_fstar
W2189T W222T	HCA HCA	chr19 chr12	42797003 25302582	42292851 25149648	G C	T A	CIC CASC1	p.S1154l p.A1835	Missense_Mutation Missense_Mutation	SNV	0,166666667	t_lod_fstar t_lod_fstar
#222T	HCA	chrX	20183015	20164897	A	1	RPS6KA3	NA NA	Splice_Site	SNV	0,253521127	PASS
#222T	HCA	chrX	20183016	20164898	c	T	RP56KA3	NA NA	Splice_Site	SNV	0,27027027	PASS
#222T	HCA:	chr6	47202493	47234757	С	A	TNFRSF21	p.V551L	Missense_Mutation	SNV	0,111111111	t_lod_fstar
#222T	HCA	chr6	144999583	144678447	A	C	UTRN	p.K2507N	Missense_Mutation	SNV	0,111607143	PASS
#222T	HCA	chr1	200946009	200976881	G	T	KIF21B	p.V1446V	Silent	SNV	0,107142857	t_lod_fstar
#222T	HCA	chr17	3438936	3535642	C	A	TRPV3	p.A2395	Missense_Mutation	SNV	0,142857143	t_lod_fstar
#222T #222T	HCA	chr17 chr11	39973440 119217031	41817188 119346321	G	T	FKBP10 MFRP	p.G126W	Missense_Mutation Silent	SNV	0,125	t_lod_fstar PASS
#222T	HCA HCA	chr11	2622230	2622230	C	A	VLDLR	p.P36P p.A14E	Missense_Mutation	SNV	0,214285714	t_lod_fstar
#222T	HCA	chr8	10383213	10525703	c	A	PRSS55	p.R405	Missense_Mutation	SNV	0,2	PASS
#222T	HCA	chr15	24922279	24677132	С	T	NPAP1	p.A422V	Missense_Mutation	SNV	0,124378109	PASS
#222T	HCA	chr10	120863641	119104129	CGCGGCGGCGGAAGATG	C	FAM45A	NA.	Start_Codon_Del	DEL	0,15	PASS
#222T	HCA	chr3	48453957	48412548	c	A	PLXNB1	p.V1643L	Missense_Mutation	SNV	0,108695652	PASS
#222T	HCA	chr3	164712149	164994361	T	c	SI	p.S15795	Silent	SNV	0,105263158	PASS
#222T #222T	HCA HCA	chr22 chr19	51065642 36530307	50627214 36039405	G T	C C	ARSA THAP8	p.P137P	Silent Missense Mutation	SNV	0,133333333	PASS
#222T	нса	chr19	44351117	43846965	A	c	ZNF283	p.Q197R p.K122Q	Missense_Mutation	SNV	0,134615385	PASS
#2615T	HCA	chr10	134659633	132846129	c	A	TTC40	p.Q2122H	Missense_Mutation	SNV	0,272727273	PASS
#2615T	HCA	chr20	37174999	38546356	A	G	RALGAPB	p.H943R	Missense_Mutation	SNV	0,189393939	PASS
#2615T	HCA	chr14	77605915	77139572	A	Т	ZDHHC22	p.F56Y	Missense_Mutation	SNV	0,123809524	PASS
#2615T	HCA	chr1	28223561	27897050	С	A	RPA2	p.l.160L	Silent	SNV	0,125	t_lod_fstar
#2615T	HCA	chr1	180022207	180053072	G	Т	CEP350	p.\$1632i	Missense_Mutation	SNV	0,281818182	PASS
#2615T	HCA	chr1	236979804 26722021	236816504 26864504	Α	T	MTR	p.E242V	Missense_Mutation	SNV	0,169230769	PASS PASS
#2615T #2615T	HCA HCA	chr8	26722021 38205493	26864504 38347975	C A	C C	ADRA1A WHSC1L1	p.V156I p.L66R	Missense_Mutation Missense_Mutation	SNV	0,181818182 0.172932331	PASS PASS
#2615T	HCA	chr6	3123976	3123742	c	A	BPHL	p.1651	Missense_Mutation	SNV	0,14084507	PASS
#2615T	нса	chr6	56472969	56608171	A	T	DST	p.L1942I	Missense_Mutation	SNV	0,269230769	PASS
#2615T	HCA	chr11	113103452	113232730	т	С	NCAM1	p.\$352P	Missense_Mutation	SNV	0,179487179	PASS
#2615T	HCA	chr4	75681110	74755900	С	Т	втс	p.G80G	Silent	SNV	0,266666667	PASS
#2615T	HCA	chr4	76878739	75957586	T	c	SDAD1	p.E567E	Silent	SNV	0,17777778	PASS
#2615T	HCA	chr4	90872904 94690579	89951753	T	A	MMRN1	NA - COCOU	Splice_Site	SNV	0,112676056	PASS
#2615T #2615T	HCA HCA	chr4 chr7	94690579 29918696	93769428 29879080	G G	T	GRID2 WIPF3	p.G860V p.G99*	Missense Mutation Nonsense Mutation	SNV	0,142857143	PASS PASS
#2615T	HCA	chr7	73254374	73840044	AT	A	WBSCR27	p.H155fs	Frame_Shift_Del	DEL	0,275862069	PASS
#2615T	HCA	chr17	38572320	40416068	A	G	TOP2A	p.V90A	Splice_Site	SNV	0,206896552	PASS
#2615T	HCA	chrX	99596960	100341962	G	A	PCDH19	p.A930V	Missense_Mutation	SNV	0,170731707	PASS
W2615T	HCA	chrX	142716743	143628927	C	T	SLITRK4	p.E728K	Missense_Mutation	SNV	0,143478261	PASS
#2615T	HCA	chrX	153247645	153982194	С	T	TMEM187	p.P44P	Silent	SNV	0,243902439	PASS
#343T #343T	HCA HCA	chr3	41266137 49053706	41224646 49016273	C	A C	CTNNB1 DALRD3	p.545Y p.Y405C	Missense_Mutation Missense Mutation	SNV	0,185430464	PASS PASS
#343T	HCA	chr3	96945109	97226265	T	A	EPHA6	p.A372A	Splice_Site	SNV	0,3	PASS
#343T	HCA	chr12	55887053	55493269	G	A	OR6C68	p.A298T	Missense Mutation	SNV	0,2109375	PASS
#343T	HCA	chr12	57572189	57178406	A	т	LRP1	p.E1470V	Missense_Mutation	SNV	0,191304348	PASS
#343T	HCA	chr12	117962850	117525045	G	A	KSR2	p.R676C	Missense_Mutation	SNV	0,226600985	PASS
#343T	HCA	chr9	112025368	109263088	T	С	EPB41L4B	p.Y198C	Missense_Mutation	SNV	0,285714286	PASS
#343T	HCA	chr9	115337209									PASS
100000				112574929	G	c	KIAA1958	p.K283N	Missense_Mutation	SNV	0,29245283	
#343T	HCA	chr13	86369328	85795193	T	c	SLITRK6	p.Y439C	Missense_Mutation	SNV	0,265957447	PASS
#343T	нса	chr13 chr4	86369328 24558015	85795193 24556392	T C	C A	SLITRK6 DHX15	p.Y439C p.M240I	Missense_Mutation Missense_Mutation	SNV	0,265957447 0,217391304	PASS PASS
#343T #343T	HCA HCA	chr13 chr4 chr4	86369328	85795193	T C A	c	SLITRK6	p.Y439C p.M240I p.N454T	Missense_Mutation	SNV SNV SNV	0,265957447	PASS
#343T	нса	chr13 chr4	86369328 24558015 86916168	85795193 24556392 85995015	T C	C A C	SLITRK6 DHX15 ARHGAP24	p.Y439C p.M240I	Missense_Mutation Missense_Mutation Missense_Mutation	SNV	0,265957447 0,217391304 0,18018018	PASS PASS PASS
#343T #343T #343T #343T #343T	HCA HCA HCA HCA	chr13 chr4 chr4 chr17 chr17 chr17	86369328 24558015 86916168 2599524 20149372 36490917	85795193 24556392 85995015 2696230 20246059 38335034	T C A C T C	C A C A C G	SLITRKG DHX15 ARHGAP24 CLUH SPECC1 GPR179	p.Y439C p.M240l p.N454T p.E735* p.L829L p.V548V	Missense_Mutation Missense_Mutation Missense_Mutation Nonsense_Mutation Silent Splice_Site	SNV SNV SNV SNV SNV	0,265957447 0,217391304 0,18018018 0,115384615 0,154471545 0,226415094	PASS PASS PASS t_lod_fstar PASS PASS PASS
#343T #343T #343T #343T #343T	HCA HCA HCA HCA HCA	chr13 chr4 chr4 chr17 chr17 chr17 chr17	86369328 24558015 86916168 2599524 20149372 36490917 72436516	85795193 24556392 85995015 2696230 20246059 38335034 74440377	T C A C T C C C	C A C G A A	SLITRKG DHX15 ARHGAP24 CLUH SPECC1 GPR179 GPRCSC	p.Y439C p.M240l p.N454T p.E735* p.L829L p.V548V p.P246T	Missense_Mutation Missense_Mutation Missense_Mutation Nonsense_Mutation Silent Splice_Site Missense_Mutation	SNV SNV SNV SNV SNV SNV	0,265957447 0,217391304 0,18018018 0,115384615 0,154471545 0,226415094 0,12244898	PASS PASS PASS t_lod_fstar PASS PASS PASS PASS
#343T #343T #343T #343T #343T #343T	HCA HCA HCA HCA HCA HCA	chr13 chr4 chr4 chr17 chr17 chr17 chr17 chr8	86369328 24558015 86916168 2599524 20149372 36490917 72436516 77617928	85795193 24556392 85995015 2696230 20246059 38335034 74440377 76705693	T C A C T C	C A C G A GA	SLITRK6 DHX15 ARHGAP24 CLUH SPECC1 GPR179 GPRCSC ZFHX4	p.Y439C p.M240l p.N454T p.E735* p.L829L p.V548V p.P246T p.K536fs	Missense_Mutation Missense_Mutation Missense_Mutation Nonsense_Mutation Silent Splice_Site Missense_Mutation Frame_Shift_Ins	SNV SNV SNV SNV SNV SNV SNV SNV	0,265957447 0,217391304 0,18018018 0,115384615 0,154471545 0,226415094 0,12244898 0,203208556	PASS PASS PASS t_lod_fstar PASS PASS PASS PASS PASS
#343T #343T #343T #343T #343T #343T #343T	HCA HCA HCA HCA HCA HCA HCA HCA	chr13 chr4 chr4 chr4 chr17 chr17 chr17 chr17 chr17 chr8 chr8	86369328 24558015 86916168 2599524 20149372 36490917 72436516 77617928 127569184	85795193 24556392 85995015 2696230 20246059 38335034 74440377 76705693 126556939	T C A C T C C C G T T	C A C G A GA C C	SLITRK6 DHX15 ARHGAP24 CLUH SPECC1 GPR179 GPRCSC ZFHX4 FAM84B	p.Y439C p.M240I p.N454T p.E735* p.I829L p.V548V p.P246T p.K536fs p.I151V	Missense_Mutation Missense_Mutation Missense_Mutation Nonsense_Mutation Silent Splice_Site Missense_Mutation Frame_Shift_ins Missense_Mutation	SNV SNV SNV SNV SNV SNV SNV SNV SNV	0,265957447 0,217391304 0,18018018 0,115384615 0,154471545 0,226415094 0,12244898 0,203208556 0,223140496	PASS PASS PASS t_lod_fstar PASS PASS PASS PASS PASS PASS PASS PAS
#343T #343T #343T #343T #343T #343T #343T #343T #343T #343T	HCA HCA HCA HCA HCA HCA HCA HCA	chr13	86369328 24558015 86916168 2599524 20149372 36490917 72436516 77617928 127569184 43188575	85795193 24556392 85995015 2696230 20246059 38335034 74440377 76705693 126556939 43220837	T C A A C C T C C C C C C C C C C C C C	C A C G A A GA C C T T	SLITRK6 DHX15 ARHGAP24 CLUH SPECCI GPR179 GPRCSC ZFHX4 FAM848 CUL9	p. Y439C p.M240I p.N454T p.E735* p.L829L p.V548V p.P246T p.K536fs p.1151V p.R2172C	Missense_Mutation Missense_Mutation Missense_Mutation Missense_Mutation Nonsense_Mutation Silent Splice_Site Missense_Mutation Frame_Shit_Ins Missense_Mutation Missense_Mutation Missense_Mutation	SNV SNV SNV SNV SNV SNV SNV SNV SNV SNV	0,265957447 0,217391304 0,18018018 0,115384615 0,1548471545 0,226415094 0,12244898 0,203208556 0,233140496 0,202702703	PASS PASS PASS Lod_fitar PASS PASS PASS PASS PASS PASS PASS PAS
#343T #343T #343T #343T #343T #343T #343T	HCA HCA HCA HCA HCA HCA HCA HCA	chr13 chr4 chr4 chr4 chr17 chr17 chr17 chr17 chr17 chr8 chr8	86369328 24558015 86916168 2599524 20149372 36490917 72436516 77617928 127569184	85795193 24556392 85995015 2696230 20246059 38335034 74440377 76705693 126556939	T C A C T C C C G T T	C A C G A GA C	SLITRK6 DHX15 ARHGAP24 CLUH SPECC1 GPR179 GPRCSC ZFHX4 FAM84B	p.Y439C p.M240I p.N454T p.E735* p.I829L p.V548V p.P246T p.K536fs p.I151V	Missense_Mutation Missense_Mutation Missense_Mutation Nonsense_Mutation Silent Splice_Site Missense_Mutation Frame_Shift_ins Missense_Mutation	SNV SNV SNV SNV SNV SNV SNV SNV SNV	0,265957447 0,217391304 0,18018018 0,115384615 0,154471545 0,226415094 0,12244898 0,203208556 0,223140496	PASS PASS PASS t_lod_fstar PASS PASS PASS PASS PASS PASS PASS PAS
#343T #343T #343T #343T #343T #343T #343T #343T #343T #343T	HCA	chr13 chr4 chr4 chr4 chr17 chr17 chr17 chr17 chr8 chr8 chr6 chr10	86369328 24558015 869161658 2599524 20149372 36490917 724345516 77617928 127569184 43188575 17891740	85795193 24556392 85995015 2696230 20246059 38335034 74440377 76705693 126556939 43220837 17849736	T C A A C C C C C C C C C C C C C C C C	C A C G A A GA C T A A	SLITRK6 DHX15 ARHGAP24 CLUH SPECCI GPR179 GPRCSC ZFHX4 FAM84B CU19 MRC1L1	p. Y439C p.M240I p.N454T p.E735* p.L829L p.V548V p.P246T p.K536fs p.L151V p.R2172C p.F407L	Missense_Mutation Missense_Mutation Missense_Mutation Norsense_Mutation Silent Splice_Site Missense_Mutation Frame_Shift_ins Missense_Mutation Missense_Mutation Missense_Mutation Missense_Mutation	SNV	0,265957447 0,217391304 0,18018018 0,115384615 0,154471545 0,226415094 0,12244898 0,203208556 0,223140496 0,20272703 0,219858156	PASS PASS PASS Lod_fstar PASS PASS PASS PASS PASS PASS PASS PAS
#343T #343T #343T #343T #343T #343T #343T #343T #343T #343T #343T	HCA HCA HCA HCA HCA HCA HCA HCA HCA HCA	chr13 chr4 chr4 chr17 chr17 chr17 chr17 chr17 chr17 chr8 chr8 chr8 chr6 chr10 chr2	86369328 24558015 86916168 2599524 20149372 36490917 72436516 77617928 127569184 43188575 12891740	85795193 24556392 85995015 2696230 20246059 38335034 74440377 76705693 126556939 43220837 17849736 1496133	T C A C C C C C C C C C C C C C C C C C	C A C C A A C C A A GA A GA C C T A A T	SLITRKE DHX15 ARHGAP24 CLUH SPECCI GPR179 GPRCSC ZFHX4 FAM84B CUL9 MRCIL1 TPO	p. Y439C p. M240I p. N454T p. F335* p. L829L p. V548V p. P246T p. K5365 p. 1151V p. R2172C p. F407L p. D717D	Missense_Mutation Missense_Mutation Missense_Mutation Nonsense_Mutation Silent Splice_Site Missense_Mutation Frame_Shift_Ins Missense_Mutation Missense_Mutation Missense_Mutation Missense_Mutation Missense_Mutation Silent	SNV	0,265957447 0,217391304 0,18018018 0,115384615 0,154471545 0,226415094 0,102244898 0,203208556 0,223140496 0,202702703 0,219858156 0,115384615	PASS PASS t_lod_fstar PASS PASS PASS PASS PASS PASS PASS PAS
### ##################################	HCA HCA HCA HCA HCA HCA HCA HCA HCA HCA	chr13 chr4 chr4 chr4 chr17 chr17 chr17 chr17 chr17 chr8 chr8 chr6 chr10 chr2 chr2	86369328 24550015 86916168 2599524 20149372 36490917 72436516 776737928 127569384 43188575 17891740 1499905 74776576 128605191	85795193 24556392 85995015 2696230 20246059 38335034 74440377 74705693 126556399 43220837 17849736 1496133 74549449	T C A A C C C C C C C G G	C A C C A A C C T A A T A A A	SUTRIKE DHX15 ABHCAR24 CLUH SPECC1 GPR179 GPRCSC ZFRX4 FAM848 CU9 MRC111 TPO LOX13 IL18RAP POLR20	p. Y439C p.M2401 p.N454T p.E735* p.E235; p.E246T p.E246T p.E3565; p.E151V p.R2172C p.F4077; p.G204G p.P459T p.A108V	Missense_Mutation Missense_Mutation Missense_Mutation Nonsense_Mutation Silent Spike_Site Missense_Mutation Frame_Shift_Ins Missense_Mutation Missense_Mutation Missense_Mutation Silent Silent	SW S	0,263957447 0,27391304 0,18018018 0,115384615 0,154471545 0,226415094 0,12244898 0,22020556 0,223140496 0,202702703 0,115384615 0,11584615 0,11584615 0,11584615 0,11584615	PASS PASS PASS PASS t_lod_fstar PASS PASS PASS PASS PASS PASS PASS PAS
### ##################################	HCA	chv13 chv4 chv4 chv4 chv4 chv17 chv17 chv17 chv17 chv18 chv8 chv8 chv8 chv10 chv2 chv10 chv2 chv2 chv2 chv2 chv2 chv2 chv1	86380328 24550015 86916168 2599524 20199372 3640917 72436516 77617928 127569184 43186575 17891740 1499905 7477576 103667472 128608191 39845104	85795193 24556392 85995015 2696230 20246059 38335034 74440377 76705693 126556939 43220837 17849736 1496133 74549449 102451012 127850617 38379432	T C A A C C C C C C C C C C C C C C C C	C A C C G A A C C T T A A A A A A	SLITRIG DHXIS ARHCAR24 CLUH SPECCI GPR179 GPRCSC ZFIXX4 FAN848 CUL9 MRCLL1 TPO LOXL3 IL18RAP POLR2D MACS1	p. Y430C p.M240l p.M240l p.M354T p. E235* p. E239l p.Y340T p.Y340T p.Y340T p.R336fs p.H351V p.R212C p.F407L p.O717D p.G204G p.P459T p.A108V p.A4507A	Missense, Mutation Missense, Mutation Missense, Mutation Monemes, Mutation Nonemes, Mutation Silent Spilice, Site Missense, Mutation Frame, Shift, Ins Missense, Mutation Silent	SWV	0,163857447 0,17391304 0,18018018 0,1554871545 0,256415094 0,12244898 0,222140496 0,222140496 0,223140496 0,15584615 0,15584615 0,15584615 0,15584615 0,15584615 0,15584615 0,15584615 0,15584615 0,15584615	PASS PASS PASS \$\frac{1}{2}\lod \ftar PASS PASS PASS PASS PASS PASS PASS PAS
### ##################################	HCA	dw13 chr4 chr4 chr4 chr4 chr4 chr4 chr17 chr17 chr17 chr17 chr8 chr8 chr6 chr10 chr2 chr2 chr2 chr2 chr2 chr2 chr1 chr1	8509328 2458015 8093168 2599534 20149372 38490917 72436516 77617928 12759184 4318575 17891740 1499905 74776576 1280149 13985104 179528824	85795193 24556192 85995015 2696230 20246059 38315034 7440377 76705693 126556939 43220837 17849736 1496133 74549449 102451012 127850617 39379432	T C C C C C C C C C C C C C C C C C C C	C A C C A A GA A A A A T T	SLITRIG SLITRIG ANHGAP24 CLUH SPECCI GPR179 GPRCSC ZFHX4 FAMB48 CUI9 MRCILI TPO LOXI3 ILIBRAP POLR2D MAGF1 NPHS2	p. Y439C p.M2401 p.M2401 p.M2401 p.W3402 p.V3402 p.Y2461 p.K33645 p.1151V p.R2172C p.F4072 p.D717D p.G204G p.P4597 p.A106V p.A4507A p.P179H	Missense, Mutation Missense, Mutation Missense, Mutation Missense, Mutation Missense, Mutation Silent Silent Missense, Mutation Frame, Shift, Ins Missense, Mutation Missense, Mutation Missense, Mutation Silent Missense, Mutation Silent Silent Missense, Mutation Missense, Mutatio	SW S	0.265957447 0.217391304 0.18010018 0.115384615 0.155471545 0.226415094 0.202208556 0.222404996 0.202208556 0.222404996 0.202207273 0.219858156 0.115588415 0.119565227 0.9241717318	PASS PASS PASS PASS † Jod Star PASS PASS PASS PASS PASS PASS PASS PAS
### ##################################	HCA	chv13 chv4 chv4 chv4 chv4 chv17 chv17 chv17 chv17 chv18 chv8 chv8 chv8 chv10 chv2 chv10 chv2 chv2 chv2 chv2 chv2 chv2 chv1	86380328 24550015 86916168 2599524 20199372 3640917 72436516 77617928 127569184 43186575 17891740 1499905 7477576 103667472 128608191 39845104	85795193 24556392 85995015 2696230 20246059 38335034 74440377 76705693 126556939 43220837 17849736 1496133 74549449 102451012 127850617 38379432	T C A A C C C C C C C C C C C C C C C C	C A C C A A C C T T A A A A A T T A A A A	SLITRIG DHXIS ARHCAR24 CLUH SPECCI GPR179 GPRCSC ZFIXX4 FAN848 CUL9 MRCLL1 TPO LOXL3 IL18RAP POLR2D MACS1	p.Y430C p.N2401 p.N2401 p.N2401 p.N2401 p.V3402 p.V3402 p.V3402 p.Y2407 p.R2172C p.F4071 p.R2172C p.F4071 p.R2172C p.F4507 p.R35066 p.R3507 p.	Missense, Mutation Missense, Mutation Missense, Mutation Monemes, Mutation Nonemes, Mutation Silent Spilice, Site Missense, Mutation Frame, Shift, Ins Missense, Mutation Silent	SWV	0,163857447 0,17391304 0,18018018 0,1554871545 0,256415094 0,12244898 0,222140496 0,222140496 0,223140496 0,15584615 0,15584615 0,15584615 0,15584615 0,15584615 0,15584615 0,15584615 0,15584615 0,15584615	PASS PASS PASS \$\frac{1}{2}\log \frac{1}{2}\text{tar} \text{ PASS} PASS PASS PASS PASS PASS PASS PASS
### ##################################	HCA	dw13 chr4 chr4 chr4 chr4 chr4 chr17 chr17 chr17 chr17 chr8 chr8 chr6 chr6 chr10 chr2 chr2 chr2 chr2 chr2 chr2 chr1 chr1 chr1 chr1 chr1 chr1 chr1 chr1	85109328 85109328 80931518 80931518 20169372 36409917 72436516 77617928 43189575 17891740 1499905 74776576 139805194 139805104 1398051 139805104 139805104 139805104 139805104 139805104 139805104 139805104 139805104 139805104 139805104 139805104 139805104 1398051 139805104 139805104 139805104 139805104 139805104 139805104 139805104 139805104 139805104 139805104 139805104 139805104 1398051	85795193 24556392 85995015 2696230 20246059 38335034 76440377 76705693 126556939 4322037 17849736 1495133 7459149 102451012 127850617 39379412 179559689 38816502	T C C C C C C C C C C C C C C C C C C C	C A C C A A GA A A A A T T	SLITRIG SLITRIG SLITRIG ARHGAP24 CLUH SPECCI GPR179 GPRCSC ZFNX4 FANS84B CU19 MRCILI TPO LONE ILIBRAP POLRZD MACFI NPHS2 ECH1 C1904781	p. Y430C p.M4240 p.M4240 p.M454T p.F325* p.F325* p.F325* p.F325* p.F325* p.F326T p.F336* p.F336* p.F336* p.F336* p.F336* p.F336* p.F336* p.F337C p.F4077 p.G2046 p.F45073 p.A108V p.A45073 p.A2045 p.A192A	Missense, Mutation Missense, Mutation Missense, Mutation Missense, Mutation Missense, Mutation Silent Silent Missense, Mutation Missense, Missense, Mutation Missense, Mutation Missense, Missense, Missense, Mutation Missense, M	5NV 5NV 5NV 5NV 5NV 5NV 5NV 5NV 5NV 5NV	0,26957447 0,21791304 0,18018018 0,11584615 0,154471545 0,226415004 0,12244898 0,02020556 0,222140496 0,202702703 0,219858156 0,11584615 0,11584615 0,11584615 0,11584615 0,11584615 0,11584617 0,020207020	PASS PASS PASS PASS \$\frac{1}{2}\log \frac{1}{2}\text{tar} \text{ PASS} PASS PASS PASS PASS PASS PASS PASS
### ##################################	HCA	cht3 cht4 cht4 cht4 cht4 cht7 cht37 cht37 cht37 cht37 cht8 cht8 cht8 cht8 cht9 cht2 cht2 cht2 cht2 cht2 cht2 cht2 cht2	8509328 24558015 8693168 2599524 20149372 3690917 72436516 77617928 127569184 43185875 17891740 1499905 7477576 103067472 128608191 39805104	85795193 24556922 89995015 2696230 20246059 38335034 74440377 76705693 126556939 4320837 17849736 1196133 74549449 107451012 127850617 3379432 17959689 38816502 50659321	T C C C C C C C C C C C C C C C C C C C	C A A C A A A A A A A A A A A A A A A A	SLITRIG SLITRIG DIXIS ARHCAP24 CLUH SPECCI GPR179 GPRCSC ZFRX4 FAMS48 CLU9 MRCILI TPO LONL3 ILISRAP POLRZD MACFI NPHS2 ECH1	p.Y430C p.N2401 p.N2401 p.N2401 p.N2401 p.V3402 p.V3402 p.V3402 p.Y2407 p.R2172C p.F4071 p.R2172C p.F4071 p.R2172C p.F4507 p.R35066 p.R3507 p.	Missense, Mutation Missense, Mutation Missense, Mutation Missense, Mutation Normerne, Mutation Silvent Silvent Missense, Mutation Frame, Shirt, Ins Missense, Mutation Missense, Mutation Missense, Mutation Silvent Missense, Mutation	58V 58V 58V 58V 58V 58V 58V 58V	0.26957447 0.217391304 0.18018018 0.11584615 0.155471545 0.226415094 0.01244898 0.01204556 0.022344096 0.022344096 0.023244096 0.023244096 0.023245096 0.115584615 0.119658217 0.2 0.201117318 0.125207092 0.255294118	PASS PASS PASS PASS PASS PASS PASS PASS
# # # # # # # # # # # # # # # # # # #	HCA	dw13 dw42 dw47 dw47 dw47 dw47 dw47 dw47 dw47 dw47	85,09228 2455,0015 86916168 86916168 20169372 36409017 72436516 77617928 41388575 17891740 1499905 17891740 1499905 17891740 1499905 1787576 1386575 13865191 3845104 17952824 339307142 51163378 345104 17952824 345104 17952824 345104	85795193 2455592 85995015 2056230 20266059 38315034 74440377 76705693 125556939 43220837 17849736 1495133 7459449 102451012 127656617 39379432 179559669 3881502 50595121 3379448 158010369 158010369 148010369 158010369 148010369	T C C C C C C C C C C C C C C C C C C C	C A C C A A G A C C T A A T A A A A C C T T T A A A A	SLITRIG DINIS ARHGAP24 CLUH SPECCI OPHIT9 GPRCSC ZFIXA FAMSHB CUI9 MRCILI TPO LONIS ILISRAP POIRZD MACFI NMHE ECHI CUPSTSI MACFI MSANTOI GOLIMA MSANTOI GOLIMA MSANTOI GOLIMA MSANTOI GOLIMA MSANTOI COLIMA MSANTOI COLI	p. y4390C p.N4240 p.N4240 p.N4541 p. R5735* p. L8297, p. V346V p. P32407 p. N53461 p. N53461 p. R53461 p. R53461 p. R53461 p. R53461 p. R54772 p. R54772 p. R5497 p.	Missense, Mutation Missense, Mutation Missense, Mutation Missense, Mutation Silver Splice, Ste Missense, Mutation Frame, Shift, Ins Missense, Mutation Silver Silve	58V 58V 58V 58V 58V 58V 58V 58V 58V 58V	0.25957447 0.317991304 0.18018018 0.18018018 0.15384615 0.154471545 0.226459004 0.01203855 0.01244898 0.01203855 0.023340496 0.022340496 0.022340496 0.023340496 0.0233594113 0.115384615 0.1159555217 0.02 0.01117318 0.01507692 0.035294118 0.01507692 0.035294118 0.01507687	PASS PASS PASS PASS PASS PASS PASS PASS
# # # # # # # # # # # # # # # # # # #	HCA	dw13 dw4 dw4 dw47 dw47 dw47 dw47 dw47 dw47 d	88,093,28 24558015 890,141,68 25995,24 20,1693,72 36,690917 72,465316 43,185,75 1796,77928 127,569184 43,185,75 1796,774 189905 10,906,747 12,966,819 13,965,104 13,975,104 14,975,104 14,9	85795193 24556392 85995015 2666230 20246059 38335034 74440377 76705693 126556939 126556939 126556939 126556939 126556939 127550617 33379432 127550617 33379432 1324988 38816502 1336498 1481010549 243350072	T C C C C C C C C C C C C C C C C C C C	G A G G A G G A G G A G A G A T T A A A A	SLITRIG DHOLS ABHGAP24 CLUH SPECCI SPECCI GPPL79 GPPCSC ZPNS4 FAMS88 CUL9 MRCL11 TPO LONG LUSSUP MAGF1 NPHS2 ECH1 MSANTD1 GOUIM4 hpt-02 NOTOH3	B 1939C B NASAT B E 1235 B E 1	Missense, Mutation Missense, Mutation Missense, Mutation Missense, Mutation Silent Spiles, Silent Spiles, Silent Missense, Mutation Frame, Shift, Ins. Missense, Mutation Silent Missense, Mutation Silent Missense, Mutation Spiles, Silent Missense, Mutation Spiles, Silent Missense, Mutation Spiles, Silent Missense, Mutation Spiles, Silent Missense, Mutation Missense, Mutati	58V	0,25957447 0,217991304 0,310018018 0,310018018 0,151084615 0,154871545 0,254871545 0,222454094 0,22244694 0,22244694 0,22244694 0,222346046 0,222346046 0,222346046 0,223346046 0,223346046 0,223346046 0,23346046 0,23346046 0,23346046 0,23346046 0,23346046 0,23346046 0,2335294118 0,152307692 0,252394111111111 0,152307692 0,35329418 0,152307692 0,35329418 0,152307692 0,35329418 0,152307692 0,35329418 0,152307692 0,35329418 0,152307692 0,35329418 0,152307692 0,35329418 0,152307692 0,35329418 0,152307692 0,35329418 0,152307692 0,35329418 0,152307692 0,35329418 0,152307692 0,35329418 0,152307692 0,35329418 0,45625	PASS PASS PASS PASS PASS PASS PASS PASS
# # # # # # # # # # # # # # # # # # #	HCA	ch+13 ch+4 ch+4 ch+4 ch+2 ch+2 ch+2 ch+17 ch+17 ch+17 ch+18 ch+18 ch+18 ch+18 ch+2 ch+2 ch+2 ch+2 ch+2 ch+2 ch+1 ch+1 ch+1 ch+1 ch+1 ch+1 ch+1 ch+1	85(69328 24550015 86016168 2599524 20149372 36409017 72436516 77617928 127569384 43188575 17891740 149905 74776576 103067472 128608191 39845104 179528824 51163378 51	82795133 2455432 245542 2	T C C C C C C C C C C C C C C C C C C C	C A C C G A G A C C T A A T A A A A C C T T A A A A A	SLITRIG DIXLS ARHCAP24 CLUH SPECIA GPRISS GPRISS ZPIXAI FANNIBB CUI-9 MRC11 TPO LONI-3 ILIBRAP POLRZD MACF1 NPHS2 ECH1 CUI-9 MSANTD1 GOUM4 sept-02 NOTCH3 SURGO7	p. Y439C p.N4240 p.N4240 p.N454T p.E735* p. L1238 p.Y548Y p.F246T p.K3366 p.1151V p.R2172C p.F497, p.D717D p.G204G p.P459T p.A108V p.A4507A p.P459T p.A4507A p.P459T p.A5507A p.P450	Missense, Mutation Missense, Mutation Missense, Mutation Missense, Mutation Silent Splice, Ste Missense, Mutation Silent Splice, Ste Missense, Mutation Silent Silent Missense, Mutation Silent Silent Missense, Mutation Silent S	9W 9	0.155957447 0.127991304 0.18018018 0.115984615 0.155984615 0.155984615 0.125441595 0.226415094 0.202100556 0.223440996 0.20210020556 0.2021040996 0.202702703 0.219868156 0.115984615 0.1159847107 0.2 0.201117318 0.1929207692 0.201117318 0.1929207692 0.11598415 0.1159847107 0.2 0.201117318 0.1929207692 0.1159847107 0.1	PASS PASS PASS PASS Lod, Marr PASS PASS PASS PASS PASS PASS PASS PA
# # # # # # # # # # # # # # # # # # #	HCA	dw13 dw4 dw47 dw47 dw47 dw47 dw47 dw47 dw47	88,093,28 24558015 890,141,68 25995,24 20,1693,72 36,690917 74,465316 43,185,75 1796,77928 127,569184 43,185,75 1796,774 189905 10,906,747 12,966,191 396,510 1795,2824 393,07142 315,1225 1677,28157 242,289487 13,2812,59 13,2812,59 13,2812,59 13,2812,59 13,2812,59 14,2812,59	85795139 24554912 8999015 12965230 20246059 23846059 24846059 27466057 27466057 12855699 27565697 12855699 27566017 12766017 12766017 12766017 12766017 12766017 12766017 12766017 12766017 12766017 12766017 13851602 38816502 14601039 24150072 15157048 3769258 3769258	T C C C C C C C C C C C C C C C C C C C	G A C G A G G A G A A A A A A A A A A A	SLITRIG DH015 ABHGAP24 CLUH SPECCI GPR179 GPRCSC ZPRV4 FAMBHB LONG MRCLI TPO LONG LONG LONG MRCLI TPO LONG MRCLI TPO LONG MRCLI TPO LONG MRCLI TPO LONG MRCSD MACGI MPHSZ ECHI CSPRGS MAGGI MSANTDI GOUIM4 Sept-02 N0TCH3 ZNRGO7 CYPPI	P. Y-90C P. NA240 P. NA547 P. E.	Missense, Mutation Missense, Mutation Missense, Mutation Missense, Mutation Silent Spiles, Site Missense, Mutation Frame, Shift, Jins Missense, Mutation Silent Missense, Mutation Missense, Mutat	98V 98V 98V 98V 98V 98V 98V 98V	0.25957447 0.217991304 0.310018018 0.310018018 0.1510384615 0.154871545 0.25481504 0.22244698 0.22244698 0.22244698 0.22244698 0.22244698 0.22234698 0.22314696 0.115965217 0.19565217 0.19	PASS PASS PASS PASS PASS PASS PASS PASS
# # # # # # # # # # # # # # # # # # #	HCA	ch+13 ch+4 ch+4 ch+4 ch+2 ch+2 ch+2 ch+17 ch+17 ch+17 ch+18 ch+18 ch+18 ch+18 ch+2 ch+2 ch+2 ch+2 ch+2 ch+2 ch+1 ch+1 ch+1 ch+1 ch+1 ch+1 ch+1 ch+1	85(69328 24550015 86016168 2599524 20149372 20149372 36409017 72436516 177617928 127569384 43188575 17891740 1499905 74776576 103067472 128608191 39845104 179528824 51163378	82795133 2455432 245542 2	T C C C C C C C C C C C C C C C C C C C	C A C C G A G A C C T A A T A A A A C C T T A A A A A	SLITRIG DHOLIS ABHGAP24 CLUH SPECC1 GPRL19 GPRLSC ZPINX4 FAN848 CLU9 MRCLIL TPO LONL3 IL18RAP POLR2D MACF1 NPHS2 ECH1 C19-dR1 MSANTO1 GOLIM4 sept-02 NOTICH3 ZNESGO7 CYPP1 IRXS	p. Y439C p.N4240 p.N4240 p.N454T p.E735* p. L1238 p.Y548Y p.F246T p.K3366 p.1151V p.R2172C p.F497, p.D717D p.G204G p.P459T p.A108V p.A4507A p.P459T p.A4507A p.P459T p.A5507A p.P450	Missense, Mutation Missense, Mutation Missense, Mutation Missense, Mutation Silent Splice, Ste Missense, Mutation Silent Splice, Ste Missense, Mutation Silent Silent Missense, Mutation Silent Silent Missense, Mutation Silent S	9W 9	0.155957447 0.127991304 0.18018018 0.115984615 0.155984615 0.155984615 0.125441595 0.226415094 0.202100556 0.223440996 0.20210020556 0.2021040996 0.202702703 0.219868156 0.115984615 0.1159847107 0.2 0.201117318 0.1929207692 0.201117318 0.1929207692 0.11598415 0.1159847107 0.2 0.201117318 0.1929207692 0.1159847107 0.1	FMSS FMSS FMSS FMSS FMSS FMSS FMSS FMSS
# # # # # # # # # # # # # # # # # # #	HCA	dw13 dw4	85(69328 86(69328) 86016168 8290524 20149372 20149372 36409017 72436516 177637928 127569384 43188575 17891740 1490905 74776576 103067472 128608191 197528824 51163378 51	85795139 \$5795139 \$5995015 \$2995015 \$20950	T C C C C C C C C C C C C C C C C C C C	C A C C G G A C C T A A T A A A A A C C T T A A A T T A A A C C T T A A A C C T T C C C C	SLITRIG DHOLS ABHGAP24 CLUH SPECCI GPR179 GPRCSC 2PRV4 FAMBHB LONG MRCLI TPO LONG LONG LONG MRCLI TPO LONG MRCLI TPO LONG MRCLI TPO LONG MRCSD MACSI MPHS2 ECHI CSPPCSC MACSI MSANTOI GOUIM4 Sept-02 NOTCH3 ZNRGO7 CYPPI	P 1930 P 1930	Missense, Mutation Missense, Mutation Missense, Mutation Missense, Mutation Silent Splice, Ste Missense, Mutation Silent Splice, Ste Missense, Mutation Silent Missense, Mutation Missense, Mutation Missense, Mutation Missense, Mutation	59V 59V 59V 59V 59V 59V 59V 59V 59V 59V	0.25557447 0.187991304 0.80018018 0.185984615 0.155984615 0.155984615 0.125441595 0.225415094 0.222446996 0.222446996 0.202702703 0.219684156 0.1059847107 0.2 0.20117318 0.195927107 0.2 0.219270799 0.219270799 0.219270799 0.219270799 0.219270799 0.219270799 0.219270799 0.255294118	PASS PASS PASS PASS PASS PASS PASS PASS
# # # # # # # # # # # # # # # # # # #	HCA	dw13 dw4 dw47 dw47 dw47 dw47 dw47 dw47 dw47	88,093,28 24558015 890,141,68 2599,524 201,693,72 36,699,917 72,446516 776,7928 1275,693,84 43,386,75 1790,766 1,499,965 1,499,766 1,499	85795139 24554912 8999015 12965230 20246059 23845059 1285	T C C C C C C C C C C C C C C C C C C C	G A G G G A G G A G G A A T T A A A A A	SLITRIG SHITRIG DHXIS ABHGAP24 CLUH SPECCI GPRI39 GPRCSC 2PRX4 FAARSH8 CULS TOOLS LURA FAARSH8 LONG LONG LONG LONG MACCI TPO MACCI MACC	P. Y-190C P. NA240 P. NA547 P. E. ST375 P. LI278 P. LI278 P. LI278 P. P. P. Met P. P. P. Met P. P. P. Met P. P. P. Met	Missense, Mutation Missense, Mutation Missense, Mutation Missense, Mutation Silent Spiles, Site Missense, Mutation Frame, Shift, Jins Missense, Mutation Silent Missense, Mutation Silent Missense, Mutation Silent Missense, Mutation	98V 98V 98V 98V 98V 98V 98V 98V	Q.55957447 Q.117991304 Q.18018018 Q.18018018 Q.151984615 Q.151984615 Q.151984615 Q.12544598 Q.12244698 Q.12244698 Q.12244698 Q.12244698 Q.12194655 Q.119565217 Q.19565217 Q.1956527 Q.19567 Q.1956527 Q.1956527 Q.1956527 Q.1956527 Q.1956527 Q.1956527 Q.1	PASS PASS PASS PASS PASS PASS PASS PASS
# #447	HCA	cht3 cht4 cht4 cht4 cht4 cht4 cht27 cht37 cht37 cht37 cht37 cht37 cht37 cht36 cht6 cht3 cht2 cht2 cht2 cht2 cht2 cht2 cht2 cht2	85,093,28 24550015 80916168 2599524 20149372 36409017 72436516 177637928 127569384 43188575 17891740 149905 74775576 13905747 12808391 13905747 2508391 15728254 15728254 15728254 15728254 15728254 15728254 15728254 15728254 15728254 15728254 15728255 15728254 15728255 15728255 15728255 15728255 15728255 15728255 15728255 15728255 1572825 157285 157	65795139 65795139 6595015 12056015 12056015 12056019 1205601	T C C C C C C C C C C C C C C C C C C C	C A C C A C G A C C T A T A A A A C T A A A A A T A A A A	SLITRIG DH0315 ABHGAP24 CLUH SPECC1 GPR179 GPRCSC ZPIXA FAN848 CLU9 MRCL11 TPO LONL3 LLSRAP POLR2D MACF1 NPHS2 ECH1 C39-d81 MSANTD1 GOLIM4 Sept-02 NOTICH3 ZNEGO7 CYPP1 IRXS SLCSRAR S	P 1930C P 1	Missense, Mutation Missense, Mutation Missense, Mutation Missense, Mutation Silent Splice, Ste Missense, Mutation Silent Splice, Ste Missense, Mutation Silent Missense, Mutation Silent Missense, Mutation Silent Missense, Mutation Silent Missense, Mutation Missense, Mutation Missense, Mutation Silent Missense, Mutation Missense, Mutation Silent Missense, Mutation Missense, Mutation Silent Missense, Mutation Missense, Mutation Silent Missense, Mutation Missense	59V 59V 59V 59V 59V 59V 59V 59V 59V 59V	0.155957447 0.187991304 0.18018018 0.185984615 0.155984615 0.155984615 0.125441595 0.125441596 0.122444998 0.1201905566 0.223404996 0.207072703 0.219858156 0.1155984615 0.1159847107 0.2 0.201117318 0.19592747 0.15592747 0.15592747 0.15592747 0.15592747 0.15592747 0.15592747 0.15592747 0.15592747 0.15592747 0.15592747	PASS PASS PASS PASS PASS PASS PASS PASS
# # # # # # # # # # # # # # # # # # #	HCA	cht3 cht4 cht4 cht4 cht4 cht7 cht7 cht7 cht7 cht7 cht8 cht8 cht8 cht8 cht8 cht8 cht8 cht8	85(93)28 85(93)28 85034158 85034158 20149372 20149372 20149372 364690917 7246515 77617928 137599184 43388575 17891740 1499965 14776576 100067472 1286605151 39845104 33907142 33907142 35102378 3451225 167728157 242289487 3451225 34507185 345	85795139 24559120 24559120 24559120 24559120 245	T C C C C C C C C C C C C C C C C C C C	G A G G G A G G A G G A G A A A A A A A	SLITRIG DH015 ABHGAP24 CLUH SPECC1 GPR129 GPRCSC 2PR04 FAR888 GUS9 MRCLI1 TPO LORL3 LIBRAP POL82D MAGF1 RPP152 EO11 MAGF1 MSST EO11 EO11 EO11 EO11 EO11 EO11 EO11 EO1	P. YING P. NAME P. NAME P. NAME P. NAME P. LETA P. LET	Missens, Mutation Missens, Mutation Missens, Mutation Missens, Mutation Silent Spiles, Sile Missens, Mutation Frame, Shift, Jin Missense, Mutation Missense, Mutation Silent Silent Silent Missense, Mutation Silent Missense, Mutation Silent Missense, Mutation Missense, Mutation Missense, Mutation Missense, Mutation Missense, Mutation Missense, Mutation Silent Missense, Mutation	98V 98V 98V 98V 98V 98V 98V 98V	Q.55957447 Q.117991304 Q.18018018 Q.18018018 Q.15159184615 Q.15159184615 Q.15159184615 Q.226415094 Q.12244699 Q.12244699 Q.12244699 Q.12244699 Q.12246995 Q.121958156 Q.119585157 Q.119585157 Q.11958157 Q.1295817107 Q.1501117118 Q.15207092 Q.152741099 Q.152741099 Q.152745099 Q.15274509	PASS PASS PASS PASS PASS PASS PASS PASS
# #4917 # #491	HICA HICA HICA HICA HICA HICA HICA HICA	cht3 cht4 cht4 cht4 cht4 cht4 cht27 cht37 cht37 cht37 cht37 cht37 cht37 cht37 cht30	85,093,28 82455015 80916168 1299524 20149372 20149372 36409017 72436516 177637928 127569384 43188575 17891740 13995510 139965104 13952824 13952742 13952824 13952742 13952824 13952742 13952824 139	85795139 85795139 15955139 159	T C C C C C C C C C C C C C C C C C C C	C A A C C T A A A A A A C C T A A G C T T A A A A A T T A A A A T T A A A A	SLITRIG DH0315 ABHGAP24 CLUH SPECC1 GPR179 GPRCSC ZPIXA FAN848 CLU9 MRC111 TPO LON13 L188AP POLR2D MAC51 NPH52 ECH1 C19-r81 MSANTD1 GOLIM4 Sept-02 NOTICH3 L288AP RESCO CVPP1 RSS SLISBAR SSLISBAR SSLISB	P. Y-930C P. M149C P.	Missense, Mutation Missense, Mutation Missense, Mutation Missense, Mutation Silent Splice, Ste Missense, Mutation Silent Splice, Ste Missense, Mutation Silent Missense, Mutation Silent Missense, Mutation Silent Missense, Mutation Missense, Missense, Mutation Missense, Mutation M	59V 59V 59V 59V 59V 59V 59V 59V 59V 59V	0.155957447 0.127991304 0.18038018 0.115984615 0.15584615 0.15584615 0.15584615 0.1256415094 0.122444998 0.202109556 0.2231404996 0.202702703 0.219854156 0.115984615 0.115984615 0.115984615 0.115984615 0.115984615 0.1159847107 0.2 0.201117318 0.1929207992 0.201117318 0.1929207992 0.201117318 0.1929207992 0.201117318 0.1929207992 0.201117318 0.1929207992 0.201117318 0.1929207992 0.201117318 0.1929207992 0.201117318 0.1929207992 0.201117318 0.1929207992 0.201117318 0.1929207992 0.201117318 0.1929207992 0.201117318 0.2012076998 0.3929150605 0.39291	PASS PASS PASS PASS PASS PASS PASS PASS
# # # # # # # # # # # # # # # # # # #	HCA	cht3 cht4 cht4 cht4 cht4 cht7 cht7 cht7 cht7 cht7 cht8 cht8 cht8 cht8 cht8 cht8 cht8 cht8	85(93)28 85(93)28 85034158 85034158 20149372 20149372 20149372 364690917 7246515 77617928 137599184 43388575 17891740 1499965 14776576 100067472 1286605151 39845104 33907142 33907142 35102378 3451225 167728157 242289487 3451225 34507185 345	85795139 24559120 24559120 24559120 24559120 245	T C C C C C C C C C C C C C C C C C C C	G A G G G A G G A G G A G A A A A A A A	SLITRIG DH015 ABHGAP24 CLUH SPECC1 GPR129 GPRCSC 2PR04 FAR888 GUS9 MRCLI1 TPO LORL3 LIBRAP POL82D MAGF1 RPP152 EC011 MSSTED MSST	P. YING P. NAME P. NAME P. NAME P. NAME P. P	Missens, Mutation Missens, Mutation Missens, Mutation Missens, Mutation Silent Spiles, Sile Missens, Mutation Frame, Shift, Jin Missense, Mutation Missense, Mutation Silent Silent Silent Missense, Mutation Silent Missense, Mutation Silent Missense, Mutation Missense, Mutation Missense, Mutation Missense, Mutation Missense, Mutation Missense, Mutation Silent Missense, Mutation	98V 98V 98V 98V 98V 98V 98V 98V	Q.55957447 Q.117991304 Q.18018018 Q.18018018 Q.15159184615 Q.15159184615 Q.15159184615 Q.226415094 Q.12244699 Q.12244699 Q.12244699 Q.12244699 Q.12246995 Q.121958156 Q.119585157 Q.119585157 Q.11958157 Q.1295817107 Q.1501117118 Q.15207092 Q.152741099 Q.152741099 Q.152745099 Q.15274509	PASS PASS PASS PASS PASS PASS PASS PASS
# # # # # # # # # # # # # # # # # # #	HCA	cht3 cht4 cht4 cht4 cht4 cht7 cht7 cht77 cht77 cht77 cht77 cht8 cht8 cht8 cht6 cht8 cht9 cht7 cht9 cht9 cht9 cht9 cht9 cht9 cht9 cht9	85,093,28 82455015 80916168 2995524 20149372 20149372 36409017 72436516 177637928 127569384 43188575 17891740 1499905 74776576 103067472 128608191 13952824 51163378 517728157 17	65795139 65795139 65795139 6595015 6595015 6595015 620	T C C C C C C C C C C C C C C C C C C C	C A C C A C G A C C A C C A C C A C C A A A A	SLITRIG DH015 ABHGAP24 CLUH SPECC1 GPR129 GPRCSC 2PR04 FAR886B CLUS MRCLL1 TPO LORL3 LERAP POLAZD MARCH MRCH MRCH MRCH MRCH MRCH MRCH MRCH M	P. YING P. NAME P. NAME P. NAME P. NAME P. P	Missense, Mutation Missense, Mutation Missense, Mutation Missense, Mutation Missense, Mutation Spiler, Silent Spiler, Silent Missense, Mutation	59V 59V 59V 59V 59V 59V 59V 59V 59V 59V	0.155957447 0.127991304 0.18038018 0.18038018 0.15588615 0.154871545 0.125415094 0.12244698 0.12244698 0.12244698 0.12244698 0.12244698 0.12020556 0.121588615 0.1159847107 0.2 0.2192146996 0.115984615 0.1159847107 0.2 0.201117318 0.1929207992 0.201117318 0.1929207992 0.19987107 0.15987107 0.000000000000000000000000000000000	PASS PASS PASS PASS PASS PASS PASS PASS
# #4917 # #491	HCA	cht3 cht4 cht4 cht4 cht4 cht4 cht27 cht37 cht37 cht37 cht37 cht37 cht37 cht37 cht30 cht40 cht30 cht40	85(93)28 85(93)28 8503158 8503158 8503158 20149272 20149272 364690917 72446515 77637928 127599184 43388575 17691740 1499905 74776276 103067472 103067473 139845104 33907142 33907142 33907142 3505125 147728157 242299487 3505125 147728157 242299487 3505125 147728157 242299487 3505125 157728157 242299487 3505125 5406731 84056652 3505125 5406731 84056652 3505125 5406731 84056652 3505125 5406731 84056652 3505125 5406731 84056652 3505125 5406731 84056652 3505125 5406731 84056652 3505125 5406731 84056652 3505125 5406731 84056652 3505125 5406731 84056652 3505125 5406731 84056652 3505125 5406731 84056652 3505125 5406731 84056652 3505125 5406731 84056652 3505125 5406731 84056652 3505125 5406731 84056652 3505125 5406731 84056652 3505125 5406731 84057505 5406751 5	85795139 24559512 26559512 2006020 2006050 200	T C C C C C C C C C C C C C C C C C C C	C A C C A C G A C C A C C A C C A C C A A A A	SLITRIG DH015 ABHGAP24 CLUH SPECC1 GPR179 GPRCSC ZPIXA FAN848 CLU9 MRC111 TPO LON13 L188AP POL820 MAC51 NPH52 ECH1 C19-r81 MSANTD1 GOLIM4 Sept-02 NOTICH3 L288AP RESCO CVPP1 RSS SLISBAB SLISB	P. Y-9302 P. M-9302 P. M-9302 P. M-9302 P. L1279 P. M-9302 P. M-930	Missense, Mutation Missense, Mutation Missense, Mutation Missense, Mutation Silent Splice, Ste Missense, Mutation Silent Splice, Ste Missense, Mutation Missense, Mutation Missense, Mutation Missense, Mutation Silent Silent Missense, Mutation Missense, Mutation Silent Missense, Mutation	98V 98V 98V 98V 98V 98V 98V 98V	Q.55957447 Q.117991304 Q.18018018 Q.18018018 Q.15159184G15 Q.15159184G15 Q.15159184G15 Q.15159184G15 Q.1254401904 Q.1224401904 Q.1224401904 Q.1224401904 Q.11591854156 Q.11591854116 Q.1159185416 Q.1159186416 Q.1159186	FMSS FMSS FMSS FMSS FMSS FMSS FMSS FMSS
# # # # # # # # # # # # # # # # # # #	HCA	cht3 cht4 cht4 cht4 cht4 cht4 cht7 cht7 cht7 cht7 cht7 cht8 cht8 cht6 cht6 cht6 cht7 cht7 cht7 cht7 cht7 cht7 cht8 cht6 cht6 cht7 cht7 cht7 cht7 cht7 cht8 cht6 cht7 cht7 cht7 cht7 cht7 cht7 cht7 cht7	88,093,28 24558015 893,14158 2939,524 201493,72 201493,72 201493,72 201493,72 201493,72 201493,72 2146515 2776,7928 127597184 431885,75 17891740 1499905 747762,76 103067473 13965104 13965104 33907142 33907142 33907142 33907142 3451225 147728157 24229487 3590714	85795139 24554512 245	T C C C C C C C C C C C C C C C C C C C	G A G G A G G A G G A G G A A A A A A A	SLITRIG DH015 ABHGAP24 CLUH SPECC1 GPR129 GPRCSC 2PNS4 FAR8H8 CUS S MRCLI1 TPO CUS S MRCLI CLIPMS1 TRUS S CSG07131 CLIPMS1 CLIPMS1 CLIPMS1 TRUS S CSG07131 CLIPMS1 CLIPMS1 TRUS S CSG07131 CLIPMS1 TRUS S SCSSSS S SCSSSS S SCSSSS S SCSSSS S SCSSSS S SCSSSS S SSSSS S SSSSS S SSSSS S SSSSS S S	P. YING P. NAME P. NAME P. NAME P. NAME P. P	Missense, Mutation Missense, Mutation Missense, Mutation Missense, Mutation Silent Spiler, Silent Spiler, Silent Missense, Mutation Missense, Muta	98V	Q.55957447 Q.117991304 Q.18018018 Q.18018018 Q.115984615 Q.1518984615 Q.1518984615 Q.1518984615 Q.12544898 Q.12244898 Q.12244898 Q.12244898 Q.121898415 Q.115985415 Q.115985415 Q.115985415 Q.115985415 Q.115985415 Q.115985415 Q.115985415 Q.115985415 Q.115985417 Q.155964111111111 Q.18813160 Q.12459597 Q.15596360 Q.1159853604 Q.12595597 Q.151813605 Q.12459597 Q.151813605 Q.1	PASS PASS PASS PASS PASS PASS PASS PASS
# # # # # # # # # # # # # # # # # # #	HCA	cht3 cht4 cht4 cht4 cht4 cht4 cht27 cht37 cht37 cht37 cht37 cht37 cht37 cht37 cht37 cht30 cht30 cht2 cht2 cht2 cht2 cht2 cht2 cht2 cht3 cht3 cht3 cht3 cht3 cht3 cht3 cht3	85,093,28 80,093,28 80,016,168 80,016,168 2,5995,24 201493,72 364,090,17 724,365,16 127,569,184 43,1885,75 1,789,174 1,78	65795131 65795131 6595015 1595015 1205015 1205015 1205015 1205019 1450	T C C C C C C C C C C C C C C C C C C C	G A C G A G G A G G A A C T T A A A A A T T A A A C T T A A A A	SLITRIG DHOLIS ABHGAP24 CLUH SPECC1 GPR179 GPRCSC ZPIXA FAN848 CUS MRCLIL TFO LONL I TFO LONL I SERAP POLRZD MACFI NPHS2 CCH CSPCCI NOTCHS SCHOOL SCHOOL NGCCI NGCCI NFPLI RXS SLISSAR SCHOOL S	P. Y-9300 P. M-9401 P. M-9	Missense, Mutation Missense, Mutation Missense, Mutation Missense, Mutation Silent Splice, Ste Missense, Mutation Silent Splice, Ste Missense, Mutation Silent Missense, Mutation Silent Missense, Mutation Silent Missense, Mutation Missense, Mutation Silent Missense, Mutation Miss	59V 59V 59V 59V 59V 59V 59V 59V 59V 59V	0.155957447 0.127991304 0.18038018 0.18038018 0.15588615 0.154871545 0.125415094 0.12244898 0.22244898 0.22244898 0.22244898 0.22244898 0.22244898 0.222244898 0.222248989 0.2222248989 0.2222248989 0.22222248989 0.22222248989 0.22222248989 0.22222248989 0.22222248989 0.22222248989 0.222222418 0.222222418 0.222222418 0.222222418 0.222222418 0.2222248 0.222248 0.2222248 0.2222248 0.2222248 0.2222248 0.2222248 0.2222248 0.2222248 0.2222248 0.2222248 0.2222248 0.2222248 0.22248 0.22248 0.22248 0.22248 0.22248 0.22248 0.22248 0.22248 0.22248 0.22248 0.22248 0.22248 0.22248 0.22248 0.22248 0.22248	FMSS FMSS FMSS FMSS FMSS FMSS FMSS FMSS
# # # # # # # # # # # # # # # # # # #	HCA	dw13 dw42 dw47 dw47 dw47 dw47 dw47 dw47 dw47 dw47	88,093,28 893,161,68 893,161,68 2939,524 201,937,2 201,937,2 36,600,017 72,4465,16 776,179,28 137,593,184 433885,75 1769,174,0 1769,762,76 103,007,472 103,007,4	85795139 24559129 245	T C C C C C C C C C C C C C C C C C C C	G A G G A G G A G G A G G A A A A A A A	SLITRIG DH015 ABHGAP24 CLUH SPECCI GPR129 GPR53C ZPR04 FAR848 GUIS MRCLI LORI LORI LORI LORI LORI LORI MRCLI LORI MRCLI LORI LORI MRCLI MRCL	P. YING P. NAME P. NAME P. NAME P. NAME P. P	Missense, Mutation Missense, Mutation Missense, Mutation Missense, Mutation Missense, Mutation Spiler, Silent Spiler, Silent Missense, Mutation Mi	98V	0.25957447 0.217991304 0.10018018 0.10018018 0.15584615 0.154872545 0.154872545 0.226415094 0.22244098 0.22244098 0.22244098 0.22244098 0.23246098 0.2323404096 0.2323404096 0.2323404096 0.232370793 0.15585415 0.115965217 0.15687217 0.15687217 0.15687217 0.157867217	PASS PASS PASS PASS PASS PASS PASS PASS
# #497	HCA	cht3 cht4 cht4 cht4 cht4 cht4 cht27 cht37 cht37 cht37 cht37 cht37 cht37 cht37 cht37 cht37 cht30 cht36 cht46 cht36 cht46 cht47	85,093,28 80,093,28 80,016,168 80,016,168 20,995,24 20,149,172 36,400,017 72,436,516 127,569,184 43,188,75 1,789,174 43,188,75 1,789,174 1,795,786 1,795,786 1,795,786 1,795,786 1,795,786 1,795,786 1,795,786 1,795,786 1,795,786 1,795,786 1,795,786 1,795,786 1,795,786 1,795,786 1,795,786 1,795,786 1,795,786 1,795,786 1,796,786 1,79	85795131 \$5795132 \$5995015 \$5995015 \$2046020 \$20460	T C C C C C C C C C C C C C C C C C C C	G A C G A G G A C G A C G A A C T A A A A A A A T A A A A C T A A A A	SLITRIG SHITRIG DH0315 ABHGAP24 CLUH SPECC1 GPR179 GPRCSC ZPIXA FAN848 CU.9 MRCILI TFO LONL3 IL188AP POLR2D MACF1 NPH52 ECH1 C19-dB1 MSANTD1 GOLIMA LSP6 MSANTD1 GOLIMA SPICO2 NOTICH3 ZNEGO7 CYPP1 IRXS SLCSSA8 SCO91311 CEPTM11 CEO'1163 INPPL1 ORCL RFWD2 MORG MORG SPINERY LUEP4 LUEP4 LUEP4 LUEP4 LUEP4 LUEP5 PLCE1 SLCDIB3 SLCDIB3 SLCDIB5 SLCDIB5 SLCDIB5 SLCDIB6 SPINERY LUEP4 LUEP4 LUEP5 PLCE1 SLCDIB3 SLCDIB5 SL	P. Y-9302 P. M-9302 P. M-9302 P. M-9302 P. L1229 P.	Missense, Mutation Missense, Mutation Missense, Mutation Missense, Mutation Silent Splice, Ste Missense, Mutation Silent Splice, Ste Missense, Mutation Missense, Mutation Missense, Mutation Missense, Mutation Missense, Mutation Silent Missense, Mutation Missense, Mutation Silent Missense, Mutation Missens	59W	0.155957447 0.127991304 0.18038018 0.18038018 0.15584615 0.15471545 0.125441594 0.122444998 0.122444998 0.122444998 0.1201205556 0.222440996 0.122346996 0.120120556 0.12012072703 0.19854156 0.115584615 0.1159847107 0.2 0.201117318 0.1992707992 0.199371070 0.11591111111 0.399728477 0.15 0.406215 0.40	FMSS FMSS FMSS FMSS FMSS FMSS FMSS FMSS
# # # # # # # # # # # # # # # # # # #	HCA	dw13 dw4 dw4 dw47 dw47 dw47 dw47 dw47 dw47 d	85(93)28 85(93)28 85(93)26 85(93)26 85(93)26 20149372 20149372 20149372 36(400)17 724(65)16 77(5)7928 137(93)26 137(93)26 149(996) 747(67)6 149(996) 747(67)6 149(996) 747(67)6 149(996) 149(996) 149(996) 149(996) 149(996) 149(996) 149(996) 149(996) 149(996) 149(996) 149(996) 149(996) 149(996) 149(996) 149(996) 151(23) 151(23) 152(25)	85795139 24559129 24559129 24559129 24559129 24650129 246	T C C C C C C C C C C C C C C C C C C C	G A G G A G G A G G A G G A A A A A A A	SLITRIG DH015 ABHGAP24 CLUH SPECCI GPR129 GPR53C ZPR04 FANSH8 CLUS MRCLLI MRCLL	P. YING P. NAME P. NAME P. NAME P. NAME P. P	Missense, Mutation Missense, Mutation Missense, Mutation Missense, Mutation Missense, Mutation Silent Splice, Site Missense, Mutation Silent Missense, Mutation Silent Missense, Mutation Missense, Mutatio	98V	Q.55957447 Q.127991304 Q.18018018 Q.18018018 Q.15384615 Q.154871545 Q.154871545 Q.154871545 Q.12544898 Q.12244898 Q.12244898 Q.12244898 Q.1234898415 Q.115965217 Q.1586415 Q.115965217 Q.1586415 Q.115965217 Q.1586415 Q.115965217 Q.1586415 Q.12765567 Q.115965217 Q.1586415 Q.12765567 Q.115965217 Q.1586415 Q.12765567 Q.1586415 Q.12765567 Q.1586415 Q.12765567 Q.1586415 Q.15865667 Q.1586567 Q.15865667 Q.15865667 Q.15865667 Q.15865667 Q.15865667 Q.1586567 Q.1586567 Q.1586567 Q.158667 Q.15866	PASS PASS PASS PASS PASS PASS PASS PASS
# #497	HCA	cht3 cht4 cht4 cht4 cht4 cht4 cht27 cht37 cht37 cht37 cht37 cht37 cht37 cht37 cht37 cht37 cht30 cht36 cht46 cht36 cht46 cht47	85,093,28 80,093,28 80,016,168 80,016,168 2,999,524 201493,72	85795131 \$5795132 \$5995015 \$5995015 \$2046020 \$20460	T C C C C C C C C C C C C C C C C C C C	G A G G A G G A G G A G G A A G G A	SLITRIG SHITRIG DH0315 ABHGAP24 CLUH SPECC1 GPR179 GPRCSC ZPIXA FAN848 CU.9 MRCILI TFO LONL3 IL188AP POLR2D MACF1 NPH52 ECH1 C19-dB1 MSANTD1 GOLIMA LSP6 MSANTD1 GOLIMA SPICO2 NOTICH3 ZNEGO7 CYPP1 IRXS SLCSSA8 SCO91311 CEPTM11 CEO'1163 INPPL1 ORCL RFWD2 MORG MORG SPINERY LUEP4 LUEP4 LUEP4 LUEP4 LUEP4 LUEP5 PLCE1 SLCDIB3 SLCDIB3 SLCDIB5 SLCDIB5 SLCDIB5 SLCDIB6 SPINERY LUEP4 LUEP4 LUEP5 PLCE1 SLCDIB3 SLCDIB5 SL	P. Y-9302 P. M-9302 P. M-9302 P. M-9302 P. L1229 P.	Missense, Mutation Missense, Mutation Missense, Mutation Missense, Mutation Silent Splice, Ste Missense, Mutation Silent Splice, Ste Missense, Mutation Missense, Mutation Missense, Mutation Missense, Mutation Missense, Mutation Silent Missense, Mutation Missense, Mutation Silent Missense, Mutation Missens	59W	0.155957447 0.127991304 0.18038018 0.18038018 0.15584615 0.15471545 0.125441594 0.122444998 0.122444998 0.122444998 0.1201205556 0.222440996 0.122346996 0.120120556 0.12012072703 0.19854156 0.115584615 0.1159847107 0.2 0.201117318 0.1992707992 0.199371070 0.11591111111 0.399728477 0.15 0.406215 0.40	PASS PASS PASS PASS PASS PASS PASS PASS
# #497	HCA	ch+13 ch+4 ch+4 ch+4 ch+2 ch+4 ch+17 ch+17 ch+17 ch+17 ch+18 ch+6 ch+10 ch+10 ch+2 ch+2 ch+2 ch+2 ch+2 ch+2 ch+2 ch+1 ch+1 ch+1 ch+1 ch+1 ch+1 ch+3 ch+3 ch+3 ch+3 ch+3 ch+3 ch+3 ch+3	85,093,28 80,093,28 80,016,168 80,016,168 2,5995,24 201493,72 364,090,17 724,365,16 127,569,184 431885,75 1789,174 139,000,77 128,008,191 139,000,191 139,000,191 139,000,191 139,000,191 139,000,191 139,000,191 149,000,191 150,000,19	65795139 65795139 65795139 6595015 6595015 12665203 12066	T C C C C C C C C C C C C C C C C C C C	C A A C C A A C G A A C C T A A A A A A A A A A A A A A A	SLITRIG SHAPE SHITRIG DHOLIS ABHGAP24 CLUH SPECCI GPRIT9 GPRESC ZPINX4 FAN848 CLU9 MRGLIL TFO LONI3 ILIBRAP POLRZD MAGGI NPHSZ ECHI CSPGTS MYSSZ CCHI CSPGTS MYSSZ	P. Y-9302 P. M-9302 P. M-9302 P. M-9302 P. L1229 P.	Missense, Mutation Missense, Mutation Missense, Mutation Missense, Mutation Silent Splice, Ste Missense, Mutation Silent Splice, Ste Missense, Mutation Missense, Mutation Missense, Mutation Missense, Mutation Silent Missense, Mutation Missense, Mutation Missense, Mutation Silent Missense, Mutation Missense, Mutation Silent Missense, Mutation	59W	0.155957447 0.127991304 0.18038018 0.18038018 0.15588615 0.154871545 0.125415094 0.12244898 0.12024	FMSS FMSS FMSS FMSS FMSS FMSS FMSS FMSS
# # # # # # # # # # # # # # # # # # #	HCA	dw13 dw42 dw47 dw47 dw47 dw47 dw47 dw47 dw47 dw47	85(93)28 85(93)28 85(93)26 85(93)26 85(93)26 85(93)26 2019372 2019372 36(900)17 72(465)16 77(517928 127(93)26 127(93)26 149(905) 747(95)26 149(905) 159(105) 15	85795139 24559129 24559129 24559129 24559129 24650139 24650139 241	T C C C C C C C C C C C C C C C C C C C	G A G G A G G A G G A G G A A A A A A A	SLITRIG DH015 ABHGAP24 CLUH SPECCI GPR129 GPRCSC ZPR04 FANSH8 CLUS MRCLI1 TFO LORI LUS MRCLI1 TFO LORI LUS MRCLI1 TFO LORI LUS MRCLI1 TFO LORI LUS MRCLI1 TFO LORI MRCLI M	P. YING P. NAME P. NAME P. NAME P. NAME P. P	Missense, Mutation Missense, Mutation Missense, Mutation Missense, Mutation Missense, Mutation Silent Splice, Site Missense, Mutation Silent Missense, Mutation Missense, Mutation Missense, Mutation Missense, Mutation Silent Missense, Mutation Missense, Mutatio	98V	Q.55957447 Q.127991304 Q.18018018 Q.18018018 Q.15384615 Q.154872545 Q.154872545 Q.12544098 Q.12244098 Q.12244098 Q.12244098 Q.12244098 Q.123584615 Q.13585415 Q.13585415 Q.13585415 Q.13585415 Q.13585417 Q.15585417 Q.15585	PASS PASS PASS PASS PASS PASS PASS PASS
# #447	HICA HICA HICA HICA HICA HICA HICA HICA	ch+13 ch+4 ch+4 ch+4 ch+27 ch+17 ch+17 ch+17 ch+17 ch+18 ch+18 ch+18 ch+18 ch+18 ch+18 ch+18 ch+19 ch+20 ch+	85,093,28 80,093,28 80,016,168 80,016,168 2,5995,24 201493,72	85795139 85795139 8599515 85995015 1266210 12064010 12064	T C C C C C C C C C C C C C C C C C C C	C A A C C T A A A A A A A A A A A A A A	SLITRIG DHOLIS ABHGAP24 CLUH SPECCI GPRI179 GPRI279 GPRI279 GPRI270 GPRI279 GPRI270 MRCILI TPO LONL3 ILIBRAP POLR2D MACGI NFM152 ECHI C19-of81 MSANTD1 GOLIMA LSPS SLICESAB LUFFM1 LCPFM1 LCPM1 LCCG-of183 L	P. 1930C P. 1940C P.	Missense, Mutation Missense, Mutation Missense, Mutation Missense, Mutation Silent Splice, Ste Missense, Mutation Silent Splice, Ste Missense, Mutation Missense, Mutation Silent Silent Silent Missense, Mutation Missense, Mutation Missense, Mutation Silent Missense, Mutation Missense, Mu	59V 59V 59V 59V 59V 59V 59V 59V	0.155957447 0.127991304 0.18038018 0.18038018 0.15588615 0.15588615 0.15588615 0.125615094 0.12244898 0.120329556 0.223140496 0.12032956 0.223140496 0.1032937107 0.2 0.19987107 0.2 0.20117318 0.1929207992 0.19987107 0.1003127 0.1003	FMSS FMSS FMSS FMSS FMSS FMSS FMSS FMSS
# # # # # # # # # # # # # # # # # # #	HCA	chr13 chr4 chr4 chr4 chr4 chr4 chr17 chr17 chr17 chr17 chr18 chr8 chr8 chr8 chr8 chr8 chr8 chr1 chr2 chr1 chr2 chr1 chr2 chr1 chr2 chr1 chr1	85(93)28 85(93)28 85(93)26 85(93)26 85(93)26 85(93)26 2019372 2019372 36(90)27 72(465)16 77(517928 1275(93)84 43188575 17891740 1499905 74776576 1499905 1499905 1499905 1499905 14952024 158(0819) 158(0819) 158(0819) 158(0819) 158(103)78 158(103	85795139 24559129 24559129 24559129 24559129 24650139 246	T C C C C C C C C C C C C C C C C C C C	G A G G A G G A G G A G G A A A A A A A	SLITRIG DH015 ABHGAP24 CLUH SPECCI GPR129 GPRCSC ZPIXIA FANSHB CLUS MRCILI TFO LORI LIBRAP POIRZO MACFI ROWS MRCILI TO LORI MR	P. YING P. NAME P. NAME P. NAME P. NAME P. P	Missense, Mutation Missense, Mutation Missense, Mutation Missense, Mutation Missense, Mutation Silent Splice, Site Missense, Mutation Missense, Mutation Missense, Mutation Missense, Mutation Silent Silent Silent Missense, Mutation Missense, Mutation Missense, Mutation Silent Missense, Mutation Silent Missense, Mutation Missense, Mutation Silent Missense, Mutation Silent Missense, Mutation Missense, Mutation Missense, Mutation Silent Missense, Mutation Missense, Mut	98V	Q.55957447 Q.127991304 Q.18018018 Q.18018018 Q.151984615 Q.151984615 Q.151984615 Q.151984615 Q.151984615 Q.151984615 Q.151984615 Q.151985415 Q.151985516 Q.151985615 Q.151985615	PASS PASS PASS PASS PASS PASS PASS PASS
# #447	HCA	ch+13 ch+4 ch+4 ch+4 ch+27 ch+17 ch+17 ch+17 ch+17 ch+18 ch+18 ch+18 ch+18 ch+18 ch+18 ch+18 ch+18 ch+19 ch+21 ch+19 ch+21 ch+21 ch+22 ch+	85,093,28 80,093,28 80,014,58 80,014,58 20,014,58 20,014,58 20,014,58 20,014,58 20,014,58 20,014,58 20,014,58 20,014,58 21,756,018 43,188,75 1,789,174 1,798,174	65795139 65795139 65795139 6595015 6595015 1206020 120	T C C C C C C C C C C C C C C C C C C C	C A A C C A A C C A A C C A A C C T A A A A	SLITRIG SLITRIG DH0IS ABHGAP24 CLUH SPECCI GPRIT9 GPRISC ZPIXX4 FAN848 CLUS MRCILI TO LONL3 ILIBRAP POLR2D MACGI NPHS2 ECHI CSPORT MSANTDI GOLIMA LSPS MSANTDI GOLIMA LSPS CONTONS SLIEBRAP RPHS2 ECHI CSPORT MSANTDI GOLIMA LSPS CONTONS SLIEBRAP RPHS2 LUZPA LUZ	P. 1930C P. 1945C P.	Missense, Mutation Missense, Mutation Missense, Mutation Missense, Mutation Silent Splice, Ste Missense, Mutation Silent Splice, Ste Missense, Mutation Missense, Mutation Missense, Mutation Missense, Mutation Silent Missense, Mutation Missense, Mutation Missense, Mutation Missense, Mutation Silent Missense, Mutation Missense, Mutation Silent Missense, Mutation Mi	59V	0.25957447 0.177910104 0.18018018 0.18018018 0.151588615 0.151588615 0.151588615 0.151588615 0.125615004 0.12244898 0.120180556 0.22146096 0.12244898 0.120185615 0.195847157 0.2 0.195847157 0.2 0.195847167 0.2 0.20117318 0.195973477 0.1558415 0.40625 0.301754098 0.392156863	PASS PASS PASS PASS PASS PASS PASS PASS
# # # # # # # # # # # # # # # # # # #	HCA	dw13 dw42 dw47 dw47 dw47 dw47 dw47 dw47 dw47 dw47	85(93)28 85(93)28 85(93)28 85(93)26 85(93)26 85(93)26 2019372 2019372 36(90)21 72(465)16 77(517928 1275(93)84 43188575 17891740 1499905 74776576 1499905 14776576 1580(319) 1595(32)2 1595(32	85795139 24559129 24559129 24559129 24559129 24560129 245	T C C C C C C C C C C C C C C C C C C C	G A G G A G G A G G A G G A A G G A	SLITRIG DH015 ABHGAP24 CLUH SPECCI GPR129 GPRCSC ZPIXIA FANSHB CUIS MRCILI TFO LORI3 MRCILI	P. YING P. NAME P. NAME P. NAME P. NAME P. P	Missense, Mutation Missense, Mutation Missense, Mutation Missense, Mutation Missense, Mutation Silent Splice, Site Missense, Mutation Silent Missense, Mutation Missense, Mutation Missense, Mutation Missense, Mutation Silent Silent Missense, Mutation Missense, Mutation Silent Missense, Mutation Silent Missense, Mutation Missense, Mutation Silent Missense, Mutation Spile, Silent Missense, Mutation Spile, Silent Missense, Mutation Spile, Silent Missense, Mutation Spile, Silent Missense, Mutation Spile Silent Silent Missense, Mutation Spile Silent Silent Missense, Mutation Missense, Mutation Spile Silent Missense, Mutation Missense, Mutation Spile Silent Missense, Mutation Missense, Mutation Missense, Mutation Missense, Mutation Spile Silent Missense, Mutation Missense, Mu	98V	Q.55957447 Q.127991304 Q.18018018 Q.18018018 Q.151984615 Q.151984615 Q.151984615 Q.151984615 Q.151984615 Q.151984615 Q.151984615 Q.151985415 Q.1519855541 Q.15198555541 Q.1519855541 Q.1519855541 Q.1519855541 Q.1519855541 Q.1519855541 Q.1519855541 Q.1519855541 Q.15198555541 Q.1519855	PASS PASS PASS PASS PASS PASS PASS PASS
# #447	HICA HICA HICA HICA HICA HICA HICA HICA	ch+13 ch+4 ch+4 ch+4 ch+4 ch+17 ch+17 ch+17 ch+17 ch+17 ch+18 ch+6 ch+10 ch+2 ch+2 ch+2 ch+2 ch+2 ch+2 ch+2 ch+1 ch+1 ch+1 ch+1 ch+1 ch+1 ch+1 ch+1	85,093,28 80,093,28 80,014,58 80,014,58 20,014,58 20,014,58 20,014,58 20,014,58 20,014,58 20,014,58 20,014,58 20,014,58 21,756,018 43,188,75 1,789,174	65795139 65795139 65795139 65795139 65795139 65795135 65795135 65795135 65795135 65795135 65795137 657	T C C C C C C C C C C C C C C C C C C C	C A A C C T A A A A A A A A A A A A A A	SLITRIG DHOLIS ABHGAP24 CLUH SPECCI GPRIT9 GPRESC ZPIXXA FANSHB CLUS MRCILI TPO LONL3 H.188AP POLRZD MACGI ROYNE MSATDI GOLIMA LSPS COMMISS SCHOOL MSATDI GOLIMA LSPS SCHOOL MSATDI GOLIMA L	P. Y-9300 P. AVASC PANASC PANA	Missense, Mutation Missense, Mutation Missense, Mutation Missense, Mutation Silent Splice, Ste Missense, Mutation Silent Splice, Ste Missense, Mutation Missense, Mutation Silent Silent Silent Missense, Mutation Missense, Mutation Silent Missense, Mutation Misse	59V	0.155957447 0.127991304 0.18038018 0.18038018 0.15588615 0.15588615 0.15588615 0.125615094 0.12244898 0.120329556 0.223140496 0.12032956 0.223140496 0.1032987107 0.2 0.19987107 0.2 0.20117318 0.192307692 0.19987107 0.199	FMSS FMSS FMSS FMSS FMSS FMSS FMSS FMSS
# # # # # # # # # # # # # # # # # # #	HCA	dw13 dw42 dw47 dw47 dw47 dw47 dw47 dw47 dw47 dw47	85(93)28 85(93)28 85(93)28 85(93)26 85(93)26 85(93)26 2019372 2019372 36(90)21 72(465)16 77(517928 1275(93)84 43188575 17891740 1499905 74776576 1499905 14776576 1580(319) 1595(32)2 1595(32	85795139 24559129 24559129 24559129 24559129 24560129 245	T C C C C C C C C C C C C C C C C C C C	G A G G A G G A G G A G G A A A A A A A	SLITRIG DH015 ABHGAP24 CLUH SPECCI GPR129 GPRCSC ZPIXIA FANSHB CUIS MRCILI TFO LORI3 MRCILI	P. YINDC P. NAME P. NAME P. NAME P. NAME P. P	Missense, Mutation Missense, Mutation Missense, Mutation Missense, Mutation Missense, Mutation Silent Splice, Site Missense, Mutation Silent Missense, Mutation Missense, Mutation Missense, Mutation Missense, Mutation Silent Silent Missense, Mutation Missense, Mutation Silent Missense, Mutation Silent Missense, Mutation Missense, Mutation Silent Missense, Mutation Spile, Silent Missense, Mutation Spile, Silent Missense, Mutation Spile, Silent Missense, Mutation Spile, Silent Missense, Mutation Spile Silent Silent Missense, Mutation Spile Silent Silent Missense, Mutation Missense, Mutation Spile Silent Missense, Mutation Missense, Mutation Spile Silent Missense, Mutation Missense, Mutation Missense, Mutation Missense, Mutation Spile Silent Missense, Mutation Missense, Mu	98V	Q.55957447 Q.127991304 Q.18018018 Q.18018018 Q.151984615 Q.151984615 Q.151984615 Q.151984615 Q.151984615 Q.151984615 Q.151984615 Q.151985415 Q.1519855541 Q.15198555541 Q.1519855541 Q.1519855541 Q.1519855541 Q.1519855541 Q.1519855541 Q.1519855541 Q.1519855541 Q.15198555541 Q.1519855	PASS PASS PASS PASS PASS PASS PASS PASS
# # # # # # # # # # # # # # # # # # #	HCA	dw13 dw4 dw4 dw4 dw47 dw47 dw47 dw47 dw47 dw	85(93)28 85(93)28 859(14)58 859(14)58 2019372 2019372 2019372 36(909)17 72(465)16 77(517928 127590184 43188575 17891740 1499905 74776576 1499905 14776576 1580(819) 1595(824) 1595(85795139 85795139 24559129 85995015 15965010 20046019 201	T C C C C C C C C C C C C C C C C C C C	G A G G A G G A G G A G G A A A A A A	SLITRIG OHOLIS ABHGAP24 CUH SPECCI CUH SPECCI CUH SPECCI CUH SPECCI CPRIST GPRESC ZPIXA FANSHB CUIS MRCILI TYO LORI3 BEBRAP POLRZO MRCILI TYO LORI3 LEBRAP POLRZO MRCILI TYO MRCILI CUPTAL GREY BEBRAP RESC CONTIST CONTIST RESC MRCILI RES	P. Y-9300 P. AVASC PANASC PANA	Missense, Mutation Missense, Mutation Missense, Mutation Missense, Mutation Missense, Mutation Silent Splice, Sile Missense, Mutation Silent Missense, Mutation Silent Missense, Mutation Missense, Mutatio	98V	Q.25957447 Q.127991304 Q.18018018 Q.18018018 Q.15384615 Q.154871545 Q.154871545 Q.154871545 Q.126415004 Q.122446908 Q.122446908 Q.122446908 Q.12346908 Q.12346908 Q.12346908 Q.12352616 Q.12746908 Q.135884615 Q.135884615 Q.135884615 Q.135884615 Q.12765957 Q.135884615 Q.12765957 Q.135884615 Q.12765957 Q.1358747 Q.1358747 Q.1358747 Q.1358747 Q.1358747 Q.1358747 Q.1358747 Q.1358747 Q.1358747 Q.135875941 Q.135876574 Q.13587677	PASS PASS
# #447	HCA	ch+13 ch+4 ch+4 ch+4 ch+4 ch+17 ch+17 ch+17 ch+17 ch+17 ch+18 ch+18 ch+18 ch+18 ch+18 ch+18 ch+18 ch+19 ch+1	85,093,28 82455015 80916168 2959524 20149372 20149372 36490917 72436516 177637928 127569184 43188575 17891740 1499905 74775576 103067472 128608191 103067472 128608191 103067472 128608191 103067472 12808191 103067472 103067472 103067472 103067472 103067472 103067472 103067472 103067472 10306481 10306482	85795139 85795139 85995015 85995015 1266020 1206020 12	T C C C C C C C C C C C C C C C C C C C	G A G G A G G A G G A G G A A	SLITRIG DHOLIS ABHGAP24 CLUH SPECCI GPRIT9 GPRESC ZPIXXA FANSHB CLUS MRCILI TPO LONL3 H.188AP POLR2D MACGI RPHS2 ECH C199-dBI MSANTD1 GOLIMA LSPB-C2 NOTCH3 ZNESC CVPPI IRXS SLCSBAB CNOTCH3 LSPB-CCI RPMU2 MCCI RPMU3 MCCI	P. N. 1930 P. N. 1940 P. P. 1944	Missense, Mutation Missense, Mutation Missense, Mutation Missense, Mutation Silent Splice, Ste Missense, Mutation Silent Splice, Ste Missense, Mutation Missense, Mutation Silent Silent Missense, Mutation Missense, Mutation Silent Missense, Mutation Misse	59V	0.255957447 0.127991304 0.80018018 0.10018018 0.115984615 0.155984615 0.155984615 0.125615094 0.12244898 0.120180556 0.221440996 0.120180556 0.221404996 0.120180556 0.221404996 0.1015984615 0.115984615 0.115984615 0.115984615 0.115984615 0.115984615 0.115984615 0.115984615 0.115984615 0.115984615 0.115984615 0.115985611 0.11591566217 0.1159111111 0.199778477 0.1501809859 0.116111111111 0.199778477 0.1161111111 0.199778477 0.1161111111 0.199778479 0.1161111111 0.199778479 0.1161111111 0.199778479 0.11611111110 0.1161878810 0.1178681514 0.1178681514 0.1178681514 0.1178681514 0.0187879 0.11611118812 0.01878797 0.0108839393 0.117578605 0.115984615 0.115984615	FMSS
# # # # # # # # # # # # # # # # # # #	HCA	dw13 dw42 dw47 dw47 dw47 dw47 dw47 dw47 dw47 dw47	85(69)28 85(69)28 859(16)58 859(16)58 859(16)58 20149372 20149372 364690917 72446516 471673928 127590184 43188575 17891740 1499905 74776576 1499905 14776576 1596(28)51 1595(28)24 1595(28)24 1595(28)25	85795139 85995131 24559132 85995135 159652130 20046059 20146	T C C C C C C C C C C C C C C C C C C C	G A G G A G G A G G A G G A A A A A A A	SLITRIG DH015 ABHGAP24 CUH SPECT CUH SPECT CUH SPECT CUH SPECT COPICS CO	P. YING P. NAME P. NAME P. NAME P. NAME P. NAME P. P	Missense, Mutation Missense, Mutation Missense, Mutation Missense, Mutation Missense, Mutation Silent Splice, Site Missense, Mutation Silent Missense, Mutation Missense, Mutation Missense, Mutation Silent Silent Missense, Mutation Silent Missense, Mutation Silent Missense, Mutation Missense, Mutat	98V	Q.55957447 Q.127991304 Q.18018018 Q.18018018 Q.18018018 Q.151804615	PASS PASS
# #447	HCA	ch+13 ch+4 ch+4 ch+4 ch+27 ch+17 ch+17 ch+17 ch+17 ch+18 ch+18 ch+18 ch+18 ch+18 ch+18 ch+18 ch+18 ch+19 ch+	85,093,28 82455015 80916168 8290524 20149372 20149372 20149372 36409017 72436516 77637928 127569184 43188575 17801740 13905747 139068191 139067472 139068191 139067472 139067472 139068191 139067472 139068191 139068191 139069742 139068191 139069742 139069742 139069742 139069742 139069742 14	65795139 657	T C C C C C C C C C C C C C C C C C C C	C A A C C A A C C A A C C A A A A A A A	SLITRIG SHITRIG DIOLIS ABHGAP24 CLUH SPECCI GPRI179 GPRI279 GPRESC ZPISXA FANSHB CLUS MRCILI TPO LONL3 ILIBRAP POLR2D MACGI NPHS2 ECHI CSPORT MSANTDI GOLIMA LSPRAP MSANTDI GOLIMA LSPRAP FOLR2D MSANTDI GOLIMA LSPRAP FOLR2D MSANTDI GOLIMA LSPRAP FOLR2D MSANTDI GOLIMA LSPRAP FOLR2D MSANTDI GOLIMA LSPRAP LSPRAP LUFPA	P. NYSEC PARTY CONTROL OF THE	Missense, Mutation Missense, Mutation Missense, Mutation Missense, Mutation Silent Splice, Ste Missense, Mutation Silent Splice, Ste Missense, Mutation Missense, Mutation Missense, Mutation Missense, Mutation Silent Missense, Mutation Missense, Mutation Missense, Mutation Silent Missense, Mutation Missense, Muta	59V	0.255957447 0.127991304 0.80018018 0.10018018 0.115984615 0.155984615 0.155984615 0.125615094 0.12244898 0.120180556 0.2231404996 0.120180556 0.2231404996 0.120180556 0.2231404996 0.115984615 0.115984615 0.115984615 0.115984615 0.115984615 0.115984615 0.115984615 0.115984615 0.115984615 0.115984615 0.115984615 0.115984615 0.115985611 0.115985611 0.115985611 0.115985611 0.115985611 0.115985611 0.115985611 0.115985611 0.115985611 0.115985611 0.115985611 0.115985611 0.115985611 0.115985611 0.115985611 0.11598611	FMSS FMSS FMSS FMSS FMSS FMSS FMSS FMSS

March Marc													
Column						С				Silent			
March Col.							A			-			
Column							T						
March													
March													
March Marc	#835T	HCA	chr5	161322780	161895774	С	Т	GABRA1		Missense_Mutation	SNV	0,365853659	PASS
March 1975 1976													
ACC						-							
Part													
APP													
APP													
APP	#835T	HCA	chr1	45266767	44801095	G	T	PLK3	p.S126S		SNV	0,136363636	t_lod_fstar
APP 1997 1							Т						
March													
March						C							
APT						c							
APT													
APP	#873T		chr19	53456092	52952839	A	С		p.\$34\$		SNV	0,196721311	PASS
APP										2020			
Georgia													
March 190						C							
APT						G							
Prof. 190. 190. 1700000 170000 170000 170000 170000 170000 170000 1700000 1700000 1700000 1700000 170000 170000 170000 170000 170000 170000 170000 170000 1	#873T	нса	chr17	7125555	7222236	c	Т		p.A271V		SNV	0,184210526	PASS
APP		HCA			28906130				p.G438W	Missense_Mutation			
March													
Decomposition Color													
General Color													
Corp. Co. Co. 193860 193860 Co. T. Out. D. Out													
	#2729T	HCA	chr3	23932048	23890557	С	Т	UBE2E1	p.A178V	Missense_Mutation	SNV	0,129770992	PASS
Property	#2729T	HCA	chr3		132631366	A		ACAD11	p.N272K	Missense_Mutation	SNV		
Column						T			p.L328P				
Company Column						C							
## Control						G							
1977 50. 60.0 7													
	#2729T	HCA		75014848	74722507	G		CYP1A1	p.V197V	Silent	SNV	0,22459893	PASS
Degree Col.						-							
Design													
Control Column													
Description Color	#375T	HCA	chr1	226019594	225831893	G	С	EPHX1			SNV	0,293650794	
1977 Mo. 1962 1989733 1999134 5 5 1999134 5 1999134 5 5 1999134 5 1 5 1 5	#375T		chr1	236758942		G	A	HEATR1		Missense_Mutation	SNV	0,266666667	PASS
Part													
Part													
\$2577													
1977													
PROF. MCG	#375T	HCA	chr6	43006153	43038415	c	A	CUL7			SNV	0,285714286	PASS
#2977										Missense_Mutation			
##877		HCA	chr7	150707754	151010666	C	T	NOS3	n P9195	Missense Mutation	SNV	0,328358209	PASS
#2977			7.00	55 (60,000) 550 550	1000000000		0.00				1800000		
##FFT MCA							G	INTS10	p.N185S	Missense_Mutation			
#377	#375T	нса	chr9	15578911	15578913	G	т	INTS10 CCDC171	p.N1855 p.R81L	Missense_Mutation Missense_Mutation	SNV	0,27777778	PASS
## 1977 INCA 69-23 13180073 13180073 13180073 C FAMODIA PAGE MARCON PAGE MARCON PAGE PAG	#375T #375T	HCA HCA	chr9 chr9	15578911 125612078	15578913 122849799	G G	T C	INTS10 CCDC171 RC3H2	p.N1855 p.R81L p.P1135R	Missense_Mutation Missense_Mutation Missense_Mutation	SNV	0,277777778 0,303571429	PASS PASS
## 1977 HGA	#375T #375T #375T #375T	HCA HCA HCA	chr9 chr9 chr11	15578911 125612078 85722154 122817384	15578913 122849799 86011111 122946676	G G G	T C	INTS10 CCDC171 RC3H2 PICALM	p.N1855 p.R81L p.P1135R p.N228K	Missense_Mutation Missense_Mutation Missense_Mutation Missense_Mutation	SNV SNV SNV SNV	0,27777778 0,303571429 0,313253012	PASS PASS PASS
#377	#375T #375T #375T #375T #375T	HCA HCA HCA HCA	chr9 chr9 chr11 chr11 chr12	15578911 125612078 85722154 122817384 19282742	15578913 122849799 86011111 122946676 19129808	G G C	T C C T A	INTS10 CCDC171 RC3H2 PICALM C11orf63 PLEKHAS	p.N1855 p.R81L p.P1135R p.N228K p.Q605* p.A3A	Missense_Mutation Missense_Mutation Missense_Mutation Missense_Mutation Nonsense_Mutation Silent	SNV SNV SNV SNV	0,27777778 0,303571429 0,313253012 0,280991736 0,277777778	PASS PASS PASS PASS PASS
## 1977 HGA	#375T #375T #375T #375T #375T #375T	HCA HCA HCA HCA HCA	chr9 chr9 chr11 chr11 chr12 chr12	15578911 125612078 85722154 122817384 19282742 111800732	15578913 122849799 86011111 122946676 19129808 111362928	G G C G	T C C T A C C	INTS10 CCDC171 RC3H2 PICALM C11orf63 PLEKHAS FAM109A	p.N18SS p.R81L p.P113SR p.N228K p.Q60S* p.A3A p.A167G	Missense_Mutation Missense_Mutation Missense_Mutation Missense_Mutation Nonsense_Mutation Silent Missense_Mutation	SNV SNV SNV SNV SNV	0,27777778 0,303571429 0,313253012 0,280991736 0,277777778 0,28042328	PASS PASS PASS PASS PASS PASS PASS
## 1975	#375T #375T #375T #375T #375T #375T #375T	HCA HCA HCA HCA HCA HCA	chr9 chr9 chr11 chr11 chr12 chr12 chr12 chr13	15578911 125612078 85722154 122817384 19282742 111800732 22077064	15578913 122849799 86011111 122946676 19129808 111362928 21502925	G G C G G	T C C T A C C	INTS10 CCDC171 RC3H2 PICALM C11orf63 PLEKHAS FAM109A MICU2	p.N1855 p.R81L p.P1135R p.N228K p.Q605* p.A3A p.A167G NA	Missense_Mutation Missense_Mutation Missense_Mutation Missense_Mutation Missense_Mutation Silent Missense_Mutation Silent Missense_Mutation Splice_Site	SNV SNV SNV SNV SNV SNV	0,27777778 0,303571429 0,313253012 0,280991736 0,277777778 0,28042328 0,288135593	PASS PASS PASS PASS PASS PASS PASS PASS
## 1975	#375T #375T #375T #375T #375T #375T #375T #375T	HCA HCA HCA HCA HCA HCA HCA	chr9 chr9 chr11 chr11 chr12 chr12 chr12 chr13	15578911 125612078 85722154 122817384 19282742 111800732 22077064 77742575	15578913 122849799 86011111 122946676 19129808 111362928 21502925 77168440	G G G G G C	T	INTS10 CCDC171 RC3H2 PICALM C11orf63 PLEKHAS FAM109A MICU2 MYCBP2	p.N1855 p.R81L p.P1135R p.N228K p.Q605* p.A3A p.A167G NA p.V1996V	Missense_Mutation Missense_Mutation Missense_Mutation Missense_Mutation Nonsense_Mutation Silent Missense_Mutation Splice_Site Silent	SNV SNV SNV SNV SNV SNV SNV	0,27777778 0,303571429 0,313253012 0,280991736 0,277777778 0,28042328 0,288135593 0,292307692	PASS PASS PASS PASS PASS PASS PASS PASS
##5757 HCA dr-99 \$1886852 1867752 G A \$12985 pp. 2578 Monore phetron 9W 0.25 PASS ##5757 HCA dr-20 6486624 M05085 A T T \$1CLAS p. M353. Monore phetron 9W 0.244 PASS ##5757 HCA dr-20 6486624 M05085 A T T \$1CLAS p. M353. Monore phetron 9W 0.244 PASS ##5757 HCA dr-20 6486791 6535039 C A BREC p. PASS ##5757 HCA dr-20 6486791 6535039 C A BREC p. PASS ##5757 HCA dr-20 6486791 6535039 C A A BREC p. PASS ##5757 HCA dr-20 6486791 6535039 C A A BREC p. PASS ##5757 HCA dr-20 6486791 FASS ##5757 HCA dr-20 12884664 L2488791 FASS ##5757 HCA dr-20 12884664 FASS ##5757 HCA dr-20 12884664 FASS ##5757 HCA dr-20 12884664 FASS HCA dr-20 12884664 FA	#375T #375T #375T #375T #375T #375T #375T #375T #375T	HCA HCA HCA HCA HCA HCA HCA	chr9 chr9 chr11 chr11 chr12 chr12 chr13 chr13 chr14	15578911 125612078 85722154 122817384 19282742 111800732 22077064 77742575 33015139	15578913 122849799 86011111 122946676 19129808 111362928 21502925 77168440 32545933	G G G G C C C C	T C C T A C T T A A	INTS10 CCDC171 RC3H2 PICALM C11orf63 PLEKHAS FAM109A MICU2 MYCBP2 AKAP6	p.N1855 p.R811 p.P1135R p.N228K p.Q605* p.A3A p.A167G NA p.Y1996V p.S427*	Missense_Mutation Missense_Mutation Missense_Mutation Missense_Mutation Nonsense_Mutation Silent Missense_Mutation Splice_Site Silent Nonsense_Mutation	SNV SNV SNV SNV SNV SNV SNV SNV	0,27777778 0,303571429 0,313253012 0,280991736 0,277777778 0,28042328 0,288135593 0,292307692 0,295081967	PASS PASS PASS PASS PASS PASS PASS PASS
#3777	#375T #375T #375T #375T #375T #375T #375T #375T #375T #375T #375T	HCA HCA HCA HCA HCA HCA HCA HCA HCA	chr9 chr9 chr11 chr11 chr12 chr12 chr13 chr13 chr14 chr15 chr15	15578911 125612078 85722154 122817384 19282742 111800732 22077064 77742575 33015139 24921470 56032607	15578913 122849799 86011111 122946676 19129808 111362928 21502925 77168440 32545933 24676323 55740409	G G C C C G G T T	T C C T T A C C T T T A T T C C	INTS10 CCDC171 RC3H2 PICALM C11orf63 PLEKHAS FAM109A MICU2 MYCBP2 AKAP6 NPAP1 PRTG	p.N1855 p.R811 p.P1135R p.N228K p.N228K p.Q605* p.A32 p.A167G NA p.V1996V p.S427* p.W152C p.S124G	Missense_Mutation Missense_Mutation Missense_Mutation Missense_Mutation Nonsense_Mutation Silent Missense_Mutation Silent Silent Nonsense_Mutation Missense_Mutation Missense_Mutation Missense_Mutation Missense_Mutation	SNV	0,27777778 0,303571429 0,313253012 0,280991736 0,287777778 0,28042328 0,283135593 0,292307692 0,275081967 0,1772727273 0,263157895	PASS PASS PASS PASS PASS PASS PASS PASS
##575T HGA d-920 (\$8870T) 633839 C A A GORDADA pM39 (\$0.00000000000000000000000000000000000	#375T #375T #375T #375T #375T #375T #375T #375T #375T #375T #375T #375T #375T	HCA HCA HCA HCA HCA HCA HCA HCA HCA HCA	chr9 chr9 chr1 chr11 chr11 chr12 chr12 chr13 chr13 chr14 chr15 chr15 chr17	15578911 125612078 85722154 122817384 19282742 111800732 22077064 77742575 33015139 24921470 56032607 79663962	15578913 122849799 8601111 122946676 19129808 111362928 21502925 77168440 32545933 24676323 5574009 81696932	G G G G G G G G G G G G G G G G G G G	T C C T T A C C T T T A A T C C A A	INTS10 CCDC171 RC3H2 PICALM C11orf63 PLEKHAS FAM109A MICU2 MYCBP2 AKAP6 NPAP1 PRTG HGS	p.N1855 p.R811 p.P1135R p.N228K p.Q605* p.A34 p.A167G NA p.V1996V p.S427* p.W152C p.S124G p.G6065	Missense, Mutation Missense, Mutation Missense, Mutation Missense, Mutation Noniense, Mutation Silien Missense, Mutation Splice, Site Silien Nonsense, Mutation Missense, Mutation Missense, Mutation Missense, Mutation Missense, Mutation Missense, Mutation	SNV SNV SNV SNV SNV SNV SNV SNV SNV SNV	0,27777778 0,303571429 0,313253012 0,280991736 0,277777778 0,28042328 0,288135593 0,292307692 0,295081967 0,1727272727 0,263157895 0,178217822	PASS PASS PASS PASS PASS PASS PASS PASS
#3757	#375T #375T #375T #375T #375T #375T #375T #375T #375T #375T #375T #375T #375T #375T	HCA HCA HCA HCA HCA HCA HCA HCA HCA HCA	chr9 chr9 chr9 chr11 chr11 chr12 chr12 chr13 chr13 chr14 chr15 chr15 chr15 chr17 chr19	15578911 125612078 885722154 122817384 19282742 111800732 22077064 77742575 33015139 24921470 56032607 79663962 18186562	15578913 122849799 86011111 122946676 19129808 21502925 77168440 32545933 24676323 55740409 81696932 18075752	G G G G G G G G G G G G G G G G G G G	T C C T A A T C C A A A A	INTSIO CCOC171 RCSH2 PICALM C11orf63 FAM109A MICU2 MYCBP2 AKAP6 NPAP1 PRTG HGS IL12RB1	p.N1855 p.R81L p.P1135R p.N228K p.Q605* p.A3A p.A167G NA p.V1996V p.S427* p.W152C p.S1246 p.G6065 p.P2335	Missense, Mutation Missense, Mutation Missense, Mutation Missense, Mutation Missense, Mutation Nonsense, Mutation Silent Missense, Mutation Splice, Sife Silent Nonsense, Mutation Missense, Mutation	SNV	0,27777778 0,303571429 0,31325012 0,280991736 0,277777778 0,2804328 0,288435593 0,292307692 0,295081967 0,172727273 0,263157895 0,78217822 0,25	PASS PASS PASS PASS PASS PASS PASS PASS
#3975T HGA	#375T #375T #375T #375T #375T #375T #375T #375T #375T #375T #375T #375T #375T #375T #375T	нса нса нса нса нса нса нса нса нса нса	chr9 chr9 chr9 chr9 chr11 chr11 chr12 chr13 chr13 chr13 chr13 chr14 chr15 chr15 chr17 chr19 chr20	15578911 125612078 85722154 122817384 19282742 111800732 22077064 77742575 33015139 24921470 56032607 79663962 18186562 44664524	15578913 122849799 86011111 122946676 19129808 111362928 21502925 77158440 32545933 24676323 55740409 81696932 40075752	G G G C C C G G G G G G G G G G G G G G	T C C T T A A T T C C A A A T T	INTSIO CCDC171 RCH2 PICALM CC10-f63 PLEGHAS FAM109A MYCBP2 AKAP6 PRTG HGS EL12RB1 SC12AS	p.N1855 p.R81L p.P1315R p.N228K p.N228K p.Q665* p.A3A p.A1676 NA p.V1996V p.S427* p.W152C p.S1226 p.G6665 p.P2335 p.M353L	Missense, Mutation Missense, Mutation Missense, Mutation Missense, Mutation Missense, Mutation Noneme, Mutation Silent Missense, Mutation Spiles, Site Silent Missense, Mutation	\$W \$W \$W \$W \$W \$W \$W \$W \$W \$W	0,27777778 0,303571429 0,31325012 0,280991736 0,27777778 0,287777778 0,28235593 0,292307692 0,295081967 0,172727273 0,263157895 0,178217822 0,25	PASS PASS PASS PASS PASS PASS PASS PASS
#397F HGG CHX 13506977 131277879 C T 1 (05F1 p.#13840 Money, Mackinn 9W 0,07389542 PASS #4107 HGG Ch2 21544546 21478406 G A A HACA2 p.11671 Steet 9W 0,82738952 PASS #41107 HGG Ch2 21544546 22478406 G A A ABGA2 p.11671 Steet 9W 0,828181882 PASS #41107 HGG Ch4 112577382 13125400 G A A LAMAA p.AOV Money, Mackinn 9W 0,72738252 PASS #41107 HGG Ch4 112577382 13125400 G A A LAMAA p.AOV Money, Mackinn 9W 0,32355012 PASS #41107 HGG Ch4 112577382 13125400 G A A LAMAA p.AOV Money, Mackinn 9W 0,33355012 PASS #41107 HGG Ch4 112577382 13125400 G A A LAMAA p.AOV Money, Mackinn 9W 0,33355012 PASS #41107 HGG Ch4 112577482 13125400 G A A LAMAA p.AOV Money, Mackinn 9W 0,33355012 PASS #41107 HGG Ch4 112577482 13125400 HGG A A MINTON PASS #41107 HGG Ch4 112577482 13125400 HGG A A MINTON PASS #41107 HGG Ch4 112577482 1310112879 A G C AMNTON PASS #41107 HGG Ch4 112577482 1310112879 A G C AMNTON PASS #41107 HGG Ch4 112577482 HGG Ch4 1125774	#375T #375T #375T #375T #375T #375T #375T #375T #375T #375T #375T #375T #375T #375T #375T #375T	HCA	chr9 chr9 chr9 chr9 chr11 chr11 chr12 chr12 chr13 chr13 chr13 chr14 chr15 chr17 chr19 chr20 chr20 chr20	15578911 125612078 85722154 122817384 13282742 111800732 22077064 77742575 33015139 24921470 79663962 18185562 44664524 61867691	15578913 122849799 86011111 122946676 19179808 211502925 77168440 32545933 24676323 5570409 81596932 18075752 46035885 6336333	G G G G G G G G G G G G G G G G G G G	T C C C T A A C T A A A A A A A A A A A	INTSID CCDC171 RCSH2 PICALM CCLOFGS PLEDIAS FAMIDDA MICU2 MYCBP2 AXAP6 NPAP1 PRTG HGS EL12R81 SIC12AS BIRC7	p.N1855 p.R81L p.P135R p.N258R p.N258R p.0565* p.A3A p.A167G NA p.V1996V p.S427* p.W152C p.S1246 p.G6665 p.P2335 p.M1531 p.R81L	Missense, Mutation Missense, Mutation Missense, Mutation Missense, Mutation Missense, Mutation Missense, Mutation Silent Missense, Mutation Splice, Site Silent Missense, Mutation Missense, Missense, Mutation Missense, Miss	SW S	0,27777778 0,0057429 0,01325012 0,280991736 0,28091736 0,28042328 0,28833599 0,292307692 0,292307692 0,292307692 0,172727273 0,172727273 0,172727273 0,172727273 0,263157895 0,178217822 0,25	PASS PASS PASS PASS PASS PASS PASS PASS
##1107 HCA 0h2 17995999 177272777 G A TN p_A0050V Morres_Mariston 9V 0,271292855 PASS ##1107 HCA 0h2 118905767 13447279 G T ABCT1 p_11677 Select 9V 0,34129299 PASS ##1107 HCA 0h2 118905767 13447279 G T ABCT1 p_11677 Select 9V 0,34129299 PASS ##1107 HCA 0h2 118275782 I 112274280 G A A MATCH p_11677 Select 9V 0,34129299 PASS ##1107 HCA 0h2 0.71274782 112274280 G A A MATCH p_11677 Select 9V 0,311274282 PASS ##1107 HCA 0h2 0.71274282 G C C MARCH p_11677 Select 0.7127428 PASS ##1107 HCA 0h2 0.7127427 110112279 A G A MARCH p_11677 Select 0.7127428 G C C MARCH p_11677 Select 0.712742 PASS ##1107 HCA 0h2 0.7127427 110112279 A G G MARCH p_11677 Select 0.712742 PASS ##1107 HCA 0h2 0.7127427 110112279 A G G MARCH p_11677 Select 0.712742 PASS ##1107 HCA 0h2 0.7127427 110112279 A G G MARCH p_11677 Select 0.712742 PASS ##1107 HCA 0h2 0.7127427 110112279 A G G MARCH p_11677 Select 0.712742 PASS ##1107 HCA 0h2 0.7127427 110112279 A G G MARCH p_11677 Select 0.712742 PASS ##1107 HCA 0h2 0.7127427 110112279 A G G MARCH p_11677 Select 0.712742 PASS ##1107 HCA 0h2 0.7127427 Select 0.7127427 PASS ##1107 HCA 0h2 0.7127427 Select 0.7127427 PASS ##1107 HCA 0h2	# 2075T # 2075	HCA	chr9 chr9 chr9 chr9 chr9 chr11 chr12 chr12 chr12 chr13 chr14 chr15 chr15 chr15 chr17 chr19 chr20 chr20 chr20 chr22 chr22	15578911 125612078 85722154 122817384 13922742 111800732 22077064 77742575 30015139 24921470 56032607 79653962 18185562 44664524 44664524 61867691 24896797 38352784	15578913 122849799 86011111 122946676 19129808 11185/2025 77168440 2254933 52740409 18169093 18075752 4607333 55740409 18169093 18075752 46073385 6328319 2440829 37956777	G G G G G G G G G G G G G G G G G G G	T C C T T A A A A A A A A	INTSID CCDC171 RCD142 PICALM C11cr65 FLEGIAS FLEGIAS FMIDDA MICU2 MYCBP2 AKAP6 NAP1 PRTG HGS ILIZRB1 SLC12A5 BIRCT ADDRAZA POURZF	p.N1855 p.R81L p.P115R p.N128R p.N228R p.N258C p.A3A p.167G NA p.Y1996V p.S427 p.W152C p.S1246 p.G6665 p.P3385 p.M1531 p.F81L p.M1939 p.O9N	Missense, Mutation Missense, Mutation Missense, Mutation Missense, Mutation Nomense, Mutation Nomense, Mutation Spire, Silver Missense, Mutation Spire, Silver Stere Nomense, Mutation Missense, Missense, Missense	SW S	0,37777778 0,30357429 0,31353012 0,280991736 0,280913736 0,292307692 0,295081967 0,172727273 0,66137895 0,1721727273 0,66137895 0,1721727273 0,66137895 0,2503157895 0,246 0,255033557 0,246	PASS PASS PASS PASS PASS PASS PASS PASS
##107 H/G ch2 21548564 2247840 G A A RICA12 p.11677 Seriet Sev Q.88181812 PASS H#107 H/G ch3 18907075 13418797 G T AG73 p.11877 Seriet Sev Q.88181812 PASS H#107 H/G ch6 11257362 1122490 G A A LAMA4 p.AAV Miscense, Parkation Sev Q.84782939 PASS H#107 H/G ch6 11257362 1122490 G A A LAMA4 p.AAV Miscense, Parkation Sev Q.84782939 PASS H#107 H/G ch6 ch7 11275762 1122490 G A A LAMA4 p.AAV Miscense, Parkation Sev Q.84782930 PASS H#107 H/G ch7 11001879 A G C ANNOTON PARKATION Sev Q.84782935 PASS H#107 H/G ch7 11001879 A G C ANNOTON PARKATION Sev Q.84782935 PASS H#107 H/G ch7 11001879 A G C ANNOTON PARKATION Sev Q.84782935 PASS H#107 H/G ch7 11001879 A G C ANNOTON PARKATION Sev Q.84782935 PASS H#107 H/G ch7 11001879 A G C G SESTI D.A2786K Miscense, Parkation Sev Q.848445735 PASS H#107 H/G ch7 11001879 A G G C G SESTI D.A2786K Miscense, Parkation Sev Q.848445735 PASS H#107 H/G ch7 11001879 A G G C G SESTI D.A2786K Miscense, Parkation Sev Q.848445735 PASS H#107 H/G ch7 11001879 A G G C G G SESTI D.A2786K Miscense, Parkation Sev Q.848445735 PASS H#107 H/G ch7 11001879 A G G C G G G A LACTOR PARKATION Sev Q.84844573 PASS H#107 H/G ch7 11001879 A G G C G G C G G C G G C G G C G G C G G C G G C G	#375T #375T	HCA HCA HCA HCA HCA HCA HCA HCA HCA HCA	chr9 chr9 chr9 chr11 chr11 chr12 chr12 chr13 chr13 chr13 chr13 chr14 chr15 chr15 chr15 chr17 chr19 chr20 chr20 chr22 chr22 chr22 chr27 chr20 chr	15578911 126412078 125612078 125612078 125212154 12322742 111800732 22077064 77742575 33015139 24021470 56022607 79663962 18186562 44654524 61867691 24836797 38352784	15578913 122849799 86011111 122946676 19129808 111362928 21502925 77168440 32545933 24676323 55740409 81696932 4003885 63236333 24440829 37956777 71132434	G G G G G G G G G G G G G G G G G G G	T C C T T A A A A A A A A	INTSID CCDC173 RC3H2 PICALM C11cr68 PLEGHAS FAM109A MMCU2 AXAPE NPAT1 PPTG HS S1C12AS S1C12AS POURZF ADDRAZA POURZF MMCD12	p.N1855 p.881L p.P11358 p.N228K p.N228K p.N228K p.N228K p.G6665 p.A3A p.A1676 NA p.A1676 p.Y1996V p.S5427* p.W152C p.G6665 p.P2338 p.M1531 p.M1939 p.M1531 p.M1939 p.D98N p.T14377	Missense, Mutation Missense, Mutation Missense, Mutation Missense, Mutation Missense, Mutation Missense, Mutation Silent Missense, Mutation Silent Nomenne, Mutation Nomenne, Mutation Missense, Mutation M	98V 98V 98V 98V 98V 98V 98V 98V 98V 98V	0,27777778 0,313753012 0,318253012 0,280991736 0,28091736 0,28042328 0,28833599 0,292307692 0,295207692 0,3157272723 0,172727273 0,172727273 0,263157895 0,78217822 0,055 0,2223131475 0,255033557 0,27272773 0,255033557 0,27272773	PASS PASS PASS PASS PASS PASS PASS PASS
##1017 HCG ch/s 18590767 134187979 G T ABCTS p.01897 Mesone_Mutation SN 0,3429293 PASS ##1017 HCG ch/s dr 11257362 11225490 G A A MAPITO p.1616/W Mesone_Mutation SN 0,31253012 PASS ##1017 HCG ch/s 4271914 4,264771 G A A MAPITO p.1616/W Mesone_Mutation SN 0,31253012 PASS ##1017 HCG ch/s 0,3729318 G C A MAPITO p.1616/W Mesone_Mutation SN 0,31253012 PASS ##1017 HCG ch/s 0,47291 110123797 A G G RBM00 p.1236 Mesone_Mutation SN 0,31253012 PASS ##1017 HCG ch/s 0,4729 11012379 A G G RBM00 p.1236 Mesone_Mutation SN 0,2440782 PASS ##1017 HCG ch/s 0,472 11012379 A G G RBM00 p.1236 Mesone_Mutation SN 0,2440782 PASS ##1017 HCG ch/s 1 6172699 ch/s 0,55166 G A MAPITO A MAPITO PASS ##1017 HCG ch/s 1 6172699 ch/s 0,55166 G G A MAPITO A MAPITO PASS ##1017 HCG ch/s 1 6172699 ch/s 0,59518 C G G RST1 p.1236K Mesone_Mutation SN 0,223797823 PASS ##1017 HCG ch/s 1 6172699 ch/s 0,59518 C G G RST1 p.1236K Mesone_Mutation SN 0 2,23797823 PASS ##1017 HCG ch/s 1 25584307 5497823 G T T TSA1 p.1246 Mesone_Mutation SN 0 2,23797823 PASS ##1017 HCG ch/s 1 25584307 5497823 G T T TSA1 p.1246 Mesone_Mutation SN 0 2,03797823 PASS ##1017 HCG ch/s 1 25584307 5497823 G T T T G G CMPTAB p.1025K Mesone_Mutation SN 0 0,037973724 PASS ##1017 HCG ch/s 1 25584307 5497823 G T T T G G CMPTAB p.1025K Mesone_Mutation SN 0 0,037973744 PASS ##1017 HCG ch/s 1 25584307 75431340 C G G CPP1 p.123 Mesone_Mutation SN 0 0,037973744 PASS ##1017 HCG ch/s 1 25584307 75431340 C G G CPP1 p.123 Mesone_Mutation SN 0 0,037973744 PASS ##1017 HCG ch/s 1 25584307 75431340 C G G CPP1 p.123 Mesone_Mutation SN 0 0,037417344 PASS ##1017 HCG ch/s 1 25584307 75431340 C G C C C C C C C C C C C C C C C C C	# 2075T # 2075	HCA	chr9 chr9 chr9 chr11 chr12 chr12 chr12 chr13 chr13 chr13 chr13 chr13 chr13 chr13 chr15 chr15 chr15 chr15 chr15 chr17 chr19 chr20 chr	15578911 125612078 85722154 122817384 119282742 111800732 22077064 77743575 33015139 24921470 56012607 79663962 18185652 444645524 61867691 248216779 38352784 79552284 139068773	15578913 122846799 8601111 122946676 19129808 111362928 77168440 21502925 77168440 81596932 18075752 46075885 63236139 2440829 37956777 71112434 131274799	G G G G G G G G G G G G G G G G G G G	T C C C T T A A T T A A A T T T T	INTSID CCCC172 RC3H2 RC3H2 RC3H2 RC4HM PICALM C11-ort63 PLEONAS FAM1030A MRCU2 MYC8P2 ACAP6 NNPAP1 PRTG HGS B122861 S12285 SIRC7 ADDR-22A POURZF MWD12 IGSF1	p.N1855 p.8811 p.P11354 p.P1288 p.05657 p.A3A p.A1676 NA p.V1996V p.54277 p.W152C p.51246 p.65665 p.P2335 p.M1531 p.F811 p.M1531 p.F811 p.M1531 p.D99N p.T14377 p.R118840	Missense, Mutation Missense, Mutation Missense, Mutation Missense, Mutation Nomense, Mutation Nomense, Mutation Select Missense, Mutation Select Missense, Mutation M	50V 50V 50V 50V 50V 50V 50V 50V 50V 50V	0,27777778 0,28057429 0,31355012 0,380991736 0,277777778 0,28042328 0,293307692 0,295081967 0,172727273 0,65157895 0,752131475 0,248 0,258 0,25903557 0,272727273 0,46157895 0,2491358	PASS PASS PASS PASS PASS PASS PASS PASS
##1107 MCA clef 11257392 11254000 G A LAMA4 p.A2V Moseney, Mariston 9NV 0,31353012 PASS ##1107 MCA clef 42756144 42861771 G A RRF107 P.15164 MSeney, Mariston 9NV 0,31353012 PASS ##1107 MCA clef 0,3758256 37219328 G C ARR0100A pV1150, MSeney, Mariston 9NV 0,32467325 PASS ##1107 MCA clef 0,3758256 37219328 G C ARR0100A pV1150, MSeney, Mariston 9NV 0,23467535 PASS ##1107 MCA clef 0,3758256 S 51560 G A RRM0 0,1758465 PASS ##1107 MCA clef 11 535660 S 51560 G A BRM0 0,1758465 PASS ##1107 MCA clef 11 535660 S 51560 G A BRM0 0,1758465 PASS ##1107 MCA clef 11 535660 S 51560 G A BRM0 0,1758465 PASS ##1107 MCA clef 11 535660 S 51560 G A BRM0 0,1758465 PASS ##1107 MCA clef 12 53568307 S 5697623 G T T T59A1 p.R146 Silver 9NV 0,224607619 PASS ##1107 MCA clef 12 59893810 S 6697623 G T T T59A1 p.R146 Silver 9NV 0,22779797 PASS ##1107 MCA clef 12 59893810 S 6690508 G A B SCT1 p.R750C MSeney, Mariston 9NV 0,207707923 PASS ##1107 MCA clef 12 59893810 S 6697623 G T T T59A1 p.R146 Silver 9NV 0,207707923 PASS ##1107 MCA clef 12 59893810 S 6697623 G T T T59A1 p.R146 Silver 9NV 0,207707927 PASS ##1107 MCA clef 12 59893810 S 6697623 G T T T59A1 p.R146 Silver 9NV 0,207707927 PASS ##1107 MCA clef 12 5784747 75831349 C C G G GFF140 p.R102 MSeney, Mariston 9NV 0,30790478 PASS ##1107 MCA clef 12 7584747 75831349 C C G G GFF140 p.R102 MSeney, Mariston 9NV 0,30790478 PASS ##1107 MCA clef 12 59873786 S 585545 C GACTCCCACCA C C MAG01 p.R1422 MSeney, Mariston 9NV 0,303444276 PASS ##1107 MCA clef 12 508674 S 585645 S 585645 C C C MAG01 p.R1422 Silver 9NV 0,303444276 PASS ##1107 MCA clef 12 508674 S 585645 S 585645 C C C MAG01 p.R1422 Silver 9NV 0,303444276 PASS ##1107 MCA clef 12 508674 S 585645 S 5856	#375T #375T	HCA	chr9 chr9 chr9 chr9 chr11 chr11 chr12 chr12 chr13 chr13 chr13 chr13 chr13 chr14 chr15 chr15 chr17 chr19 chr20 chr20 chr20 chr22 chr20 chr2	15578911 12541278 85722154 122817384 122817384 122817384 11380732 11380732 11380732 124921470 1565962 1585962 14865424 4665424 4665424 1586797 38552784 15968777 38552784 15968777	15578013 122849799 86011111 122946676 13129866 131362928 2150925 77168440 32545933 24475323 4605885 6328539 2446029 37956777 2446029 37956777 71132434 131274799	G G G G G G G G G G G G G G G G G G G	T C C T T A A A A T T A A A A T T A A A A	INTSID CCDC177 RC3H2 PICALM C11crf63 PLEGHAS FAM109A MICU2 MYC8P2 AKAP6 H9AP1 H95 L12R81 SLC12A5 BIRC7 ADDRA2A MC012 IGSF1 TTN	p.NIESS p.RISL p.P11358 p.N228K p.Q1605* p.A3A p.A1676 NA p.V1996V p.S427* p.W152C p.S1246 p.G6065 p.P3335 p.M153L p.RISL p.M1939 p.M1931 p.RISL p.M1931 p.RISL p.M1931 p.RISL	Missense, Mutation Missense, Mutation Missense, Mutation Missense, Mutation Missense, Mutation Nonemer, Mutation Sier Missense, Mutation Missense, Mutation Sier Sier Sier Missense, Mutation	58V 58V 58V 58V 58V 58V 58V 58V 58V 58V	0,77777728 0,20091736 0,313253012 0,313253012 0,313253012 0,320991736 0,277777778 0,28042338 0,28213593 0,292307692 0,295681967 0,177272773 0,2613157895 0,178217822 0,25 0,2131475 0,248 0,255033557 0,272727273 0,27272727 0,27272727 0,27272727 0,272727273 0,2727272727 0,272727273 0,2727272727 0,27272727 0,27272727 0,27272727 0,27272727 0,27272727 0,27272727 0,27272727 0,2727 0,272727 0,272	PASS PASS PASS PASS PASS PASS PASS PASS
##1107 HGA dr30 \$73768756 \$73719328 G C ANDDOOR \$P\$1150, Mosconey, Mostation \$9N\$ 0,324675325 PASS ##1107 HGA dr31 \$132768757 \$100812879 A G RBMDO BT3264 Mosconey, Mostation \$9N\$ 0,234675257 PASS ##1107 HGA dr31 \$51560 S1560 G A BMDO BT3264 Mosconey, Mostation \$9N\$ 0,244047619 PASS ##1107 HGA dr31 \$51560 S1560 G A BMDO BT3264 Mosconey, Mostation \$9N\$ 0,224047619 PASS ##1107 HGA dr31 \$51560 S51560 G A BMDO BT3264 PASS ##1107 HGA dr31 \$55560 S51560 G A T \$15941 BALL STATE BALL STAT	# 2051 # 2051 # 2051 # 2053 #	HCA	chr9 chr9 chr9 chr11 chr11 chr12 chr12 chr13 chr13 chr13 chr13 chr13 chr13 chr14 chr15 chr15 chr15 chr17 chr19 chr20 chr	155789211 125612078 85722154 122817894 13982747 131800732 22077064 27743575 77743575 33051519 24921470 79653962 4604524 4604524 4604524 131805679 24836797 38352784 7355288 130408773 13953288	15578013 122840799 8001111 122946076 19129080 11185928 21502925 77168440 2255933 24676123 55740409 8169612 4003585 63236339 2440829 37956777 11712434 131224799 13728772 147278940	G G G G G G G G G G G G G G G G G G G	T C C T T A A A A A A A A A A A A A A A	INTSUD CCCC171 RCH2 RCH2 RCH2 RCHM C11erf63 PLECHA C11erf63 PLECHA FAM100A MYCU2 MYCBP2 AKAP6 RNAP1 PRTG HGS BLIZRB1 SLC1245 BRICT ADORAZA POLRZF MWD12 IGSF1 TTN ABCA12	p.N1855 p.8811 p.P.11358 p.N228K p.N228K p.05655 p.AMA p.A167G NA p.V1996V p.54277 p.W152C p.51246 p.65665 p.P2335 p.M1531 p.F811 p.M1938 p.D9N p.T43177 p.R1184Q p.A0068V p.16471	Missense, Mutation Missense, Mutation Missense, Mutation Missense, Mutation Noncerne, Mutation Noncerne, Mutation Select Missense, Mutation Select Missense, Mutation Silvert	50V 50V 50V 50V 50V 50V 50V 50V 50V 50V	0,27777778 0,280357429 0,31355012 0,380991736 0,280313593 0,292307692 0,2920313593 0,292037692 0,172727273 0,65157895 0,782131475 0,248 0,255033557 0,272727273 0,26157895 0,275131475 0,248 0,25903557 0,27727273 0,261578955 0,27727273 0,261578955 0,27727273 0,261578955 0,27727273 0,261578955 0,27727273 0,261578955 0,277297825 0,3771897825 0,3771897825 0,31818181812	PASS PASS PASS PASS PASS PASS PASS PASS
##110T HGA dr10 11237637 110912879 A G R8M300 p.T8284 Moseney, Mackston SW 0.2444657 PASS ##110T HGA dr11 535160 55160 G A URCCS p.R2091 MSeney, Mackston SW 0.24446719 PASS ##110T HGA dr11 0.1726900 15190518 C G G R5T1 p.N2966 MSeney, Mackston SW 0.242707923 PASS ##110T HGA dr11 0.1726900 15190518 C G G R5T1 p.N2966 MSeney, Mackston SW 0.222707923 PASS ##110T HGA dr12 SS88837 S5476323 G T T T55941 p.R14R Sket SW 0.022727927 PASS ##110T HGA dr12 SS88837 S5476323 G T T T55941 p.R14R Sket SW 0.022727927 PASS ##110T HGA dr12 SS88837 S5476323 G T T T55941 p.R14R Sket SW 0.022727927 PASS ##110T HGA dr12 SS8837 S547632 G T T T55941 p.R14R Sket SW 0.022727927 PASS ##110T HGA dr12 SS89331M S660058 G A SSCANA p.R120 MSeney, Mackston SW 0.022000712 PASS ##110T HGA dr12 SS57604 G T T MS12 p.R141T Sket SW 0.022707472 PASS ##110T HGA dr14 SS57604 G T T MS12 p.R141T Sket SW 0.022707472 PASS ##110T HGA dr14 SS577604 G T T MS12 p.R141T Sket SW 0.022707474 PASS ##110T HGA dr14 SS577604 G T T MS12 p.R141T Sket SW 0.023546474 PASS ##110T HGA dr14 SS577604 G T T MS12 p.R141T Sket SW 0.023546474 PASS ##110T HGA dr14 SS577604 G T MS12 p.R141T Sket SW 0.023546474 PASS ##110T HGA dr14 SS577604 G T MS12 p.R141T Sket SW 0.03546474 PASS ##110T HGA dr14 SS577604 G T MS12 p.R141T Sket SW 0.03546474 PASS ##110T HGA dr14 SS577604 G T MS12 p.R141T Sket SW 0.03546474 PASS ##110T HGA dr14 SS577604 G T MS12 p.R141T Sket SW 0.03546474 PASS ##110T HGA dr14 SS577604 G T MS12 p.R141T Sket SW 0.03546474 PASS ##110T HGA dr14 SS577604 G T MS12 p.R141T Sket SW 0.03546474 PASS ##110T HGA dr14 SS577604 G T MS12 p.R141T Sket SW 0.03546474 PASS ##110T HGA dr14 SS577604 G T MS12 p.R141T Sket SW 0.03546474 PASS ##110T HGA dr14 SS577604 G T MS12 p.R141T Sket SW 0.03546474 PASS ##110T HGA dr14 SS577604 G T MS12 p.R141T Sket SW 0.03546474 PASS ##110T HGA dr14 SS577604 G T MS12 p.R141T Sket SW 0.03546474 PASS ##110T HGA dr14 SS577604 G T MS12 p.R141T Sket SW 0.03546474 PASS ##110T HGA dr12 SS577604 G T MS12 PASS PASS PASS PASS PASS PASS PASS PAS	# 235T #	HCA	chr8 chr8 dr41 dr41 dr41 dr41 dr41 dr41 dr41 dr41	15578911 12561279 8572154 12281784 1982745 111800732 2207766 111800732 2207766 177343575 33035139 24921470 79663962 4665524 61867691 24867677 38832784 79532284 13966973 119593296 119593499 119593499 119593499 119593499 119593499	15578013 122849799 80011111 122946676 19129008 19129008 21502025 21502025 23502025 24676123 24676123 24676123 24676123 24005885 6326459 2440829 2440829 2440829 21122498 13122499 13122499 13122498 1312249 1312249 13122498 1312249 131224	G G G G G G G G G G G G G G G G G G G	T C C C C C C C C C C C C C C C C C C C	INTSID CCDC171 RCHQ RCHQ RCHQ PICALM C11orf63 FLEDIAS FAM100A MICU2 MYCBP2 AAAP6 RPAP1 PPTG HCS 8127881 S1C12A5 BIRC7 AD08A2A POUR3F MED12 IGSF1 TTN ABCG12	p.N1855 p.R81L p.P.1135R p.N228R p.N228R p.0665* p.A3AA p.A1676 NA p.V19960/ NA p.V19960 p.5427* p.W152C p.651246 p.66665 p.P.2335 p.M153L p.R61L p.M1938 p.099N p.T14377 p.R118440 p.A6068V p.116471 p.D1869 p.118647 p.D1869	Missense, Mutation Missense, Mutation Missense, Mutation Missense, Mutation Missense, Mutation Normerse, Mutation Splice, Splice Silent Missense, Mutation	58V	0_37777778 0_31937429 0_31937429 0_31937429 0_31937429 0_32937777778 0_27777778 0_27777778 0_27272773 0_2293270702 0_329307602	PASS PASS PASS PASS PASS PASS PASS PASS
##110T HGA drill 5151660 51560 G A LIRCG BRIZDH Moseney, Mastero NV 0,24407619 PASS ##110T HGA drill 5172690 5159518 C G G BST1 PASS ##110T HGA drill 5172690 5159518 C G G T T TSPAI DRILL NO. Moseney, Mastero NV 0,223772737 PASS ##110T HGA drill 5172690 5159518 C G T T TSPAI DRILL NO. Moseney, Mastero NV 0,223772737 PASS ##110T HGA drill 5172690 10176178 T G G GRPTAB PASS ##110T HGA drill 5172692 10176178 T G G GRPTAB PASS ##110T HGA drill 5172692 T PASS ##110T HGA drill 51	# #375T # #375T # #375T # #375T # #375T #3	HCA	chr9 chr9 chr9 chr9 chr11 chr11 chr11 chr12 chr12 chr13 chr13 chr13 chr13 chr14 chr15 chr15 chr15 chr15 chr15 chr15 chr17 chr19 chr20 chr2	15578911 15541078 85722154 85722154 122817384 12382742 111800732 22077064 77743575 33015139 24921470 7563962 13185562 44654524 46654524 46654524 131856791 24806797 24806797 138352784 139408779 1155328 1155328 1155328 1155328 1155328 1155328 1155328 1155328 1155328 1155328 1155328 1155328 11	15578013 122849799 86011111 122966676 13129808 1111862928 21509275 77168440 2254933 24676323 24676323 24676323 24676323 24676323 24676323 24676323 24676323 24676323 13075752 246035885 2446829 2767677 71132434 131274799 13127479 13127479 13127479 13127479 131274799 1312747747 1312747 1312747 1312747 1312747 1312747 1312747 1312747 1312747 1312747 1312747 1312747 131274 131274 131274 131274 131274 1	G G G G G G G G G G G G G G G G G G G	T C C C T T T A A A A T T A A A A A A A	INTSID CCCC171 RCH2 RCH2 PCALM CTLOrES PLEASE PLEAS	p.N1855 p.N811 p.P.1115A p.N228K p.N228K p.N228K p.N228K p.N228K p.N5655 p.AJA p.A1676 NA p.X15960 p.X1596 p.W1526 p.W1526 p.W1526 p.W1526 p.W1526 p.W1526 p.W1526 p.W1527 p.W1526 p.W	Missense, Mutation Missense, Mutation Missense, Mutation Missense, Mutation Missense, Mutation Nonemer, Mutation Nonemer, Mutation Silver Silver Silver Silver Silver Missense, Mutation	58V 58V 58V 58V 58V 58V 58V 58V 58V 58V	0,77777728 0,30357429 0,313253012 0,380912736 0,380912736 0,277777778 0,26042328 0,2777777778 0,26042328 0,295061967 0,172727273 0,260157895 0,272131475 0,260157895 0,272131475 0,260157895 0,272131475 0,260157895 0,272131475 0,260157895 0,272131475 0,272727273 0,260157895 0,372727273 0,26015895 0,372727273 0,26015895 0,372727273 0,381818182 0,37253825 0,342592593 0,342592593 0,342592593	PASS PASS PASS PASS PASS PASS PASS PASS
##110T HCA drill 6179690 5199018 C G G BST1 p.N296K Moseney, Mostation 9NV 0,22970923 PASS ##110T HCA drill 55588875 59797323 G T TISPAI p.R18K Sket 9NV 0,229709277 PASS ##110T HCA drill 5558875 59797323 G T TISPAI p.R18K Sket 9NV 0,2297097277 PASS ##110T HCA drill 5192595 107071178 T G G SCCANA p.V250 Moseney, Mostation 9NV 0,210907527 PASS ##110T HCA drill 5192595 107071178 T G G SCCANA p.V250 Moseney, Mostation 9NV 0,210907527 PASS ##110T HCA drill 5795754 T FAST3149 C G G GFP1 p.R2Q Moseney, Mostation 9NV 0,27970744 PASS ##110T HCA drill 5795747 57574345 5767004 G T M912 p.R121T Sket 9NV 0,303404276 PASS ##110T HCA drill 5795744 FASS ##110T HCA drill 579574 FASS ##110T HCA drill 5795744 FASS ##110T HCA drill 579574	# #375T # #375	HCA	chr8 chr8 dr41 dr41 dr41 dr41 dr41 dr41 dr41 dr41	15578911 125612078 8572154 122817884 1982745 1382745 111800732 2007064 277741575 3005139 24921470 79663962 4606522 4606522 4606523 4606523 138352784 79532284 13906773 139352784 13936773 139352784 13936773 139352784 13936773 139352784 13936773 139352784 13936773 139352784 13936773 139352784 13936773 139352784 13936773 139352784 13936773 139352784 13936773 139352784 13936773 139352784 13936773 1393	15578013 122849799 80011111 122946676 19129008 19129008 21520225 21520225 2352023 24676123 24676123 24676123 24676123 24005885 6326353 2440829 2440829 2440829 21122498 1132249 1132249 1132249 1132249 1132249 1132249 1132249 1132249 113224080 42861771 2712928	G G G G G G G G G G G G G G G G G G G	T C C C C C C C C C C C C C C C C C C C	INTSID CCCC171 RCH2 RCH2 RCH2 PICALM C11orf63 FLEIGHS FEEDHAS FAM100A MCU2 MYCBP2 ACAP6 RNAP1 PRTG HCS 8122R81 S1C12AS BIRC7 ADDRAZA POURZF MED12 ASCA12 ASC	p.N1855 p.N81L p.P.1135A p.N228K p.N228K p.N228K p.0565* p.A3AA p.A1676 NA p.V1996V p.5127* p.W152C p.G6065 p.P.2335 p.M153L p.G6065 p.P.2335 p.M153L p.F61L p.M1939 p.T61647 p.G0568V p.116471 p.D1869V p.116471 p.D1869V p.224V p.R161W p.P.224V p.R161W p.P.224V p.R161W p.V1150L	Missense, Mutation Missense, Mutation Missense, Mutation Missense, Mutation Missense, Mutation Normense, Mutation Normense, Mutation Splice, Splice Silent Missense, Mutation Missense, Mitation Missense,	58V	0,27777778 0,30574429 0,318251012 0,318251012 0,318251012 0,32891786 0,22804338 0,288433593 0,328433593 0,3282307692 0,3292307692 0,3292307692 0,3292307692 0,3292307692 0,3292307692 0,3292307692 0,3292307692 0,3292307692 0,329237693 0,329237693 0,3292372727273 0,32693158 0,37272727273 0,32693158 0,37272727273 0,32693158 0,37272727273 0,38181818182 0,34292959 0,3182551012 0,318253012 0,318253012 0,318253012 0,318253012 0,318253012	PASS PASS PASS PASS PASS PASS PASS PASS
##110T HGA dri22 59598867 5-9678623 G T T T59A1 p.1.148 Siete SN 0.227927277 PASS ##110T HGA dri22 5959886 98000058 G A SLC2AA p.17250 Missense, Mination SN 0.237927277 PASS ##110T HGA dri22 101254956 101761178 T G G GRPFAB p.810285 Missense, Mination SN 0.0120007722 PASS ##110T HGA dri22 101254956 101761178 T G G GRPFAB p.810285 Missense, Mination SN 0.0120007722 PASS ##110T HGA dri21 57574046 7574777 75383190 C G G G GPF1 p.120 Missense, Mination SN 0.030707744 PASS ##110T HGA dri21 57574046 55574700 G T T MISS p.12011 Six	#2557 #2557	HCA	chr9 chr9 chr9 chr9 chr9 chr9 chr11 chr11 chr11 chr12 chr12 chr13 chr13 chr13 chr13 chr13 chr13 chr15 chr15 chr15 chr15 chr15 chr15 chr15 chr15 chr16	15578921 15578921 8572154 8572154 15282742 15282744 1528274	1528919 1528919 1528979 1529197 152919	G G G G G G G G G G G G G G G G G G G	T C C C C C C C C C C C C C C C C C C C	INTSID CCCC171 RCH2 RCH2 PCALM C11orf63 P1E914S F1E914S FMA100A MCU2 MYCBP2 MYC	p.N1855 p.N811 p.P11158 p.N228E p.N228E p.05055 p.A3A p.1676 p.A1676 p.V1996V p.S1276 p.S124G	Missense, Mutation Missense, Mutation Missense, Mutation Missense, Mutation Missense, Mutation Nonemer, Mutation Nonemer, Mutation Silver Silver Silver Silver Silver Missense, Mutation Missense, Missense, Missense, Missense, Missense, Missense, Missense, Missense, Missense, Miss	58V	0,277777778 0,377777778 0,31375402 0,31375402 0,31875402 0,31875403 0,389317602 0,379017777738 0,389335593 0,38933593 0,38933593 0,38933593 0,38933593 0,38933593 0,2469313782 0,25 0,25 0,248 0,248 0,255 0,31873872 0,275 0,27613782 0,27613782 0,27613782 0,27613782 0,27613782 0,318738925 0,318738925 0,318738925 0,318738925 0,3187389474 0,3124673325	PASS PASS PASS PASS PASS PASS PASS PASS
##107 HCA	# 235T #	HCA	chr8 chr8 dr41 dr41 dr41 dr41 dr41 dr41 dr41 dr41	15578911 125612078 8572154 122817884 15982742 11800782 22077664 111800782 22077664 277743575 33035139 24921470 79663962 4466522 4186562 4186562 4186562 11876562 11876562 11876562 11876562 11876562 11876562 11876562 11876562 11876562 11876562 11876562 11876562 11876562 11876662 11876662 1187762 1187662 1187762 1187662 1187762 1187662 1187662 1187762 1187662 1187762 1187662 1187762 1187662 1187762 1187662 1187762 1187762 1187762 1187762 1187662 1187762	15578013 12289799 80011111 122946676 19129008 19129008 21502025 21502025 21502025 21502025 21502025 21502025 240013 24001	G G G G G G G G G G G G G G G G G G G	T C C C C C C C C C C C C C C C C C C C	INTSID CCCC171 RCH2 RCH2 RCH2 PICALM C11orf63 FLEIGHS FEEIGHS FAM100A MICU2 MYCBP2 AXAP6 RNAP1 PRTG HCS S1C12AS BIRC7 ADDRAZA POURTF TN ABCG12 ABCG3 ABCG12 ABCG3 ARNEJOO RBMA2A RNH170 ARNEJOO RBMA2O RBMA2O RBMA2O LERECG6	p.N1855 p.N81L p.P.1135A p.N228K p.N228K p.N228K p.0565* p.A3AA p.A1676 NA p.V1996V p.S1272 p.W152C p.G6065 p.P.2335 p.M153L p.G6065 p.P.2335 p.M153L p.R781L p.M1939 p.T06065 p.P.116477 p.D.1869V p.116477 p.D.1869V p.116471 p.D.1869V p.P.115407 p.P.1154	Missense, Mutation Missense, Mutation Missense, Mutation Missense, Mutation Missense, Mutation Normone, Mutation Normone, Mutation Splice, Splice Silent Missense, Mutation Missense, Missense, Missense, Missense, Missense, Missense, Missense, Missense, Missense	58V	0,77777778 0,30537429 0,313251012 0,313251012 0,313251012 0,32937777778 0,77777778 0,77777778 0,2727777778 0,282135109 0,329307602 0,32930	PASS PASS PASS PASS PASS PASS PASS PASS
##10T MAA	# 275T #	HEA	chr8 chr8 dr41 dr41 dr41 dr41 dr41 dr41 dr41 dr41	155789214 125612078 85722154 122817884 13982742 111800732 22077064 177343575 33035139 24921470 79663962 44665524 4666524 4666524 13805677 73835286 13805777 138352784 13905777 13953286 13756386 1375686 137568 13	15578013 12289799 80011111 122946676 19129008 19129008 21502025 21502025 21502025 21502025 21502025 246023	G G G G G G G G G G G G G G G G G G G	T C C C C C C C C C C C C C C C C C C C	INTSID CCCC171 RCH2 RCH2 RCH2 PICALM C11orf65 PLEDIAS FREIDAS FAMIDDA MUCU2 MYCBP2 AXAP6 RNAP1 PRTG HGS 8122881 S1C12AS BIRCT ADDRAZA POURZF MED12 ASCA12 ASCA13 ASCA12 ASCA13 ARRITO AR	p.N1855 p.881L p.P.1135R p.N228R p.N228R p.0565* p.A3AA p.A1676 NA p.V19960 NA p.V19960 p.5927* p.W152C p.66665 p.P.2335 p.M153L p.6761L p.M1939 p.7681L p.M1939 p.7681L p.M1939 p.7681L p.M1939 p.7681L p.M1939 p.7681L p.M1939 p.766680 p.716570 p.715677 p.D1897 p.71677 p.	Missense, Mutation Missense, Mutation Missense, Mutation Missense, Mutation Normone, Mutation Normone, Mutation Splice, Splice Silent Missense, Mutation	58V	0,27777778 0,31937429 0,31937429 0,31937429 0,31937429 0,32937777778 0,27777778 0,27777778 0,27272777 0,27272777 0,27272777 0,27272777 0,27272777 0,27272777 0,2727277 0,2727277 0,2727277 0,2727277 0,2727277 0,2727277 0,2727277 0,2727277 0,2727277 0,27272727 0,2727273 0,2727273 0,2727273 0,2727273 0,2727273 0,2727273 0,2727273 0,2727273 0,2727273 0,2727273 0,2727273 0,2727273 0,2727273 0,2727273 0,2727273 0,2727273 0,2727273 0,2727273 0,272727273 0,272727273 0,272727273 0,272727273 0,272727273 0,272727273 0,272727273 0,272727273 0,272727273 0,272727273 0,272727273 0,272727273 0,272727273 0,272727273 0,272727273 0,272727273 0,272727273 0,2727272727	PASS PASS PASS PASS PASS PASS PASS PASS
##110T HGA drift 55275486 5767706 G T M912 p.1731T Siete SN 0.335448276 PASS ##110T HGA drift 55215486 \$1555425 GATCCCCCCCA C GAG01 p.17902281 b.175706 b.17	#375T	HCA	chr9 chr9 chr9 chr9 chr9 chr9 chr11 chr11 chr12 chr12 chr12 chr13 chr13 chr13 chr13 chr13 chr15 chr15 chr15 chr15 chr15 chr15 chr15 chr16 chr17	15578911 15582748 8572154 152817884 15282742 111800732 22077064 17744575 33015139 24021470 56032607 7764595 24021470 56032607 79653962 18185562 44664524 61867691 24867677 38852784 130088773 1305284	15278913 13289799 86011111 122946676 19119808 19119808 111382928 21502925 27502925 27502925 27502925 27502925 27502925 27502925 27750292	G G G G G G G G G G G G G G G G G G G	C T T A A A A A T T A A A A C C G A A G G T T A A A A A T T A A A A T T T A A A A A T T T A A A A A T T T A A A A A T T T A A A A A T T T A A A A A T T T A A A A A T T T T A A A A A T T T T A A A A A T	INTSID CCCC171 RCH2 RCH2 RCH2 PCALM C11orf83 P1E9US FREGUS FMATIONA MCU2 MYCBP2 MYCBP2 HOAP1 PHTG HOS RLIZERS BIRC7 ADDRAZA POURZE MMCU2 IGSF1 TTN ABCA12 ABG73 LAMA4 RNF170 ABKRD30 ARKRD30A RRMSD30A RRMSD30A RRMSD30A RRMSD30 LRRCS6 BEST1 TESPA1	p.N1855 p.N811 p.P.11154 p.P.1228K p.N2228K p.06955 p.A3AA p.A1676 NA p.Y1996V NA p.Y1996V p.M1526 p.M1526 p.M1526 p.M1528 p.M1528 p.M1528 p.M1528 p.M1528 p.M1528 p.M1528 p.M1528 p.M1528 p.M1538 p.M	Missense, Mutation Missense, Mutation Missense, Mutation Missense, Mutation Nonense, Mutation Nonense, Mutation Nonense, Mutation Silve Silve Silve Silve Silve Silve Missense, Mutation	58V	0,277777778 0,31375492 0,31375492 0,31375492 0,31375492 0,319391760 0,277777778 0,2737777778 0,283335593 0,389335993 0,389335993 0,389335993 0,389335993 0,389335993 0,31932318475 0,248 0,256 0,256 0,2762727273 0,26157895 0,2762727273 0,26157895 0,2762792793 0,315789474 0,32467325 0,315789474 0,31267325 0,315789474 0,31267325 0,315789474 0,31267325 0,315789474 0,2267325 0,315789474 0,2267325 0,315789474 0,2267325 0,2167326760 0,2167676923 0,2167676923	PASS PASS PASS PASS PASS PASS PASS PASS
## # ## # ## # # # # # # # # # # # #	# 275T #	HEA	chr8 chr8 dr41 dr41 dr41 dr41 dr41 dr41 dr41 dr41	15578911 125612078 8572154 122817884 15982742 111800732 22077664 111800732 22077664 277743575 33035139 24021470 79663962 4606528 4606528 4606528 4606528 13806507 73805286 13806773 13805773 13805775 1380575 138	15578013 122899799 80011111 122946676 19129008 19129008 21502025 21502025 21502025 21502025 21502025 246023	G G G G G G G G G G G G G G G G G G G	T C C C C C C C C C C C C C C C C C C C	INTSID CCCC171 RCH2 RCH2 RCH2 PICALM C11orf63 FLEIGHS FEEDHS FAMIDDA MUCU2 MYCBP2 ACAP6 RNAP1 PRTG HCS E122R81 S1C12AS BIRCT ADDRAZA ADDRAZA ADRAZA ADRAZA ADRAZA ADRAZA ADRAZA ADRAZA ADRAZA RNE170 ADRAZA BRAZO LERGGG BEST1 TESPA1 S1C22A3 SCRPTAB	p.N1855 p.N81L p.P.1135A p.N228R p.N228R p.N228R p.0565* p.A3AA p.A1676 NA p.V1996V p.M152C p.S1246 p.G6665 p.P.2335 p.M153L p.G6665 p.P.2335 p.M153L p.R761L p.M1939 p.T0676 p.R161W p.R16477 p.D189V p.R16477 p.D189V p.R16470 p.R26W p.R164W p.R164	Missense, Mutation Missense, Mutation Missense, Mutation Missense, Mutation Normense, Mutation Normense, Mutation Normense, Mutation Splice, Splice Silent Missense, Mutation Missense, Mitation Missense, Mitation Missense, Mitation Missense, Mitation Missense,	58V	0,27777778 0,319357429 0,319357429 0,319357429 0,319357429 0,32930792 0,329309792 0,32930792 0,3	PASS PASS PASS PASS PASS PASS PASS PASS
B110T	#375T	HCA	chr9 chr9 chr9 chr9 chr9 chr9 chr11 chr11 chr12 chr12 chr13 chr13 chr13 chr13 chr13 chr15 chr15 chr15 chr15 chr15 chr16	15578911 1578911 1578911 1578911 1578911 1578911 1578911 15787184 15782742	15578913 122849799 86011111 122946676 191128008 191128008 191128008 19128040 191280 191280 191280 191280 191280	G G G G G G G G G G G G G G G G G G G	C T T A A A A A T T A A A A C C G A A G G T T A A A A C C G G A A G C C C C C C C C C	INTSID CCCC171 RCH2 RCH2 RCH2 PCALM C11orf83 P1E9US FMA1DDA MUU2 MYGBP2 MYGBP2 MYGBP3 MA2AP6	p.N1855 p.N811 p.P.11158 p.N228K p.N228K p.N228K p.N228K p.N228K p.N328 p.N457C NA p.V1996V NA p.V1996V p.M152C p.G6065 p.M153K p.M15X p.M153K	Missense, Mutation Missense, Mutation Missense, Mutation Missense, Mutation Missense, Mutation Nonense, Mutation Nonense, Mutation Select Silect Missense, Mutation	58V	0,277777778 0,31375402 0,31375402 0,31375402 0,31375402 0,319037602 0,39037602 0,39037602 0,39037602 0,39037602 0,39037602 0,39037602 0,39037602 0,39037602 0,3157893 0,246 0,248 0,256 0,3157893 0,27693936 0,27693936 0,3169542 0,316789474 0,32673235 0,316789474 0,32673235 0,315789474 0,3267325 0,315789474 0,3267325 0,315789474 0,3267325 0,315789474 0,3267325 0,315789474 0,3267325 0,315789474 0,3267325 0,315789474 0,3267325 0,315789474 0,3267325 0,315789474 0,3267325 0,315789474 0,3267325 0,315789474 0,3267325 0,315789474 0,3267325 0,315789474 0,3267325 0,315789474 0,3267325 0,315789474 0,3267325 0,315789474 0,3267325 0,3267325 0,3267325 0,3267325 0,3267325 0,	PASS PASS PASS PASS PASS PASS PASS PASS
B4110T HCA	# 275T #	HEA	chr8 chr8 dr41 dr41 dr41 dr41 dr41 dr41 dr41 dr41	15578911 125612078 8572154 122817884 15982742 111800782 22077664 111800782 22077664 277743575 33035139 24021470 79663962 4606528 4606528 4606528 4606528 13806507 73805286 13806773 13905286 13905707 11257582 47716914 137508256 11257687 5572680 1572687 157	15578013 122890799 80011111 122946674 19179008 19179008 2152922 21529225 21529225 25702025 257025 2	G G G G G G G G G G G G G G G G G G G	T C C C C C C C C C C C C C C C C C C C	INTSID CCCC171 RCH2 RCH2 RCH2 PICALM C11orf65 FLEIGHS FLEIGHS FAMIDDA MUCU2 MYCBP2 AAAP6 RNAP1 PRTG HGS 8122881 S1C12A5 BIRCT ADDRA2A POURZF MED12 ABC12 ABC12 ABC12 ABC12 ABC12 ABC13 ABC12 ABC13 ABC12 ABC13 ABC	p.N1855 p.N81L p.P.1135A p.N228R p.N228R p.N228R p.0565* p.A3AA p.A1676 NA p.V1996V p.M152C p.S1246 p.G6665 p.P.2335 p.M153L p.G6665 p.P.2335 p.M153L p.R661L p.M1939 p.T161W p.A0068V p.116647 p.D189V p.116647 p.D189V p.116670 p.P.224V p.R161W p.N266R p.P.1150A p.R769H p.N296K p.R162W p.V1150C p.R162W p.R161W p.V1150C p.R162W	Missense, Mutation Missense, Mutation Missense, Mutation Missense, Mutation Normone, Mutation Normone, Mutation Normone, Mutation Splice, Splice Silent Missense, Mutation	58V	0,27777778 0,319357429 0,319357429 0,319357429 0,319357429 0,32903796 0,32903796 0,32903796 0,32903796 0,32903796 0,32903796 0,32903796 0,32903796 0,32903796 0,32903797 0,32903797 0,329037 0,32903797 0,329037 0,339037 0	PASS PASS PASS PASS PASS PASS PASS PASS
Billion	# 275T #	HEA	chr8 chr8 dr41 dr41 dr41 dr41 dr41 dr41 dr41 dr41	15578911 125612798 8572154 122817884 1982742 112807864 1982742 22077864 22077864 24071479 24071479 24071479 24071479 24081479 240	15578013 122890799 80011111 122846674 19178068 19178089 215780292 21502925 21502925 21502925 21502925 21502925 21502925 21502925 21502925 2160292 21607512 2	G G G G G G G G G G G G G G G G G G G	C T T T A A A A T T A A A A T T A A A A	INTSID CCCC171 RCH2 RCH2 RCH2 PICALM C11orf65 PLEDIAS FAMIDDA MUU2 MYCBP2 AAAP6 NPAP1 PPTG HGS E122R81 S1C12AS BIRC7 ADDRA2A POURZF MED12 ABC12 ABC12 ABC13 ABC12 ABC13	p.N1855 p.N81L p.P.1135A p.N228K p.N228K p.N228K p.N228K p.M35A p.A1676 NA p.V1996V NA p.V1996V p.S1272 p.W152C p.G6065 p.P3335 p.M153L p.G6065 p.P3335 p.M153L p.R61L p.M1939 p.T0606V p.T1437T p.D186V p.A0068V p.T1437T p.T144T p.	Missense, Mutation Missense, Mutation Missense, Mutation Missense, Mutation Normense, Mutation Normense, Mutation Normense, Mutation Normense, Mutation Splice, Splice Silent Missense, Mutation Missense, Mitation Missense, Mutation Missense, Mutation Missense, Mutation Missense, Mitation Missense,	58V	0,77777778 0,305374429 0,313251012 0,313251012 0,313251012 0,328037672 0,338037672 0,338037672 0,338037672 0,338037672 0,338037672 0,338037672 0,338037672 0,338037672 0,338037672 0,338037672 0,338037672 0,338037672 0,338037672 0,338037672 0,338037672 0,338037672 0,338037672 0,338037672 0,3380377544	PASS PASS PASS PASS PASS PASS PASS PASS
B1110T	#275T	HCA	chr9 chr9 chr9 chr9 chr9 chr9 chr9 chr9	15578911 15578911 15578911 15578911 157812798 1572154 15722742 15722742 15722742 15722742 15722742 15722742 15722742 15722742 15722742 15722742 15722742 1572274275 1572274275 1572274275	15578913 13289799 86011111 122946676 19129068 19129068 1912908	G G G G G G G G G G G G G G G G G G G	C T T T A A A A T T A A A A T T A A A A	INTSID CCCC171 RCH2 RCH2 RCH2 RCH2 RCH3 RCH2 RCH3 RCH3 RESUS RESUS RM100A MM012 MM013 MM01	p.N1855 p.N811 p.P11158 p.N228E p.N228E p.N228E p.06055 p.A3A p.A1676 NA p.V1996V NA p.V1996V p.M1526 p.M1526 p.M1526 p.M1528 p.M1528 p.M1528 p.M1528 p.M1528 p.M1528 p.M1528 p.M1528 p.M1528 p.M1538	Missense, Mutation Missense, Mutation Missense, Mutation Missense, Mutation Nonense, Mutation Nonense, Mutation Nonense, Mutation Silver Silver Silver Missense, Mutation Missense, Muta	58N	0,277777778 0,377777778 0,310757429 0,310574429 0,310574429 0,310574429 0,310574429 0,310574429 0,310574429 0,310574429 0,31057427273 0,41057427273 0,41057427273 0,41057427273 0,41057427273 0,41057427273 0,41057427273 0,41057427273 0,41057427273 0,41057427273 0,41057427273 0,41057427273 0,41057427273 0,41057427473 0,41057427473 0,41057427473 0,41057427473 0,41057427473 0,410574274747 0,41057427474 0,41057427474 0,41057427474 0,41057427474 0,410574274 0,41057	PASS PASS PASS PASS PASS PASS PASS PASS
BR110T HGA	# 275T #	HEA	chr8 chr8 dr41 dr41 dr41 dr41 dr41 dr41 dr41 dr41	15578911 12541278 8572154 12281784 13982742 2007064 111800732 2207064 2407054 24021479 240214	15578013 12289799 80011111 12284676 1912806 1912806 2152925 2152925 2152925 255933 2545933 2545933 2545933 2545933 2545933 25459 25459 2545	G G G G G G G G G G G G G G G G G G G	T C C C C C C C C C C C C C C C C C C C	INTSID CCCC171 RCH2 RCH2 RCH2 PICALM C11orf65 PLEDIAS FREIDAS	p.N1855 p.N81L p.P.1135A p.N228R p.N228R p.N228R p.G6665 p.A3AA p.A1676 NA p.V1996V p.M152C p.G6665 p.F233S p.M153L p.G6665 p.F233S p.M153L p.G6665 p.F233S p.M153L p.G6665 p.F233S p.M153L p.F681L p.M1939 p.T6667 p.R161W p.A6066V p.R16647 p.R165W	Missense, Mutation Missense, Mutation Missense, Mutation Missense, Mutation Normone, Mutation Normone, Mutation Normone, Mutation Splice, Splice Silent Missense, Mutation Missense, Mitation Missense, Mitation Missense, Mitation Missense, Mitation Missense, Mit	58V	0,77777778 0,305374429 0,319251429 0,319251429 0,319251429 0,319251429 0,3292307692	PASS PASS PASS PASS PASS PASS PASS PASS
BILIDT	#275T	HCA	chr9 chr9 chr9 chr9 chr9 chr9 chr9 chr9	15578911 1578911 1578911 1578911 1578911 1578911 1578911 157871584 1572154 157	15578913 12289799 86011111 122946676 19129008 1912908 191290	G G G G G G G G G G G G G G G G G G G	C T T T A A A A T T A A A A T T A A A C C C C	INTSID CCCC171 RCH2 RCH2 RCH2 RCH2 RCH3 RCH2 RCH3 RCH3 RFEGWS FMM100A MM012 MYGBP2 MYGBP2 MYGBP3 MAAPA NAPA NAPA NAPA NAPA NAPA NAPA NAP	p.N1855 p.N811 p.P.1158 p.N228E p.N228E p.N228E p.05055 p.A3A p.A1676 NA p.V1996V NA p.V1996V p.M152C p.G6065 p.F2335 p.M1531 p.M1532 p.M1531 p.M1532 p.M1531 p.M1532 p.M1531 p.M1532 p.M1532 p.M1533	Missense, Mutation Missense, Mutation Missense, Mutation Missense, Mutation Nonense, Mutation Nonense, Mutation Nonense, Mutation Silver Silver Silver Silver Missense, Mutation Missens	\$80	0,277777778 0,310774797 0,31075429 0,3105742	PASS PASS PASS PASS PASS PASS PASS PASS
B1110T HCA	# 275T #	HEA	chr8 chr8 dr41 dr41 dr41 dr41 dr41 dr41 dr41 dr41	15578911 12541278 8572154 12281784 13281784 13282742 2007064 111800792 22007064 17783575 33055139 24021470 54023407 24054767 2405797 2	15578013 12289799 86011111 12284676 1912806 1912806 2152925 2152925 2152925 2756840 2555933 24676123 2576409 81569032 4407525 4407525 4407525 4407525 10075352 4407525 10075352 10075352 1107535	G G G G G G G G G G G G G G G G G G G	T C C C C C A A A A A A A A A A A A A A	INTSID CCCC171 RCH2 RCH2 RCH2 PCALM C11orf65 PLEDIAS FREIDAS FAMIDOA MCU2 MYCBP2 AAAP6 RNAP1 PTG HGS E122R81 S1C12AS BIRCT ADORAZA ADORAZA ADORAZA ADORAZA ADORAZA ADORAZA RNE170 ABCA12	p.N1855 p.N81L p.P.1135A p.N228R p.N228R p.N228R p.N228R p.N228R p.N228R p.N228R p.N228R p.N34A p.N1996V NA p.V1996V NA p.V1996V p.N152C p.G6065 p.P.233S p.M153L p.G6065 p.P.233S p.M153L p.R61L p.M1939 p.R161W p.A0068V p.R16477 p.D189V p.R16474 p.R165W p.R16474 p.R165W p.R16474 p.R165W	Missense, Mutation Missense, Mutation Missense, Mutation Missense, Mutation Normense, Mutation Normense, Mutation Normense, Mutation Splice, Splice Silent Missense, Mutation Missense, Mitation Missense, Mitation Missense, Mitation Missense, Mitation Missense,	58V	0,77777778 0,303574429 0,313251012 0,313251012 0,313251012 0,313251012 0,32337692 0,3237692 0,	PASS PASS PASS PASS PASS PASS PASS PASS
FSSIT HGA	#275T	HCA	chr9 chr9 chr9 chr9 chr9 chr9 chr9 chr9	15578911 1578911 1578911 1578911 1578911 1578911 1578911 15787158 1572154 1572	15578913 122849799 86011111 122946676 19129008 1912908 1912	G G G G G G G G G G G G G G G G G G G	C T T T A A A A T T A A A A T T A A A A	INTSID CCCC171 RCH2 RCH2 RCH2 RCH2 RCH3 RCH2 RCH3 RCH3 RCH3 RCH3 RCH3 RCH3 RCH3 RCH3	p.N1855 p.N811 p.P11158 p.N228K p.N228K p.N228K p.N228K p.N228K p.N228K p.N228K p.N228K p.N238K p.N238K p.N1996V NA p.V1996V p.N1996V p.N1996V p.N1996V p.N1996V p.N1996V p.N1996V p.N1996V p.N1998V p.N1	Missense, Mutation Missense, Mutation Missense, Mutation Missense, Mutation Nonense, Mutation Nonense, Mutation Nonense, Mutation Select Silent Missense, Mutation Mi	\$80	0,277777778 0,319251429 0,319251429 0,319251429 0,319251429 0,319251429 0,319251429 0,329217692 0,329217692 0,329217692 0,3292137692 0,3292137692 0,3292137692 0,3292137692 0,3292137692 0,3292137475 0,248 0,25503957 0,272727273 0,31925925 0,31	PASS PASS PASS PASS PASS PASS PASS PASS
F531T HGA	#275T	HCA	chr9 chr9 chr9 chr9 chr9 chr9 chr9 chr9	15578911 1578911 1578911 1578911 1578911 1578911 1578911 15787158 1572154 1572154 1572154 1572154 1572154 1572154 1572154 1572154 1572154 1572154 1572155 1572156 1572157 1572156 1572156 1572156 1572156 1572156 1572156 1572156 1572157 1572156 1572156 1572156 1572157 1572156 1572156 1572156 1572157 1572156 1572157 1572156 1572157 1572156 1572157 1572156 1572157 1572156 1572157 1572156 1572157 1572156 1572157 1572156 1572157 1572156 1572157 1572	15578913 15289799 80011111 122946676 19129008 111262928 111262928 11529295 111262928 11529295 12559295 12559295 12559295 12559295 12559295 12559295 12676123	G G G G G G G G G G G G G G G G G G G	C T T T A A A A T T T A A A A T T T A A A C G G A G G T T T T A A A A T T T A A A A	INTSID CCCC171 RCH2 RCH2 RCH2 RCH2 RCH3 RCH2 RCH3 RCH3 RCH3 RCH3 RCH3 RCH3 RCH3 RCH3	p.N1855 p.N811 p.P1158 p.N228K p.N228K p.N228K p.N228K p.N228K p.N228K p.N228K p.N238K p.N238K p.N239K p.N1996V	Missense, Mutation Missense, Mutation Missense, Mutation Missense, Mutation Nonense, Mutation Nonense, Mutation Nonense, Mutation Select Silent Missense, Mutation	\$80	0,277777778 0,310757429 0,310757429 0,310757429 0,310757429 0,310757429 0,310757429 0,310757429 0,32076727273 0,32076727273 0,32076727273 0,32076727273 0,32076727273 0,32076727273 0,32076727273 0,32076727273 0,32076727273 0,32076727273 0,32076727273 0,32076727273 0,32076727273 0,32076727273 0,32076727273 0,32076727273 0,32076727273 0,32076727273 0,32076727273 0,32076727273 0,32076727273 0,32076727273 0,32076727273 0,3207672727273 0,32076727273 0,32076727273 0,32076727273 0,32076727273 0,32076727273 0,32076727273 0,32076727273 0,32076727273 0,3207672727273 0,32076727273 0,32076727273 0,32076727273 0,32076727273 0,32076727273 0,32076727273 0,32076727273 0,32076727273 0,3207672727	PASS PASS PASS PASS PASS PASS PASS PASS
F538T	# 275T #	HEA	chr8 chr8 dr41 dr41 dr41 dr41 dr41 dr41 dr41 dr41	15578911 12541278 8572154 12921784 19922742 2207766 111800792 2207766 17783575 33055139 24051470 56032607 79863952 44664521 4666521 4666521 4666521 18186652 4666521 18186652 1818652 18186652 18186652 18186652 18186652 18186652 18186652 181865	15578013 12289799 80011111 12284676 1912808 1912808 2152928 2152928 2152928 2152928 2554593 2545033 2545033 2545033 2545033 2545033 2545033 2545033 2545033 2545033 2545033 2545033 2545033 254503 254	G G G G C C C G G G G G G G G G G G G G	T C C C C C C C C C C C C C C C C C C C	INTSID CCDC171 RCHQ RCHQ RCHQ RCHQ RCHQ RCHQ RCHQ RCHQ	p.N1855 p.N811 p.P11354 p.N228E p.N228E p.05655 p.A3AA p.A1676 NA p.V19960 NA p.V19960 p.51272 p.W152C p.51246 p.65665 p.P2335 p.M1531 p.67611 p.M1939 p.714377 p.114377 p.114377 p.114377 p.114374 p.11617 p.	Missense, Mutation Missense, Mutation Missense, Mutation Missense, Mutation Normone, Mutation Normone, Mutation Splice, Splice Silent Missense, Mutation Missense, Mu	\$8V \$8V	0,77777778 0,303574429 0,313251012 0,313251012 0,313251012 0,313251012 0,32337692 0,3237692 0,3337692 0,	PASS PASS PASS PASS PASS PASS PASS PASS
#533T HCA chrk 1307286469 106327922 GA G AIMP1 p.1516 frame_SMP_Dol DEL 0,184724099 PASS	#275T	HCA	chr9 chr9 chr9 chr9 chr9 chr9 chr9 chr9	15578921 15578921 15578921 15578921 15578921 1578921 1578921 1578921 1578921 1578921 1578921 1578921 1578921 1578921 1578921 1578921 1578921 1578921 1578921 1578922 157892	15578913 15289799 152916676 15129099 152916676 15129099 152916676 15129099	G G G G G G G G G G G G G G G G G G G	C T T T A A A A T T A A A A T T A A A A	INTSID CCCC171 RCH2 RCH2 RCH2 RCH2 RCH3 RCH2 RCH3 RCH2 RCH3 RCH3 RCH3 RCH3 RCH3 RCH3 RCH3 RCH3	p.N1855 p.N811 p.P11158 p.N228K p.N228K p.N228K p.N228K p.N228K p.N228K p.N228K p.N228K p.N238K p.N238K p.N1996V p.N1996	Missense, Mutation Missense, Mutation Missense, Mutation Missense, Mutation Nonense, Mutation Nonense, Mutation Nonense, Mutation Select Silent Missense, Mutation	\$80	0,277777778 0,313251012 0,318251012 0,31825102 0,31825102 0,3183135593 0,3283135593 0,3283135593 0,3283135593 0,3283135593 0,318313593 0,318313593 0,318313593 0,318313593 0,318313593 0,318313593 0,318313159 0,318313169 0,318313169 0,318313169 0,318313169	PASS PASS PASS PASS PASS PASS PASS PASS
FSSIT HCA	#375T	HEA	chr8 chr8 dr41 dr41 dr41 dr41 dr41 dr41 dr41 dr41	15578911 12541278 8572154 12281784 1982742 1982742 1982743 1982742 111800792 2207764 17783575 33055139 24021470 5402307 7766552 44664524 4666524 4666524 1188652 4686797 12885797 17852284 1890977 17852284 1890977 17852284 1890977 17852284 1785284 1785284 1785284 1785	15578013 12289799 80011111 12284676 1912808 1912808 2152928 2152928 2152928 2152928 2554593 2545033 2545033 2545033 2545033 2545033 2545033 2545033 2545033 2545033 2545033 2545033 2545033 254503 254	G G G G G G G G G G G G G G G G G G G	T C C C C A A A A A A A A A A A A A A A	INTS10 CCCC172 RCH2 RCH2 RCH2 RCH2 RCH2 RCH2 RCH3 RCH2 RCH3 RCH2 RCH3 RCH2 RCH3 RCH3 RCH2 RCH3 RCH3 RCH3 RCH3 RCH3 RCH3 RCH3 RCH3	p.N1855 p.N811 p.P11354 p.N228E p.N228E p.N228E p.N228E p.N228E p.N228E p.N228E p.N258E p.N33A p.A1676 NA p.Y1996V p.S3272 p.W152C p.S3235 p.M1531 p.G6665 p.P2335 p.M1531 p.R6665 p.P2335 p.M1531 p.R6665 p.P2335 p.M1531 p.R66665 p.P2335 p.M1531 p.R66665 p.P3355 p.M1531 p.R66665 p.P3355 p.M1531 p.R7137 p.R11840 p.A0068V p.R1161W p.R1163C p.R1028C p.R103W p.Y11500 p.R10285 p.R104W	Missense, Mutation Missense, Mutation Missense, Mutation Missense, Mutation Normense, Mutation Normense, Mutation Normense, Mutation Splice, Steel Silent Missense, Mutation Missense, M	\$8V \$8V	0,77777778 0,303574429 0,313251012 0,313251012 0,313251012 0,313251012 0,32337692 0,3237692 0,3237692 0,3237692 0,3237692 0,3237692 0,3237692 0,3237692 0,3237692 0,3237692 0,3237692 0,3237692 0,3237692 0,3237692 0,3237692 0,3237692 0,3237692 0,3237692 0,3237692 0,333759474 0,33375774 0,3337577777776 0,33375777777777777777777777777777777777	PASS PASS PASS PASS PASS PASS PASS PASS
F531T HCA	#275T	HCA	chr9 chr9 chr9 chr9 chr9 chr9 chr9 chr9	15578921-1 15578921-1 15578921-1 15578921-1 15578921-1 152782-1 152782-1 15282-14 15	15578913 122849799 86011111 122946676 19129008 1912908 1912	G G G G G G G G G G G G G G G G G G G	C T T T A A A A A A A A A A A A A A A A	INTSID CCCC171 RCH2 RCH2 RCH2 RCH2 RCH3 RCH2 RCH3 RCH2 RFAMIDOA MCU2 MYCBP2 AAAP6 NRAF1 NRAF1 RS LC2AS RCH2 RCH2 RCH2 RCH2 RCH3 RCH2 RCH3 RCH2 RCH3 RCH3 RCH3 RCH3 RCH3 RCH3 RCH3 RCH3	p.N1855 p.N811 p.P1158 p.N228E p.N228E p.N228E p.N228E p.N228E p.N228E p.N228E p.N228E p.N238E p.N239E p.N338 p.N1538	Missense, Mutation Missense, Mutation Missense, Mutation Missense, Mutation Nonense, Mutation Nonense, Mutation Nonense, Mutation Select Silent Missense, Mutation	\$80	0,277777778 0,318751429 0,318751429 0,318751429 0,318751429 0,318751429 0,318751429 0,318751429 0,328731429 0,328731429 0,32873157692 0,32873157692 0,32873157692 0,32873157692 0,32873157692 0,32873157692 0,32873157692 0,32873157692 0,32873157692 0,32873157692 0,32873157692 0,32873157692 0,32873157692 0,318789474 0,32874578325 0,318789474 0,32874578325 0,318789474 0,32874578325 0,318789474 0,32874578325 0,318789474 0,32874578325 0,318789474 0,32874578325 0,318789474 0,32874578325 0,318789474 0,32874578325 0,318789474 0,32874578325 0,318789474 0,32874578325 0,318789474 0,32874578325 0,318789474 0,32874578325 0,3187884656 0,3187887817 0,328745788886666 0,03878813117 0,31878833117 0,31878833117 0,3187833117 0,3187833117 0,3187833117 0,3187833117 0,3187833117 0,3187833117 0,3187833117 0,3187833117 0,3187833117 0,3187833117 0,3187833117	PASS PASS PASS PASS PASS PASS PASS PASS
F538T HCA	# 275T #	HEA	chr8 chr8 dr41 dr41 dr41 dr41 dr41 dr41 dr41 dr41	15578911 12541278 8572154 122817884 1982742 1982742 1982742 111800792 22077664 17783575 33055139 24021470 54023207 1188562 1486521 44664524 4664524 4664524 1188562 14886797 14882284 14886797 14882284 14782284 14782	15578013 12289799 86011111 12284676 1912806 1912806 1912806 2152922 2152922 2152922 2152922 2152922 24676123 2576009 81569032 4607612 24676123 2576009 81569032 4607512 4607512 4607512 4607512 4607512 1007512 1107512 1107512 11072800 1112249 11072800 1112249 11072800 1112249 11072800 1112249 11072800 1112249 11072800 1112249 11072800 1112249 11072800 1112249 11072800 1112249 11072812 1107281	G G G G C C C G G G G G G G G G G G G G	T C C C C C C C C C C C C C C C C C C C	INTSID CCCC172 RCH2 RCH2 RCH2 RCH2 RCH2 RCH3 RCH2 RCH3 RCH2 RCH3 RCH2 RCH3 RCH3 RCH3 RCH3 RCH3 RCH3 RCH3 RCH3	p.N1855 p.N81L p.P.1135A p.N228R p.N228R p.N228R p.N228R p.N228R p.N5655 p.A3AA p.A1676 NA p.V1996V NA p.V1996V p.S1272 p.W152C p.S1246 p.G6665 p.P.2335 p.M153L p.R61L p.M1939 p.T61L p.M1939 p.M19315 p.M1939 p.M19315	Missense, Mutation Missense, Mutation Missense, Mutation Missense, Mutation Normone, Mutation Normone, Mutation Normone, Mutation Splice, Silver Silver Missense, Mutation Missense, Mitation Missense, Mitation Missense, Mitation Missense, Mitation Missense, Mit	SNV	0,77777778 0,303574429 0,313251012 0,313251012 0,313251012 0,313251012 0,32337692 0,33337692 0,3333	PASS PASS PASS PASS PASS PASS PASS PASS
F531T HGA	# 275T #	HEA	chr8 chr8 dr41 dr41 dr41 dr41 dr41 dr41 dr41 dr41	155789211 15541278 8572154 1572154 1572154 1572154 1572154 1572154 1572154 1572154 1572154 1572154 1572154 1572155 157215 1	15578013 12289799 86011111 12284676 191280678 191280678 191280678 191280678 23502925 23502925 24502925 24502925 24502925 24502925 24502925 24502925 24502925 24502925 24502925 2450292	G G G G G C C C G G G G G G G G G G G G	T C C C C C C C C C C C C C C C C C C C	INTSID CCCC172 RCH2 RCH2 RCH2 RCH2 RCH2 RCH2 RCH3 RCH2 RCH3 RCH2 RCH3 RCH2 RCH3 RCH3 RCH3 RCH3 RCH3 RCH3 RCH3 RCH3	p.N1855 p.N81L p.P11354 p.N228R p.N228R p.N228R p.N228R p.N228R p.N228R p.N258 p.A3AA p.A1676 NA p.V1996V p.A3AA p.A1676 NA p.V1996V p.S1227 p.W152C p.S1246 p.G6665 p.P233S p.M153L p.R61L p.M1939 p.R0668V p.R161W p.A0668V p.R16477 p.D189V p.R161W p.R16477 p.R1844 p.R0668V p.R16477 p.R161W p.R16477 p.R161W p.R16477 p.R161W p.R16477 p.R161W p.R16477 p.R161W p.R16477 p.R161W p.R16477 p.R16477 p.R16477 p.R16477 p.R16477 p.R16477 p.R16477 p.R16470 p.R16477 p.R16477 p.R16477 p.R16477 p.R16470 p.R16477 p.R16470 p.R164	Missense, Mutation Missense, Mutation Missense, Mutation Missense, Mutation Normense, Mutation Normense, Mutation Normense, Mutation Normense, Mutation Splice, Silver Silver Missense, Mutation Missense, Mitation Missense, Mutation Missense, Mutation Missense, Mitation Missense,	\$8V \$8V	0,27777778 0,31925102 0,319251429 0,319251429 0,319251429 0,319251429 0,329237692 0,32937692 0,33933333	PASS PASS PASS PASS PASS PASS PASS PASS
F538T HCA Chr9 104317117 101554855 G T RNF20 p.A721S Missene, Mutation SNV 0,178571429 PASS #6538T HCA Chr11 55335630 S5386134 G T 084A15 p.G68V Missene, Mutation SNV 0,18809524 PASS #6538T HCA Chr15 33175516 3148313 G T OTUDA p.A921E Missene, Mutation SNV 0,158839333 PASS #6538T HCA Chr15 99672706 9912501 C A SYRM p.Q1380K Missene, Mutation SNV 0,14 Clustered events	#275T	HGA	chr9 chr9 chr9 chr9 chr9 chr9 chr9 chr9	15578911 15578911 15578911 15578911 15578911 15781784 15782742 1578274 15782742 1578274 157827	15578913 12289799 86011111 122946676 19129008 1912908 19129	G G G G G G G G G G G G G G G G G G G	C T T T A A A A T T A A A C C G A G G T T T A A A A A A A A A A A A A	INTSID CCCC171 RCH2 RCH2 RCH2 RCH2 RCH3 RCH2 RCH3 RCH2 RCH3 RCH3 RCH2 RCH3 RCH3 RCH3 RCH3 RCH3 RCH3 RCH3 RCH3	p.N1855 p.N811 p.P1158 p.N228C p.05055 p.A3A p.A1676 NA p.V1996V P.M152C p.G6065 p.P233S p.M153L p.F811 p.M153L p.F811 p.M153C p.M	Missense, Mutation Missense, Mutation Missense, Mutation Missense, Mutation Missense, Mutation Nonense, Mutation Nonense, Mutation Silver Silver Silver Silver Missense, Mutation	\$80	0,277777778 0,277777778 0,3182917459 0,3182917469 0,3182917469 0,3182917469 0,3182917469 0,278277273 0,2782174728 0,2881335593 0,3881335593 0,388135593 0,37829327273 0,255 0,27821727273 0,255 0,27821727273 0,255 0,27821727273 0,255 0,27821727273 0,27821727273 0,27821727273 0,27821727273 0,27821727273 0,27821727273 0,27821727273 0,27821727273 0,27821727273 0,27821727273 0,27821727273 0,27821727273 0,3782172727 0,378217272 0,3782172 0,378217272 0,3	PASS PASS PASS PASS PASS PASS PASS PASS
F538T HCA	# 275T #	HEA	chr8 chr8 dr41 dr41 dr41 dr41 dr41 dr41 dr41 dr41	15578911 12541278 8572154 122817884 1982742 2007054 111800722 2207054 111800722 2207054 111800722 2207054 11180572 24021479 56032697 79569952 18186552 44664521 18186552 181865552 18186552 1818	15578013 12289799 86011111 12284676 191280678 191280678 191280678 191280678 23502925 23502925 24502925 24502925 24502925 24502925 24502925 24502925 24502925 24502925 24502925 2450292	G G G G G G G G G G G G G G G G G G G	T C C C A A A A A A A A A A A A A A A A	INTSID CCCC172 RCH2 RCH2 RCH2 RCH2 RCH2 RCH3 RCH2 RCH3 RCH2 RCH3 RCH2 RCH3 RCH3 RCH3 RCH3 RCH3 RCH3 RCH3 RCH3	p.N1855 p.N81L p.P1135A p.N228R p.N228R p.N228R p.N228R p.N228R p.N228R p.N228R p.N228R p.N34A p.N1996V NA p.V1996V NA p.V1996V p.S1272 p.W152C p.S1246 p.G6665 p.P2335 p.M153L p.R61L p.M1939 p.R0668V p.P3335 p.N153L p.R61L p.M1939 p.D09N p.T1437T p.D189V p.R1161W p.A0068V p.R16477 p.D189V p.R161W p.N296K p.R161W p.V250C p.R102W p.R1161W p.V250C p.R102B p.R1069C p.R1028C p.R1069C	Missense, Mutation Missense, Mutation Missense, Mutation Missense, Mutation Normone, Mutation Normone, Mutation Normone, Mutation Splice, Silver Silver Silver Missense, Mutation Missen	58V	0,27777778 0,310251429 0,310251429 0,310251429 0,310251429 0,310251429 0,310251429 0,310251429 0,320270777778 0,3207777778 0,3207777778 0,3207707778 0,3207707778 0,32077077778 0,320770777778 0,320770777778 0,320770777778 0,320770777777 0,320770777777 0,32077077777 0,32077077777 0,3207707777 0,320770777 0,320770777 0,320770777 0,320770777 0,320770777 0,320770777 0,32077077 0,320770777 0,3207707 0,320770	PASS PASS PASS PASS PASS PASS PASS PASS
#533T HCA chr15 31775516 31483313 G T OTUD7A p.A921E Missener_Mutation SW 0,15833333 PASS #538T HCA chr15 99672706 99132501 C A SYMM p.Q1380K Missener_Mutation SW 0,14 clustered_events	# # # # # # # # # # # # # # # # # # #	HCA	chr9 chr9 chr9 chr9 chr9 chr9 chr9 chr9	15578911 15578911 15578911 15578911 15578911 15781	15578913 12289799 80011111 122946676 19129008 19129008 19129008 19129008 19129008 2456933 24676123 25764009 18169093 18075752 4003585 63236139 18075752 4003585 63236139 18075752 18169093 18174799 18169093 18174799 18169093 18169093 18174799 18169093 18169093 18174799 18169093 181690 181690 181690 181690 181690 181690 181690 181690 181690 181690 181690 181690 181690 1816	G G G G G G G G G G G G G G G G G G G	C C C C C C C C C C C C C C C C C C C	INTSID CCCC171 RCH2 RCH2 RCH2 RCH2 RCH2 RCH3 RCH2 RCH3 RCH2 RCH3 RCH2 RCH3 RCH3 RCH3 RCH3 RCH3 RCH3 RCH3 RCH3	p.N1855 p.N811 p.P.1158 p.N228C p.05055 p.A3A p.A1676 NA p.V19960 NA p.V19960 NA p.V19960 p.S227 p.W152C p.G6055 p.P.2335 p.M1531 p.F811 p.M1531 p.F811 p.M1532 p.M1531 p.F811 p.M1531 p.F811 p.M1532 p.M1531 p.R1617 p.R16477 p.R16477 p.R16477 p.R16477 p.R16477 p.R16477 p.R16477 p.R16477 p.R16477 p.R16590 p.R16500 p.R16677 p.R1677 p.R1678 p.R1687	Missense, Mutation Missense, Mutation Missense, Mutation Missense, Mutation Missense, Mutation Nonense, Mutation Nonense, Mutation Sieler Sieler Sieler Sieler Sieler Missense, Mutation	\$80	0,277777778 0,3107777778 0,3107777778 0,3107777778 0,3107777778 0,3107777778 0,3107777778 0,3107777778 0,3107777778 0,3107777778 0,3107777778 0,3107777778 0,3107777778 0,31077777778 0,31077777778 0,31077777778 0,31077777778 0,31077777777 0,31077777777 0,3107777777 0,3107777777 0,3107777777 0,3107777777 0,310777777 0,310777777 0,31077777 0,31077777 0,31077777 0,3107777 0,3107777 0,3107777 0,3107777 0,310777 0,310777 0,310777 0,310777 0,310777 0,310777 0,310777 0,310777 0,310777 0,310777 0,310777 0,310777 0,310777 0,310777 0,3107 0,3107 0,3107 0,3107 0,3107 0,3107 0,3107 0,3107 0,3107 0,3107 0,3107 0,3107 0,3107 0,31	PASS PASS PASS PASS PASS PASS PASS PASS
	# 275T #	HEA	chris	15578911 12541278 8572154 12921784 19922742 2007054 111800792 2207054 111800792 24021479 56032607 1895595 1485652 1485	15578013 12289799 80011111 122946676 19129008 19129008 111367028 21502925 21502925 27506400 32556933 24670123 55740409 3556933 46035365 4784071 11012479 110	G G G G G C C C G G G G G G G G G G G G	T C C C C A A A A A A A A A A A A A A A	INTSID CCCC172 RCH2 RCH2 RCH2 RCH2 RCH2 RCH2 RCH3 RCH2 RCH3 RCH2 RCH3 RCH2 RCH3 RCH3 RCH2 RCH3 RCH3 RCH3 RCH3 RCH3 RCH3 RCH3 RCH3	p.N1855 p.N81L p.P1135A p.N228R p.N228R p.N228R p.N228R p.N228R p.N228R p.N228R p.N228R p.N250P p.A3A p.A1676 NA p.Y1996V p.S1272 p.W152C p.S1246 p.G6665 p.P2335 p.M153L p.R611 p.M1939 p.R06685 p.P3335 p.M153L p.R611 p.M1939 p.R0688V p.R161W p.A0688V p.R16477 p.R1844Q p.A0688V p.R16477 p.R161W p.R16477 p.R161W p.R16477 p.R161W p.R16477 p.R161W p.R16477 p.R161W p.R16477 p.R16477 p.R16477 p.R16479	Missense, Mutation Missense, Mutation Missense, Mutation Missense, Mutation Normone, Mutation Normone, Mutation Normone, Mutation Splice, Silver Silver Missense, Mutation Missense, Mut	58V	0,27777778 0,31037429 0,310374429 0,310374429 0,310374429 0,310374429 0,310374429 0,310374429 0,32037602 0,33037602 0,330377602 0,3303777777777777777777777777777777777	PASS PASS PASS PASS PASS PASS PASS PASS
## P533T HCA chr15 99672716 99132511 G C SYNM p.51383T Missense_Mutation SNV 0,139303483 clustered_events	#275T	HCA	chr9 chr9 chr9 chr9 chr9 chr9 chr9 chr9	15578911 15578911 15578911 15578911 15578911 15578911 1578911	15578913 12289799 80011111 122946676 19129008 19129008 19129008 19129008 19129008 2456933 24676123 2576903 18075752 4003585 63236139 18075752 4003585 63236139 18075752 18075752 18169032 18174799 18169032 18174799 18169032 18174799 1817479	G G G G G G G G G G G G G G G G G G G	C T T T A A A A A A A A A A A A A A A A	INTSID CCCC171 RCH2 RCH2 RCH2 RCH2 RCH3 RCH2 RCH3 RCH3 RCH2 RCH3 RCH3 RCH3 RCH3 RCH3 RCH3 RCH3 RCH3	p.N1855 p.N811 p.P.1158 p.N828E p.N228E p.05055 p.A3A p.A1676 NA p.V19960 NA p.V19960 NA p.V19960 p.S227 p.W152C p.G6055 p.P.2335 p.M1531 p.F821 p.M1531 p.F821 p.M1532 p.M1531 p.F821 p.M1531 p.F821 p.M1532 p.M1531 p.F821 p.M1532 p.M1532 p.M1532 p.M1532 p.M1533 p.M15333 p.M1533 p.M15333 p.M1	Missense, Mutation Missense, Mutation Missense, Mutation Missense, Mutation Missense, Mutation Nonense, Mutation Nonense, Mutation Silver Silver Silver Missense, Mutation	\$80	0,277777778 0,277777778 0,318751429	PASS PASS PASS PASS PASS PASS PASS PASS
	# # # # # # # # # # # # # # # # # # #	HCA	chr9 chr9 chr9 chr9 chr9 chr9 chr9 chr9	15578921 15578921 15578921 15578921 15578921 1578921 1578921 1578921 1578921 1578921 1578921 1578921 1578921 1578921 1578921 1578921 1578921 1578921 1578921 1578921 1578921 1578921 1578921 1578922 1578922 1578922 1578922 1578922 1578922 1578922 1578922 1578922 1578922 1578922 1578922 157892 1578	15578913 12289799 86011111 122946676 19129008 1912908 1912	G G G G G G G G G G G G G G G G G G G	C T T T T T T T T T T T T T T T T T T T	INTSID CCCC171 RCH2 RCH2 RCH2 RCH2 RCH3 RCH2 RCH3 RCH3 RCH3 RCH3 RCH3 RCH3 RCH3 RCH3	p.N1855 p.N811 p.P1158 p.N828K p.N228K p.N228K p.N228K p.N228K p.N228K p.N228K p.N228K p.N228K p.N2396 p.N33A p.N167K p.N1996 p.N1998	Missense, Mutation Missense, Mutation Missense, Mutation Missense, Mutation Missense, Mutation Nonense, Mutation Nonense, Mutation Siene Missense, Mutation Siene Siene Nonense, Mutation Missense, Mutatio	\$80	0,277777778 0,277777778 0,3187931429 0,3187831429 0,3187931429 0,3187931429 0,3187931429 0,3187931429 0,3187831439 0,3187831439 0,3187831439 0,3187831439 0,318783143833333 0,3188387937 0,31883833333 0,31883833333 0,31883833333 0,31883833333 0,31883833333	PASS PASS PASS PASS PASS PASS PASS PASS

#533T												
#533T		,							-			
	HCA	chr18	6942159	6942160		A	LAMA1	p.P3049P	Silent	SNV	0,2	PASS
#533T	HCA	chr19	8209815	8144931	C	A	FBN3	p.G163W	Missense_Mutation	SNV	0,134146341	PASS
#533T	HCA	chr20	60791598	62216542	C	G	HRH3	p.E268Q	Missense_Mutation	SNV	0,219251337	PASS
#533T	HCA	chr21	38853060	37480758	A	T	DYRK1A	p.K150*	Nonsense_Mutation	SNV	0,129496403	PASS
#533T	HCA	chrX	43628600	43769353		G	MAOB	p.G434A	Missense_Mutation	SNV	0,233766234	PASS
							IFRD2					
#477T	HCA	chr3	50327178	50289747	С	810		p.G2525	Missense_Mutation	SNV	0,354037267	PASS
#477T	HCA	chr5	90670828	91375011	С	ст	ARRDC3	p.E261fs	Frame_Shift_Ins	INS	0,29535865	PASS
#477T	HCA	chr5	179192901	179765900	A	G	MAML1	p.N2975	Missense_Mutation	SNV	0,189189189	PASS
#477T	HCA	chr7	27169940	27130321	G	A	HOXA4	p.P138L	Missense_Mutation	SNV	0,315	PASS
#477T	HCA	chr9	101818612	99056330	G	С	COL15A1	p.G1088A	Missense_Mutation	SNV	0,311111111	PASS
#477T	HCA	chr11	66360237	66592766	Т	G	CCDC87	p.184L	Missense_Mutation	SNV	0,338541667	PASS
#477T	HCA	chr12	82147918	81754139	T.	c	PPFIA2	p.D28G	Missense Mutation	SNV	0.312977099	PASS
#477T	HCA	chr14	21955825	21487666	G	T	TOX4	p.G97G	Silent	SNV	0,395061728	PASS
#477T	HCA	chr14	100759653	100293316	T	G	SLC25A29	p.K47T	Missense_Mutation	SNV	0,340425532	PASS
#477T	HCA	chr15	68582798	68290460	C	T	FEM1B	p.L368F	Missense_Mutation	SNV	0,282926829	PASS
#477T	HCA	chr17	27250972	28923954	G	C	PHF12	p.Q224E	Missense_Mutation	SNV	0,304	PASS
#477T	HCA	chr17	28887667	30560649	т	c	TBC1D29	p.D37D	Slent	SNV	0.12605042	PASS
#477T	HCA	chr18	3452206	3452208	Т	A	TGIF1	p.577T	Missense_Mutation	SNV	0,207729469	PASS
#477T	HCA	chr18	51807184	54280814	6	c	POLL	p.G236A	Missense_Mutation	SNV	0,207729409	PASS
									Missense_Mutation			
#477T	HCA	chrX	3544551	3626510	G	T	PRIOX	p.P242T	Missense_Mutation	SNV	0,240310078	PASS
#477T	HCA	chrX	38158213	38298960	T	C	RPGR	p.E414G	Missense_Mutation	SNV	0,159292035	PASS
#477T	HCA	chrX	48682656	48824246	C	T	HDAC6	p.111771	Silent	SNV	0,142857143	PASS
#477T	HCA	chrX	123514498	124380648	c	T	TENM1	p.R2689Q	Missense_Mutation	SNV	0,196296296	PASS
#757T	HCA	chr2	17696551	17515284	G	A	RAD51AP2	p.H1044H	Silent	SNV	0,293577982	PASS
#757T	HCA	chr2	241818194	240878777	G		AGXT	p.A3795	Missense_Mutation	SNV	0,252941176	PASS
#757T	HCA	chr3	170102544	170384756	A	G	SKIL	p.\$474G	Missense_Mutation	SNV	0,276923077	PASS
#757T	HCA	chr4	105412445	104491288	T	C	CXXC4	p.H3R	Missense_Mutation	SNV	0,243589744	PASS
#757T	HCA	chr4	144106702	143185549	A	G	USP38	p.L33L	Silent	SNV	0,25	PASS
#757T	HCA	chr5	82948586	83652767	C	T	HAPLN1	p.RS3K	Missense_Mutation	SNV	0,220858896	PASS
#757T	HCA	chr6	83884141	83174422	TTTCTTATC	т	PGM3	p.DKK315fs	Frame_Shift_Del	DEL	0,169230769	PASS
#757T	HCA	chr8	128428420	127416175	G	A	POUSF1B	p.V103V	Silent	SNV	0,285223368	PASS
						-						
#757T	HCA	chr9	2029049	2029049	G	-	SMARCA2	p.A9A	Silent	SNV	0,247863248	PASS
#757T	HCA	chr9	100132979	97370697	A	С	CCDC180	p.E1458D	Missense_Mutation	SNV	0,253846154	PASS
#757T	HCA	chr9	125437820	122675541	C	T	OR1L3	p.R138C	Missense_Mutation	SNV	0,220183486	PASS
#757T	HCA	chr9	138413373	135521527	T	c	LCN1	p.L10L	Silent	SNV	0,113402062	events;homologous_mag
#757T	HCA	chr10	26446370	26157441	A	G	MYO3A	p.T975T	Silent	SNV	0,272727273	PASS
#757T	HCA	chr11	56230241	56462765	G	c	OR5M9	p.L213V	Missense_Mutation	SNV	0.130434783	events;homologous_mag
#757T	HCA	chr11	32136794	31983860	A	G	KIAA1551	p.1969V	Missense Mutation	SNV	0,130434783	PASS PASS
#757T #757T	HCA HCA	chr12 chr12	32136794 43925997	31983860 43532194	A G		KIAA1551 ADAMTS20		Missense_Mutation Splice Site	SNV	0,267605634	PASS
						A		p.T152M				
#757T	HCA	chr12	101005823	100612045	G	T	GAS2L3	p.G117C	Missense_Mutation	SNV	0,268292683	PASS
#757T	HCA	chr13	37014210	36440073	T	A	CCNA1	p.L330M	Missense_Mutation	SNV	0,278145695	PASS
#757T	HCA	chr16	24564879	24553558	GTA	G	RBBP6	NA NA	Splice_Site	DEL	0,12345679	str_contraction
#757T	HCA	chr19	813708	813708	G	т	LPPR3	p.A340D	Missense_Mutation	SNV	0,258333333	PASS
#757T	HCA	chr19	40711106	40205199	c	G	MAP3K10	p.A364G	Missense_Mutation	SNV	0,25	PASS
	HCA		53270093	52766840				p.A364G	Missense Mutation	SNV	0,122994652	
#757T		chr19		52766840	c	A	ZNF600	p.E306*	Nonsense_Mutation			PASS
#757T	HCA	chr22	21153976	20799688	G	С	PI4KA	p.1543M	Missense_Mutation	SNV	0,293650794	PASS
#757T	HCA	chr22	26299739	25903772	G	A	MYO18B	p.A1698T	Missense_Mutation	SNV	0,368852459	PASS
#757T	HCA	chrX	16170753	16152630	c	A	GRPR	p.H380Q	Missense_Mutation	SNV	0,328571429	PASS
#757T	HCA	chrX	49142604	49286142	c	T	PPP1R3F	p.14841	Silent	SNV	0,243781095	PASS
#1896T	HCA	chr1	22921760	22595267	С	A	EPHA8	p.C547*	Nonsense Mutation	SNV	0,236686391	PASS
#1896T	HCA	chr1	158812095	158842305			MNDA	p.LS1S	Missense Mutation	SNV	0,174193548	
					- 1							events;homologous_mag
#1896T	HCA	chr1	201798426	201829298	c	T	IPO9	p.T301	Missense_Mutation	SNV	0,146666667	PASS
#1896T	HCA	chr1	204945884	204976756	C	A	NFASC	p.L5981	Missense_Mutation	SNV	0,190082645	PASS
#1896T	HCA	chr1	235969637	235806337	G	A	LYST	p.A933A	Silent	SNV	0,264516129	events;homologous_ma
#1896T	HCA	chr1	237656304	237493004	T	c	RYR2	p.R626R	Silent	SNV	0,192307692	PASS
#1896T	HCA	chr1	243809241	243645939	A	G	AKT3	p.I128T	Missense Mutation	SNV	0,278787879	PASS
#1896T	HCA	chr2	11364587	11224461	С	т	ROCK2	NA	Splice_Site	SNV	0,23255814	PASS
#1896T	HCA	chr2	24480865	24257996	A	c	ITSN2	p.V927G	Missense Mutation	SNV	0,227272727	PASS
						1000						
#1896T	HCA	chr2	42719980	42492840	G	A	KCNG3	p.S221F	Missense_Mutation	SNV	0,179310345	PASS
#1896T	HCA	chr2	55544847	55317711	. A	T	CCDC88A	p.L1152H	Missense_Mutation	SNV	0,176829268	PASS
#1896T	HCA	chr2	74043167	73816040	A	c	C2orf78	p.K606T				PASS
#1896T	HCA	chr2	113482966	112725389	G	A			Missense_Mutation	SNV	0,221052632	
#1896T	HCA	chr2	116066861				NTSDC4	p.K6061 p.S298S	Missense_Mutation Silent	SNV		PASS
#1896T	HCA			115309285	C	T	NTSDC4 DPP10	p.S298S p.A36V			0,221052632	
#1896T		chr2	238296631	115309285 237387988	C			p.S298S p.A36V	Silent	SNV	0,221052632 0,18556701	PASS
	HCA		238296631	237387988		T T	DPP10 COL6A3	p.S298S p.A36V p.K302K	Silent Missense_Mutation Silent	SNV SNV SNV	0,221052632 0,18556701 0,223880597 0,183098592	PASS events;homologous_ma PASS
HIDOCT	HCA	chr3	238296631 32030572	237387988 31989080	C A	T T G	DPP10 COL6A3 ZNF860	p.S298S p.A36V p.K302K p.M1V	Silent Missense_Mutation Silent Start_Codon_SNV	SNV SNV SNV	0,221052632 0,18556701 0,223880597 0,183098592 0,225165563	PASS events;homologous_mag PASS PASS
#1896T	HCA	chr3	238296631 32030572 33895418	237387988 31989080 33853926	C A T	T T G	DPP10 COL6A3 ZNF860 PDCD6IP	p.S298S p.A36V p.K302K p.M1V p.A646A	Silent Missense_Mutation Silent Start_Codon_SNV Silent	SNV SNV SNV SNV	0,221052632 0,18556701 0,223880597 0,183098592 0,225165563 0,217391304	PASS events;homologous_mag PASS PASS PASS
#1896T	HCA HCA	chr3 chr3 chr3	238296631 32030572 33895418 156877726	237387988 31989080 33853926 157159937	C A T G	T T G C	DPP10 COL6A3 ZNF860 PDCD6IP CCNL1	p.S298S p.A36V p.K302K p.M1V p.A646A p.T53fs	Silent Missense_Mutation Silent Start_Codon_SNV Silent Frame_Shift_Ins	SNV SNV SNV SNV SNV INS	0,221052632 0,18556701 0,223880597 0,183098592 0,225165563 0,217391304 0,177083333	PASS avents;homologous_maj PASS PASS PASS PASS PASS
#1896T #1896T	HCA HCA	chr3 chr3 chr3 chr4	238296631 32030572 33895418 156877726 74274520	237387988 31989080 33853926 157159937 73408803	C A T G AAAGT	T T G C	DPP10 COL6A3 ZNF860 PDCD6IP CCNL1 ALB	p.S298S p.A36V p.K302K p.M1V p.A646A p.T53fs p.K161fs	Silent Missense_Mutation Silent Start_Codon_SNV Silent Frame_Shift_ins Splice_Site	SNV SNV SNV SNV SNV INS DEL	0,221052632 0,18556701 0,223880597 0,183098592 0,225165563 0,217391304 0,177083333 0,212121212	PASS pvents;homologous_maj PASS PASS PASS PASS PASS ST_contraction
#1896T #1896T #1896T	HCA HCA HCA	chr3 chr3 chr3 chr4 chr5	238296631 32030572 33895418 156877726 74274520 38523524	237387968 31989080 33853926 157159937 73408803 38523422	C A T G AAAGT T	T T G C	DPP10 COL6A3 ZNF860 PDCD6IP CCNL1 ALB LIFR	p.S2985 p.A36V p.K302K p.M1V p.A646A p.T53fs p.K161fs p.K186K	Silent Missense_Mutation Silent Start_Codon_SNV Silent Frame_Shift_Ins Splice_Site Silent	SNV SNV SNV SNV SNV INS DEL SNV	0,221052632 0,18556701 0,223880597 0,183098592 0,225165563 0,217391304 0,177083333 0,212121212 0,304878049	PASS svents; homologous_mag PASS PASS PASS PASS PASS PASS Str_contraction PASS
#1896T #1896T #1896T #1896T	HCA HCA HCA HCA	chr3 chr3 chr3 chr4 chr5 chr5	238296631 32030572 33895418 156877726 74274520 38523524 76373371	237387968 31989080 33853926 157159937 73408803 38523422 77077546	C A T G AAAGT T A	T T G C	DPP10 COL6A3 ZNF860 PDCDGIP CCNL1 ALB LIFR ZBED3	p. S298S p. A36V p. K302K p. M3V p. A646A p. T53fs p. K161fs p. K186K p. P111P	Silent Missense_Mutation Silent Start_Codon_SNV Silent Frame_Shift_ins Splice_Site Silent Silent	SNV SNV SNV SNV SNV INS DEL SNV SNV	0,221052632 0,18556701 0,223880597 0,183098592 0,225165563 0,217391304 0,177083333 0,212121212 0,304878049 0,315789474	PASS pvents;homologous_map PASS PASS PASS PASS PASS PASS PASS PAS
#1896T #1896T #1896T	HCA HCA HCA	chr3 chr3 chr3 chr4 chr5	238296631 32030572 33895418 156877726 74274520 38523524	237387968 31989080 33853926 157159937 73408803 38523422	C A T G AAAGT T	T T G C	DPP10 COL6A3 ZNF860 PDCD6IP CCNL1 ALB LIFR	p.S2985 p.A36V p.K302K p.M1V p.A646A p.T53fs p.K161fs p.K186K	Silent Missense_Mutation Silent Start_Codon_SNV Silent Frame_Shift_Ins Splice_Site Silent	SNV SNV SNV SNV SNV INS DEL SNV	0,221052632 0,18556701 0,223880597 0,183098592 0,225165563 0,217391304 0,177083333 0,212121212 0,304878049	PASS svents; homologous_mai PASS PASS PASS PASS PASS PASS Str_contraction PASS
#1896T #1896T #1896T #1896T	HCA HCA HCA HCA HCA	chr3 chr3 chr3 chr4 chr5 chr5 chr5	238296631 32030572 33895418 156877726 74274520 38523524 76373371	237387968 31989080 33853926 157159937 73408803 38523422 77077546	C A T G AAAGT T A	T T G G C GT A C T T	DPP10 COL6A3 ZNF860 PDCDGIP CCNL1 ALB LIFR ZBED3	p. S2985 p. A36V p. K302K p. M1V p. A646A p. T53fs p. K161fs p. K186K p. P111P p. T3833T	Silent Missense_Mutation Silent Start_Codon_SNV Silent Frame_Shift_ins Splice_Site Silent Silent	SNV SNV SNV SNV SNV INS DEL SNV SNV	0,221052632 0,18556701 0,223880597 0,183098592 0,225165563 0,217391304 0,177083333 0,212121212 0,304878049 0,315789474	PASS avents;homologous_ma PASS PASS PASS PASS PASS Str_contraction PASS PASS PASS
#1896T #1896T #1896T #1896T #1896T	HCA HCA HCA HCA HCA HCA	chr3 chr3 chr3 chr4 chr5 chr5 chr5 chr5	238296631 32030572 33895418 156877726 74274520 38523524 76373371 79058976 140228923	237387988 31989080 33853926 157159937 73408803 38523422 77077546 79763153 140849338	C A T G AAAGT T A	T T T G C A A	DPP10 COL6A3 ZNF860 PDCDGIP CCNL1 ALB LIFR Z8ED3 CMYA5 PCDHA9	p.52985 p.A36V p.K302K p.M1V p.A646A p.T53fs p.K161fs p.K186K p.P111P p.T3833T p.F281L	Silent Missense_Mutation Silent Start_Coden_SNV Silent Frame_Shift_Ins Splice_Site Silent Silent Silent Missense_Mutation	SNV	0,221052632 0,18556701 0,223880597 0,183998592 0,225165563 0,217391304 0,177083333 0,212121212 0,304878049 0,315789474 0,103719424 0,153846154	PASS vvents;homologous_maj PASS PASS PASS PASS PASS PASS PASS PAS
#1896T #1896T #1896T #1896T #1896T #1896T #1896T	нса нса нса нса нса нса нса нса	chr3 chr3 chr4 chr5 chr5 chr5 chr5 chr5 chr5	238296631 32030572 33895418 156877726 74274520 38523524 765373371 79058976 140228923 169310146	237387988 31989080 33853926 157159937 73408803 38523422 77077546 79763153 140849338 169883142	C A T G AAAGT T A C C C	T T G G C GT A C C T C C	DPP10 COL6A3 ZNF860 PDCDGIP CCNL1 ALB LIFR Z8ED3 CMYA5 PCDHA9 FAM1968	p.S2985 p.A36V p.K302K p.M3V p.A646A p.T53fs p.K161fs p.K186K p.P111P p.T3833T p.F281L p.E253*	Silent Missense_Mutation Silent Silent Start_Coden_SNV Silent Frame_Shift_Ins Splice_Site Silent Silent Silent Missense_Mutation Norsense_Mutation	SNV	0,221052632 0,18556701 0,223880597 0,183098592 0,217391304 0,177083333 0,2112121121 0,304878049 0,315789474 0,100719424 0,153846154 0,221374046	PASS vvents;homologous_maj PASS PASS PASS PASS PASS Str_contraction PASS PASS Lod_fstar Lod_fstar PASS
#1896T #1896T #1896T #1896T #1896T #1896T #1896T #1896T	нса нса нса нса нса нса нса нса нса	chr3 chr3 chr3 chr4 chr5 chr5 chr5 chr5 chr5 chr5 chr5	238296631 32030572 33895418 156877726 74274520 38523524 76573371 79058976 140228923 169310146 32084264	237387988 31989080 33853926 157159937 73408803 38523422 77077546 79763153 140849338 169883142 32116487	C A T G AAAGT T A	T T G G C GT A A C C T T C A A A T T	DPP10 COL6A3 ZNF860 PDCDGIP CONL1 ALB LIFR Z8ED3 CMYAS PCOHA9 FAM1966 ATF68	p. S2985 p. A36V p. K302K p. M1V p. A646A p. T536: p. K166f: p. K186K p. P111P p. T3833T p. F281L p. E253* p. A655A	Silent Missense_Mutation Silent Start_Codon_SNV Silent Frame_Shift_Ins Splice_Site Silent Silent Silent Missense_Mutation Nonese_Mutation Silent Silent	SWV	0,221652632 0,18556701 0,18568097 0,183098992 0,225165563 0,177093304 0,177093303 0,212121212 0,304878049 0,100719424 0,100719424 0,153846154 0,18302439	PASS avents;homologous_maj PASS PASS PASS PASS ST_contraction PASS \$tr_contraction PASS \$t_lod_fstar t_lod_fstar \$t_lod_fstar \$t_lod_fs
#1896T #1896T #1896T #1896T #1896T #1896T #1896T #1896T #1896T	HCA	chr3 chr3 chr3 chr4 chr5 chr5 chr5 chr5 chr5 chr5 chr6 chr6 chr6	238296631 32030572 33895418 156877726 74274520 38523524 76373371 79058976 140228923 169310146 32084264 47925536	237387988 31989080 33853926 157159937 73408803 38523422 77077546 79763153 140849338 169831142 32116487 47885938	C A T G AAAGT T A G G C C C C G G T T	T T T G C A A	DPP10 COL6A3 ZNR860 PDCD6IP CCNL1 ALB LIFR Z8E03 CMYAS PCDHA9 FAM1968 PKD1L1	p. \$2985 p. A36V p. K302X p. M1V p. A646A p. T5365 p. K1645 p. K1665 p. K186K p. P111P p. T38337 p. F2811 p. E253* p. E253* p. E253* a. T385A	Silent Missense, Mutation Silent Start, Codon, SNV Silent Missense, Mutation Nonsense, Mutation Missense, Mutation Missense, Mutation Missense, Mutation	SWV	0,221652632 0,88556701 0,223889597 0,183098592 0,225165563 0,217931304 0,177083333 0,212121212 0,3104780499 0,315789474 0,1553846154 0,2221374046 0,18902439 0,1914839302	PASS pents/monologous_mai pass PASS PASS PASS PASS PASS PASS PASS SIT_contraction T_contraction PASS PASS PASS PASS PASS PASS PASS PAS
#1896T #1896T #1896T #1896T #1896T #1896T #1896T #1896T #1896T #1896T	HCA	chr3 chr3 chr3 chr4 chr5 chr5 chr5 chr5 chr5 chr5 chr6 chr6 chr7 chr7	238296631 32030572 33895418 156877726 74274520 38523524 76373371 79058976 140228923 169310146 32084264 47925536 97867838	237387988 31989080 33853926 157159937 73408803 38523422 77077546 79763153 140849338 169883142 32116487 47885938 98238526	C A T G AAAGT T A A G C C C G T T C C C C C C C C C C C C C	T T G G C GT A A C C T T C A A A T T	DPP10 COL6A3 ZNR8KO PDCDGIP CCNL1 ALB LIFR ZBED3 CMYAS PCDHA9 FAM196B ATF68 PKD1L1 TECPR1	p. S2985 p. A36V p. K302X p. M1V p. A646A p. T336; p. K161f; p. K166K p. P111P p. T38337 p. F281L p. E253* p. A625A p. T385A p. Y36VM	Silent Missense, Mutation Silent Start, Codon, SNV Silent Frame, Shift, Ins Spilee, Site Silent Silent Silent Missense, Mutation Missense, Mutation Missense, Mutation Missense, Mutation Missense, Mutation Missense, Mutation	SWV	0,221652632 0,8856701 0,223880597 0,383098592 0,225165693 0,217391304 0,177083333 0,212121212 0,304678049 0,155789474 0,1007394 0,1007394 0,	PASS PASS PASS PASS PASS PASS PASS PASS
#1896T #1896T #1896T #1896T #1896T #1896T #1896T #1896T #1896T #1896T #1896T	HCA	chr3 chr3 chr3 chr4 chr5 chr5 chr5 chr5 chr5 chr5 chr6 chr7 chr7 chr7	238296631 32030572 33895418 156877726 74274520 38523524 76373371 79058976 140228923 169310146 32084264 47925536 97867838 96051511	237387988 33199080 33853926 157159937 73408803 38523422 77077546 79763153 140649338 169883142 32116487 47885938 9328526 93285229	C A T G AAAGT T A G G C C C C G G T T	T T G G C GT A A C C T T C A A A T T	DPP10 COL6A3 2NR800 PDCDGIP CON.1 AlB LUFR 28ED3 CMWAS PCDHA9 FAM1968 AT168 PKD111 TECPR1 WWK2	p. \$2985 p. A36V p. K302X p. M1V p. A646A p. T5365 p. K1645 p. K1665 p. K186K p. P111P p. T38337 p. F2811 p. E253* p. E253* p. E253* a. T385A	Silent Missense, Mutation Silent Start, Codon, SVV Silent Frame, Shift, Ins Splice, Site Silent Silent Silent Missense, Mutation Monesce, Mutation Missense, Mutation	SW S	0,216/5/63/2 0,1855/6701 0,22880997 0,188098992 0,225165/689 0,217991304 0,177083333 0,212121212 0,04678049 0,155984074 0,100719424 0,100719424 0,155984054 0,2121374046 0,18092459 0,180851064 0,19125/6893	PASS PASS PASS PASS PASS PASS PASS PASS
#1896T #1896T #1896T #1896T #1896T #1896T #1896T #1896T #1896T #1896T	HCA	chr3 chr3 chr3 chr4 chr5 chr5 chr5 chr5 chr5 chr5 chr6 chr6 chr7 chr7	238296631 32030572 33895418 156877726 74274520 38523524 76373371 79058976 140228923 169310146 32084264 47925536 97867838	237387988 31989080 33853926 157159937 73408803 38523422 77077546 79763153 140849338 169883142 32116487 47885938 98238526	C A T G AAAGT T A A G C C C G T T C C C C C C C C C C C C C	T T G G C GT A A C C T T C A A A T T	DPP10 COL6A3 ZNR8KO PDCDGIP CCNL1 ALB LIFR ZBED3 CMYAS PCDHA9 FAM196B ATF68 PKD1L1 TECPR1	p. S2985 p. A36V p. K302X p. M13V p. A646A p. T336; p. K161f; p. K166K p. P111P p. T38337 p. F281L p. E253* p. A625A p. T385A p. Y340M	Silent Missense, Mutation Silent Start, Codon, SVV Silent Frame, Shift, Ins Splice, Site Silent Silent Silent Missense, Mutation Monesce, Mutation Missense, Mutation	SWV	0,216/5/63/2 0,1855/6701 0,22880997 0,188098992 0,225165/689 0,217991304 0,177083333 0,212121212 0,04678049 0,155984074 0,100719424 0,100719424 0,155984054 0,2121374046 0,18092459 0,180851064 0,19125/6893	PASS PASS PASS PASS PASS PASS PASS PASS
#1896T #1896T #1896T #1896T #1896T #1896T #1896T #1896T #1896T #1896T #1896T #1896T	HCA	chr3 chr3 chr4 chr5 chr5 chr5 chr5 chr5 chr5 chr5 chr5	28296631 2020572 33895418 156877726 74274520 38253524 76373371 79058976 14022823 169310146 3204264 47925536 97867838 96051511 5786533	237387988 33989080 33853926 157159937 73408803 38523422 77077546 79763153 140649338 169883142 4788593 98238526 5746690	C A T T G A A A A A A A A A A A A A A A A	T T G G G G T A C C T T C C C C T T T C C C T T T C C C T T T C C C T T T C C C T T T C C C T T T C C C T	DPFID COLGA3 ZNR800 PDCDGIP CONLI ALB LIFR Z8ED3 CMYAS FDMA9 FAM1966 ATT68 PKDILI TECPRI VNKZ FAM208	p. S2985 p. A36V p. K302X p. M3V p. A646A p. T53f p. K1615 p. K1645 p. F13837 p. K1645 p. F2811 p. E253* p. A625A p. T388A p. V340M p. A1529V p. A10000	Silent Missene, Mutation Silent Seart, Coden, SW Silent Missense, Mutation	SW S	0,221053632 0,8856701 0,233889597 0,183098592 0,225165563 0,217391304 0,177083333 0,212121212 0,30478049 0,153846154 0,153846154 0,18302439 0,18302439 0,18302439 0,18302439 0,18302439 0,18302439 0,18302439 0,18302439 0,18302439	PASS PASS PASS PASS PASS PASS PASS PASS
#1896T #1896T #1896T #1896T #1896T #1896T #1896T #1896T #1896T #1896T #1896T #1896T #1896T #1896T	HCA	chr3 chr3 chr3 chr4 chr4 chr5 chr5 chr5 chr5 chr5 chr6 chr6 chr7 chr7 chr9 chr30 chr30	28296631 3200572 33895418 15687726 74274520 38523524 76573371 7958976 140228923 140228923 3520464 47925536 97867838 986051511 3094564 3094563 3094565 3094565 3094565 3094565 3094565	237387988 3399080 33853926 157159937 73408803 38523422 77077546 78763153 140849338 140849338 23216487 47855938 98238526 93289229 30625620	C A A T G A A A A G T T A A A A G T T A A A G T T A A C C C C C C C C C C C C C C C C	T T G G C G T A A A T T G G C T T A A C C C C C C C C C C C C C C C	DPPID COLGAS 2N98GO PDCOGAS 2N98GO PDCOGAS 2N98GO PDCOGAS 2N98GO PDCOGAS 2N98GO PDCOGAS 2N98GO PDCOGAS 2N99GO P	p.52985 p.A36V p.K302X p.M1V p.A646A p.T53fs p.K161fs p.K161fs p.K186K p.P111P p.T3833T p.F2811 p.E253* p.A625A p.T385A p.V340M p.A1529V p.A100000 p.A256	Silent Missense, Mutation Silent Sort. Coden, SW Silent Silent Frame, Shift, Ins Splice, Ste Silent Silent Silent Silent Missense, Mutation	SWV SWV SWV SWW SWW SWW SWW SWW SWW SWW	0,21655612 0,18556701 0,22880597 0,181098592 0,225165659 0,217991304 0,177083333 0,212121212 0,304878974 0,10073924 0,105846154 0,2221374046 0,18092439 0,19489362 0,19489362 0,19586154 0,19596164 0,	PASS PASS PASS PASS PASS PASS PASS PASS
#1896T #1896T #1896T #1896T #1896T #1896T #1896T #1896T #1896T #1896T #1896T #1896T #1896T #1896T	HCA HCA HCA HCA HCA HCA HCA HCA HCA HCA	chr3 chr3 chr3 chr3 chr4 chr4 chr5 chr5 chr5 chr5 chr5 chr5 chr6 chr7 chr6 chr7 chr9 chr10 chr10 chr10 chr10 chr10	238296631 3200572 33895418 15687726 74274520 3823524 76973371 79058976 140028923 169910146 32084264 47925536 97807838 97807838 97807838 97807838 97807838 97807838 97807838	237387988 31999080 33853926 157159937 73408803 38523422 77077546 79763153 140649338 169883142 47885938 9228526 932856 932856 932856 932856 932856 932856 932856 932856	C A T T G A A A G C C C G G G G G G G G G G G G	T T G G C T A A A A T T C T T T A A C T T T T T	DPF10 COL6A3 ZN8860 PDC06IP CCNL1 ALB LIFR 28ED3 CMYA5 PC0H49 FAM1968 AT168 AT168 AT161 TECPR1 WWK2 FAM2086	p. 52985 p. A36V p. K102X p. M13V p. A666A p. T53f p. K1615 p. K1615 p. K186X p. F1317 p. F2811 p. F2833T p. F2811 p. F2835 p. A625A p. T385A p. V340M p. A1529V	Silent Missense, Mutation Silent Seart, Coden, SW Silent Silent Frame, Shift, Ins Fisher, Silent Silent Silent Silent Silent Missense, Mutation Missense, Missense Missense, Missense Missense, Missense Missense Missense Missense Missense Missense Missense Misse	58V 58V 58V 58V 58V 18S 58V 58V 58V 58V 58V 58V 58V 58V 58V 58V	0.221652612 0.18555701 0.223889597 0.223889597 0.223655659 0.277991304 0.177093333 0.212212122 0.304678049 0.315789474 0.15902439 0.15902439 0.15902439 0.15902459 0.15902459 0.15902459 0.15902459 0.15902459 0.1590250 0.1590	PASS PASS PASS PASS PASS PASS PASS PASS
#1896T #1896T #1896T #1896T #1896T #1896T #1896T #1896T #1896T #1896T #1896T #1896T #1896T #1896T #1896T	HCA	chr3 chr3 chr3 chr3 chr4 chr5 chr5 chr5 chr5 chr5 chr5 chr5 chr5	28296631 3200572 33895418 15687726 36523524 7627357 79058976 140228923 169310146 32084264 4792536 97807838 96051511 5786953 39318549 8487642 44925463	237387988 33989380 33853926 157159937 73408803 38523422 77077546 159833142 32116487 47885938 47885938 5786690 30629620 30629620 4731815	C A T T A A G G C C C G G G G G C C C C C C C C	T T G G C G T A A A A T T C C T T A A A A A A T T C C T T A A A A	DPPID COLEAS ZNIBEO PDCDEIP CCNL1 ALB LURR ZBED3 CANYAS PCDHA9 FAM1968 ATTE68 PKDL11 TECPR1 WNK2 FAM208 LYZL2 CLY20 CDAN1	B. 52985 B. A36V p. K302X p. K302X p. M16V p. A466A p. T53fb p. K186X p. F131F p. T38337 p. F2831 p. E2533 p. A4625A p. T385A p. V340M p. A1529V p. A1029C p. A1029C p. A229G p. R1072R p. 525151	Silent Missense, Mutation Silent Start, Coden, SW Start, Coden, SW Silent Frame, Shift, Ins Splice, Site Silent Silent Silent Missense, Mutation M	58V 58V 58V 58V 58V 68V 68V 58V 58V 58V 58V 58V 58V 58V 58V 58V 5	0.221652612 0.18556701 0.22880997 0.188098992 0.225165569 0.217931304 0.1177083333 0.212121212 0.310478049 0.315789474 0.100739424 0.153846154 0.22374046 0.153846154 0.22374046 0.153846154 0.22374046 0.153846154 0.22374046 0.153846154 0.22374046 0.153846154 0.22374046 0.153846154 0.2237404 0.153846154 0.2237404 0.153846154 0.153	PASS PASS PASS PASS PASS PASS PASS PASS
#1896T #1896T #1896T #1896T #1896T #1896T #1896T #1896T #1896T #1896T #1896T #1896T #1896T #1896T #1896T #1896T #1896T #1896T	HCA	chr3 chr3 chr3 chr3 chr4 chr4 chr5 chr5 chr5 chr5 chr5 chr5 chr5 chr5	238296631 3200572 33895418 15687726 38223524 76273377 79058976 14022823 169310146 32084264 47925536 97867838 96051511 5788053 98051511 5788053 88487642 43024013 52024076	237387988 33989080 33853926 157159937 73408803 38523422 77077545 79763153 140649338 169893142 32116487 4785593 99238526 99238526 5746690 8003865 42731815 52416279	C A T T A A A A A A A A A A A A A A A A	T T G G C G T A A T T C G C T T T A A C C T T A A C C T T A A C C T T A A C C T T A A C C T T A A C C T T A A C C T T A A C C T T A A C C C T T A C C C C	DPPI0 COLEGA ZNY860 PDCD6IP CON11 ALB LIFR Z8ED3 CMYAS PCDH49 FAM1958 AT168 PDD111 TECPR1 TECPR1 TMXCI FAM208 LYRZ CMY25 CDAN1 MYOSA	p. 52985 p. A36V p. K302K p. M10V p. A666A p. T5365 p. K1665 p. K1665 p. K1665 p. F1281 p. T3833T p. F2811 p. F2831 p. F2815 p. A625A p. T385A p. Y340M p. A1529V p. A1090E p. A	Silent Missens, MutaSon Silent Start, Codon, SW Start, Silent Missens, MutaSon	58V 58V 58V 58V 58V 58V 58V 58V 58V 58V	0.221652612 0.18555291 0.222889597 0.222889597 0.222865595 0.277991304 0.177093333 0.212212122 0.304678049 0.315789474 0.150913424 0.150913424 0.15091424 0.150915064 0.19156893 0.272727273 0.13267133 0.162161162 0.015094702 0.15094705	PASS Ventickomologicus, may PASS PASS PASS PASS PASS #############
#1896T #1896T #1896T #1896T #1896T #1896T #1896T #1896T #1896T #1896T #1896T #1896T #1896T #1896T #1896T #1896T #1896T #1896T	HCA	chr3 chr3 chr3 chr4 chr6 chr6 chr6 chr6 chr5 chr5 chr5 chr6 chr6 chr7 chr9 chr9 chr1 chr1 chr1 chr1 chr1 chr1 chr1 chr1	288796631 3080572 30805418 15687725 74274520 38523524 76523372 79058976 140228923 169310146 97807838 97807838 98051511 3084564 47925536 9780783 98051511 52708476 47205476 9780783 978	22 78 7988 23 78 7988 3385 926 15715 9937 74408803 3852 3422 77077546 7976 3153 1698 3142 478 859 38 982 1852 6 932 892 9 366 9 366 9 366 9 366 9 366 9 367 9 368 9 3	C A T G AMGT T A G C C G G G T C C C C T T T T T T T T T	T T G G G G G G G G G G G G G G G G G G	DPF0 COL643 DPF0 COL643 DPF0 COL643 DPF0 COL64 DP	р. 5.2985 р. 8.3667 р. 8.1026X р. 8.1026X р. 8.1026X р. 8.1036X р. 8.1036X р. 8.1036X р. 9.111P р. 7.38337 р. 7.2811 р. 2.72537 р. 2.7254X р. 1.7254X р. 1.7254	Missens, Mutation Silent Silent Silent Silent Silent Silent Silent Silent Silent Frame, Shift, Ins Silent Silent Silent Silent Silent Silent Silent Missens, Mutation Missense, Mutation	58V 58V 58V 58V 58V 58V 58V 58V 58V 58V	0.21653612 0.18556701 0.22880997 0.22880997 0.22195569 0.221978304 0.717088303 0.717078830 0.71707883	PASS PASS PASS PASS PASS PASS PASS PASS
#1896T #1896T #1896T #1896T #1896T #1896T #1896T #1896T #1896T #1896T #1896T #1896T #1896T #1896T #1896T #1896T #1896T #1896T	HCA	chr3 chr3 chr3 chr3 chr4 chr4 chr5 chr5 chr5 chr5 chr5 chr5 chr5 chr6 chr7 chr7 chr7 chr7 chr1 chr1 chr1 chr1 chr1 chr1 chr15 chr15 chr15 chr15 chr15 chr16 chr1 chr2 chr10 chr10 chr15 ch	238296631 3200572 33895418 15687726 38223524 76273377 79058976 14022823 169310146 32084264 47925536 97867838 96051511 5788053 98051511 5788053 88487642 43024013 52024076	237387988 33989080 33853926 157159937 73408803 38523422 77077545 79763153 140649338 169893142 32116487 4785593 99238526 99238526 5746690 8003865 42731815 52416279	C A T T A A A A A A A A A A A A A A A A	T T G G C G T A A T T C G C T T T A A C C T T A A C C T T A A C C T T A A C C T T A A C C T T A A C C T T A A C C T T A A C C T T A A C C C T T A C C C C	DPPI0 COLEGA ZNY860 PDCD6IP CON11 ALB LIFR Z8ED3 CMYAS PCDH49 FAM1958 AT168 PDD111 TECPR1 TECPR1 TMXCI FAM208 LYRZ CMY25 CDAN1 MYOSA	B. 52985 P. A36V P. A36V p. K102X p. MILY p. A646A p. K166X p. K16CX p. K166X p. K16CX p. K166X p. K16CX p. K166X	Silent Missens, MutaSon Silent Start, Codon, SW Start, Silent Missens, MutaSon	58V 58V 58V 58V 58V 58V 58V 58V 58V 58V	0.221652612 0.18555291 0.222889597 0.222889597 0.222865595 0.277991304 0.177093333 0.212212122 0.304678049 0.315789474 0.150913424 0.150913424 0.15091424 0.150915064 0.19156893 0.272727273 0.13267133 0.162161162 0.015094702 0.15094705	PASS Ventickomologicus, may PASS PASS PASS PASS PASS #############
#1896T #1896T #1896T #1896T #1896T #1896T #1896T #1896T #1896T #1896T #1896T #1896T #1896T #1896T #1896T #1896T #1896T #1896T	HCA	chr3 chr3 chr3 chr4 chr6 chr6 chr6 chr6 chr5 chr5 chr5 chr6 chr6 chr7 chr9 chr9 chr1 chr1 chr1 chr1 chr1 chr1 chr1 chr1	288796631 3080572 30805418 15687725 74274520 38523524 76523372 79058976 140228923 169310146 97807838 97807838 98051511 3084564 47925536 9780783 98051511 52708476 47205476 9780783 978	22 78 7988 23 78 7988 3385 926 15715 9937 74408803 3852 3422 77077546 7976 3153 1698 3142 478 859 38 982 1852 6 932 892 9 366 9 366 9 366 9 366 9 366 9 367 9 368 9 3	C A T G AMGT T A G C C G G G T C C C C T T T T T T T T T	T T G G G G G G G G G G G G G G G G G G	DPF0 COL643 DPF0 COL643 DPF0 COL643 DPF0 COL64 DP	B. 52985 P. A36V P. A36V p. K102X p. MILY p. A646A p. K166X p. K16CX p. K166X p. K16CX p. K166X p. K16CX p. K166X	Missens, Mutation Silent Silent Silent Silent Silent Silent Silent Silent Silent Frame, Shift, Ins Silent Silent Silent Silent Silent Silent Silent Missens, Mutation Missense, Mutation	58V 58V 58V 58V 58V 58V 58V 58V 58V 58V	0.21653612 0.18556701 0.22880997 0.22880997 0.22195569 0.221978304 0.717088303 0.717078830 0.71707883	PASS PASS PASS PASS PASS PASS PASS PASS
#1896T	HICA HICA HICA HICA HICA HICA HICA HICA	thr3 thr3 thr3 thr4 thr4 thr4 thr5 thr5 thr5 thr5 thr6 thr9 thr9 thr10 thr10 thr15 thr15 thr15 thr15 thr15 thr15 thr15 thr15 thr16 thr16 thr16 thr16	288796431 238796431 33875418 156877276 38523524 76273377 79058976 140228923 169310146 32084264 47925536 97807583 5788653 30918549 68457642 4920536 68457642 684576442 68457644444 68457644444 68457644444 68457644444 68457644444 68457644444 6845764444 6845764444 68457644444 6845764444 684576444 684576444 684576444 684576444 6845764444 68457644444 684576444 684576444 684576444 68457644 68457644 68457644 68457644 6845764 6845764 6845764 6845764 6845764 6845764 6845764 684	22 78 7988 22 78 7988 385 926 385 926 157 159937 74408803 385 23422 77077546 7976 3153 16983142 32116487 4785938 982 18526 932 18526 932 18526 932 18526 942 18526 952	C A T G G AMGT T A G C C C G G T T C C C C C C C C C C C C	T T G G G G G G G G G G G G G G G G G G	DPFID OCIOSA 3 2 NOS 4 N	P. 52985 P. A36V P. A36V D. MIV D. A646A P. T53H D. K161H D	Silent Missense, Mutation Mi	5W 5	0.21653612 0.18556701 0.22880997 0.22880997 0.22195563 0.271978394 0.777088393 0.77121222 0.04678099 0.10579404 0.15894154 0.158948154 0.158948154 0.158948154 0.15892489 0	PASS PASS PASS PASS PASS PASS PASS PASS
#1896T	HICA HICA HICA HICA HICA HICA HICA HICA	chr3 chr3 chr4 chr3 chr4 chr5 chr5 chr5 chr5 chr5 chr5 chr5 chr6 chr6 chr7 chr2 chr2 chr3 chr3 chr3 chr3 chr3 chr3 chr3 chr3	28296631 3200572 33895418 3895418 74274520 38523524 76028977 79058976 14022823 169310146 9780788 96051511 5786653 3038546 47925586 96051511 5786653 3038546 4792556 6732746 6824876 7736746 8848764 8848764 88	227387988 3199080 3885926 15715997 7246880 3855926 7246880 38523422 7707754 14068931 14068931 14068931 10983142 7785938 98238526 9823856 98238526 98238526 9823856 9823856 9823856 9823856 9823856 9823856 9823856 9823856 9823856 9823856 9823856 9823856 9823856 98238	C A A T G G AMAGT T T C C C C C C C C C C C C C C C C C	T T T G G G T A A C C T T T A A C C T T T G G G G G T T T G G G G G G G	DPF0 DPF0 DPF0 DPF0 DPF0 DPF0 DPF0 DPF0	B. 52985 B. A36V B. MILY D. MILY D. A646A D. PTSH: D. K1615	Silvert Missense, Mutation Silvert Missense, Mutation Miss	58V 58V 58V 58V 58V 58V 58V 58V 58V 58V	0.21653632 0.18556701 0.22880597 0.185098592 0.225165563 0.277913034 0.177083333 0.217212122 0.0047009 0.315788474 0.10073494 0.10073494 0.2221374046 0.18902459 0.191256891 0.1912577771 0.1912577771 0.1912577771 0.19125777711	PASS Ventishomologicus, ma Ventishomologicus, ma PASS PASS PASS PASS PASS ST_CONTROLOGIC PASS ST_CONTROLOGIC PASS PASS PASS PASS PASS PASS PASS PAS
#1896T	HCA	(hr) (hr) (hr) (hr) (hr) (hr) (hr) (hr)	382956611 382956611 382956611 38895418 15687726 74274520 74274520 74274520 74274520 169310146 32084264 32084265 978078387 97807838 9780788 97807838 9780788 9780788 978078 978078 9780788 9780788 9780788 9780788 978078 978078 978078 9780788 9780788	23787988 23787989 23787989 23787989 23787989 23787989 23853926 23853926 23853926 23853926 23853926 23853926 279707546 279763153 140689338 140689338 9238526 238526 258526	C A T G G AMGT T A G C C G G G T T C C C C C C C C C C C C	T T G G T T T G G T T T T T T T T T T T	DPP10 COL633 ZNR960 PDCD6P CCN11 ANE LIFR ZBC03 CMACS FCORAS FM1986 ATT68 FM1986 LY72 CF230 CDAN1 MYOSA GPR139 KCTD19 ADAD2 sept-09 ACT19	P. 52985 P. A36V P. A36V P. A36V P. MIV D. MIV D. A646A P. T518- P. K1615- P. K1615- P. K1616- P. T38337 P. F2811 P. F2813 P. F2813 P. F281- P. F2813 P. F281- P.	Silent Missense, Mutation Sart, Codon, SNV Silent Sart, Codon, SNV Silent Missense, Mutation Missense, Muta	5W 5	0.21653612 0.18556701 0.22880997 0.22880997 0.22195563 0.271978394 0.777088393 0.771978394 0.100779424 0.10077944	PASS PASS PASS PASS PASS PASS PASS PASS
#1890T #1890T	HICA HICA HICA HICA HICA HICA HICA HICA	chr3 chr3 chr3 chr4 chr4 chr4 chr5 chr5 chr5 chr5 chr5 chr5 chr6 chr7 chr7 chr9 chr9 chr30 chr30 chr30 chr312 chr35 chr36 chr36 chr36 chr37 chr3	282796531 382906572 383955418 38395418 74274520 38523524 79058976 74274520 38523524 79058976 74274520 3208266 47275536 9780788 96051511 5789653 30318549 4720556 4720556 4720556 4720556 4720556 4720556 4720556 4720556 4720556 4720556 4720556 4720556 4720556 4720556 4720556 4720556 4720556 4720556 47206 47206 472066 47206 472066 472066 472066 472066 47	227347988 3399080 38859026 15715997 72468803 38559026 72468803 38523422 77077546 77075153 14068933 14068933 14068933 14068933 5746690	C A A A A A A A A A A A A A A A A A A A	G G G G T T T C C C T T C C C T T C C C T	DPF01 DPF02 DPF03 ZNR800 PPCDGP CONL1 LIFR LIFR LIFR LIFR LIFR LIFR LIFR LIFR	B. 52985 B. A36V B. A36V B. MILY D. A64GA D. PTSH: D. K1615: D. K1615:	Missens, Mutation Silvert Missens, Mutation Silvert Missens, Mutation	58V 58V 58V 58V 58V 58V 58V 58V	0.21653632 0.18556701 0.22880597 0.185098592 0.225165563 0.271991304 0.177083333 0.217191304 0.177083333 0.217121212 0.304678049 0.315788474 0.105738451 0.221374046 0.18502459 0.191898362 0.185051604 0.191256873 0.185051604 0.191256873 0.195067050 0.196051064 0.191256873 0.19606705 0.19606705 0.19606705 0.19606705 0.19602707 0.155609170 0.156909187 0.159609187	PASS Ventishomologicus, ma Ventishomologicus, ma PASS PASS PASS PASS PASS ST_CONTROLOGIC PASS PASS PASS PASS PASS PASS PASS PAS
#1996T	HICA HICA HICA HICA HICA HICA HICA HICA	(hr) (hr) (hr) (hr) (hr) (hr) (hr) (hr)	382956611 382956611 382956613 38895418 15687726 74274520 74274520 74274520 16921024 76973377 169310246 3204264 3204265 97807838	227347988 331999000 33853926 157159927 74068903 38534926 77077546	C A T T G AMGT T A G C C C G G T C C C C C C C C C C C C C	T T G G G G G G G G G G G G G G G G G G	DPP10 COL633 ZN#860 ZN#860 PDCDEP CCN11 ANE LIFR ZBEO3	P. 52985 P. A36V P. A36V P. K102X P. MIV P. M46KA P. T516 P. K1615 P. K1615 P. K1615 P. K1616 P. T38337 P. F2811 P. F2831 P. F3837	Silent Missense, Mutation Service, Silent Service, Silent Service, Silent Missense, Mutation Mi	5W 5	0.21653612 0.18556701 0.22880997 0.22880997 0.22165563 0.271978394 0.777088393 0.771978394 0.17078393 0.17121222 0.1047708393 0.17121222 0.1047708393 0.105773404 0.10577344 0.10577344 0.10577344 0.10577344 0.10577344 0.1057744 0.1057	PASS PASS PASS PASS PASS PASS PASS PASS
#1890T #1890T	HICA HICA HICA HICA HICA HICA HICA HICA	chr3 chr3 chr3 chr4 chr4 chr4 chr5 chr5 chr5 chr5 chr5 chr5 chr6 chr7 chr7 chr9 chr9 chr30 chr30 chr30 chr312 chr35 chr36 chr36 chr36 chr37 chr3	282796531 382906572 383955418 38395418 74274520 38523524 79058976 74274520 38523524 79058976 74274520 3208266 47275536 9780788 96051511 5789653 30318549 4720556 4720556 4720556 4720556 4720556 4720556 4720556 4720556 4720556 4720556 4720556 4720556 4720556 4720556 4720556 4720556 4720556 4720556 47206 47206 472066 47206 472066 472066 472066 472066 47	227347984 3199080 3885926 15715997 7240803 3852422 77077546 77077545 77075153 10983142 4788938 98238526 9823856 98238526 9823856 98238526 98238526 98238526 98238526 98238526 98238526 98238526 98238526 98238526 98238526 98238526 98238526 98238526 98238526	C A A A A A A A A A A A A A A A A A A A	G G G G T T T C C C T T C C C T T C C C T	DPF01 DPF02 DPF03 ZNR800 PPCDGP CONL1 LIFR LIFR LIFR LIFR LIFR LIFR LIFR LIFR	B. 52985 B. A36V B. A36V B. MILY D. A64GA D. TSSB D. K1615	Missens, Mutation Silvert Missens, Mutation Silvert Missens, Mutation	58V 58V 58V 58V 58V 58V 58V 58V	0.21653632 0.18556701 0.22880997 0.128109592 0.225165563 0.275165563 0.17191304 0.177083333 0.171212121 0.304678049 0.315788474 0.100739424 0.100739424 0.100739424 0.121374046 0.155846514 0.221374046 0.1580851064 0.191256813 0.180851064 0.191256813 0.180851064 0.191256813 0.180851064 0.191256813 0.180851064 0.191256813 0.1908702 0.180851064 0.191256813 0.1908702 0.1908702 0.1908702 0.1908702 0.1908703 0	PASS
#1996T	HICA HICA HICA HICA HICA HICA HICA HICA	(hr) (hr) (hr) (hr) (hr) (hr) (hr) (hr)	382956611 382956611 382956613 38895418 15687726 74274520 74274520 74274520 16921024 76973377 169310246 3204264 3204265 97807838	227347988 331999000 33853926 157159927 74068903 38534926 77077546	C A T T G AMGT T A G C C C G G T C C C C C C C C C C C C C	T T G G G G G G G G G G G G G G G G G G	DPP10 COL633 ZN#860 ZN#860 PDCDEP CCN11 ANE LIFR ZBEO3	B. 52985 B. A36V B. A36V B. MILY D. A64GA D. TSSB D. K1615	Silent Missense, Mutation Service, Silent Service, Silent Service, Silent Missense, Mutation Mi	5W 5	0.21653612 0.18556701 0.22880997 0.22880997 0.22165563 0.271978394 0.777088393 0.771978394 0.17078393 0.17121222 0.1047708393 0.17121222 0.1047708393 0.105773404 0.10577344 0.10577344 0.10577344 0.10577344 0.10577344 0.1057744 0.1057	PASS
19957 19957	HCA	(hr) (hr) (hr) (hr) (hr) (hr) (hr) (hr)	382966611 382966611 382966611 38896418 38896418 156877726 74274520 74274520 74274520 160910914 32082426 160910914 32082426 97807838 97807815 9780783 9	23747884 23747884 237478980 33857926 33857926 33857926 33857926 33857926 3777754 3777754 377	C A A A A A A A A A A A A A A A A A A A	G G G G G G G G G G G G G G G G G G G	DPP10 COL633 ZN#860 PDCDEP CCN1 ALE IFR ZREG3 CMYA5 FCOHA9 FAM1986 AIT68 POD111 TECPR1 VWN2 FAM208 LYRL2 CEP20 CDAN1 MYOSA GPR139 KCTD19 ADA02 Lept-09 ACT19 DCAF15 ZN#850 ZN#850 ZN#850 ZN#850 ZN#850	B. 52985 B. A36V B. A36V B. A36V B. MIV B. A646A B. T53B B. K161B B.	Silent Missense, Mutation Sart, Codon, SNV Silent Sart, Codon, SNV Silent Missense, Mutation Missens	\$W \$	0.21653612 0.18556701 0.22880997 0.22880997 0.221865691 0.22165569 0.221978304 0.77708333 0.771212122 0.00670099 0.315798474 0.100739424 0	PASS PASS PASS PASS PASS PASS PASS PASS
1991 1992 1992 1992 1992 1992 1992 1992	HICA HICA HICA HICA HICA HICA HICA HICA	chr3 chr3 chr3 chr4 chr4 chr4 chr5 chr5 chr5 chr5 chr5 chr5 chr5 chr6 chr7 chr7 chr9 chr3 chr30	28279651 38296618 38296572 38895418 156377735 74274520 38523524 76272377 76252976 76252976 76252976 7625297 76	227347984 3199080 38959026 157159977 7468803 3855926 777545 777545 7776313 1406933 1406933 1406933 1406933 1406933 747659 7476593 747659 747659 747659 747659 747659 747659 747659 74769 74769	C A A T G G AMAGT T T T C C C C C C C C C C C C C C C C	G G G G G G G G G G G G G G G G G G G	DPF10	B. 52985 P. A36V p. A36V p. A36V p. MIVY p. A646A p. T518- p. T1518- p	Missens, Mutation Missens, Mut	58V 58V 58V 58V 58V 58V 58V 58V	0.21653632 0.18556701 0.22880997 0.128109592 0.225165563 0.271791304 0.177083333 0.171212121 0.301673009 0.315788474 0.100739424 0.100739424 0.100739424 0.100739424 0.100739424 0.100739424 0.100739424 0.100739424 0.100739424 0.100739424 0.100739424 0.100739424 0.100739424 0.100739424 0.100739424 0.100739424 0.100739427 0.100739429 0.1007394	PASS
19957 19957	HICA HICA HICA HICA HICA HICA HICA HICA	(hr) (hr) (hr) (hr) (hr) (hr) (hr) (hr)	382956611 382956611 382956611 38895418 15687726 74274520 74274520 74274520 74274520 169310146 3208223 169310146 3208256 97807837 169310146 3208256 9780783 978	237347884 237387986 237387986 33853926 157159927 74068903 38534926 77077546 7707545 169893142 277077546 169893142 32116487 4785938 98238526 98238526 8923852	C A A A A A A A A A A A A A A A A A A A	T T G G G G G G G G G G G G G G G G G G	DPP10 COL633 ZN#860 PDCDEP CCN1 ALE IFR ZREG3 CMYA5 FCOHA9 FAM1986 AIT68 FMOH39	P. 52985 P. A36V P. A36V P. A36V P. MIV D. MIV D. A646A P. T516 P. K1615 P. K1615 P. K1616 P. T38337 P. F2811 P. F2813 P. F2813 P. F2815 P. F2816 P.	Silent Missense, Mutation Sart, Codon, SNV Silent Sart, Codon, SNV Silent Missense, Mutation	58V 58V 58V 58V 58V 58V 58V 58V 58V 58V	0.21653612 0.18556701 0.22880997 0.22880997 0.22165563 0.221978394 0.77708333 0.771212122 0.0067009 0.315798474 0.100739424 0.	PASS
1991 1992 1992 1992 1992 1992 1992 1992	HICA HICA HICA HICA HICA HICA HICA HICA	chr3 chr3 chr3 chr4 chr4 chr4 chr5 chr5 chr5 chr5 chr5 chr5 chr5 chr6 chr7 chr7 chr9 chr3 chr30	28279651 38296618 38296572 38895418 156377735 74274520 38523524 76272377 76252976 76252976 76252976 7625297 76	227347984 3199080 38959026 157159977 7468803 3855926 777545 777545 7776313 1406933 1406933 1406933 1406933 1406933 747659 7476593 747659 747659 747659 747659 747659 747659 747659 74769 74769	C A A T G G AMAGT T T T C C C C C C C C C C C C C C C C	G G G G G G G G G G G G G G G G G G G	DPF10	B. 52985 P. A36V p. A36V p. A36V p. MIVY p. A646A p. T518- p. T1518- p	Missens, Mutation Silvert Missens, Mutation Silvert Missens, Mutation	58V 58V 58V 58V 58V 58V 58V 58V	0.21653632 0.18556701 0.22880997 0.128109592 0.225165563 0.271791304 0.177083333 0.171212121 0.301673009 0.315788474 0.100739424 0.100739424 0.100739424 0.100739424 0.100739424 0.100739424 0.100739424 0.100739424 0.100739424 0.100739424 0.100739424 0.100739424 0.100739424 0.100739424 0.100739424 0.100739424 0.100739427 0.100739429 0.1007394	PASS

Abbreviations:
REF-reference
RLT-altered
VAF-Variant Allele Fraction
HCA-hepatocellular adenoma
SNV-Single Nucleotide Variant
DEL-deletion
INS-insertion

		er Alterations from					An along the same	Barra Abdan 2010 - III		
sample #1343T	chr chr1	start_hg19 861348	end_hg19 33116108	nMarkers 3655	URR 0.3214	GNL 0	drivHCC_Schulze2015_genes	Beroukhim2010andZack201	cytoStart 1-25-22	cytoEnd
#1343T	chr1	33117588	33138436	3655	-0,1569	-1	ARID1A,RPL22		1p36.33 1p35.1	1p35.1 1p35.1
#1343T	chr1	33146349	249212472	13778	0,2534	0	COL11A1		1p35.1	1944
#1343T	chr2	40221	242842554	13479	0,2463	0	ACVR2A,NFE2L2,EPHA4,APOB		2p25.3	2q37.3
#1343T	chr3	239470	14528614	837	0,2914	0			3p26.3	3p25.1
#1343T	chr3	14535253	14552745	8	0,5896	1			3p25.1	3p25.1
#1343T	chr3	14554324	197769162	10087	0,2549	0	CTNNB1,BAP1,PDE12,KLF15,SETD2		3p25.1	3q29
#1343T	chr4	53291	190947044	7106	0,2312	0	ALB,FGA,GABRA2,IRF2		4p16.3	4q35.2
#1343T	chr5	140602	180687559	7964	0,246	0	ATP10B,MEF2C,IL6ST,DOCK2,ADAMTS19,TERT		5p15.33	5q35.3
#1343T	chr6	203615	32292448	2171	0,2576	0			6p25.3	6p21.32
W1343T	chr6	32299746	32299958	5	-0,27	-1			6p21.32	6p21.32
W1343T W1343T	chr6	32301759 195642	170892714 158937319	6955 8245	0,2363 0,2659	0	CDKN1A,EEF1A1,SPATS1,VEGFA MET		6p21.32 7p22.3	6q27 7q36.3
#1343T	chr8	190866	146280815	6120	0,2566	0	SLURP1,MYC		8p23.3	8q24.3
#1343T	chr9	214910	141017498	6913	0,279	0	CDKN2A,TSC1,MTAP,PTPN3		9p24.3	9q34.3
W1343T	chr10	226000	105727306	5466	0,2534	0	PTEN		10p15.3	10q24.33
#1343T	chr10	105750514	105759665	5	-0,2096	-1			10q24.33	10q24.33
#1343T	chr10	105761266	135373624	1678	0,2584	0			10q24.33	10q26.3
#1343T	chr11	193118	134856548	9816	0,2861	0	HMBS		11p15.5	11q25
#1343T	chr12	208345	57937660	5329	0,2622	0	ARID2,CDKN1B		12p13.33	12q13.3
#1343T	chr12	57937922	57957439	5	-0,2369	-1		,	12q13.3	12q13.3
W1343T W1343T	chr12	57957942 19600450	133811687 115091029	5109 3185	0,2492	0	HNF1A RB1		12q13.3	12q24.33
#1343T	chr13 chr14	20201689	107282930	5910	0,2267	0	RB1		13q12.11 14q11.2	13q34 14q32.33
#1343T	chr15	20170066	65677372	3585	0,2578	0	+			15q22.31
#1343T	chr15	65678941	65703532	9	0,6384	1			15q11.1 15q22.31	15q22.31
#1343T	chr15	65735572	102389376	2590	0,2723	0			15q22.31	15q26.3
W1343T	chr16	96492	90142284	6877	0,3149	0	AXIN1,TSC2,BRD7		16p13.3	16q24.3
#1343T	chr17	6088	81052160	9708	0,3079	0	TP53		17p13.3	17q25.3
#1343T	chr18	163380	77941018	2792	0,2345	0			18p11.32	18q23
#1343T	chr19	282222	45202658	6042	0,359	0	KEAP1		19p13.3	19q13.32
#1343T	chr19	45204710	45206790	3	1,1022	1			19q13.32	19q13.32
#1343T	chr19	45207426	59083958	2468	0,3458	0	SEPW1,TMEM160		19q13.32	19q13.43
#1343T #1343T	chr20 chr21	68379 9825922	62906077 48084620	4377 1825	0,2999	0	DNAIC5 DYRK1A		20p13 21p11.2	20q13.33 21q22.3
#1343T	chr21	17060842	48084620 51219140	1825 3567	0,2816	0	ZNRF3.CLDN5		21p11.2 22q11.1	21q22.3 22q13.33
#1343T	chrX	2700138	154774846	5886	0,2544	0	RPS6KA3		Xp22.33	Xq28
#1424T	chr1	762224	249213866	16643	0,1836	0	ARID1A,RPL22,COL11A1		1p36.33	1944
#1424T	chr2	40221	242842554	12939	0,1685	0	ACVR2A,NFE2L2,EPHA4,APOB		2p25.3	2q37.3
W1424T	chr3	239468	197769154	10510	0,1737	0	CTNNB1,BAP1,PDE12,KLF15,SETD2		3p26.3	3q29
#1424T	chr4	53291	190862085	6995	0,1542	0	ALB,FGA,GABRA2,IRF2		4p16.3	4q35.2
#1424T	chr5	143266	180687559	7686	0,1639	0	ATP10B,MEF2C,IL6ST,DOCK2,ADAMTS19,TERT		5p15.33	5q35.3
#1424T	chr6	203615	170891556	8750	0,1723	0	CDKN1A,EEF1A1,SPATS1,VEGFA		6p25.3	6q27
#1424T #1424T	chr7	195642 891633	891069 896016	43	0,2455	0		7-22.2	7p22.3	7p22.3
#1424T	chr7	891633 899892	158930780	5 7713	-0,2418 0.1806	-1 0	MET	7p22.3	7p22.3 7p22.3	7p22.3 7q36.3
#1424T	chr8	183094	665934	24	0,1695	0	MEI		8p23.3	8p23.3
#1424T	chr8	676520	960314	6	0,5142	1			8p23.3	8p23.3
#1424T	chr8	1497320	146280027	5886	0,1682	0	SLURP1,MYC		8p23.3	8q24.3
#1424T	chr9	213464	141017498	6463	0,1916	0	CDKN2A,TSC1,MTAP,PTPN3		9p24.3	9q34.3
#1424T	chr10	226000	135378996	6784	0,1719	0	PTEN		10p15.3	10q26.3
W1424T	chr11	193118	134257636	9184	0,2006	0	HMBS		11p15.5	11q25
#1424T	chr12	208345	133810818	9447	0,1767	0	ARID2,HNF1A,CDKN1B		12p13.33	12q24.33
#1424T	chr13	19752446	115091029	3118	0,1598	0	RB1		13q12.11	13q34
#1424T #1424T	chr14 chr15	20201689 20450269	107283203 102389376	5294 5542	0,1835 0,1812	0			14q11.2 15q11.1	14q32.33 15q26.3
W1424T	chr15	97088	90142284	6368	0,1812	0	AXIN1,TSC2,BRD7		16p13.3	15q26.3 16q24.3
#1424T	chr17	6088	81052160	9153	0,2144	0	TP53		17p13.3	17q25.3
#1424T	chr18	163380	77960704	2674	0,155	0			18p11.32	18q23
#1424T	chr19	287612	9768755	1623	0,27	0			19p13.3	19p13.2
#1424T	chr19	9770098	9939531	12	-0,0062	0			19p13.2	19p13.2
#1424T	chr19	9959820	23445054	2105	0,2483	0	KEAP1		19p13.2	19p12
#1424T	chr19	23505878	23506923	5	0,7402	1			19p12	19p12
#1424T	chr19	23543160	23578141	5	0,1661	0			19p12	19p12
#1424T	chr19	23648920	23651150	8	0,7238	1	PERMIT TO LOCAL		19p12	19p12
#1424T	chr19	23674706	59083958	4242	0,2364	0	SEPW1,TMEM160 DNAIC5		19p12	19q13.43
#1424T #1424T	chr20 chr21	68379 9825921	62906077 48084620	4131 1719	0,2063	0	DNAJCS DYRKIA		20p13 21p11.2	20q13.33 21q22.3
W1424T	chr21	17061701	48084620 51179116	3329	0,1873	0	ZNRF3,CLDN5		21p11.2 22q11.1	21q22.3 22q13.33
#1424T	chrX	2700138	154774846	5668	0,1723	0	RPS6KA3		Xp22.33	Xq28
#1439T	chr1	762224	115323180	8942	0,06	0	ARID1A,RPL22,COL11A1		1p36.33	1p13.2
#1439T	chr1	115399236	115453070	13	-0,3479	-1			1p13.2	1p13.2
#1439T	chr1	115454151	249213866	8201	0,0437	0			1p13.2	1q44
#1439T	chr2	40221	216981473	11188	0,0211	0	ACVR2A,NFE2L2,APOB		2p25.3	2q35
#1439T	chr2	216982491	216997078	6	-0,3037	-1			2q35	2q35
#1439T	chr2	217002856	227963462	820	0,0991	0	EPHA4		2q35	2q36.3
#1439T #1439T	chr2	227964370 227974184	227973970 242842554	10 1323	-0,329 0,0785	-1 0	+		2q36.3 2q36.3	2q36.3 2q37.3
#1439T	chr2	239468	15614707	965	0,0785	0			2q36.3 3p26.3	3p25.1
#1439T	chr3	15616536	15631082	5	-0,4631	-1			3p25.1	3p25.1
#1439T	chr3	15633146	25666232	241	0,0278	0			3p25.1	3p24.2
#1439T	chr3	25668107	25671880	7	-0,3414	-1			3p24.2	3p24.2
#1439T	chr3	25672360	197769154	9605	0,0382	0	CTNNB1,BAP1,PDE12,KLF15,SETD2		3p24.2	3q29
#1439T	chr4	53291	100257920	4235	0,0202	0	ALB,GABRAZ		4p16.3	4q23
#1439T	chr4	100260802	100268952	6	-0,5787	-1			4q23	4q23
#1439T	chr4	100273822	190862085	3006	-0,0029	0	FGA,IRF2		4q23	4q35.2
#1439T	chr5	143266	180687559	7905	0,0248	0	ATP10B,MEF2C,IL6ST,DOCK2,ADAMTS19,TERT		5p15.33	5q35.3
#1439T	chr6	203615 195642	170891556 158930780	9040 8008	0,0328	0	CDKN1A,EEF1A1,SPATS1,VEGFA MET		6p25.3	6q27 7q36.3
#1439T #1439T	chr7	195642	158930780	8008 4723	0,0482	0	WEI		7p22.3 8p23.3	7q36.3 8q24.12
#1439T	chr8	120770347	120768300	5	-0,4619	-1			8p23.3 8q24.12	8q24.12 8q24.12
#1439T	chr8	120795746	146280027	1367	0,0907	0	SLURP1,MYC		8q24.12	8q24.3
W1439T	chr9	213464	141017498	6652	0,0626	0	CDKN2A,TSC1,MTAP,PTPN3		9p24.3	9q34.3
#1439T	chr10	226000	135381590	6994	0,0329	0	PTEN		10p15.3	10q26.3
#1439T	chr11	193811	17316942	1718	0,0882	0			11p15.5	11p15.1
#1439T	chr11	17317704	17332784	5	-0,4254	-1			11p15.1	11p15.1
#1439T	chr11	17333448	134257636	7727	0,0681	0	HMBS		11p15.1	11q25
W1439T	chr12	208345	133810818	9744	0,0485	0	ARID2,HNF1A,CDKN1B		12p13.33	12q24.33
	chr13	19752446	115091029	3259	0,011	0	RB1		13q12.11	13q34
#1439T		2025								
	chr14 chr15	20201689 20462622	107283203 102389376	5490 5712	0,0414	0			14q11.2 15q11.1	14q32.33 15q26.3

#1439T	chr17	6088	81052160	9366	0,0888	0	TP53		17p13.3	17q25.3
#1439T	chr18	163380	77960704	2777	0,019	0	1135		18p11.32	18q23
#1439T	chr19	287612	55898654	7702	0,1184	0	KEAP1,SEPW1,TMEM160		19p13.3	19q13.42
W1439T	chr19	55899440	55949952	7	0,4976	1		19q13.42	19q13.42	19q13.42
#1439T	chr19	55964714	59083958	408	0,0885	0		-0	19q13.42	19q13.43
#1439T	chr20	68379	62906077	4185	0,083	0	DNAIC5		20p13	20q13.33
#1439T	chr21	9825921	48084620	1760	0,0602	0	DYRK1A		21p11.2	21q22.3
#1439T	chr22	17056656	51179116	3376	0,1121	0	ZNRF3,CLDN5		22q11.1	22q13.33
#1439T	chrX	2700138	154774846	5805	0,038	0	RPS6KA3		Xp22.33	Xq28
#1896T	chr1	69550	179972365	15352	0,9489	0	ARID1A,RPL22,COL11A1,JAK1,NRAS		1p36.33	1q25.2
W1896T	chr1	179975645	180010328	11	1,2772	1			1q25.2	1q25.2
#1896T #1896T	chr1	180010867 41618	249211681 242814646	4649 14755	0,9365	0	ACVR2A,NFE2L2,EPHA4,APOB,ALK		1q25.2	1944
#1896T	chr2 chr3	361505	197765488	11526	0,945	0	CTNNB1,BAP1,KLF15,SETD2,FANCD2,TNFSF10,PIK3CA		2p25.3 3p26.3	2q37.3 3q29
#1896T	chr4	53384	113242	7440	0,9403	0	ETHNOT, BAFT, KEFTS, SET DZ, FANCOZ, THESPTO, FIKSCA		4p16.3	4p16.3
#1896T	chr5	92369	58147085	2100	0,931	0	IL6ST,TERT		5p15.33	5q11.2
#1896T	chr5	58270699	58295339	10	0.5714	-1		PDE4D	5q11.2	5q11.2
#1896T	chr5	58334742	180794757	6411	0,9466	0	ATP10B,MEF2C,DOCK2,ADAMTS19,APC,MAP1B		5q11.2	5q35.3
#1896T	chr6	292550	65149150	4971	0,937	0	CDKN1A,VEGFA		6p25.3	6q12
#1896T	chr6	65300999	117203561	2022	0,5869	-1	EEF1A1,FRK		6q12	6q22.1
W1896T	chr6	117215189	117641112	27	0,908	0			6q22.1	6q22.1
#1896T	chr6	117642489	170893528	2605	0,5848	-1		PARK2	6q22.1	6q27
#1896T	chr7	193502	158937438	9099	0,9459	0	MET,HGF,EGFR,KMT2C,BRAF,NUP205		7p22.3	7q36.3
#1896T	chr8	116555	146279474	6482	0,9425	0	MYC,RSPO2		8p23.3	8q24.3
#1896T	chr9	14874	141016186	7831	0,9367	0	CDKN2A,TSC1,NOTCH1,PTPN3		9p24.3	9q34.3
#1896T	chr10	93526	135440158	7983	0,9443	0	PTEN		10p15.3	10q26.3
#1896T	chr11	193127	134257498	10910	0,9391	0	HMBS,FGF19,IGF2,CDKN1C,ATM		11p15.5	11q25
#1896T	chr12	176326	133810818	11030	0,9446	0	ARIDZ,HNF1A,GLI1,KMT2D,KRAS,PTPRB		12p13.33	12q24.33
#1896T #1896T	chr13 chr13	19748151 96624880	96622441 96675948	2447 9	0,9564 0,5276	-2	RB1,MYCBP2		13q12.11 13q32.1	13q32.1 13q32.1
#1896T	chr13	96684184	115090537	919	0,5276	0			13q32.1 13q32.1	13q32.1 13q34
#1896T	chr13	19378084	105995651	5765	0,9226	0	DICER1		13q32.1 14q11.2	13q34 14q32.33
W1896T	chr14	20740212	103995651	6835	0,9435	0	JICER I		14q11.2 15q11.2	14q32.33 15q26.3
#1896T	chr16	97494	90142284	8255	0,9504	0	AXIN1,TSC2,BRD7		16p13.3	16q24.3
#1896T	chr17	193127	81052161	11559	0,9476	0	TP53,STAT3,ERBB2,NF1		17p13.3	17q25.3
#1896T	chr18	158706	78005195	2946	0,9477	0			18p11.32	18q23
#1896T	chr19	111138	59082559	11156	0,9554	0	KEAP1,CCNE1,JAK3,KMT2B,DNAJB1,PRKACA		19p13.3	19q13.43
W1896T	chr20	68379	62904763	4751	0,9432	0	GNAS		20p13	20q13.33
#1896T	chr21	10959769	42218566	1028	0,5849	-1	DYRK1A	ERG,DSCAM	21p11.1	21q22.2
#1896T	chr21	42540347	48084246	888	0,9134	0			21q22.2	21q22.3
#1896T	chr21	10969099	45658349	83	0,9341	0			21q22.3	21p11.1
#1896T	chr22	19378084	51220669	4045	0,9377	0	ZNRF3,NF2		22q11.21	22q13.33
#1896T	chrX	200918	155239777	6794	0,5725	-1	RPS6KA3	DMD	Xp22.33	Xq28
#1896T	chrY	150918	59342783	121	0,6128	-1			Yp11.32	Yq12
#2189T	chr1	721657	249212472	18794	0,0814	0	ARID1A,RPL22,COL11A1		1p36.33	1q44
#2189T	chr2	40221	242842554	14271	0,0887	0	ACVR2A,NFE2L2,EPHA4,APOB		2p25.3	2q37.3
#2189T	chr3	239470	197769162	11532	0,0849	0	CTNNB1,BAP1,PDE12,KLF15,SETD2		3p26.3	3q29
#2189T	chr4	53291	190947577	7422	0,0977	0	ALB,FGA,GABRA2,IRF2		4p16.3	4q35.2
#2189T	chr5	140602	177054498	7964	0,0893	0	ATP10B,MEF2C,IL6ST,DOCK2,ADAMTS19,TERT		5p15.33	5q35.3
W2189T W2189T	chr5	177163594 177310749	177309702 180687559	6 402	0,6198	1			5q35.3	5q35.3
#2189T	chr5	203615	170892714	9687	0,0673	0	CDKN1A,EEF1A1,SPATS1,VEGFA		5q35.3 6p25.3	5q35.3 6q27
#2189T	chr7	195642	158937319	9014	0,0861	0	MET		7p22.3	7q36.3
#2189T	chr8	190866	145001461	6115	0,0961	0	SLURP1,MYC		8p23.3	8q24.3
#2189T	chr8	145001756	145006648	6	-0,3399	-1	January, mrs		8q24.3	8q24.3
#2189T	chr8	145007120	146280815	359	0,0421	0			8q24.3	8q24.3
#2189T	chr9	172880	141070232	7493	0,0739	0	CDKN2A,TSC1,MTAP,PTPN3		9p24.3	9q34.3
#2189T	chr10	226000	135439464	7604	0,0891	0	PTEN		10p15.3	10q26.3
#2189T	chr11	193118	134856548	10639	0,0777	0	HMBS		11p15.5	11q25
#2189T	chr12	208345	133811687	11105	0,0888	0	ARID2,HNF1A,CDKN1B		12p13.33	12q24.33
#2189T	chr13	19600450	115091029	3312	0,0947	0	RB1		13q12.11	13q34
#2189T	chr14	20201689	107283203	6272	0,0871	0			14q11.2	14q32.33
#2189T	chr15	20170066	83936934	5539	0,0836	0			15q11.1	15q25.2
#2189T	chr15	83951925	84241383	5	-0,3938	-1			15q25.2	15q25.2
#2189T	chr15	84245414	102389376	1092	0,082	0				15q26.3
#2189T	chr16								15q25.2	Todeoro
#2189T	chr17	97096	90161144	7691	0,0721	0	AXIN1,TSC2,BRD7		15q25.2 16p13.3	16q24.3
#2189T		6088	81083508	7691 10854	0,0702	0	AXIN1,TSC2,BRD7 TP53		15q25.2 16p13.3 17p13.3	16q24.3 17q25.3
	chr18	6088 117194	81083508 9593818	7691 10854 489	0,0702 0,0973	0 0			15q25.2 16p13.3 17p13.3 18p11.32	16q24.3 17q25.3 18p11.22
#2189T	chr18 chr18	6088 117194 9595083	81083508 9593818 9814052	7691 10854 489 5	0,0702 0,0973 -0,348	0 0 0 -1			15q25.2 16p13.3 17p13.3 18p11.32	16q24.3 17q25.3 18p11.22 18p11.22
#2189T	chr18 chr18 chr18	6088 117194 9595083 9815165	81083508 9593818 9814052 77941018	7691 10854 489 5 2450	0,0702 0,0973 -0,348 0,098	0 0 0 -1 0	TPS3		15q25.2 16p13.3 17p13.3 18p11.32 18p11.22 18p11.22	16q24.3 17q25.3 18p11.22 18p11.22 18q23
#2189T #2189T	chr18 chr18 chr18 chr19	6088 117194 9595083 9815165 107510	81083508 9593818 9814052 77941018 59083958	7691 10854 489 5 2450 10017	0,0702 0,0973 -0,348 0,098 0,0612	0 0 0 -1 0	TP53 KEAP1,SEPW1,TMEM160		15q25.2 16p13.3 17p13.3 18p11.32 18p11.22 18p11.22 18p13.3	16q24.3 17q25.3 18p11.22 18p11.22 18q23 19q13.43
#2189T #2189T #2189T	chr18 chr18 chr18 chr19 chr20	6088 117194 9595083 9815165 107510 68379	81083508 9593818 9814052 77941018 59083958 62906077	7691 10854 489 5 2450 10017 4715	0,0702 0,0973 -0,348 0,098 0,0612 0,1037	0 0 0 -1 0 0	TP53 KEAPI,SEPWI,TMEM160 DNAVCS		15q25.2 16p13.3 17p13.3 18p11.32 18p11.22 18p11.22 19p13.3 20p13	16q24.3 17q25.3 18p11.22 18p11.22 18q23 19q13.43 20q13.33
#2189T #2189T #2189T #2189T	chr18 chr18 chr18 chr19 chr20 chr21	6088 117194 9595083 9815165 107510 68379 9825922	81083508 9593818 9814052 77941018 59083958	7691 10854 489 5 2450 10017 4715 1947	0,0702 0,0973 -0,348 0,098 0,0612 0,1037 0,082	0 0 0 -1 0 0 0	TP53 KEAPLSEPWI,TMEMISO DNAJC5 DYRKIA		15q25.2 16p13.3 17p13.3 18p11.32 18p11.22 18p11.22 19p13.3 20p13 21p11.2	16q24.3 17q25.3 18p11.22 18p11.22 18q23 19q13.43 20q13.33 21q22.3
#2189T #2189T #2189T #2189T #2189T	chr18 chr18 chr18 chr19 chr20	6088 117194 9595083 9815165 107510 68379 9825922 17060842	81083508 9593818 9814052 77941018 59083958 62906077 48084620 51219140	7691 10854 489 5 2450 10017 4715 1947 4004	0,0702 0,0973 -0,348 0,098 0,0612 0,1037 0,082 0,0691	0 0 0 -1 0 0 0	TP53 KEAPI,SEPWI,TMEM160 DNAUCS		15q25.2 16p13.3 17p13.3 18p11.32 18p11.22 18p11.22 19p13.3 20p13	16q24.3 17q25.3 18p11.22 18p11.22 18q23 19q13.43 20q13.33
#2189T #2189T #2189T #2189T	chr18 chr18 chr18 chr19 chr20 chr21 chr21	6088 117194 9595083 9815165 107510 68379 9825922	81083508 9593818 9814052 77941018 59083958 62906077 48084620	7691 10854 489 5 2450 10017 4715 1947	0,0702 0,0973 -0,348 0,098 0,0612 0,1037 0,082	0 0 0 -1 0 0 0	TP53 KEAPLSEPWI,TMEMIEO DNAUCS DYRKIA ZNRF3,CLDNS		15q25.2 16p13.3 17p13.3 18p11.32 18p11.22 18p11.22 19p13.3 20p13 21p11.2 22q11.1 Xp22.33	16q24.3 17q25.3 18p11.22 18p11.22 18q23 19q13.43 20q13.33 21q22.3 22q13.33
#2189T #2189T #2189T #2189T #2189T #2189T	chr18 chr18 chr18 chr19 chr20 chr21 chr22 chrX	6088 117194 9595083 9815165 107510 68379 9825922 17060842 2700138	81083508 9593818 9814052 77941018 59083958 62906077 48084620 51219140 154774846	7691 10854 489 5 2450 10017 4715 1947 4004 4595	0,0702 0,0973 -0,348 0,098 0,0612 0,1037 0,082 0,0691	0 0 0 -1 0 0 0 0	TP53 KEAPLSEPWI,TMEMIEO DNAUCS DYRKIA ZNRF3,CLDNS		15q25.2 16p13.3 17p13.3 18p11.32 18p11.22 18p11.22 19p13.3 20p13 21p11.2 22q11.1	16q24.3 17q25.3 18p11.22 18p11.22 18q23 19q13.43 20q13.33 21q22.3 22q13.33 Xq28
#2189T #2189T #2189T #2189T #2189T #2189T #2189T #2189T	chr18 chr18 chr18 chr19 chr20 chr21 chr22 chrX chrY	6088 117194 9595083 9815165 107510 68379 9825922 17060842 2700138 2655318	81083508 9593818 9814052 77941018 59083958 62906077 48084620 51219140 154774846 24457064	7691 10854 489 5 2450 10017 4715 1947 4004 4595	0,0702 0,0973 -0,348 0,098 0,0612 0,1037 0,082 0,0691 0,0774	0 0 0 -1 0 0 0 0 0	TP53 KEAPI,SEPWI,TMEMISO DNAUCS DYAKIA ZNIF3,CLONS RPSOKAS		15q25.2 16p13.3 17p13.3 18p11.32 18p11.22 18p11.22 19p13.3 20p13 21p11.2 22q11.1 Xp22.33 Yp11.31	16q24.3 17q25.3 18p11.22 18p11.22 18q23 19q13.43 20q13.33 21q22.3 22q13.33 Xq28 Yq11.223
#2189T #2189T #2189T #2189T #2189T #2189T #2189T #222T	chr18 chr18 chr18 chr19 chr20 chr21 chr22 chrX chrY chr1	6088 117194 9595083 9815165 107510 68379 9825922 17060842 2700138 2655318 861348	81083508 9593818 9814052 77941018 59083958 62906077 48084620 51219140 154774846 24457064 203012574	7691 10854 489 5 2450 10017 4715 1947 4004 4595	0,0702 0,0973 -0,348 0,098 0,0612 0,1037 0,082 0,0691 0,0774 0,0874	0 0 0 -1 0 0 0 0 0 0	TP53 KEAPI,SEPWI,TMEMISO DNAUCS DYAKIA ZNIF3,CLONS RPSOKAS		15q25.2 16p13.3 17p13.3 18p11.32 18p11.22 18p11.22 19p13.3 20p13 21p11.2 22q11.1 xp22.33 Yp11.31 1p36.33	16q24.3 17q25.3 18p11.22 18p11.22 18q23 19q13.43 20q13.33 21q22.3 22q13.33 Xq28 Yq11.223 1q32.1
#2189T #2189T #2189T #2189T #2189T #2189T #2189T #222T #222T #222T	chr18 chr18 chr19 chr20 chr21 chr21 chr21 chr22 chrX chrY chr1 chr1	6088 117194 9595083 9815165 107510 68379 9825922 17060842 2700138 2655318 861348 203013543 402058 402058	81083508 9593818 9814052 77941018 99083958 99083958 48084620 51219140 154774846 22457064 203012574 203018848 249212472 242842554	7691 10854 489 5 2450 10017 4715 1947 4004 4595 145 14887 5 3054	0,0702 0,0973 -0,348 0,098 0,0612 0,1037 0,082 0,0691 0,0774 0,0874 0,1045 -0,3601 0,1154 0,1314	0 0 0 -1 0 0 0 0 0 0 0 0 0 0	TP53 KEAPI,SEPWI,TMEMISO DNAUCS DYNKLA ZNRF3,CLONS RP56KA3 ARIDIA, RP122,COLIIAI ACVR2A,NF212,EPHAI,APOB		15q25.2 16p13.3 17p13.3 18p11.32 18p11.22 18p11.22 19p13.3 20p13 21p11.2 22q11.1 Xp22.33 Yp11.31 1p36.33 1q32.1 2p25.3	16q24.3 17q25.3 18p11.22 18p11.22 18q23 19q13.43 20q13.33 21q22.3 22q13.33 Xq28 Yq11.223 1q32.1
#2189T #2189T #2189T #2189T #2189T #2189T #2189T #2189T #222T #222T #222T #222T	chr18 chr18 chr18 chr18 chr19 chr20 chr21 chr22 chrX chrY chr1 chr1 chr1 chr1 chr1 chr2 chr3	6088 117194 9595083 9815165 107510 68379 9825922 17060842 2700138 2655318 861348 203013543 203020658 40221 239470	81083508 9593818 9514052 77941018 59083958 62906077 48084620 51219140 154774846 24457064 203012574 203018848 249212472 249212472 197769162	7691 10854 489 5 2450 10017 4715 1947 4004 4595 145 14887 5 3054 13571 11085	0,0702 0,0973 -0,348 0,098 0,0612 0,1037 0,082 0,0691 0,0774 0,0874 0,1154 0,1154 0,1314 0,1225	0 0 0 -1 0 0 0 0 0 0 0 0 0 0 0 0 0	TP53 KEAPJ,SEPWI,TMEMISO DNAUCS DYRKIA ZNRF3,CLDNS RPSOKAS ARIDIA,RPJ2Z,COLIIAI ACVRZA,NFEZIZ,EPHAA,APOB CTNBB_BAPJ,POEZ,KEJTS,SETOZ		15q25.2 16p13.3 17p13.3 18p11.32 18p11.22 18p11.22 19p13.3 20p13 21p11.2 22q11.1 Xp22.33 Yp11.31 1p36.33 1q32.1 1q32.1 2p25.3 3p26.6	16q24.3 17q25.3 18p11.22 18p11.22 18p11.22 18q23 19q13.43 20q13.33 21q22.3 22q13.33 ×q28 yq11.223 1q32.1 1q44 2q37.3 3q29
#2189T #2189T #2189T #2189T #2189T #2189T #2189T #222T #222T #222T #222T #222T	chr18 chr18 chr18 chr18 chr19 chr20 chr21 chr22 chrX chrY chr1 chr1 chr1 chr1 chr1 chr1 chr2 chr3 chr4	6088 117194 9959083 9815165 107510 68379 9825922 17060842 2700138 2655318 861348 203013543 203020658 40221 239470 53291	81083508 9593818 9814052 77941018 59083958 62296077 48084620 51219140 154774846 24457064 203012574 203012848 249212472 242842554 197769162 190947044	7691 10854 489 5 2450 10017 4715 1947 4004 4595 145 14887 5 3054 13571 11085 7105	0,0702 0,0973 -0,348 0,098 0,0612 0,0691 0,0691 0,0774 0,087 0,0874 0,1045 -0,3601 0,1154 0,1154 0,1154 0,1225 0,1423	0 0 0 -1 0 0 0 0 0 0 0 0 0 0 0	TP53 KEAP1.SEPW1,TMEM160 DNAUCS DYNKLA ZNNF3.CLONS RP56KA3 ARIDIA.RP12.COL11A1 ACVR2A,NFE12.FPHA4.APOB CTNNB1.BAP1.PG12.KKT35.SETD2 ALB.RGA.GABRARAJRF2 ALB.RGA.GABRARAJRF2		15q25.2 16p13.3 17p13.3 18p11.32 18p11.22 18p11.22 12p11.2 22q11.1 Xp22.33 Yp11.31 1q36.33 1q32.1 2p25.3 3p26.3 4p16.3	16q24.3 17q25.3 18p11.22 18p11.22 18q23 19q13.43 20q13.33 21q22.3 22q13.33 Xq28 Yq11.223 1q32.1 1q32.1 1q44 2q37.3 3q29 4q35.2
#2189T #2189T #2189T #2189T #2189T #2189T #2189T #2189T #222T #222T #222T #222T #222T #222T #222T	chr18 chr18 chr18 chr19 chr20 chr21 chr21 chr22 chrX chrY chr1 chr1 chr1 chr1 chr1 chr2 chr3 chr4 chr5	6088 117194 9995083 9815165 107510 68379 9825922 17060842 2700138 2655318 861348 203013543 203020658 40221 239470	81083508 9593818 9814052 77941018 9814052 77941018 62906077 48084520 154774846 24457064 203012574 203012574 203012574 203012574 197769162 197769162 197769162 197769162	7691 10854 489 5 2450 10017 4715 1947 4004 4595 14887 5 3054 13571 11085 705 8014	0,0702 0,0973 -0,348 0,098 0,0612 0,1037 0,082 0,0691 0,0774 0,0874 0,1045 -0,3601 0,1154 0,1314 0,1225 0,1423 0,1312	0 0 0 0 0 0 0 0 0 0 0 0 0 0 0 0 0 0 0	TP53 KEAPI, SEPWI, TMEMISO DNACS DYRKIA ZNRF3, CLONS RP50KAS ARIDIA, RPL22, COLIIA1 ACV22A, NFEZIZ, EPHAA, APOB CTNNB1, BAP1, POEIZ, RLF15, SETD2 ALB, GRAGABRAZ, IRF2 ATPIDB, MEZEZ, LISET, DOCAZ, ADAMMSTS, TERT		15q25.2 16p13.3 17p13.3 18p11.32 18p11.22 18p11.22 19p13.3 20p13 21p11.2 22q11.1 Xp22.33 Yp11.31 1p36.33 1q32.1 1q32.1 1q32.1 5p15.3 3p26.3 4p16.3	16q24.3 17q25.3 18p11.22 18p11.22 18p11.22 18q23 20q13.33 21q22.3 22q13.33 4q28 Yq11.223 1q32.1 1q32.1 1q44 2q37.3 3q29 4q48 2q37.3 3q29 4q58.3
#21897 #21897 #21897 #21897 #21897 #21897 #21897 #22207 #22207 #22207 #22207 #22207 #22207 #22207 #22207	chv18 chv18 chv18 chv19 chv20 chv20 chv21 chv22 chrX chrY chr1 chr1 chr1 chr1 chr1 chr2 chr3 chr4 chr4 chr5 chr6	6088 117194 9595083 9815165 107510 68379 9825922 17060842 2700138 2655318 861348 203013543 203020658 40221 239470 53291 140602 203615	81083508 9593818 9814052 77941018 59083958 62906077 48084620 51219140 154774846 24457064 2457064 203018848 249212472 203018848 249212472 197947044 180687559 170892714	7691 10854 489 5 5 2450 10017 4715 1947 4004 4595 145 14887 5 3054 13571 11085 7105 8014	0,0702 0,0973 -0,348 0,098 0,0612 0,1037 0,082 0,0691 0,0774 0,0874 0,1045 -0,3601 0,1154 0,1225 0,1423 0,1312 0,1232	0 0 0 -1 0 0 0 0 0 0 0 0 0 0 0 0 0 0 0 0	TP53 KEAP1.SEPW1,TMEM160 DNAUCS DYNKLA ZNNF3.CLONS RP56KA3 ARIDIA.RP12.COL11A1 ACVR2A,NFE12.FPHA4.APOB CTNNB1.BAP1.PG12.KKT35.SETD2 ALB.RGA.GABRARAJRF2 ALB.RGA.GABRARAJRF2		15q25.2 16p13.3 17p13.3 18p11.32 18p11.22 18p11.22 19p13.3 20p13 21p11.2 22q11.1 Xp22.33 Yp11.3 1p36.33 1q32.1 1q32.1 2p25.3 3p26.3 4p16.3 5p15.33 6p25.3	16q24.3 17q25.3 18p11.22 18p11.22 18p23 19q13.43 20q13.33 21q22.3 22q2.3 24q2.3 1q22.3 1q22.3 1q22.3 2q28 Yq11.223 1q32.1 1q44 2q32.3 2q28 4q35.2 5q25.3 6q27
#2189T #2189T #2189T #2189T #2189T #2189T #2189T #2189T #222T #222T #222T #222T #222T #222T #222T	chr18 chr18 chr18 chr19 chr20 chr20 chr21 chr2 chrX chrY chr1 chr1 chr1 chr1 chr1 chr2 chr3 chr4 chr5 chr6 chr7	6088 117194 9959083 9815165 9815165 68379 9825922 17060842 2700138 2655518 861348 203001543 2030020658 40221 239470 53291 140602 203615	81083508 9593818 9814052 779341018 59083958 62906077 48084620 51219140 154774846 24457064 203012574 203012574 203012848 249212472 242842554 197769162 190947044 180687559 170892714	7691 10854 489 5 5 2450 10017 4715 1947 4004 4595 14887 5 13571 11085 8014 9230	0,0702 0,0973 -0,348 0,098 0,0612 0,062 0,0691 0,0774 0,0874 0,1045 -0,3601 0,1154 0,1314 0,1225 0,1423 0,1312 0,1423 0,1312 0,1312 0,1312 0,1423 0,1312	0 0 0 -1 0 0 0 0 0 0 0 0 0 0 0 0 0 0 0 0	TP53 KEAPI, SEPWI, TMEMISO DNACS DYRKIA ZNRF3, CLONS RP50KAS ARIDIA, RPL22, COLIIA1 ACV22A, NFEZIZ, EPHAA, APOB CTNNB1, BAP1, POEIZ, RLF15, SETD2 ALB, GRAGABRAZ, IRF2 ATPIDB, MEZEZ, LISET, DOCAZ, ADAMMSTS, TERT		15cg5.2 16p13.3 17p13.3 18p11.32 18p11.22 18p11.22 18p11.22 18p11.22 19p13.3 20p13 22p11.1 22q11.1 xp22.33 yp11.31 1p86.33 1q32.1 1q32.1 2p25.3 3p26.3 4p16.3 5p15.33 6p25.3 7p22.3	16q24.3 17q25.3 18p11.22 18p11.22 18p13.2 19q13.43 20q13.33 21q22.3 21q22.3 1q32.1 1q32.1 1q44 2q37.3 3q29 4q35.2 5q35.3
#2189T #2189T #2189T #2189T #2189T #2189T #2189T #222T #222T #222T #222T #222T #222T #222T #222T #222T	chr18 chr18 chr18 chr19 chr20 chr20 chr21 chr22 chrX chr1 chr1 chr1 chr1 chr1 chr2 chr3 chr4 chr5 chr6 chr7	6088 117194 9595083 9815165 107510 68379 9825922 17060842 2700138 861348 203020658 40221 239470 53291 140602 203615 193386	81083508 9593818 9514052 777941018 59083958 62906077 48084620 51219140 154774846 203012574 203012574 203012574 1180687559 170892714 100244414 100253126	7691 10854 489 5 5 2450 10017 4715 1947 4004 4595 1485 14887 5 3054 13571 11085 7105 8014 9230 4910 6	0,0702 0,0973 -0,348 0,098 0,0612 0,1037 0,082 0,0991 0,0774 0,1045 -0,3601 0,1154 0,1154 0,1154 0,1154 0,1225 0,1423 0,1423 -0,0624 -0,0624	0 0 0 0 0 0 0 0 0 0 0 0 0 0 0 0 0 0 0	TP53 KEAP1.SEPW1,TMEM160 DNACCS DVRKIA 2NR13,CLONS RP50KA3 ARID1A,RP122,COL11A1 ACVB2A,NTE12,EPHAA,APOB CTNNE1,BAP1,POE1,RLS15,SETD2 ALS,GGAGARD2,RP2 AFPLOB,MET2C,LISST,DOCK2,ADAMTS19,TERT CONNIA, EEFIAL,SPATS1,VEGFA		15;05:2 16;013:3 170;13.3 18;01:12:3 18;01:12:1 18;01:12:1 18;01:12:1 18;01:12:1 18;01:12:1 18;01:12:1 19;01:3 10;01:1	16q24.3 17q25.3 18p11.22 18p11.22 18p11.22 18q23 20q13.33 21q22.3 22q13.33 Xq28 Yq11.22 1q22.1 1q32.1 1q32.1 1q42.1 1q44 2q37.3 3q29 4q35.2 5q25.3 6q27 7q22.1
#2189T #2189T #2189T #2189T #2189T #2189T #2189T #2189T #222T #222T #222T #222T #222T #222T #222T #222T #222T #222T	chr18 chr18 chr18 chr19 chr20 chr20 chr21 chr22 chr1 chr1 chr1 chr1 chr1 chr1 chr1 chr2 chr3 chr4 chr4 chr5 chr6 chr7 chr7 chr7 chr7	6088 111794 9555083 9815165 107510 68379 9825922 2700138 265318 265318 265318 40221 228470 5329 140602 229013661 10234664	81093508 99214052 77941018 9908998 62906077 4808450 51219140 154772846 24457064 200112574 200112574 20011888 249212472 242841556 197799162 19094704 110082714 110082714 110082714 110082715	7691 10854 489 5 5 10017 4715 1947 4004 4595 145 5 3054 13371 11085 7018 8014 4910 6	0.0702 0.0873 -0.348 0.089 0.098 0.091 0.0012 0.0024 0.0074 0.0074 0.0074 0.0154 0.1154 0.1154 0.1225 0.1312 0.1423 0.1423 0.1423 0.1423 0.1424 0.1525 0.1526 0	0 0 0 1 1 0 0 0 0 0 0 0 0 0 0 0 0 0 0 0	TP53 KEAPI,SEPWI,TMEMISO DNAUCS DYRKIA ZNRSJ,CLONS RPSGKA3 ARIDIA,RP122,COLIAI ACV82A,NF212,EPHA4,APOB CTNNB1,BAP1,PB212,KF15,SETD2 ALBJ,GAG,BABR2,JR12 ATP108,MF52L,LIST,DOCK2,ADAMTS19,TERT CONNIA,EEFIAL,SPATS1,VEGFA		15-05-2 16-01-3 16-01-3 16-01-12 18-01-12 18-01-12 18-01-12 18-01-12 18-01-12 18-01-12 18-01-12 18-01-13 18-01-13 18-01-3 18-01-13 18-01-3 1	16q24.3 17q25.3 18p11.22 18p11.22 18p13.3 12q13.43 22q13.33 22q13.33 xq28 Yq11.223 1q32.1 1q32.1 1q44 2q37.3 3q29 4q35.2 5q35.3 6q27 7q22.1
#2189T #222T	chr18 chr18 chr18 chr19 chr20 chr20 chr21 chr22 chrX chr1 chr1 chr1 chr1 chr1 chr2 chr3 chr4 chr5 chr4 chr5 chr6 chr7 chr7 chr7 chr7 chr7 chr7 chr8	6088 11794 9595083 9815165 107510 107	82003508 9598185 9598185 9598395 5298697 4800450 51219140 51217486 5245704 20011584 2445704 20011584 24921247 242825 199947044 19994704	7691 10854 489 5 5 10017 4715 1947 4004 4595 145 14887 15801 11085 7105 8014 9230 4910 6 3887 6220	0.0702 0.0973 0.098 0.098 0.098 0.0091 0.0074 0.0091 0.0774 0.1055 0.1154 0.1154 0.1225 0.1225 0.1225 0.1227 0.0574 0	0 0 0 0 0 0 0 0 0 0 0 0 0 0 0 0 0 0 0	TP53 KEAPI,SEPWI,TMEMISO DNACS DVAKIA ZNRF3,CLDNS RPSGRAS ARIDIA,RPL22,COLIIAI ACVR2A,NFE212,EPHAA,APOB CTNMB1,BAP1,POE1Z,RIP15,SETD2 ALB,GGA,GBARAZ,RIP2 ATPIOS,MERZ_LOST,DOEA,DAMMISI,FIERT CDKNIA,EEFIAI,SPATSI,VEGFA MET SLUPPJ,MYC		15-95-2 16-91-3 179-13-3 189-11-2 189-11-2 189-11-2 189-11-2 189-11-2 199-13-3 20-91-1 22-91-1 192-2-3 79-12-3 193-3 194-3 194-3 19	16q24.3 17q25.3 18p11.22 18p11.22 18p11.23 19q13.43 20q13.33 21q22.3 22q13.33 22q13.33 1q32.1 1q32.1 1q44 2q37.3 3q29 4q35.2 5q25.3 6q27 7q22.1 7q22.1
#21897 #21897 #21897 #21897 #21897 #21897 #21897 #22207	chv18 chv18 chv18 chv19 chv20 chv21 chv22 chv2 chv2 chv1 chv1 chv1 chv1 chv1 chv1 chv1 chv1	6088 111794 9555083 9815165 107510 68379 9825922 2700138 265318 265318 265318 40221 228470 5329 140602 229013661 10234664	81005308 9959818 9959818 9914052 77941018 9908938 62996077 4808450 51219140 2457064 200105848 2457064 200105848 197799162 19799162 19799162 19799162 19799162 19799162 1979917 19799714 100244414 1002461559 115997719	7691 10854 489 5 5 2450 10017 4715 1947 4004 4595 145 153571 11085 7105 8014 9230 4910 6 3887 6220	0.0702 0.0897 -0.348 0.098 0.098 0.091 0.0091 0.0074 0.0874 0.0874 0.0874 0.1154 0.1154 0.1225 0.1423 0	0 0 0 0 0 0 0 0 0 0 0 0 0 0 0 0 0 0 0	TP53 KEAPI,SEPWI,TMEMISO DNAUCS DYRKIA ZNRSJ,CLONS RPSGKA3 ARIDIA,RP122,COLIAI ACV82A,NF212,EPHA4,APOB CTNNB1,BAP1,PB212,KF15,SETD2 ALBJ,GAG,BABR2,JR12 ATP108,MF52L,LIST,DOCK2,ADAMTS19,TERT CONNIA,EEFIAL,SPATS1,VEGFA		15-93-2 15-93-3 15-91-3 15-91-3 15-91-3 15-91-12 15-91-12 15-91-12 15-91-13 15-91-3 15	16q24.3 17q25.3 18p11.22 18p11.22 18p11.22 18q13.3 19q13.43 20q13.33 21q22.3 22q3.33 xq28 yq11.223 1q32.1 1q32.1 1q32.1 1q42.1 2q37.3 3q29 4q55.2 5q55.3 6q27 7q22.1 7q36.3 8q24.3
#21897 #21897 #21897 #21897 #21897 #21897 #21897 #21897 #21897 #21897 #21897 #21897 #21897 #22217 #22217 #22217 #22217 #22217 #22217 #22217 #22217 #22217 #22217 #22217 #22217 #22217 #22217 #22217 #22217 #22217 #22217 #2221	chv18 chv18 chv18 chv19 chv20 chv21 chv21 chv21 chv2 chv7 chv1 chv1 chv1 chv1 chv1 chv1 chv1 chv1	6088 117294 117294 117294 1952083 9815165 107510 107510 68379 9825952 17006942 2700138 2655318 2655318 2651349 203010549 10201055 1100353661 1100253661 1100253661	82003508 9598185 9598185 9598395 5298697 4800450 51219140 51217486 5245704 20011584 2445704 20011584 24921247 242825 199947044 19994704	7691 10954 489 5 5 2450 10017 4715 1947 4004 4595 14887 5 14887 5 10017	0.0702 0.0703 0.0813 0.098 0.098 0.0812 0.0891 0.0774 0.0774 0.1055 0.1154 0.1225 0.1225 0.1225 0.1226 0.1226 0.1226 0.1226 0.1226 0.1227 0.1227 0.1228 0.1228	0 0 0 0 0 0 0 0 0 0 0 0 0 0 0 0 0 0 0	TP53 KEAPI,SEPWI,TMEMISO DNACS DVRKIA ZNRF3,CLONS RPSGKA3 ARIDIA,RPL22,COLIJA1 ACVB2A,NFEZI2,EPHA4,APOB CTINNBLBAPI,PDEZ,RAFIS,SETD2 ALB,FGA,GABRA2,IRF2 APIDB,MRF2C,LIGST,DOCKZ,DAMMISI9,TERT CDKNIA,EEFIAI,SPATSI,VEGFA MET SLURPI,MYC CDKNIA,MYCPPTPN3		15-95-2 16-913-3 17913-3 18911-12 18911-12 18911-12 18911-12 18911-12 18911-12 18911-12 18911-12 18911-12 18911-12 18911-12 18911-12 18911-12 19911-13 190-3-3	16q24.3 17q25.3 18p11.22 18p11.22 18p11.22 18q13.3 19q13.43 20q13.33 21q22.3 22q13.33 Xq28 Yq11.223 1q32.1 1q42.1 1q44 2q37.3 3q29 4q47.7 2q37.3 5q25 5q25.3 6q27 7q22.1 7q22.1 7q22.3
#21897 #21897 #21897 #21897 #21897 #21897 #21897 #21897 #21897 #21897 #2227 #2277 #2227 #227 #227 #2227 #2227 #2227 #2227 #2227 #2227 #2227 #2227 #2227 #2227 #2227 #2227 #2227 #2227 #2227 #2227 #2227 #27 #	chv18 chv18 chv18 chv19 chv19 chv20 chv21 chv21 chv2 chv3 chv1 chv1 chv1 chv1 chv1 chv1 chv2 chv2 chv2 chv2 chv3 chv4 chv2 chv4 chv5 chv6 chv7 chv7 chv7 chv7 chv7 chv7 chv7 chv7	6088 10784 9595083 9815165 107510 107510 107510 68379 9825952 17006842 2700138 265518 20500569 40221 239470 239470 10024860 10024860 10024860 100258661 10026866 218910 12734018	81005308 9959818 99518165 9951816 9951816 995085958 62996077 49608450 51219140 151774846 24517064 24517064 24517064 24517064 24517064 24517064 19779162 19799162 19799162 19799162 19799162 19799162 19799170162 1	7691 10854 489 5 10017 4715 1947 4004 4595 1487 13871 13107 13887 6 6 3887 6 3887 7 7 7 2354	0.0702 0.0873 -0.348 0.0897 -0.348 0.098 0.0912 0.0137 0.0274 0.074 0.074 -0.1154 0.1154 0.1225 -0.060 0.1423 0.1423 -0.0624 -0.066 0.1286 0.1286 0.1286	0 0 0 0 0 0 0 0 0 0 0 0 0 0 0 0 0 0 0	TP53 KEAP1.SEPW1,TMEM160 DNAUCS DYNKLA ZNNF3.CLONS RP56KA3 ARIDIA,RP12.COL11A1 ACVR2A,NFE112,EPHA4.APOB CTNNR1,BAP1.P0E12,KF15,SET02 ARIBGAGABRAZ,RR12 AFP106,MFF2C,MSF1,DOCK2.ADAMTS19,TERT CDKNIA,EF1A1.SPATS1,VEGFA MET SLUPPJ,MYC CDKNIA,MFFAPTFN3 TSC1		15:05:2 16:013:3 17:013.3 28:01.12 18:01.12 18:01.12 18:01.12 18:01.12 18:01.12 18:01.12 18:01.12 18:01.12 18:01.13 20:013 12:18:11 22:18:11 22:18:11 22:18:11 22:18:11 22:18:11 22:18:11 22:18:18 22:18:18:18 22:18:18:18 22:18:18:18 22:18:18:18 22:18:18:18 22:18:18:18 22:18:18:18 22:18:18:18 22:18:18:18 22:18:18:18 22:18:18:18 22:18:18:18 22:18:18:18 23:18:18 23:18 23:18	16q24.3 17q25.3 18p11.22 18p11.2 18q12.3 19q13.43 20q13.33 21q22.3 22q13.33 74q2.3 14q2.1 14q2.1 14q2.1 14q2.1 14q2.1 14q2.1 14q3.5 14q
#21897 #21897 #21897 #21897 #21897 #21897 #21897 #21897 #21897 #21897 #21897 #22217 #2217 #22	chr18 chr18 chr18 chr19 chr20 chr21 chr21 chr21 chr21 chr2 chr1 chr1 chr1 chr1 chr1 chr1 chr2 chr3 chr4 chr5 chr6 chr7 chr7 chr7 chr7 chr8 chr7 chr9 chr9 chr9 chr9 chr9 chr9 chr9 chr9	6088 11779 3959083 9815165 107510 107	81093508 99314052 77941018 9098398 62906677 90906977 90906977 90906977 90906977 90906977 90906977 909069 909069 9090697 9090697 9090697 9090697 9090697 909069	7691 10954 489 5 5 5 10017 4715 1947 4004 499 14887 14887 13971 11085 7105 8014 4910 6 1387 6220 4735 7 2334	0.0702 0.0973 -0.348 0.098 0.098 0.0061 0.0072 0.0074 0.0074 0.1045 -0.3601 0.1154 0.1225 0.1225 0.1226 0.1226 0.1236	0 0 0 0 0 0 0 0 0 0 0 0 0 0 0 0 0 0 0	TP53 KEAPI,SEPWI,TMEMISO DNACS DVRKIA ZNR3,CLONS RP56KA3 ARIDIA,RP1,2C,COLIJA1 ARIDIA,RP1,2C,COLIJA1 ACVR2A,NF212,EPHA4,APOB CTNNB1,BAPI,PDE1,RV13,SETD2 ALB,FGA,GABRA2,JRF2 ATP10B,MF2F2,CLSS,DOCK2,ADAMTS19,TERT CONNIA, EEFIAI,SPATSI,VEGFA MET SLURPJ,MYC COKKIGA,MTAP,FPN3 TSC1 PFEN		15-95-2 15-913-3 15-9	16q24.3 18p11.22 18p11.22 18p11.23 18q13.23 19q13.43 20q13.33 Xq28 Val1.223 1q32.1 1
#21897 #21897 #21897 #21897 #21897 #21897 #21897 #21897 #21897 #22217 #2217 #2217 #2217 #2217 #22217 #22217 #22217 #22217 #22217 #22217 #22217 #22217 #22217 #22217 #22217 #22217 #22217 #22217 #22217 #22217 #22217 #22217	thr18 thr18 thr18 thr19 thr20 thr20 thr21 thr21 thr2 thr3 thr1 thr1 thr1 thr1 thr2 thr3 thr4 thr4 thr4 thr4 thr5 thr6 thr7 thr8 thr9 thr9 thr9 thr9 thr9 thr9 thr9 thr9	6088 17294 955083 9815165 107510 107510 107510 68379 9825922 17006842 2700138 265318 200213643 20020568 40221 239470 100244650 100244650 100254664 110234666 214910 117734618	81005308 9959818 9959818 9814052 77941018 90085958 62956077 48004620 51219140 15477484 20511284 20411284 20411284 19779162 19794104 19084104 19084104 19084104 19084104 19084104 146279982 12720847 12720847 12720847 114017489	7691 10854 489 5 10954 489 100017 4715 1947 4004 4599 1488 5 10017 14887 14887 14887 14887 14887 1605 17105 18014 1871 1871 1871 1871 1871 1871 1871 18	0.0702 0.0873 -0.348 0.098 0.091 0.091 0.091 0.091 0.0774 0.0774 0.1145 -0.1601 0.1144 0.1225 -0.0624 -0.066 0.1246 -0.124 -0.066 0.1246 0.1246 0.1247 -0.066 0.067 -0.067 -0.067	0 0 0 0 0 0 0 0 0 0 0 0 0 0 0 0 0 0 0	TP53 KEAPI.SEPWI,TMEMI60 DNACCS DYRKIA ZNNF3,CLONS RP56KA3 ARIDIA.RPJ2,COLI1A1 ACVR2A,NFE12,EPMA,AFOB CTNNB1,BAPI.PD12,KR115,SETD2 AIR JAB AND		15:05:2 16:013:3 17:013.3 28:01.13:2 18:01.12:2 18:01.12:2 18:01.12:2 18:01.12:2 18:01.12:2 18:01.12:3 18:01.12:3 18:01.12:3 18:01.13:3 18:01.1	16q24.3 17q25.3 18p11.22 18p11.22 18p11.22 18q23 19q13.43 20q13.33 21q22.3 22q13.33 Xq28 Yq11.223 1q32.1 1q32.1 1q32.1 1q42.1 1q42.1 1q42.1 1q42.1 1q42.1 1q42.1 1q42.1 1q42.1 1q42.1 1q43.2 1q
#21897 #21897 #21897 #21897 #21897 #21897 #21897 #21897 #21897 #21897 #21897 #22217 #2217 #22	chr18 chr18 chr18 chr19 chr20 chr21 chr21 chr21 chr21 chr2 chr1 chr1 chr1 chr1 chr1 chr1 chr2 chr3 chr4 chr5 chr6 chr7 chr7 chr7 chr7 chr8 chr7 chr9 chr9 chr9 chr9 chr9 chr9 chr9 chr9	6088 11779 3959083 9815165 107510 107	81093508 99314052 77941018 9098398 62906677 90906977 90906977 90906977 90906977 90906977 90906977 909069 909069 9090697 9090697 9090697 9090697 9090697 909069	7691 10954 489 5 5 5 10017 4715 1947 4004 499 14887 14887 13971 11085 7105 8014 4910 6 1387 6220 4735 7 2334	0.0702 0.0973 -0.348 0.098 0.098 0.0061 0.0072 0.0074 0.0074 0.1045 -0.3601 0.1154 0.1225 0.1225 0.1226 0.1226 0.1236	0 0 0 0 0 0 0 0 0 0 0 0 0 0 0 0 0 0 0	TP53 KEAPI,SEPWI,TMEMISO DNACS DVRKIA ZNR3,CLONS RP56KA3 ARIDIA,RP1,2C,COLIJA1 ARIDIA,RP1,2C,COLIJA1 ACVR2A,NF212,EPHA4,APOB CTNNB1,BAPI,PDE1,RV13,SETD2 ALB,FGA,GABRA2,JRF2 ATP10B,MF2F2,CLSS,DOCK2,ADAMTS19,TERT CONNIA, EEFIAI,SPATSI,VEGFA MET SLURPJ,MYC COKKIGA,MTAP,FPN3 TSC1 PFEN		15-95-2 16-913-3 16-913-3 17913-3 18-91-12-2 18-91-12-2 18-91-12-2 18-91-12-2 18-91-12-2 18-91-12-2 18-91-12-2 18-91-12-2 18-91-13-1 18-91-3 1	16q24.3 17q25.3 18p11.22 18p11.22 18p12.3 19q13.49 20q13.33 Xq28 Yq11.222 1q32.1 1q42.1 1q42.1 1q42.1 1q42.1 1q22.1 1q32.1 1q44 2q37.3 6q27 7q22.1 7q22.1 7q22.1 7q22.1 7q36.3 8q4.3 9q33.3 9q33.3 9q33.3 9q33.3 10q26.3 11q25.1
#21897 #21897 #21897 #21897 #21897 #21897 #21897 #21897 #21897 #21897 #21897 #21897 #2227 #227 #227 #227 #227 #	chv18 chv18 chv18 chv18 chv19 chv20 chv21 chv21 chv1 chv1 chv1 chv1 chv1 chv1 chv1 chv	6088 11779 959083 9815165 107510 107510 107510 108379 9825952 17006842 2700138 68379 2825922 17006842 2700138 681348 203020658 681348 203020658 100244650 100254661 100254650 110254650 110254650 110254650 12724013 12724400 12724013	81093508 9593818 9914052 77941018 95083958 62906077 4808450 51219140 15477846 2457064 200112574 200112574 200112574 10043746 10054759 179892714 10054754 10054759 179892714 10054754 12720947 12720947 12720947 12720947 12720947 13548930 11548930 11548930 11548930	7691 10854 489 5 2450 10017 4715 1947 4004 4595 14887 5 3054 13571 11085 7105 8014 4910 6 6 3887 6 2230 4910 7 2354 6 7 2356 10161	0.0702 0.0873 -0.348 0.089 0.098 0.091 0.001 0.002 0.0024 0.0074 0.0074 0.0074 0.0154 0.1154 0.1154 0.1225 0.1312 0.1	0 0 0 0 0 0 0 0 0 0 0 0 0 0 0 0 0 0 0	TP53 KEAPI.SEPWI,TMEMI60 DNACCS DYRKIA ZNNF3,CLONS RP56KA3 ARIDIA.RPJ2,COLI1A1 ACVR2A,NFE12,EPMA,AFOB CTNNB1,BAPI.PD12,KR115,SETD2 AIR JAB AND		15:05:2 16:013:3 17:013.3 28:01.13:2 18:01.12:2 18:01.12:2 18:01.12:2 18:01.12:2 18:01.12:2 18:01.12:3 18:01.12:3 18:01.12:3 18:01.13:3 18:01.1	16q24.3 17q25.3 18p11.22 18p11.22 18p11.22 19q13.43 20q13.33 21q22.3 22q13.33 Xq28 Yq11.223 1q32.1 1q32.1 1q32.1 1q42.1 1q42.1 1q44 2q37.3 3q29 4q35.2 5q35.3 6q27 7q22.1 7q36.3 8q24.3 9q33.3 9q33.3 9q33.3 9q34.3 10q66.3
#21897 #21897 #21897 #21897 #21897 #21897 #21897 #21897 #21897 #22217 #2217 #2217 #221	chv18 chv18 chv18 chv19 chv20 chv21 chv21 chv2 chv1 chv1 chv1 chv1 chv1 chv1 chv2 chv2 chv2 chv2 chv2 chv2 chv2 chv2	6088 117294 595083 9815165 107510 107510 107510 68379 98279522 17006842 2700138 2655318 863148 203011543 203011543 203012655 103026565 10324656 10324660 1193188 117230418 117230418 117230418 117230418 117230418 117230418	81005308 9959818 9959818 9814052 77941018 9006959 62950677 48004620 51219140 15177486 204517064 205012574 202012584 197799152 19789718 190547084 190547088 190547084 1	7691 10954 489 5 5 10017 4715 1947 4004 4595 14887 14887 5 14887 1601 13871 11085 8014 9230 4910 6 6 3887 6220 4735 77 2354 2354 2354	0.0702 0.0973 -0.348 0.0987 -0.0981 0.0991 0.0091 0.0091 0.0091 0.0091 0.0091 0.0144 0.1144 0.1125 0.1144 0.125 0.0142 0.0142 0.0064 0.0774 0.0774 0.0774 0.0774 0.0774 0.0774 0.0774 0.0774 0.1144 0.1125 0.0475 0.0475 0.0475	0 0 0 0 0 0 0 0 0 0 0 0 0 0 0 0 0 0 0	TP53 KEAP1.SEPW1,TMEM160 DNACCS DVRKIA ZNN33,CLONS RP5GKA3 ARID1A.RP122.COL11A1 ACVR2A.NF1212.EPHAA,APOB CTNNB1_BAP1.P0121.K1151.SETD2 AGGAGRAPAZITY AFPIDS.MF521_CHEST_DOCK2_ADAMMTS1_PTERT CDKN1A.EEF1A1_SPATS1_VEGFA MET SURP1_MYC CDKN2A_MTAP.PTPN3 TSC1 PTEN HM85 ARID2.CDKN1B		15-95-2 16-913-3 18-91-13-2 18-91-13-2 18-91-13-2 18-91-13-2 18-91-13-2 18-91-13-2 18-91-13-2 18-91-13-2 18-91-13-3 18-91-13-3 18-91-13-3 18-91-13-3 18-91-13-3 18-91-13-3 18-91-13-3 18-91-13-3 18-91-13-3 18-91-13-3 18-91-13-3 11-91-5 20-91-3 20-91-3 20-9	16q24.3 17q25.3 18p11.22 18p11.22 18p11.22 18q13.3 19q13.43 20q13.33 21q22.3 22q13.33 Xq28 Yq11.22.1 1q32.1 1q32.1 1q32.1 1q44 2q37.3 3q29 4q35.2 5q35.3 6q27 7q22.1 7q36.3 8q24.3 9q33.3 9q34.3 1q32.1 1q25.1 1q26.3 1q26.
#21897 #21897 #21897 #21897 #21897 #21897 #21897 #21897 #21897 #21897 #21897 #22217 #2217 #2217 #2217 #22217 #22217 #22217 #22217 #22217 #22217 #22217 #22217 #2221	chv18 chv18 chv18 chv18 chv19 chv20 chv21 chv21 chv2 chvX chvY chv1 chv1 chv1 chv1 chv1 chv2 chv3 chv6 chv6 chv7 chv7 chv7 chv7 chv7 chv8 chv9 chv9 chv9 chv9 chv10 chv1	6088 11729 11729 11759 9851565 9851565 107510 68379 9825952 17006842 2700138 265318 265318 265318 265318 265318 1002465 1002465 10024661 10024561 110235461	81005308 9593818 9514652 77941018 95083918 62966077 48084520 51219140 15477484 24657064 24051276 24084570 15477484 2408127 15477484 2408127 15477484 100018888 19994704 19994704 190947	7691 10854 489 5 2450 10017 4715 1947 4004 4595 14887 5 3054 13571 11085 7105 8014 4910 6 4910 6 4725 7 5226 10151 77286	0.0702 0.0873 -0.348 0.0893 0.0982 0.0982 0.0991 0.00174 0.0874 0.0874 0.0874 0.1154 0.1154 0.1225 0.1312 0.1312 0.1225 0.0423 0.0527 0.0527 0.0527 0.0527 0.0527 0.0528	0 0 0 0 0 0 0 0 0 0 0 0 0 0 0 0 0 0 0	TP53 KEAPI,SEPWI,TMEMIGO DNAUCS DVAKUA 2NRF3,CLORS RP56KA3 ARIDIA,8P1,2C,COLIAI ARIDIA,8P1,2C,COLIAI ACVR2A,NF212,EPHA4,APOB CTNNB1,BAP1,PDE12,K151,5,ETD2 ALB,RGA,GABRAZ,RR72 ATPIOR,MEF2C,USST,DOCK2,ADAMTS19,TERT CDN11A,EEFIAI,SPATS1,VEGFA MET SURPJ,MYC CDKN2A,MTAP,PTPN3 TSC1 PTEN 1HMBS ARIDZ,COPIIB HNES ARIDZ,COPIIB		15:05:2 16:013:3 16:013:3 18:01:12:1 18:01:12:1 18:01:12:1 18:01:12:1 18:01:12:1 18:01:12:1 18:01:12:1 18:01:12:1 18:01:12:1 18:01:12:1 18:01:13:1 18:01:1	16024.3 18011.22 18011.22 18011.22 18011.22 18021.3 18021.3 1902.
#21897 #21897 #21897 #21897 #21897 #21897 #21897 #21897 #21897 #22217 #2217 #22	chv18 chv18 chv18 chv19 chv20 chv21 chv21 chv2 chv2 chv2 chv1 chv1 chv1 chv1 chv1 chv1 chv2 chv2 chv2 chv2 chv2 chv2 chv2 chv2	6088 11794 9595083 9815165 107510 9785083 9815165 107510 9825922 17066842 2700138 68379 9825922 17066842 2700138 68139 9825922 17066842 230013643 1000145 100015 1000015 100015 100015 1000015 1000015 1000015 1000015 1000015 1000015 10	81005308 9959818 9959818 9814052 77941018 9908995 62956077 4808452 5119140 511	7691 10954 489 5 5 10017 4715 1947 4004 4595 14887 5 14887 5 8014 13571 11065 8014 9210 6 6 887 7 7 2254 4735 7 7 2254 10161 6788 8811	0.0702 0.0703 -0.488 0.0963 -0.0961 0.0961 0.0962 0.0961 0.0974 0.0774 0.0144 0.1154 0.1314 0.1314 0.1314 0.1312 0.0423 0	0 0 0 0 0 0 0 0 0 0 0 0 0 0 0 0 0 0 0	TP53 KEAPI,SEPWI,TMEMIGO DNAUCS DVAKUA 2NRF3,CLORS RP56KA3 ARIDIA,8P1,2C,COLIAI ARIDIA,8P1,2C,COLIAI ACVR2A,NF212,EPHA4,APOB CTNNB1,BAP1,PDE12,K151,5,ETD2 ALB,RGA,GABRAZ,RR72 ATPIOR,MEF2C,USST,DOCK2,ADAMTS19,TERT CDN11A,EEFIAI,SPATS1,VEGFA MET SURPJ,MYC CDKN2A,MTAP,PTPN3 TSC1 PTEN 1HMBS ARIDZ,COPIIB HNES ARIDZ,COPIIB		15-95-2 16-913-3 18-91-12-2 18-91-12-2 18-91-12-2 18-91-12-2 18-91-12-2 18-91-12-2 18-91-12-2 18-91-12-2 18-91-12-2 18-91-12-2 18-91-12-2 18-91-12-2 18-91-12-2 18-91-13-3 18-91	16q24.3 17q25.3 18p11.22 18p11.22 18p12.3 18q23 19q13.43 20q13.33 21q22.3 22q13.33 24q22.3 22q13.33 24q27 1q22.1 1q24.1 1q24.1 1q24.7 1q25.2 1q27.7 1q26.3 6q27 7q22.1 7q26.3 8q24.3 9q33.3 9q34.3 10q26.3 11q25 11q25 11q26 11q
#21897 #21897 #21897 #21897 #21897 #21897 #21897 #21897 #21897 #21897 #21897 #21897 #2221	chv18 chv18 chv18 chv18 chv19 chv20 chv21 chv2 chv2 chv7 chv1 chv1 chv1 chv2 chv3 chv4 chv3 chv6 chv6 chv7 chv7 chv7 chv7 chv7 chv7 chv7 chv7	6088 117294 117294 1952083 9815165 107510 68379 9825922 17006842 2700138 2655318 2655318 2655318 265148 203010569 10024560 1100253661 1100253661 1100253661 1100253661 127230018 127234018 127234018 127234018 127234018 127234018 127234018 127234018	81005308 9959818 9959818 9914052 77941018 99089398 62996077 4808450 51219140 24457064 200016848 24457064 200016848 2421247 200016848 197709162 197909162 197	7691 10854 489 15 2450 10017 4715 1947 4004 4595 14887 5 10854 14887 5 10954 13571 11085 7705 8014 4910 6 7230 4910 6 7235 7 7 7 2354 7286 10161 6 779 8 817 8817 8817	0.0702 0.0873 -0.348 0.0893 -0.098 0.0981 0.0091 0.0091 0.0074 0.0874 0.0874 0.0154 0.1154 0.1154 0.1152 0.1152 0.1225 0.0627 0.1225 0.0627 0.1226 0.1226 0.1226 0.1226 0.1226 0.1226 0.1226	0 0 0 0 0 0 0 0 0 0 0 0 0 0 0 0 0 0 0	TP53 KEAPI,SEPWI,TMEMIGO DNAUCS DVAKUA 2NRF3,CLORS RP56KA3 ARIDIA,8P1,2C,COLIAI ARIDIA,8P1,2C,COLIAI ACVR2A,NF212,EPHA4,APOB CTNNB1,BAP1,PDE12,K151,5,ETD2 ALB,RGA,GABRAZ,RR72 ATPIOR,MEF2C,USST,DOCK2,ADAMTS19,TERT CDN11A,EEFIAI,SPATS1,VEGFA MET SURPJ,MYC CDKN2A,MTAP,PTPN3 TSC1 PTEN 1HMBS ARIDZ,COPIIB HNES ARIDZ,COPIIB		15-95-2 16-913-3 16-913-3 18-91-12-1 18-91-12-1 18-91-12-1 18-91-12-1 18-91-12-1 18-91-12-1 18-91-12-1 18-91-12-1 18-91-12-1 18-91-13-1 18-91-1	16q24.3 17q25.3 18p11.22 18p11.22 18p11.23 19q13.43 20q13.33 21q22.3 22q13.33 1q22.1 1q32.1 1
#21897 #21897 #21897 #21897 #21897 #21897 #21897 #21897 #21897 #21897 #21897 #22217 #2217 #22	chv18 chv18 chv18 chv19 chv19 chv20 chv21 chv21 chv2 chv2 chv2 chv2 chv1 chv1 chv1 chv1 chv1 chv1 chv2 chv2 chv2 chv2 chv2 chv2 chv2 chv2	6088 11779 959083 9815165 107510 1075	81003508 9593818 9914052 77941018 95083958 62906077 48008450 51219140 154778846 24457064 200112594 200112594 200112594 201012594 100447044 100647559 179892714 100647564 100647569 179892714 100234114 100234116 1158997319 115897319 115897319 1158997319 1158997319 1158997319 1158997319 1158997319 115897319 115899731 115899731 11589731 1	7691 10954 489 5 5 10017 489 10017 1097 10017 1947 4004 4004 4595 14887 5 3054 13371 11085 7105 8014 4910 6 6 3387 6220 4735 7 7286 10161 10161 68 8 3817 3162 6019 3817 3162	0.0702 0.0702 0.0873 -0.348 0.0893 0.098 0.0991 0.0092 0.0991 0.0074 0.0074 0.0074 0.0074 0.0074 0.0074 0.0074 0.0074 0.0074 0.0074 0.0074 0.0074 0.0078 0.0078 0.0078 0.0078 0.0078 0.0078 0.0078 0.0078 0.0078 0.0078	0 0 0 0 0 0 0 0 0 0 0 0 0 0 0 0 0 0 0	TP53 KEAPI,SEPWI,TMEMISO DNACS DNACS DVRKIA ZNR3,CLONS RP56KA3 ARIDIA,RP1,2,COLIJA1 ACVR2A,NF212,EPHA4,APOB CTNNB1,BAPI,PDE1,RV13,SETD2 ALB,GGA,GABRA2,JRF2 ATP108,MF27,CLIST,DOCK2,ADAMTS19,TERT CONNIA, EEFIAI,SWATSI,VEGFA MET SLURPI,MYC COKKIGA,MTAP,PFN3 TSC1 PFTN HM85 ARID2,CONIB HNF3A RB1		15-95-2 16-913-3 17913-3 18911-12 18911-12 18911-12 18911-12 18911-12 18911-12 18911-12 18911-12 18911-12 18911-12 18911-12 18911-12 18911-12 18911-12 18911-13 18911	16024.3 17025.3 18011.22 18011.22 18011.22 18011.23 18023 19011.43 19011.43 21022.3 22013.33 Xq28 4011.222 1492.1
#21897 #21897 #21897 #21897 #21897 #21897 #21897 #21897 #21897 #21897 #21897 #21897 #21897 #2221	chv18 chv18 chv18 chv19 chv20 chv21 chv22 chvX chv1 chv1 chv1 chv1 chv1 chv1 chv2 chv2 chv2 chv3 chv4 chv4 chv5 chv6 chv7 chv7 chv7 chv7 chv7 chv7 chv1 chv1 chv1 chv1 chv1 chv2 chv2 chv2 chv3 chv4 chv5 chv6 chv7 chv7 chv7 chv7 chv7 chv7 chv7 chv7	6088 6088 985165 985165 985165 107510 68379 9825922 17006842 2700138 265318 861348 220013543 220013543 220013543 10025465 100254664 1900666 112724601 12724601	81005308 9959818 9951815 9951819 9951819 9951819 9951819 1397181 1397181	7691 10954 489 5 10954 489 10017 10954 10017 1947 4715 1947 4004 45995 1488 5 10017 13571 11085 1005 11085 7105 80114 715 8014 715 8016 6 887 6220 4715 7288 8817 2354 7288 8817 2354 7286 881	0.0702 0.0873 -0.348 0.0897 -0.348 0.098 0.0912 0.0137 0.092 0.0991 0.0774 0.0774 0.0774 0.1154 0.1154 0.1225 -0.1660 0.1144 0.1225 -0.056 0.1286	0 0 0 0 0 0 0 0 0 0 0 0 0 0 0 0 0 0 0	TP53 KEAP1.SEPW1,TMEM160 DNAUCS DYNKIA ZNRF3.CLONS RP56KA3 ARIDIA.RP12Z.COL11A1 ACVR2A,NF21Z.FPHAA,APOB CTNNB1,BAP1.P021_XKT31_SETD2 ARIBAGA,GRARAZ,TR12 ATP106,MEF2C_MEST_DOCK2_ADAMTS19,TERT CONNIA.EFF1A1.SPATS1,VEGFA MET SLURP1_AWC CONNAA_MTAP.FPTN3 TSC1 PFEN HMB5 ARID2.CON1B HNF3A RB1 AWN1,TSC2_BRD7		15-93-2 15-93-2 15-91-3 17-91-3 17-91-3 17-91-3 18-91-12 18-91-12 18-91-12 18-91-12 18-91-12 18-91-12 18-91-12 18-91-12 18-91-12 18-91-13	16q24.3 17q25.3 18p11.22 18p11.2 18q13.3 19q13.43 20q13.33 21q22.3 22q13.33 Xq28 Yq11.223 1q32.1 1q32.1 1q32.1 1q42.1 1q44.2 2q37.3 3q29 4q35.2 5q55.3 6q27 7q22.1 7q22.1 7q22.3 2q33.3 9q33.3 9q33.3 9q33.3 9q33.3 10q26.3 11q24.3 12q26.3 12

#222T	chr21	9825922	48084620	1860	0,1021	0	DYRK1A		21p11.2	21q22.3
#222T	chr22	17063472	51219140	3796	0,0617	0	ZNRF3,CLDN5		22q11.1	22q13.33
#222T	chrX	2700138	154774846	4077	0.0988	0	RPS6KA3		Xp22.33	Xq28
#222T	chrY	2655318	23548182	122	0,1171	0			Yp11.31	Yq11.223
#2615T	chr1	721657	84641485	7908	-0,1422	0	ARID1A,RPL22		1p36.33	1p31.1
#2615T	chr1	84644854	84650824	5	-0,6937	-1			1p31.1	1p31.1
#2615T	chr1	84662362	249212472	11080	-0,1442	0	COL11A1		1p31.1	1q44
#2615T	chr2	40221	242946533	14500	-0,1369	0	ACVR2A,NFE2L2,EPHA4,APOB		2p25.3	2q37.3
#2615T	chr3	239470	197769162	11715	-0,1481	0	CTNNB1,BAP1,PDE12,KLF15,SETD2		3p26.3	3q29
#2615T	chr4	53291	190947577	7639	-0,1399	0	ALB,FGA,GABRA2,IRF2		4p16.3	4q35.2
W2615T	chr5	140602	180687559	8569	-0,1418	0	ATP10B,MEF2C,IL6ST,DOCK2,ADAMTS19,TERT		5p15.33	5q35.3
#2615T	chr6	203615	170892714	9829	-0,1491	0	CDKN1A,EEF1A1,SPATS1,VEGFA		6p25.3	6q27
#2615T	chr7	195642	21521641	1107	-0,142	0			7p22.3	7p15.3
#2615T	chr7	21551452	21913004	78	-0,4883	-1			7p15.3	7p15.3
#2615T	chr7	21920414	158937319	7891	-0,1479	0	MET		7p15.3	7q36.3
W2615T	chr8	190866	25286210	1236	-0,1195	0			8p23.3	8p21.2
#2615T	chr8	25287278	25298140	7	-0,4595	-1			8p21.2	8p21.2
#2615T	chr8	25301829	146280815	5333	-0,143	0	SLURP1,MYC		8p21.2	8q24.3
#2615T	chr9	172880	141017498	7493	-0,1447	0	CDKN2A,TSC1,MTAP,PTPN3	3	9p24.3	9q34.3
#2615T	chr10	226000	135439464	7728	-0,1406	0	PTEN		10p15.3	10q26.3
W2615T	chr11	193118	134856548	10634	-0,14	0	HMBS		11p15.5	11q25
#2615T	chr12	208345	133811687	11259	-0,1439	0	ARID2,HNF1A,CDKN1B		12p13.33	12q24.33
#2615T	chr13	19600450	115091029	3427	-0,1414	0	RB1		13q12.11	13q34
#2615T	chr14	20201689	107282930	6363	-0,1442	0			14q11.2	14q32.33
#2615T	chr15	20170066	102389376	6697	-0,2156	0			15q11.1	15q26.3
W2615T	chr16	96492	90161144	7575	-0,142	0	AXIN1,TSC2,BRD7		16p13.3	16q24.3
#2615T	chr17	6088	81052160	10743	-0,1434	0	TP53		17p13.3	17q25.3
#2615T	chr18	117194	77960704	3010	-0,1396	0			18p11.32	18q23
#2615T	chr19	107510	59083958	9643	-0,151	0	KEAP1,SEPW1,TMEM160		19p13.3	19q13.43
#2615T	chr20	68379	62906077	4681	-0,1397	0	DNAICS		20p13	20q13.33
#2615T	chr21	9825922	48084620	1968	-0,2622	0	DYRKIA		21p11.2	21q22.3
#2615T	chr22	17060354	51219140	3957	-0,1405	0	ZNRF3,CLDN5		22q11.1	22q13.33
W2615T	chrX	2700138	154774846	6320	-0,1478	0	RPS6KA3		Xp22.33	Xq28
#2729T	chr1	69550	110260004	10019	0,7148	0	ARID1A,RPL22,COL11A1		1p36.33	1p13.3
#2729T	chr1	110279742	110282886	8	0,4017	0			1p13.3	1p13.3
#2729T	chr1	110293018	146739131	1452	0,6656	0			1p13.3	1q21.1
#2729T	chr1	146740489	146747844	5	0,2869	-1			1q21.1	1q21.1
W2729T	chr1	146751781	153752390	1079	0,6864	0			1q21.1	1q21.3
#2729T	chr1	153782720	153791332	8	0,3793	0			1q21.3	1q21.3
#2729T	chr1	153792146	155156470	414	0,7253	0			1q21.3	1q22
#2729T	chr1	155158648	155165847	11	1,084	1			1q22	1q22
#2729T	chr1	155166918	186289497	3159	0,6621	0			1q22	1q31.1
#2729T	chr1	186291497	186300672	7	0,199	-1			1q31.1	1q31.1
#2729T	chr1	186301401	249211681	4128	0,6744	0			1q31.1	1944
#2729T	chr2	41618	242814646	15016	0,6699	0	ACVR2A,NFE2L2,EPHA4,APOB		2p25.3	2q37.3
#2729T	chr3	361505	126451993	7694	0,6925	0	CTNNB1,BAP1,PDE12,KLF15,SETD2		3p26.3	3q21.3
#2729T	chr3	126571531	127295700	42	1,0134	1			3q21.3	3q21.3
#2729T	chr3	127295876	197765488	3970	0,6496	0			3q21.3	3q29
#2729T	chr4	53384	113242	7572	0,639	0			4p16.3	4p16.3
W2729T	chr5	92369	180018436	8550	0,6607	0	ATP10B,MEF2C,IL6ST,DOCK2,ADAMTS19,TERT		5p15.33	5q35.3
#2729T	chr5	180030291	180058730	30	0,9596	0			5q35.3	5q35.3
#2729T	chr5	180076516	180794757	64	0,6987	0			5q35.3	5q35.3
#2729T	chr6	292550	170893528	9752	0,6671	0	CDKN1A,EEF1A1,SPATS1,VEGFA		6p25.3	6q27
#2729T	chr7	193502	158937438	9228	0,6899	0	MET		7p22.3	7q36.3
#2729T	chr8	116555	146279474	6599	0,6813	0	SLURP1,MYC		8p23.3	8q24.3
#2729T	chr9	14874	141016186	7940	0,7144	0	CDKN2A,TSC1,MTAP,PTPN3		9p24.3	9q34.3
#2729T	chr10	93526	76854535	3792	0,6631	0			10p15.3	10q22.2
#2729T	chr10	76855443	76865526	5	0,9547	0			10q22.2	10q22.2
#2729T	chr10	76867858	135440158	4289	0,7022	0	PTEN		10q22.2	10q26.3
#2729T	chr11	193127	73078727	7167	0,7508	0			11p15.5	11q13.4
#2729T	chr11	73100204	73118632	11	1,0292	1		3	11q13.4	11q13.4
#2729T	chr11	73120619	126141442	3458	0,6621	0	HMBS		11q13.4	11q24.2
#2729T	chr11	126142919	126160823	10	1,0376	1			11q24.2	11q24.2
#2729T	chr11	126162692	134257498	376	0,7098	0			11q24.2	11q25
#2729T	chr12	176326	133810818	11199	0,6758	0	ARID2,HNF1A,CDKN1B		12p13.33	12q24.33
#2729T	chr13	19748151	115090537	3441	0,6518	0	RB1		13q12.11	13q34
#2729T	chr14	19378084	105995651	5880	0,6873	0			14q11.2	14q32.33
#2729T	chr15	20740212	28625712	347	0,7131	0			15q11.2	15q13.1
#2729T	chr15	28626388	28630829	11	1,0531	1			15q13.1	15q13.1
#2729T	chr15	28632272	91354536	6127	0,698	0			15q13.1	15q26.1
#2729T	chr15	91358420	91456914	52	0,9726	1			15q26.1	15q26.1
#2729T	chr15	91459420	102462803	417	0,6783	0			15q26.1	15q26.3
#2729T	chr16	97494	74487148	7072	0,7501	0	AXIN1,TSC2,BRD7		16p13.3	16q23.1
							, touris, tous, enter			16q23.1
#2729T	chr16	74490600	74683065	34	0,4966	0	7.0012,1302,0107		16q23.1	
#2729T	chr16	74685919	90142284	1215	0,7763	0			16q23.1 16q23.1	16q24.3
#2729T #2729T	chr16 chr17	74685919 193127	90142284 17716738	1215 2969	0,7763 0,7384	0	TP53		16q23.1 16q23.1 17p13.3	16q24.3 17p11.2
#2729T #2729T #2729T	chr16 chr17 chr17	74685919 193127 17716983	90142284 17716738 17720361	1215 2969 9	0,7763 0,7384 1,1405	0 0 1			16q23.1 16q23.1 17p13.3 17p11.2	16q24.3 17p11.2 17p11.2
#2729T #2729T #2729T #2729T	chr16 chr17 chr17 chr17	74685919 193127 17716983 17720670	90142284 17716738 17720361 19648361	1215 2969 9 418	0,7763 0,7384 1,1405 0,7811	0 0 1			16q23.1 16q23.1 17p13.3 17p11.2 17p11.2	16q24.3 17p11.2 17p11.2 17p11.2
#2729T #2729T #2729T #2729T #2729T	chr16 chr17 chr17 chr17 chr17	74685919 193127 17716983 17720670 19679691	90142284 17716738 17720361 19648361 19752700	1215 2969 9 418 23	0,7763 0,7384 1,1405 0,7811 0,512	0 0 1 0			16q23.1 16q23.1 17p13.3 17p11.2 17p11.2 17p11.2	16q24.3 17p11.2 17p11.2 17p11.2 17p11.2
#2729T #2729T #2729T #2729T #2729T #2729T	chr16 chr17 chr17 chr17 chr17 chr17	74685919 193127 17716983 17720670 19679691 19753071	90142284 17716738 17720361 19648361 19752700 19769095	1215 2969 9 418 23	0,7763 0,7384 1,1405 0,7811 0,512 1,0394	0 0 1 0 0			16q23.1 16q23.1 17p13.3 17p11.2 17p11.2 17p11.2 17p11.2	16q24.3 17p11.2 17p11.2 17p11.2 17p11.2 17p11.2
#2729T #2729T #2729T #2729T #2729T #2729T	chr16 chr17 chr17 chr17 chr17 chr17 chr17	74685919 193127 17716983 17720670 19679691 19753071 19770685	90142284 17716738 17720361 19648361 19752700 19769095 37226189	1215 2969 9 418 23 3 1806	0,7763 0,7384 1,1405 0,7811 0,512 1,0394 0,7324	0 0 1 0 0 0			16q23.1 16q23.1 17p13.3 17p11.2 17p11.2 17p11.2 17p11.2 17p11.2	16q24.3 17p11.2 17p11.2 17p11.2 17p11.2 17p11.2 17p11.2
#2729T #2729T #2729T #2729T #2729T #2729T #2729T #2729T	chr16 chr17 chr17 chr17 chr17 chr17 chr17 chr17 chr17 chr17	74685919 193127 17716983 17720670 19679691 19753071 19770685 37228721	90142284 17716738 17720361 19648361 19752700 19769095 37226189 37234233	1215 2969 9 418 23 3 1806	0,7763 0,7384 1,1405 0,7811 0,512 1,0394 0,7324 1,0145	0 0 1 0 0 1 0			16q23.1 16q23.1 17p13.3 17p11.2 17p11.2 17p11.2 17p11.2 17p11.2 17p11.2	16q24.3 17p11.2 17p11.2 17p11.2 17p11.2 17p11.2 17p11.2 17q12 17q12
#2729T #2729T #2729T #2729T #2729T #2729T #2729T #2729T #2729T	chr16 chr17	74685919 193127 17716983 17720670 19679691 19753071 19770685 37228721 37235387	90142284 17716738 17720361 19648361 19752700 19769095 37226189 37234233 60663541	1215 2969 9 418 23 3 1806 2 3437	0,7763 0,7384 1,1405 0,7811 0,512 1,0394 0,7324 1,0145 0,724	0 0 1 0 0 1 0 NA			16q23.1 16q23.1 17p13.3 17p11.2 17p11.2 17p11.2 17p11.2 17p11.2 17p11.2 17q12	16q24.3 17p11.2 17p11.2 17p11.2 17p11.2 17p11.2 17p11.2 17q12 17q12 17q22 17q23.2
#2729T #2729T #2729T #2729T #2729T #2729T #2729T #2729T #2729T #2729T	chr16 chr17	74685919 193127 17716983 17720670 19679691 19753071 19770685 37228721 37235387 60673991	90142284 17716738 17720361 19648361 19752700 19769095 37226189 37234233 60663541 60689839	1215 2969 9 418 23 3 1806 2 3437 6	0,7763 0,7384 1,1405 0,7811 0,512 1,0394 0,7324 1,0145 0,724 0,4401	0 0 1 0 0 1 0 NA 0			16q23.1 16q23.1 17p13.3 17p11.2 17p11.2 17p11.2 17p11.2 17p11.2 17p11.2 17q12 17q12 17q12	16q24.3 17p11.2 17p11.2 17p11.2 17p11.2 17p11.2 17q12 17q12 17q23.2 17q23.2
#2729T #2729T #2729T #2729T #2729T #2729T #2729T #2729T #2729T #2729T #2729T	chr16 chr17	74685919 193127 17716983 17720670 19679691 19753071 19770685 37228721 37235387 60673991 60705223	90142284 17716738 17720361 19648361 19752700 19769095 37226189 37234233 60663541 60689839 74303563	1215 2969 9 418 23 3 1806 2 3437 6	0,7763 0,7384 1,1405 0,7811 0,512 1,0394 0,7324 1,0145 0,724 0,4401 0,7482	0 0 1 0 0 1 0 NA 0			16q23.1 16q23.1 17p13.3 17p11.2 17p11.2 17p11.2 17p11.2 17p11.2 17p11.2 17q12 17q12 17q12 17q23.2	16q24.3 17p11.2 17p11.2 17p11.2 17p11.2 17p11.2 17q12 17q12 17q12 17q23.2 17q23.2 17q25.1
#2729T #2729T #2729T #2729T #2729T #2729T #2729T #2729T #2729T #2729T #2729T #2729T #2729T	chr16 chr17 chr17 chr17 chr17 chr17 chr17 chr17 chr17 chr17 chr17 chr17 chr17	74685919 193127 17716983 17720670 19679691 19730671 19770685 37228721 37235387 60673991 60705223 74307702	90142284 17716738 17720361 19648361 19752700 19769095 37226189 37234233 60663541 60689839 74303563 74326689	1215 2969 9 418 23 3 1806 2 3437 6 1760 6	0,7763 0,7384 1,1405 0,7811 0,512 1,0394 0,7324 1,0145 0,724 0,4401 0,7482 0,4126	0 0 1 0 0 1 0 NA 0 0			16q23.1 16q23.1 17p13.3 17p11.2 17p11.2 17p11.2 17p11.2 17p11.2 17q12 17q12 17q12 17q23.2 17q23.2	16q24.3 17p11.2 17p11.2 17p11.2 17p11.2 17p11.2 17q12 17q12 17q12 17q23.2 17q23.2 17q25.1
#2729T #2729T #2729T #2729T #2729T #2729T #2729T #2729T #2729T #2729T #2729T #2729T #2729T #2729T	chr16 chr17 chr17 chr17 chr17 chr17 chr17 chr17 chr17 chr17 chr17 chr17 chr17 chr17	74685919 193127 17716983 17726670 19679691 19753071 19770685 37228721 37235387 60673991 60705223 74307702 74328430	90142284 17716738 17720361 19648361 19752700 19769095 37226189 37234233 60663541 60689839 74303563 74326689	1215 2969 9 418 23 3 1806 2 3437 6 1760 6 808	0,7763 0,7384 1,1405 0,7811 0,512 1,0394 0,7324 1,0145 0,724 0,4401 0,7482 0,4126	0 0 1 0 0 1 0 NA 0 0 0			16q23.1 16q23.1 17p13.3 17p11.2 17p11.2 17p11.2 17p11.2 17p11.2 17p11.2 17p12 17q12 17q23.2 17q23.2 17q23.2 17q25.1	16q24.3 17p11.2 17p11.2 17p11.2 17p11.2 17p11.2 17p11.2 17q12 17q12 17q23.2 17q23.2 17q25.1 17q25.1
#2729T #2729T #2729T #2729T #2729T #2729T #2729T #2729T #2729T #2729T #2729T #2729T #2729T #2729T #2729T #2729T	chr16 chr17 chr17 chr17 chr17 chr17 chr17 chr17 chr17 chr17 chr17 chr17 chr17 chr17 chr17 chr17	74685919 193127 17716983 17726970 19679691 19775085 37228721 37235387 60673991 60705223 74307702 74328430 79571664	90142284 17716738 177720361 19648361 19752700 19769095 372246189 37234233 60663541 60669393 74303563 74326889 795567410 79596791	1215 2969 9 4118 23 3 1806 2 3437 6 1760 6 808 7	0,7763 0,7384 1,1405 0,7811 0,512 1,0394 0,7324 1,0145 0,724 0,4401 0,7482 0,4126 0,8273 0,4409	0 0 1 0 0 0 1 1 0 NA 0 0 0			16q23.1 16q23.1 17p13.3 17p11.2 17p11.2 17p11.2 17p11.2 17p11.2 17q11.2 17q12 17q12 17q23.2 17q23.2 17q25.1 17q25.1	16q24.3 17p11.2 17p11.2 17p11.2 17p11.2 17p11.2 17q12 17q12 17q12 17q23.2 17q23.2 17q25.1 17q25.3
#2729T #2729T #2729T #2729T #2729T #2729T #2729T #2729T #2729T #2729T #2729T #2729T #2729T #2729T #2729T #2729T #2729T	chr16 chr17 chr17 chr17 chr17 chr17 chr17 chr17 chr17 chr17 chr17 chr17 chr17 chr17 chr17 chr17 chr17	74685919 193127 17716983 177716983 17772670 19679691 19773671 19770685 37228721 37235387 60673921 60705223 74307702 74328430 79571664 79603949	90142284 17716738 17720361 19648361 19752700 19769055 37226189 37234233 60663341 60663341 74326689 79557410 79596791 81052161	1215 2969 9 418 23 3 1806 2 3437 6 1760 6 808 7	0,7763 0,7384 1,1405 0,7811 0,512 1,0394 0,7324 1,0145 0,724 0,4126 0,4126 0,8273 0,4409 0,8839	0 0 1 0 0 1 0 0 NA 0 0 0 0			16q23.1 16q23.1 17p13.3 17p11.2 17p11.2 17p11.2 17p11.2 17p11.2 17p11.2 17q12 17q12 17q23.2 17q23.2 17q25.1 17q25.1 17q25.3	16q24.3 17p11.2 17p11.2 17p11.2 17p11.2 17p11.2 17q12 17q12 17q23.2 17q23.2 17q25.1 17q25.3 17q25.3
#2729T #2729T #2729T #2729T #2729T #2729T #2729T #2729T #2729T #2729T #2729T #2729T #2729T #2729T #2729T #2729T #2729T	chr16 chr17 chr17 chr17 chr17 chr17 chr17 chr17 chr17 chr17 chr17 chr17 chr17 chr17 chr17 chr17 chr17 chr17 chr17	74685919 193127 17716983 17720670 19679691 19770685 37228721 37235387 60673991 60705223 74307702 74328430 79571664 79603349 158706	90142284 17716738 17720361 19648361 19752700 19769095 37226189 37224233 60663341 60689839 74303563 74326689 79567410 79596791 81052161 61558762	1215 2969 9 418 23 3 1806 2 3437 6 1760 6 808 7	0,7763 0,7384 1,1405 0,7811 0,512 1,0394 0,7324 1,0145 0,7224 0,4401 0,7482 0,4126 0,8273 0,4409 0,8339 0,6362	0 0 1 1 0 0 1 0 NA 0 0 0 0 0 0 0 0 0 0 0 0 0 0 0 0 0			16q23.1 16q23.1 17p13.3 17p11.2 17p11.2 17p11.2 17p11.2 17p11.2 17q12 17q12 17q23.2 17q23.2 17q25.1 17q25.1 17q25.3	16q24.3 17p11.2 17p11.2 17p11.2 17p11.2 17p11.2 17q12 17q12 17q12 17q23.2 17q23.2 17q25.1 17q25.3 17q25.3 17q25.3 17q25.3
#2729T #2729T #2729T #2729T #2729T #2729T #2729T #2729T #2729T #2729T #2729T #2729T #2729T #2729T #2729T #2729T #2729T #2729T #2729T #2729T	chr16 chr17 chr17 chr17 chr17 chr17 chr17 chr17 chr17 chr17 chr17 chr17 chr17 chr17 chr17 chr17 chr17 chr17 chr17	74685919 193127 17716983 177726670 19679691 197730671 19770687 37228721 37225387 60673991 60705223 74307702 74328430 79571664 79603949 158706 61562558	90142284 17716738 17720361 19648361 19752700 19752700 19752905 37226189 37234233 60663541 60669839 74303563 74326689 79567410 79596791 81052161 61558762 61554389	1215 2969 9 418 23 3 1806 2 3437 6 1760 6 808 7 457 457	0,7763 0,7384 1,1405 0,7811 0,512 1,0394 0,7324 1,01145 0,724 0,4401 0,7482 0,4126 0,8839 0,8839 0,9883	0 0 1 0 0 1 1 0 0 0 0 0 0 0 0 0 0 0 0 0			16q23.1 16q23.1 17p13.3 17p11.2 17p11.2 17p11.2 17p11.2 17p11.2 17p11.2 17q12 17q12 17q23.2 17q25.1 17q25.1 17q25.3 17q25.3 17q25.3 17q25.3	16q24.3 17p11.2 17p11.2 17p11.2 17p11.2 17p11.2 17p11.2 17q12 17q12 17q12 17q23.2 17q25.1 17q25.1 17q25.3 17q25.3 17q25.3 17q25.3 18q21.33
#2229T #2729T	chr16 chr17 chr17 chr17 chr17 chr17 chr17 chr17 chr17 chr17 chr17 chr17 chr17 chr17 chr17 chr17 chr17 chr17 chr18 chr18	74685919 193127 17716983 17720670 19679691 19770685 37228721 37235387 60673991 60705223 74328430 74307702 74328430 158706 61562558 61565020	90142284 17716738 17720361 19648361 19752700 19769095 37226189 37234233 60663541 60689839 7430563 74326689 79567410 181052161 61558762 61564389 78005195	1215 2969 9 418 23 3 1806 2 2 3437 6 1760 6 808 7 457 2649 2	0,7763 0,7384 1,1405 0,7811 0,512 1,0394 0,7324 1,0145 0,724 0,4401 0,7482 0,4126 0,8273 0,4839 0,6362 0,6804	0 0 1 1 0 0 1 1 0 NA 0 0 0 0 0 0			16q23.1 16q23.1 17p13.3 17p11.2 17p11.2 17p11.2 17p11.2 17p11.2 17p11.2 17q12 17q12 17q23.2 17q25.1 17q25.1 17q25.3 17q25.3 18q21.33	16q24.3 17p11.2 17p11.2 17p11.2 17p11.2 17p11.2 17q12 17q12 17q23.2 17q23.2 17q25.1 17q25.3 17q25.3 17q25.3 18q21.33 18q21.33
#2729T #2729T	chr16 chr17 chr17 chr17 chr17 chr17 chr17 chr17 chr17 chr17 chr17 chr17 chr17 chr17 chr17 chr17 chr17 chr18 chr18 chr18	74685919 193127 17716983 17720670 19679691 19730671 19770685 37228721 37235287 60673991 60705223 74307702 74328430 79571664 79603949 158706 61562558 61565020 111138	90142284 177716738 177720361 19648361 197522700 19769095 372246189 37234233 60663341 6068939 74303563 74326689 79567410 79596791 81052161 61558762 61564389 78005195	1215 2969 9 418 23 3 1806 2 1760 6 808 7 457 2649 2 1862	0,7763 0,7384 1,1405 0,7811 0,512 1,0394 0,7324 1,0145 0,724 0,4401 0,7482 0,4126 0,8273 0,4409 0,8839 0,6362 0,9883 0,6804 0,8228	0 0 1 1 0 0 1 1 0 0 0 0 0 0 0 0 0 0 0 0			16q23.1 16q23.1 17p13.3 17p11.2 17p11.2 17p11.2 17p11.2 17p11.2 17q12 17q12 17q12 17q23.2 17q23.2 17q25.1 17q25.3 17q25.3 17q25.3 17q25.3 17q25.3	16q24.3 17p11.2 17p11.2 17p11.2 17p11.2 17p11.2 17p11.2 17q12 17q12 17q23.2 17q25.1 17q25.3 17q25.3 17q25.3 17q25.3 18q21.33 18q21.33 18q21.33
#229T #2729T	chr16 chr17 chr18 chr18 chr18 chr18 chr18 chr19 chr19	74685919 193127 1771:0883 1777:0683 1777:0670 1967:9691 1977:0685 37228721 37235387 60073991 60075223 74307702 74328430 79571664 79503949 158706 61562558 61565020 111138	90142284 17716738 17720361 19648361 19752700 19769095 37224189 37234233 60663541 60669393 743026689 79567410 79596791 81052161 61558762 61564389 78005195 6833733 6890523	1215 2969 9 418 23 3 1806 2 3437 6 6 808 7 457 2649 2 361 1862	0,7763 0,7384 1,1405 0,7811 0,512 1,0394 0,723 1,0145 0,724 0,4401 0,7482 0,4401 0,7482 0,4409 0,8273 0,4409 0,8339 0,6362 0,9883 0,6804 0,8228 0,3765	0 0 1 1 0 0 0 0 0 0 0 0 0 0 0 0 0 0 0 0	TPS3		16q23.1 16q23.1 17p13.3 17p11.2 17p11.2 17p11.2 17p11.2 17p11.2 17p12.1 17q12.1 17q23.2 17q23.2 17q25.1 17q25.3 17q25.3 18q21.33 18q21.33 19p13.3	16q24.3 17p11.2 17p11.2 17p11.2 17p11.2 17p11.2 17p11.2 17q12 17q12 17q12 17q25.1 17q25.1 17q25.1 17q25.3 17q25.3 17q25.3 17q25.3 17q25.3 18q21.3 18q21.3 18q21.3 18q21.3
#229T #229T	ch16 ch27 ch27 ch27 ch27 ch27 ch27 ch27 ch27	74685919 193127 17716983 177716987 177716987 177716987 19579697 19573697 19	90142244 17716738 17720361 19648851 19648851 1976905 37226189 37234233 60663541 60669893 74303563 7430369 74303563 6663989 6663989 6663989 6663989 6663989 6663989 6663989 6663989 6663989 6663989 6663989 6663989 6663989 6663989 6663989	1215 2969 9 418 23 3 1806 2 2 3437 6 1760 6 808 7 7 2649 2 111 1862 111 1315	0,7763 1,1405 1,1405 0,7811 1,5105 1,512 1,0394 0,7324 1,0145 0,724 0,4401 0,7482 0,4409 0,8273 0,4409 0,8273 0,4409 0,823 0,6862 0,9883 0,6862 0,9883 0,6862 0,9883 0,6862 0,7317	0 0 0 1 1 0 0 0 0 0 0 0 0 0 0 0 0 0 0 0			16q23.1 16q25.1 17p13.3 17p11.2 17p11.2 17p11.2 17p11.2 17p11.2 17q12 17q12 17q12 17q23.2 17q23.2 17q25.3 17q25.3 18q21.33 18q21.33 18q21.33 18q21.33 19p13.3	16q24.3 17p11.2 17p11.2 17p11.2 17p11.2 17p11.2 17p11.2 17q12 17q22.2 17q25.3 17q25.1 17q25.3 17q25.3 17q25.3 18q21.33 18q21.33 18q21.33
#2295 #2795 #2795 #2796 #2797	cht16 cht17 cht18 cht19 cht19 cht19 cht18 cht18 cht18 cht18 cht19	74685919 193127 17716983 17726670 19575961 19750670 195750071 19750071 19750072 19750072 1725887 1725887 172670 17407702 174128430 179571666 1555000 1155706 1555000 1155706 1555000 1155716 1555706	90142284 17716738 1770361 19648361 19648361 1976905 37226129 37234233 60665819 7430563	1215 2969 9 418 418 23 3 1806 2 2 3437 6 6 808 7 7 457 2649 2 361 11 1315	0.7763 0.7384 1.1405 0.7811 1.1405 0.7811 0.912 1.0394 1.0145 0.7224 1.0145 0.7426 0.4401 0.4402 0.4327 0.6162 0.8273 0.6862 0.8282 0.3765 0.7317	0 0 1 0 0 0 1 0 0 0 0 0 0 0 0 0 0 0 0 0	TPS3		16q23.1 16q23.1 17p13.3 17p11.2 17p11.2 17p11.2 17p11.2 17p11.2 17p11.2 17q12 17q12 17q12 17q23.2 17q25.1 17q25.1 17q25.3 17q25.3 18q11.3 18q11.3 18q11.3 19p13.3	16q243 17p112 17p112 17p112 17p112 17p112 17p112 17q12 17q12 17q25 17q25 17q25 17q25 17q25 17q25 17q25 17q25 17q25 17q25 17q25 17q25 18q21 18q21 18q23 18q23 18q23 18q23 18q23 18q23 18q13
#2295 #2295 #2295 #2295 #2296 #2296 #2296 #2296 #2297	ch16 ch27 ch27 ch27 ch27 ch27 ch27 ch27 ch27	7465819 7465819 719117	90142284 1772081 1772081 13648861 139648861 13760955 3722413 60668364 60668364 60668364 60668364 60668364 60668364 60668364 60668364 60668364 60668364 60668364 60668364 60668364 60668364 7822669 78567410 7856764 6068364 60	1215 2969 9 418 23 3 1806 2 24 3437 6 1760 6 1760 2 361 361 1862 111 1315 9	0.7763 0.7384 1.1405 0.7381 1.1405 0.7811 0.9312 1.0194 0.9721 1.0195 0.722 0.4416 0.8273 0.4416 0.8273 0.4601 0.8383 0.6802 0.8228 0.8228 0.7317 1.0657	0 0 0 1 1 0 0 0 0 0 0 0 0 0 0 0 0 0 1 1 0	TPS3		16q23.1 16q23.1 17p13.3 17p11.2 17p11.2 17p11.2 17p11.2 17p11.2 17p11.2 17p11.2 17q12 17q12 17q23.2 17q23.2 17q25.1 17q25.1 17q25.3 18p11.32 18q21.33 19p13.3 19p13.3 19p13.3 19p13.2	16q243 17p112 17p112 17p112 17p112 17p112 17p112 17p112 17q12 17q23 17q23 17q25 17q2
#2295 #2795 #27297	cht16 cht17 cht18 cht18 cht18 cht18 cht19	74685919 193127 17716983 17726070 19579607 19579607 19573071 19573071 19570503 19726872 1972687 1972687 1972687 1972687 1972687 1972687 1972687 1972687 1972687 1972687 1972687 1972687 19727 19	90142244 17716781 17710781 19648861 19648861 1976905 37226189 3722428 3722428 3722428 3722428 3722428 3722428 3722428 3722428 3722428 3722618	1215 2969 9 418 23 3 1806 2 2 3437 6 6 1760 6 808 7 457 2699 2 3 361 1862 1862 1862 1863 1863 1863 1863 1863 1863 1863 1863	0.7763 0.7284 1.1405 0.7381 1.1405 0.7811 0.912 1.0394 0.7224 0.4401 0.4482 0.4401 0.4482 0.8273 0.6562 0.8238 0.6004 0.8228 0.3765 0.8221 0.7311 0.0457	0 0 0 1 1 0 0 0 0 0 0 0 0 0 0 0 0 0 0 0	TPS3		16q23.1 16q23.1 17p13.3 17p11.2 17p11.2 17p11.2 17p11.2 17p11.2 17p12.2 17q12 17q12 17q23.2 17q25.1 17q25.1 17q25.3 17q25.3 18q21.33 18q21.33 19p13.3 19p13.3 19p13.3	16q243 17p112 17p112 17p112 17p112 17p112 17p112 17q12 17q12 17q25
#2295 #2295	ch16 ch27 ch47 ch47 ch47 ch47 ch47 ch47 ch47 ch4	7465819 193127 17716983 17726670 1971670 19776687 19776687 19776687 19776687 19776687 37228721 27252721 274507702 274527430 74507702 745274430 79651949 1156706 61562558 61562558 61562558 61565550 111188 6896481 11567154 42931576	90142284 17720951 17720951 19648861 19760955 3722423 60668541 7432689 77557210 18052761	1215 2969 9 418 23 3 1806 6 11760 6 808 7 457 467 261 11862 11 1315 9 4554 6	0.7763 0.7384 1.1405 0.7384 1.1405 0.512 1.0394 1.0394 1.0145 0.7224 0.4401 0.7422 0.4426 0.4426 0.4426 0.4426 0.84839 0.6662 0.9883 0.06602 0.7317 1.0454	0 0 0 1 1 0 0 0 0 0 0 0 0 0 0 0 0 0 0 0	TPS3 KEAP1 SEPWI.TMEM160		16e23.1 16e23.1 16e23.1 17ep1.3 17ep1.2 17ep1.2 17ep1.1 17ep1.2 17ep1.2 17ep1.2 17ep1.2 17ep1.2 17ep1.2 17ep1.2 17ep1.3 17ep1.2 17ep2.3 17ep2.3 17ep2.3 17ep2.3 17ep2.3 17ep2.3 17ep2.3 17ep2.3 17ep2.3 18ep1.3 18ep1.3 18ep1.3 18ep1.3 19ep1.3	16q243 17p112 17p112 17p112 17p112 17p112 17p112 17p112 17q12 17q25 17q2
#2295 #2295 #27297	chris	74685919 193127 17716983 17726670 19579671 19579671 19579671 19579671 19579672 19579672 1977085 37228721 37228872 7432740 74307702 74328430 79571564 7960940 158706 61562558 61556200 111138 6833941 6833941 1557126 11555513 42927178 43015566	90142284 17716781 17716781 19648861 1976985 1976995 37226189 3722428 60669819 74315583 7432689 79567410 79596791 81052161 61558782 6155878	1215 2969 9 418 23 3 1806 2 2 3437 6 1760 6 808 7 457 2649 2 361 111 1315 9 4554 451 454 4813	0.7763 0.7384 1.1405 0.7381 1.1405 0.7511 0.512 1.0394 0.7324 0.4410 0.7482 0.4420 0.4420 0.8491 0.6460 0.8883 0.6504 0.6228 0.3765 0.7317 0.4126 0.4277 0.4274 0.4274 0.4274 0.4474 0.4474 0.4474 0.4474 0.4474 0.4474 0.4474 0.4474 0.4474 0.4474 0.4474 0.4474 0.4474 0.4474 0.4474 0.4474 0.4474 0.4474 0.7474	0 0 0 1 1 0 0 0 0 0 0 0 0 0 0 0 0 0 0 0	TPS3		16q23.1 16q23.1 16q23.1 17p13.3 17p11.2 17p11.2 17p11.2 17p11.2 17p11.2 17p11.2 17p11.2 17p11.2 17p11.1 17p11.1 17p11.1 17q12 17q12 17q13.2 17q23.2 17q23.3 17q25.3 18q21.33 18q21.33 18q21.33 18q21.33 19p13.3 19p13.3 19p13.3 19p13.2 19p13.3 10p13.3 10p1	166243 170112 170112 170112 170112 170112 170112 170112 170112 170212 170232 170232 170253 17
#2295 #2295 #2295 #2295 #2297	ch16 ch27 ch47 ch47 ch47 ch47 ch47 ch47 ch47 ch4	7465819 193127 1771083 17720670 197107 17710883 17720670 19730071 19730071 19770685 37228721 37228721 3723587 4007702 74307702 74307702 14	90142284 17720851 17720851 19648861 19752700 19762095 37324233 60668361 7432689 7432	1215 2969 9 418 23 3 1806 1806 6 808 7 7 457 2669 2 1862 111 1315 9 45554 6 3494 4813	0.7763 0.7384 1.1405 0.7384 1.1405 0.512 1.0994 0.512 1.0994 0.7224 0.4401 0.7482 0.4426 0.8273 0.4409 0.8873 0.4409 0.8883 0.6802 0.6802 0.7882 0.4909 0.8783 0.4009 0.8783 0.4009 0.8783 0.4009 0.8783 0.4009 0.8783 0.7883 0.7883 0.7883 0.7883 0.7883 0.7883 0.7883 0.7883 0.7883 0.7883 0.7883 0.7883 0.7883 0.7883 0.7883	0 0 0 1 1 0 0 0 0 0 0 0 0 0 0 0 0 0 0 0	TPS3 TPS3 KEAP1 KEAP1 SEPWI,TMEMIGO DNMCS		16e23.1 16e23.1 16e23.1 17e3.3 17e3.1 17e3.1 17e3.1 17e3.1 17e3.1 17e3.1 17e3.1 17e3.2 17e3.2 17e3.2 17e3.2 17e3.2 17e3.3 18e3.3 18e3.3 18e3.3 18e3.3 19e3.3	16q243 17p112 17p112 17p112 17p112 17p112 17p112 17q112 17q12 17q22 17q22 17q25 17q2
#2295 #2295 #27297	chris	74685919 193127 17716983 17726670 19579671 19579671 19579671 19579671 19579672 19579672 1977085 37228721 37228872 7432740 74307702 74328430 79571564 7960940 158706 61562558 61556200 111138 6833941 6833941 1557126 11555513 42927178 43015566	90142284 17716781 17716781 19648861 1976985 1976995 37226189 3722428 60669819 74315583 7432689 79567410 79596791 81052161 61558782 6155878	1215 2969 9 418 23 3 1806 2 2 3437 6 1760 6 808 7 457 2649 2 361 111 1315 9 4554 451 454 4813	0.7763 0.7384 1.1405 0.7381 1.1405 0.7511 0.512 1.0394 0.7324 0.4410 0.7482 0.4420 0.4420 0.8491 0.6460 0.8883 0.6504 0.6228 0.3765 0.7317 0.4126 0.4277 0.4274 0.4274 0.4274 0.4474 0.4474 0.4474 0.4474 0.4474 0.4474 0.4474 0.4474 0.4474 0.4474 0.4474 0.4474 0.4474 0.4474 0.4474 0.4474 0.4474 0.4474 0.7474	0 0 0 1 1 0 0 0 0 0 0 0 0 0 0 0 0 0 0 0	TPS3 KEAP1 SEPWI.TMEM160		16q23.1 16q23.1 16q23.1 17p13.3 17p11.2 17p11.2 17p11.2 17p11.2 17p11.2 17p11.2 17p11.2 17p11.2 17p11.1 17p11.1 17p11.1 17q12 17q12 17q13.2 17q23.2 17q23.3 17q25.3 18q21.33 18q21.33 18q21.33 18q21.33 19p13.3 19p13.3 19p13.3 19p13.2 19p13.3 10p13.3 10p1	166243 170112 170112 170112 170112 170112 170112 170112 170112 170212 170232 170232 170253 17

110000000000000000000000000000000000000		200	900000000000000000000000000000000000000	AND THE				1	000000000
#2729T	chr22	44589692	44601673	5	1,2762	1		22q13.31	22q13.31
#2729T	chr22	44602252	50757413	520	0,8338	0		22q13.31	22q13.33
#2729T #2729T	chr22 chr22	50765329 50857352	50854553 51220669	5 209	0,5585	0		22q13.33 22q13.33	22q13.33 22q13.33
#2729T	chr22 chrX	200918	155239777	6821	0,9167	0	RPS6KA3	Z2q13.33 Xp22.33	22q13.33 Xq28
#2729T	chrY	150918	59342783	129	0,7476	0	RESONAS	Xp22.33 Yp11.32	Yq12
#343T	chr1	762325	249212472	19104	-0,0445	0	ARID1A,RPL22,COL11A1	1p36.33	1944
#343T	chr2	40221	228996748	13267	-0,0558	0	ACVR2A.NFE2L2.EPHA4.APOB	2p25.3	2q36.3
#343T	chr2	229034976	229889758	5	0,3338	1		2q36.3	2q36.3
#343T	chr2	230020606	242946533	1397	-0,0251	0		2q36.3	2q37.3
#343T	chr3	239470	197769162	11848	-0,05	0	CTNNB1,BAP1,PDE12,KLF15,SETD2	3p26.3	3q29
#343T	chr4	53291	190947044	7745	-0,0651	0	ALB,FGA,GABRA2,IRF2	4p16.3	4q35.2
#343T	chr5	140602	180687559	8641	-0,0562	0	ATP10B,MEF2C,IL6ST,DOCK2,ADAMTS19,TERT	5p15.33	5q35.3
#343T	chr6	203615	170892714	9917	-0,0552	0	CDKN1A,EEF1A1,SPATS1,VEGFA	6p25.3	6q27
#343T	chr7	195642	158937319	9109	-0,0482	0	MET	7p22.3	7q36.3
#343T	chr8	190866	146280815	6666	-0,0483	0	SLURP1,MYC	8p23.3	8q24.3
#343T	chr9	213465	141017498	7569	-0,0319	0	CDKN2A,TSC1,MTAP,PTPN3	9p24.3	9q34.3
#343T	chr10	226000	33093984	1706	-0,0637	0		10p15.3	10p11.22
#343T	chr10	33103339	33144303	10	-0,3936	-1	VVIII)	10p11.22	10p11.22
#343T	chr10	33165390	135438930	6072	-0,0485	0	PTEN	10p11.22	10q26.3
#343T #343T	chr11	193118	134856548 49920264	10763	-0,0322	0	HMBS	11p15.5	11q25
#343T	chr12 chr12	208345	49920264	3864 27	-0,0599 0.1715	0	ARID2,CDKN1B	12p13.33	12q13.12 12q13.12
#343T	chr12	49976851	133811687	7477	-0,0485	0	HNF1A	12q13.12 12q13.12	12q13.12 12q24.33
#343T	chr13	19600450	115091029	3459	-0,0613	0	RB1	13q12.11	13q34
#343T	chr14	20201689	107282930	6439	-0,0448	0		14q11.2	14q32.33
#343T	chr15	20170066	56676189	3091	-0,0513	0	1	15q11.1	15q21.3
#343T	chr15	56680694	56719870	6	-0,4976	-1		15q21.3	15021.3
#343T	chr15	56720736	102389376	3639	-0,0438	0		15q21.3	15q26.3
#343T	chr16	96492	90142284	7652	-0,0096	0	AXIN1,TSC2,BRD7	16p13.3	16q24.3
#343T	chr17	6088	81052160	10797	-0,0215	0	TP53	17p13.3	17q25.3
#343T	chr18	117194	77960704	3035	-0,0638	0		18p11.32	18q23
#343T	chr19	281462	603755	58	0,0527	0		19p13.3	19p13.3
#343T	chr19	617298	619252	5	-0,4547	-1		19p13.3	19p13.3
#343T	chr19	620018	59083958	9824	0,0058	0	KEAP1,SEPW1,TMEM160	19p13.3	19q13.43
#343T	chr20	68379	62906077	4752	-0,0231	0	DNAICS	20p13	20q13.33
#343T	chr21	9825922	10862908	8	0,2309	0	0.00000000	21p11.2	21p11.2
#343T	chr21	10906821	48084620	1998	-0,0429	0	DYRKIA	21p11.1	21q22.3
#343T	chr22	17060842	51219140	4000	-0,0055	0	ZNRF3,CLDN5	22q11.1	22q13.33
#343T	chrX	2700138	38013775	1294	-0,067	0	RP56KA3	Xp22.33	Xp11.4
#343T	chrX	38016215	38080049	7	0,2686	1		Xp11.4	Xp11.4
#343T	chrX	38080636	154774846	5066	-0,0496	0		Xp11.4	Xq28
#375T	chr1	69550	249211681	20300 14999	0,5141	0	ARID1A,RPL22,COL11A1	1p36.33	1q44
#375T #375T	chr2 chr3	41618 361505	242814646 197765488	11710	0,528	0	ACVR2A,NFE2L2,EPHA4,APOB	2p25.3 3p26.3	2q37.3 3q29
#375T	chr4	53384	113242	7579	0,5218	0	CTNNB1,BAP1,PDE12,KLF15,SETD2	4p16.3	4p16.3
#375T	chr5	92369	180794757	8653	0,5295	0	ATP10B,MEF2C,IL6ST,DOCK2,ADAMTS19,TERT	5p15.33	5q35.3
#375T	chr6	292550	170893528	9755	0,5263	0	CDKN1A,EEF1A1,SPATS1,VEGFA	6p25.3	6q27
#375T	chr7	193502	158937438	9218	0,519	0	MET	7p22.3	7q36.3
#375T	chr8	116555	146279474	6615	0,5275	0	SLURP1,MYC	8p23.3	8q24.3
#375T	chr9	15115	141016186	7934	0,5081	0	CDKN2A,TSC1,MTAP,PTPN3	9p24.3	9q34.3
#375T	chr10	93526	135440158	8080	0,5253	0	PTEN	10p15.3	10q26.3
#375T	chr11	193127	134257498	11034	0,503	0	HMBS	11p15.5	11q25
#375T	chr12	176326	133810818	11185	0,52	0	ARID2,HNF1A,CDKN1B	12p13.33	12q24.33
#375T	chr13	19748151	115090537	3449	0,5412	0	RB1	13q12.11	13q34
#375T	chr14	19378084	105995651	5872	0,5232	0		14q11.2	14q32.33
#375T	chr15	20740212	102462803	6952	0,5138	0		15q11.2	15q26.3
#375T	chr16	97494	90142284	8318	0,4943	0	AXIN1,TSC2,BRD7	16p13.3	16q24.3
#375T	chr17	193127	81052161	11695	0,5022	0	TP53	17p13.3	17q25.3
#375T	chr18	158706	78005195	3008	0,5374	0		18p11.32	18q23
#375T	chr19	111138	59082559	11245	0,4781	0	KEAP1,SEPW1,TMEM160	19p13.3	19q13.43
#375T	chr20	68379	62904763	4804	0,5005	0	DNAIC5	20p13	20q13.33
#375T	chr21	45658349	48083380	2024	0,5156	0		21q22.3	21q22.3
#375T	chr22	19378084	51220669	4098	0,4866	0	ZNRF3,CLDN5	22q11.21	22q13.33
#375T	chrX	200918	155239777	6818 129	0,5278	0	RPS6KA3	Xp22.33	Xq28
#375T #4110T	chr1	150918 69550	59342783 861358	4	0,514 1.0004	0		Yp11.32	Yq12 1p36.33
#4110T	chr1	865626	16174604	2055	0,6521	0	RPL22	1p36.33 1p36.33	1p36.33
#4110T	chr1	16199471	16248794	8	1,1079	0	275.666	1p36.33 1p36.21	1p36.21 1p36.13
#4110T	chr1	16258673	20209117	636	0,7031	0	1	1p36.21 1p36.13	1p36.13
#4110T	chr1	20216952	20209117	6	1.0811	0		1p36.13	1p36.13
#4110T	chr1	20216932	21151642	118	0,6577	0		1p36.13	1p36.13
#4110T	chr1	21155703	21329221	27	1,0715	0		1p36.12	1p36.12
#4110T	chr1	21546536	21978293	68	0,6922	0		1p36.12	1p36.12
#4110T	chr1	22005921	22141103	26	0,9417	0		1p36.12	1p36.12
#4110T	chr1	22142501	22338951	116	0,5931	0		1p36.12	1p36.12
#4110T	chr1	22405024	22417965	5	1,2045	1		1p36.12	1p36.12
#4110T	chr1	22446777	22469377	5	0,5076	-1		1p36.12	1p36.12
#4110T	chr1	22816790	24666205	275	0,7384	0		1p36.12	1p36.11
#4110T	chr1	24668684	24673087	5	0,3998	-2		1p36.11	1p36.11
#4110T	chr1	24674000	52822085	3378	0,7769	0	ARID1A	1p36.11	1p32.3
#4110T	chr1	52822736	52830258	15	0,5537	-1		1p32.3	1p32.3
#4110T	chr1	52838950	92798989	2065	0,9813	0	1	1p32.3	1p22.1
#4110T	chr1	92801944	92948987	10	0,6942	0		1p22.1	1p22.1
#4110T	chr1	92979370	94033353	100	1,011	0		1p22.1	1p22.1
#4110T #4110T	chr1	94037313	94140328 94370112	12	0,7156 1,0509	0		1p22.1 1p22.1	1p22.1 1p22.1
#4110T	chr1	94335454	94370112	50	0,7872	0		1p22.1 1p22.1	1p22.1
#4110T	chr1	94374656	109486568	618	1,0456	0	COL11A1	1p22.1 1p22.1	1p22.1 1p13.3
#4110T	chr1	109490286	110091402	167	0,7753	0	COLLINI	1p22.1 1p13.3	1p13.3
#4110T	chr1	110116380	110091402	8	1,236	1		1p13.3 1p13.3	1p13.3
#4110T	chr1	110116380	110146071	16	0,7241	0		1p13.3 1p13.3	1p13.3
#4110T	chr1	110146650	110170096	8	0,7241	-2	1	1p13.3 1p13.3	1p13.3
#4110T	chr1	110170460	110172942	157	0,345	-2	1	1p13.3 1p13.3	1p13.3
#4110T	chr1	110173360	111439315	10	1,2216	1		1p13.3 1p13.3	1p13.3
#4110T	chr1	111440472	178754717	5209	0.8644	0	1	1p13.3	1p13.3
#4110T	chr1	178777221	178871293	18	1,2377	1		1q25.2	1q25.2 1q25.2
#4110T	chr1	178777221	180080214	139	0,9776	0	-	1q25.2 1q25.2	1q25.2 1q25.2
	chr1	180124175	180243517	19	0,6056	0		1925.2	1q25.2
#4110T	chr1	180257575	227504795	3210	0,9034	0		1q25.2 1q25.2	1942.13
#4110T #4110T			229580705	218	0,6052	0		1q42.13	1942.13
	chr1	227751411							
#4110T		227751411 229584905	249211681	1160	0,9355	0		1q42.13	1944
#4110T #4110T	chr1				0,9355 0,8699	0	APOB		1q44 2p21

		-								
#4110T	chr2	42483706	42950102	43	0,9732	0			2p21	2p21
#4110T	chr2	42980526	43655305	25	0,6642	0			2p21	2p21
#4110T #4110T	chr2	43657397 44050005	44047147 44104983	66 23	1,004 0,6916	0			2p21 2p21	2p21 2p21
#4110T	chr2	44030005	71188102	1281	0,6916	0			2p21 2p21	2p21 2p13.3
#4110T	chr2	71188774	71216096	16	0,5383	-1			2p13.3	2p13.3
#4110T	chr2	71216912	71658508	52	0,9384	0			2p13.3	2p13.2
#4110T	chr2	71660354	72411260	69	0,6617	0			2p13.2	2p13.2
W4110T	chr2	72562113	72968515	14	1,1042	0			2p13.2	2p13.2
#4110T	chr2	73052983	73118571	4	0,7621	0			2p13.2	2p13.2
W4110T	chr2	73145241	73228681	12	0,4386	-1			2p13.2	2p13.2
#4110T	chr2	73247381	113420521	2555	0,8747	0			2p13.2	2q13
#4110T	chr2	113479431	113484285	14	0,6052	0			2q13	2q13
#4110T	chr2	113487243	127658960	455	0,9011	0			2q13	2q14.3
#4110T	chr2	127806156	127834242	19	0,5056	-1			2q14.3	2q14.3
W4110T	chr2	127864478	128065268	24	0,7882	0			2q14.3	2q14.3
#4110T #4110T	chr2	128066250 128177554	128100704 128244184	15 10	1,1511 0,5838	0			2q14.3 2q14.3	2q14.3 2q14.3
#4110T	chr2	128246783	128262794	10	1,0431	0			2q14.3 2q14.3	2q14.3 2q14.3
#4110T	chr2	128281310	128466358	65	0,5826	0			2q14.3 2q14.3	2q14.3 2q14.3
W4110T	chr2	128467110	130877828	107	0.9363	0			2q14.3	2q21.1
#4110T	chr2	130897195	131130763	66	0,6237	0			2q21.1	2q21.1
#4110T	chr2	131221053	131261410	14	1,134	0			2q21.1	2q21.1
#4110T	chr2	131266548	131369311	14	0,5922	0			2q21.1	2q21.1
#4110T	chr2	131374420	131403793	12	1,1482	0			2q21.1	2q21.1
W4110T	chr2	131412554	131976236	29	0,7567	0			2q21.1	2q21.1
#4110T	chr2	131981226	132120911	13	1,0611	0			2q21.1	2q21.1
#4110T	chr2	132233774	132558487	20	0,614	0			2q21.1	2q21.2
#4110T	chr2	133066889	172844218	1866	1,0238	0	ACVRZA		2q21.2	2q31.1
#4110T	chr2	172848182	173330329	17	0,62	0			2q31.1	2q31.1
#4110T	chr2	173332248	176860299	201	0,9678	0			2q31.1	2q31.1
#4110T	chr2	176866953	177134378	23	0,6445	0	AUTON		2q31.1	2q31.1
W4110T	chr2	177161612	238738003	4410 554	0,9301	0	NFE2L2,EPHA4		2q31.1 2q37.3	2q37.3
#4110T #4110T	chr2	238742713	242814646 42642528	554 2296	0,6255	0	CTNNB1		2q37.3 3n26.3	2q37.3 3n22.1
#4110T #4110T	chr3	361505 42659099	42642528 42687424	2296	0,8687 1,1469	0	CINNBI	+	3p26.3 3p22.1	3p22.1 3p22.1
#4110T	chr3	42659099	42687424 47456400	563	0,7767	0	SETD2		3p22.1 3p22.1	3p22.1 3p21.31
#4110T	chr3	47456629	47456400	8	0,7767	-2	36106		3p21.31	3p21.31
#4110T	chr3	47462470	48982595	445	0,6596	0			3p21.31	3p21.31
#4110T	chr3	48999079	49011191	6	1,0004	0			3p21.31	3p21.31
#4110T	chr3	49012275	52233357	860	0,6761	0			3p21.31	3p21.2
#4110T	chr3	52236636	52242181	6	1,0347	0			3p21.2	3p21.2
#4110T	chr3	52245433	52574470	271	0,5965	0	BAP1		3p21.2	3p21.1
#4110T	chr3	52582165	129599253	3427	0,9139	0	PDE12,KLF15		3p21.1	3q22.1
#4110T	chr3	129694765	129817082	10	0,5649	0			3q22.1	3q22.1
#4110T	chr3	130092515	183862702	2464	0,9855	0			3q22.1	3q27.1
#4110T	chr3	183873504	184552484	243	0,6445	0			3q27.1	3q27.2
#4110T	chr3	184556518	195269787	558	0,9627	0			3q27.2	3q29
#4110T	chr3	195295889	195778934	51	0,6045	0			3q29	3q29
W4110T	chr3	195780359 195934321	195925703 195955065	19	0,9857	-1			3q29	3q29 3q29
#4110T	chr3	195934321	195955065	213	0,4649	-1			3q29 3q29	3q29 3q29
#4110T	chr4	53384	493201	18	0,8803	0			4p16.3	4p16.3
#4110T	chr4	494287	2835493	414	0,5807	0			4p16.3	4p16.3
#4110T	chr4	2877740	2901074	8	1,0107	0			4p16.3	4p16.3
W4110T	chr4	2906663	8608545	518	0,6867	0			4p16.3	4p16.1
#4110T	chr4	8609073	108871490	3756	1,0076	0	ALB,GABRA2		4p16.1	4q25
#4110T	chr4	108911154	108984802	12	0,6882	0			4q25	4q25
#4110T	chr4	113242	108985516	2560	1,0053	0			4q25	4p16.3
#4110T	chr5	92369	5423071	317	0,597	0	TERT		5p15.33	5p15.32
#4110T	chr5	5440017	5454708	7	1,3268	1			5p15.32	5p15.32
#4110T	chr5	5457649	38427232	1024	0,9518	0			5p15.32	5p13.1
#4110T	chr5	38431334	38463062	8	0,5742	0		_	5p13.1	5p13.1
#4110T #4110T	chr5	38464011 54468447	54459964 54528282	480	1,0259	-1				5q11.2
#4110T	chr5								5p13.1	F-11 3
#4110T	chr5	54520161		11 3093	0,5425		MEESC HEST ADAMTS 10		5q11.2	5q11.2 5q31.1
#4110T		54529161 132096589	132094514	3093	1,0015	0	MEF2C,IL6ST,ADAMTS19		5q11.2 5q11.2	5q31.1
#4110T		132096589	132094514 132161344	3093 17	1,0015 0,6011	0			5q11.2 5q11.2 5q31.1	5q31.1 5q31.1
#4110T	chr5	132096589 132197764	132094514 132161344 160973611	3093	1,0015 0,6011 0,8551	0	MEF2C,IL6ST,ADAMTS19 ATP108		5q11.2 5q11.2 5q31.1 5q31.1	5q31.1 5q31.1 5q34
		132096589	132094514 132161344	3093 17 2170	1,0015 0,6011	0 0 0			5q11.2 5q11.2 5q31.1	5q31.1 5q31.1 5q34 5q34
#4110T	chr5 chr5	132096589 132197764 161113014	132094514 132161344 160973611 161530964	3093 17 2170 22	1,0015 0,6011 0,8551 1,1868	0 0 0	ATP10B		5q11.2 5q11.2 5q31.1 5q31.1 5q34	5q31.1 5q31.1 5q34
#4110T #4110T	chr5 chr5 chr5 chr5 chr5	132096589 132197764 161113014 161569246 175779688 175913423	132094514 132161344 160973611 161530964 175777678 175906223 175956775	3093 17 2170 22 487	1,0015 0,6011 0,8551 1,1868 0,8763	0 0 0 1 0 -1	ATP10B		5q11.2 5q11.2 5q31.1 5q31.1 5q34 5q34	5q31.1 5q31.1 5q34 5q34 5q35.2
#4110T #4110T #4110T	chr5 chr5 chr5 chr5 chr5 chr5	132096589 132197764 161113014 161569246 175779688 175913423 175957145	132094514 132161344 160973611 161530964 175777678 175906223 175956775 178017051	3093 17 2170 22 487 22 13 401	1,0015 0,6011 0,8551 1,1868 0,8763 0,5508 0,9187 0,6394	0 0 0 1 0 -1 0	ATP10B		5q11.2 5q11.2 5q31.1 5q31.1 5q34 5q34 5q34 5q35.2 5q35.2 5q35.2	5q31.1 5q31.1 5q34 5q34 5q35.2 5q35.2 5q35.2 5q35.2 5q35.3
#4110T #4110T #4110T #4110T	chr5 chr5 chr5 chr5 chr5 chr5 chr5	132096589 132197764 161113014 161569246 175779688 175913423 175957145 178030688	132094514 132161344 160973611 161530964 175777678 175906223 175956775 178017051 178139841	3093 17 2170 22 487 22 13 401	1,0015 0,6011 0,8551 1,1868 0,8763 0,5508 0,9187 0,6394 1,0027	0 0 0 1 0 -1 0 0	ATP10B		5q11.2 5q11.2 5q31.1 5q31.1 5q34 5q34 5q35.2 5q35.2 5q35.2 5q35.2 5q35.2	5q31.1 5q31.1 5q34 5q34 5q35.2 5q35.2 5q35.2 5q35.2 5q35.3
#4110T #4110T #4110T #4110T	chr5 chr5 chr5 chr5 chr5 chr5 chr5 chr5	132096589 132197764 161113014 161569246 175779688 175913423 175957145 178030688 178152425	132094514 132161344 160973611 161530964 175777678 175906223 175906775 178017051 178139841 179334762	3093 17 2170 22 487 22 13 401 12	1,0015 0,6011 0,8551 1,1868 0,8763 0,5508 0,9187 0,6394 1,0027 0,7078	0 0 0 1 0 -1 0 0 0	ATP10B		5q11.2 5q11.2 5q31.1 5q31.1 5q34 5q34 5q35.2 5q35.2 5q35.2 5q35.3 5q35.3	5q31.1 5q31.1 5q34 5q34 5q35.2 5q35.2 5q35.2 5q35.2 5q35.3 5q35.3
#4110T #4110T #4110T #4110T #4110T	chr5 chr5 chr5 chr5 chr5 chr5 chr5 chr5	132096589 132197764 161113014 161569246 175779688 175913423 175957145 178030688 178152425 179382662	132094514 132161344 160973611 161530964 175777678 175906223 175956775 178017051 178139841 179334762 179529107	3093 17 2170 22 487 22 13 401 12 160	1,0015 0,6011 0,8551 1,1868 0,8763 0,5508 0,9187 0,6394 1,0027 0,7078 0,9974	0 0 0 1 0 -1 0 0 0	ATP10B		5q11.2 5q11.2 5q11.1 5q31.1 5q34.1 5q34 5q34 5q35.2 5q35.2 5q35.2 5q35.3 5q35.3	5q31.1 5q34.1 5q34 5q34 5q35.2 5q35.2 5q35.2 5q35.3 5q35.3 5q35.3
#4110T #4110T #4110T #4110T	chr5 chr5 chr5 chr5 chr5 chr5 chr5 chr5	132096589 132197764 161113014 161569246 175779688 175913423 175957145 178030688 178152425	132094514 132161344 160973611 161530964 175777678 175906223 175906775 178017051 178139841 179334762	3093 17 2170 22 487 22 13 401 12	1,0015 0,6011 0,8551 1,1868 0,8763 0,5508 0,9187 0,6394 1,0027 0,7078	0 0 0 1 0 -1 0 0 0	ATP10B		5q11.2 5q11.2 5q31.1 5q31.1 5q34 5q34 5q35.2 5q35.2 5q35.2 5q35.3 5q35.3	5q31.1 5q31.1 5q34 5q34 5q35.2 5q35.2 5q35.2 5q35.2 5q35.3 5q35.3
#4110T #4110T #4110T #4110T #4110T #4110T #4110T	chr5 chr5 chr5 chr5 chr5 chr5 chr5 chr5	132096589 132197764 161113014 161569246 175779688 175913423 175957145 178030688 178152425 179382662 179538518	132094514 132151344 160973611 161530964 175777678 175906223 175956775 178017051 178139841 179334762 179529107 180794757 43276509	3093 17 2170 22 487 22 13 401 12 160 11 151 3929	1,0015 0,6011 0,8551 1,1868 0,8763 0,5508 0,9187 0,6394 1,0027 0,7078 0,974 0,7158 0,7782	0 0 0 1 1 0 -1 0 0 0 0	ATP10B		5q11.2 5q11.1 5q31.1 5q34.1 5q34 5q34 5q35.2 5q35.2 5q35.2 5q35.3 5q55.3 5q55.3 5q55.3	5q31.1 5q34.1 5q34 5q34 5q35.2 5q35.2 5q35.2 5q35.3 5q35.3 5q35.3 5q35.3 5q35.3
#4110T #4110T #4110T #4110T #4110T #4110T #4110T #4110T #4110T	chr5 chr5 chr5 chr5 chr5 chr5 chr5 chr5	132096589 132197764 16113014 161569246 175779688 175913423 175957145 178030688 178152425 179382662 179538518 292550 43306568	132094514 132161344 160973611 161530964 175777678 175906223 175956775 178017051 178139841 179334762 179529107 180794757 43276509 43320164	3093 17 2170 22 487 22 13 401 12 160 11 151 3929 6	1,0015 0,6011 0,8551 1,1868 0,8763 0,5508 0,9187 0,6394 1,0027 0,7078 0,9974 0,7158 0,7782	0 0 0 1 1 0 0 0 0 0 0	ATP108 DOCK2 CDKN1A		5q11.2 5q11.2 5q31.1 5q31.1 5q34 5q34 5q35.2 5q35.2 5q35.2 5q35.2 5q35.3 5q35.3 5q35.3 5q35.3 6p21.1	Sq31.1 Sq31.1 Sq34 Sq34 Sq35.2 Sq35.2 Sq35.2 Sq35.3 Sq35.3 Sq35.3 Sq35.3 Sq35.3 Sq25.3
#4110T #4110T #4110T #4110T #4110T #4110T #4110T #4110T #4110T	chr5 chr5 chr5 chr5 chr5 chr5 chr5 chr5	132096589 132197764 161113014 161569246 175779688 175913423 178030688 178152425 179382662 179538518 292550 43306568	132094514 132161344 160973611 161530964 175777678 175906223 175956775 178017051 178139841 179334762 179529107 180794757 43276509 43276509 43320164 44364127	3093 17 2170 22 487 22 13 401 12 160 11 151 3929 6	1,0015 0,6011 0,8551 1,1868 0,8763 0,5508 0,9187 0,6394 1,0027 0,7078 0,7974 0,7158 0,7782 1,0521 0,7153	0 0 0 1 0 -1 0 0 0 0 0 0 0	DOCKZ DOCKZ CDKNIA SPATSI,VEGFA		5q11.2 5q11.2 5q31.1 5q31.1 5q34 5q34 5q35.2 5q35.2 5q35.2 5q35.2 5q35.3 5q35.3 5q35.3 5q25.3 5q25.3 5q25.3 5q25.3 5q25.3 5q25.3 5q25.3	5q31.1 5q31.1 5q34 5q35.2 5q35.2 5q35.2 5q35.2 5q35.3 5q35.3 5q35.3 5q35.3 5q21.1 6p21.1
#4110T #4110T #4110T #4110T #4110T #4110T #4110T #4110T #4110T #4110T #4110T	chr5 chr5 chr5 chr5 chr5 chr5 chr5 chr5	132096589 132197764 161113014 161569246 175779688 175957145 178030688 178152425 179382662 17938518 292550 43306568 43323142 44371655	132094514 132161344 160973611 161530964 175777678 175906223 175956775 178017051 1781139841 179334762 179529107 43276509 43320164 44364127 100010771	3093 17 2170 22 487 22 13 401 12 160 11 151 3929 6 272 2020	1,0015 0,6011 0,8551 1,1868 0,8763 0,5508 0,9187 0,6394 1,0027 0,7078 0,9974 0,7158 0,7782 1,0521 0,7782	0 0 0 1 0 -1 0 0 0 0 0 0 0 0 0	ATP108 DOCK2 CDKN1A		5q11.2 5q11.1 5q31.1 5q31.1 5q34.1 5q34.5 5q35.2 5q35.2 5q35.2 5q35.2 5q35.3 5q35.3 5q35.3 6p25.3 6p21.1 6p21.1	5q31.1 5q31.1 5q34 5q34 5q35.2 5q35.2 5q35.2 5q35.3 5q35.3 5q35.3 5q35.3 6p21.1 6p21.1 6q16.2
#4110T #4110T #4110T #4110T #4110T #4110T #4110T #4110T #4110T	chr5 chr5 chr5 chr5 chr5 chr5 chr5 chr5	132096589 132197764 161113014 161569246 175779688 175913423 178030688 178152425 179382662 179538518 292550 43306568	132094514 132161344 160973611 161530964 175777678 175906223 175956775 178017051 178139841 179334762 179529107 180794757 43276509 43276509 43320164 44364127	3093 17 2170 22 487 22 13 401 12 160 11 151 3929 6	1,0015 0,6011 0,8551 1,1868 0,8763 0,5508 0,9187 0,6394 1,0027 0,7078 0,7974 0,7158 0,7782 1,0521 0,7153	0 0 0 1 0 -1 0 0 0 0 0 0 0	DOCKZ DOCKZ CDKNIA SPATSI,VEGFA		5q11.2 5q11.2 5q31.1 5q31.1 5q34 5q34 5q35.2 5q35.2 5q35.2 5q35.2 5q35.3 5q35.3 5q35.3 5q25.3 5q25.3 5q25.3 5q25.3 5q25.3 5q25.3 5q25.3	5q31.1 5q31.1 5q34 5q35.2 5q35.2 5q35.2 5q35.2 5q35.3 5q35.3 5q35.3 5q35.3 5q21.1 6p21.1
#4110T #4110T #4110T #4110T #4110T #4110T #4110T #4110T #4110T #4110T #4110T #4110T	chr5 chr5 chr5 chr5 chr5 chr5 chr5 chr5	132096589 132197764 161113014 1611509246 175779688 175913423 175957145 179837662 17938518 292550 43306568 43323142 44371655 100368974	132094514 132161344 132161344 160973611 161530964 175777678 175906223 175956775 178017051 178139841 179334762 179529107 180794757 43276509 43276509 43264127 100010771 100061772	3093 17 2170 22 487 22 13 401 12 160 11 151 3929 6 272 2020 5 9	1,0015 0,6011 0,8551 1,1868 0,8763 0,5508 0,9187 0,6394 1,0027 0,7078 0,974 0,7158 0,7782 1,0181 0,6114 0,9945	0 0 0 1 1 0 0 0 0 0 0 0 0 0 0 0 0 0 0 0	DOCKZ DOCKZ CDKNIA SPATSI,VEGFA		5q11.2 5q11.2 5q11.1 5q31.1 5q34.1 5q34.5 5q34 5q35.2 5q35.2 5q35.2 5q35.2 5q35.3 5q55.3 5q55.3 5q55.3 6p21.1 6p21.1 6p21.1 6p21.1 6p21.2	5q31.1 5q31.1 5q31.1 5q34 5q34 5q35.2 5q35.2 5q35.3 5q35.3 5q35.3 5q35.3 5q35.3 6p21.1 6p21.1 6p21.1 6q16.2 6q16.2 6q16.3
#4110T #4110T #4110T #4110T #4110T #4110T #4110T #4110T #4110T #4110T #4110T	chr5 chr5 chr5 chr5 chr5 chr5 chr5 chr5	132096589 132197764 161113014 161569246 175779688 175913423 175957145 178030688 178152425 179538518 292550 43306568 43323142 44371655 100016388	132094514 132161344 132161346 160973611 161530964 175777678 175906223 175956775 178017051 178139841 179334762 179529107 180794757 43276509 43276509 43230164 44364127 100010771	3093 17 2170 22 487 22 13 401 12 160 11 151 3929 6 272 2020 5	1,0015 0,6011 0,8551 1,1868 0,8763 0,5508 0,9187 0,6394 1,0027 0,7078 0,7158 0,7782 1,0521 0,7153 1,0181 0,6114	0 0 0 1 0 -1 0 0 0 0 0 0 0 0 0	DOCKZ DOCKZ CDKNIA SPATSI,VEGFA		Sq11.2 Sq11.2 Sq31.1 Sq31.1 Sq34.5 Sq35.2 Sq35.2 Sq35.2 Sq35.2 Sq35.3 Sq35.3 Sq35.3 Sq25.3 Sq25.3 Sq25.3 Sq25.3 Sq25.3	5q31.1 5q31.1 5q34 5q34 5q35.2 5q35.2 5q35.2 5q35.3 5q35.3 5q35.3 5q35.3 6p21.1 6p21.1 6p21.1 6q16.2
#4110T #4110T #4110T #4110T #4110T #4110T #4110T #4110T #4110T #4110T #4110T #4110T #4110T	chr5 chr5 chr5 chr5 chr5 chr5 chr5 chr5	132096589 132197764 161113014 161569246 175779688 175913423 175957145 178030688 178152425 179382662 179382662 179382164 4323142 43271655 100016388 100368974 100896075	13204514 132161344 132161344 169773611 161530964 175777678 175906223 175906723 175906775 178017051 178019941 179334762 179529107 1380794757 43276509 43276509 43230164 44364127 100019771 100051772 100051772 100057778	3093 17 2170 22 487 22 13 401 12 160 111 151 3929 6 272 2020 5 9	1,0015 0,6011 0,8551 1,1868 0,8763 0,5508 0,9187 0,6394 1,0027 0,7078 0,9974 0,7158 1,0521 0,7153 1,0181 0,6114 0,9945 0,72	0 0 0 1 0 0 0 0 0 0 0 0 0 0 0 0 0 0 0 0	DOCKZ DOCKZ CDKNIA SPATSI,VEGFA		5911.2 5911.2 5931.1 5931.1 5931.1 5934 5935.2 5935.2 5935.2 5935.2 5935.3 5935.3 5935.3 6921.1 6921.1 6921.1 6921.1 6921.1 6916.2 6916.2	\$q31.1 \$q31.1 \$q31.4 \$q34 \$q34 \$q34 \$q35.2 \$q35.2 \$q35.2 \$q35.3 \$q35.3 \$q35.3 \$q35.3 \$q35.3 \$q35.3 \$q35.1 \$q21.1 \$q16.2 \$q16.2 \$q16.2 \$q16.3 \$q16.3
#4110T	chr5 chr5 chr5 chr5 chr5 chr5 chr5 chr5	132096589 132197764 16113014 161569246 175779688 175913423 175957145 178030688 179135245 179382662 179382662 179382662 199382550 43305568 43305568 43305568 100368874 10086875 100964130 10996175 100964130	132094514 13215344 100975611 101975611 101979611 101979611 1019796223 17906223 17906223 17906223 17906224 179062705 178017051 178017051 178017051 10007071 10007071 100095718 100005777 100095718 100065778	3093 17 2170 227 487 22 13 401 12 160 11 151 3929 6 272 2020 5 9 10 293 45	1.0015 0.6011 0.8551 1.1888 0.8763 0.5508 0.9187 0.5508 0.9187 0.01987 0.7078 0.9197 0.7078 0.7158 0.7758 0.7153 1.0821 1.0021 1.0021 1.0021 1.0021 0.9552	0 0 0 1 1 0 0 0 0 0 0 0 0 0 0 0 0 0 0 0	DOCKZ DOCKZ CDKNIA SPATSI,VEGFA		5q11.2 5q11.2 5q11.1 5q31.1 5q31.1 5q34.1 5q34.5 5q34.5 5q35.2 5q35.2 5q35.2 5q35.3 5q35.3 5q35.3 5q35.3 6p21.1 6p21.1 6p21.1 6p21.1 6p21.1 6p21.1 6p21.1 6p21.1 6p21.1 6p21.1 6p21.1 6p21.1 6p21.1	\$q31.1 \$q31.1 \$q34 \$q34 \$q35.2 \$q35.2 \$q35.2 \$q35.3
#4110T	chrs chrs chrs chrs chrs chrs chrs chrs	13209/5699 132197764 131197764 15119014 15159746 17597342 17597342 17597342 17597342 17597342 17597342 17597342 17597342 17597342 17597342 10096439 100016389 100016389 10006439 10096475 10096439 10096475	131096514 13101314 13101314 13101314 100973611 101510964 137596223 137596223 137596223 137596223 137596223 137597675 137617051 137813841 1378134762 14325059 43325054 4434177 100061772 100061772 10006971385 10086521 1008751385 10086552 10086552	3093 17 2170 2170 22 487 22 13 401 12 160 11 151 27 2020 5 9 10 283 45 2920 11	1.0015 0.6011 0.8551 1,1366 0.8763 0.8763 0.5768 0.5768 0.5768 0.9187 0.6394 1.0027 0.7778 0.7728 0.7715 1.0021 0.7753 1.0021 0.7153 1.0181 0.6114 0.6954 0.772 0.795 0.	0 0 0 1 1 0 0 0 0 0 0 0 0 0 0 0 0 0 0 0	DOCKZ DOCKZ CDKNIA SPATSI,VEGFA		5q11.2 5q31.1 5q31.1 5q31.1 5q31.1 5q31.1 5q34 5q34 5q34 5q34 5q35.2 5q35.2 5q35.2 5q35.3 5q55.3 5q55.3 5q55.3 6q21.1 6q16.2 6q16.3 6q21.6 6q16.3 6q21.6 6q21.6 6q21.6 6q21.6	\$q31.1 \$q31.1 \$q34.1 \$q34.5 \$q34.5 \$q35.2 \$q35.2 \$q35.2 \$q35.2 \$q35.3 \$q35.3 \$q35.3 \$q35.3 \$q35.3 \$q35.3 \$q35.3 \$q36.5 \$q36.6 \$q16.6 \$q16.6 \$q16.6 \$q16.6 \$q21 \$q21 \$q21 \$q21 \$q21 \$q21 \$q21 \$q21
#4110T	chrs chrs chrs chrs chrs chrs chrs chrs	13200/GS99 132197746 15113014 15113014 15113014 15113014 15113014 15113014 17579688 17931423 17931423 17931423 17931423 17931423 17938164 24310368 43310344 44371655 100368974 100368974 100368974 100368974 11003697126 10956137 110956137 110956137	1320e514 13215344 10079761 16097961 161530964 175706223 175906223 175906223 175906223 175917675 178017051 178017051 178017051 178017051 178017051 178017051 178017051 178017051 178017051 178017051 178017051 178017051 179017051 179017051 179017051 179017051 179017051 179017051 179017051 179017051 179017051	3093 17 2170 22 7 487 22 13 401 10 110 111 151 3929 6 222 2020 5 9 10 293 45 45 2920 111	1.0015 0.6011 0.8551 1.1868 0.8763 0.5508 0.5508 0.5108 0.9187 0.6304 1.0027 0.7078 0.9778 0.7782 0.7158 0.7158 0.7158 0.7158 0.7158 0.7159 0.	0 0 0 1 1 0 0 0 0 0 0 0 0 0 0 0 0 0 0 0	DOCKZ DOCKZ CDKNILA SPATSI_VEGFA EEFIAI		5911.2 5911.1 5911.1 5911.1 5911.1 5911.1 5931.1 5934.1 5935.2 5935.2 5935.2 5935.2 5935.3 5935.3 5935.3 5935.3 5935.3 6921.1	\$q31.1 \$q34.1 \$q34.4 \$q34.5 \$q35.2 \$q35.2 \$q35.2 \$q35.2 \$q35.3 \$q
#41107 #41107 #41107 #41107 #41107 #41107 #41107 #41107 #41107 #41107 #41107 #41107 #41107 #41107 #41107 #41107 #41107	chrs chrs chrs chrs chrs chrs chrs chrs	132097649 132197764 15113014 15150746 15150746 17579785 17597182	13206514 132161516 132161516 10097611 1015109064 117577762 17597675 178017051 17984762 17984762 17984762 17984762 17984762 10001777 10001772 100087218 100984151 100986000 10098718 100981551 1798592 170185518	3093 17 2170 22 487 22 18 487 22 19 19 19 19 19 19 19 19 19 19 19 19 19	1.0015 0.6011 0.8551 1.1866 0.8763 0.8763 0.8763 0.5508 0.5508 0.9187 0.6394 1.0027 0.7078 0.9187 0.7153 1.0521 0.7153 1.06114 0.9944 0.10552 0.9552 0.8552 0.8552 0.8552	0 0 0 1 1 0 0 0 0 0 0 0 0 0 0 0 0 0 0 0	DOCKZ DOCKZ CDKNIA SPATSI,VEGFA		5911.2 5931.1 5931.1 5931.1 5931.1 5931.1 5934 5934 5935.2 5935.2 5935.2 5935.3 5935.3 5935.3 5925.3 6921.1 6921.1 6921.1 6916.2 6916.3 6921.1 6916.2 6916.3 6921.1 6916.9 6916.3 6921.1 6916.9 6916.3 6921.1 6917 6927 7922.3	\$431.1 \$431.1 \$431.1 \$434.5 \$434.5 \$435.2 \$435.2 \$435.2 \$435.3 \$4
#41107 #41107	chrs chrs chrs chrs chrs chrs chrs chrs	132006699 132197746 16113014 161190246 16113014 161690246 17579688 17591423 17591423 17591423 175915423 178915423	1320e514 13216344 132163344 16097961 161530964 175777628 175906223 175906223 175906223 175906224 17595677 178017051	3093 177 22170 22 487 22 13 401 112 160 111 151 3929 6 6 272 2020 5 9 10 233 45 292 2020 111 121 2020 2020 2020 2030 2030	1.0015 0.0011 0.8551 1.1868 0.8763 0.5508 0.5508 0.5508 0.9187 0.6394 1.0027 0.7078 0.9772 1.0027 0.7153 1.0021 0.7154 0.6114 0.9945 0.72 0.055 0.9552 0.9552 0.9552 0.9552	0 0 0 1 1 0 0 0 0 0 0 0 0 0 0 0 0 0 0 0	DOCKZ DOCKZ CDKNILA SPATSI_VEGFA EEFIAI		5911.2 5911.1 5911.1 5911.1 5911.1 5911.1 5931.1 5934 5934 5935.2 5935.2 5935.2 5935.3 5935.3 5935.3 5935.3 6921.1 6921.1 6921.1 6921.1 6921.1 6921.1 6921.1 6921.1 6921.1 6927 7922.3	\$q31.1 \$q34.1 \$q34.4 \$q34.5 \$q34.5 \$q35.2 \$q35.2 \$q35.2 \$q35.2 \$q35.3 \$q
#41107 #41107	chrs chrs chrs chrs chrs chrs chrs chrs	13209/GS99 132197764 15113014 151569246 15159341 151569246 175913423 175913423 175913423 175913423 175913423 175913423 175913424 17591344 17591344 17591344 17591344 17591344 17591344 17591344 17591344 17591344 175914	131009514 131019514 131019514 131019514 131019514 131019514 131019514 131019514 131019514 131019514 131019514 131019515 13101951 131019515 13101951 13	3093 3093 77 2170 22 487 487 22 13 401 12 160 111 151 3929 5 9 10 2020 5 9 11 12 2020 13 44 14 151 151 152 2020 153 164 175 175 175 175 175 175 175 175	1.0015 0.6011 0.8551 1.1856 0.6763 0.8763 0.8763 0.8763 0.5508 0.9187 0.6194 0.7158 0.7158 0.7158 1.0027 0.7778 0.7158 0.7158 0.7158 0.7159	0 0 0 1 1 0 0 0 0 0 0 0 0 0 0 0 0 0 0 0	DOCKZ DOCKZ CDKNILA SPATSI_VEGFA EEFIAI		5q11.2 5q31.1 5q31.1 5q31.1 5q31.1 5q31.1 5q34 5q34 5q35.2 5q35.2 5q35.2 5q35.2 5q35.3 5q55.3 6q21.1 6q21.1 6q21.1 6q21.1 6q21.6 6q16.2 6q16.3 6q21 6q27 6q27 7q22.3 7q22.3	\$q31.1 \$q34 \$q34 \$q34 \$q35 \$q35 \$q35.2 \$q35.2 \$q35.2 \$q35.3 \$q35.
#41107 #41107 #41107 #41107 #41107 #41107 #41107 #41107 #41107 #41107 #41107 #41107 #41107 #41107 #41107 #41107 #41107 #41107 #41107 #41107	chrs chrs chrs chrs chrs chrs chrs chrs	132006699 132197744 161113014 161169246 151595246 17579688 17591423 17591423 175915552 175915552 175915552 175915552 175915552 175915552 175915552	1320e514 13216341 13216341 13216341 13216341 16097261 161530964 175777728 175976723 175976723 175976723 175976724 17595476 175954	3093 177 227 487 222 133 401 112 160 111 151 153 2929 6 6 2722 2020 5 9 9 10 293 45 292 11 293 293 11 293 293 11 293 293 11 293 293 293 293 293 293 293 293 293 293	1.0015 0.0011 0.8551 1.11668 0.8763 0.5768 0.5768 0.5768 0.5768 0.9187 0.6394 1.0027 0.7078 0.7782 1.0027 0.7782 0.7753 0.7159 0.7154 0.0114 0.9985 0.715 0.0144 0.9985 0.715 0.055 0.756 0.758 0.1149 0.9985 0.758 0.8884 0.8884 0.8881	0 0 0 1 1 0 0 0 0 0 0 0 0 0 0 0 0 0 0 0	DOCKZ DOCKZ CDKNILA SPATSI_VEGFA EEFIAI		5911.2 5911.1 5911.1 5911.1 5911.1 5911.1 5931.1 5934 5934 5935.2 5935.2 5935.2 5935.3 5935.3 5935.3 6921.1	\$931.1 \$931.1 \$934 \$934 \$935.2 \$935.2 \$935.2 \$935.2 \$935.3
#41107 #41107	chrs chrs chrs chrs chrs chrs chrs chrs	13209/GS99 132197764 1611301764 161169746 1151569746 1151569746 117577968 175913423 175913423 175913423 175913423 175913423 175913423 175913423 175913423 175913423 175913643 100016388 100016388 100016388 100016388 100016381 10096171 1009	13209514 13209514 14209514 10097561 1615100964 17577762 17597672 17596775 170017051 1790472 17904775 14070475 1	3093 307 2170 22170 22 487 487 22 13 401 11 151 151 3929 6 222 2020 5 9 10 203 45 2920 11 11 11 11 11 11 11 11 11 11 11 11 11	1.0015 0.6011 0.8551 1.1868 0.6763 0.5769 0.5769 0.5769 0.5769 0.5769 0.778 0.	0 0 0 1 1 0 0 0 0 0 0 0 0 0 0 0 0 0 0 0	DOCKZ DOCKZ CDKNILA SPATSI_VEGFA EEFIAI		5q11.2 5q31.1 5q31.1 5q31.1 5q31.1 5q31.1 5q31.1 5q34 5q34 5q35.2 5q35.2 5q35.2 5q35.2 5q35.3 5q35.3 6q21.1	\$931.1 \$931.1 \$934.1 \$934.5 \$935.2 \$935.2 \$935.2 \$935.2 \$935.3 \$9
#41107 #41107 #41107 #41107 #41107 #41107 #41107 #41107 #41107 #41107 #41107 #41107 #41107 #41107 #41107 #41107 #41107 #41107 #41107 #41107	chrs chrs chrs chrs chrs chrs chrs chrs	132006699 132197744 161113014 161169246 175796881 17591423 17591423 17591542	13206514 13216314 13216314 13216314 13216314 16097361 161530964 175796723 17596773 17596773 175976723 17596773 17597659 17595777 17607051 17595777 17607051 17595777 17607051 17595777 17607051 1759577 17607051 1759577 17607051 1779575 176096600 17777755 176096600 17777755 176096600 17777755 176096600 17777755 176096600 17777755 176096600 17777755 176096600 17777957 176096701	3093 17 17 17 17 17 22 487 22 13 401 11 12 160 11 151 151 151 152 2020 5 9 10 203 45 204 205 205 205 205 205 205 205 205	1.0015 0.6011 0.8551 1,1668 0.8763 1,1668 0.8763 0.5508 0.9187 0.6394 1.0027 0.7782 1.0027 0.7782 1.0027 0.7782 0.7153 0.6114 0.9945 0.72 0.05552 0.4704 0.8944 0.8944 0.8944 0.8944 0.8944 0.8944 0.8944 0.8944 0.8944 0.8944 0.8944 0.8944 0.8944 0.8944 0.8951 1.1893	0 0 0 1 1 0 0 0 0 0 0 0 0 0 0 0 0 0 0 0	DOCKZ DOCKZ CDKNILA SPATSI_VEGFA EEFIAI		Sq11.2 Sq11.2 Sq11.2 Sq11.1 Sq11.2 Sq11.1 Sq11.2 Sq15.2 Sq15.3 Sq	\$931.1 \$931.1 \$934 \$934 \$935.2 \$935.2 \$935.2 \$935.2 \$935.3
MedilOT MedilO	chrs chrs chrs chrs chrs chrs chrs chrs	132097689 13219774 15113014 15113014 15113014 15113014 15113014 17579881 17931423 17931423 17931423 17931525 17938516 293551 17938516 1093617	1320e514 13215344 10073611 161530964 157577678 178017051	3093 17 2170 2170 22 487 22 13 401 11 151 151 152 2020 5 9 10 10 203 45 203 11 11 151 151 151 151 151 151 151 151	1.0015 0.6011 1.8561 1.1856 0.8763 0.8763 0.5508 0.5508 0.5508 0.9974 0.7782 0.9974 0.7785 1.0027 0.778 0.9944 0.7851 1.0021 0.9744 0.9455 0.9944 0.9552 0.9952 0.9552 0.8704 0.8568 0.8568 0.8568 0.8568	0 0 0 0 1 1 0 0 0 0 0 0 0 0 0 0 0 0 0 0	DOCKZ DOCKZ CDKNILA SPATSI_VEGFA EEFIAI		5911.2 5911.2 5911.1 5931.1 5931.1 5931.1 5934.1 5934.5 5935.2 5935.2 5935.2 5935.2 5935.3 5935.3 5935.3 5935.3 6921.1 6921.1 6921.1 6921.1 6921.1 6921.1 6921.1 6921.1 6921.1 6921.1 7936.1 7922.3 7922.3 7922.3 7932.3 7936.1 7936.1	\$931.1 \$931.1 \$934.1 \$934.5 \$935.2 \$935.2 \$935.2 \$935.3 \$9
##1107 ##1107	chrs chrs chrs chrs chrs chrs chrs chrs	132006699 132197744 161113014 161569246 151518014 151569246 17579888 175931423 175931423 175931423 175931423 175931423 175931423 175931423 17593142 17593142 17593142 17593142 17593142 17593141	131009514 131019514 131019514 10097301 10197301 10197301 10197301 10197301 175906723 175906723 175907051 175906723 175907051 175914705 175914705 175914705 175914705 175914705 10001777 100001772 100001772 100001772 100001773 1000001773 100001773 100001773 100001773 100001773 100001773 100001773 100001773 100001773 100001773 100001773 100001773 100001773 1000001773 1000001773 1000001773 10000000000	3093 17 1277 17 177 18 17 18 18 18 18 18 18 18 18 18 18 18 18 18	1.0015 0.6011 0.8551 1.1366 0.8763 0.8763 0.5768 0.5768 0.5768 0.5778 0.6778 0.7778 0.7778 0.7781 0.7781 0.7782 0.7785 0.7782 0.7785 0.7786 0.7786 0.7786 0.7787 0.7788 0.7789 0.7789 0.8518 1.1993 0.9591 1.0317 0.9591	0 0 0 0 1 1 0 0 0 0 0 0 0 0 0 0 0 0 0 0	ATP108 DOCK2 CDKN1A CDKN1A SPATSI_VEGFA EEFIA1 MET		Sq11.2 Sq11.2 Sq11.2 Sq11.1 Sq11.2 Sq11.1 Sq11.2 Sq15.2 Sq15.3 Sq	\$q31.1 \$q34.1 \$q34.5 \$q34.5 \$q34.5 \$q34.5 \$q35.2 \$q35.2 \$q35.2 \$q35.3 \$q36.1 \$q36.1 \$q36.1 \$q36.1 \$q36.1 \$q36.1 \$q36.1 \$q36.1 \$q36.3 \$q
##1107 ##1107	chrs chrs chrs chrs chrs chrs chrs chrs	13200/GS99 132197744 15113014 15113014 15113014 15113014 15113014 15113014 175779688 17931423 17931423 17931423 17931423 17931423 17931423 17931423 17931424 17931518 100368974 100368974 100368974 100368974 100368974 101368971	1320e514 132163344 132163344 16097961 161530964 175702728 175906223 175906773 178017051 17801705	3093 177 22170 22 487 22 13 401 12 160 111 151 152 272 2020 203 45 9 10 10 293 45 292 113 121 121 131 131 131 131 13	1.0015 0.6011 1.8561 1.1856 0.8763 0.8763 0.5508 0.5508 0.5508 0.9974 0.7782 0.9974 0.7785 1.0027 0.778 0.9944 0.7851 1.0021 0.9744 0.9455 0.9944 0.9552 0.9952 0.9552 0.8704 0.8568 0.8568 0.8568 0.8568	0 0 0 0 1 1 0 0 0 0 0 0 0 0 0 0 0 0 0 0	DOCKZ DOCKZ CDKNILA SPATSI_VEGFA EEFIAI		Sq11.2 Sq11.1 Sq	\$q31.1 \$q34.1 \$q34.5 \$q34.5 \$q34.5 \$q35.2 \$q35.2 \$q35.2 \$q35.3 \$q36.1 \$q
#41107 #41107	chrs chrs chrs chrs chrs chrs chrs chrs	132006699 132197744 161113014 161569246 151518014 151569246 17579888 175931423 175931423 175931423 175931423 175931423 175931423 175931423 17593142 17593142 17593142 17593142 17593142 17593141	131009514 131019514 131019514 10097301 10197301 10197301 10197301 10197301 175906723 175906723 175907051 175906723 175907051 175914705 175914705 175914705 175914705 175914705 10001777 100001772 100001772 100001772 100001773 1000001773 100001773 100001773 100001773 100001773 100001773 100001773 100001773 100001773 100001773 100001773 100001773 100001773 1000001773 1000001773 1000001773 10000000000	3093 17 1277 17 177 18 17 18 18 18 18 18 18 18 18 18 18 18 18 18	1.0015 0.0011 0.8551 1.1868 0.8763 0.5508 0.5508 0.5508 0.5508 0.9187 0.6394 1.0027 0.7078 0.9772 0.7153 1.0021 0.7153 0.6114 0.9445 0.726 0.7550 0.7550 0.7750	0 0 0 0 1 1 0 0 0 0 0 0 1 1 0 0 0 0 0 0	ATP108 DOCK2 CDKN1A CDKN1A SPATSI_VEGFA EEFIA1 MET		Sq11.2 Sq11.2 Sq11.2 Sq11.1 Sq11.2 Sq11.1 Sq11.2 Sq15.2 Sq15.3 Sq	\$931.1 \$931.1 \$931.6 \$934.5 \$934.5 \$935.2 \$935.2 \$935.2 \$935.3 \$9
#41107 #41107	chrs chrs chrs chrs chrs chrs chrs chrs	13209/GS99 132197764 16113017 161506746 17577688 175913423 175913423 175913423 175913423 175913423 175913423 175913423 175913423 175913423 175913423 175913423 175913423 175913423 17591343 17591343 17591343 17591343 17591343 17591343 17591343 17591343 17591343 17591343 17591343 17591343 17591343 17591343 17591354 1759	131096514 13101514 13101514 13101514 10097501 10097501 1015109964 17579672 17590775 178017051 17993776 179937776 1799377	3093 17 2170 22 487 22 180 401 11 190	1.0015 0.6011 0.8551 1.1868 0.8763 0.8763 0.5768 0.5768 0.5768 0.5768 0.5778 0.1027 0.7778 0.7778 0.7759 1.0027 0.7759	0 0 0 0 1 1 0 0 0 0 0 0 0 0 0 0 0 0 0 0	ATP108 DOCK2 CDKN1A CDKN1A SPATSI_VEGFA EEFIA1 MET		5q11.2 5q31.1 5q31.1 5q31.1 5q31.1 5q31.1 5q31.1 5q34 5q34 5q35.2 5q35.2 5q35.2 5q35.2 5q35.3 5q55.3 6q21.1 6q21.6 6q21 6q21.6 6q21 6q21 6q21 6q21 6q21 6q21 6q21 6q2	\$q31.1 \$q34.1 \$q34.5 \$q34.5 \$q34.5 \$q35.2 \$q35.2 \$q35.2 \$q35.2 \$q35.3 \$q36.1 \$q
#41107 #41107	chrs chrs chrs chrs chrs chrs chrs chrs	13209/GS-99 132197764 1611907164 161190746 161190746 161190746 17591842 17591842 17591842 17591842 17591842 17591842 17591842 17591842 17591864 17591864 17591864 17591864 10006675 10006675 10006675 1006671 100676130 109761726 100676130 109761726 100676130 109761726 100676130 109761726 100676130 109761726 10076130 100	137096514 132163341 132163341 132163341 160973611 161530964 1515777628 175906223 175906773 178017051 178017051 17803762	3093 17 2170 22 7 487 22 13 401 13 401 151 152 160 272 2020 5 9 10 293 45 2920 11 29 11 29 11 29 2020 5 10 27 21 21 29 2020 10 203 203 203 203 203 203 203 203 203 20	1.0015 0.6011 0.8551 1.1886 0.6763 0.8763 0.8763 0.8763 0.5508 0.9767 0.9778 0.9187 0.0778 0.9974 0.7158 0.7158 0.7159 0.7159 0.7159 0.72 1.0027 0.707 0.9944 0.9944 0.9944 0.9944 0.9944 0.9944 0.9945 0.72 0.0552 0.4704 0.8541 1.1893 0.9551 1.011 0.9551 0.0554 0.9564 0.9564 0.9564 0.9564 0.9574 0.9564 0.9574 0.9564 0.9564 0.9574	0 0 0 0 0 0 0 0 0 0 0 0 0 0 0 0 0 0 0	DOCKZ DOCKZ CDKN1A CDKN1A SPATSI,VEGFA EEFJA1 MET		5q11.2 5q31.1 5q31.1 5q31.1 5q31.1 5q31.1 5q31.1 5q31.1 5q34 5q34 5q35.2 5q35.2 5q35.2 5q35.2 5q35.3 5q35.3 6q21.1	\$931.1 \$931.1 \$931.6 \$934.5 \$934.5 \$935.2 \$935.2 \$935.2 \$935.3 \$9
##1107 ##1107	chrs chrs chrs chrs chrs chrs chrs chrs	132006699 132197746 16113014 16169246 17579688 17591423 17591423 17591423 17591423 17591423 17691423 17691423 17691423 17691423 17691423 17691423 17691423 17691423 17691423 17691423 17691423 17691423 17691423 17691423 17691423 17691424 1	13209514 13206154 13206154 13206154 10097611 1015109964 17577678 17596775 17007051 17596775 17007051 17939762 17939762 179397675 10007071 10006772 10006772 10006772 10006772 10006772 10006773 10006772 10006773	3093 177 22170 227 487 222 133 401 112 160 111 151 152 2020 5 9 10 203 45 2020 11 29 7103 13 13 167 211 21 21 2020 203 203 31 31 31 31 31 32 37 37 37 37 37	1.0015 0.0011 0.8551 1.11668 0.8763 0.5508 0.5508 0.5508 0.5508 0.9187 0.6394 1.0027 0.7078 0.9774 0.7753 1.0027 0.7753 0.114 0.9945 0.7159 0.114 0.9945 0.114 0.9945 0.114 0.9945 0.114 0.9945 0.8581 0.8581 0.8581 0.8584 0.8584 0.8584 0.8584 0.8584 0.8584 0.8585 0.8584 0.8584 0.8584 0.8585 0.8584 0.8585 0.8584 0.8585 0.8584 0.8585 0.8584 0.8585 0.8584 0.8585 0.8584	0 0 0 0 0 0 0 0 0 0 0 0 0 0 0 0 0 0 0	DOCKZ DOCKZ CDKN1A CDKN1A SPATSI,VEGFA EEFJA1 MET		5q11.2 5q11.1 6q11.1 6q21.1 6q	\$931.1 \$931.1 \$931.4 \$934 \$934 \$934 \$935.2 \$935.2 \$935.2 \$935.3 \$935.3 \$935.3 \$935.3 \$935.3 \$935.3 \$921.1 \$936.1 \$936.1 \$736.1 \$

#4110T #4110T										
	chr9	22451487	33369940	216	0,9766	0			9p21.3	9p13.3
	chr9	33385146	33528782	41	0,5776	0			9p13.3	9p13.3
#4110T #4110T	chr9	33529084 95285002	95280063 95526906	1911 26	0,8896 0,6284	0			9p13.3 9q22.31	9q22.31 9q22.31
#4110T	chr9	95609672	95765252	6	0,6284	0				9q22.31 9q22.31
#4110T	chr9	95766351	96214594	68	0,5902	0			9q22.31 9q22.31	9q22.31 9q22.31
#4110T	chr9	96233546	96318768	12	0,8708	0			9q22.31	9022.31
#4110T	chr9	96320200	96846934	33	0,5548	-1			9q22.31	9q22.32
W4110T	chr9	96847618	97054686	10	0,9707	0			9q22.32	9q22.32
#4110T	chr9	97055304	97090898	9	0,5588	-1			9q22.32	9q22.32
#4110T	chr9	97137156	98638327	81	0,8572	0			9q22.32	9q22.32
#4110T	chr9	98643363	98691074	10	1,2649	1			9q22.32	9q22.32
#4110T	chr9	98703784	125946412	1762	0,8809	0	PTPN3		9q22.32	9q33.3
#4110T	chr9	126118587	126164140	16	0,5056	-1			9q33.3	9q33.3
#4110T	chr9	126165725	126692176	19	0,9365	0			9q33.3	9q33.3
N4110T	chr9	126774687	127662779	77	0,6556	0			9q33.3	9q33.3
#4110T	chr9	127670703	129246281	105	0,9246	0			9q33.3	9q33.3
#4110T	chr9	129265499	131122691	405	0,6514	0			9q33.3	9q34.11
#4110T #4110T	chr9	131133677 131150137	131140350 141016186	2164	1,1149 0,6261	0	TSC1	7	9q34.11 9q34.11	9q34.11 9q34.3
W4110T	chr10	93526	43326429	1867	0,932	0	1301		10p15.3	10q11.21
#4110T	chr10	43572743	43623638	21	0,5511	-1			10q11.21	10q11.21
#4110T	chr10	43650928	94821123	2675	0,8629	0	PTEN		10q11.21	10q23.33
#4110T	chr10	94821879	94835650	10	0,5339	-1			10q23.33	10q23.33
#4110T	chr10	94836377	131973150	3039	0,8613	0			10q23.33	10q26.3
W4110T	chr10	131973307	135440158	335	0,5854	0			10q26.3	10q26.3
#4110T	chr11	193127	2950365	788	0,5128	-1		11p15.5	11p15.5	11p15.4
#4110T	chr11	2970492	20104639	1597	0,8525	0			11p15.4	11p15.1
#4110T	chr11	20112488	20114695	3	1,1747	1			11p15.1	11p15.1
#4110T	chr11	20117266	20181687	13	0,6625	0			11p15.1	11p15.1
#4110T	chr11	20385408	44255729	747	0,9882	0			11p15.1	11p11.2
#4110T	chr11	44257884	45957239	97	0,6437	0			11p11.2	11p11.2
#4110T	chr11 chr11	45958083 46105743	46100701 46760886	14 118	0,9916	0			11p11.2	11p11.2 11p11.2
#4110T	chr11	46761056	46760886	45	1,0581	0			11p11.2 11p11.2	11p11.2
#4110T	chr11	46886043	66394035	2717	0,7122	0			11p11.2	11q13.2
#4110T	chr11	66407389	66444345	7	1,0282	0			11q13.2	11q13.2
W4110T	chr11	66453459	66512302	37	0,6111	0			11q13.2	11q13.2
#4110T	chr11	66515919	66568537	6	1,1514	0			11q13.2	11q13.2
#4110T	chr11	66571563	71529240	646	0,6322	0			11q13.2	11q13.4
#4110T	chr11	71529866	71701703	12	0,9883	0			11q13.4	11q13.4
#4110T	chr11	71705832	72539979	203	0,6765	0			11q13.4	11q13.4
#4110T	chr11	72540391	72726892	17	1,0229	0			11q13.4	11q13.4
#4110T	chr11	72794763	73371847	51	0,6482	0			11q13.4	11q13.4
#4110T	chr11	73372579	74862435	183	0,9211	0			11q13.4	11q13.4
#4110T	chr11	74873765	75526511 76730798	80	0,6361	0			11q13.4	11q13.5
#4110T	chr11	75562987		58	0,9469	0			11q13.5	11q13.5
#4110T #4110T	chr11 chr11	76731344 76940236	76938935 120207969	65 2450	0,6136	0	HMBS		11q13.5	11q13.5
N4110T	chr11	120276839	120310884	11	1,1938	1	nwio3		11q13.5 11q23.3	11q23.3 11q23.3
#4110T	chr11	120312471	124761326	328	0.8679	0			11q23.3	11q24.2
#4110T	chr11	124761630	124767656	11	0,4675	-1			11q24.2	11q24.2
#4110T	chr11	124789780	133781841	441	0,8495	0			11q24.2	11q25
#4110T	chr11	133790465	133816055	17	0,5592	-1		11q25	11q25	11q25
#4110T	chr11	133826617	134257498	111	0,7966	0			11q25	11q25
#4110T	chr12	176326	112600259	8885	0,8882	0	ARID2,CDKN1B		12p13.33	12q24.13
#4110T	chr12	112600957	112610570	9	0,4597	-1			12q24.13	12q24.13
#4110T	chr12	112613602	112684792	38	0,8602	0			12q24.13	12q24.13
#4110T	chr12	112685310	112696992	10	1,1457	0	1000000		12q24.13	12q24.13
#4110T	chr12	112699171	133810818	2029	0,7472	0	HNF1A		12q24.13	12q24.33
#4110T	chr13	19748151	115090537	3346	0,9396	0	RB1	\	13q12.11	13q34
#4110T	chr14	19378084	71478237	3278	0,8883	0			14q11.2	14q24.2
#4110T #4110T	chr14 chr14	71479811 71500201	71495463 75276291	6 387	1,3736 0,8248	0			14q24.2 14q24.2	14q24.2 14q24.3
#4110T	chr14	75276659	75302041	12	1,1989	1			14q24.3	14q24.3
#4110T	chr14	75321920	103470313	1635	0,8597	0			14q24.3	14q32.32
#4110T	chr14	103474851	103803509	32	0,5102	-1				14q32.32
#4110T	chr14	103804737			0,8092	0			14q32.32	
#4110T	chr14	103004737	104518369	128	0,0092	0			14q32.32 14q32.32	14q32.33
#4110T		104552149	104518369 105995651	264	0,5105	-1				14q32.33 14q32.33
	chr15			264 4726					14q32.32	
#4110T	chr15	104552149 20740212 73590821	105995651 73585810 73660219	264 4726 10	0,5106 0,8692 0,5673	-1 0 0			14q32.32 14q32.33 15q11.2 15q24.1	14q32.33 15q24.1 15q24.1
#4110T	chr15 chr15	104552149 20740212 73590821 73735606	105995651 73585810 73660219 73855587	264 4726 10 8	0,5106 0,8692 0,5673 1,2202	-1 0 0			14q32.32 14q32.33 15q11.2 15q24.1 15q24.1	14q32.33 15q24.1 15q24.1 15q24.1
#4110T #4110T	chr15 chr15 chr15	104552149 20740212 73590821 73735606 73862627	105995651 73585810 73660219 73855587 82431091	264 4726 10 8 879	0,5106 0,8692 0,5673 1,2202 0,753	-1 0 0 1			14q32.32 14q32.33 15q11.2 15q24.1 15q24.1 15q24.1	14q32.33 15q24.1 15q24.1 15q24.1 15q25.2
#4110T #4110T #4110T	chr15 chr15 chr15 chr15	104552149 20740212 73590821 73735606 73862627 82444285	105995651 73585810 73660219 73855587 82431091 82533677	264 4726 10 8 879 14	0,5106 0,8692 0,5673 1,2202 0,753 1,1445	-1 0 0 1 0			14q32.32 14q32.33 15q11.2 15q24.1 15q24.1 15q24.1 15q24.1	14q32.33 15q24.1 15q24.1 15q24.1 15q25.2 15q25.2
#4110T #4110T #4110T #4110T	chr15 chr15 chr15 chr15 chr15	104552149 20740212 73590821 73735606 73862627 82444285 82545074	105995651 73585810 73660219 73855587 82431091 82533677 90233835	264 4726 10 8 879 14 562	0,5106 0,8692 0,5673 1,2202 0,753 1,1445 0,801	-1 0 0 1 0 0			14q32.32 14q32.33 15q11.2 15q24.1 15q24.1 15q24.1 15q25.2 15q25.2	14q32.33 15q24.1 15q24.1 15q24.1 15q25.2 15q25.2 15q26.1
#4110T #4110T #4110T #4110T	chr15 chr15 chr15 chr15 chr15 chr15	104552149 20740212 73590821 73735606 73862627 82444285 82545074 90245129	105995651 73585810 73660219 73855587 82431091 82533677 90233835 90258269	264 4726 10 8 879 14 562 5	0,5106 0,8692 0,5673 1,2202 0,753 1,1445 0,801 1,1258	-1 0 0 1 0 0 0			14q32.32 14q32.33 15q11.2 15q24.1 15q24.1 15q24.1 15q24.1 15q25.2 15q25.2	14q32.33 15q24.1 15q24.1 15q24.1 15q25.2 15q25.2 15q26.1 15q26.1
#4110T #4110T #4110T #4110T #4110T	chr15 chr15 chr15 chr15 chr15 chr15 chr15	104552149 20740212 73590821 73735606 73862627 82444285 82545074 90245129 90260161	105995651 73585810 73660219 73855587 82431091 82533677 90233835 90258269 90809575	264 4726 10 8 879 14 562 5	0,5106 0,8692 0,5673 1,2202 0,753 1,1445 0,801 1,1258 0,6636	-1 0 0 1 0 0 0 0			14q32.32 14q32.33 15q11.2 15q24.1 15q24.1 15q24.1 15q24.1 15q25.2 15q26.1 15q26.1	14q32.33 15q24.1 15q24.1 15q24.1 15q25.2 15q25.2 15q26.1 15q26.1
M4110T M4110T M4110T M4110T H4110T M4110T M4110T	chr15	104552149 20740212 73590821 73735606 73862627 82444285 82545074 90245129 90260161 90814720	105995651 73585810 73660219 73855587 82431091 82533677 9023835 90258269 90809575 91147648	264 4726 10 8 879 14 562 5 87 46	0,5106 0,8692 0,5673 1,2202 0,753 1,1445 0,801 1,1258 0,6636 0,968	-1 0 0 1 0 0 0 0 0			14q32.32 14q32.33 15q11.2 15q24.1 15q24.1 15q24.1 15q25.2 15q25.2 15q26.1 15q26.1	14q32.33 15q24.1 15q24.1 15q24.1 15q25.2 15q25.2 15q26.1 15q26.1 15q26.1
#4110T #4110T #4110T #4110T #4110T	chr15 chr15 chr15 chr15 chr15 chr15 chr15	104552149 20740212 73590821 73735606 73862627 82444285 82545074 90245129 90260161	105995651 73585810 73660219 73855587 82431091 82533677 90233835 90258269 90809575	264 4726 10 8 879 14 562 5	0,5106 0,8692 0,5673 1,2202 0,753 1,1445 0,801 1,1258 0,6636	-1 0 0 1 0 0 0 0			14q32.32 14q32.33 15q11.2 15q24.1 15q24.1 15q24.1 15q24.1 15q25.2 15q26.1 15q26.1	14q32.33 15q24.1 15q24.1 15q24.1 15q25.2 15q25.2 15q26.1 15q26.1
#4110T #4110T #4110T #4110T #4110T #4110T #4110T #4110T	chr15	104552149 20740212 73590821 73735606 73862627 82444285 82545074 90245129 90260161 90814720 91150660	105995651 73585810 73660219 73655587 82431091 82533677 90233835 90258269 90809575 91147648 91185268	264 4726 10 8 879 14 562 5 87 46	0,5106 0,8692 0,5673 1,2202 0,753 1,1445 0,801 1,1258 0,6636 0,968 0,6909	-1 0 0 1 0 0 0 0 0 0			14q32.32 14q32.33 15q11.2 15q24.1 15q24.1 15q24.1 15q25.2 15q26.1 15q26.1 15q26.1	14q32.33 15q24.1 15q24.1 15q24.1 15q25.2 15q25.2 15q26.1 15q26.1 15q26.1 15q26.1
#4110T #4110T #4110T #4110T #4110T #4110T #4110T #4110T #4110T	chr15	104552149 20740212 73590821 73790821 73735606 73862627 82444285 82545074 90245129 90260161 90814720 91150660 91150660 91150672 91358420 91504924	105995651 73585810 73660219 73855587 82431091 82533677 90233835 90258269 9009575 91147648 91185268	264 4726 10 8 879 14 562 5 87 46 9 20 88	0,5106 0,8692 0,5673 1,2202 0,753 1,1445 0,801 1,1258 0,6636 0,968 0,6909 1,005 0,5901	-1 0 0 1 1 0 0 0 0 0 0 0 0 0			14q32.32 14q32.33 15q11.2 15q24.1 15q24.1 15q24.1 15q25.2 15q26.1 15q26.1 15q26.1	14q32.33 15q24.1 15q24.1 15q24.1 15q25.2 15q25.2 15q26.1 15q26.1 15q26.1 15q26.1 15q26.1
M4110T M4110T M4110T M4110T M4110T M4110T M4110T M4110T M4110T M4110T M4110T M4110T M4110T	chr15 chr16	104552149 20740212 73590821 73590821 73735606 73862627 82444285 82545074 90245129 90260161 91150660 91290672 91358420 9150924 97494	105995651 73585810 73565219 7366219 7365587 82431091 82533677 9023835 90258269 90809575 91147648 91185268 91354270 102467803 23091379	264 4726 10 8 879 14 562 5 87 46 9 20 88 379 3055	0,5106 0,8692 0,5673 1,2202 0,753 1,1445 0,801 1,1258 0,6636 0,968 0,6909 1,005 0,5901 0,8669 0,6967	-1 0 0 1 1 0 0 0 0 0 0 0 0 0 0 0 0 0 0 0	AXIN1,TSC2		14q32.32 14q32.33 15q11.2 15q24.1 15q24.1 15q24.1 15q25.2 15q25.2 15q25.2 15q26.1 15q26.1 15q26.1 15q26.1 15q26.1 15q26.1	14q32.33 15q24.1 15q24.1 15q24.1 15q25.2 15q25.2 15q26.1 15q26.1 15q26.1 15q26.1 15q26.1 15q26.1 15q26.1
M4110T M4110T M4110T M4110T M4110T H4110T H4110T M4110T	chr15 chr16 chr16	104552149 20740212 73590821 73735606 73862627 82444285 82545074 90260161 90814720 91150660 91150660 91150692 91504924 97494 23093819	105995651 73585810 73585810 73680219 73855587 82431091 82533677 90233835 90258269 90809575 91147648 91185268 91354336 91504270 102462803 90391379 23117580	264 4726 10 8 879 14 562 5 87 46 9 20 88 379 3055 9	0,5106 0,8692 0,5673 1,2202 0,753 1,1445 0,801 1,1258 0,6636 0,968 0,6909 1,005 0,5901 0,8609 0,6909 1,1276	-1 0 0 0 1 1 0 0 0 0 0 0 0 0 0 0 0 0 0 0	AXIN1,TSC2		14q32.32 14q32.33 15q11.2 15q24.1 15q24.1 15q24.1 15q25.2 15q26.1 15q26.1 15q26.1 15q26.1 15q26.1 15q26.1 15q26.1 15q26.1	14q32.33 15q24.1 15q24.1 15q24.1 15q25.2 15q25.2 15q26.1 15q26.1 15q26.1 15q26.1 15q26.1 15q26.1 15q26.1 15q26.1 15q26.1
M4110T	chr15 chr16 chr16 chr16	104552149 20740212 73590821 73735606 73862627 82444285 82545074 90245129 90245129 91150660 91290672 91358420 91504924 97494 23093819 23119435	105995651 73885810 73860219 73860219 73855587 82431091 82533677 90233835 90258269 90809575 91147648 91354270 102462803 23091379 23117580	264 4726 10 8 879 14 562 5 87 46 9 20 88 379 3055 9	0,5106 0,8692 0,5673 1,2202 0,753 1,1445 0,801 1,1258 0,6636 0,968 0,6999 1,005 0,5901 0,8609 0,6967 1,1276 0,7477	-1 0 0 0 1 0 0 0 0 0 0 0 0 0 0 0 0 0 0 0	ARINI,TSC2		14q32.32 14q32.33 15q11.2 15q24.1 15q24.1 15q24.1 15q25.2 15q25.2 15q26.1 15q26.1 15q26.1 15q26.1 15q26.1 15q26.1 15q26.1 15q26.1 15q26.1 15q26.1	14g32.33 15g24.1 15g24.1 15g24.1 15g25.2 15g25.2 15g26.1 15g26.1 15g26.1 15g26.1 15g26.1 15g26.1 15g26.1 15g26.1 15g26.1 15g26.3 16g12.2 16g12.2
M4110T	chv15 chv16 chv16 chv16 chv16 chv16 chv16	104552149 20740212 73590821 73735606 73862627 82544285 82545074 90245129 90260161 90814720 91150660 91290672 91358420 97494 23093819 23119435 2339689	10:995651 73585810 73680219 73680219 73855587 82431091 82533677 90233835 90258269 90809575 91147648 91354536 91504270 102462803 230931379 23117580 23995491 29458235	264 4726 10 8 879 14 562 5 87 46 9 20 88 88 379 3055 9	0,5106 0,8692 0,5673 1,2202 0,753 1,1445 0,801 1,1258 0,6636 0,968 0,6909 1,005 0,5901 0,8609 0,6967 1,1276 0,7477 0,9927	-1 0 0 0 1 1 0 0 0 0 0 0 0 0 0 0 0 0 0 0			14q32.32 14q32.33 15q11.2 15q24.1 15q24.1 15q25.2 15q26.1 15q26.1 15q26.1 15q26.1 15q26.1 15q26.1 15q26.1 15q26.1 15q26.1 15q26.1 15q26.1 15q26.1 15q26.1 15q26.1 15q26.1	14q32.33 15q24.1 15q24.1 15q24.1 15q25.2 15q25.2 15q26.1 15q26
M4110T	chr15 chr16 chr16 chr16 chr16 chr16 chr16 chr16	104552149 20740212 73590821 73735606 73862627 82444285 82545074 90245129 90260161 90814720 91150660 91290672 91358420 91504924 97494 23093819 23119435 23119435	105995651 7388810 73868219 73865219 73855587 82431091 82533677 90233835 90258269 90809575 91147626 91354536 91354536 91504270 102462803 23091379 23117580 23995491 23995491	264 4726 10 8 879 14 562 5 87 46 9 20 88 8379 3055 9	0,5106 0,8692 0,5673 1,2202 0,753 1,1445 0,801 1,1258 0,6636 0,968 0,6909 1,005 0,5901 0,8609 0,6967 1,1276 0,7477 0,7477	-1 0 0 0 1 0 0 0 0 0 0 0 0 0 0 0 0 0 0 0	AXIN1_TSC2 BRD7		14q32.32 14q32.33 15q11.2 15q24.1 15q24.1 15q24.1 15q26.1 15q2	1492.33 15q24.1 15q24.1 15q24.1 15q25.2 15q25.2 15q26.1 15q26.1 15q26.1 15q26.1 15q26.1 15q26.1 15q26.1 15q26.3 15q26.1 15q26.3 15q26.3 15q26.3 15q26.3 15q26.3 15q26.3
#4110T	chr15 chr16	104552149 20740212 73550821 7373500821 73735606 738862627 82444285 90245129 90245129 90245129 91150660 91150662 91504924 97494 23033819 2319435 23956889 2445503 56792508	10:995651 73585810 73660219 73865587 82431091 82533677 90233835 90258269 90809575 91147648 91185268 91354536 91504270 102462803 23091379 23117580 23935491 29458235 56782249	264 4776 10 8 879 14 562 5 87 46 9 20 88 379 3055 9 1389 20	0,5106 0,8692 0,5673 1,2202 0,753 1,1445 0,6636 0,998 0,6909 1,005 0,8901 0,8609 0,6909 1,005 0,8901 0,8609 0,6909 1,075 1,1276 0,7477 0,9927 0,754 1,0301	-1 0 0 0 0 1 1 0 0 0 0 0 0 0 0 0 0 0 0 0			14q32.32 14q32.32 15q11.2 15q24.1 15q24.1 15q24.1 15q26.1 15q25.2 15q26.1 15q2	14q22.33 15q24.1 15q24.1 15q24.1 15q25.2 15q25.2 15q26.1 15q26
M4110T	chv15 chv16	104552149 20740212 773590821 77375506 7735606 773867627 82444285 82545074 90245129 90245129 90245129 9150402 91150607 911507 9115	10999651 73868310 73860219 73855587 82431091 82533677 9023836 9080975 9116758 9116758 9116758 9116758 91150227 10246383 2393591 2393591 2393591 2393591 2393591 2395591 56782249	264 4726 10 8 879 14 562 5 87 46 9 20 88 379 3055 9 1389 20 403	0,5106 0,8692 1,2702 1,2702 0,601 1,1445 0,603 1,1445 0,603 0,609 1,005 0,009 1,005 0,009 1,005 0,009 1,005 0,009 1,005 0,009 1,005 0,009 1,005 0,009 1,005 0,009 1,005 0,009 1,005 0,009 1,005 0,009 1,005 0,009 1,005 0,009 1,005 0,009 1,005 0,009 0,0	-1 0 0 0 0 0 0 0 0 0 0 0 0 0 0 0 0 0 0 0			14q12.12 14q12.32 15q11.2 15q24.1 15q24.1 15q24.1 15q25.2 15q25.2 15q26.1 15q2	14q22.33 15q24.1 15q24.1 15q24.2 15q25.2 15q25.2 15q26.1 15q26.1 15q26.1 15q26.1 15q26.1 15q26.1 15q26.1 15q26.2 15q26.2 15q26.3 15q26
#4110T	chv15 chv16	104552149 20740212 73550821 7373500821 73735606 738862627 82444285 90245129 90245129 90245129 91150660 91150662 91504924 97494 23033819 2319435 23956889 2445503 56792508	1.0999651 7385810 73660219 7385537 82431091 8233367 90258289 9080975 9118758 9118758 911902270 10246289 9280975 92935815 95562229 956878466 95550479	264 4726 10 8 879 14 552 5 5 87 46 9 20 88 88 379 379 9 3055 9 3055 9 3055 9 20 403 44	0.5106 0.8692 0.5673 1.2702 1.2702 1.2702 1.1445 1.1455 0.6636 0.6909 1.005 0.5901 1.005 0.6667 1.1276 0.7447 0.9227 0.7544 1.0301 0.6719	-1 -1 -0 -0 -0 -0 -0 -0 -0 -0 -0 -0 -0 -0 -0			14q12.22 14q12.22 14q11.2 15q24.1 15q24.1 15q24.1 15q24.1 15q24.1 15q26.1 1	1492.2 33 15924.1 15924.1 15924.1 15925.2 15925.2 15925.2 15926.1 1592
#4110T	chris	104552149 20740212 72550821 72735666 77385667 82544285 8255574 90245129 9024015 9034770 91354072 91354	10999651 73868310 73860219 73855587 82431091 82533677 9023836 9080975 9116758 9116758 9116758 9116758 91150227 10246383 2393591 2393591 2393591 2393591 2393591 2395591 56782249	264 4726 10 8 879 14 562 5 87 46 9 20 20 88 83 379 20 5 9 20 40 3 9 1389 20 40 40 40 40 40 40 40 40 40 40 40 40 40	0,5106 0,8692 1,2702 1,2702 0,601 1,1445 0,603 1,1445 0,603 0,609 1,005 0,009 1,005 0,009 1,005 0,009 1,005 0,009 1,005 0,009 1,005 0,009 1,005 0,009 1,005 0,009 1,005 0,009 1,005 0,009 1,005 0,009 1,005 0,009 1,005 0,009 1,005 0,009 1,005 0,009 0,0	-1 -1 -0 -0 -0 -0 -0 -0 -0 -0 -0 -0 -0 -0 -0			14q12.12 14q12.32 15q11.2 15q24.1 15q24.1 15q24.1 15q24.1 15q25.2 15q26.1 15q2	1492.33 15924.1 15924.1 15924.1 15925.2 15925.2 15926.1 15926.
#4110T	chv15 chv16	104552149 20740212 77375062 77375062 8244285 82545074 90245129 90260151 90260151 91150660 91150660 91150660 911506924 923819 220938319 22115945 22996989 2495928 56895288	1.0999651 73555810 73660219 73855587 73855810 73860219 73855587 7385587 73813107 82333077 9025829 9025829 9025829 91137648 91137648 911354536 911354536 911354536 91504270 1040280 23093139 2309	264 4726 10 8 879 14 552 5 5 87 46 9 20 88 88 379 379 9 3055 9 3055 9 3055 9 20 403 44	0.5106 0.8992 0.5673 1.2202 1.2202 1.2202 1.2202 1.2445 1.2445 1.258 1.265 1.265 1.265 1.265 1.265 1.276 1.276 1.277 1.275	-1 -1 -0 -0 -0 -0 -0 -0 -0 -0 -0 -0 -0 -0 -0			14422.21 14422.31 14422.31 15411.7 15424.1 15424.1 15424.1 15425.1 15425.1 15425.1 15426.1 154	1492.33 15924.1 15924.1 15924.1 15925.2 15925.2 15925.2 15926.1 15926.
M4110T M4	chv15 chv16	104552149 10452149 10552149 10	1.0999651 73565810 73660219 7385587 7385810 73860219 7385587 7385587 73823197 73823197 90258249 9080575 91187588 91187588 91187588 91187588 91187588 91592170 101445893 22091379 23117995 58578466 58578466 58578466 58578466	264 4726 10 8 879 14 552 5 87 46 9 9 20 88 8 379 3055 9 1389 20 403 404 404 118	0.5106 0.8992 0.5973 1.2202 1.2202 1.2202 1.2445 1.1445 0.6656 0.9699 1.005 0.9890 0.6997 1.1276 0.6997 1.1276 0.6997 1.1276 0.6997 1.1276 0.6997 1.1276 0.6997 1.1276 0.6997 1.1276 0.6997 1.1276 0.7477 0.9927 0.9927 0.744 1.0048 0.7473 1.0048 0.7473 1.0048	-1 -0 -0 -0 -0 -0 -0 -0 -0 -0 -0 -0 -0 -0			14q12.12 14q12.32 15q11.2 15q24.1 15q24.1 15q24.1 15q24.1 15q25.2 15q26.1 15q2	14q32.33 15q24.1 15q24.1 15q24.1 15q24.1 15q25.2 15q25.1 15q26
#41107 #41107	ch/15 ch/16	104552149 20740212 73550821 73735666 77385667 7386667 7386667 90245129 9024016 91150607 91150	1.0999651 73555810 73660219 73650219	264 4726 10 8 879 14 15 562 5 87 46 9 20 88 379 3005 9 11889 20 403 441 18 32	0.5106 0.8992 0.5678 1,2202 0,753 1,1445 0,6616 0,6636	-1 -1 -0 -0 -0 -0 -0 -0 -0 -0 -0 -0 -0 -0 -0			14q12.12 14q12.32 14q12.31 15q14.1 15q24.1 15q24.1 15q24.5 15q25.2 15q25.1 15q26.1 15q	14q22.33 15q24.1 15q24.1 15q24.1 15q25.2 15q25.2 15q25.2 15q26.1 15q26
#4107 #41107	chv15 chv16	104552J49 10552J49 10552J49 10552J49 10552J49 10552566 173735666 173735666 173735666 18244285 1824529 190080161 1900814720 1910860 191296672 191398420 19150492 191998420 19150492 191998420 19150492 191998420 19150492 19	1.0999651 73558310 73660219 73855367 73558310 73660219 73855367 73833507 73833507 90158269 90089575 91147648 91185268 91185268 91185268 91185268 91504270 1004270 1004270 20193379 23117590 23995491 23417590 566752 5878466 65038659 77327004	264 4726 10 8 879 14 14 55 562 57 46 9 20 88 379 3095 9 636 9 1389 20 44 18 32 1642	0.5106 0.8992 0.5673 1.2202 1.2202 1.2445 1.1445 1.1445 0.6686 0.6686 0.6686 0.6890 1.005 0.5901 0.6890 0.6897 1.107 0.7477 0.9227 0.7477 0.921 1.0088 0.743 1.0048 0.744 1.0048 0.7467 1.0445	-1 -0 -0 -0 -0 -0 -0 -0 -0 -0 -0 -0 -0 -0			14q12.23 14q12.33 15q11.2 15q11.2 15q24.1 15q24.1 15q24.1 15q25.2 15q25.2 15q26.1 15q2	1492.33 15024.1 15024.1 15024.1 15025.2 15025.2 15025.2 15026.1 15026.
#41107 #41107	chris	104552149 20740212 737506821 737506821 737506821 737860627 82444285 8224507 9026015 90150692 9120067 91150692 91150692 9120067 9120067 9120067 9120067 9120067 9135450 913540	10999651 7356540 7356540 73660219 73660219 73650219 23855547 24313091 82533677 90258209 90258209 91347648 9134536 9134536 9134536 9135456 9135456 9135456 9135456 9135456 9135456 9135456 9135456 9135456 9135456 9135456 9135456 9135456 9135456 9135456 9135456 9135456 9135456 913546 9	264 4726 10 8 879 14 562 562 5 87 46 9 20 88 379 3055 9 636 9 11889 20 403 44 18 18 12 1642 15 1005	0.5106 0.8692 0.5673 1.2202 0.5673 1.1245 0.753 1.1445 0.6616 0.968 0.6636 0.969 0.0909 1.005 0.8699 0.9901 0.8699 0.9901 0.8777 0.7447 1.1090 0.7467 1.10462 0.7467	1 0 0 0 0 0 0 0 0 0 0 0 0 0 0 0 0 0 0 0			14q12.12 14q12.32 14q12.31 15q14.1 15q24.1 15q24.1 15q24.1 15q26.1 15q	14q22.33 15q24.1 15q24.1 15q24.1 15q24.1 15q25.2 15q25.2 15q26.1 15q26
#41107 #41107	chv15 chv16 chv17 chv17 chv17	104552149 10552149 10552149 10552149 10552149 1055266 107375666 107386672 107464285 107467485 1074674285 107467485 1074674285 107467485 1	1.0999651 73555810 73660219 73855587 73855810 73860219 73855587 782431091 82333077 90389275 91147648 91187648 91187648 91187648 91504270 1046280 2303399 23033399 23033399 23033399 23033399 24033399 25056782249 566782249 566782249 566782249 574034074 7404349 7404349 7404349 7404349 7404349	264 4726 10 8 99 14 14 55 52 52 54 46 9 20 88 379 3055 9 1389 20 403 44 18 32 1642 15 1005 404 15	0.5106 0.8992 0.3673 1,2202 0.3673 1,2202 0.3673 1,1445 0.6636 0.6636 0.6636 0.6636 0.6636 0.6636 1,065 0.5802 0.0667 1,105 0.754 1,001 0.0714 1,001	-1 -1 -0 -0 -0 -0 -0 -0 -0 -0 -0 -0 -0 -0 -0			14412.23 14412.23 15411.2 15411.1 15424.1 15424.1 15425.2 15425.2 15425.1 15426.1 1542	14q22.33 15q24.1 15q24.1 15q24.1 15q25.2 15q25.2 15q26.1 15q26
#41107 #41107	chris	104523149 20740212 73550821 73750621 73750621 737862627 82444285 8255507 90260151 90814720 91350420 91	10999651 73565810 73660219 73660219 73650219 7385587 28431091 82533677 90358209 903699757 91147648 911547546 9156470 10464203 23093139 23117580 23955917 23117580 55550479 55616752 55713866 65036559 77327064 77401419 90142284	264 4726 10 8 879 14 562 562 579 46 9 20 88 379 3055 9 1389 3055 1189 20 403 44 18 18 32 1642 151 1005	0.5106 0.8692 0.5671 1.2202 0.5673 1.1445 0.753 1.1445 0.8610 0.8610 0.8660 0.8690 0.8600 0.8600 0.8600 0.9901 1.1276 0.754 1.1276 0.7477 1.10301 0.6719 0.6828 0.6828 0.68590 0.86590 0.9901 0.9901	-1 -0 -0 -0 -0 -0 -0 -0 -0 -0 -0 -0 -0 -0			14q12.22 14q12.23 14q11.2 15q24.1 15q24.1 15q24.1 15q24.1 15q24.1 15q26.1 15q2	14q22.33 15q24.1 15q24.1 15q24.1 15q25.2 15q25.2 15q25.2 15q26.1 15q26.1 15q26.1 15q26.1 15q26.1 15q26.1 15q26.1 15q26.1 15q26.1 15q26.1 15q26.1 15q26.1 15q26.1 15q26.3 15q26
#41107 #41107	chris	104552149 20752117 273506821 77375666 77385667 90245129 90245129 9024015 9034770 9034770 91354029 9135	1.0999651 73555810 73660219 73855587 73855810 73860219 73855587 82431091 82333077 9025829 9025829 90809575 91147648 91354536 91354536 91354536 91354536 91354536 91354536 91354536 91504270 101402803 20013739 23013739 23013739 23013739 23013739 23013739 23117580 6008659 7740419 90142234 2344818 2356001 3427574 2316560	264 4726 10 8 879 14 16 552 562 20 88 87 20 88 99 20 379 3055 9 11889 20 403 44 18 32 1642 15 1005 404 17 32	0.5106 0.8992 0.5673 1.2202 0.5673 1.2202 1.2202 0.6016 0.6016 0.6036 0.6036 0.6036 0.6036 0.6036 0.5001 1.005 0.5001 1.005 0.5001 1.005 0.5001 1.005 0.5001 1.005 0.5001 1.005 0.5001 1.005 0.5001 1.005 0.5001 1.1276 0.7477 0.7427 0.754 1.0092 0.7423 0.754 1.0048 0.7431 1.0048 0.7432 0.7447 0.7544 0.5004 0.60528 0.60599 0.60528 0.60599 0.60599 0.60594	-1 -1 -0 -0 -0 -0 -0 -0 -0 -0 -0 -0 -0 -0 -0			14q12.12 14q12.32 15q11.2 15q24.1 15q24.1 15q24.1 15q24.5 15q25.2 15q26.1 15q2	14q22.33 15q24.1 15q24.1 15q25.2 15q25.2 15q25.2 15q25.2 15q26.1 15q26
#41107 #41107	chris	104552J49 104552J49 17375666 17375666 17375666 17375666 17375666 17375666 173866767 18244285 182454594 19024139 19026016 190341720 1913660 19136607 19136607 19136607 19136607 19136607 19136607 19136607 191360807 191360807 191360807 191360807 191360807 191360807 191360807 191360807 191360807 191360807 191360807 19136080808 191360807 19136080808 19136080808 1913608080808080808080808080808080808080808	1.0999651 7355810 73660219 73650310 73660219 7385587 24315091 82333677 90089757 91147648 91185268 91185268 91185268 91185268 91185268 91504270 10046280 24091379 24117500 24995491 2491225 56678466 56038659 77327004 77401479 90142284 2456600 24595600 3427574	264 4726 4726 10 8 879 14 455 55 87 46 9 20 88 379 3055 9 1389 20 43 44 15 15 1005 404 15 407 32 94	0.5106 0.8992 0.5673 1.2202 1.2202 1.2202 1.2445 1.1445 1.1445 1.1445 1.1445 1.1445 1.1445 1.1658	-1 -1 -0 -0 -0 -0 -0 -0 -0 -0 -0 -0 -0 -0 -0			1442.2.3 1442.2.3 1442.2.3 1442.2.3 15411.7 15424.1 15424.1 15424.1 15424.1 15425.1 15426.1 15	14q22.33 15q24.1 15q24.1 15q24.1 15q24.1 15q25.2 15q25.2 15q25.1 15q26.1 15q26.1 15q26.1 15q26.1 15q26.1 15q26.1 15q26.1 15q26.1 15q26.1 15q26.1 15q26.1 15q26.1 15q26.1 15q26.1 15q26.3 15q26
#41107 #41107	chris	104552149 20752117 273506821 77375666 77385667 90245129 90245129 9024015 9034770 9034770 91354029 9135	1.0999651 73555810 73660219 73855587 73855810 73860219 73855587 82431091 82333077 9025829 9025829 90809575 91147648 91354536 91354536 91354536 91354536 91354536 91354536 91354536 91504270 101462803 22001379 2301579	264 4726 10 8 879 14 16 552 562 20 88 87 20 88 99 20 379 3055 9 11889 20 403 44 18 32 1642 15 1005 404 17 32	0.5106 0.8992 0.5673 1.2202 0.5673 1.2202 1.2202 0.6016 0.6016 0.6036 0.6036 0.6036 0.6036 0.6036 0.5001 1.005 0.5001 1.005 0.5001 1.005 0.5001 1.005 0.5001 1.005 0.5001 1.005 0.5001 1.005 0.5001 1.005 0.5001 1.1276 0.7477 0.7427 0.754 1.0092 0.7423 0.754 1.0048 0.7431 1.0048 0.7432 0.7447 0.7544 0.5001 0.60528 0.60536 0.60536 0.60536 0.60536 0.60536 0.60536	-1 -1 -0 -0 -0 -0 -0 -0 -0 -0 -0 -0 -0 -0 -0			14q12.12 14q12.32 15q11.2 15q24.1 15q24.1 15q24.1 15q24.5 15q25.2 15q26.1 15q2	14q22.33 15q24.1 15q24.1 15q25.2 15q25.2 15q25.2 15q25.2 15q26.1 15q26

#4110T #4110T										
	chr17	38546316	38569496	26	1,0852	0	I		17q21.2	17q21.2
	chr17	38572288	38721656	23	0,6619	0			17q21.2 17q21.2	17q21.2
#4110T	chr17	38785141	39165178	103	1,0012	0			17q21.2	17q21.2
#4110T	chr17	39183145	43176827	1145	0,7077	0			17q21.2	17q21.31
#4110T	chr17	43180404	43190028	5	0,9945	0			17q21.31	17q21.31
#4110T	chr17	43190306	46926676	494	0,7525	0			17q21.31 17q21.31	17q21.31
#4110T	chr17	46928495	46940284	8	1.1	0			17q21.32	17q21.32
#4110T	chr17	46970799	47376030	65	0.7543	0			17q21.32	17q21.32
N4110T	chr17	47388746	47481620	5	1,0566	0			17q21.32	17q21.32
#4110T	chr17	47482460	74300551	2936	0,7803	0			17q21.33	17q25.1
#4110T	chr17	74300993	74344636	11	1,0662	0			17q25.1	17q25.1
#4110T	chr17	74349699	74621950	64	0,6243	0			17q25.1	17q25.1
#4110T	chr17	74622132	74865146	40	0,9235	0				17q25.2
#4110T	chr17	74868938	76046341	51	0,6844	0			17q25.1	
		76060911	76098590			0		3	17q25.2	17q25.3
#4110T	chr17			16	0,9753				17q25.3	17q25.3
W4110T	chr17	76099565	81052161	1098	0,6523	0			17q25.3	17q25.3
#4110T	chr18	158706	78005195	2931	0,9326	0		emica	18p11.32	18q23
#4110T	chr19	111138	4409328	1276	0,5579	-1		STK11	19p13.3	19p13.3
#4110T	chr19	4418045	4428774	5	1,0347	0		4	19p13.3	19p13.3
#4110T	chr19	4429519	5594045	188	0,5992	0			19p13.3	19p13.3
N4110T	chr19	5595440	5616465	12	0,9603	0			19p13.3	19p13.3
#4110T	chr19	5621363	6680221	285	0,6298	0			19p13.3	19p13.3
#4110T	chr19	6681997	6686217	6	1,0519	0			19p13.3	19p13.3
#4110T	chr19	6686835	9449932	725	0,6572	0			19p13.3	19p13.2
#4110T	chr19	9451819	9643561	23	1,0479	0	022009	2	19p13.2	19p13.2
N4110T	chr19	9644579	11373094	585	0,6516	0	KEAP1		19p13.2	19p13.2
#4110T	chr19	11407008	11436168	8	0,9701	0			19p13.2	19p13.2
#4110T	chr19	11446185	19767881	2181	0,6553	0			19p13.2	19p13.11
#4110T	chr19	19768181	29698760	143	0,9855	0			19p13.11	19q12
#4110T	chr19	29703919	40030364	1587	0,6742	0		-	19q12	19q13.2
#4110T	chr19	40093216	40276556	19	0,9691	0			19q13.2	19q13.2
#4110T	chr19	40316540	40487155	57	0,6538	0	-		19q13.2	19q13.2
N4110T	chr19	40504275	40595168	15	0,9618	0			19q13.2	19q13.2
#4110T	chr19	40698279	44306500	811	0,6579	0			19q13.2	19q13.31
#4110T	chr19	44339700	45016968	87	0,9312	0			19q13.31	19q13.31
#4110T	chr19	45017289	59082559	3222	0,6636	0	SEPW1,TMEM160		19q13.31	19q13.43
#4110T	chr20	68379	21319704	1309	0,8446	0			20p13	20p11.22
#4110T	chr20	21321424	21369944	14	1,2502	1		<u></u>	20p11.22	20p11.22
#4110T	chr20	21376860	30309739	230	0,7142	0			20p11.22	20q11.21
#4110T	chr20	30345333	30382278	13	1,0919	0			20q11.21	20q11.21
#4110T	chr20	30385263	62904763	3214	0,7359	0	DNAICS		20q11.21	20q13.33
#4110T	chr21	45104483	48083380	583	0,589	0			21q22.3	21q22.3
#4110T	chr21	45103207	45658349	1428	0,8758	0			21q22.3	21q22.3
#4110T	chr22	17443694	36013257	2014	0,7133	0	ZNRF3,CLDN5		22q11.1	22q12.3
#4110T	chr22	17288796	19378084	15	1,0868	0			22q11.21	22q11.1
#4110T	chr22	36052497	36357632	22	1,0228	0			22q12.3	22q12.3
#4110T	chr22	36424380	43204834	1126	0,6885	0			22q12.3	22q13.2
#4110T	chr22	43206884	43243579	11	0,9483	0			22q13.2	22q13.2
#4110T	chr22	43253154	45741395	245	0,6615	0		Į.	22q13.2	22q13.31
W4110T	chr22	45745643	45804685	20	1,0054	0			22q13.31	22q13.31
#4110T	chr22	45809394	46068002	28	0,6905	0			22q13.31	22q13.31
#4110T	chr22	46085688	46238964	10	1,049	0			22q13.31	22q13.31
#4110T	chr22	46239550	51220669	598	0,5577	-1		22q13.32	22q13.31	22q13.33
#4110T	chrX	200918	152105010	6116	0,9113	0	RPS6KA3		Xp22.33	Xq28
#4110T	chrX	152106662	153881655	543	0,5757	0			Xq28	Xq28
#4110T	chrX	153906513	155239777	136	0,9255	0			Xq28	Xq28
#4110T	chrY	150918	59342783	128	0,6972	0			Yp11.32	Yq12
#471T	chr1	762224	249213866	17232	-0,0459	0	ARID1A,RPL22,COL11A1		1p36.33	1944
#471T	chr2	40221	242842554	13340	-0,0279	0	ACVR2A,NFE2L2,EPHA4,APOB		2p25.3	2q37.3
#471T	chr3	239468	123022972	6746	-0,0396	0	CTNNB1,BAP1,PDE12,SETD2		3p26.3	3q21.1
#471T	chr3	123036915	123071353	8	-0,3889	-1			3q21.1	3q21.1
#471T	chr3	123086820	197769154	4121	-0,0261					3q29
#471T	chr4					0	KLF15		3q21.1	
#471T		53291	190862085	7182	-0,0164	0	KLF15 ALB,FGA,GABRA2,IRF2			4q35.2
	chr5			7182 7880			ALB,FGA,GABRA2,IRF2		3q21.1 4p16.3	4q35.2 5q35.3
	chr5	53291	190862085		-0,0164 -0,0227	0			3q21.1	
#471T #471T		53291 143266	190862085 180687559	7880	-0,0164	0	ALB,FGA,GABRA2,IRF2 ATP10B,MEF2C,IL6ST,DOCK2,ADAMTS19,TERT		3q21.1 4p16.3 5p15.33	5q35.3
#471T	chr6	53291 143266 203615	190862085 180687559 170891556 158935187 146280027	7880 9011	-0,0164 -0,0227 -0,0285	0 0	ALB,FGA,GABRAZ,IRF2 ATP10B,MEF2C,ILEST,DOCK2,ADAMTS19,TERT CDKNIA,EEF1A1,SPATS1,VEGFA MET SLURP1,MYC		3q21.1 4p16.3 5p15.33 6p25.3	5q35.3 6q27
#471T #471T	chr6 chr7	53291 143266 203615 195642	190862085 180687559 170891556 158935187	7880 9011 8044	-0,0164 -0,0227 -0,0285 -0,0501	0 0 0	ALB,FGA,GABRAZ,IRF2 ATP10B,MEF2C,IL6ST,DOCK2,ADAMTS19,TERT CDKN1A,EEF1A1,SPATS1,VEGFA MET		3q21.1 4p16.3 5p15.33 6p25.3 7p22.3	5q35.3 6q27 7q36.3
#471T #471T #471T	chr6 chr7 chr8	53291 143266 203615 195642 183094	190862085 180687559 170891556 158935187 146280027	7880 9011 8044 6109	-0,0164 -0,0227 -0,0285 -0,0501 -0,0313	0 0 0 0	ALB,FGA,GABRAZ,IRF2 ATP10B,MEF2C,ILEST,DOCK2,ADAMTS19,TERT CDKNIA,EEF1A1,SPATS1,VEGFA MET SLURP1,MYC		3q21.1 4p16.3 5p15.33 6p25.3 7p22.3 8p23.3	5q35.3 6q27 7q36.3 8q24.3
#471T #471T #471T #471T	chr6 chr7 chr8 chr9	53291 143266 203615 195642 183094 213464	190862085 180687559 170891556 158935187 146280027 139888074	7880 9011 8044 6109 6397	-0,0164 -0,0227 -0,0285 -0,0501 -0,0313 -0,0482	0 0 0 0	ALB,FGA,GABRAZ,IRF2 ATP10B,MEF2C,ILEST,DOCK2,ADAMTS19,TERT CDKNIA,EEF1A1,SPATS1,VEGFA MET SLURP1,MYC		3q21.1 4p16.3 5p15.33 6p25.3 7p22.3 8p23.3 9p24.3	5q35.3 6q27 7q36.3 8q24.3 9q34.3
#471T #471T #471T #471T	chr6 chr7 chr8 chr9 chr9	53291 143266 203615 195642 183094 213464 139888322	190862085 180687559 170891556 158935187 146280027 139888074 139905490	7880 9011 8044 6109 6397	-0,0164 -0,0227 -0,0285 -0,0501 -0,0313 -0,0482 -0,6406	0 0 0 0 0 0	ALB,FGA,GABRAZ,IRF2 ATP10B,MEF2C,ILEST,DOCK2,ADAMTS19,TERT CDKNIA,EEF1A1,SPATS1,VEGFA MET SLURP1,MYC		3q21.1 4p16.3 5p15.33 6p25.3 7p22.3 8p23.3 9p24.3 9q34.3	5q35.3 6q27 7q36.3 8q24.3 9q34.3
#471T #471T #471T #471T #471T #471T #471T	chr6 chr7 chr8 chr9 chr9	53291 143266 203615 195642 183094 213464 139888322 139906382 226000 193118	190862085 180687559 170891556 158935187 146280027 139888074 139905490 141017498 135381590 47361271	7880 9011 8044 6109 6397 10 287 6998 3164	-0,0164 -0,0227 -0,0285 -0,0501 -0,0313 -0,0482 -0,6406 -0,1484	0 0 0 0 0 0 0	ALB_FGA_CABRAZ_BEZ ATPIOB_MEF2C_LEST_DOCEZ_ADAMTS19_TERT CONNIA_EFEALS_WATS11_VEFA MET SLURP1_MYC CONNIZA_TSC1_MTAP_PTPN3		3q21.1 4p16.3 5p15.33 6p25.3 7p22.3 8p23.3 9p24.3 9q34.3	5q35.3 6q27 7q36.3 8q24.3 9q34.3 9q34.3
#471T #471T #471T #471T #471T #471T	chr6 chr7 chr8 chr9 chr9 chr9 chr9	53291 143266 203615 195642 183094 213464 139888322 139906382 226000 193118 47362742	190862085 180687559 170891556 158935187 146280027 139888074 139905490 141017498 135381590	7880 9011 8044 6109 6397 10 287 6998	-0,0164 -0,0227 -0,0285 -0,0501 -0,0313 -0,0482 -0,6406 -0,1484 -0,0327	0 0 0 0 0 0 0 -1 0 0	ALB_FGA_CABRAZ_BEZ ATPIOB_MEF2C_LEST_DOCEZ_ADAMTS19_TERT CONNIA_EFEALS_WATS11_VEFA MET SLURP1_MYC CONNIZA_TSC1_MTAP_PTPN3		3q21.1 4p16.3 5p15.33 6p25.3 7p22.3 8p23.3 9p24.3 9q34.3 9q34.3	5q35.3 6q27 7q36.3 8q24.3 9q34.3 9q34.3 9q34.3
#471T #471T #471T #471T #471T #471T #471T	chr6 chr7 chr8 chr9 chr9 chr9 chr10 chr11	53291 143266 203615 195642 183094 213464 139888322 139906382 226000 193118	190862085 180687559 170891556 158935187 146280027 139888074 139905490 141017498 135381590 47361271	7880 9011 8044 6109 6397 10 287 6998 3164	-0,0164 -0,0227 -0,0285 -0,0501 -0,0313 -0,0482 -0,6406 -0,1484 -0,0327 -0,05	0 0 0 0 0 0 0 -1 0	ALB_FGA_CABRAZ_BEZ ATPIOB_MEF2C_LEST_DOCEZ_ADAMTS19_TERT CONNIA_EFEALS_WATS11_VEFA MET SLURP1_MYC CONNIZA_TSC1_MTAP_PTPN3		3q21.1 4p16.3 5p15.33 6p25.3 7p22.3 8p23.3 9p24.3 9q34.3 10p15.3 11p15.5	5q35.3 6q27 7q36.3 8q24.3 9q34.3 9q34.3 9q34.3 10q26.3 11p11.2
#471T #471T #471T #471T #471T #471T #471T #471T	chr6 chr7 chr8 chr9 chr9 chr9 chr10 chr11 chr11	53291 143266 203615 195642 183094 213464 139888322 139906382 226000 193118 47362742	190862085 180687559 170891556 158935187 146280027 13988074 139905490 141017498 135381590 47361271 47374186	7880 9011 8044 6109 6397 10 287 6998 3164 12	-0,0164 -0,0227 -0,0285 -0,0501 -0,0313 -0,0482 -0,6406 -0,1484 -0,0327 -0,05 -0,4033	0 0 0 0 0 0 0 -1 0 0	ALB_FGA_CABRAZ_BEZ ATPIOB_MEF2C_LEST_DOCEZ_ADAMTS19_TERT CONNIA_EFEALS_APS15_VEFA MET SLURP_I_MYC CONNIZ_ATSCI_MTAP_PTPN3		3q21.1 4p16.3 5p15.33 6p25.3 7p22.3 8p23.3 9p24.3 9q34.3 10p15.3 11p15.5 11p11.2	5q35.3 6q27 7q36.3 8q24.3 9q34.3 9q34.3 10q26.3 11p11.2 11p11.2
#471T #471T #471T #471T #471T #471T #471T #471T #471T #471T #471T	chr6 chr7 chr8 chr9 chr9 chr9 chr10 chr11 chr11	53291 143266 203615 195642 183094 213464 139888322 139906382 226000 193118 47362742 47376754	190862085 180687559 170891556 158935187 146280027 139888074 139905490 141017498 135381590 47361271 47374186 61534692 61544848 63978199	7880 9011 8044 6109 6397 10 287 6998 3164 12 764	-0,0164 -0,0227 -0,0285 -0,0501 -0,0501 -0,0482 -0,6406 -0,1484 -0,0327 -0,05 -0,4033 -0,0455	0 0 0 0 0 0 0 -1 0 0	ALB_FGA_CABRAZ_BEZ ATPIOB_MEF2C_LEST_DOCEZ_ADAMTS19_TERT CONNIA_EFEALS_APS15_VEFA MET SLURP_I_MYC CONNIZ_ATSCI_MTAP_PTPN3		3q21.1 4p16.3 5p15.33 6p25.3 7p22.3 8p23.3 9p24.3 9q34.3 10p15.3 11p15.5 11p11.2	5q35.3 6q27 7q36.3 8q24.3 9q34.3 9q34.3 10q26.3 11p11.2 11p11.2
#471T #471T #471T #471T #471T #471T #471T #471T #471T #471T #471T	chr6 chr7 chr8 chr9 chr9 chr9 chr10 chr11 chr11 chr11	53291 143266 203615 195642 183094 213464 213464 13988322 139906382 226000 193118 47362742 47376754 61536762	190862085 180687559 170891556 158935187 146280027 139888074 139905490 141017498 135381590 47361271 47374186 61534692 61543848 63978199 63991393	7880 9011 8044 6109 6397 10 287 6998 3164 12 764 6	-0,0164 -0,0227 -0,0285 -0,0501 -0,0313 -0,0482 -0,6406 -0,1484 -0,0327 -0,05 -0,403 -0,0455 -0,7842	0 0 0 0 0 0 0 -1 0 0 0	ALB_FGA_CABRAZ_BEZ ATPIOB_MEF2C_LEST_DOCEZ_ADAMTS19_TERT CONNIA_EFEALS_APS15_VEFA MET SLURP_I_MYC CONNIZ_ATSCI_MTAP_PTPN3		3q21.1 4p16.3 5p15.33 6p25.3 7p22.3 8p23.3 9p24.3 9q34.3 10p15.3 11p15.5 11p11.2 11q12.2	5q35.3 6q27 7q36.3 8q24.3 9q34.3 9q34.3 10q26.3 11p11.2 11q12.2 11q12.2
#471T #471T #471T #471T #471T #471T #471T #471T #471T #471T #471T	chr6 chr7 chr8 chr9 chr9 chr9 chr10 chr11 chr11 chr11	53291 143266 203615 195642 183094 213464 139888322 139906382 226000 193118 47362742 47376754 61536762 61544836	190862085 180687559 170891556 158935187 146280027 139888074 139905490 141017498 135381590 47361271 47374186 61534692 61544848 63978199	7880 9011 8044 6109 6397 10 287 6998 3164 12 764 6 482	-0,0164 -0,0227 -0,0285 -0,0501 -0,0313 -0,0482 -0,6406 -0,1484 -0,0327 -0,05 -0,4033 -0,0455 -0,7842 -0,0794	0 0 0 0 0 0 0 0 0 0 0 0 0 0 0 0 0 0 0	ALB_FGA_CABRAZ_BEZ ATPIOB_MEF2C_LEST_DOCEZ_ADAMTS19_TERT CONNIA_EFEALS_APS15_VEFA MET SLURP_I_MYC CONNIZ_ATSCI_MTAP_PTPN3		3q21.1 4p16.3 5p15.33 6p25.3 7p22.3 8p23.3 9p24.3 9q34.3 10p15.3 11p15.5 11p11.2 11p11.2 11q12.2	5q35.3 6q27 7q36.3 8q24.3 9q34.3 9q34.3 10q26.3 11p11.2 11q12.2 11q12.2 11q13.1
#471T #471T #471T #471T #471T #471T #471T #471T #471T #471T #471T #471T #471T	chr6 chr7 chr8 chr9 chr9 chr9 chr10 chr11 chr11 chr11 chr11 chr11	53291 143266 203615 195642 183094 213464 139888322 139906382 226000 193118 47362742 47376754 61536762 63987062	190862085 180687559 170891556 158935187 146280027 138988074 139905490 131905490 141017498 135381590 47361271 47374186 61534692 61543848 63978199 63991393 134257636 138810818	7880 9011 8044 6109 6397 10 287 6998 3164 12 764 6 482	-0,0164 -0,0227 -0,02285 -0,0501 -0,0313 -0,0482 -0,6406 -0,1484 -0,0327 -0,603 -0,403 -0,7842 -0,7842 -0,7842 -0,7944 -0,7944	0 0 0 0 0 0 0 -1 0 0 0 0 -1 0 0 -1 0 0	ALB_FGA_GABBAQ_JREZ ATP108_MFEZ_LISEST_DOCK2_ADAMTS19_TERT CONNIA_EEF_ALS_WATS1_VEGFA MET SURP3_IMVC CONN2A_TSC1_MTAP_PTPN3 PTEN		3q21.1 4p16.3 5p15.33 6p25.3 7p22.3 8p23.3 9p24.3 9q34.3 10p15.3 11p15.5 11p11.2 11q11.2 11q12.2 11q12.2 11q13.1	5q35.3 6q27 7q36.3 8q24.3 9q34.3 9q34.3 10q26.3 11p11.2 11q12.2 11q12.2 11q12.2 11q13.1
#471T #471T #471T #471T #471T #471T #471T #471T #471T #471T #471T #471T #471T #471T #471T #471T	chr6 chr7 chr8 chr9 chr9 chr9 chr10 chr11 chr11 chr11 chr11 chr11 chr11	53291 143266 203615 195642 183094 213464 139888322 139906382 226600 193118 47362742 47376754 61536762 65987062 63987062 63987062 63987062	190862085 180687559 170891556 158935187 146/280027 139888074 139905490 141017498 135381590 47361271 47374186 61534692 61543848 63978199 3398193 134257636	7880 9011 8044 6109 6397 10 287 6998 3164 12 764 6 482 8 5131	-0,0164 -0,0227 -0,02285 -0,0501 -0,0313 -0,0492 -0,6406 -0,1494 -0,0327 -0,05 -0,4033 -0,07842 -0,0794 -0,0794 -0,0578	0 0 0 0 0 0 0 0 0 0 0 0 0 0 0 0 0 0 0	ALB/GA_GABAG_JRF2 ATPIOB_MEFC_LIISTS_DOCK_ADAMTS19_TERT CONN_EEF_LIST_SOCK_TOPE MET SLIPP_I_MYC CONN_ZA_TSC_I_MTAP_PTPNB PTEN HMBS		3q21.1 4p16.3 5p15.33 6p25.3 7p22.3 8p23.3 9p24.3 9q34.3 10p15.3 11p15.5 11p11.2 11q12.2 11q12.2 11q12.1 11q13.1 11q13.1 12p13.33 13q12.11	5q35.3 6q27 7q36.3 8q24.3 9q34.3 9q34.3 10q26.3 11p11.2 11p11.2 11q12.2 11q12.2 11q13.1 11q25
#471T #471T #471T #471T #471T #471T #471T #471T #471T #471T #471T #471T #471T #471T #471T #471T #471T	chr6 chr7 chr8 chr9 chr9 chr9 chr9 chr11 chr11 chr11 chr11 chr11 chr11 chr11 chr11 chr11	53291 143266 203615 193642 183094 213464 139888322 226000 193118 47367242 47376754 61536762 61544836 63987062 208345 19752446	190862085 180687559 170891556 158935187 146280027 139888074 139888074 135881590 47361271 47374186 61534692 61543848 6397819 63991393 134257636 134810818 115091029	7880 9011 8044 6109 6397 10 287 6998 3164 12 764 6 482 8 15131 9752	-0,0164 -0,0227 -0,0285 -0,0501 -0,0313 -0,0482 -0,6406 -0,1484 -0,0327 -0,057 -0,7842 -0,07842 -0,0578 -0,0578 -0,0578 -0,0578 -0,0578	0 0 0 0 0 0 0 0 0 0 0 0 0 0 0 0 0 0 0	ALB/GA_GABAQ_JRF2 ATPJOB_MEF2_LIBST_DOCK2_ADAMTS19_TERT CONNIA_CEF_IA1_SWATS1_MEGA MET SUMP1_MYC CONNIA_TSC1_MTAP_PTPN3 PTEN PTEN HMBS AND2_MNT3_ACDINIB		3q21.1 4p16.3 5p15.33 6p25.3 7p22.3 8p23.3 9p24.3 9q34.3 10p15.3 11p15.5 11p11.2 11q11.2 11q12.2 11q13.1 12p13.33	5q35.3 6q27 7q36.3 8q24.3 9q34.3 9q34.3 10q26.3 11p11.2 11p11.2 11q12.2 11q12.2 11q13.1 11q13.1 11q25 12q24.33
#471T #471T #471T #471T #471T #471T #471T #471T #471T #471T #471T #471T #471T #471T #471T #471T	chr6 chr7 chr8 chr9 chr9 chr9 chr10 chr11 chr11 chr11 chr11 chr11 chr11 chr11 chr11 chr11	53291 143266 203615 195642 183094 213464 139888322 139906382 226600 193118 47362742 47376754 61536762 65987062 63987062 63987062 63987062	190862085 180687559 170891556 158935187 146280027 139905490 141017498 135981590 47361271 47374186 61554692 61543848 63991393 134257636 13810818 115091029	7880 9011 8044 6109 6397 10 287 6998 3164 12 764 6 8 5131 9752 3215	-0,0164 -0,0227 -0,02285 -0,0501 -0,0313 -0,0482 -0,6406 -0,1484 -0,0327 -0,05 -0,4033 -0,0455 -0,7842 -0,0794 -0,0578 -0,0794 -0,0578 -0,0578 -0,0578 -0,0462 -0,0462 -0,0462	0 0 0 0 0 0 0 0 0 0 0 0 0 0 0 0 0 0 0	ALB/GA_GABAQ_JRF2 ATPJOB_MEF2_LIBST_DOCK2_ADAMTS19_TERT CONNIA_CEF_IA1_SWATS1_MEGA MET SUMP1_MYC CONNIA_TSC1_MTAP_PTPN3 PTEN PTEN HMBS AND2_MNT3_ACDINIB		3q21.1 4p16.3 5p15.33 6p25.3 7p22.3 8p23.3 9p24.3 9q34.3 10p15.3 11p15.5 11p11.2 11q12.2 11q12.2 11q12.1 11q13.1 11q13.1 12p13.33 13q12.11	5q35.3 6q27 7q36.3 8q24.3 9q34.3 9q34.3 9q34.3 10q26.3 11p11.2 11p11.2 11q12.2 11q12.2 11q12.1 11q13.1 11q25 12q24.33 13q34
#471T #471T #471T #471T #471T #471T #471T #471T #471T #471T #471T #471T #471T #471T #471T #471T #471T	chr6 chr7 chr8 chr9 chr9 chr9 chr10 chr11	53291 143266 203615 193642 183094 213464 139888322 226000 193118 47367242 47376754 61536762 61544836 63987062 208345 19752446	190862085 180687559 170891556 158935187 146280027 139888074 139888074 135881590 47361271 47374186 61534692 61543848 6397819 63991393 134257636 134810818 115091029	7880 9011 8044 6109 6397 10 287 6998 3164 6 6 482 8 5131 9752 8 3215 5490 5760	-0,0164 -0,0227 -0,0285 -0,0501 -0,0402 -0,0402 -0,0406 -0,1484 -0,0327 -0,05 -0,0433 -0,0455 -0,7842 -0,0794 -0,5691 -0,0794 -0,5691 -0,0184 -0,0184 -0,0184	0 0 0 0 0 0 0 0 0 0 0 0 0 0 0 0 0 0 0	ALB/GA_GABAQ_JRF2 ATPJOB_MEF2_LIBST_DOCK2_ADAMTS19_TERT CONNIA_CEF_IA1_SWATS1_MEGA MET SUMP1_MYC CONNIA_TSC1_MTAP_PTPN3 PTEN PTEN HMBS AND2_MNT3_ACDINIB		3q21.1 4p16.3 5p15.33 6p25.3 7p22.3 8p23.3 9p24.3 9q34.3 10p15.3 11p15.5 11p11.2 11q12.2 11q12.2 11q13.1 11q13.1 11q13.1 12p13.33 13q12.11 14q11.2	5q35.3 6q27 7q36.3 8q24.3 9q34.3 9q34.3 9q34.3 10q26.3 11p11.2 11q12.2 11q12.2 11q13.1 11q13.1 11q25 12q24.33
#471T #471T #471T #471T #471T #471T #471T #471T #471T #471T #471T #471T #471T #471T #471T #471T #471T	chr6 chr7 chr8 chr9 chr9 chr9 chr10 chr11	53291 143266 203615 195642 183094 213464 139888322 139906382 22600 193138 47362742 47376754 61536762 61544836 63987062 63987062 63987062 208845 19752446 20201689	190862085 180687559 170891556 1589835187 146230027 1398965490 141017498 135381590 47361271 47374186 61534892 61543848 63978199 63991393 134257636 133810818 115091029 107282930 107282930	7880 9011 8044 6109 6397 10 287 6998 3164 12 764 6 482 8 5131 9752 3215 5490 5760	-0,0164 -0,0227 -0,02285 -0,0501 -0,0313 -0,0482 -0,6406 -0,1484 -0,0327 -0,055 -0,4033 -0,0403 -0,7842 -0,0794 -0,0578 -0,058 -0,07842 -0,0784 -0,0578 -0,0584 -0,0584 -0,0584 -0,0584 -0,0584 -0,0584 -0,0584 -0,0584 -0,0584 -0,0584 -0,0584 -0,0407 -0,0462 -0,0407 -0,0452	0 0 0 0 0 0 0 0 0 0 0 0 0 0 0 0 0 0 0	ALB/GA_GABRA_JRF2 ATPIOB.MEEG_IGIST DOOK2_ADMITS19_TERT CONNIA_EEFIAL_SPATS1_VEGFA MET SLIPPI_MYC CONN2A_TSCI_MTAP_PTPN3 PTEN PTEN HMBS ANIDZ_MYS_ACDMYIB RB1		3q21.1 4p16.3 5p15.33 6p25.3 7p22.3 8p23.3 9p24.3 9p34.3 10p15.3 11p11.2 11p11.2 11q12.2 11q12.2 11q13.1 11q13.1 11q13.1 14q11.2 14q11.2	5q35.3 6q27 7q36.3 8q24.3 9q34.3 9q34.3 10q26.3 11p11.2 11p11.2 11q12.2 11q13.1 11q13.1 11q3.1
#471T #471T #471T #471T #471T #471T #471T #471T #471T #471T #471T #471T #471T #471T #471T #471T #471T #471T #471T	chr6 chr7 chr8 chr8 chr9 chr9 chr9 chr10 chr11	53291 143266 203615 195642 1183094 213664 13980832 226000 199118 47367742 47370754 61534762 61534836 663902102 208345 2020189 20450269	190662085 180687559 170891556 158985187 146280027 139895490 141017498 135981590 47361271 47374186 61534692 61543848 63978199 63991393 134257636 134810818 13590129 107282930 107282930 107282930 107282930	7880 9011 8044 6109 6397 10 287 6998 3164 6 6 482 8 5131 9752 8 3215 5490 5760	-0.0164 -0.0227 -0.0227 -0.0227 -0.0285 -0.0513 -0.0482 -0.0513 -0.0482 -0.055 -0.0482 -0.055 -0.055 -0.055 -0.055 -0.055 -0.055 -0.0578 -0.0678 -0.0678 -0.0678 -0.0678 -0.0679 -0.0679 -0.0679 -0.0679 -0.0679 -0.0679 -0.0679	0 0 0 0 0 0 0 0 0 0 0 0 0 0 0 0 0 0 0	ALB/GA_GABAG_JERP ATPIOB_MEFC_LIBST_DOCK_ADAMTS19_TERT CONTA_EEFT_ALS_PATS_LYEGA MET SUMP_I_MYC CDNN2A_TSC1_MTAP_PTINB PTEN PTEN HMBS ARID_J_NINE_A_CONNIB RB1 AMN1_TSC2_RRD7		3e21.1 4916.3 5915.38 6e25.3 7522.3 8e23.3 9e24.3 9e24.3 9e24.3 10e15.9 11e15.5 11e11.2 11e12.2 11e12.2 11e12.2 11e12.2 11e12.1 11e13.3 12e13.3 12e13.	5q35.3 6q27.7q36.3 8q24.3 9q24.3 9q34.3 9q34.3 11p11.2 11p11.2 11q12.2 11q12.2 11q12.2 11q13.1 11q25 12q24.3 14q32.3 15q24.3
8471Y	chr6 chr7 chr8 chr9 chr9 chr9 chr10 chr11	53291 53291 53296 203615 195642 183094 183094 123464 13988822 139906382 226000 199118 47367742 47376774 61519762 615967062 63987062	190867085 180687595 118987556 158987587 138985187 144280027 1399858074 13995490 141017498 13938190 4774186 61554892 61554892 61554892 6155492 133810818 133810818 133810818 133810818 133810818 133810818 133810818 133810818 133810818 133810818 133810818 133810818 133810818 133810818 133810818 133810818 133810818	7880 9011 8044 6109 6397 10 287 110 287 12 764 6 8 8 5131 9752 3215 5490 5760 6647	-0,0164 -0,0227 -0,0227 -0,0285 -0,0501 -0,0501 -0,0482 -0,1484 -0,027 -0,063 -0,0455	0 0 0 0 0 0 0 0 0 0 0 0 0 0 0 0 0 0 0	ALB/GA_GABAG_JERP ATPIOB_MEFC_LIBST_DOCK_ADAMTS19_TERT CONTA_EEFT_ALS_PATS_LYEGA MET SUMP_I_MYC CDNN2A_TSC1_MTAP_PTINB PTEN PTEN HMBS ARID_J_NINE_A_CONNIB RB1 AMN1_TSC2_RRD7		3e21.1 426.5 3 5 5 5 5 5 5 5 5 5 5 5 5 5 5 5 5 5 5	5q35.3 6q27 7q36.3 8q24.3 8q24.3 9q34.3 9q34.3 10q26.3 11p11.2 11q12.2 11q12.2 11q12.2 11q13.3 11q13.3 11q3.3 13q34 14q32.33 15q26.3 15q26.3
8471Y	chr6 chr7 chr8 chr9 chr9 chr9 chr9 chr9 chr9 chr11	\$3291 140266 203615 195642 195642 1396602 13988832 13990582 22500 199118 47362754 6536762 6397062 20845 20201689 20400689 20400689 608666 6086762 6096762 6096762 6096762 6096762 6096762 6096762 6096762 6096762 6096762 6096762 6096762 6096762 6096762 6096	190867085 180687599 170891556 139981587 146280027 1399858074 139905490 141017488 135981590 14781271 14781271 135881590 14781271 1478171 14781271 14	7880 9011 8044 6109 6397 10 287 11 287 764 6 482 8 5131 5131 5450 6647 2559 9	-0.0164 -0.0227 -0.0227 -0.0227 -0.0285 -0.0501 -0.0612 -0.0612 -0.0620	0 0 0 0 0 0 0 0 0 0 0 0 0 0 1 1 0 0 0 1 1 0	ALB/GA_GABAG_JERP ATPIOB_MEFC_LIBST_DOCK_ADAMTS19_TERT CONTA_EEFT_ALS_PATS_LYEGA MET SUMP_I_MYC CDNN2A_TSC1_MTAP_PTINB PTEN PTEN HMBS ARID_J_NINE_A_CONNIB RB1 AMN1_TSC2_RRD7		3e21.1 4g16.3 5915.8 6625.3 7p22.3 6625.3 7p22.3 8e23.3 9g24.3 10615.3 11615.5 11611.2 11612.2 11612.2 11612.1 11613.1 11613.3 11615.5 11611.2 11612.2 11612.2 11613.3 11615.5 11611.2 11613.3 11615.5 11611.2 11613.3	5q35.3 6q27.7q36.3 8q24.3 9q34.3 9q34.3 10q26.3 11p11.2 11p11.2 11q12.1 11q13.1 11q13.1 11q25 12q24.3 13q34 14q22.33 15q26.3 16q24.3 17p11.2
8671Y	chr6	\$3291 143266 203615 195642 135094 213464 13988822 13990582 22600 193118 4736742 47376734 61536762 6154836 6387062 63970102 20201689 20450269 97088 6088 18156693	1908/2055 11068/1595 11068/1595 11089/1556 11899/1556 11899/1557 11998/8074 11017/209 11990/450 141017/209 1479/1156 11534/59 1479/1156 11534/59 11	7880 9011 8044 6109 6397 10 287 11 287 764 6 6 482 8 15131 9752 3215 5490 6647 2559 9	-0,0164 -0,0227 -0,0285 -0,0501 -0,0501 -0,0402 -0,0406 -0,1484 -0,0527 -0,0649 -0,064	0 0 0 0 0 0 0 0 0 0 0 0 0 0 0 0 0 0 0	ALB/GA_GABAG_JERP ATPIOB_MEFC_LIBST_DOCK_ADAMTS19_TERT CONTA_EEFT_ALS_PATS_LYEGA MET SUMP_I_MYC CDNN2A_TSC1_MTAP_PTINB PTEN PTEN HMBS ARID_J_NINE_A_CONNIB RB1 AMN1_TSC2_RRD7		3e21.1 4e36.3 5 5 5 5 5 5 5 5 5 5 5 5 5 5 5 5 5 5 5	\$q35.3 6q27 7q36.3 8q24.3 8q24.3 9q34.3 9q34.3 9q34.3 10q26.3 11p11.2 11q12.2 11q12.2 11q12.2 11q13.3 11q13.1 11q25 12q24.33 13q34.3 13q34.3 13q34.3 13q34.3 15q26.3 15q26.3 15q26.3 15q26.3 15q26.3 15q26.3 17p11.2 17p11.2 17p11.2 17p11.2 17p15.3 17q25.3 17p15.3 17q25.3
##211 ##21 ##21	chr6 chr3 chr8 chr9 chr9 chr9 chr9 chr9 chr9 chr9 chr9 chr11	\$3291 143266 203615 195642 183094 213664 13988832 13990582 22600 193118 4732754 61357052 6397002 20845 1930888 22500 193118 973674 6257052 6397002 20845 193704 2001889 2045029 97088 6397082 19388 19	190867085 180687599 170891556 189895187 146280027 1398968074 139905490 141017488 139905490 147841271 14774146 147841271 147874146 14784187 1478418 147	7880 9011 8044 6109 6397 10 287 6998 3164 12 764 6 482 8 5131 9752 3215 5490 6647 2559 9 92 7756	-0.0164 -0.0227 -0.0227 -0.0227 -0.0285 -0.0501 -0.0402 -0.0402 -0.0402 -0.0402 -0.0503 -0.0455 -0.0455 -0.0455 -0.0455 -0.0455 -0.0455 -0.0456 -0.0457 -0.065	0 0 0 0 0 0 0 0 0 0 0 0 0 0 0 0 0 0 0	ALB/GA_GABAG_JRF2 ATPIOB_METC_LISTS_TOOKZ_ADAMTS19_TERT CONN_ETC_LISTS_TOOKZ_ADAMTS19_TERT CONN_ETC_LISTS_TOOKZ_ADAMTS19_TERT SURPT_JAMTC CONN_ETC_LISTS_TOOK_ETC_LISTS_TOOKS_TOOKS_ETC_LISTS		3e21.1 4e36.3 5p15.33 6e25.3 3 6e25.3 3 6e25.3 3 6e25.3 3 6e25.3 16e25.3 16e25	\$485.3 \$427 \$748.3 \$424.
## ## ## ## ## ## ## ## ## ## ## ## ##	chr6 chr6 chr8 chr8 chr8 chr9 chr9 chr9 chr9 chr9 chr9 chr11 chr12 chr13 chr14 chr15 chr16 chr17 chr17 chr17 chr17 chr18	\$3291 143266 203615 195642 135094 213464 13988822 13990582 123506 193118 47367754 61536762 6154836 63987062 63987062 63987062 63987062 1957446 195744 1957446 195744 19574 19574 195744 19574	1908/2055 11068/1595 170891556 158985187 146280027 139888074 139905490 47761271 15841899 47761271 47374186 61534092 61534084 61991388 11050109 1072899 10728999 10728999 10728999 1072899 10728999 1072899 10728999 1072899 1072899 1072899 1072899 1072899 107289 107	7880 9011 8044 6109 9011 10 10 10 10 10 12 764 6 6 482 8 15131 9752 3215 5490 5760 6647 2559 9 9 2756	-0,0164 -0,0227 -0,0227 -0,0285 -0,0501 -0,0410 -0,041	0 0 0 0 0 0 0 0 0 0 0 0 0 0 0 0 0 0 0	ALB/GA_GABAQ_JRF2 ATPIOB_MEFC2_LISST_DOCK2_ADAMTS19_TERT CONTAL_EFFTA_LS/ATS1_MEFCA MET SUMP1_MYC CONN2A_TSC1_MTAP_PTIN3 PTEN PTEN HMBS ARIO_2_MWF3_ACCENTB RB1 AXIN_1,TSC2_BB07 TPS3 KEAP1_SEPW1_TMEM160		3q211 4q163 5 epi3.3 5 epi3.3 3 epi3.3 3 epi3.3 3 epi3.3 3 epi3.3 10015 3 11015 5 11011 2 11012 2 11012 2 11012 2 11012 11013 1 1013 1	\$485.3 \$6427 7486.8 \$8243.3 \$9434.3 9434.3 9434.3 9434.3 10426.3 11p11.2 11p11.2 11q12.2 11q12.2 11q13.1 11q2.4 11q13.1 11q2.6 11q13.1 11q2.6 11q13.1 11q2.7 11q13.1 11q2.8 11q13.1 11q2.8
##271T ##27T ##2	chr6	\$3291 143266 203615 195642 183094 213664 13988812 13996882 22600 193118 47370754 6154636 6397002 20845 1975246 4736742 47370762 6397002 20845 1975246 6397002 20845 1975246 197524 19	190867085 180687599 170891556 189895187 118985187 118985187 118985674 118985674 118985674 118985674 118985674 118985674 11898574	7880 9011 8044 6109 10 10 287 6998 3164 425 8 482 8 15131 9752 3215 5400 6647 2599 9 6927 2756 8466	-0,0164 -0,0225 -0,0225 -0,0225 -0,0513 -0,0410 -0,0410 -0,0410 -0,1484 -0,033 -0,0455	0 0 0 0 0 0 0 0 0 0 0 0 0 0 0 0 0 0 0	ALB/GA_GABAG_JRF2 ATPIOR_MER_GIST_DOVX_ADAMTS19_TERT CONNIA_GEF_LAL_SPATS1_VEGFA MET SLUPP_J.MYC CONNIA_TSC_J.MTAP_PTPN3 PTEN PTEN HMBS ARIO_2_NNS_A_CDKN1B RB1 ANN_I_TSC_J.BRD7 TPS3 KEAP1_SEPWI_TMEM160 DNAICS		3e21.1 4e36.3 5915.3 3 6e25.3 5e25.3	\$485.3 \$6427 7486.3 8924.3 9424.3 9424.3 9424.3 9424.3 9424.3 10026.8 11011.2 11011.2 11011.2 11011.3 11012.3 11013.3 11025 12024.3
## ## ## ## ## ## ## ## ## ## ## ## ##	chr6 chr8 chr8 chr8 chr8 chr9 chr9 chr9 chr9 chr9 chr9 chr11 chr15 chr16 chr16 chr17 chr17 chr17 chr17 chr18 chr19 chr19 chr19 chr19 chr19 chr21	\$3291 148266 203615 195642 139640 213464 13988832 13990582 225600 193118 47367754 6135762 6136762 63987102 20201689 2040009 97088 608 608 608 608 608 608 608 608 608	190687295 170891556 170891556 159891587 1398958074 139905490 47361271 4737148 6153482 615348 6153482 6153482 6153482 615348 615348 615348 615348 615348 615348	7880 9011 8044 6109 9011 8044 6109 10 287 10 287 6998 3164 6 482 8 15131 55131 559 9752 3215 5490 96927 2756 6847 88466 4465	-0,0164 -0,0227 -0,0227 -0,0227 -0,0239 -0,0402 -0,0402 -0,0402 -0,0402 -0,0402 -0,0402 -0,0403 -0,0452 -0,045	0 0 0 0 0 0 0 0 0 0 0 0 0 0 0 0 0 0 0	ALB/GA_GABAQ_JRF2 ATPIOB_MEFC_LIBST_DOCK_ADAMTS19_TERT CONTA_CEFT_ALS_ATS1_MEGA MET SLUPP_I_MYC CONN_ZATSCI_MTAP_PTPN3 PTEN HMBS ARID_JINFIA_COUNTB RB1 ANIN_TSC_BRD7 TPS3 KEAP1_SEPW1_TMEM150 DNAICS DVAKEA		3q211 4q163 5 5 5 5 5 5 5 5 5 5 5 5 5 5 5 5 5 5 5	\$485.3 \$6427 \$746.8 \$844.3 \$944.3 \$944.3 \$944.3 \$944.3 \$944.3 \$100,26.3 \$11911.2 \$11911.2 \$11412.2 \$11412.2 \$11412.3 \$11413.1 \$1143.3 \$1242.4 \$1344.4 \$154
##21TT ##22TT ##2TT ##22TT ##2TT ##22TT ##2TT ##22TT ##22TT ##22TT ##22TT ##22TT ##22TT ##22TT ##22TT ##22T	chr6	\$3291 143266 203615 195642 183094 213464 13988822 13990582 226000 193118 4736724 67357052 61534762 61534762 61534762 1937054 61536762 1937054 61536762 1937054 61536762 1937054 61536762 1937054 61536762 1937054 1937	190867085 180687599 170891556 189895187 118985187 118985187 118985674 118985674 118985674 118985674 118985674 118985674 11898574	7880 9011 9011 9044 6109 6397 10 287 6998 1164 112 764 6 482 8 15131 5131 5131 5170 6647 2559 97 2756 8466 425 1783	-0,0164 -0,0225 -0,0225 -0,0225 -0,0225 -0,0311 -0,0442 -0,0317 -0,0406 -0,1484 -0,0327 -0,05 -0,0327 -0,05 -0,0402 -0	0 0 0 0 0 0 0 0 0 0 0 0 0 0 0 0 0 0 0	ALB/GA_GABAG_JRF2 ATPIOL/MEZ_GISTO DOVZ_ADAMTS19_TERT CONNIA_GEF_LAL_SPATS1_VEGFA MET SLUPP_JAPC CONNZA_TSC1_MTAP_PTPN3 PTEN PTEN HMBS ANID_2.NNT_A_CON1B RB1 ANIL_TSC2_BRD7 TP53 KEAP_LSEPVL_TMEM_ISG0 DVARCS		3e21.1 426.5 3 5 5 5 5 5 5 5 5 5 5 5 5 5 5 5 5 5 5	\$485.3 6427 7486.3 8424.3 9424.3 9424.3 9424.3 9424.3 9424.3 9424.3 10026.8 11011.2 11011.2 11011.2 11012.1 11012.1 11012.1 11012.1 11012.1 11013.1 11025 12024.3 15026.3 16024.3 17011.2 17011.3 18023
## ## ## ## ## ## ## ## ## ## ## ## ##	chr6 chr7 chr8 chr9 chr9 chr9 chr9 chr9 chr9 chr9 chr9 chr11	53291 143266 203615 195642 195642 195642 1396615 1396882 13996582 13996582 225600 193118 47357754 61536762 6154836 63997102 203435 1970246 20201689 6088 6088 6088 18166613 18166613 18166613 18166613 18166613 18166613 18166613	190867085 180687595 170891556 159891587 139895187 146280027 139888074 139905490 47961271 4797418 135881590 47961271 4797418 135881590 165991899 1679918 1679918	7880 9011 8044 6109 9011 8044 6109 10 287 10 287 6998 3164 6 6 482 8 8 5131 5131 5131 5131 5131 5490 9752 9215 5490 9752 9215 5490 9752 9752 9752 9752 9752 9753 9752 9753 9752 9753 9753 9754 9755	-0.0164 -0.0227 -0.0227 -0.0227 -0.0227 -0.0238 -0.05013 -0.0482 -0.05013 -0.0482 -0.0503 -0.0402 -0.0503 -0.0402 -0.0503 -0.0403 -0.0503 -0.0403 -0.0503 -0.0603	0 0 0 0 0 0 0 0 0 0 0 0 0 0 0 0 0 0 0	ALB/GA_GABAG_JRF2 ATPIOB_MEFC_LIBST_DOCK2_ADAMTS19_TERT CONTA_EEF_ALS_PATS1_VEGFA MET SLUPP_JMYC CDNN2ATSC_JMTAP_PTINB PTEN PTEN HMBS ARID_JNNEA_CDN1B RB1 AMN1_TSC_JRRD7 TPS3 KEAP_LSEPAU_TIMEM160 DNAICS DYSKIA ZNIS_CLONS BRSSGA3		3q211 4q163 5 5 5 5 5 5 5 5 5 5 5 5 5 5 5 5 5 5 5	\$985.3 6927 7966.8 8924.3 9934.3 9934.3 9934.3 10026.3 11911.2 11911.2 11911.2 11912.2 11012.2 11012.2 11012.2 11012.2 11012.1 1102.3 1
##21TT ##22TT ##	chr6	\$3291 144266 203615 195642 138094 213464 13988822 13990582 226600 193118 4736754 6736756 6535762 203686 20368 203686 2036	190867085 170891556 170891556 170891556 1109031587 1109031587 139988074 139905490 141017298 13988074 141017298 1450402 1470417298 1470417298 1470417299 147041729 1470	7880 9011 9011 9014 6109 6397 10 287 6998 112 764 6 6 482 8 15131 5131 5131 5153 5160 6647 2559 9 16927 2756 48465 4855 1783 48665 487 5807	-0,0164 -0,0228 -0,0228 -0,0228 -0,0011 -0,0440 -0,044	0 0 0 0 0 0 0 0 0 0 0 0 0 0 0 0 0 0 0	ALB/GA_GABAG_JRF2 ATPIOB_MEFC_LIBST_DOCK2_ADAMTS19_TERT CONTA_EEF_ALS_PATS1_VEGFA MET SLUPP_JMYC CDNN2ATSC_JMTAP_PTINB PTEN PTEN HMBS ARID_JNNEA_CDN1B RB1 AMN1_TSC_JRRD7 TPS3 KEAP_LSEPAU_TIMEM160 DNAICS DYSKIA ZNIS_CLONS BRSSGA3		3q21.1 4q16.3 5p15.3 3 6p25.3 5 6p25.3	\$935.3 6927 7966.8 8924.3 9924.3 9924.3 9924.3 10026.8 11011.2 11011.2 11011.2 11011.2 11011.2 11012.2 11012.2 11012.2 11012.2 11013.3 11013.1 1103.3 1103.4 1103.3 15026.3 15026.3 1501.3 1502.3 17011.2 17012.3 18023 12013.33 12023.3 12023.3
### ### ### ### ### ### ### ### ### ##	chr6	\$3291 143266 203615 195642 1396612 1396612 1396612 1396613 13988812 139905182 225600 193118 47362742 47376754 65356762 63987102 208345 20201689 20401689 20401689 18166613 1616603 18166613 1616603 18166613 1616603 18166613 1616603 18166613 1616603	190867.085 1806875.95 170891556 170891556 139915187 146280027 139888074 139905490 141017488 139905490 14781271	7880 9011 8044 6109 9011 8044 6109 10 10 12 764 6 482 8 81 5131 5131 5131 5131 5131 5131 5131	-0.0164 -0.0227 -0.0227 -0.0227 -0.0228 -0.0513 -0.0482 -0.0513 -0.0482 -0.053 -0.0482 -0.053 -0.0482 -0.053 -0.0482 -0.053 -0.0482 -0.053 -0.0482 -0.053 -0.0482 -0.0483 -0.0483 -0.0483 -0.0483 -0.0483 -0.0483 -0.0483 -0.0483 -0.0483	0 0 0 0 0 0 0 0 0 0 0 0 0 0 0 0 0 0 0	ALB/GA,GABRAZ,BRZ ATPIOR,METZ,LISTS,DOCKZ,ADAMTS19,TERT CONNIA,EEFLALSPATSL,VEGFA MET SLUPPI,MYC CONNIA,TSCI,MYAP,PTINB PTEN PTEN HMBS ARIOZ,INSTA,CDONIB RB1 ANINI,TSCZ,BRD7 TPS3 KEAPI,SEPWI,TMEMIGO DNALCS DYAKIA ZNIFJ,CLONS RPSGRA3 ARIDJA,RPJZ2		3e21.1 4g16.3 5p15.33 6g67.3 7p22.3 8g23.3 9g24.3 9g34.3 9g34.3 10015.3 11015.5 11011.2 11011.2 11011.2 11011.2 11011.2 11011.2 11011.2 11011.2 11011.2 11011.2 11011.2 11011.1 11013.3 12013.3 12013.3 12013.3 17011.2 18013.3 17011.2 18011.3 17011.2 18011.3 17011.2 18011.3 17011.2 18011.3 17011.2 18011.3 17011.2 18011.3 17011.2 18011.3 17011.2 18011.3 17011.2 18011.3 17011.2 18011.3 17011.2 18011.3 17011.2 18011.3 17011.2 18011.3 17011.2 18011.3 17011.2 18011.3 17011.	Sq85.3 6q27 7q86.3 8q24.3 9q34.3 9q34.3 9q34.3 10q26.3 11p11.2 11p11.2 11p11.2 11q12.1 11q12.1 11q13.1 11q25 12q24.3 13q44 14q12.33 15q26.3 15
##271T ##277T ##277T ##277T ##277T	chr6 chr6 chr8 chr8 chr8 chr8 chr9 chr9 chr9 chr9 chr9 chr9 chr9 chr11 chr12 chr13 chr14 chr15 chr16 chr17 chr17 chr17 chr17 chr17 chr17 chr18 chr18 chr19 chr20 chr21 c	\$3291 143266 203615 195642 1350642 1350642 1390682 11990582 12990582 123606 193118 47367754 61536762 6154836 63987062 63987062 63987062 2001689 2045069 193746 1937	1908/2055 1708/2055 1708/2055 1708/2055 1898/2055 1898/2055 1898/2055 1398/2056 1398/2	7880 9011 8044 6109 9011 8044 6109 10 10 10 10 11 10 12 12 14 12 14 15 13 164 15 13 164 17 18 16 17 18 16 17 18 18 18 18 18 18 18 18 18 18 18 18 18	-0.0164 -0.0227 -0.0227 -0.0227 -0.0285 -0.0501 -0.0410 -0.0410 -0.0410 -0.0410 -0.045	0 0 0 0 0 0 0 0 0 0 0 0 0 0 0 0 0 0 0	ALB/GA,GABRAZ,BRZ ATPIOR,METZ,LISTS,DOCKZ,ADAMTS19,TERT CONNIA,EEFLALSPATSL,VEGFA MET SLUPPI,MYC CONNIA,TSCI,MYAP,PTINB PTEN PTEN HMBS ARIOZ,INSTA,CDONIB RB1 ANINI,TSCZ,BRD7 TPS3 KEAPI,SEPWI,TMEMIGO DNALCS DYAKIA ZNIFJ,CLONS RPSGRA3 ARIDJA,RPJZ2		3e21.1 4e16.3 5p15.33 6e25.3 6e25.3 8e23.3 9e24.3 9e24.3 9e24.4 10e15.3 11e15.5 11e11.2 11e11.2 11e12.2 11e12.3 12e13.3 12e12.3 12e13.3 12e12.3 12e13.3 12e23.3 12e23.3 12e23.3 12e23.3 12e23.3	\$985.3 6927 7986.8 8924.3 9934.3 9934.3 9934.3 10026.8 11p11.2 11p11.2 11q12.2 11q12.2 11q12.2 11q12.2 11q12.3 11q13.1 11q2.5 12q24.3 13q4 14q2.4 15q2.4 17p11.2 17p11.2 17p11.2 17p11.2 17p11.2 17p11.2 17p13.3 15q2.6 3 1
## ## ## ## ## ## ## ## ## ## ## ## ##	chr6	\$3291 143266 203615 195642 183004 1318648 1380882 13990582 226000 193118 47327054 61536762 61536762 63992102 208345 1930888 6088 6088 6088 1816663 1816655 588379 5885921 17061701 2700138	1908/2055 170891556 170891556 189895187 146280027 139888074 139905490 141017488 139805490 147017488 1398187 147361271 14737186 135481590 147361271 14737186 13348188 135481590 107389991 107389976 10738991 107389976 107389786 107389976 107389786 10	7880 9011 8044 6109 9011 8044 6109 10 10 12 764 66 482 8 815131 5131 5131 5131 5131 5131 5131	-0.0164 -0.0227 -0.0227 -0.0227 -0.0227 -0.0239 -0.0511 -0.04402 -0.04502 -0.051 -0.04502 -0.055 -0.04502 -0.055 -0.04502 -0.04502 -0.055 -0.04502 -0.055 -0.04502 -0.055 -0.04502 -0.055 -0.04502 -0.055 -0.04502 -0.055 -0.04502 -0.055 -0.04502 -0.055 -0.04602 -0.055 -0.04602 -0.055 -0.04602 -0.055 -0.04602 -0.055 -0.04602 -0.055 -0.04602 -0.055 -0.04602 -0.055 -0.04602 -0.055 -0.04602 -0.055 -0.04602 -0.055 -0.05	0 0 0 0 0 0 0 0 0 0 0 0 0 0 0 0 0 0 0	ALB/GA,GABRAZ,BRZ ATPIOR,METZ,LISTS,DOCKZ,ADAMTS19,TERT CONNIA,EEFLALSPATSL,VEGFA MET SLUPPI,MYC CONNIA,TSCI,MYAP,PTINB PTEN PTEN HMBS ARIOZ,INSTA,CDONIB RB1 ANINI,TSCZ,BRD7 TPS3 KEAPI,SEPWI,TMEMIGO DNALCS DYAKIA ZNIFJ,CLONS RPSGRA3 ARIDJA,RPJZ2		3e21.1 4e16.3 5p15.33 6e25.3 6e25.3 8e23.3 9e24.3 9e24.3 9e24.4 10e15.8 11e15.5 11e11.2 11e11.2 11e11.2 11e11.2 11e11.2 11e11.2 11e11.2 11e11.2 11e11.2 11e11.3 11e13.3 12e11.3 12e11.	\$935.3 6927 7q36.3 8924.3 9934.3 9934.3 9934.3 10026.3 11p11.2 11p11.2 11q12.2 11q12.2 11q12.2 11q12.2 11q13.1 11q2.3 11q13.1 11q2.3 12q24.33 15q26.3 17p11.2 17p11.2 17p11.2 17p11.3 13q34 14q2.3 15q26.3 15q26.3 17p11.2 17p11.2 17q25.3 18q23.3 17q21.3
## ## ## ## ## ## ## ## ## ## ## ## ##	chr6	\$3291 143266 203615 195642 183094 13180642 183094 13180642 13968822 226500 193118 6736724 6736724 6736762 65367062 63972002 20845 197088 6088 18156693 18166613 1816613 1816613 1816613 1816613 1816613 1816613 181613	190867085 120867085 120867085 170891556 139895187 140891556 139895187 139888074 139905490 141017248 13980549 14784181 143905490 14784181 143905490 14784181 143905490 14784181 143905490 14784181 143905490 14784181 148905481 148905481 148905481 148905481 148805481 148805681	7880 9011 8044 6109 10 10 28 11 10 27 10 28 11 164 11 12 12 764 64 482 8 13164 15131 5131 5131 5480 6647 2559 9 16927 2756 8466 1783 8466 1783 4219 1807 17734 130	-0.0164 -0.0225 -0.0225 -0.0225 -0.0225 -0.0250 -0.0317 -0.0402 -0.0402 -0.0402 -0.0402 -0.05 -0.0402 -0.05 -0.0402 -0.05 -0.0403 -0.055 -0.0403	0 0 0 0 0 0 0 0 0 0 0 0 0 0 0 0 0 0 0	ALB/GA,GABRAZ,BRZ ATPIOR,METZ,LISTS,DOCKZ,ADAMTS19,TERT CONNIA,EEFLALSPATSL,VEGFA MET SLUPPI,MYC CONNIA,TSCI,MYAP,PTINB PTEN PTEN HMBS ARIOZ,INSTA,CDONIB RB1 ANINI,TSCZ,BRD7 TPS3 KEAPI,SEPWI,TMEMIGO DNALCS DYAKIA ZNIFJ,CLONS RPSGRA3 ARIDJA,RPJZ2		3e21.1 4e36.3 5 5 5 5 5 5 5 5 5 5 5 5 5 5 5 5 5 5 5	\$485.3 \$6427 7486.3 8924.3 9424.3 9424.3 9424.3 9424.3 9424.3 10426.3 11911.2 11911.2 11911.2 11911.3 11413.1 11413.
## ## ## ## ## ## ## ## ## ## ## ## ##	chr6	\$3291 148266 203615 195642 135054 213464 13988832 13990582 225600 193118 47367754 6135762 6135762 6135762 63987062 63987	1908/2055 170891556 170891556 189895187 146280027 139888074 139905490 141017488 139805490 147017488 1398187 147361271 14737186 135481590 147361271 14737186 13348188 135481590 107389991 107389976 10738991 107389976 107389786 107389976 107389786 10	7880 9011 8044 6109 9011 8044 6109 10 10 12 764 66 482 8 815131 5131 5131 5131 5131 5131 5131	-0.0164 -0.0227 -0.0227 -0.0227 -0.0227 -0.0238 -0.00313 -0.0482 -0.00313 -0.0482 -0.053 -0.0402 -0.055 -0.0402 -0.055 -0.0402 -0.055 -0.0402 -0.0578 -0.0402 -0.0678	0 0 0 0 0 0 0 0 0 0 0 0 0 0 0 0 0 0 0	ALB/GA_GABAG_JERP2 ATPIOR_MEFC_LIBST_DOCK_ADAMTS19_TERT CONTA_EEFT_ALS_PATS_LYEGA MET SUMP_I_MYC CONN2ATSCI_MTAP_PTINB PTEN PTEN HMBS ARID_J_NET_A_CON1IB RB1 AMNI_TSCI_RRD7 TPS3 KEAPI_SEPUL_TIMEMISO DNAICS DYNEIA ZNIRS_CIONS RPSGA3 ARIDIA_RPZ2 COL11AL_JAKI_ARAS		3e21.1 4e16.3 5p15.33 5p15.33 6p26.3 7p22.3 8e23.3 9p24.3 9p24.3 3e015.3 11p15.5 11p11.2 11q12.2 11q12.2 11q12.2 11q12.2 11q12.1 11q13.1 11q13.1 11q13.1 11q13.1 11q13.1 11q13.1 11q13.1 12p13.3 13q12.11 14q11.2 15q11.2 15q11.2 15q11.2 15q11.2 15q11.3 15q12.3 1p16.3 1p1	\$485.3 6627 7q86.8 8q24.3 9q34.3 9q34.3 9q34.3 10q26.8 11p11.2 11p11.2 11q12.2 11q12.2 11q12.2 11q12.2 11q12.2 11q12.2 11q12.1 11q2.3 11q12.3 11q2.3 11q2.3 11q2.3 12q34.3 13q34 14q22.33 15q26.3 15q12.3 17p11.2 17q25.3 18q23.3 19q13.48 20q13.33 22q13.33 42q2.3 11q2.2 11q2.2 11q2.2 11q2.3 1
## ## ## ## ## ## ## ## ## ## ## ## ##	chr6	\$3291 143266 203615 195642 1395642 1395642 13986832 13986832 13980582 225500 193118 47357754 6154635 63987062 6	190687295 170891556 170891556 159891587 1398958074 139905490 47361271 139888074 139905490 47361271 47371418 63991393 47361271 47371418 63991393 134215768 134215768 134216768 13	7880 9011 8044 6109 9011 8044 6109 10 10 10 10 10 11 11 10 10 10 10 10 10	-0.0164 -0.0225 -0.0225 -0.0225 -0.0225 -0.0250 -0.0317 -0.0402 -0.0402 -0.0402 -0.0402 -0.05 -0.0402 -0.05 -0.0402 -0.05 -0.0403 -0.055 -0.0403	0 0 0 0 0 0 0 0 0 0 0 0 0 0 0 0 0 0 0	ALB/GA,GABRAZ,BRZ ATPIOR,METZ,LISTS,DOCKZ,ADAMTS19,TERT CONNIA,EEFLALSPATSL,VEGFA MET SLUPPI,MYC CONNIA,TSCI,MYAP,PTINB PTEN PTEN HMBS ARIOZ,INSTA,CDONIB RB1 ANINI,TSCZ,BRD7 TPS3 KEAPI,SEPWI,TMEMIGO DNALCS DYAKIA ZNIFJ,CLONS RPSGRA3 ARIDJA,RPJZ2		3921.1 4916.3 5915.33 6925.3 6925.3 8923.3 9924.3 9934.3 10015.3 11015.5 11011.2 11011.2 11011.2 11011.2 11011.2 11011.2 11011.2 11011.2 11011.2 11011.1 11013.3 12013.3 13011.1 14013.3 12013	\$485.3 6627 7q86.3 8q24.3 9q34.3 9q34.3 9q34.3 10q26.3 11p11.2 11p11.2 11p11.2 11p11.2 11p11.2 11q12.1 11q12.1 11q13.1 11q25 12q24.3 13q44 14q12.3 15q26.3 18q23 19q13.3 18q23 19q13.3 18q23 19q13.3 19q13.3 1q21.2 1p11.2 1q24.3 1q22.3 1q21.3
##211 ##211	chr6	\$3291 143266 203615 195642 183094 1318064 1318064 1318064 1318064 131808812 13960812 13960812 13960812 13960812 13960812 13960812 13960812 13960812 13960812 13960812 13960812 13960812 13960818 13960812 13960818	190867085 170891556 170891556 18905187 170891556 118905187 1189058074 118905490 1140107498 118905490 1470107498 118905490 1470107498 118905490 1470107498 118905490 1181554092	7880 9011 8044 6109 9011 10 8044 6109 110 287 6998 13164 112 764 6 81 81 15131 9752 3215 5400 5700 6647 2559 9 2756 4265 1783 1480 1480 1480 1480 1580 17734 130 131 131 1308	-0.0164 -0.0225 -0.0225 -0.0225 -0.0225 -0.0225 -0.0225 -0.0225 -0.0225 -0.0406 -0.1484 -0.05 -0.0406 -0.1484 -0.05 -0.0	0 0 0 0 0 1 1 0 0 0 0 0 0 0 0 0 0 0 0 0	ALB/GA_GABAG_JERP2 ATPIOR_MEFC_LIBST_DOCK_ADAMTS19_TERT CONTA_EEFT_ALS_PATS_LYEGA MET SUMP_I_MYC CONN2ATSCI_MTAP_PTINB PTEN PTEN HMBS ARID_J_NET_A_CON1IB RB1 AMNI_TSCI_RRD7 TPS3 KEAPI_SEPUL_TIMEMISO DNAICS DYNEIA ZNIRS_CIONS RPSGA3 ARIDIA_RPZ2 COL11AL_JAKI_ARAS		3e21.1 4e16.3 5p15.33 5p15.33 6p26.3 7p22.3 8e23.3 9p24.3 9p24.3 3e015.3 11p15.5 11p11.2 11q12.2 11q12.2 11q12.2 11q12.2 11q12.1 11q13.1 11q13.1 11q13.1 11q13.1 11q13.1 11q13.1 11q13.1 12p13.3 13q12.11 14q11.2 15q11.2 15q11.2 15q11.2 15q11.2 15q11.3 15q12.3 1p16.3 1p1	\$485.3 6627 7q16.8 8q24.3 9q34.3 9q34.3 9q34.3 10q26.8 11p11.2 11p11.2 11p11.2 11q12.2 11q12.2 11q12.1 11q13.1 11q2.3 11q13.1 11q2.3 11q13.1 11q2.3 11q13.1 11q2.3 11q13.1 13q34 14q2.3 15q13.3 15q13.3 15q13.3 15q13.3 15q13.3 12q13.3 12q23.3 12q23.
## ## ## ## ## ## ## ## ## ## ## ## ##	chr6	\$3291 143266 203615 195642 1395642 1395642 1395642 1395642 1395682 1395682 1395682 1395682 1395682 1395682 1395682 1395682 1395682 1395682 1395682 1395682 1395683 1395683 1395683 1395683 1395683 1395683 1395683 1395683 1395683 1395683 1395683 1395683 1395683 1395838 139588 1	190862085 180683759 170891556 130981587 139981587 146280027 1399868074 139905490 47961271 4737418 4737418 4737418 4737418 135881590 147061271 1470748 13588159 1470748 13888 138810818 138810818 138810818 138810818 1389159 1072829 1072829 1072	7880 9011 8044 6109 9011 8044 6109 10 10 10 10 10 10 10 11 10 10 10 10 10	-0.0164 -0.0227 -0.0227 -0.0227 -0.0228 -0.0513 -0.0482 -0.0513 -0.0482 -0.0533 -0.0482 -0.0533 -0.053	0 0 0 0 0 0 0 0 0 0 0 0 0 0 0 0 0 0 0	ALB/GA_GABAG_JRF2 ATPIOR_MEFC_LIRST_DOCK_ADAMTS19_TERT CONTA_EEF_LALSPATS1_VEGFA MET SLURP_I_MYC CONN2ATSCI_MTAP_PTINB PTEN PTEN HMBS ARID_J_NETA_CON1B RB1 ANN1_TSC2_RRD7 TPS3 KEAP_I_SEPM_I_TMEM160 DOWALCS DYRKLA 2NHS_CLONS RPSGAS3 ARIDJA_RP122 COLITAL_JAKI_MRAS		3q211 4q163 3 49163 3	\$485.3 6627 7q86.3 8q24.3 9q34.3 9q34.3 9q34.3 10q26.3 11p11.2 11p11.2 11p11.2 11p11.2 11p11.2 11q12.1 11q12.1 11q13.1 11q25 12q24.3 13q44 14q12.3 15q26.3 18q23 19q13.3 18q23 19q13.3 18q23 19q13.3 19q13.3 1q21.2 1p11.2 1q24.3 1q22.3 1q21.3

		00000	400704757	2524	0.707		Lan		F-45.00	F-05 0
#477T	chr5	92369 292550	180794757 34495187	8584 2779	0,787	0	10B,MEF2C,IL6ST,DOCK2,ADAMTS19,TERT,APC,MAP1B	1	5p15.33 6p25.3	5q35.3 6p21.31
#477T	chr6	34496537	34499471	6	1,2468	1			6p21.31	6p21.31
#477T	chr6	34500253	170893528	6914	0,7887	0	CDKN1A,EEF1A1,FRK,VEGFA		6p21.31	6q27
#477T	chr7	193502	158937438	9157	0,7981	0	MET,HGF,EGFR,KMT2C,BRAF,NUP205		7p22.3	7q36.3
#477T	chr8	116555	145279474	6562	0,79	0	MYC,RSPO2		8p23.3	8q24.3
#477T	chr9	14874	24925	10	1,0987	1			9p24.3	9p24.3
#477T #477T	chr9	117460 19378811	19378439 19446348	755 8	0,7801 1,1304	0			9p24.3 9p22.1	9p22.1 9p22.1
#477T	chr9	19450541	141016186	7115	0,818	0	CDKN2A,TSC1,NOTCH1,PTPN3		9p22.1	9q34.3
#477T	chr10	93526	135440158	8033	0,7951	0	PTEN		10p15.3	10q26.3
#477T	chr11	193127	134257498	10963	0,812	0	HMBS,FGF19,IGF2,CDKN1C,ATM		11p15.5	11q25
#477T	chr12	176326	133810818	11121	0,7984	0	ARID2,HNF1A,GLI1,KMT2D,KRAS,PTPRB		12p13.33	12q24.33
#477T	chr13	19748151	115090537	3406	0,7849	0	RB1,MYCBP2		13q12.11	13q34
#477T	chr14	19378084	105995651	5838	0,7979	0	DICER1		14q11.2	14q32.33
#477T	chr15	20740212	102462803	6904	0,809	0			15q11.2	15q26.3
#477T	chr16	97494	90142284	8279	0,8274	0	AXIN1,TSC2,BRD7		16p13.3	16q24.3
#477T	chr17 chr17	193127 36285820	36104703 42852092	4961 1715	0,8151	0	TP53,NF1 STAT3,ERBB2		17p13.3 17q12	17q12 17q21.31
#477T	chr17	36285821	36287166	66	1,1272	1	37313,61002		17q12	17q12
#477T	chr17	42852630	42854910	8	1,222	1			17q21.31	17q21.31
#477T	chr17	42855147	81052161	4882	0,8265	0			17q21.31	17q25.3
#477T	chr18	158706	78005195	2978	0,7742	0			18p11.32	18q23
#477T	chr19	111138	59082559	11208	0,8098	0	KEAP1,CCNE1,JAK3,KMT2B,DNAJB1,PRKACA		19p13.3	19q13.43
#477T	chr20	68379	62904763	4777	0,8204	0	GNAS		20p13	20q13.33
#477T	chr21	45658349	45953687	1636	0,7892	0			21q22.3	21q22.3
#477T	chr21	45959609	46117485	17	0,5079	0			21q22.3	21q22.3
#477T #477T	chr21 chr22	46131389 19378084	48084246 51220669	367 4061	0,8129	0	ZNRF3,NF2		21q22.3 22q11.21	21q22.3
#477T	chrX	200918	120012716	5067	0,8273	0	RPS6KA3		22q11.21 Xp22.33	22q13.33 Xq24
#477T	chrX	120064205	120119012	24	1,0672	0			Xq24	Xq24
#477T	chrX	120182377	134928918	515	0,7015	0			Xq24	Xq26.3
#477T	chrX	134856765	134930218	28	1,0739	0			Xq26.3	Xq26.3
#477T	chrX	134947481	153421889	817	0,7248	0			Xq26.3	Xq28
#477T	chrX	153424346	153520465	23	1,0386	0	-		Xq28	Xq28
#477T	chrX	153524279	155239777	342	0,7585	0			Xq28	Xq28
#477T	chrY	150918	59342783 9833391	127 1289	0,8571	0	RPL22		Yp11.32	Yq12
#533T	chr1	69550			0,6154		RPLZZ		1p36.33	1p36.22
#533T #533T	chr1	9883746 10132179	10093740 249211681	21 19068	0,88	0	ARID1A,COL11A1		1p36.22 1p36.22	1p36.22 1q44
#533T	chr2	41618	242814646	15102	0.5864	0	ACVR2A,NFE2L2,EPHA4,APOB		2p25.3	2q37.3
#533T	chr3	361505	197765488	11764	0,5875	0	CTNNB1,BAP1,PDE12,KLF15,SETD2		3p26.3	3q29
#533T	chr4	53384	113242	7626	0,574	0			4p16.3	4p16.3
#533T	chr5	92369	180794757	8692	0,5912	0	ATP10B,MEF2C,IL6ST,DOCK2,ADAMTS19,TERT		5p15.33	5q35.3
#533T	chr6	292550	170893528	9806	0,5894	0	CDKN1A,EEF1A1,SPATS1,VEGFA		6p25.3	6q27
#533T	chr7	193502	124482939	6785	0,6152	0	MET		7p22.3	7q31.33
#533T	chr7	124487024	124493109	3	0,9194	1			7q31.33	7q31.33
#533T #533T	chr7	124499088 116555	158937438 146279474	2484 6644	0,5885	0	SLURP1,MYC		7q31.33 8p23.3	7q36.3
#533T	chr9	14874	75407188	2305	0,5876	0	CDKN2A,MTAP		8p23.3 9p24.3	8q24.3 9q21.13
#533T	chr9	75420362	75450878	7	0,2213	-1	Companying		9q21.13	9021.13
#533T	chr9	75516160	141016186	5671	0,6057	0	TSC1,PTPN3		9q21.13	9q34.3
#533T	chr10	93526	18827201	1022	0,6142	0			10p15.3	10p12.31
#533T	chr10	18828406	18874950	5	1,3626	1			10p12.31	10p12.31
#533T	chr10	18885197	135440158	7110	0,5915	0	PTEN		10p12.31	10q26.3
#533T	chr11	193127	47767777	3769	0,5883	0			11p15.5	11p11.2
#533T	chr11	47772528	47808056	11	0,9216	1			11p11.2	11p11.2
#533T	chr11 chr11	47809796 55029766	51411920 55036766	98 5	0,5947	0			11p11.2	11p11.12
#533T #533T	chr11	55111170	134257498	7188	1,1514	0	HMBS		11q11 11q11	11q11 11q25
#533T	chr12	176326	133810818	11258	0,6078	0	ARID2,HNF1A,CDKN1B		12p13.33	12q24.33
#533T	chr13	19748151	115090537	3468	0,5744	0	RB1		13q12.11	13q34
#533T	chr14	19378084	105995651	5909	0,6029	0			14q11.2	14q32.33
#533T	chr15	20740212	102462803	6998	0,5997	0			15q11.2	15q26.3
#533T	chr16	97494	90142284	8346	0,6399	0	AXIN1,TSC2,BRD7		16p13.3	16q24.3
#533T	chr17	193127	6544475	1247	0,6579	0			17p13.3	17p13.1
#533T	chr17	6545114	6547883	4	0,2709	-1			17p13.1	17p13.1
#533T	chr17	6553350 36981427	36977240	3964 6	1,0434	0	TP53		17p13.1	17q12
#533T #533T	chr17	37008921	37006671 81052161	6524	0,6342	0	1		17q12 17q12	17q12 17q25.3
#533T	chr18	158706	43604614	1834	0,5901	0			18p11.32	18q21.1
#533T	chr18	43619963	43708066	23	0,8353	0			18q21.1	18q21.1
#533T	chr18	43796204	78005195	1174	0,5682	0			18q21.1	18q23
#533T	chr19	111138	5729919	1544	0,6878	0			19p13.3	19p13.3
#533T	chr19	5733924	5776249	17	0,9816	1			19p13.3	19p13.3
#533T	chr19 chr19	5778537 56166495	56163954 56172480	9286 5	0,7011	0	KEAP1,SEPW1,TMEM160		19p13.3	19q13.42
#533T #533T	chr19 chr19	56166495	56172480	420	0,275	-1 0	1		19q13.42 19q13.42	19q13.42 19q13.43
#533T	chr19	68379	30137895	1565	0,5771	0	1		20p13	20q11.21
#533T	chr20	30142591	30253821	12	0,8962	1		BCL2L1	20q11.21	20q11.21
#533T	chr20	30309739	62904763	3255	0,6219	0	DNAICS		20q11.21	20q13.33
#533T	chr21	45658349	48084246	2054	0,6027	0			21q22.3	21q22.3
#533T	chr22	19378084	51220669	4110	0,6304	0	ZNRF3,CLDN5		22q11.21	22q13.33
#533T	chrX	200918	48830651	2036	0,5996	0	RPS6KA3		Xp22.33	Xp11.23
#533T	chrX	48831644	48844572	14	0,8847	0	+		Xp11.23	Xp11.23
#533T	chrX	48846072	155239777	4552	0,585	0			Xp11.23	Xq28
#533T #623T	chrY chr1	150918 717420	59342783 33134894	555 3196	0,5867	0	ARID1A,RPL22		Yp11.32 1p36.33	Yq12 1p35.1
#623T	chr1	33135125	33134894	7	-0,1143	0	ANIVARIAN ANIVAR		1p36.33 1p35.1	1p35.1
#623T	chr1	33149635	159860325	8131	0,143	0	COL11A1		1p35.1	1q23.2
#623T	chr1	159863017	159921553	17	0,443	1			1q23.2	1q23.2
#623T	chr1	159922172	249149602	5985	0,1362	0			1q23.2	1q44
#623T	chr1	249149795	249211681	7	0,449	1			1q44	1q44
#623T	chr2	41602	243037096	13813	0,122	0	ACVR2A,NFE2L2,EPHA4,APOB		2p25.3	2q37.3
#623T	chr3	361504	197847544	10647	0,1384	0	CTNNB1,BAP1,PDE12,KLF15,SETD2		3p26.3	3q29
#623T	chr4	53383	190946966	7234	0,09	0	ALB,FGA,GABRA2,IRF2		4p16.3	4q35.2
#623T	chr5	143251	180687764	7921	0,1218	0	ATP10B,MEF2C,IL6ST,DOCK2,ADAMTS19,TERT		5p15.33	5q35.3
#623T	chr6	140294 195642	170892713 158935187	9130 8092	0,1321	0	CDKN1A,EEF1A1,SPATS1,VEGFA MET		6p25.3	6q27 7g36 3
	chr7	195642 163585	158935187 146279464	8092 5762	0,143	0	MET SLURP1.MYC		7p22.3 8p23.3	7q36.3 8q24.3
#623T #623T		117444	141071146	6753	0,1642	0	CDKN2A,TSC1,MTAP,PTPN3		9p24.3	9q34.3
#623T #623T	chr9									
#623T	chr9 chr10	93566	32751620	1625	0,1216	0			10p15.3	10p11.22
#623T #623T				1625 15	0,1216 -0,1993	0 -1			10p15.3 10p11.22	10p11.22 10p11.22

March Marc	#6227	-b-10	27420740	37488685	15	0.1000		Ī		10-11 21	10-11-21
March Marc	#623T #623T	chr10	37438740 37490207		15 5505	-0,1988 0,1478	-1	PTEN		10p11.21 10p11.21	10p11.21 10q26.3
March Marc	#623T	chr11	193811	45992792	2661	0,1654	0			11p15.5	
MATERIAL											
Section Color											
SEPT Color Septem Sept								HMBS			
Section Sect								ARID2,CDKN1B			
March Marc								19974			
March Marc											
Marcia	#623T	chr14	19110319	106236157	5549						
Marcia M											
March Marc											
March Marc											
March Marc	#623T	chr15	28520085	63579683	2958	0,1318	0				100
March 1967 1969											
Reg									3		
MATERIAL CAMPA											
Harris			81841	1889347	338			AXIN1			
Bear 1998											
March 1990				-				TSC2,BRD7			
Mary 1.97			100000000000000000000000000000000000000			700,000,000					
REGIT CHOP	#623T	chr17	11293	81052160	9104	0,1986		TP53			17q25.3
BREET											
RADIT								KEAP1,SEPW1,TMEM160			
Mart Column				200000000000000000000000000000000000000							
MATI	#623T	chr20	5564947	62934540	3532	0,1887	0			20p12.3	20q13.33
Mary Color			+								
REST											
PFSFI	17/2000	1 1 1 1 1 1 1 1 1 1 1 1 1 1 1 1 1 1 1 1	100000000000000000000000000000000000000	1 - 1 - 1 - 1 - 1 - 1 - 1 - 1 - 1 - 1 -	7	10000000		nr:JONA3			
PATE Oct	#750T		721657					ARID1A,RPL22		1p36.33	1p35.2
PROF. OPI. 1906005 1906005 6 4,1775 -1											
PATE Orl 15000000 15000000 15000000 15000000 18 0.00000 1.000000 1.000000 1.0000000 1.0000000 1.00000000 1.0000000000											
PSF								COL11A1			
PROFIT 0-02 20191291 21195685 3139 0.277 0 ACMPANTELEPHALADOR 29273	#750T	chr1	150484120	150532308	18	-0,0668					
Profit Oct											
Profit Gold								ACVR2A,NFE2L2,EPHA4,APOB	2027.2		
PSST									2457.5		
## PST	#750T	chr3	239470	38524787	1924	0,2569	0			3p26.3	
Profit chi 1 1987-1986 1977-1986 131 0.0865 0 ABJEGACHINA 1529 3929 2927 1577 chi 1 1987-1986 1977-1986 1590 0.0858 0 ABJEGACHINA 1577 0.954 0.1118 0.958 0 ABJEGACHINA 1577 0.954 0.958 0.958 0 ABJEGACHINA 1577 0.954 0.958 0.958 0.958 0 ABJEGACHINA 1577 0.954 0.958 0.9											
Profit cht 15977056 15977056 15170562 1511 0.3005 0								CTNNB1,BAP1,PDE12,KLF15,SETD2			
# F9FT					77						
## PSPT 695 14182700 14182800 3 0.0213 0.0 ## PSPT 695 14182700 150 566 0.0272 0 0 5611.3 5413.3 ## PSPT 695 14182700 150 566 0.0272 0 0 5611.3 5413.3 ## PSPT 695 15072890 15073700 56 0.0272 0 0 5613.3 5413.3 ## PSPT 695 15072890 15073700 5 0 0.0218 0 0 APPEND.DOCK2 5413.3 5413.3 ## PSPT 695 15072890 13073700 1302 0.0218 0 CNDHARFFALSANSLYGFA 6.65.3 6627. ## PSPT 697 1506 15072890 1302 0.0218 0 0 CNDHARFFALSANSLYGFA 6.65.3 6627. ## PSPT 697 1506 1507289 1302 0.0218 0 0 CNDHARFFALSANSLYGFA 6.65.3 6627. ## PSPT 697 1506 1507289 1302 0.0218 0 0 MRT 6.0218.3 6627. ## PSPT 697 1506 13096 1300729 1302 0.0232 0 0 MRT 6.0218.3 6627. ## PSPT 697 1506 13096 1300729 1302 0.0232 0 0 MRT 6.0218.3 6627. ## PSPT 697 1506 130096 1300729 1302 0.0232 0 0 MRT 6.0218.3 6627. ## PSPT 697 1506 130096 1300729 1302 0.0232 0 0 MRT 6.0218.3 6627. ## PSPT 698 1506 130096 1300729 1302 0.0232 0 0 MRT 6.0218.3 6627. ## PSPT 698 1508 130096 1300729 1302 0.0232 0 0 MRT 6.0218.3 6627. ## PSPT 698 1508 1300729 1302 0.0232 0 0 MRT 6.0218.3 6627. ## PSPT 698 1508 1300729 1302 0.0232 0 0 MRT 6.0218.3 6627. ## PSPT 698 1508 1300729 1300 0.0275 0 0 MRC 6.0212.3 6811.2	#750T	chr4	53291	190947577	6954	0,3118	0	ALB,FGA,GABRA2,IRF2		4p16.3	4q35.2
## PSPT chr chr 1418F414 18732730 956 0.2472 0					5590	100000000000000000000000000000000000000		MEF2C,IL6ST,ADAMTS19,TERT			
## 250FT					3 956						
#798T											
#750T chr? 195642 650702 19 0.1857 1 792.33 791.12 #750T chr? 6555756 156937919 5662 0.2489 0 MET 791.12 791.12 #750T chr8 19566 3707478 1721.0.2522 0 MET 791.13 791.13 #750T chr8 19566 3707248 3275085 10 0.2499 0 MET 791.13 791.13 #750T chr8 197248 3275085 10 0.2575 0 MET 891.13 891.13 #750T chr8 3707248 3275085 10 0.2775 0 Bg.1.13 #750T chr8 3827349 3275085 10 0.2775 0 Bg.1.13 #750T chr8 3827349 3275085 10 0.2775 0 MTC 891.13 891.13 #750T chr8 3827349 3275085 10 0.2775 0 MTC 891.13 891.13 #750T chr8 3827349 3275085 0 MTC 891.13 891.13 #750T chr8 3827349 3275085 0 MTC 891.13 891.13 #750T chr8 3827349 3275085 0 MTC 891.13 891.23 #750T chr8 3827349 327508 0 MTC 891.13 891.23 #750T chr8 3827349 327508 0 MTC 891.13 892.33 #750T chr8 3827492 327508 0 MTC 891.13 892.33 #750T chr8 10.1250999 146280815 0.5 0.04 0 SURPT 882.43 892.43 #750T chr9 2.1000 14610708 771.7 0.2148 0 CONDATKI,MTAPTPN3 992.43 992.43 #750T chr9 2.1000 14610708 771.7 0.2148 0 CONDATKI,MTAPTPN3 992.43 992.43 #750T chr10 8845810 8845310 19 0.6551 1 1 100.12 1 1	#750T	chr5	156741411	180687559	1362	0,2118	0	ATP10B,DOCK2		5q33.3	5q35.3
#750T chr								CDKN1A,EEF1A1,SPATS1,VEGFA			
## 1950T chr					* *******						
P750T								MET			
#750T ch8 37703248 3870536 110 0.2715 0 891.23 891.23 891.23 8750T ch8 3877152 32387182 7 -0.107 -1 1 MC 891.23 891.23 891.23 8750T ch8 13877152 32387182 32387184 3862 0.3172 0 MC 891.28 894.3 894.3 894.3 89750T ch8 14210099 34620815 675 0.04 0 SUBPI 892.43 894.3 894.3 89750T ch9 234910 341012498 7711 0.2148 0 COMPLATING PTMS 99.43.3 894.3 89750T ch9 234910 341012498 7711 0.2248 0 COMPLATING PTMS 99.43.3 894.3 19750T ch9 234910 88414510 8845210 19 -0.0512 11 1 1 1 1 1 1 1 1 1 1 1 1 1 1 1 1 1		chr8	190866	37641778	1721	0,2522	0			8p23.3	
#750T ch8 38271452 38275818 7 -0.107 -1 MrC 8911.23 89243 8750T ch8 1827752 13286774 3602 0.3172 0 MrC 8911.23 89243 8750T ch8 12120099 314020815 075 0.04 0 SLUBPI 89243 89243 8750T ch9 212000 31010789 7117 0.2184 0 CONGATSCLMTAP.PTM3 9.9243 99243 8750T ch70 22600 88277586 3971 0.2598 0 FERN 10913.2 10023.2 6750T ch70 8845301 99 -0.0512 1 FERN 10913.2 10023.2 6750T ch70 8845301 99 -0.0512 1 FERN 10913.2 10023.2 6750T ch70 8845301 99 -0.0512 1 FERN 10913.2 10023.2 6750T ch70 8845301 99 -0.0512 1 FERN 10913.2 10023.2 6750T ch70 8845301 99 -0.0512 1 FERN 10913.2 10023.2 6750T ch70 99651128 33543544 2522 0.2360 0 FERN 10913.2 10024.2 6750T ch70 99651128 33543544 2522 0.2360 0 FERN 10913.2 10024.2 6750T ch71 10913.2 6750T ch71 1											
9750T											
#750T ch/9 214910 141017488 7117 0.2148 0 CONN2ATSCLMTAPFFNS 99,043 99,43 99,43 9750T ch/10 881530 8823210 19 -0,0512 -1 1 10013 2 10023 2 100								MYC			
##50T chr10 22000 8827586 3671 0.2598 0 1001.3 100232 100232 ##50T chr10 8845451 9965606 5 0.2595 0 PTEN 100232 100232 ##50T chr10 9664077 99656706 5 0.2529 1.1 1 1 1 1 1 1 1 1 1 1 1 1 1 1 1 1 1	#750T	chr8	142190899		675	0,04		SLURP1			
##50T ch10 88416510 8845211 09 -0.0512 -1 100242 100242 100242 100242 1750T ch10 9966077 9965076 5 -0.2509 1 1 1 1 1 1 1 1 1 1								CDKN2A,TSC1,MTAP,PTPN3			
##50T chr10 98640977 98656706 5 0,2559 1 1 1 1 1 1 1 1 1 1 1 1 1 1 1 1 1 1											
##50T chr10 99661328 13549664 2522 0,2368 0 100,242 100,242 100,242 100,263								PTEN			
#750T chr1	#750T	chr10	99640077	99656706	5	-0,2509	-1			10q24.2	10q24.2
#750T cht1 6756162 6399814 10 -0,1101 -1 11q131 11q131 11q131 11q131 11											
## ## ## ## ## ## ## ## ## ## ## ## ##											
#F50T		-	007.002.00					HMBS			
#750T cht2 49950A0 54792431 93 0.883 0 1224132 1224131								ARID2,CDKN1B			
#750T											
#750T ch12 5479800 133198073 5835 0,252 0 HHF1A 120433 1204313 120433 4750T ch12 13319815 133197804 6 0-3137 -1 120433 120433 120433 120433 120433 #750T ch12 13319815 133191887 159 0,1572 0 #811 120433 120433 120433 120433 #750T ch13 2000M50 115091029 3095 0,3087 0 #811 1304111 13044 #750T ch14 2000M69 30728303 5961 0,2461 0 #811 120433 120433 120433 #750T ch15 2017006 30239376 6299 0,2395 0 #811 120433 120433 #750T ch16 50326661 50328567 6299 0,2395 0 #810 1204323 #750T ch16 50326661 5033855 7 - 0,133 -1 #870T ch16 50326661 5033855 0 #870T ch16 50326661 503355 0 #870T ch16 50326661 50326661 50326667 50326 0 #870T ch16 50326661 50326667 50326 0 #870T ch16 50326661 50326667 50326 0 #870T ch16 5032667 50326 0 #870T ch16 50326667 50326 0 #870T ch16 5032667 50326 0 #											
##50T cht2 133196500 133197894 6 -0.3137 -1 12024.33 1202								HNF1A			
##50T		chr12	133196300	133197894	6		-1		12q24.33	12q24.33	12q24.33
#750T child 20201689 107283203 5961 0,2461 0 14q12.3 14q12.3 1 #750T chil6 97096 50324469 3989 0,1477 0 ANNI,TSC2 16q13.3 16q12.1 #750T chil6 50324661 50328852 7 - 0,133 -1											
##50T chris 2017056 10.289376 529 0.2395 0								MB1			
##50T chr16 97096 93024649 3989 0,1477 0 ANNI,TSC2 169133 156122 ##50T chr16 50328651 50338852 7 0,193 -1 ##50T chr16 50338455 93051444 3409 0,1705 0 BRD7 169121 169213 ##50T chr16 50338455 91051144 3409 0,1705 0 BRD7 16921 119133 170523 ##50T chr17 6088 81052160 10417 0,1688 0 TPS3 179113 170523 ##50T chr18 117194 77910108 2745 0,2988 0 TPS3 179113 170523 ##50T chr19 107510 59083958 9626 0,1109 0 KIAPI,SPRI,TIMENGO 159133 1991343 ##50T chr20 68379 62056077 4528 0,188 0 DNAICS 0,0013 ##50T chr20 68379 62056077 4528 0,188 0 DNAICS 0,0013 ##50T chr21 9823922 48084620 1859 0,2181 0 DYRKIA 219112 210223 ##50T chr22 2760842 2663888 915 0,1007 0 CLDN5 229111 221023 ##50T chr22 24765236 45732350 2375 0,1469 0 ZNRF3 2291123 2291123 ##50T chr22 24765236 45732350 2375 0,1469 0 ZNRF3 229112 2291133 ##50T chr22 4590848 2129140 576 0,0072 0 CLDN5 229113 2291131 ##50T chr22 4590848 51219140 576 0,0071 0 RPS6A3 ##50T chr2 4590848 51219140 576 0,0071 0 RPS6A3 ##50T chr2 4590841 51219140 576 0,0071 0 RPS6A3 ##50T						-					
##50T chr16 5938455 90161144 3409 0.705 0 8BD7 16q121 16q243 ##50T chr17 6668 81051160 10417 0.1698 0 7953 17p133 17q253 ##50T chr18 117194 77941018 2745 0.2998 0 ##50T chr18 117194 77941018 2745 0.2998 0 ##50T chr19 107510 59983958 9626 0.1109 0 ##50T chr20 68379 62966077 4528 0.188 0 ##50T chr20 68379 62966077 4528 0.188 0 ##50T chr20 107510 59983958 9926 0.1097 0 ##50T chr21 992392 4808420 1859 0.2181 0 ##50T chr21 992392 4808420 1859 0.2181 0 ##50T chr22 2469838 24761522 11 ##50T chr22 24765236 4572250 2375 0.1469 0 ##50T chr22 24765236 4572250 2375 0.1469 0 ##50T chr22 24765236 4572250 2375 0.1469 0 ##50T chr22 4598418 51219140 576 0.6071 0 ##50T chr22 4598418 51219140 576 0.6071 0 ##50T chr2 45986418 51219140 576 0 ##50T chr2 45986418 51219140 576 0 ##50T chr2 4					3989		0	AXIN1,TSC2			
#750T cht7 6088 \$1052160 10417 0,1698 0 TP53 179133 179253 #750T cht8 117194 77941018 2745 0,2998 0 1891.32 18921 #750T cht9 107510 59933958 9626 0,1109 0 KEAP1,SEPWI,TMEMIGO 199133 1991348 #750T cht20 68379 62966077 4528 0,188 0 DNACS 20913 201333 #750T cht21 9925922 4094620 1899 0,2181 0 DWKIA 219112 219223 #750T cht22 17966842 2698388 915 0,1097 0 CLONS 229111 2219123 #750T cht22 24082888 915 0,1097 0 CLONS 229111 2219123 #750T cht22 24082888 915 0,1097 0 CLONS 229111 2219123 #750T cht22 24082588 24765322 11 0,4377 0 CLONS 229112 2219134 #750T cht22 2476536 45792250 2375 0,1449 0 781873 2291123 #750T cht22 4785361 28904884 20 0,4072 0 229131 #750T cht22 4590418 51219140 576 0,0671 0 229131 #750T cht22 4590418 51219140 576 0,0671 0 875643								0000	1		
#750T ch/18 117194 77941018 2745 0,2998 0 1801132 18023 #750T ch/19 107510 59083958 9626 0,1109 0 KEAPLSEPVLIMIMISO 199133 1941343 1941343 4750T ch/20 68379 6;295(6077 4528 0,188 0 DNAICS 20913 2094133 4750T ch/21 9925922 48084620 1859 0,2181 0 DNAICS 220114 2;210123 4750T ch/22 10706842 2,468888 915 0,1087 0 CLONS 22411 2;240123 4750T ch/22 24608288 24765152 11 0,4377 0 CLONS 224112 2;241123 2;241134 4750T ch/22 24608288 24765152 11 0,4377 0 22415 2 224123 2;24113 4750T ch/22 24763236 45732250 2375 0,1449 0 278673 2224123 2;24133 4750T ch/22 457865136 45732250 2375 0,1449 0 278673 2224123 2;24133 4750T ch/22 45786518 20 0,0072 0 288678 2224123 2;24133 4750T ch/22 45786518 51219140 576 0,0671 0 22415 22415 2;24133 4750T ch/22 4578648 20 0,0072 0 22415 3 22413 3 4750T ch/22 4578648 120 20 0,072 0 22415 3 22413 3 4750T ch/22 4578648 1972 0,2715 0 RP566A3 8,223 8,78123 4750T ch/K 4909404 49105675 9 -0,2016 11 8750T ch/K 4909404 49105675 9 -0,2016 11 8750T ch/K 49107417 51640936 112 0,2726 0 RP156A3 8,223 8,781123 4750T ch/K 49107417 51640936 112 0,2726 0 RP156A3 8,223 8,781123 4750T ch/K 49107417 51640936 112 0,2726 0 RP156A3 8,781123 8,781											
##50T chi 9 107510 9983998 9626 0.1109 0 KEAPLSFPMITMEMIGO 1991.3 1991.34 1991.34 197510 chi 9 107510 95083998 9626 0.1109 0 KEAPLSFPMITMEMIGO 1991.3 1991.34 1991.34 19750T chi 9 107510 0.188 0 DWACS 20013 20013.3 1991.34 19750T chi 9 107510 0.188 0 DWACS 20013 20013.3 19750T chi 9 107510 0.1859 0.2181 0 DYRKIA 21911.2 2192.3 19750T chi 9 107510 0.1859 0.1087 0 CLONS 22011.1 2211.2 19750T chi 9 107510 0.1859 0.1087 0 CLONS 22011.1 2211.2 19750T chi 9 107510 0.1859 0.1489 0 2781873 22011.2 19750T chi 9 107510 0.1859 0.0072 0 22011.3 19750T chi 9 107510 0.18590884 20 0.0072 0 22013.3 19750T chi 9 107510 0.18590884 20 0.0072 0 22013.3 19750T chi 9 107510 0.18590884 20 0.0072 0 107510 0.1859						-					
#750T chr21 9825922 48084620 1859 0.2181 0 0YKKIA 21p11.2 21p22.3 #750T chr22 17008842 24082888 915 0,1087 0 CLDN5 22p11.3 22p11.2 22p11.2 #750T chr22 24765236 45732250 2375 0,1469 0 2NRF3 22p11.2 22p11.23 22p11.3 #750T chr22 43765236 45732250 2375 0,1469 0 2NRF3 22p11.2 22p11.23 22p11.3 #750T chr22 43765216 45732250 2375 0,1469 0 2NRF3 22p11.23 22p11.31 #750T chr22 4580418 512p140 576 0,0671 0 22p11.31 22p13.31 22p13.31 #750T chr32 4580484 9.0 0,072 0 2P1.2 2p1.3 2p1.3 2p1.3 #750T chr32 4580418 512p140 576 0,0671 0 2p1.3 2p1.3 2p1.3 2p1.3 4750T chr32 4580418 512p140 576 0,0671 0 8P56A3 8p2.3 8p1.2 2p1.3 4750T chr32 4580418 512p140 576 0,0671 0 8P56A3 8p2.3 8p1.2 3p1.2	#750T	chr19	107510	59083958	9626	0,1109	0			19p13.3	19q13.43
#750T chr22 17060842 26628888 915 0,1087 0 CLDN5 22q11.1 22q11.23 #750T chr22 24690288 24761522 11 0,4377 0 22q11.23 22q11.23 1750T chr22 24690288 24761522 11 0,4377 0 22q11.23 22q11.23 1750T chr22 24765236 4573250 0,2375 0,1449 0 70 2NRF3 22q11.23 22q13.31 18750T chr22 4578512 45304684 20 0,4072 0 2NRF3 22q13.31 22q13.31 22q13.31 18750T chr22 4580418 51219140 576 0,0671 0 22q13.31 22q13.31 22q13.31 18750T chr2 2701038 4909848 1972 0,2715 0 RP590A3 18720A 1872											
#750T chr22 24690258 24763522 11 0,4377 0 2241123 2241123 2241123 4750T chr22 24765236 45732250 2375 0,1469 0 218F3 2241123 2241123 2241123 4750T chr22 4578512 6580488 20 0,4072 0 2241331 2241331 4750T chr22 4580418 51219140 576 0,0671 0 2241331 2241331 4750T chr8 270138 4909848 91972 0,2715 0 RP5603 2241331 2241331 4750T chr8 470038 4809848 91972 0,2715 0 RP5603 82233 38,78123 4750T chr8 4909844 49105675 9 -0,2016 -1 8750T chr8 4909844 49105675 9 -0,2016 -1 8750T chr8 49107417 5160936 112 0,2726 0 81123 4751123 4750T chr8 49107417 5160936 112 0,2726 0 81123 4750T chr8 49107417 5160936 112 0,2726 0 81123 4750T chr8 49107417 5160936 112 0,0726 0											
#750T chr2 2476336 4573250 2375 0.1449 0 278873 2291131 2291331 8750T chr2 45739512 4580488 20 0.4072 0 2291331 2291331 2291333 4750T chr2 4580948 51219140 576 0.0671 0 2201331 2291333 4750T chr3 270018 4090848 1972 0.2715 0 87560A3 0.2233 591133 4750T chr3 49909404 49105675 9 0.2016 1 891123 8750T chr3 4910747 5180956 112 0.2726 0 9 0.2726 0 0.2726 0 0.2726 0 0.2726 0 0.2726											
#750T chr2 4580948 51219140 576 0.0671 0 2201331 2201333 278307 chr3 7270138 4099844 1972 0.2715 0 8P56K43 %22.33 %211.23 8750T chr3 4099804 49105675 9 -0.2016 -1 8P56K43 %21.23 %211.23 %211.23 %211.23 %212.23 %250T chr3 4910747 51860956 112 0.2726 0 8911.23 %211.23 %211.23 %211.24 %250T chr3 5184129 5.6277378 6 -0.0809 -1 8911.23 %211.25 %	#750T	chr22	24765236		2375	0,1449	0	ZNRF3		22q11.23	22q13.31
#750T chrX 2700138 49098548 1972 0,2715 0 RP56KA3 Xp22.33 Xp11.23 #750T chrX 49099404 49105675 9 -0,2016 -1 Ps11.23 Xp11.23 #750T chrX 49107417 51640936 112 0,2726 0 Xp11.23 Xp11.22 #750T chrX 51641249 52677378 6 -0,0809 -1 Xp1 Xp1.22 Xp11.22											
#750T chrK 48099404 49105675 9 -0,2016 -1 Kp11.23 Xp11.23 #750T chrK 48107417 51640956 112 0,2726 0 Kp11.23 Xp11.23 Xp								Rbzekas			
#750T chrX 49107417 \$1640936 112 0,2726 0 Xp11.22 Xp11.22 Xp11.22 #750T chrX \$1641249 \$2677378 6 -0,0809 -1 Xp11.22 Xp11.22 Xp11.22											
			49107417		112						Xp11.22
χρ11.22 Xq28											
	#/SUI	Cnr.X	52081349	134774646	3800	0,25/4	U	1	L	Ap11.22	ждга

#757T #757T #757T	0.900	60777	24027	0.00	0.000	70277	100011 00100 0		4-90	
	chr1	69550	249211681	20304	0,6618	0	ARID1A,RPL22,COL11A1,JAK1,NRAS		1p36.33	1q44
#757T	chr2	41618	242814646	15037	0,6698	0	ACVR2A,NFE2L2,EPHA4,APOB,ALK		2p25.3	2q37.3
	chr3	361505	197765488	11714	0,6711	0	CTNNB1,BAP1,KLF15,SETD2,FANCD2,TNFSF10,PIK3CA		3p26.3	3q29
#757T	chr4	53384	113242	7594	0,6696	0			4p16.3	4p16.3
#757T	chr5	92369	180794757	8649	0,6691	0	10B,MEF2C,IL6ST,DOCK2,ADAMTS19,TERT,APC,MAF	18	5p15.33	5q35.3
#757T	chr6	292550	117150079	7094	0.6552	0	CDKN1A,EEF1A1,FRK,VEGFA		6p25.3	6q22.1
#757T	chr6	117198550	117593637	23	0,2028	-1			6q22.1	6q22.1
#757T		117609810	117645537		0,5867					
	chr6			10		0			6q22.1	6q22.1
#757T	chr6	117647482	117725517	29	0,1954	-1			6q22.1	6q22.1
#757T	chr6	117730775	170893528	2613	0,6668	0			6q22.1	6q27
#757T	chr7	193502	158937438	9235	0,6615	0	MET,HGF,EGFR,KMT2C,BRAF,NUP205		7p22.3	7q36.3
#757T	chr8	116555	146279474	6612	0,6679	0	MYC,RSPO2		8p23.3	8q24.3
#757T	chr9	14874	141016186	7946	0,6606	0	CDKN2A,TSC1,NOTCH1,PTPN3		9p24.3	9q34.3
#757T	chr10	93526	135370294	8093	0,667	0	PTEN		10p15.3	10q26.
#757T	chr10	135370616	135373626	6	1,0887	2			10q26.3	10q26.
#757T	chr10	135378997	135440158	5	0,6815	0			10q26.3	10q26.
#757T	chr11	193127	134257498	11028	0,656	0	HMBS,FGF19,IGF2,CDKN1C,ATM		11p15.5	11q25
#757T	chr12	176326	133810818	11210	0,6667	0	ARID2,HNF1A,GLI1,KMT2D,KRAS,PTPRB		12p13.33	12q24.3
#757T	chr13	19748151	115090537	3449	0,6716	0	RB1,MYCBP2		13q12.11	13q34
		19378084	104433107	5584						
#757T	chr14	-			0,6596	0	DICER1		14q11.2	14q32.3
#757T	chr14	104436918	104460898	6	1,1162	2			14q32.33	14q32.3
#757T	chr14	104462115	105995651	288	0,6257	0			14q32.33	14q32.3
#757T	chr15	20740212	102462803	6943	0,6637	0			15q11.2	15q26.
#757T	chr16	97494	90142284	8326	0.6511	0	AXIN1,TSC2,BRD7			16q24.
200000000	50010000	1	200000000000000000000000000000000000000	2012/1920	10000000				16p13.3	100000000000000000000000000000000000000
#757T	chr17	193127	81052161	11692	0,6561	0	TP53,STAT3,ERBB2,NF1		17p13.3	17q25.
#757T	chr18	158706	78005195	3022	0,6676	0			18p11.32	18q23
#757T	chr19	111138	59082559	11244	0,6383	0	KEAP1,CCNE1,JAK3,KMT2B,DNAJB1,PRKACA		19p13.3	19q13.4
#757T	chr20	68379	62904763	4813	1,01	1	GNAS	BCL2L1,ZNF217,20q13.33	20p13	20q13.
#757T	chr21	45658349	48084246	2031	0,6508	0		,,	21q22.3	21q22
		19378084		4095			ZNDES NES			
#757T	chr22	-	51220669	1000000	0,6493	0	ZNRF3,NF2		22q11.21	22q13.
#757T	chrX	200918	155239777	6822	0,6001	0	RPS6KA3	<u> </u>	Xp22.33	Xq28
#757T	chrY	150918	59252516	118	0,4603	0			Yp11.32	Yq12
#757T	chrY	59272417	59342783	12	0,7472	0			Yq12	Yq12
#835T	chr1	861348	249212472	19263	-1,0751	0	ARID1A,RPL22,COL11A1		1p36.33	1944
#835T	chr2	40221	242842554	14692	-1,0726	0	ACVR2A,NFE2L2,EPHA4,APOB		2p25.3	2q37.
-		-		7.00000000					5.25000000	7.77
#835T	chr3	239470	197769162	11873	-1,0763	0	CTNNB1,BAP1,PDE12,KLF15,SETD2		3p26.3	3q29
#835T	chr4	53291	190947044	7735	-1,0695	0	ALB,FGA,GABRA2,IRF2		4p16.3	4q35.
#835T	chr5	140602	180687559	8651	-1,0709	0	ATP10B,MEF2C,IL6ST,DOCK2,ADAMTS19,TERT		5p15.33	5q35.
#835T	chr6	203615	68598996	5143	-1,0792	0	CDKN1A,SPATS1,VEGFA		6p25.3	6q12
#835T	chr6	69348939	93967210	1151	-1,5062	-1	EEF1A1			
							EEFIAI		6q12	6q16.
#835T	chr6	93967909	167608890	3440	-1,0738	0			6q16.1	6q27
#835T	chr6	167704934	168070076	16	-1,5068	-1			6q27	6q27
#835T	chr6	168187893	168764159	71	-2,0972	-1			6q27	6q27
#835T	chr6	168910680	170866070	120	-1,5087	-1			6q27	6q27
#835T	chr6	170871100	170892714	11	-1.0903	0			6027	6q27
							MET			
#835T	chr7	193386	158937319	9196	-1,0631	0			7p22.3	7q36.
#835T	chr8	190866	146280815	6700	-1,0766	0	SLURP1,MYC		8p23.3	8q24.
#835T	chr9	213465	141070232	7640	-1,0757	0	CDKN2A,TSC1,MTAP,PTPN3		9p24.3	9q34.
#835T	chr10	226000	135438930	7841	-1,0726	0	PTEN		10p15.3	10q26
#835T	chr11	193118	134856548	10894	-1,0807	0	HMBS		11p15.5	11q2
#835T	chr12	208345	133811687	11410	-1,0865	0	ARID2,HNF1A,CDKN1B		12p13.33	12q24
#835T	chr13	19600450	115091029	3456	-1,0658	0	RB1		13q12.11	13q3
#835T	chr14	20201689	107283203	6477	-1,0745	0			14q11.2	14q32
#835T	chr15	20170066	102389376	6766	-1,0867	0			15q11.1	15q26
#835T	chr16	96492	90161144	7793	-1,0816	0	AXIN1,TSC2,BRD7		16p13.3	16q24
#835T	chr17	6088	81052160	10955	-1,0804	0	TP53		********	
#0331		8800			*1,0804				170122	
		******					11.50	3	17p13.3	17q25
#835T	chr18	117194	77960704	3041	-1,0592	0			18p11.32	18q2
#835T	chr18 chr19	281462	77960704 59083958	10169	-1,0592 -1,0731	0	KEAP1,SEPW1,TMEM160			
#835T									18p11.32	18q2 19q13
#835T #835T	chr19	281462	59083958	10169	-1,0731	0	KEAP1,SEPW1,TMEM160		18p11.32 19p13.3	18q2 19q13 20q13
#835T #835T #835T	chr19 chr20 chr21	281462 68379 9825922	59083958 62906077 48084620	10169 4809 2008	-1,0731 -1,0721 -1,0665	0 0	KEAP1,SEPW1,TMEM160 DNAICS DYRKIA		18p11.32 19p13.3 20p13 21p11.2	18q2 19q13 20q13 21q22
#835T #835T #835T #835T	chr19 chr20 chr21 chr22	281462 68379 9825922 17060842	59083958 62906077 48084620 51219140	10169 4809 2008 4075	-1,0731 -1,0721 -1,0665 -1,0738	0 0 0	KEAP1,SEPW1,TMEM160 DNAICS DYRCIA ZNRF3,CLDNS		18p11.32 19p13.3 20p13 21p11.2 22q11.1	18q2 19q13 20q13 21q2; 22q13
#835T #835T #835T #835T #835T	chr19 chr20 chr21 chr22 chrX	281462 68379 9825922 17060842 2700138	59083958 62906077 48084620 51219140 154774846	10169 4809 2008 4075 6399	-1,0731 -1,0721 -1,0665 -1,0738 -1,069	0 0 0 0	KEAP1,SEPW1,TMEM160 DNAICS DYRK1A ZNRF3,CLDNS RPS6KA3		18p11.32 19p13.3 20p13 21p11.2 22q11.1 Xp22.33	18q2 19q13 20q13 21q2; 22q13 Xq2;
#835T #835T #835T #835T #835T #835T	chr19 chr20 chr21 chr22 chrX chr1	281462 68379 9825922 17060842 2700138 762325	59083958 62906077 48084620 51219140 154774846 249212472	10169 4809 2008 4075 6399 18763	-1,0731 -1,0721 -1,0665 -1,0738 -1,069 -0,2675	0 0 0 0	KEAP1,SEPW1,TMEM160 DNAICS DYRKIA ZNEF3,CLDNS RPSGKA3 ARIDIA,RPL22,COL11A1		18p11.32 19p13.3 20p13 21p11.2 22q11.1 Xp22.33 1p36.33	18q2 19q13 20q13 21q2 22q13 Xq2
#835T #835T #835T #835T #835T #835T	chr19 chr20 chr21 chr22 chrX	281462 68379 9825922 17060842 2700138	59083958 62906077 48084620 51219140 154774846	10169 4809 2008 4075 6399	-1,0731 -1,0721 -1,0665 -1,0738 -1,069	0 0 0 0	KEAP1,SEPW1,TMEM160 DNAICS DYRK1A ZNRF3,CLDNS RPS6KA3		18p11.32 19p13.3 20p13 21p11.2 22q11.1 Xp22.33	18q2 19q13 20q13 21q2 22q13 Xq2
#835T #835T #835T #835T #835T #835T #873T	chr19 chr20 chr21 chr22 chrX chr1	281462 68379 9825922 17060842 2700138 762325	59083958 62906077 48084620 51219140 154774846 249212472	10169 4809 2008 4075 6399 18763	-1,0731 -1,0721 -1,0665 -1,0738 -1,069 -0,2675	0 0 0 0	KEAP1,SEPW1,TMEM160 DNAICS DYRKIA ZNEF3,CLDNS RPSGKA3 ARIDIA,RPL22,COL11A1		18p11.32 19p13.3 20p13 21p11.2 22q11.1 Xp22.33 1p36.33	18q2 19q13 20q13 21q2; 22q13 Xq2; 1q4 2q37
#835T #835T #835T #835T #835T #873T #873T	chr19 chr20 chr21 chr22 chrX chr1 chr2 chr2 chr3	281462 68379 9825922 17060842 2700138 762325 40221 239470	59083958 62906077 48084620 51219140 154774846 249212472 242842554 197769162	10169 4809 2008 4075 6399 18763 14284 11615	-1,0731 -1,0721 -1,0665 -1,0738 -1,069 -0,2675 -0,2698 -0,2735	0 0 0 0 0 0	KEAPI,SEPNI,TMEMISO DMAICS DVRKLA ZWEJS,CLINS RUSSONS ARIDARRAZ,COLITAL ACURZA,REZZ,EPHALAPOB CTNBS,BARZ-POETZ,RETS,SETD2		18p11.32 19p13.3 20p13 21p11.2 22q11.1 Xp22.33 1p36.33 2p25.3 3p26.3	18q2 19q13 20q13 21q2; 22q13 Xq2; 1q4 2q37 3q2;
#835T #835T #835T #835T #835T #835T #873T #873T #873T	chr19 chr20 chr21 chr22 chrX chr1 chr2 chr3 chr4	281462 68379 9825922 17060842 2700138 762325 40221 239470 53291	59083958 62906077 48084620 51219140 154774846 249212472 242842554 197769162 190947044	10169 4809 2008 4075 6399 18763 14284 11615 7541	-1,0731 -1,0721 -1,0665 -1,0738 -1,069 -0,2675 -0,2698 -0,2735 -0,2773	0 0 0 0 0 0	KEAPJ,SEPNI,TMEMISO DNACS DVRKIA ZMEBJ,CIDNS RPSGOA ARIDA,RP12,COLITAL ACVRZA,NETRIZ,EPNALAPOS CTINBI,RAPI,POZI,RIJS,SETD2 AB,GAGBRAZ,BEZ AB,GAGBRAZ,BEZ AB,GAGBRAZ,BEZ		18p11.32 19p13.3 20p13 21p11.2 22q11.1 Xp22.33 1p36.33 2p25.3 3p26.3 4p16.3	18q2 19q13 20q13 21q2: 22q13 Xq2 1q4 2q37 3q2 4q35
#835T #835T #835T #835T #835T #835T #873T #873T #873T #873T	chr19 chr20 chr21 chr22 chrX chr1 chr2 chr3 chr4 chr5	281462 68379 9825922 17060842 2700138 762325 40221 239470 53291 140602	59083958 62906077 48084620 51219140 154774846 249212472 242842554 197769162 190947044 180687559	10169 4809 2008 4075 6399 18763 14284 11615 7541 8421	-1,0731 -1,0721 -1,0665 -1,0738 -1,069 -0,2675 -0,2698 -0,2735 -0,2773 -0,2731	0 0 0 0 0 0 0	KEAPL, SEPVI, TMEMIGO DIVACS OYRKIA ZNRF3, CLIDNS RP56033 ARIDA, RP12, COLITAL ACWEA, ARE REZ, EPIMA, APOB CTNNB, BAPL, POTEZ, RF15, SETO2 ALB, F04, GABRAZ, RF2 APPLOB, METZ, LISTS, DOCKZ, ADAM/S19, TERT		18p11.32 19p13.3 20p13 21p11.2 22q11.1 Xp22.33 1p36.33 2p25.3 3p26.3 4p16.3 5p15.33	18q2 19q13 20q13 21q2: 22q13 Xq2 1q4 2q37 3q2 4q35 5q35
#835T #835T #835T #835T #835T #873T #873T #873T #873T #873T	chr19 chr20 chr21 chr22 chrX chr1 chr2 chr3 chr4 chr5 chr6	281462 68379 9825922 17060842 2700138 762325 40221 239470 53291 140602 203615	59083958 62906077 48084620 51219140 154774846 249212472 242842554 197769162 190947044 180687559 92231416	10169 4809 2008 4075 6399 18763 14284 11615 7541 8421 6118	-1,0731 -1,0721 -1,0665 -1,0738 -1,069 -0,2675 -0,2698 -0,2735 -0,2773 -0,2773 -0,2731 -0,2706	0 0 0 0 0 0 0 0	KEAPJ,SEPNI,TMEMISO DNACS DVRKIA ZMEBJ,CIDNS RPSGOA ARIDA,RP12,COLITAL ACVRZA,NETRIZ,EPNALAPOS CTINBI,RAPI,POZI,RIJS,SETD2 AB,GAGBRAZ,BEZ AB,GAGBRAZ,BEZ AB,GAGBRAZ,BEZ		18p11.32 19p13.3 20p13 21p11.2 22q11.1 Xp22.33 1p36.33 2p25.3 3p26.3 4p16.3 5p15.33 6p25.3	18q2 19q13 20q13 21q2; 22q13 Xq2 1q4 2q37 3q2 4q35 5q35
#835T #835T #835T #835T #835T #873T #873T #873T #873T #873T #873T	chr19 chr20 chr21 chr21 chr22 chrX chr1 chr2 chr3 chr4 chr4 chr5 chr6 chr6	281462 68379 9825922 17060842 2700138 762325 40221 239470 53291 140602 203615 93951498	59083958 62906077 48084620 51219140 154774846 249212472 242842554 197769162 190947044 180687559 92231416 105736700	10169 4809 2008 4075 6399 18763 14284 11615 7541 6118	-1,0731 -1,0721 -1,0665 -1,0738 -1,069 -0,2675 -0,2698 -0,2735 -0,2731 -0,2706 -0,5049	0 0 0 0 0 0 0 0 0	KEAPL, SEPVI, TMEMIGO DIVACS OYRKIA ZNRF3, CLIDNS RP56033 ARIDA, RP12, COLITAL ACWEA, ARE REZ, EPIMA, APOB CTNNB, BAPL, POTEZ, RF15, SETO2 ALB, F04, GABRAZ, RF2 APPLOB, METZ, LISTS, DOCKZ, ADAM/S19, TERT		18p11.32 19p13.3 20p13 21p11.2 22q11.1 Xp22.33 1p36.33 2p25.3 3p26.3 4p16.3 5p15.33 6p25.3 6q16.1	18q2 19q13 20q13 21q2; 22q13 Xq2; 1q4 2q37 3q2; 4q35 5q35 6q1;
#835T #835T #835T #835T #835T #873T #873T #873T #873T #873T #873T	chr19 chr20 chr21 chr22 chrX chr1 chr2 chr3 chr4 chr5 chr6	281462 68379 9825922 17060842 2700138 762325 40221 239470 53291 140602 203615	59083958 62906077 48084620 51219140 154774846 249212472 242842554 197769162 190947044 180687559 92231416	10169 4809 2008 4075 6399 18763 14284 11615 7541 8421 6118	-1,0731 -1,0721 -1,0665 -1,0738 -1,069 -0,2675 -0,2698 -0,2735 -0,2773 -0,2773 -0,2731 -0,2706	0 0 0 0 0 0 0 0	KEAPL, SEPVI, TMEMIGO DIVACS OYRKIA ZNRF3, CLIDNS RP56033 ARIDA, RP12, COLITAL ACWEA, ARE REZ, EPIMA, APOB CTNNB, BAPL, POTEZ, RF15, SETO2 ALB, F04, GABRAZ, RF2 APPLOB, METZ, LISTS, DOCKZ, ADAM/S19, TERT		18p11.32 19p13.3 20p13 21p11.2 22q11.1 Xp22.33 1p36.33 2p25.3 3p26.3 4p16.3 5p15.33 6p25.3	18q2 19q13 20q13 21q2; 22q13 Xq2 1q4 2q37 3q2 4q35 5q35 6q1 6q2
#835T #835T #835T #835T #835T #873T #873T #873T #873T #873T #873T #873T	chr19 chr20 chr21 chr21 chr22 chrX chr1 chr2 chr3 chr4 chr4 chr5 chr6 chr6	281462 68379 9825922 17060842 2700138 762325 40221 239470 53291 140602 203615 93951498	59083958 62906077 48084620 51219140 154774846 249212472 242842554 197769162 190947044 180687559 2214116 105736700 170892714	10169 4809 2008 4075 6399 18763 14284 11615 7541 8421 6118 269 3314	-1,0731 -1,0721 -1,0665 -1,0738 -1,069 -0,2675 -0,2698 -0,2735 -0,2731 -0,2731 -0,2706 -0,6049 -0,2715	0 0 0 0 0 0 0 0 0 0 0	KEAPL, SEPVI, TMEMIGO DIVACS OYRKIA ZNRF3, CLIDNS RP56033 ARIDA, RP12, COLITAL ACWEA, ARE REZ, EPIMA, APOB CTNNB, BAPL, POTEZ, RF15, SETO2 ALB, F04, GABRAZ, RF2 APPLOB, METZ, LISTS, DOCKZ, ADAM/S19, TERT		18p11.32 19p13.3 20p13 21p11.2 22q11.1 Xp22.33 1p36.33 2p25.3 3p26.3 4p16.3 5p15.33 6p25.3 6q16.1	18q2 19q13 20q13 21q2; 22q13 Xq2 1q4 2q37 3q2 4q35 5q35 6q1 6q2
#835T #835T #835T #835T #835T #835T #835T #835T #835T #873T	chr19 chr20 chr21 chr22 chrX chr1 chr2 chr3 chr4 chr5 chr6 chr6 chr6 chr7	281462 68379 9825922 17060842 2700138 762325 40021 239470 53291 140602 203615 93951498 105770558	59083958 62906077 48084620 51219140 154774846 19774946 197769162 190947044 180687559 92231416 105736700 170892714 158937319	10169 4809 2008 4075 6399 18763 14284 11615 7541 8421 6118 269 3314	-1,0731 -1,0721 -1,0665 -1,0738 -1,069 -0,2675 -0,2678 -0,2735 -0,2773 -0,2773 -0,2773 -0,2773 -0,2771 -0,2706 -0,6049 -0,2715 -0,2685	0 0 0 0 0 0 0 0 0 0 0 0	KEAPJ,SEPNI,TMEMIGO DNAICS DYNKIA ZWEFS,CLONS RPSGOA3 ARIDARREZ,COLITAL ACWEZA,WEZZ,EPHAA,APOB CTINBILBAPI,POEZ,BAFJ,SETD2 ABAF,GAGBRAZ,REZ APT-108,GAGBRAZ,REZ APT-108,MEZC,LIGST,DOCKZ,ADAMTSI9,TERT CDNIA, EEFIAI,SPATSI,VEGFA MET		18p11.32 19p13.3 20p13 21p11.2 22q11.1 %p22.33 1p36.33 2p25.3 3p26.3 4p16.3 5p15.33 6p25.3 6q16.1 6q21	18q2 19q13 20q13 21q2 22q13 Xq2 1q4 2q37 3q2 4q35 5q35 6q1 6q2 6q2 7q36
#835T #835T #835T #835T #835T #835T #835T #835T #835T #873T	chr19 chr20 chr21 chr22 chr22 chr3 chr1 chr2 chr3 chr4 chr6 chr6 chr6 chr6 chr7 chr8	281462 68379 9825922 17060842 2700138 762325 402211 239470 53291 140602 203615 93951498 105770558 195642	59083958 62906077 48084620 51219140 154774846 249212472 242842554 197769162 199947044 180687559 92237416 105736700 170892714 158937319 146280815	10169 4809 2008 4075 6399 18763 14284 11615 7541 8421 6118 269 3314 8937 6533	-1,0731 -1,0721 -1,0721 -1,0665 -1,0738 -1,069 -0,2675 -0,2698 -0,2735 -0,2773 -0,2773 -0,2706 -0,6049 -0,2685 -0,2689	0 0 0 0 0 0 0 0 0 0 0 0 0 0 0	ELAPJ,SEPNJ,TMEMIGO DNAICS DYKKIA ZWEFS,CLIMS RIPSGOAJ ARIDJARP122,COLIJA1 ACVEZA,MEZIZ,EPHAA,APOB CTINBL,BARJ,DOS,ZA,BT,SSTD2 ALB,GA,GABRAJ,BOSZ,ALB,TS,STD2 ALB,GA,GABRAJ,BOSZ,ALB,TS,GABATSIJ,YEBT CDNIIA,EEFAAI,SPATSI,VEGFA MET SURDI,MYC		18p11.32 19p13.3 20p13 21p11.2 22q11.1 Xp22.33 1p36.33 2p25.3 3p26.3 4p16.3 5p15.33 6p25.3 6q16.1 6q21 7p22.3 8p23.3	18q2 19q13 20q13 21q2; 22q13 Xq2 1q4 2q37 3q2 4q35 6q1 6q2 7q36
#835T #835T #835T #835T #835T #835T #835T #835T #835T #873T	chr19 chr20 chr21 chr22 chr22 chrX chr1 chr2 chr3 chr4 chr5 chr6 chr6 chr6 chr6 chr7 chr8 chr9	281462 68379 9825922 17060842 2700138 7623325 40221 239470 53291 140602 203615 93951498 105770558 195642 190866 214910	59083958 62906077 48084620 51219140 154774846 249212472 242842554 197769162 199947044 180687559 92231416 105736700 170892714 158937319 146220815 141017498	10169 4809 2008 4075 6399 18763 14284 11615 7541 8421 6118 269 3314 8937 6533 7440	-1,0731 -1,0721 -1,0665 -1,0738 -1,069 -0,2675 -0,2698 -0,2735 -0,2773 -0,2706 -0,699 -0,2715 -0,2689 -0,2689 -0,2689	0 0 0 0 0 0 0 0 0 0 0 0 0 0 0 0 0 0 0	KEAPJ, SEPNJ, TMEMISO DNAICS DWKILS ZWEFS, CLONS RPSSOA ARIDARPA2Z, COLISIA ACVEZA, MEZI, ZEPMAA, APOS CTNNBLBAPL, POEIZ, RETS, SETD2 AB, SGA, GABRAZ, JRRZ APPLIBA, MEZC, JLEST, SOCKZ, ADAMTS19, TERT CDNIAL, EEFIAL, SPATSI, VEGFA MET SLIRPI, MYC CONNA, TSC, JATTAP, PTRIS		18p11.32 19p13.3 20p13 21p11.2 21p11.1 Np22.33 1p36.33 2p25.3 3p26.3 4p16.3 5p15.33 6p25.3 6q16.1 6q21 7p22.3 8p23.3 9p24.3	18q2 19q13 21q2; 22q13 22q13 3q2 4q35 5q35 6q1 6q2 6q2 7q36 8q24
#835T #835T #835T #835T #835T #835T #835T #873T #873T #873T #873T #873T #873T #873T #873T #873T	chr19 chr20 chr21 chr22 chrX chr22 chr3 chr3 chr4 chr5 chr6 chr6 chr6 chr6 chr7 chr8 chr9 chr10	281462 68379 9825922 17060842 2700138 762325 40221 239470 53291 140602 203615 93951498 105770558 195642 190866 214910 226000	59083958 62906077 48084620 51219140 154774846 249212472 242843554 197769162 190947044 180687559 92231416 105736700 170892714 15893737319 146280815 141017498	10169 4809 2008 4075 6399 18763 14284 11615 7541 8421 6118 269 3314 8937 6533 7440 7635	-1,0731 -1,0721 -1,0665 -1,0738 -1,0738 -0,2675 -0,2698 -0,2735 -0,2731 -0,2736 -0,6049 -0,2715 -0,2685 -0,2689 -0,2689 -0,2684 -0,2644	0 0 0 0 0 0 0 0 0 0 0 0 0 0 0 0 0 0 0	EEAPJ.SEPNJ.TMEMISO DINAICS DYRKIA 2NAF3.CLONS RUSSOKS ARIDLARPA2.ZCOLITAI ACVEZA.NETZL.SEPHALAPOB CTINBLE.RAPL.DEST.ZE.ST.DE ALS.FG.G.GRARJ.RETZ. ALS.FG.GRARJ.RETZ.LETS.TDE ALS.FG.GRARJ.RETZ.LETS.TDE ALS.FG.GRARJ.SETZ.TDE SURPL.MYC CONNIA_EEFIALSPATSI,VEGFA MET SURPL.MYC CONNIA_TSC.J.MYC.DEST.		18p11.32 19p13.3 20p13 21p11.2 22q11.1 Kp22.33 1p36.33 2p25.3 3p26.3 4p16.3 5p15.33 6p25.3 6q16.1 6q21 7p22.3 8p23.3 9p24.3 10p15.3	18q2 19q13 20q13 21q2: 22q13 3q2 24q35 3q2 4q35 5q35 6q1 6q2 6q2 7q36 8q24 9q34
#835T #835T #835T #835T #835T #835T #835T #873T #873T #873T #873T #873T #873T #873T #873T #873T	chr19 chr20 chr21 chr22 chr22 chrX chr1 chr2 chr3 chr4 chr5 chr6 chr6 chr6 chr6 chr7 chr8 chr9	281462 68379 9825922 17060842 2700138 7623325 40221 239470 53291 140602 203615 93951498 105770558 195642 190866 214910	59083958 62906077 48084620 51219140 154774846 249212472 242842554 197769162 199947044 180687559 92231416 105736700 170892714 158937319 146220815 141017498	10169 4809 2008 4075 6399 18763 14284 11615 7541 8421 6118 269 3314 8937 6533 7440	-1,0731 -1,0721 -1,0665 -1,0738 -1,069 -0,2675 -0,2698 -0,2735 -0,2773 -0,2706 -0,699 -0,2715 -0,2689 -0,2689 -0,2689	0 0 0 0 0 0 0 0 0 0 0 0 0 0 0 0 0 0 0	KEAPJ, SEPNJ, TMEMISO DNAICS DWKILS ZWEFS, CLONS RPSSOA ARIDARPA2Z, COLISIA ACVEZA, MEZI, ZEPMAA, APOS CTNNBLBAPL, POEIZ, RETS, SETD2 AB, SGA, GABRAZ, JRRZ APPLIBA, MEZC, JLEST, SOCKZ, ADAMTS19, TERT CDNIAL, EEFIAL, SPATSI, VEGFA MET SLIRPI, MYC CONNA, TSC, JATTAP, PTRIS		18p11.32 19p13.3 20p13 21p11.2 21p11.1 Np22.33 1p36.33 2p25.3 3p26.3 4p16.3 5p15.33 6p25.3 6q16.1 6q21 7p22.3 8p23.3 9p24.3	18q2 19q13 20q13 21q2: 22q13 3q2 24q35 3q2 4q35 5q35 6q1 6q2 6q2 7q36 8q24 9q34
#835T #835T #835T #835T #835T #835T #835T #873T #873T #873T #873T #873T #873T #873T #873T #873T #873T	chr19 chr20 chr21 chr22 chr22 chr2 chr2 chr3 chr1 chr2 chr3 chr4 chr5 chr6 chr6 chr6 chr6 chr6 chr6 chr9 chr9 chr9 chr10 chr11	281462 68379 9825922 17060842 2700138 762325 40221 239470 53291 140602 293951498 105770558 195642 190666 214910 226000 193118	99083958 62906077 48084620 51219140 154774846 249212472 242842554 19769162	10169 4809 2008 4075 6399 18763 14284 11615 7541 8421 6118 269 3314 8937 6533 7440 7440 7635	-1,0731 -1,0721 -1,0665 -1,0738 -1,069 -0,2675 -0,2698 -0,2773 -0,2773 -0,2731 -0,2706 -0,5049 -0,2745 -0,2685 -0,2689 -0,2648 -0,2642	0 0 0 0 0 0 0 0 0 0 0 0 0 0 0 0 0 0 0	KEAPJ, SEPWI, TMEMISO DNAICS DWKILS ZWEFS, CLIDNS RPSSOAD ARIDARPA 22, COLIDAI ACVEZA, MERZA, EPHAA, APOB CTINB, JABPI, POST, LO, ES, STOZ AB, FGA, GABRAZ, JRV AB, FGA, GABRAZ, JRV CDONIA, EEFJAL, SPATS, VEGFA MET SLURPJ, MYC CDINZA, TSC, JATTAP, PTPNB PTEM HMMS		18p11.32 19p13.3 20p13 21p11.2 22q11.1 Kp22.33 1p36.33 2p25.3 3p26.3 4p16.3 5p15.33 6p25.3 6q16.1 6q21 7p22.3 8p23.3 9p24.3 10p15.3	18q2 19q13 20q13 21q2; 22q13 3q2 1q4 2q33 3q2 4q35 6q1 6q2 6q2 7q36 8q24 9q34 10q2;
#835T #835T #835T #835T #835T #835T #835T #835T #873T	chv19 chv20 chv21 chv21 chv21 chv22 chv2 chv1 chv1 chv2 chv3 chv4 chv6 chv6 chv6 chv6 chv6 chv6 chv7 chv8 chv1 chv1 chv1 chv10 chv10 chv10 chv10 chv10	281462 68379 9825922 17066842 2700138 762325 40221 239470 53291 140602 203615 93951498 105770558 195642 190666 214910 226600 193118	99083958 62906077 48084620 51219140 154774846 249212472 242842554 197769162 199047044 180687559 92231416 105736700 170892714 158937319 146200815 141017498 135438930 134856548 138811687	10169 4809 2008 4075 63399 18763 14284 11615 7541 8421 6118 269 3314 8937 6533 7440 7635	-1,0731 -1,0721 -1,0665 -1,0738 -1,0738 -0,2675 -0,2698 -0,2735 -0,273 -0,2731 -0,2706 -0,6049 -0,2735 -0,2689 -0,2689 -0,2684 -0,2644 -0,2715	0 0 0 0 0 0 0 0 0 0 0 0 0 0 0 0 0 0 0	EEAPL,SEPNI,TMEMISO DINALCS DYRKLA ZNAF3,CLONS RUSSOKS ARIDLARPA2,COLITAL ACURZA,NEZA,12,EPHALAPOB CTINBLE,MARIPLOETE,RET,SETD2 ALB,FGA,GABRAZ,RETAL,SETD2 ALB,FGA,GABRAZ,RETAL ATPIDEM,MEZ,LERS,TOOCZ,ADAMTSIB,TERT CONNIA,EEFLAL,SPATSI,VEGFA MET SLURPI,MYC CONNIA,TSC,MTAP,PTINB PIEN HMSS ARDZ,NESIA,CONNIB		18p11.32 19p13.3 20p13 21p11.2 22q11.1 Xp22.33 1p36.33 2p25.3 3p26.3 4p16.3 5p15.33 6p25.3 6q16.1 6q21 7p22.3 8p23.3 9p24.3 10p15.3	18q2 19q13 20q13 20q2 22q13 Xq2 1q4 2q37 3q25 6q1 6q2 6q2 7q36 8q24 9q34 11q2 11q2
#835T #835T #835T #835T #835T #835T #835T #835T #835T #873T	chr19 chr20 chr21 chr21 chr22 chrX chr1 chr2 chr3 chr4 chr5 chr6 chr6 chr6 chr6 chr6 chr6 chr6 chr6	281462 68379 9825922 17066842 2700138 40221 239470 53291 140602 239470 199851498 105770558 199666 214910 226000 199118 226000 199118	59083958 62996077 48084620 51219140 154774846 249312472 242842554 199769162 199947044 180687559 92231416 105736700 170892714 158937319 146208015 141017498 138483930 134855548 133811687 11501029	10169 4809 2008 4075 6399 14284 14284 14284 1518 8421 6118 269 3314 8533 7540 10613 111140 3375	-1,0731 -1,0731 -1,0665 -1,0738 -1,0699 -0,2675 -0,2793 -0,2773 -0,2773 -0,2791 -0,2796 -0,2699 -0,2685 -0,2689 -0,2684 -0,2642 -0,2642 -0,2642 -0,2715 -0,2715 -0,2715 -0,2715 -0,2715 -0,2715 -0,2715 -0,2715 -0,2715	0 0 0 0 0 0 0 0 0 0 0 0 0 0 0 0 0 0 0	KEAPJ, SEPWI, TMEMISO DNAICS DWKILS ZWEFS, CLIDNS RPSSOAD ARIDARPA 22, COLIDAI ACVEZA, MERZA, EPHAA, APOB CTINB, JABPI, POST, LO, ES, STOZ AB, FGA, GABRAZ, JRV AB, FGA, GABRAZ, JRV CDONIA, EEFJAL, SPATS, VEGFA MET SLURPJ, MYC CDINZA, TSC, JATTAP, PTPNB PTEM HMMS		18911.32 19913.3 20913 21911.12 22911.1 Xp22.33 1985.33 3026.3 4925.3 5915.33 6925.3 6925.3 8023.3 19924.3 10915.3	18q2 19q13 20q13 20q13 Xq2 1q4 2q37 3q2 4q35 5q35 6q1 6q2 7q36 8q24 9q34 10q2 11q2 12q24
#835T #835T #835T #835T #835T #835T #835T #8373T #873T	chr19 chr20 chr21 chr22 chr22 chr22 chr2 chr2 chr2 chr3 chr4 chr1 chr6 chr6 chr6 chr6 chr6 chr6 chr6 chr7 chr8 chr9 chr10 chr11 chr12 chr13 chr13 chr13 chr13	281462 68379 9825922 17006842 2700138 762325 40221 239470 53291 140602 203615 9393148 105770558 214910 226000 1919118 20845 196005	59083958 62996077 48084620 51219140 154774846 2492112472 242841254 197769162 190947044 180687559 92231416 105736700 170892714 158937319 146280815 141017498 135438930 135438930 135438930 135438930 135438930 135438930 135438930 135438930 135438930 135438930 135438930 135438930 135438930	10169 4809 2008 4007 2008 4075 6399 18763 14284 11615 7541 6118 269 3314 8827 6533 7440 7635 10613 311140 3375 6306	-1,0731 -1,0731 -1,0665 -1,0738 -1,069 -0,2675 -0,2735 -0,2735 -0,2736 -0,2736 -0,2736 -0,2736 -0,2689 -0,2689 -0,2689 -0,2689 -0,2689 -0,2642 -0,2715 -0,2764 -0,2764 -0,2775	0 0 0 0 0 0 0 0 0 0 0 0 0 0 0 0 0 0 0	EEAPL,SEPNI,TMEMISO DINALCS DYRKLA ZNAF3,CLONS RUSSOKS ARIDLARPA2,COLITAL ACURZA,NEZA,12,EPHALAPOB CTINBLE,MARIPLOETE,RET,SETD2 ALB,FGA,GABRAZ,RETAL,SETD2 ALB,FGA,GABRAZ,RETAL ATPIDEM,MEZ,LERS,TOOCZ,ADAMTSIB,TERT CONNIA,EEFLAL,SPATSI,VEGFA MET SLURPI,MYC CONNIA,TSC,MTAP,PTINB PIEN HMSS ARDZ,NESIA,CONNIB		18011.32 19013.2 20013 21011.2 22011.1 822.33 1905.3 2025.3 2025.3 2026.3 4026.3 6025.3 6016.1 6021.3 10015.3 11015.3 11015.3 12013.3 32023.3 32023.3 32023.3 32023.3 32023.3 32023.3 32023.3 32023.3 32023.3 32023.3 32023.3	18q2 19q13 20q13 21q2; 22q13 3q2 4q35 5q35 6q1 6q2 7q36 8q24 9q34 10q20 11q2 11q24 13q3 14q32
#835T #835T #835T #835T #835T #835T #835T #8373T #873T	chr19 chr20 chr21 chr21 chr22 chrX chr1 chr2 chr3 chr4 chr5 chr6 chr6 chr6 chr6 chr6 chr6 chr6 chr6	281462 68379 9825922 17066842 2700138 40221 239470 53291 140602 239470 199851498 105770558 199666 214910 226000 199118 226000 199118	90089398 62906077 48084620 53129140 15477464 242841554 19779162 197971044 190947044 190947044 150947044 150947044 150947044 150947044 150947044 15095714 150	10169 4809 2008 4075 6399 14284 14284 14284 1518 8421 6118 269 3314 8533 7540 10613 111140 3375	-1,0731 -1,0731 -1,0665 -1,0738 -1,0699 -0,2675 -0,2793 -0,2773 -0,2773 -0,2791 -0,2796 -0,2699 -0,2685 -0,2689 -0,2684 -0,2642 -0,2642 -0,2642 -0,2715 -0,2715 -0,2715 -0,2715 -0,2715 -0,2715 -0,2715 -0,2715 -0,2715	0 0 0 0 0 0 0 0 0 0 0 0 0 0 0 0 0 0 0	EEAPL,SEPNI,TMEMISO DINALCS DYRKLA ZNAF3,CLONS RUSSOKS ARIDLARPA2,COLITAL ACURZA,NEZA,12,EPHALAPOB CTINBLE,MARIPLOETE,RET,SETD2 ALB,FGA,GABRAZ,RETAL,SETD2 ALB,FGA,GABRAZ,RETAL ATPIDEM,MEZ,LERS,TOOCZ,ADAMTSIB,TERT CONNIA,EEFLAL,SPATSI,VEGFA MET SLURPI,MYC CONNIA,TSC,MTAP,PTINB PIEN HMSS ARDZ,NESIA,CONNIB		18911.32 19913.3 20913 21911.12 22911.1 Xp22.33 1985.33 3026.3 4925.3 5915.33 6925.3 6925.3 8023.3 19924.3 10915.3	18q2 19q13 20q13 21q2; 22q13 3q2 4q35 5q35 6q1 6q2 7q36 8q24 9q34 10q20 11q2 11q24 13q3 14q32
#835T #835T #835T #835T #835T #835T #835T #835T #8373T #873T	chr19 chr20 chr21 chr22 chr22 chr22 chr2 chr2 chr2 chr3 chr4 chr1 chr6 chr6 chr6 chr6 chr6 chr6 chr6 chr7 chr8 chr9 chr10 chr11 chr12 chr13 chr13 chr13 chr13	281462 68379 9825922 17006842 2700138 762325 40221 239470 53291 140602 203615 9393148 105770558 214910 226000 1919118 20845 196005	59083958 62996077 48084620 51219140 154774846 2492112472 242841254 197769162 190947044 180687559 92231416 105736700 170892714 158937319 146280815 141017498 135438930 135438930 135438930 135438930 135438930 135438930 135438930 135438930 135438930 135438930 135438930 135438930 135438930 135438930 135438930	10169 4809 2008 4007 2008 4075 6399 18763 14284 11615 7541 6118 269 3314 8827 6533 7440 7635 10613 311140 3375 6306	-1,0731 -1,0731 -1,0665 -1,0738 -1,069 -0,2675 -0,2735 -0,2735 -0,2736 -0,2736 -0,2736 -0,2736 -0,2689 -0,2689 -0,2689 -0,2689 -0,2689 -0,2642 -0,2715 -0,2764 -0,2764 -0,2775	0 0 0 0 0 0 0 0 0 0 0 0 0 0 0 0 0 0 0	EEAPL,SEPNI,TMEMISO DINALCS DYRKLA ZNAF3,CLONS RUSSOKS ARIDLARPA2,COLITAL ACURZA,NEZA,12,EPHALAPOB CTINBLE,MARIPLOETE,RET,SETD2 ALB,FGA,GABRAZ,RETAL,SETD2 ALB,FGA,GABRAZ,RETAL ATPIDEM,MEZ,LERS,TOOCZ,ADAMTSIB,TERT CONNIA,EEFLAL,SPATSI,VEGFA MET SLURPI,MYC CONNIA,TSC,MTAP,PTINB PIEN HMSS ARDZ,NESIA,CONNIB		18011.32 19013.2 20013 21011.2 22011.1 822.33 1905.3 2025.3 2025.3 2026.3 4026.3 6025.3 6016.1 6021.3 10015.3 11015.3 11015.3 12013.3 32023.3 32023.3 32023.3 32023.3 32023.3 32023.3 32023.3 32023.3 32023.3 32023.3 32023.3	18q2 19q13 20q13 20q13 22q13 22q13 3q2 4q35 6q1 6q2 7q36 8q24 9q34 10q2 11q2 12q24 13q3 14q32 11q3
#835T #835T #835T #835T #835T #835T #835T #835T #8373T	ch/19 ch/20 ch/21 ch/21 ch/22 ch/21 ch/22 ch/21 ch/22 ch/3 ch/4 ch/4 ch/5 ch/6 ch/6 ch/6 ch/6 ch/6 ch/6 ch/6 ch/6	281462 68379 9825922 1700688 762325 40221 299470 53291 1446602 29951498 105770558 1190666 1190666 206669 206669 206669 206669 206669 2076669 2076669 2076669 2076669 2076669	59089398 62906977 48084500 51319140 104774866 249312472 242841554 197769162 190941704 190941704 190941704 190941704 190941704 190941704 190941704 140941704	10169 4809 2008 4075 2008 4075 6399 18763 14284 11615 7541 8421 6118 269 3314 8937 7440 7635 10613 11140 3375 6506 6503	-1,0731 -1,0721 -1,0721 -1,0665 -1,0738 -1,069 -0,2673 -0,2698 -0,2735 -0,2731	0 0 0 0 0 0 0 0 0 0 0 0 0 0 0 0 0 0 0	KEAPJ, SEPWI, TMEMISO DNAICS DWRICH ZHEFS, CLONS RPSSOAD ARIDARPA 22, COLIAIA ACVEAA, RETAL ZEPMAA, APOB CTNNBLBAPL, POELZ, RETS, SETIOZ AB, SGA, GABRAZ, RRZ APPLIBA, METZ-CLIGAT CDRVIA, EEFFALS, PATS, LYCFA MET SLIRPI, MYC CONNA, TSCJ, MYTAP, PTPNB PTEN HMBS ARIOZ, NESA, COKNIBB BB1 ARIOZ, NESA, COKNIBB BB1 ARIOL, 15C, 2, BAD7		18011.32 19013.20013 20013.200	18q: 19q1: 19q1: 20q1: 20q1: 21q2: 22q1: 3q2 4q3: 6q1: 6q2 6q2 9q3 10q2 11q4 11q2: 11q2: 15q2: 15q2:
#835T #835T #835T #835T #835T #835T #835T #835T #8373T #873T	cht19 cht20 cht21 cht22 cht22 cht22 cht22 cht3 cht3 cht4 cht3 cht6 cht6 cht6 cht6 cht6 cht6 cht7 cht8 cht8 cht9 cht8 cht9 cht1 cht9 cht9 cht9 cht9 cht9 cht9 cht9 cht9	281462 68379 9825922 17006842 2700138 762325 40221 239470 53291 140602 203615 93951488 105770558 1195666 214910 22600 193118 203645 200666 214910 22600 193118 200766 20170666 20170666 20170666 20170666 20170666 20170666	\$9089398 62966277 48084620 531219140 15477486 249512472 24284155 197769162 199647046 1806697559 92231416 105736700 170892714 135893731 146120815 141073870 13881687 10738370 10738370 13881687 10738370 10738370 10738370 10738370 10738370 10738370 10738370 10738370 10738370 10738370 10738370 10738370 10738370 10738370 10738370 10738370 10738370 10738370	10169 2008 2008 4075 6399 18763 11615 7541 6118 421 6118 421 6118 3314 8937 6533 7440 7455 10613 11140 3375 6503 7508	-1,0731 -1,0666 -1,0738 -1,0666 -1,0738 -1,0669 -2,075 -2,075 -2,278 -2,278 -2,278 -2,278 -2,278 -2,278 -2,278 -2,278 -2,278 -2,278 -2,268 -2,	0 0 0 0 0 0 0 0 0 0 0 0 0 0 0 0 0 0 0	HEAPI,SEPNI,TMEMIGO DNAICS DVIKKIA ZWEIS,CLIMS RIPSGOLD ARIDARRIZZ,COLIDAI ACVEZA,NEZIZ,EPHAA,PAPO CTONBO,BARP,DEZ,COLIDAI ACVEZA,NEZIZ,EPHAA,PAPO ALB,GG,GABRAZ,BEZ ATPLOS,METZ,LIGST,DOCKZ,DAMTS19,TERT CDMIA_EETAL,SPATSI,VEGA MET SURPI,MYC CDMIA_ETAL,SPATSI,VEGA MET SURPI,MYC CDMIA_ETAL,SPATSI,VEGA MET SURPI,MYC CDMIA_ETAL,SPATSI,VEGA ARIDZ,MYC CDMIA_ETAL,SPATSI,VEGA MET SURPI,MYC CDMIA_ETAL,SPATSI,VEGA RB1 HMB5 ARIDZ,MYSAC,DOKIBB RB1		1801.132 1902.132 2001.13 2001.13 2001.13 2001.13 2025.3 2025.3 2025.3 2025.3 4016.3 4016.3 4016.3 4016.3 4016.3 1017.3 1	18q. 19q1i 19q1i 20q1i 20q1i Xq2 22q1i Xq2 2q3i 3q2 4q3i 5q3i 6q1 6q2 7q36 8q2/ 10q2 11qi 12q26 13qi 14q3i 15q2 15q2 11qq2
#835T #8373T	ch/19 ch/20 ch/21 ch/21 ch/21 ch/22 ch/21 ch/22 ch/3 ch/1 ch/2 ch/3 ch/4 ch/6 ch/6 ch/6 ch/6 ch/6 ch/6 ch/6 ch/6	281462 68379 9825922 17006842 2700138 763235 40221 239470 53291 140602 201615 93951498 105770542 1199666 2199666 2199666 2199666 20170666 20170666 20170666 20170666 20170666	59089398 62906977 48084510 15119140 15129140 15284515 197799162 197799162 19084704 180687599 92231416 105736700 110802714 1108075 1108	10169 4809 2008 4075 6399 18763 14763 14763 14763 14764 8421 6418 269 3314 6418 10613 3317 6533 11140 3317 6505 6106 5106 5106 5106 5106 5106 5106	-1,0731 -1,0721 -1,0721 -1,0721 -1,0721 -1,0765 -1,0789 -1,0789 -0,2773 -0,2731 -0,273	0 0 0 0 0 0 0 0 0 0 0 0 0 0 0 0 0 0 0	KEAPJ, SEPWI, TMEMISO DNAICS DWKILS ZWEFS, CLONS RIPSGOAS ARIDARPAZ, COLIDAI ACWEAN PERZA, EPHAA, PAPO CTINBI, BAPI, POSTEZ, RES, STOZ AB, FGA, GABRAZ, RIPZ APPUB, MEZC, LIGST, DOCIZ, ADAMTS19, TERT CONIA, EEFIAL, SPATS1, VICEA MET SALIRPI, MYC CONIA, TSC, LATTAP, PTPNB PTEM HMBS ARIOZ, HWEJA, CONIAB RBII ANINI, TSC, ZBRD7 TIPS3		1801.1.2 1901.3 1901.3 20013 21011.2 22013 22013 22011.2 22011.1 8,022.33 1026.3 3026.	18q; 19q13 20q131 21q2; 22q13 Xq2 1q4 2q37 3q2 4q555 5q35 6q1 6q2 10q2; 11q4 11q4 11q4 11q24
#8351 #8351 #8351 #8351 #8351 #8351 #8531 #8731 #8731 #8731 #8731 #8731 #8731 #8731 #8731 #8731 #8731 #8731 #8731 #8731 #8731	cht19 cht20 cht21 cht22 cht22 cht22 cht22 cht3 cht3 cht4 cht3 cht6 cht6 cht6 cht6 cht6 cht6 cht7 cht8 cht8 cht9 cht8 cht9 cht1 cht9 cht9 cht9 cht9 cht9 cht9 cht9 cht9	281462 68379 9825922 17006842 2700138 762325 40221 239470 53291 140602 203615 93951488 105770558 1195666 214910 22600 193118 203645 200666 214910 22600 193118 200766 20170666 20170666 20170666 20170666 20170666 20170666	\$9089398 62966277 48084620 531219140 15477486 249512472 24284155 197769162 199647046 1806697559 92231416 105736700 170892714 135893731 146120815 141073870 13881687 10738370 10738370 13881687 10738370 10738370 10738370 10738370 10738370 10738370 10738370 10738370 10738370 10738370 10738370 10738370 10738370 10738370 10738370 10738370 10738370 10738370	10169 2008 4075 2008 4075 6399 18763 14763 14763 14764 11615 6118 4421 6118 4421 6118 3314 43314 7645 7635 10613 11140 3375 6506 6509 7558 10619 2956	-1,0731 -1,0666 -1,0738 -1,0666 -1,0738 -1,0669 -2,075 -2,075 -2,278 -2,278 -2,278 -2,278 -2,278 -2,278 -2,278 -2,278 -2,278 -2,278 -2,268 -2,	0 0 0 0 0 0 0 0 0 0 0 0 0 0 0 0 0 0 0	KEAPJ,SEPNI,TMEMISO DNAICS DWRICH ZHEFS,CLONS RPSSOAD ARIDARPA2Z,COLIAIA ACVEZA,NETAZ,EPHAA,APOB CTNNBLBAPL,POEIZ,RIFS,SETD2 AB,SGA,GBRAZ,RRZ APPLIBA,METZ-CLIGST,DOCKZ,ADAMTS19,TERT CDRVIA,EEFAALSPATSL,VEGFA MET SLIRPI,MYC CDNVIA,EEFAALSPATSL,VEGFA HOMBS ARIDZ,NESZ,DATTAP,PTRNB PFEN HOMBS ARIDZ,NESZ,DATTAP,PTRNB BB1 RB1 BB1 ARINI,TSCZ,BRD7		1801.132 1902.132 2001.13 2001.13 2001.13 2001.13 2025.3 2025.3 2025.3 2025.3 4016.3 4016.3 4016.3 4016.3 4016.3 1017.3 1	18q2q21 19q1q13q2 20q1q1 22q1q2 22q1q2 2q37 3q2 2q37 3q2 2q37 3q2 4q3 4q3 4q3 4q3 4q3 4q3 4q3 4q3 4q3 4q3
#8351 #8351 #8351 #8351 #8351 #8351 #8531 #8731 #8731 #8731 #8731 #8731 #8731 #8731 #8731 #8731 #8731 #8731 #8731 #8731 #8731	ch/19 ch/20 ch/21 ch/21 ch/21 ch/22 ch/21 ch/22 ch/3 ch/1 ch/2 ch/3 ch/4 ch/6 ch/6 ch/6 ch/6 ch/6 ch/6 ch/6 ch/6	281462 68379 9825922 17006842 2700138 763235 40221 239470 53291 140602 201615 93951498 105770542 1199666 2199666 2199666 2199666 20170666 20170666 20170666 20170666 20170666	59089398 62906977 48084510 15119140 15129140 15284515 197799162 197799162 19084704 180687599 92231416 105736700 110802714 1108075 1108	10169 4809 2008 4075 6399 18763 14763 14763 14763 14764 8421 6418 269 3314 6418 10613 3317 6533 11140 3317 6505 6106 5106 5106 5106 5106 5106 5106	-1,0731 -1,0721 -1,0721 -1,0721 -1,0721 -1,0765 -1,0789 -1,0789 -0,2773 -0,2731 -0,273	0 0 0 0 0 0 0 0 0 0 0 0 0 0 0 0 0 0 0	KEAPJ, SEPWI, TMEMISO DNAICS DWKILS ZWEFS, CLONS RIPSGOAS ARIDARPAZ, COLIDAI ACWEAN PERZA, EPHAA, PAPO CTINBI, BAPI, POSTEZ, RES, STOZ AB, FGA, GABRAZ, RIPZ APPUB, MEZC, LIGST, DOCIZ, ADAMTS19, TERT CONIA, EEFIAL, SPATS1, VICEA MET SALIRPI, MYC CONIA, TSC, LATTAP, PTPNB PTEM HMBS ARIOZ, HWEJA, CONIAB RBII ANINI, TSC, ZBRD7 TIPS3		1801.1.2 1901.3 1901.3 20013 21011.2 22013 22013 22011.2 22011.1 8,022.33 1026.3 3026.	18q2q21 19q1q13q2 20q1q1 22q1q2 22q1q2 2q37 3q2 2q37 4q3 4q3 4q3 4q3 4q3 4q3 4q3 4q3 4q3 4q3
#835T #8373T	ch/19 ch/20 ch/21 ch/21 ch/21 ch/22 ch/21 ch/22 ch/3 ch/4 ch/1 ch/2 ch/3 ch/4 ch/5 ch/6 ch/6 ch/6 ch/6 ch/6 ch/6 ch/6 ch/6	281462 68379 9825922 1700688 763235 40221 239470 53291 146602 209415 19351498 10577058 19351498 10577058 193666 19366 19366 193666 1936	\$9089398 \$9089398 \$0089398 \$0089398 \$0290627 \$4004450 \$1219140 \$1219147	10169 4809 2008 4075 4809 2008 4075 6399 18763 14784 11615 7541 8421 6118 299 33114 8421 1013 1013 3317 6533 11140 3327 6536 10613 1758 10619 1758 1758 1758 1758 1758 1758 1758 1758	-1,0731 -1,0721 -1,0721 -1,0721 -1,0721 -1,0695 -1,0789 -1,069 -0,2773 -0,2773 -0,2773 -0,2773 -0,2773 -0,2773 -0,2783 -0,2689	0 0 0 0 0 0 0 0 0 0 0 0 0 0 0 0 0 0 0	KEAPJ, SEPNI, TIMEMISO DNAICS DWRILD ZNEFS, CLONG RISSONA ARIDARPAZ, COLITAL ACVEZAMERIZ, EPHALA, PAOB CTNB, BLAPL, POST, 22, ELT, SKTD2 ALB, FGA, GABRAZ, RFZ ATPOR, METZ, CLIEST, DOCCZ, ADMITSTS, TERT CDOTIA, EEFIAL, SYNTOS MET SLIRPI, MYC CDENZA, TSCI, MYTAP, PTPN3 PTEN HMBS ARIDZ, NOST, LANTAP, PTPN3 HMBS ARIDZ, NOST, LANTAP, PTPN3 HMBS ARID		1801.1.2 1901.3 20013 21011.2 22011 22011.1 22011.1 22011.1 22011.1 22011.3 2205.3	18q2q2q2q2q2q2q2q2q2q2q2q2q2q2q2q2q2q2q2
#835T #873T	cht/19 cht/20 cht/21 cht/22 cht/22 cht/23 cht/24 cht/25 cht/26 cht/26 cht/26 cht/26 cht/26 cht/26 cht/26 cht/26 cht/26 cht/27 cht/27 cht/27 cht/26 cht/27 cht/27 cht/27 cht/26 cht/27 ch	281462 68379 9825922 17006842 2700138 762325 40221 140602 230415 1995148 105770558 119562 120606 12160040 122600 199116 10570568 10570558 1057058 105	\$9083958 6:296507 48084650 5121510 15477486 2-28212472 2-2881254 197769162 19094704 11062759 9-2231416 100738700 117882714 13581739 144628815 141017488 135418930 11485815 115789733 10738970 115789733 10738970 11578973 1	10169 10069 2008 4075 6399 18763 14784 11615 8421 16118 8421 6118 9937 7541 1140 3314 3315 6533 10613 3375 6536 10619 2596 9716	-1,0731 -1,0761 -1,0761 -1,0765 -1,0768 -1,0768 -1,0768 -1,0768 -1,0769 -0,2678 -0,2778 -0,2778 -0,2778 -0,2778 -0,2778 -0,2778 -0,2778 -0,2778 -0,2778 -0,2778 -0,2778 -0,2778 -0,2778 -0,2661 -0,2661 -0,2778 -0,2661 -0,2778 -0,277	0 0 0 0 0 0 0 0 0 0 0 0 0 0 0 0 0 0 0	KEAPJ, SEPWI, TMEMISO DNAICS DWKILS ZWEFS, CLONS RIPSGOAS ARIDARPAZ, COLIDAI ACWEAN PERZA, EPHAA, PAPO CTINBI, BAPI, POSTEZ, RES, STOZ AB, FGA, GABRAZ, RIPZ APPUB, MEZC, LIGST, DOCIZ, ADAMTS19, TERT CONIA, EEFIAL, SPATS1, VICEA MET SALIRPI, MYC CONIA, TSC, LATTAP, PTPNB PTEM HMBS ARIOZ, HWEJA, CONIAB RBII ANINI, TSC, ZBRD7 TIPS3		1901.1.2 1901.3 1901.3 20013 20013 20013 2001.1 1902.3 2001.1 1902.3 200	18q2421 24q341 19q3431 24q342 24q37 34q35 44q35 64q31 10q22 11q34
#835T #833T	ch/19 ch/20 ch/21 ch/21 ch/21 ch/21 ch/21 ch/21 ch/21 ch/21 ch/3 ch/4 ch/3 ch/4 ch/5 ch/6 ch/6 ch/6 ch/6 ch/6 ch/6 ch/6 ch/6	281462 88379 9825922 1700689 763325 40221 239470 33291 140602 203615 195642 1956666 1956666 19566666 1956666 1956666 1956666 1956666 19566666 19566666 19566666 19566666 19566666 19566666 19566666 195666666 195666	\$9089388 \$2906977 4800450 4800450 114774846 1243712472 124384354 19779162 199041704 190647704 190647704 190647704 114047498 114457491 114457491 114457491 114457491 114457491 1144574	10169 4809 2008 4075 6399 18763 14763 14763 14764 11015 7541 8421 6118 8937 7540 7440 7465 11140 3314 1140 3375 6306 6593 11478 10613 2956 9716 1447 1447	-1,0731 -1,0721 -1,0721 -1,0721 -1,0721 -1,0720 -1,0729 -1,072	0 0 0 0 0 0 0 0 0 0 0 0 0 0 0 0 0 0 0	HEAP1,SEPN1,TMEMISO DNAICS DWRITA ZWRF3,CLIDNS RIPSGOA3 ARIDIARRIZZ,COLIDAI ACVEZA,MEZIZ,EPHAA,APOB CINNBLABER,DEZIZ,ELISSTD2 ALB,TGA,GAGBARZ,BEZ ATPIOR,METZ-C,REST,DOCEZ,ADAMTS19,TERT CORNIA,EEFLAI,SPATSI,VEGA MET SLIRPI,MYC CONRAZ,TSC,LANTAP,PTPN3 PTEN HMB5 ARIDZ,NNB LACONNIB RB1 ARIN,TSCZ,BRD7 TPS3 KEAP1,SEPN1,TMEMISO		1801.1.2 1901.3 20013 21011.2 20013 21011.2 22011.1 22013	18q2421424244444444444444444444444444444
#835T #873T	ch/19 ch/20 ch/21 ch/21 ch/22 ch/21 ch/22 ch/23 ch/21 ch/23 ch/23 ch/21 ch/23 ch/24 ch/25 ch/26 ch/26 ch/27 ch/26 ch/27 ch/26 ch/27 ch/26 ch/27 ch/26 ch/27 ch/27 ch/26 ch/27 ch/27 ch/26 ch/27 ch/27 ch/26 ch/27	281462 68379 9825922 17006842 2700138 762325 40221 1346602 23951498 105770558 1195666 1195666 120666 1206666 120666 120666 1206666 1206666 1206666 1206666 120666 120666 1206666 1206666 12066	59083958 59083958 62906377 4808450 51219140 5	10169 4809 2008 4075 6399 18763 118763 148763 11615 5541 8421 6118 8421 6118 1140 3314 1150 6306 6593 1140 6305 6593 7595 10619 2996 9716 14778	-1,0731 -1,0731 -1,0765 -1,0731 -1,0665 -1,0738 -1,0696 -1,0798 -2,0798 -2,2795 -2,2791 -2,279	0 0 0 0 0 0 0 0 0 0 0 0 0 0 0 0 0 0 0	ELAPI,SEPNI,TMEMISO DINALCS DYRKLA ZNAF3,CLONS RUSSOKS ARIDLARRAZ,COLITAL ACURZA,REZA,ZEPHALAPOB CTNBELBARI-DEIZ,REJS,SETD2 ALB,FGA,GABRAZ,RETAL,STATS ALPIDAM,FCILLERS,TODCZ,ADAMTSIB,TERT CONNIA,EEFLAL,SPATSI,VEGFA MET SLURPI,MYC CONNIA,TSCLA,TATA,PTINS PIEN HMBS ARID,XEPNIA,CONNIB RB1 ARID,XEPNIA,CONNIB ARID,XEPNIA,CONNIB ARID,XEPNI,TMEMISO KEAPI,SEPNI,TMEMISO DNALCS DNALCS DNALCS DNALCS DNALCS	IG, DSCAM,TMPRSSZ, PTTG	1901.1.2 1901.3 20013 20013 20013 20013 20013 20013 20013 20013 20013 20015 3006.3 4016.3 4016.3 4016.3 6021 6021 6021 10015.3 10015.3 10015.3 10015.3 10115.5 10015.3 10115.5	18q242142424242424242424242424242424242424
#835T #835T #835T #835T #835T #835T #835T #873T	ch/19 ch/20 ch/21 ch/21 ch/21 ch/21 ch/21 ch/21 ch/21 ch/21 ch/3 ch/4 ch/3 ch/4 ch/5 ch/6 ch/6 ch/6 ch/6 ch/6 ch/6 ch/6 ch/6	281462 88379 9825922 1700689 763325 40221 239470 33291 140602 203615 195642 1956666 1956666 19566666 1956666 1956666 1956666 1956666 19566666 19566666 19566666 19566666 19566666 19566666 19566666 195666666 195666	\$9089388 \$2906977 4800450 4800450 114774846 1243712472 124384354 19779162 199041704 190647704 190647704 190647704 114047498 114457491 114457491 114457491 114457491 114457491 1144574	10169 4809 2008 4075 6399 18763 14763 14763 14764 11015 7541 8421 6118 8937 7540 7440 7465 11140 3314 1140 3375 6306 6593 11478 10613 2956 9716 1447 1447	-1,0731 -1,0721 -1,0721 -1,0721 -1,0721 -1,0720 -1,0729 -1,072	0 0 0 0 0 0 0 0 0 0 0 0 0 0 0 0 0 0 0	HEAP1,SEPN1,TMEMISO DNAICS DWRITA ZWRF3,CLIDNS RIPSGOA3 ARIDIARRIZZ,COLIDAI ACVEZA,MEZIZ,EPHAA,APOB CINNBLABER,DEZIZ,ELISSTD2 ALB,TGA,GAGBARZ,BEZ ATPIOR,METZ-C,REST,DOCEZ,ADAMTS19,TERT CORNIA,EEFLAI,SPATSI,VEGA MET SLIRPI,MYC CONRAZ,TSC,LANTAP,PTPN3 PTEN HMB5 ARIDZ,NNB LACONNIB RB1 ARIN,TSCZ,BRD7 TPS3 KEAP1,SEPN1,TMEMISO	IG, DSCAN,TMPRSSQ, PTTG1	1801.1.2 1901.3 20013 21011.2 20013 21011.2 22011.1 22013	18q2 19q13 20q13

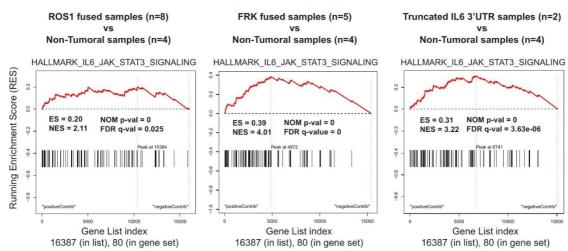
Abbreviations: IL=Gain, Normal, Los LRR=LogR ration

Supplementary Table 6: ROS1 and FRK fusions identified from RNAseq

Sample	Diagnosis	Fus_type	5prim_gen e	chr1	pos1_hg38	3prim_gen e	chr2	pos2_hg38	Supporting _reads	Oncofuse _InFrame	Oncofuse _DRIVER PROB	Oncofuse_3_DOMAINS _RETAINED	Oncofuse_3_DOMAINS _BROKEN
#1439T	HCA	TRANS	PLEKHA5	chr12	19348520	FRK	chr6	115968739	11	Yes	0.99928	Tyrosine-protein kinase, active site[Active_site]	SH2 domain[Domain]
#835T	HCA	TRANS	MIA3	chr1	222660315	FRK	chr6	115968739	58	Yes	0.99928	Tyrosine-protein kinase, active site[Active site]	SH2 domain[Domain]
#222T	HCA	TRANS	MIA2	chr14	39327023	FRK	chr6	115968739	14	Yes	0.981333	Tyrosine-protein kinase, active site[Active_site]	SH2 domain[Domain]
#873T	HCA	TRANS	LMO7	chr13	75853310	FRK	chr6	115968739	25	Yes	0.99928	Tyrosine-protein kinase, active site[Active_site]	SH2 domain[Domain]
#471T	HCA	TRANS	SEC16B	chr1	177936297	FRK	chr6	116060149	9	Yes	0.946629	Tyrosine-protein kinase, active site[Active_site]	Src homology-3 domain[Domain]
#1343T	HCA	TRANS	RBP4	chr10	93600392	ROS1	chr6	117321394	60	Yes	0.911829	Tyrosine-protein kinase, active site[Active_site]	
#1343T	HCA	TRANS	RBP4	chr10	93600392	ROS1	chr6	117324415	205	Yes	0.911829	Tyrosine-protein kinase, active site[Active_site]	Fibronectin, type III[Domain]
#375T	HCA	INV	PLG	chr6	160741418	ROS1	chr6	117324415	284	Yes	0.999594	Tyrosine-protein kinase, active site[Active_site]	Fibronectin, type III[Domain]
#2729T	HCA	INV	PLG	chr6	160718839	ROS1	chr6	117324415	21	Yes	0.996059	Tyrosine-protein kinase, active site[Active_site]	Fibronectin, type III[Domain]
#477T	HCA	TRANS	RBP4	chr10	93593822	ROS1	chr6	117321394	2	Yes	0.911829	Tyrosine-protein kinase, active site[Active_site]	
#744T	HCA	INV	PLG	chr6	160741418	ROS1	chr6	117324415	360	Yes	0.999594	Tyrosine-protein kinase, active site[Active_site]	Fibronectin, type III[Domain]
#533T	HCA	TRANS	APOB	chr2	21040937	ROS1	chr6	117320030	500	Yes	0.911829	Tyrosine-protein kinase, active site[Active_site]	
#533T	HCA	TRANS	APOB	chr2	21040937	ROS1	chr6	117326414	414	Yes	0.911829	Tyrosine-protein kinase, active site[Active site]	Immunoglobulin-like fold[Domain];Fibronectin
#4110T	HCA	INV	PLG	chr6	160741418	ROS1	chr6	117324415	147	Yes	0.999594	Tyrosine-protein kinase, active site[Active_site]	Fibronectin, type III[Domain]
#757T	HCA	INV	PLG	chr6	160741418	ROS1	chr6	117324415	21	Yes	0.999594	Tyrosine-protein kinase, active site[Active_site]	Fibronectin, type III[Domain]

Abbreviations:
HCA-Hepatocellular Adenoma
FRK-Fyn Related Src Family Tyrosine Kinase
RSI-Fyn Related Src Family Tyrosine Kinase
ROSI-ROS Proto-Oncogene 1, Receptor Tyrosine Kinase
PLEKHAS-Pleckstrin Homology Domain Containing A5
MM2-Melanoma Inhibitory Activity 2
MM3-Melanoma Inhibitory Activity 2
LM07=LMN Domain 7
SEC16B-SEC16 Homolog B, Endoplasmic Reticulum Export Factor
RBP4-Retinol Binding Protein 4
PLG- Plasminogen
APOB-Apolipoprotein B
TRANS-Translocation
INV=Inversion

Supplementary Figure 3



2. Annex 2: Supplementary data Article 4

Supplementary Information

Cyclin A2 and E1 genomic alterations define a specific subclass of hepatocellular carcinomas Bayard *et al.*

Supplementary Figures

Supplementary Figure 1. Consequences of viral insertions in CCNA2 gene

Supplementary Figure 2. Deletions associated with CCNA2 deregulation

Supplementary Figure 3. Cyclin E1 overexpression induced by viral insertions and structural rearrangements

Supplementary Figure 4. Mutational signature analysis of CCN-HCC

Supplementary Figure 5. SNP array analysis of focal duplications in CCN-HCC from the TCGA series

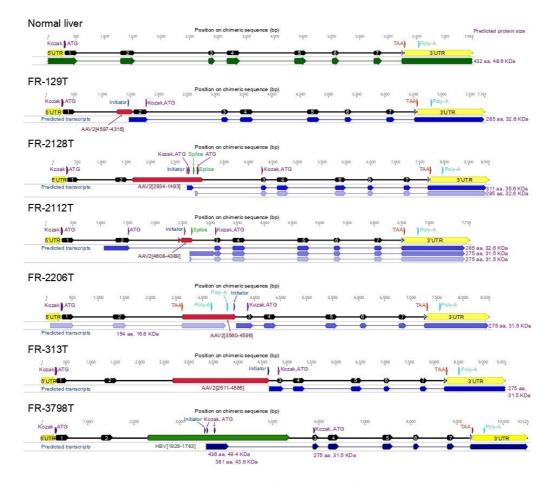
Supplementary Figure 6. Characteristic copy-number profile of CCN-HCC

Supplementary Figure 7. Examples of intra-chromosomal templated insertions and templated insertion cycles involving several chromosomes

Supplementary Figure 8. RS1 breakpoint hotspots involving highly expressed liver enzymes **Supplementary Figure 9.** Binomial regression modeling of rearrangement breakpoint density **Supplementary Figure 10.** Rearrangements affecting *TERT* promoter region in CCN-HCC

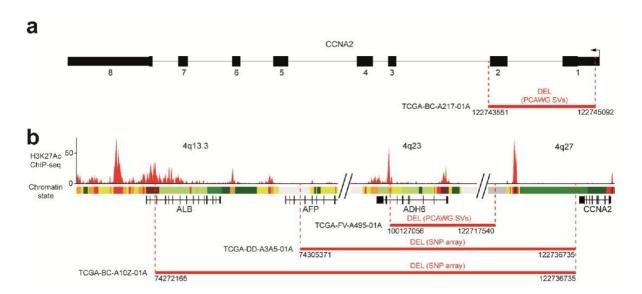
Supplementary Figure 11. Modulation of *TERT* expression by different types of genomic alterations.

Supplementary Figure 12. Rearrangement signatures identified in the pan-cancer series

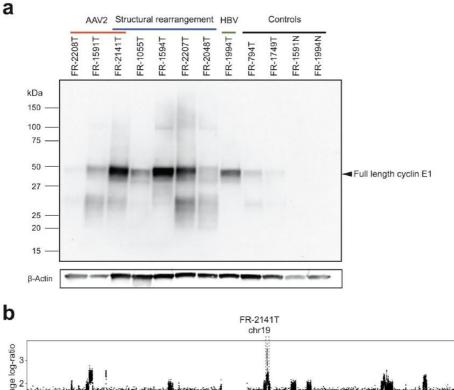


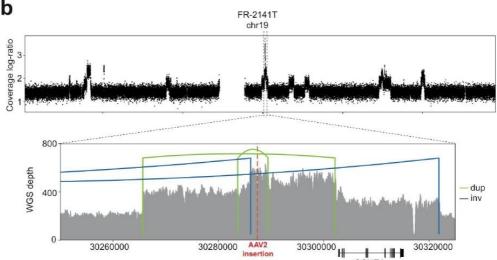
Supplementary Figure 1. Consequences of viral insertions in CCNA2 gene

Five AAV2 and 1 HBV insertions were identified in *CCNA2* in the LICA-FR series. Precise insertion boundaries were identified by WGS or viral capture, and RNA-seq reads were aligned on the chimeric sequence. Here, the different transcripts predicted by Cufflinks are represented for each case, ordered by transcript abundance. Predicted functional elements (Transcription initiator, splice and poly-A sites, Kozak sequence, initiator and terminator codons) are annotated on the chimeric DNA sequence, and the predicted protein sizes resulting from the translation of each transcript are annotated on the right. Only the most abundant abnormal transcripts were represented in **Fig. 1c**.



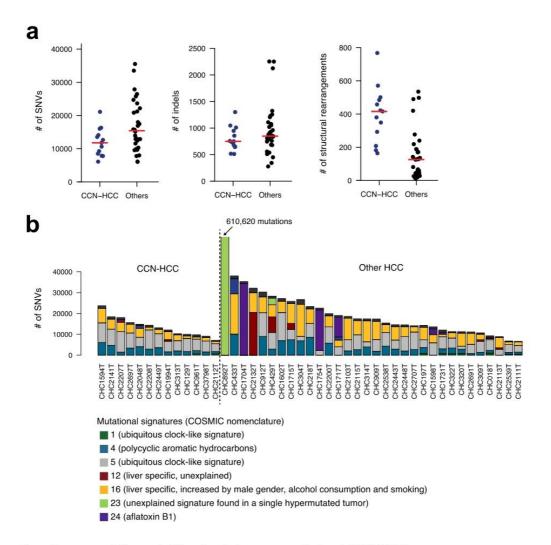
Supplementary Figure 2. Deletions associated with *CCNA2* deregulation a Focal deletion of *CCNA2* exons 1 & 2 identified in TCGA tumor TCGA-BC-A217. b Deletions identified in 3 TCGA tumors linking *CCNA2* downstream region with the highly expressed genes *ALB*, *AFP* and *ADH6*.





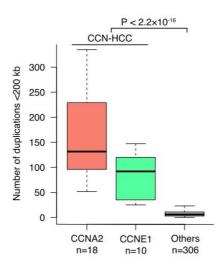
Supplementary Figure 3. Cyclin E1 overexpression induced by viral insertions and structural rearrangements

- **a** Western blot analysis of cyclin E1. Tumors with viral insertions or structural rearrangements are compared with tumors without *CCNE1* alteration and non-tumoral liver controls.
- **b** Tumor FR-2141T displays both an AAV2 insertion in *CCNE1* regulatory region and a high-level amplification of the locus. The top panel displays the coverage log-ratio along chromosome 19 in this tumor. The bottom panel displays the coverage of WGS reads aligned to the chimeric sequence of *CCNE1* locus including AAV2 insertion together with structural rearrangement breakpoints. It shows that the most strongly amplified region includes *CCNE1* regulatory region, and in particular the locus of AAV2 insertion.



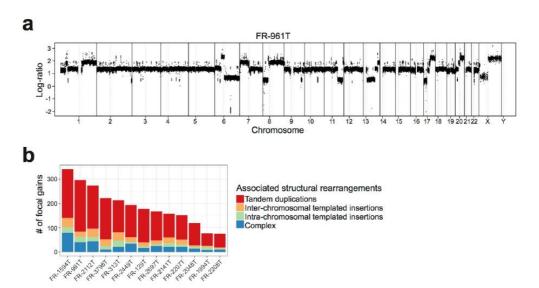
Supplementary Figure 4. Mutational signature analysis of CCN-HCC

a Comparison of the number of single-nucleotide variants (SNVs), indels and structural rearrangements in CCN-HCC vs others (LICA-FR data, 45 WGS). Red line represent median. b Contribution of the different mutational signatures known to be operative in liver cancers to the mutational burden of CCN-HCC and other HCC.



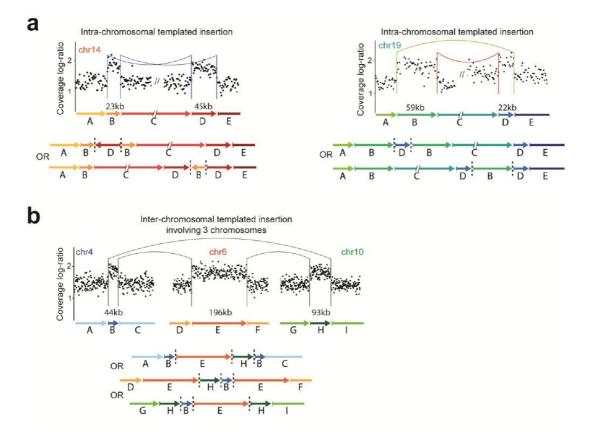
Supplementary Figure 5. SNP array analysis of focal duplications in CCN-HCC from the TCGA series.

Focal deletions (<200 kb) were quantified across 334 tumors from the TCGA series as a surrogate marker of the RS1 signature, and compared between CCNA2-activated, CCNE1-activated and other HCC. The middle bar, median; box, interquartile range; bars extend to 1.5 times the interquartile range.



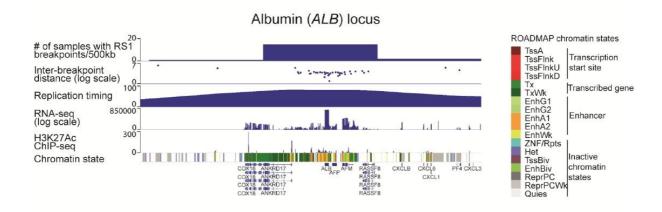
Supplementary Figure 6. Characteristic copy-number profile of CCN-HCC

- **a** Typical copy-number profile of a CCN-HCC, showing hundreds of focal gains scattered throughout the genome.
- **b** Proportion of focal gains in each CCN-HCC attributed to each rearrangement mechanism.

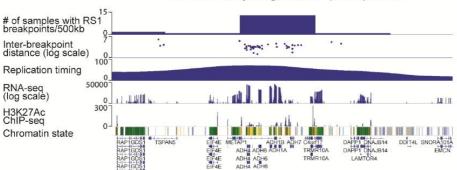


Supplementary Figure 7. Examples of intra-chromosomal templated insertions and inter-chromosomal templated insertion cycles involving several chromosomes

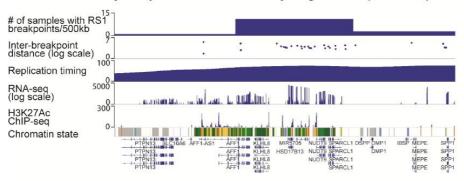
- **a** Intra-chromosomal templated insertions appear as couples of inversions (left) or deletion and duplication (right) depending on the orientation of aberrant junctions.
- **b** Example of inter-chromosomal templated insertion involving 3 different chromosomes.



Alcohol dehydrogenases (ADH) locus

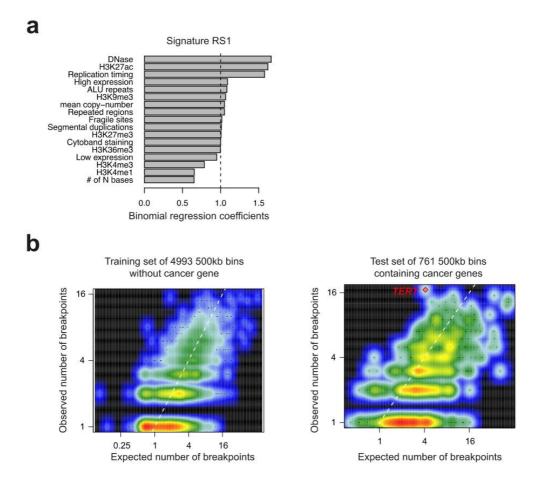


Hydroxysteroid 17-Beta dehydrogenases (HSD17B) locus



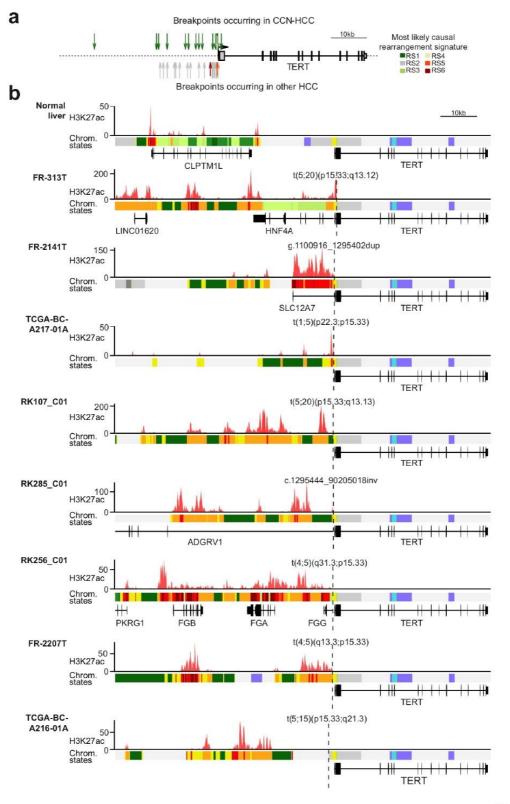
Supplementary Figure 8. RS1 breakpoint hotspots involving highly expressed liver enzymes

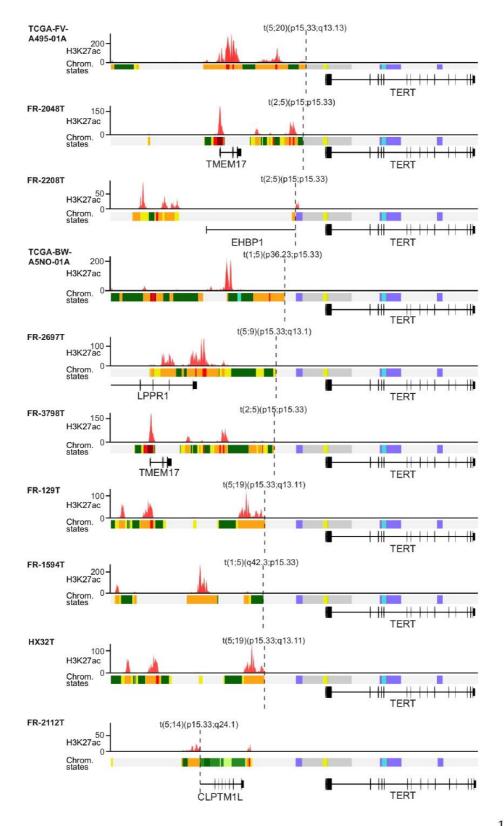
The density of RS1 breakpoints, replication timing, RNA-seq expression, H3K27Ac and ROADMAP chromatin states are displayed for 3 representative hotspots involving the very highly expressed liver enzymes albumin, alcohol dehydrogenases and hydroxysteroid 17-Beta dehydrogenases.



Supplementary Figure 9. Binomial regression modeling of rearrangement breakpoint density a Regression coefficients of the 17 genomic features used to predict the density of signature RS1 breakpoints.

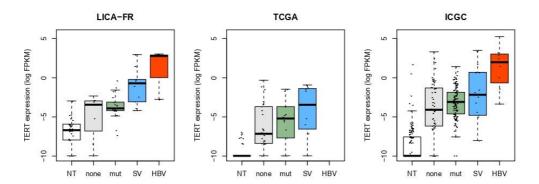
b Correlation between the number of observed RS1 breakpoints per 500 kb bin and the expected number predicted by the binomial regression model. Left: Within 4933 bins without any cancer gene used as training set. Right: Within 761 bins containing cancer genes (test set). The bin corresponding to *TERT* promoter region is highlighted in red.





Supplementary Figure 10. Rearrangements affecting *TERT* promoter region in 350 HCC genomes

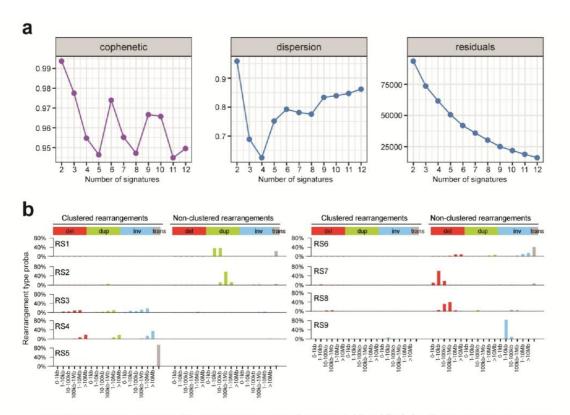
- **a** Summary of rearrangement breakpoints in *TERT* regulatory region. Each arrow indicates a rearrangement breakpoint. The color indicates the rearrangement signature of the most likely causal process. Breakpoints occurring in CCN-HCC are represented above the scheme. Those occurring in other HCC are represented below.
- **b** Functional consequences of structural rearrangements affecting *TERT* regulatory region in CCN-HCC. Chromatin states and H3K27 acetylation in normal adult liver (top) are compared with predicted chromatin states and H3K27 acetylation resulting from the 18 structural rearrangements of *TERT* regulatory regions identified in CCN-HCC. H3K27Ac chromatin immunoprecipitation sequencing (ChIP-seq) signal were obtained from the ROADMAP consortium. The color code of chromatin states is the same as in **Supplementary Fig. 8**



Supplementary Figure 11. Modulation of *TERT* expression by different types of genomic alterations.

The expression of *TERT* is shown in the 3 data sets as a function of the type of alteration identified in *TERT* promoter. Only samples with both whole genome and RNA sequencing were considered. No HBV insertion in *TERT* was identified among the 48 TCGA samples with whole genome sequencing.

NT: non-tumor liver sample; none: HCC without *TERT* alteration identified; mut: HCC with *TERT* promoter mutation; SV: HCC with structural rearrangement affecting *TERT* promoter; HBV: HCC with HBV insertion in *TERT* promoter. The middle bar, median; box, interquartile range; bars extend to 1.5 times the interquartile range.



Supplementary Figure 12. Rearrangement signatures identified in the pan-cancer ICGC series

- a Non-negative matrix factorization (NMF) metrics used to determine the optimal number of signatures. With 9 signatures, we obtain good cophenetic coefficient and dispersion score.
- **b** Frequency of the 38 structural rearrangement categories in the 9 signatures.

Description of Additional Supplementary Files

File Name: Supplementary Table 1

Description: Clinical annotations for the 160 samples of the LICA-FR series

File Name: Supplementary Table 2

Description: Main clinical characteristics of the LICA-FR, TCGA and ICGC-JP cohorts

File Name: Supplementary Table 3

Description: Viral insertions identified at CCNA2 and CCNE1 loci

File Name: Supplementary Table 4

Description: Structural rearrangements identified at CCNA2 and CCNE1 loci

File Name: Supplementary Table 5

Description: Significantly de-regulated pathways in CCN-HCC

File name: Supplementary Table 6

Description: Significantly enriched and depleted driver genes in CCN-HCC

File Name: Supplementary Table 7

Description: Contribution of rearrangement signatures to the genomes of 350 tumors

from the LICA-FR, TCGA and ICGC series

File Name: Supplementary Table 8

Description: Rearrangements affecting TERT promoter region in 350 HCC genomes

File Name: Supplementary Table 9

Description: Number of RS1 events and association with CCNA2/E1 alterations across

cancer types

Supplementary Table 1: Clinical annotations for the 160 samples of the LICA-FR series

Sample	CCNA2/E1 alteration	CCNA2/E1 alteration type	Gender	Age	Alcohol intake	Hepatitis B	Hepatitis C	Metabolic syndrome		Edmons L on grade	argest nodule diameter (mm)	Vascular invasion	Last survival status	Last survival delay (months)
BCB307T BCM257T	None CCNE1	NA AAV2	M M	59 53	no yes	yes no	no no	no no	F4 F4	I-II III-IV	30 30	no no	death from liver cancer death from liver cancer	33 29
BCM269T	None	NA	M	67	no	yes	no	no	F4	III-IV	26	no	death from liver cancer	23
CHC018T	None	NA	F	35	no	yes	no	no	F2-F3	III-IV	170	yes	death from liver cancer	35
CHC051T CHC1010T	None None	NA NA	F F	69 53	no yes	no no	yes no	no no	F4 F0-F1	III-IV III-IV	60 100	no no	death from liver cancer alive without relapse	54 56
CHC1040T		NA NA	M	73	yes	no	no	no	F2-F3	III-IV	160	yes	alive with relapse	36
CHC1041T		NA	M	69	no	no	no	no	F0-F1	I-II	100	no	alive without relapse	36
CHC1052T		NA	M	75 74	yes	no	no	no	F2-F3	III-IV	130	yes	alive without relapse	1
CHC1053T CHC1055T	None CCNE1	NA amplification	M M	68	yes yes	no no	no no	no no	F4 F2-F3	III-IV III-IV	35 200	yes yes	death from liver cancer death from liver cancer	20 6
CHC1061T		NA	F	79	no	no	no	yes	F0-F1	I-II	150	yes	alive with relapse	40
CHC1137T		NA	M	57	no	no	yes	no	F4	III-IV	60	yes	death from other etiology	8
CHC1148T CHC1180T	None	NA NA	M M	69 65	yes	no	no	no	F0-F1 F2-F3	I-II	90 30	yes	death from liver cancer alive without relapse	15 89
CHC1180T		NA NA	M	60	yes no	no no	no no	no no	F2-F3	I-II I-II	180	no no	death from liver cancer	49
CHC1185T	None	NA	M	53	yes	yes	no	no	F4	III-IV	30	no	alive without relapse	92
CHC1207T		NA	M	60	yes	no	no	no	F0-F1	1-11	210	yes	alive without relapse	66
CHC1208T CHC1210T		NA NA	M F	47 44	no no	yes yes	no no	no no	F4 F2-F3	III-IV III-IV	60 70	yes no	death from liver cancer alive without relapse	11 23
CHC1211T		NA NA	F	32	no	yes	no	no	F0-F1	III-IV	130	no	alive without relapse	82
CHC121T	None	NA	M	67	yes	no	no	yes	F0-F1	1-11	120	no	death from other etiology	110
CHC129T	CCNA2	AAV2	F	62	no	no	no	no	F0-F1	I-II	130	yes	death from liver cancer	5
CHC1530T CHC1534T	None None	NA NA	M M	64 67	yes yes	yes no	no no	no no	F2-F3 F2-F3	III-IV III-IV	75 55	yes no	death from liver cancer alive without relapse	16 53
CHC1539T		NA NA	M	45	no	no	yes	no	F4	III-IV	32	yes	alive without relapse	59
CHC1545T	None	NA	M	77	yes	no	yes	no	F4	1-11	40	no	death from liver cancer	37
CHC1548T		NA	М	55	no	yes	no	no	F4	III-IV	25	no	alive without relapse	87
CHC1568T CHC1594T		NA Pearrangement regulatory region	M F	71 76	no	yes	no	no	F4 F0-F1	III-IV	30 100	yes	death from other etiology death from other etiology	45 25
CHC15941		Rearrangement regulatory region NA	F	76 76	yes no	no yes	no no	no no	F0-F1	I-II III-IV	90	yes yes	alive without relapse	61
CHC1602T		NA.	M	71	no	no	no	no	F0-F1	1-11	75	yes	death	88
CHC1600T		NA	M	69	yes	no	no	no	F0-F1	I-II	80	yes	alive without relapse	66
CHC1704T		NA	М	43	no	yes	no	no	F2-F3	III-IV	140	yes	alive without relapse	34
CHC1603T CHC1604T		NA NA	M M	78 57	yes	no	no	no	F4 F2-F3	III-IV III-IV	50 18	yes	death from liver cancer alive with relapse	14 67
CHC16041	None None	NA NA	F	77	no no	no no	no yes	no no	F4	III-IV	100	no no	death from liver cancer	46
CHC1626T		NA	M	75	yes	no	no	yes	F0-F1	III-IV	100	yes	death from liver cancer	51
CHC1629T		NA	M	64	yes	no	no	no	F0-F1	1-11	70	yes	death	69
CHC1715T		NA NA	M	72	yes	no	no	no	F0-F1	1-11	60	no	alive without relapse	69
CHC1717T CHC1731T		NA NA	M F	50 55	no no	yes no	no no	no no	F4 F0-F1	I-II I-II	55 110	yes no	alive with relapse alive without relapse	25 21
CHC1725T		NA	F	83	no	no	yes	no	F2-F3	1-11	60	yes	alive without relapse	11
CHC1754T	None	NA	M	34	no	yes	no	no	F2-F3	III-IV	170	yes	death from liver cancer	5
CHC1732T		NA	M	49	yes	no	yes	no	F4	III-IV	60	yes	death from liver cancer	10
CHC1736T CHC1737T		NA NA	M M	58 73	no no	yes no	no no	no yes	F4 F2-F3	III-IV III-IV	45 32	yes no	death from liver cancer alive with relapse	3 61
CHC1737T		NA NA	M	55	yes	no	no	yes	F4	III-IV	50	no	death from other etiology	19
CHC1741T		NA	M	57	yes	no	no	no	F4	1-11	32	no	alive with relapse	60
CHC1742T	None	NA	M	67	no	no	no	no	F0-F1	III-IV	33	yes	death from liver cancer	17
CHC1744T CHC1745T		NA NA	M F	50 69	no no	yes no	yes yes	no yes	F4 F4	III-IV III-IV	70 60	yes yes	death from liver cancer death from other etiology	28 14
CHC1745T		NA NA	M	75	no	no	no	no	F2-F3	III-IV	40	yes	alive with relapse	65
CHC1747T		NA	M	54	yes	no	yes	no	F4	III-IV	40	yes	death from liver cancer	27
CHC1749T		NA	M	66	no	yes	no	no	F0-F1	III-IV	150	yes	alive without relapse	12
CHC1753T CHC197T	None None	NA NA	M M	65 73	no yes	no no	yes no	no no	F2-F3 F2-F3	III-IV III-IV	25 130	no yes	alive with relapse alive with relapse	112 68
CHC1756T	None	NA NA	M	73	yes	yes	no	no	F4	III-IV	45	yes	alive with relapse	144
CHC1757T		NA	M	41	yes	no	no	yes	F4	I-II	12	no	alive without relapse	66
CHC1763T		NA	М	75	yes	no	no	yes	F0-F1	III-IV	60	no	death from other etiology	21
CHC1994T		HBV	M	57	no	yes	no	no	F0-F1	III-IV	190	yes	alive with relapse	52
CHC2048T CHC2043T		Rearrangement regulatory region NA	M F	65 21	yes no	no no	no no	no no	F0-F1 F0-F1	III-IV III-IV	100 50	yes no	death from liver cancer alive without relapse	21 67
CHC2103T		NA	M	57	yes	no	yes	no	F0-F1	III-IV	28	yes	death	49
CHC2111T		NA	F	56	no	no	no	no	F0-F1	1-11	60	no	alive without relapse	61
CHC2112T CHC2128T		AAV2	F F	48 53	no	no	no	yes	F0-F1	III-IV	190	yes	death from other etiology	13 45
CHC21281 CHC2113T		AAV2 NA	M	53 61	no yes	no no	no no	yes no	F0-F1 F0-F1	I-II III-IV	200 90	yes no	alive without relapse death from other etiology	45 57
CHC2115T		NA NA	M	75	yes	no	no	yes	F0-F1	III-IV	100	yes	death from liver cancer	17
CHC2206T	CCNA2	AAV2	M	90	no	no	no	no	F0-F1	III-IV	40	no	alive without relapse	41
CHC2132T		NA NA	M	57	no	no	no	yes	F0-F1	III-IV	180	no	alive without relapse	51
CHC2135T CHC2141T		NA AAV2	F M	57 74	yes	yes no	no no	yes no	F0-F1 F2-F3	III-IV III-IV	25 65	no no	death death	36 16
CHC21411	None	NA	M	69	yes no	no no	no no	no yes	F2-F3 F0-F1	III-IV III-IV	130	no yes	death death from liver cancer	2
CHC2200T		NA	M	69	no	no	no	yes	F0-F1	III-IV	110	yes	alive with relapse	40
CHC1591T		AAV2	М	60	no	no	no	yes	F0-F1	III-IV	120	yes	death from liver cancer	46
CHC2207T		Rearrangement regulatory region	M	49	no	no	no	no	F0-F1	III-IV	90	yes	alive with relapse alive without relapse	51
CHC2208T CHC2210T		AAV2 NA	M M	53 66	no no	no no	no no	no yes	F0-F1 F0-F1	III-IV III-IV	20 50	no yes	alive without relapse death	31 43
CHC2415T		NA NA	M	68	no	no	no	yes	F0-F1	III-IV	180	yes	alive without relapse	36
CHC2443T	None	NA	M	74	yes	no	no	yes	F0-F1	III-IV	48	yes	death	24
CHC2448T		NA fusion	M	82	no	no	no	yes	F0-F1	I-II	75	yes	death from other etiology	
CHC2449T CHC2491T		fusion NA	M M	81 66	no yes	no	no no	yes no	F0-F1 F4	III-IV III-IV	90 30	no	alive with relapse death from other etiology	45 86
CHC24911 CHC2538T		NA NA	F	76	yes no	no no	no no	no yes	F2-F3	III-IV I-II	30 40	yes no	alive with relapse	86 37
CHC2539T		NA NA	F	41	no	no	no	no	F0-F1	III-IV	160	yes	alive with relapse	35
CHC253T	None	NA	M	67	no	no	no	yes	F4	III-IV	80	yes	death from other etiology	0
		NA	М	70	yes	no	no	yes	F0-F1	1-11	30	no	alive with relapse	34
	None	NA	M	74 52	no no	no no	no no	yes no	F0-F1 F0-F1	I-II III-IV	70 110	no	alive without relapse alive without relapse	28 NA
CHC2560T		N/A												
CHC2560T CHC2686T	None	NA NA	F M									yes ves		
	None None	NA NA NA	M M	76 68	no yes	no no	no no	yes yes	F0-F1 F0-F1	III-IV III-IV	120 60	yes no	NA NA	NA NA
CHC2560T CHC2686T CHC2687T	None None None	NA	M	76	no	no	no	yes	F0-F1	III-IV	120	yes	NA	NA

Sample	CCNA2/E1 alteration	CCNA2/E1 alteration type	Gender	Age	Alcohol intake	Hepatitis B	Hepatitis C	Metabolic syndrome	Fibrosis stage	Edmons on grade	Largest nodule diameter (mm)	Vascular invasion	Last survival status	Last survival delay (months)
CHC2706T	None	NA	М	70	yes	no	no	no	F4	III-IV	50	yes	alive with relapse	35
CHC2707T	None	NA	M	79	no	no	no	no	F0-F1	1-11	30	yes	alive without relapse	33
CHC2844T	None	NA NA	M	55	no	no	no	no	F0-F1	1-11	120	yes	alive without relapse	21
CHC2899T CHC3029T	None None	NA NA	M F	52 54	no no	no no	yes	no no	F4 F4	III-IV III-IV	62 70	yes	alive with relapse alive with relapse	30 26
CHC30231	None	NA NA	M	72	no	no	yes yes	no	F2-F3	I-II	45	yes no	alive without relapse	66
CHC304T	None	NA NA	M	77	yes	no	no	no	F0-F1	III-IV	180	ves	death from liver cancer	22
CHC306T	None	NA	M	68	no	no	yes	no	F4	I-II	20	no	alive without relapse	65
CHC309T	None	NA	F	69	no	no	yes	no	F2-F3	III-IV	20	yes	death from other etiology	2
CHC313T	CCNA2	AAV2	F	43	no	no	yes	no	F0-F1	III-IV	130	yes	death from liver cancer	11
CHC314T	None	NA	M	71	yes	no	yes	no	F2-F3	1-11	45	no	alive without relapse	60
CHC320T	None	NA	M	65	yes	no	yes	no	F4	III-IV	35	no	death from other etiology	1
CHC322T	None	NA	M	74	yes	no	no	no	F4	III-IV	40	no	death from liver cancer	21
CHC3238T	None	NA	F	58	no	no	no	no	F0-F1	III-IV	160	no	death from liver cancer	7
CHC327T	None	NA	M	63	no	no	yes	no	F4	1-11	25	no	death from other etiology $% \label{eq:control_eq} % \label{eq:control_eq}$	5
CHC3618T	None	NA	M	53	no	yes	no	no	F0-F1	III-IV	130	no	death from liver cancer	1
CHC3619T	None	NA	M	66	no	no	yes	no	F4	1-11	50	yes	death from liver cancer	15
CHC3620T	None	NA	М	35	no	yes	no	no	F4	III-IV	40	yes	alive	15
CHC3621T	None	NA	M	55	yes	no	no	no	F4	III-IV	60	yes	alive	11
CHC3624T	None	NA NA	M	64	no	no	no	no	F4 F4	III-IV	60	no	alive	21 7
CHC3626T	None	NA NA	M	82	yes	no	no	no		I-II	160	no	death from liver cancer	
CHC3627T CHC3628T	None None	NA NA	M M	55 86	no no	no no	yes no	no	F4 F4	I-II I-II	63 20	no no	death from liver cancer alive	20 24
CHC36281	None	NA NA	M	85	yes	no	no	yes no	F0-F1	I-II	130	no	death from liver cancer	24
CHC3633T	None	NA NA	M	70	yes	no	no	yes	F4	III-IV	110	yes	death from liver cancer	1
CHC3638T	None	NA NA	M	84	no	no	no	yes	F0-F1	III-IV	65	no	alive	28
CHC3641T	CCNE1	AAV2	M	47	no	no	no	yes	F0-F1	1-11	140	no	alive	29
CHC3643T	None	NA NA	M	53	no	yes	no	no	F0-F1	III-IV	200	no	death from liver cancer	9
CHC3644T	None	NA	М	50	yes	no	no	no	F4	III-IV	100	yes	NA	NA
CHC3647T	None	NA	M	56	no	no	yes	no	F4	III-IV	50	yes	death from other etiology	11
CHC3650T	None	NA	F	67	no	no	yes	no	F4	III-IV	110	no	death from liver cancer	1
CHC3716T	None	NA	F	53	no	no	yes	no	F4	III-IV	20	no	death from liver cancer	4
CHC3788T	None	NA	M	58	no	yes	no	no	F4	III-IV	28	yes	alive with relapse	16
CHC3798T	CCNA2	HBV	F	51	no	yes	no	no	F2-F3	III-IV	120	yes	NA	NA
CHC3825T	None	NA	M	74	no	yes	no	no	F2-F3	III-IV	43	yes	NA	NA
CHC3864T	None	NA	M	69	yes	no	no	no	F4	1-11	32	no	alive without relapse	13
CHC3880T	CCNA2	fusion	F	32	no	no	no	no	F0-F1	NA	80	yes	death from liver cancer	34
CHC3894T	None	NA	M	56	yes	no	no	no	F0-F1	III-IV	160	yes	alive	69
CHC3914T	None	NA	M	68	no	yes	no	no	F4	NA	40	no	alive	10
CHC4041T	None	NA	F	64	no	no	yes	no	F2-F3	III-IV	120	yes	death from liver cancer	0
CHC4042T CHC4043T	None None	NA NA	F M	58 72	no no	no no	no no	no	F0-F1 F0-F1	I-II III-IV	80 50	no no	death from liver cancer alive	4 11
CHC40451	None	NA NA	M	58	yes	no	no	yes yes	F2-F3	III-IV	90	no	death from liver cancer	8
CHC4049T	None	NA NA	M	42	no	yes	no	no	F4	III-IV	25	yes	alive	22
CHC40431	None	NA NA	M	72	ves	no	no	no	F0-F1	III-IV	190	no	death from liver cancer	8
CHC4055T	None	NA NA	M	62	no	no	yes	no	F4	1-11	35	yes	death from liver cancer	38
CHC429T	None	NA	F	64	no	no	no	no	FO-F1	III-IV	45	yes	alive with relapse	65
CHC432T	None	NA	M	70	yes	no	no	no	F2-F3	1-11	70	yes	death from liver cancer	34
CHC433T	None	NA	M	70	yes	no	no	yes	F0-F1	1-11	180	yes	death from liver cancer	16
CHC609T	None	NA	M	60	yes	yes	no	yes	F2-F3	III-IV	50	yes	alive with relapse	50
CHC614T	None	NA	M	61	no	no	no	yes	F0-F1	III-IV	30	yes	death from other etiology	12
CHC736T	None	NA	M	77	no	yes	no	no	F0-F1	III-IV	160	yes	alive without relapse	61
CHC793T	None	NA	M	61	no	no	no	no	F0-F1	III-IV	80	yes	death from liver cancer	37
CHC794T	None	NA	M	73	no	no	no	no	F0-F1	III-IV	160	yes	death from liver cancer	6
CHC796T	None	NA	M	76	yes	no	no	no	F2-F3	1-11	48	no	alive without relapse	31
CHC884T	None	NA	М	75	yes	no	no	no	F2-F3	III-IV	130	yes	alive without relapse	54
CHC889T	None	NA	M	71	no	no	no	yes	F2-F3	1-11	85	yes	death from other etiology	1
CHC891T	None	NA NA	F	73	no	no	no	no	F4	III-IV	45	yes	death from liver cancer	17
CHC892T	None	NA NA	F	72	no	no	no	no	F0-F1	1-11	55	no	alive with relapse	49
CHC898T	None	NA NA	M M	71 41	no	no	no	no	F2-F3 F4	III-IV I-II	80 17	yes	death from liver cancer	47
CHC900T	None	NA NA			yes	no	yes	no				no	alive without relapse	110
CHC909T	None None	NA NA	M M	70 78	no	no no	no	no no	F0-F1 F0-F1	III-IV III-IV	210 60	yes ves	alive without relapse death from liver cancer	37 26
		INA	IVI	78	yes	110	yes	110	ru-r1	III-IV	UU	yes	ueath from liver cancer	20
CHC912T CHC961T	CCNA2	fusion	М	57	yes	no	no	no	F0-F1	III-IV	190	ves	death from liver cancer	17

Supplementary Table 2: Main clinical characteristics of the LICA-FR, TCGA and ICGC-JP cohorts. For each clinical characteristic, % are given as proportion of samples with available data.

	LICA-FR	COHORT	(n=160)
--	---------	--------	---------

Age	Median [range]	66 [21-94]
Gender	M	126 (79%)
	F	34 (21%)
Etiology	Alcohol	63 (39%)
	Metabolic disease	37 (23%)
	HCV	30 (19%)
	HBV	30 (19%)
Largest nodule diameter (mm)	Median [range]	67 [12-210]
Fibrosis (METAVIR score)	F0-F1	75 (47%)
	F2-F3	32 (20%)
	F4	53 (33%)
Edmonson grade	1-11	48 (30%)
	III-IV	110 (70%)
	Not determined	2
Vascular invasion	yes	93 (58%)
	no	67 (42%)

TCGA COHORT (n=334)

Age	Median [range]	61 [16-90]
Gender	M	224 (67%)
	F	110 (33%)
Etiology	Alcohol	106 (32%)
	NAFLD*	19 (6%)
	HCV	52 (16%)
	HBV	86 (26%)
Fibrosis (Ishak score)	0 - No Fibrosis	85 (36%)
	1,2 - Portal Fibrosis	35 (15%)
	3,4 - Fibrous Speta	28 (12%)
	5 - Nodular Formation and Incomplete Cirrhosis	9 (4%)
	6 - Established Cirrhosis	78 (33%)
	Not determined	99
Histological grade	G1	50 (15%)
	G2	160 (48%)
	G3	113 (34%)
	G4	7 (2%)
	Not determined	4
Vascular invasion	Macro	14 (5%)
	Micro	80 (29%)
	None	186 (66%)
	Not determined	54

^{*}NAFLD: Non-Alcoholic Fatty Liver Disease

ICGC-JP COHORT (n=257)

Age	Median [range]	68 [31-86]
Gender	M	196 (76%)
	F	61 (24%)
Etiology	Alcohol (>60g per day)	33 (14%)
	HCV	147 (57%)
	HBV	76 (30%)
Tumor size (mm)	Median [range]	30 [8-300]
Liver fibrosis (New Inuyama Classification)	0	11 (4%)
	1	28 (11%)
	1-2	12 (5%)
	2	53 (21%)
	3	61 (24%)
	4	92 (36%)
Edmonson grade	I	21 (8%)
	I-II	11 (4%)
	П	149 (58%)
	II-III	43 (17%)
	III	30 (12%)
	IV	2 (1%)
	Not determined	1
Vascular invasion	yes	86 (34%)
	no	169 (66%)
	Not determined	2

Supplementary Table 3: Viral insertions identified at CCNA2 and CCNE1 loci.

Suj	ķΙ)1(eı	110	eı	11	d	Гу	<u> </u>	ld	l	16	•) :	V	П	dl	1.	118	se	ľ	.1()[]
Published/new	Nault <i>et al.</i> 2015	new	new	new	new	new	Fujimoto et al., 2016	new	Nault <i>et al.</i> 2015	Nault <i>et al.</i> 2015	Nault <i>et al.</i> 2015	new	new	new	new	new	TCGA, 2017	new	Fujimoto et al., 2016	Fujimoto et al., 2016			
Data used to map breakpoints	Viral catpure	Viral catpure	Viral catpure	Viral catpure	WGS	WES	RNA-seq	WES	RNA-seq	WGS	WGS	Viral catpure	Viral catpure	Viral catpure	WES	WES	WGS	WES	RNA-seq	RNA-seq	RNA-seq	WGS	WGS
Breakpoint 2 on viral genome	4585	4389	1493	4596	4597	QN	QN	4586	QN	1639	1783	4598	4379	4237	QN	4590	2849	QN	QN	ND	ND	1808	4600
Breakpoint 1 on viral genome	2611	4608	2934	3560	4316	4613	3412	4064	1807	1817	1928	4340	4599	4604	4239	4253	1674	4626	885	2453;2477;3024*	1830	2040	4386
Breakpoint 2 on human genome (hg19)	chr4:122,742,409	chr4:122,742,667	chr4:122,743,452	chr4:122,742,456	chr4:122,743,844	ND	ND	chr4:122,743,742	ND	chr4:122,742,581	chr4:122,742,755	chr19:30,303,053	chr19:30,287,316	chr19:30,304,542	ND	chr19:30,303,740	chr19:30,291,287	ND	ND	ND	ND	chr19:30,305,243	chr19:30,304,511
Breakpoint 1 on human genome (hg19)	chr4:122,742,417	chr4:122,742,660	chr4:122,743,475	chr4:122,742,478	chr4:122,743,835	chr4:122,743,570	chr4:122,742,400	chr4:122,743,756	chr4:122,743,189	chr4:122,742,221	chr4:122,742,792	chr19:30,303,035	chr19:30,287,313	chr19:30,304,532	chr19:30,291,515	chr19:30,303,743	chr19:30,291,247	chr19:30,302,891	chr19:30,300,450	chr19:30,303,439	chr19:30,302,064	chr19:30,304,909	chr19:30,304,517
Virus	AAV2	AAV2	AAV2	AAV2	AAV2	AAV2	AAV2	AAV2	HBV	HBV	HBV	AAV2	AAV2	AAV2	AAV2	AAV2	HBV	AAV2	HBV	HBV	HBV	HBV	AAV2
Human target gene	CCNA2	CCNA2	CCNA2	CCNA2	CCNA2	CCNA2	CCNA2	CCNA2	CCNA2	CCNA2	CCNA2	CCNE1	CCNE1	CCNE1	CCNE1	CCNE1	CCNE1	CCNE1	CCNE1	CCNE1	CCNE1	CCNE1	CCNE1
Sample	CHC313T	CHC2112T	CHC2128T	CHC2206T	CHC129T	TCGA-G3-AAUZ	TCGA-ZS-A9CF	TCGA-BC-A10Y	TCGA-DD-AADF	RK107	CHC3798T	CHC1591T	CHC2141T	CHC2208T	CHC3641T	BCM257T	CHC1994T	TCGA-BC-A10T	TCGA-DD-AACV	TCGA-ED-A7XO	TCGA-DD-AADV	RK256	HX032
Series	LiC1162	LiC1162	LIC1162	LiC1162	LiC1162	TCGA	TCGA	TCGA	TCGA	ICGC-JP	LiC1162	LiC1162	LiC1162	LiC1162	LiC1162	LiC1162	LiC1162	TCGA	TCGA	TCGA	TCGA	ICGC-JP	ICGC-JP

ND: Not determined

* The HBV insertion in TCGA-ED-A7XO was identified by RNA-seq. Junctions were found between chr19:30,303,439 and 3 different positions on the virus, corresponding to different splicing sites.

$\textbf{Supplementary Table 4}: \textbf{Structural rearrangements identified at CCNA2 and CCNE1} \ \textbf{loci.}$

Detail	deletion of exons 1 & 2	TET2-CCNA2 fusion	TET2-CCNA2 fusion	SNX29-CCNA2 fusion	GSTCD-CCNA2 fusion	LIPC-CCNA2 fusion	UBA6-CCNA2 fusion	KIAA1109-CCNA2 fusion	KIAA1109-CCNA2 fusion	KIAA1109-CCNA2 fusion	FAM160A1-CCNA2 fusion	TDO2-CCNA2 fusion	ANXAS-CCNA2 fusion	deletion linking ALB with the intergenic region in 3' of CCNA2	deletion linking AFP with the intergenic region in 3' of CCNA2	deletion linking ADH6 with the intergenic region in 3' of CCNA2	high-level amplification of the whole CCNE1 locus	rearrangement bringing enhancers of the RAPH1 region in CCNE1 regulatory region	CCNE1 promoter translocation with ERRF11	rearrangement bringing distal enhancers in CCNE1 regulatory region	rearrangement of regulatory region rearrangement bringing enhancers of the CYB5A region in CCNE1 regulatory region
Functional consequence	intragenic deletion	gene fusion	gene fusion	gene fusion	gene fusion	gene fusion	gene fusion	gene fusion	gene fusion	gene fusion	gene fusion	gene fusion	gene fusion	rearrangement of regulatory region	rearrangement of regulatory region	rearrangement of regulatory region	high-level amplification	rearrangement of regulatory region	rearrangement of regulatory region	rearrangement of regulatory region	rearrangement of regulatory region
Data used to map breakpoints	WGS	WGS	RNAseq	WGS	WGS	RNAseq	RNAseq	RNAseq	RNAseq	WGS	RNAseq	WGS	WGS	SNP	SNP	WGS	WES	WGS	WGS	WGS	WGS
Breakpoint 2	chr4:122745092	chr4:106090217	chr4:106068135	chr16:12307494	chr4:106634881	chr15:58703017	chr4:68566767	chr4:123075267	chr4:123075267	chr4:123091320	chr4:152403800	chr4:156815968	chr4:122617787	chr4:74272165	chr4:74305371	chr4:100065889	chr19:30314622	chr2:204506174	chr1:8076609	chr8:9176252	chr18:71877647
Breakpoint 1	chr4:122743551	chr4:122742941	chr4:122742245	chr4:122743069	chr4:122743077	chr4:122742245	chr4:122742245	chr4:122742245	chr4:122742245	chr4:122743197	chr4:122742245	chr4:122743078	chr4:122743507	chr4:122736735	chr4:122736735	chr4:122755879	chr19:30303894	chr19:30268298	chr19:30276189	chr19:30276809	chr19:30300307
Type of rearrangement	deletion	inversion	inversion*	inter-chromosomal translocation	inversion	inter-chromosomal translocation*	tandem duplication*	inversion*	inversion*	inversion	inversion*	inversion	tandem duplication	deletion	deletion	deletion	amplification	inter-chromosomal translocation	inter-chromosomal translocation	inter-chromosomal translocation	inter-chromosomal translocation
Gene	CCNA2	CCNA2	CCNA2	CCNA2	CCNA2	CCNA2	CCNA2	CCNA2	CCNA2	CCNA2	CCNA2	CCNA2	CCNA2	CCNA2	CCNA2	CCNA2	CCNE1	CCNE1	CCNE1	CCNE1	CCNE1
Sample	TCGA-BC-A217	CHC2449T	CHC3880T	CHC2697T	CHC961T	TCGA-GJ-A6C0	TCGA-DD-A3A5	TCGA-DD-A1EK	TCGA-CC-5263	TCGA-PD-A5DF	TCGA-BC-A3KG	TCGA-BC-A216	RK285	TCGA-BC-A10Z	TCGA-XR-A8TG	TCGA-FV-A495	CHC1055T	CHC2207T	CHC2048T	TCGA-BW-A5NO	CHC1594T
Series	TCGA	LIC1162	LIC1162	LiC1162	LiC1162	TCGA	TCGA	TCGA	TCGA	TCGA	TCGA	TCGA	ICGC-JP	TCGA	TCGA	TCGA	LIC1162	LiC1162	LiC1162	TCGA	LiC1162

For rearrangements identified only at the transcript level only (RNA-seq data), breakpoint locations correspond to exon boundaries on each side of the junction, and the most likely types of rearrangement were deduced from the location and orientation of gene partners.

Supplementary Table 5: Significantly de-regulated pathways in CCN-HCC.

UP-REGULATED PATHWATS							
Gene cet	Gene set tyne	Gene set size	Normalized enrichment score	Normalized	FDR q-value	FDR q-value	Description
	244		UCA-FR	TCGA	UCA-FR	TCGA	roadingo.
HALLMARK_E2F_TARGETS	Hallmark	197	6,0755	7,5188	0	0	Genes encoding cell cycle related targets of E2F transcription factors.
HALLMARK_G2M_CHECKPOINT	Hallmark	195	5,4502	6,1559	0	0	Genes involved in the G2/M checkpoint, as in progression through the cell division cycle.
REACTOME_CELL_CYCLE	REACTOME	386	5,0887	5,7322	0	0	Genes involved in Cell Cycle
REACTOME_CELL_CYCLE_MITOTIC	REACTOME	302	4,7241	5,6609	0	0	Genes involved in Cell Cycle, Mitotic
REACTOME_GENERIC_TRANSCRIPTION_PATHWAY	REACTOME	333	4,4213	5,0535	0	0	Genes involved in Generic Transcription Pathway
REACTOME_CHROMOSOME_MAINTENANCE	REACTOME	111	3,965	4,5359	0	0	Genes involved in Chromosome Maintenance
REACTOME_DNA_REPLICATION	REACTOME	185	3,9481	4,5097	0	0	Genes involved in DNA Replication
REACTOME_G2_M_CHECKPOINTS	REACTOME	41	3,517	4,0963	0	0	Genes involved in G2/M Checkpoints
REACTOME_MITOTIC_M_M_G1_PHASES	REACTOME	165	3,4981	4,0636	0	0	Genes involved in Mitotic M-M/G1 phases
REACTOME_MITOTIC_PROMETAPHASE	REACTOME	83	3,4656	3,9825	0	0	Genes involved in Mitotic Prometaphase
REACTOME_DNA_STRAND_ELONGATION	REACTOME	30	3,4275	3,9651	0	0	Genes involved in DNA strand elongation
REACTOME_DEPOSITION_OF_NEW_CENPA_CONTAINING_NUCLEOSOME!	REACTOME	26	3,1044	3,7764	1,29E-05	0	Genes involved in Deposition of New CENPA-containing Nucleosomes at the Centromere
REACTOME_MEIOSIS	REACTOME	100	3,0982	3,7687	1,28E-05	0	Genes involved in Meiosis
_EARLY_G1	REACTOME	23	3,018	3,6524	1,80E-05	0	Genes involved in G0 and Early G1
	Canonical pathway	39	2,9928	3,5532	2,38E-05	0	ATR signaling pathway
REACTOME_ACTIVATION_OF_THE_PRE_REPLICATIVE_COMPLEX	REACTOME	30	2,974	3,5156	2,34E-05	0	Genes involved in Activation of the pre-replicative complex
REACTOME_UNWINDING_OF_DNA	REACTOME	11	2,9421	3,4882	4,03E-05	0	Genes involved in Unwinding of DNA
KEGG_SYSTEMIC_LUPUS_ERYTHEMATOSUS	KEGG	124	2,935	3,4604	3,98E-05	0	Systemic lupus erythematosus
REACTOME_ACTIVATION_OF_ATR_IN_RESPONSE_TO_REPLICATION_STRE	REACTOME	35	2,9311	3,4085	3,94E-05	0	Genes involved in Activation of ATR in response to replication stress
COMBINATION	REACTOME	72	2,8936	3,3583	5,34E-05	0	Genes involved in Meiotic Recombination
WAY	Canonical pathway	47	2,8911	3,353	5,31E-05	0	Fanconi anemia pathway
	Canonical pathway	45	2,867	3,3285	7,15E-05	0	PLK1 signaling events
REACTOME_G1_S_SPECIFIC_TRANSCRIPTION	REACTOME	18	2,8521	3,3108	7,53E-05	0	Genes involved in G1/S-Specific Transcription
REACTOME_E2F_MEDIATED_REGULATION_OF_DNA_REPLICATION	REACTOME	33	2,7989	3,2926	0,00011519	0	Genes involved in E2F mediated regulation of DNA replication
REACTOME_TELOMERE_MAINTENANCE	REACTOME	89	2,7784	3,246	0,00013589	0	Genes involved in Telomere Maintenance
KEGG_CELL_CYCLE	KEGG	120	2,6965	3,2354	0,00032299	0	Cell cycle
BIOCARTA_MCM_PATHWAY	BioCarta	18	2,6002	3,1199	0,00060631	2,12E-05	CDK Regulation of DNA Replication
PINDLE	Hallmark	196	2,5385	3,0785	0,00099436	4,08E-05	Genes important for mitotic spindle assembly.
	Canonical pathway	39	2,532	3,0502	0,0010158	5,98E-05	FOXM1 transcription factor network
REACTOME_FANCONI_ANEMIA_PATHWAY	REACTOME	21	2,4473	3,0251	0,0018333	5,89E-05	Genes involved in Fanconi Anemia pathway
C_G1_G1_S_PHASES	REACTOME	129	2,4278	3,0211	0,0020988	6,85E-05	Genes involved in Mitotic G1-G1/5 phases
	Canonical pathway	71	2,4026	2,9845	0,0025517	9,57E-05	E2F transcription factor network
BIOCARTA_G2_PATHWAY	BioCarta	24	2,3998	2,9334	0,0025907	9,25E-05	Cell Cycle (SZ/M Checkpoint
REGG_DNA_REPLICATION	KEGG	30	2,3994	2,899	0,0026003	0,00011/23	UNA replication
M BHASES	Canonical patriway	2 0	7.3961	2,0000	0,0026349	0,00013464	Multiple Digitaling Generalized in Matteria G2.C2/Machanas
	Caponical pathway	ę o	2,350	2,632	0,0025699	0,0001/477	dentes involved in introduce. Cat Agringhina ass Agricos asset and and and a complex to induce the G2 (MAtransition
SISAPA	REACTOME	0 79	2,3307	2,6323	0.0046463	0.00060251	cutza, activates in teutzi-(Vegini b cumptes to middee trie 62/m transmon. Genes involved in Meiriti Synansis
REACTOME CYCLIN A B1 ASSOCIATED EVENTS DURING G2 M TRANS	REACTOME	15	2,2912	2,6798	0,0051626	0,00063702	Genes involved in Cyclin A/B1 associated events during G2/M transition
REACTOME_LAGGING_STRAND_SYNTHESIS	REACTOME	19	2,2588	2,6222	0,0063416	0,00097661	Genes involved in Lagging Strand Synthesis
SA_REG_CASCADE_OF_CYCLIN_EXPR	Canonical pathway	11	2,2242	2,51	0,0077682	0,0019643	Expression of cyclins regulates progression through the cell cycle by activating cyclin-dependent kinases.
REACTOME_EXTENSION_OF_TELOMERES	REACTOME	27	2,2002	2,4553	0,0089946	0,002975	Genes involved in Extension of Telomeres
REACTOME_S_PHASE	REACTOME	105	2,1638	2,424	0,011202	0,003654	Genes involved in S Phase
REACTOME_SYNTHESIS_OF_DNA	REACTOME	06	2,163	2,4108	0,011251	0,0039285	Genes involved in Synthesis of DNA
BIOCARTA_CELLCYCLE_PATHWAY	BioCarta	22	2,105	2,3928	0,015678	0,0043915	Cyclins and Cell Cycle Regulation
REACTOME_OLFACTORY_SIGNALING_PATHWAY	REACTOME	54	2,0453	2,3774	0,021773	0,0050119	Genes involved in Olfactory Signaling Pathway
BIOCARTA_ATRBRCA_PATHWAY	BioCarta	21	2,0238	2,3665	0,024483	0,0053759	Role of BRCA1, BRCA2 and ATR in Cancer Susceptibility
	REACTOME	23	2,0211	2,3083	0,024765	0,0075011	Genes involved in Kinesins
	Canonical pathway	13	1,9834	2,3069	0,030465	0,0075558	Cdk2, 4, and 6 bind cyclin D in G1, while cdk2/cyclin E promotes the G1/5 transition.
REACTOME_CDC6_ASSOCIATION_WITH_THE_ORC_ORIGIN_COMPLEX	REACTOME	11	1,9705	2,1614	0,032586	0,018177	Genes involved in CDG association with the ORC:origin complex
REACTOME_POL_SWITCHING	REACTOME	13	1,9699	2,1325	0,03263	0,021213	Genes involved in Polymerase switching Genes annothing collarge professive
SSIVE SYNTHESIS ON THE LAGGING STRAND	Anonical pathway	‡ £	1,9543	2,1079	0,035196	0,024326	oettes entoding Collageri plotterins. Ganes involued in Prozecetius curthesis on the lasseine strand
NEACLOUNIE_FRONCESSIVE_SINVIIIESIS_CIV_IIIE_EAGOIIIV_CIIIII	אויי טראל	7	COLC'T	6,020,0	U, coccour	1000000	GETTES TIVOLVED III PLOCESSIVE SYLLICES ON THE 1988/118 STUDIES

Gene set	Gene set type	Gene set size	Normalized enrichment score LICA-FR	Normalized enrichment score TCGA	FDR q-value LICA-FR	FDR q-value TCGA	Description
HALLMARK_OXIDATIVE_PHOSPHORYLATION	Hallmark	192	-8,5766	-3,715	0	0	Genes encoding proteins involved in oxidative phosphorylation.
HALLMARK_MYC_TARGETS_V1	Hallmark	191	-6,9431	-3,6501	0	0	A subgroup of genes regulated by MYC - version 1 (v1).
REACTOME_METABOLISM_OF_PROTEINS	REACTOME	414	-6,5794	-3,6293	0	0	Genes involved in Metabolism of proteins
REACTOME_TCA_CYCLE_AND_RESPIRATORY_ELECTRON_TRANSPORT	REACTOME	108	-6,5467	-3,5416	0	0	Genes involved in The citric add (TCA) cycle and respiratory electron transport
REACTOME_TRANSLATION	REACTOME	141	-6,4403	-3,5255	0	0	Genes involved in Translation
REACTOME_3_UTR_MEDIATED_TRANSLATIONAL_REGULATION	REACTOME	104	-6,4298	-3,5173	0	0	Genes involved in 3 - UTR-mediated translational regulation
KEGG_OXIDATIVE_PHOSPHORYLATION	KEGG	109	-6,3007	-3,4372	0	0	Oxidative phosphorylation
REACTOME_RESPIRATORY_ELECTRON_TRANSPORT_ATP_SYNTHESIS_BY_	REACTOME	74	-6,1286	-3,3745	0	0	Genes involved in Respiratory electron transport, ATP synthesis by chemiosmotic coupling, and heat production by uncoupling proteins.
REACTOME_INFLUENZA_VIRAL_RNA_TRANSCRIPTION_AND_REPLICATION	REACTOME	86	-6,0795	-3,3411	0	0	Genes involved in Influenza Viral RNA Transcription and Replication
REACTOME_METABOLISM_OF_RNA	REACTOME	247	-5,9311	-3,2594	0	0	Genes involved in Metabolism of RNA
REACTOME_PEPTIDE_CHAIN_ELONGATION	REACTOME	83	-5,7991	-3,1913	0	0	Genes involved in Peptide chain elongation
REACTOME_INFLUENZA_LIFE_CYCLE	REACTOME	131	-5,7795	-3,0016	0	0,00018015	Genes involved in Influenza Life Cycle
REACTOME_NONSENSE_MEDIATED_DECAY_ENHANCED_BY_THE_EXON_J	REACTOME	104	-5,7731	-2,9741	0	0,00026093	Genes involved in Nonsense Mediated Decay Enhanced by the Exon Junction Complex
KEGG_RIBOSOME	KEGG	81	-5,7619	-2,6431	0	0,0028391	Ribosome
REACTOME_SRP_DEPENDENT_COTRANSLATIONAL_PROTEIN_TARGETING	REACTOME	105	-5,6704	-2,5242	0	0,0056459	Genes involved in SRP-dependent cotranslational protein targeting to membrane
REACTOME_METABOLISM_OF_MRNA	REACTOME	205	-5,5643	-2,4233	0	0,0093172	Genes involved in Metabolism of mRNA
HALLMARK_MYC_TARGETS_V2	Hallmark	26	-4,589	-2,4207	0	0,0094132	A subgroup of genes regulated by MYC - version 2 (v2).
REACTOME_ACTIVATION_OF_THE_MRNA_UPON_BINDING_OF_THE_CAP	REACTOME	26	-4,4127	-2,3906	0	0,011144	Genes involved in Activation of the mRNA upon binding of the cap-binding complex and eIFs, and subsequent binding to 43S
REACTOME_FORMATION_OF_THE_TERNARY_COMPLEX_AND_SUBSEQUE	REACTOME	48	-4,1903	-2,3599	0	0,013414	Genes involved in Formation of the ternary complex, and subsequently, the 43S complex
REACTOME_CYTOSOLIC_TRNA_AMINOACYLATION	REACTOME	23	-3,8832	-2,349	0	0,014192	Genes involved in Cytosolic tRNA aminoacylation
REACTOME_TRNA_AMINOACYLATION	REACTOME	41	-3,7096	-2,3453	0	0,014476	Genes involved in tRNA Aminoacylation
REACTOME_MITOCHONDRIAL_PROTEIN_IMPORT	REACTOME	49	-3,5366	-2,3204	0	0,016459	Genes involved in Mitochondrial Protein Import
HALLMARK_REACTIVE_OXIGEN_SPECIES_PATHWAY	Hallmark	46	-3,4888	-2,3168	0	0,016849	Genes up-regulated by reactive oxigen species (ROS).
KEGG_AMINOACYL_TRNA_BIOSYNTHESIS	KEGG	41	-3,3865	-2,2181	0	0,025562	Aminoacyl-tRNA biosynthesis
KEGG_LYSOSOME	KEGG	119	-3,0686	-2,218	3,56E-06	0,025538	Lysosome
REACTOME_TRANS_GOLGI_NETWORK_VESICLE_BUDDING	REACTOME	26	-3,0595	-2,1774	1,06E-05	0,031602	Genes involved in trans-Golgi Network Vesicle Budding
KEGG_VIBRIO_CHOLERAE_INFECTION	KEGG	51	-2,5394	-2,1678	0,00049064	0,032626	Vibrio cholerae infection
KEGG_EPITHELIAL_CELL_SIGNALING_IN_HELICOBACTER_PYLORI_INFECTIK	KEGG	29	-2,4174	-2,1254	0,0011	0,039087	Epithelial cell signaling in Helicobacter pylori infection
REACTOME_RETROGRADE_NEUROTROPHIN_SIGNALLING	REACTOME	12	-2,263	-2,1124	0,0028905	0,041073	Genes involved in Retrograde neurotrophin signalling
REACTOME_INSULIN_RECEPTOR_RECYCLING	REACTOME	21	-1,9752	-2,1042	0,014178	0,042399	Genes involved in Insulin receptor recycling
REACTOME_NFKB_ACTIVATION_THROUGH_FADD_RIP1_PATHWAY_MEDI	REACTOME	11	-1,7305	-2,1028	0,044336	0,042454	Genes involved in NF-kB activation through FADD/RIP-1 pathway mediated by caspase-8 and -10

Supplementary Table 6: Significantly enriched and depleted driver genes in CCN-HCC.

LICA-FR SERIES

Gene	% alteration	% alteration	Fisher's exact	a valua
Gene	in CCN-HCC	in other HCC	test p-value	q-value
PTEN	0,50	0,078571	0,000004	0,000110
RB1	0,70	0,178571	0,000009	0,000110
TERT promoter	0,21	0,688525	0,000160	0,001331
CTNNB1	0,00	0,407143	0,001321	0,008255
TP53	0,50	0,378571	0,004942	0,024708

TCGA SERIES

Come	% alteration	% alteration	Fisher's exact	
Gene	in CCN-HCC	in other HCC	test p-value	q-value
PTEN	0,500000	0,084967	0,000000	0,000002
CDKN1A	0,392857	0,055556	0,000001	0,000004
RB1	0,571429	0,169935	0,000001	0,000004
FGA	0,357143	0,124183	0,000013	0,000066
CTNNB1	0,000000	0,316993	0,000549	0,002306
TERT promoter*	0,464286	0,715686	0,009426	0,034562
		•		

^{*}TERT promoter screening available for 186 tumors.

Supplementary Table 7: Contribution of rearrangement signatures to the genomes of 350 tumors from the LICA-FR, TCGA and ICGC series

Sample	Series	CCNA2/E1 alteration	CCNA2/E1 alteration type	# of events attributed to signature RS1	# of events attributed to signature RS2	# of events attributed to signature RS3	# of events attributed to signature RS4	# of events attributed to signature RS5	# of events attributed to signature RS
CHC2449T	LICA-FR	CCNA2	fusion	572	0	0	0	0	0
CHC1594T	LICA-FR	CCNE1	SV	524	41	39	163	0	0
CGA-BC-A217	TCGA	CCNA2	del_ex12	459	0	113	0	0	0
CHC961T	LICA-FR	CCNA2	fusion	455	0	42	62	0	0
RK107	ICGC-JP	CCNA2	HBV	424	42	48	60	43	0
CHC129T	LICA-FR	CCNA2	AAV2	414	0	0	0	32	0
						72		0	0
CGA-PD-A5DF	TCGA	CCNA2	fusion	408	44		0		
CHC3798T	LICA-FR	CCNA2	HBV	363	24	0	0	29	0
CHC313T	LICA-FR	CCNA2	AAV2	316	29	0	50	0	0
CHC2112T	LICA-FR	CCNA2	AAV2	293	81	54	119	0	0
CHC2697T	LICA-FR	CCNA2	fusion	276	0	0	0	36	0
RK285	ICGC-JP	CCNA2	fusion	275	23	0	0	54	0
CHC2207T	LICA-FR	CCNE1	SV	262	32	0	91	34	0
GA-BW-A5NO	TCGA	CCNE1	sv	215	69	0	122	0	0
HX32	ICGC-JP	CCNE1	AAV2	208	29	0	0	0	0
CHC2141T	LICA-FR	CCNE1	AAV2	199	57	0	92	0	0
CGA-FV-A495	TCGA	CCNA2	SV	190	39	76	88	0	0
CHC2048T	LICA-FR	CCNE1	SV	188	31	0	0	0	0
CGA-BC-A216	TCGA	CCNA2	fusion	171	96	38	80	60	0
CHC1994T	LICA-FR	CCNE1	HBV	123	39	15	18	13	0
CHC2208T	LICA-FR	CCNE1	AAV2	110	27	0	0	35	0
RK126	ICGC-JP	WT		95	0	0	0	68	0
			NA						
GA-DD-A4NA	TCGA	WT	NA	89	57	0	0	18	0
CHC2115T	LICA-FR	WT	NA	65	18	0	0	123	0
RK111	ICGC-JP	WT	NA	60	96	0	20	0	0
CGA-DD-A1EB	TCGA	WT	NA	56	175	0	0	0	0
CGA-ED-A459	TCGA	WT	NA	56	0	211	0	42	0
RK172	ICGC-JP	WT	NA	55	0	103	10	0	0
CHC218T	LICA-FR	WT	NA	46	29	0	0	488	0
CHC322T	LICA-FR	WT	NA NA	43	13	0	53	30	0
CHC912T	LICA-FR	WT	NA	39	0	0	122	281	0
RK023	ICGC-JP	WT	NA	34	18	0	0	105	0
RK079	ICGC-JP	WT	NA	30	0	29	15	0	6
CHC909T	LICA-FR	WT	NA	29	0	0	0	38	0
CGA-G3-A25T	TCGA	WT	NA	28	0	0	0	69	14
CHC2200T	LICA-FR	WT	NA	27	145	34	21	23	0
CHC304T	LICA-FR	WT	NA	26	9	0	30	82	0
					254	0		0	0
CGA-FV-A496	TCGA	WT	NA	26			20		
RK211	ICGC-JP	WT	NA	26	118	31	36	16	0
RK326	ICGC-JP	WT	NA	26	0	12	0	10	0
RK083	ICGC-JP	WT	NA	24	0	0	0	82	0
RK187	ICGC-JP	WT	NA	24	8	0	19	18	0
RK263	ICGC-JP	WT	NA	24	0	0	0	4	0
RK070	ICGC-JP	WT	NA	23	217	0	42	0	0
CHC314T	LICA-FR	WT	NA	22	20	0	104	11	0
		WT		22			69	8	8
CGA-DD-A1EJ	TCGA		NA		13	11			
CHC2443T	LICA-FR	WT	NA	20	12	20	53	22	0
RK019	ICGC-JP	WT	NA	20	48	105	150	0	0
RK162	ICGC-JP	WT	NA	20	5	0	4	4	0
RK191	ICGC-JP	WT	NA	19	0	39	0	6	0
RK027	ICGC-JP	WT	NA	18	18	0	35	58	0
RK207	ICGC-JP	WT	NA	18	19	32	0	52	0
CHC1754T	LICA-FR	WT	NA	17	0	89	50	30	11
CGA-G3-A25S	TCGA	WT	NA	17	0	128	65	20	15
RK229	ICGC-JP	WT	NA	17	2	0	4	4	0
CGA-DD-A3A7	TCGA	WT	NA	16	35	43	47	29	0
CGA-DD-A4NE	TCGA	WT	NA	16	0	28	93	17	0
HX27	ICGC-JP	WT	NA	16	0	0	0	11	0
RK115	ICGC-JP	WT	NA	16	0	0	2	10	6
CHC320T	LICA-FR	WT	NA	15	14	16	5	42	0
GA-BW-A5NP	TCGA	WT	NA	15	13	0	66	16	0
RK026	ICGC-JP	WT	NA NA	15	0	0	0	15	4
RK030	ICGC-JP	WT	NA	15	26	7	17	31	38
RK062	ICGC-JP	WT	NA	15	2	0	12	2	0
RK157	ICGC-JP	WT	NA	15	5	0	5	21	6
RK256	ICGC-JP	CCNE1	HBV	15	19	18	33	6	0
RK280	ICGC-JP	WT	NA	15	77	0	10	10	0
CGA-FV-A23B	TCGA	WT	NA	14	0	37	31	0	0
RK001	ICGC-JP	WT	NA	14	5	0	9	18	3
									0
RK046_2	ICGC-JP	WT	NA	14	0	6	8	44	
RK128	ICGC-JP	WT	NA	14	0	0	89	0	0
CHC2103T	LICA-FR	WT	NA	13	0	0	15	20	0
RK228	ICGC-JP	WT	NA	13	20	0	9	22	5
RK261_2	ICGC-JP	WT	NA	13	11	15	26	54	47
CHC1704T	LICA-FR	WT	NA	12	0	0	30	101	0
					0				0
CGA-CC-5261	TCGA	WT	NA	12		0	42	19	
CGA-DD-A1EI	TCGA	WT	NA	12	0	156	43	0	11
CGA-CC-A1HT	TCGA	WT	NA	12	11	0	22	44	0
RK257	ICGC-JP	WT	NA	12	4	0	8	3	0
CHC1598T	LICA-FR	WT	NA	11	7	18	33	10	0
HX28	ICGC-JP	WT	NA	11	0	30	119	0	0
RK075	ICGC-JP	WT	NA	11	11	0	39	61	0
	ICGC-JP	WT	NA	11	0	52	75	0	0
RK224									
RK224 RK266	ICGC-JP	WT	NA	11	40	0	0	39	0 6

TCGA-CC-5260	TCGA	WT	NA	10	15	17	73	11	0
RK005	ICGC-JP	WT	NA	10	0	0	62	0	6
									1000
RK087	ICGC-JP	WT	NA	10	0	9	15	15	12
RK135	ICGC-JP	WT	NA	10	0	100	31	12	39
RK277	ICGC-JP	WT	NA	10	4	0	4	24	3
RK287	ICGC-JP	WT	NA	10	61	0	34	26	0
CHC2113T									
100 100 100 100 100 100 100 100 100 100	LICA-FR	WT	NA	9	0	0	9	18	0
TCGA-FV-A3R2	TCGA	WT	NA	9	4	0	18	2	0
HX11	ICGC-JP	WT	NA	9	0	7	7	16	3
HX21	ICGC-JP	WT	NA	9	0	59	14	41	11
HX34	ICGC-JP	WT		9	0	0	0	17	2
			NA						
RK034	ICGC-JP	WT	NA	9	0	4	18	18	0
RK092	ICGC-JP	WT	NA	9	8	12	26	28	6
RK120	ICGC-JP	WT	NA	9	0	0	19	19	5
CHC309T	LICA-FR	WT	NA	8	5	0	13	12	0
TCGA-CC-5262	TCGA	WT	NA	8	0	8	5	17	0
TCGA-DD-A1EG	TCGA	WT	NA	8	7	31	71	0	7
TCGA-DD-A4NG	TCGA	WT	NA	8	0	18	27	12	0
RK028	ICGC-JP	WT	NA	8	1	0	0	7	2
									800
RK059	ICGC-JP	WT	NA	8	7	0	6	11	0
RK074	ICGC-JP	WT	NA	8	13	6	25	15	0
RK082	ICGC-JP	WT	NA	8	4	0	6	13	4
RK089	ICGC-JP	WT	NA	8	0	0	27	5	17
		WT		8	24	0		0	
RK104	ICGC-JP		NA				51		5
RK170	ICGC-JP	WT	NA	8	24	9	16	31	0
RK201	ICGC-JP	WT	NA	8	8	0	22	23	4
RK265	ICGC-JP	WT	NA	8	0	0	0	17	0
CHC892T	LICA-FR	WT	NA	7	0	0	0	12	5
									770
TCGA-DD-A1EL	TCGA	WT	NA	7	0	0	20	11	4
TCGA-FV-A3R3	TCGA	WT	NA	7	7	0	0	12	0
HX17	ICGC-JP	WT	NA	7	0	0	6	31	0
HX30	ICGC-JP	WT	NA	7	0	0	11	14	0
RK021	ICGC-JP	WT	NA	7	0	0	78	0	5
RK025	ICGC-JP	WT	NA	7	5	22	24	12	0
RK044	ICGC-JP	WT	NA	7	2	0	14	5	2
RK058	ICGC-JP	WT	NA	7	4	0	0	10	11
RK205	ICGC-JP	WT	NA	7	0	0	4	10	5
RK233_2	ICGC-JP	WT	NA	7	7	0	6	7	0
RK261_1	ICGC-JP	WT	NA	7	10	0	27	22	0
RK262	ICGC-JP	WT	NA	7	0	6	22	36	5
CHC2448T	LICA-FR	WT	NA	6	0	0	0	19	0
HX10	ICGC-JP	WT	NA	6	0	26	10	9	0
HX25	ICGC-JP	WT	NA	6	0	64	40	0	0
HX37	ICGC-JP	WT	NA	6	0	0	45	27	0
. NEECHOOL									5555
RK042	ICGC-JP	WT	NA	6	0	0	31	55	0
RK147	ICGC-JP	WT	NA	6	21	0	19	6	0
RK215	ICGC-JP	WT	NA	6	13	0	0	3	0
TCGA-FV-A2QQ	TCGA	WT	NA	5	10	38	22	8	0
TCGA-DD-A4ND	TCGA	WT	NA	5	3	35	0	6	0
TCGA-ED-A4XI	TCGA	WT	NA	5	0	0	0	70	0
TCGA-G3-A5SL	TCGA	WT	NA	5	5	3	9	11	3
HX16	ICGC-JP	WT	NA	5	4	0	19	4	5
RK007	ICGC-JP	WT	NA	5	0	0	7	18	2
									9.0
RK050	ICGC-JP	WT	NA	5	13	0	22	8	0
RK068	ICGC-JP	WT	NA	5	0	3	28	0	5
RK088	ICGC-JP	WT	NA	5	8	18	10	19	15
RK140	ICGC-JP	WT	NA	5	0	0	10	17	4
RK141	ICGC-JP	WT	NA	5	0	0	20	0	5
		200			_			-	
RK185	ICGC-JP	WT	NA	5	0	0	21	1	0
RK199	ICGC-JP	WT	NA	5	0	0	10	0	8
RK210	ICGC-JP	WT	NA	5	0	0	2	30	0
RK217	ICGC-JP	WT	NA	5	0	0	35	4	0
RK223	ICGC-JP	WT	NA	5	0	0	3	30	0
					9				
RK234	ICGC-JP	WT	NA	5		0	15	17	5
RK237	ICGC-JP	WT	NA	5	19	21	22	0	0
RK264	ICGC-JP	WT	NA	5	0	0	0	53	8
CHC1717T	LICA-FR	WT	NA	4	0	0	10	6	0
CHC1731T	LICA-FR	WT	NA	4	0	0	17	21	3
CHC2132T	LICA-FR	WT	NA	4	0	19	20	26	0
CHC429T	LICA-FR	WT	NA	4	7	0	24	14	0
HX4	ICGC-JP	WT	NA	4	3	6	20	9	4
HX26	ICGC-JP	WT	NA	4	5	0	13	6	0
RK006_1	ICGC-JP	WT	NA	4	16	0	9	17	0
RK018	ICGC-JP	WT		4	0	0	7	10	5
			NA						
RK024	ICGC-JP	WT	NA	4	0	0	14	7	0
RK037	ICGC-JP	WT	NA	4	1	0	0	10	0
RK046_1	ICGC-JP	WT	NA	4	1	0	5	14	2
RK052	ICGC-JP	WT	NA	4	0	12	0	18	0
									2000
RK118	ICGC-JP	WT	NA	4	3	0	0	15	21
RK144	ICGC-JP	WT	NA	4	5	0	1	2	0
RK150	ICGC-JP	WT	NA	4	11	0	6	3	33
RK152	ICGC-JP	WT	NA	4	17	12	6	8	6
RK156	ICGC-JP	WT	NA	4	10	0	13	5	6
RK159	ICGC-JP	WT	NA	4	3	0	12	5	0
RK181	ICGC-JP	WT	NA	4	9	0	9	22	3
RK197	ICGC-JP	WT	NA	4	8	10	30	4	0
RK216	ICGC-JP	WT	NA	4	0	12	22	0	0
INCTO		V V I	1375	-	U	14	~~	U	
DV330		NA/T	NI A	4	15			-	
RK230	ICGC-JP	WT	NA	4	15	0	0	7	4
RK230 RK232		WT WT	NA NA	4	15 11	0	0 20	7 12	4 5

Supplementary Table 8: Rearrangements affecting TERT promoter region in 350 HCC

genomes.

Breakpoint 2 chromatin state	EnhA2	EnhA1	EnhA1	TxWk	Quies	EnhA1	EnhA1	EnhWk	EnhWk	EnhA1	EnhA1	EnhG2	EnhA1	TxWk	TssFlnkU	Quies	EnhA1	TxWk	Quies	TssFlnk	EnhA1	EnhA1	EnhA2	TssA	Quies	EnhA2	Quies	EnhA2	EnhA1	Quies	ReprPCWk	EnhWk	ZNF/Rpts	TssFlnkU	EnhA1	EnhA2	EnhA2	TssA	EnhA1	EnhA1	ReprPCWk
Breakpoint 2 closest gene*	SEP15	HNF4A	GPR98	[PTPN1]	[WDR72]	[CEBPB]	[BAAT]	[TMEM17]	CTD-2540B15.12	RAD51B	SLC12A7	FGG	[ALB]	[TMEM17]	EHBP1	[ERRFI1]	[CEBPA]	[IRF2BP2]	[TRIB1]	CLPTM1L	FLNB	[RP11-404L6.2]	ADRA1A	NCLN	PLEKHG4B	[WDPCP]	[ERRFI1]	ANKH	[HS1BP3]	SLC25A21	[TERT]	SDR9C7	[PGBD2]	[OTUD1]	ALB	ZFP36L1	[TSPYL5]	PTP4A1	[BCL3]	[TOMM20]	[CCNH]
Breakpoint 2 functional category	IGR	Intron	Intron	IGR	IGR	IGR	IGR	IGR	lincRNA	Intron	Intron	Intron	IGR	IGR	Intron	IGR	IGR	IGR	IGR	5'UTR	Intron	IGR	Intron	5'UTR	Exon	IGR	IGR	Intron	IGR	Intron	IGR	Intron	IGR	IGR	5'Flank	IGR	IGR	Intron	IGR	IGR	IGR
Breakpoint 2	chr1:87326526	chr20:43039447	chr5:90205018	chr20:49035293	chr15:53763959	chr20:48901456	chr9:104109584	chr2:62698661	chr19:33772231	chr14:69147921	chr5:1100916	chr4:155527854	chr4:74249043	chr2:62710191	chr2:62926001	chr1:8224257	chr19:33770341	chr1:234994146	chr8:126644024	chr5:1345091	chr3:58007495	chr5:67466718	chr8:26665185	chr19:3185861	chr5:156985	chr2:63960694	chr1:8223434	chr5:14730258	chr2:20798818	chr14:37580176	chr5:1299728	chr12:57326014	chr1:249239943	chr10:23847990	chr4:74268328	chr14:69253156	chr8:98176329	chr6:64283298	chr19:45247948	chr1:235105047	chr5:86730606
Breakpoint 1 chromatin state	EnhWk	EnhWk	EnhWk	EnhWk	ReprPCWk	ReprPCWk	Quies	Quies	Quies	¥	EnhWk	EnhWk	EnhWk	ReprPCWk	Quies	Quies	Quies	Quies	EnhWk	EnhWk	EnhWk	EnhWk	EnhWk	ReprPCWk	ReprPCWk	ReprPCWk	ReprPCWk	ReprPCWk	ReprPCWk	ReprPCWk	ReprPCWk	ReprPCWk	ReprPCWk	Het	Quies	Quies	Quies	Quies	Quies	Quies	Quies
Distance between breakpoint 1 and TERT TSS	-120	-230	-282	-323	-1541	-5472	-13847	-14399	-16805	-34893	-240	-386	-478	-6312	-8372	-9247	-17031	-17395	15	-277	-400	-439	-590	-638	-1012	-1052	-1557	-1619	-1734	-1952	-2223	-3915	-5440	-7830	-8649	-10908	-11982	-12363	-14346	-16429	-16506
Breakpoint 1 (TERT 5' flanking region)	chr5:1295282	chr5:1295392	chr5:1295444	chr5:1295485	chr5:1296703	chr5:1300634	chr5:1309009	chr5:1309561	chr5:1311967	chr5:1330055	chr5:1295402	chr5:1295548	chr5:1295640	chr5:1301474	chr5:1303534	chr5:1304409	chr5:1312193	chr5:1312557	chr5:1295147	chr5:1295439	chr5:1295562	chr5:1295601	chr5:1295752	chr5:1295800	chr5:1296174	chr5:1296214	chr5:1296719	chr5:1296781	chr5:1296896	chr5:1297114	chr5:1297385	chr5:1299077	chr5:1300602	chr5:1302992	chr5:1303811	chr5:1306070	chr5:1307144	chr5:1307525	chr5:1309508	chr5:1311591	chr5:1311668
Most likely causal rearrangement signature	RS1	RS1	RS1	RS1	RS1	RS1	RS1	RS1	RS1	RS1	RS2	RS4	RS1	RS1	RS1	RS1	RS1	RS1	RS4	RS5	RS4	RS4	RS4	RS4	RS4	RS4	RS4	RS4	RS4	RS4	RS6	RS4	RS4								
Туре	inter-chromosomal translocation	inter-chromosomal translocation	inversion	inter-chromosomal translocation	tandem duplication	inter-chromosomal translocation	deletion	inter-chromosomal translocation	inversion	inter-chromosomal translocation	inter-chromosomal translocation	inversion	inter-chromosomal translocation	inter-chromosomal translocation	inversion	inter-chromosomal translocation	inter-chromosomal translocation	inversion	inter-chromosomal translocation	deletion																					
Cyclin.Status	CCNA2	CCNA2	CCNA2	CCNA2	CCNA2	CCNA2	CCNA2	CCNA2	CCNA2	CCNA2	CCNE1	CCNE1	CCNE1	CCNE1	CCNE1	CCNE1	CCNE1	CCNE1	Ϋ́	ΙM	ΙM	ΙM	Ϋ́	Ϋ́	ΙM	ΙM	W	ΙM	W	ΙM	M	ΙM	ΙM	ΙM	ΙM	Ϋ́	ΙM	ΙM	ΙM	M	ΤW
Sample	TCGA-BC-A217	CHC313T	RK285	RK107	TCGA-BC-A216	TCGA-FV-A495	CHC2697T	CHC3798T	CHC129T	CHC2112T	CHC2141T	RK256	CHC2207T	CHC2048T	CHC2208T	TCGA-BW-A5NO	HX32	CHC1594T	RK260	RK077	CHC1598T	RK222	RK237	RK261_1	RK012	CHC1602T	RK278	RK122	RK044	TCGA-DD-A1EI	CHC1731T	RK254	TCGA-G3-A25S	RK065	RK283	TCGA-DD-A4NE	TCGA-DD-A3A8	HX26	RK227	RK054	RK034

*For intergenic breakpoints, the name of the gene with the closest transcription start site is indicated between brackets.

Supplementary Table 9: Number of RS1 events and association with CCNA2/E1

alterations across cancer types.

Cancer type	Cancer_code	ICGC PCAWG projects regrouped	Number of tumors	Mean number of RS1 events per tumor	% of tumors with at least 50 RS1 events	Association with CCNA2/E1 rearrangement (Fisher's exact test q-value)
Acute Myeloid Leukemia	AML	LAML-KR	8	0,75	0	1
Biliary Tract Cancer	BILCA	BTCA-SG	12	3,66666667	0	П
Chronic Lymphocytic Leukemia	CLL	CLLE-ES	91	0,175824176	0	П
Chronic Myeloid Disorders	CMD	CMDI-UK	21	0,380952381	0	П
Diffuse Large B-cell Lymphoma	DLBCL	DLBC-US	7	1,571428571	0	П
Glioblastoma Multiforme	GBM	GBM-US	40	1,6	0	П
Kidney Cancer	KIRC	KIRC-US/KIRP-US/RECA-EU/KICH-US	176	727272770	0	1
Lower Grade Glioma	997	reg-ns	17	0,529411765	0	1
Oral Cancer	OCA	ORCA-IN	12	4,33333333	0	Н
Pediatric Brain Cancer	PEDBCA	PBCA-DE	204	0,828431373	0	1
Sarcoma	SARC	SARC-US	34	4,323529412	0	1
Thyroid Cancer	THYCA	THCA-US	30	0,2	0	1
Malignant Lymphoma	ML	MALY-DE	66	3,52525255	П	0,2929293
Bone Cancer	BOCA	BOCA-UK	09	4,61666667	2	1
Head and Neck Squamous Cell Carcinoma	HNSCC	HNSC-US	44	10,56818182	2	1
Pancreatic Cancer	PACA	PACA-AU/PACA-CA/PAEN-AU/PAEN-IT	307	5,296416938	2	0,890566495
Prostate Cancer	PROST	PRAD-US/PRAD-CA/PRAD-UK/EOPC-DE	278	11,83093525	2	1
Skin Cancer	SKIN	SKCM-US/MELA-AU	106	6,29245283	2	0,372675236
Colorectal Cancer	COLORECT	COAD-U S/READ-US	09	12,78333333	8	1
Liver Cancer	LIHC	LIHC-US/LICA-FR/LIRI-JP/LINC-JP	345	7,808695652	3	2,54E-10
Lung Adenocarcinoma	LUAD	LUAD-US	36	4,416666667	8	1
Bladder Cancer	BLCA	BLCA-US	23	9,434782609	4	1
Lung Squamous Cell Carcinoma	CUSC	rnsc-ns	48	22,39583333	4	1
Cervical Squamous Cell Carcinoma	CSCC	CESC-US	20	9,1	2	1
Uterine Cancer	UTCA	UCEC-US	47	13,55319149	9	1
Esophageal Cancer	ESOCA	ESAD-UK	87	22,06896552	11	0,372675236
Gastric Cancer	GASTR	STAD-US/GACA-CN	72	24,88888889	15	0,890566495
Breast Cancer	BRCA	BRCA-US/BRCA-EU/BRCA-UK	209	46,04784689	18	0,334057764
Ovarian Cancer	OVCA	OV-US/OV-AU	112	64,54464286	33	0,664892237

3. Annex 3: Article 5

Research Article Hepatic and Biliary Cancer



JOURNAL OF HEPATOLOGY

BAP1 mutations define a homogeneous subgroup of hepatocellular carcinoma with fibrolamellar-like features and activated PKA

Théo Z. Hirsch^{1,2,†}, Ana Negulescu^{1,2,†}, Barkha Gupta^{1,2}, Stefano Caruso^{1,2}, Bénédicte Noblet^{1,2}, Gabrielle Couchy^{1,2}, Quentin Bayard^{1,2}, Léa Meunier^{1,2}, Guillaume Morcrette^{1,2,3}, Jean-Yves Scoazec⁴, Jean-Frédéric Blanc^{5,6,7}, Giuliana Amaddeo⁸, Jean-Charles Nault^{1,2,9}, Paulette Bioulac-Sage^{6,7}, Marianne Ziol¹⁰, Aurélie Beaufrère¹¹, Valérie Paradis^{11,12}, Julien Calderaro^{1,2,13}, Sandrine Imbeaud^{1,2}, Jessica Zucman-Rossi^{1,2,14,*,‡}

¹Centre de Recherche des Cordeliers, Sorbonne Université, Inserm, Université de Paris, F-75006 Paris, France; ²Functional Genomics of Solid Tumors laboratory, équipe labellisée Ligue Nationale contre le Cancer, Labex Oncolmmunology, F-75006, Paris, France; ³Service de Pathologie Pédiatrique, APHP, Hôpital Robert Debré, F-75019 Paris, France; ⁴Service d'anatomie et de cytologie pathologiques, Gustave Roussy Cancer Center, F-94800 Villejuif, France; ⁵Service Hépato-Gastroentérologie et Oncologie Digestive, Hôpital Haut-Lévêque, CHU de Bordeaux, F-33000 Bordeaux, France; ⁵Service de Pathologie, Hôpital Pellegrin, CHU de Bordeaux, F-33076 Bordeaux, France; ⁻Université Bordeaux, Inserm, Research in Translational Oncology, BaRITOn, F-33076 Bordeaux, France; ⁵Service d'Hepato-Gastro-Entérologie, Hôpital Henri Mondor, APHP, Université Paris Est Créteil, Inserm U955, Institut Mondor de Recherche Biomédicale, F-94010 Créteil, France; ¹9Service d'Hépatologie, Hôpital Jean Verdier, Hôpitaux Universitaires Paris-Seine-Saint-Denis, APHP, Université Sorbonne Paris Nord, F-93140 Bondy, France; ¹1Service de pathologie, Hôpital Beaujon, APHP, F-92110 Clichy, France; ¹1Université de Paris, CNRS, Centre de Recherche Biomédicale, F-94010 Créteil, France; ¹1Faris, France; ¬1Faris, F

Background & Aims: *DNAJB1-PRKACA* fusion is a specific driver event in fibrolamellar carcinoma (FLC), a rare subtype of hepatocellular carcinoma (HCC) that occurs in adolescents and young adults. In older patients, molecular determinants of HCC with mixed histological features of HCC and FLC (mixed-FLC/HCC) remain to be discovered.

Methods: A series of 151 liver tumors including 126 HCC, 15 FLC, and 10 mixed-FLC/HCC were analyzed by RNAseq and wholegenome- or whole-exome sequencing. Western blots were performed to validate genomic discoveries. Results were validated using the TCGA database.

Results: Most of the mixed-FLC/HCC RNAseq clustered in a robust subgroup of 17 tumors, which all had mutations or translocations inactivating *BAP1*, the gene encoding BRCA1-associated protein-1. Like FLC, BAP1-HCC were significantly enriched in females, patients with a lack of chronic liver disease, and fibrotic tumors compared to non-BAP1 HCC. However, patients were older and had a poorer prognosis than those with FLC. BAP1 tumors were immune hot, showed progenitor features and did not show *DNAJB1-PRKACA* fusion, while almost none of these tumors had mutations in *CTNNB1*, *TP53* and *TERT* promoter. In contrast, 80% of the BAP1 tumors showed a chromosome gain

of *PRKACA* at 19p13, combined with a loss of *PRKAR2A* (coding for the inhibitory regulatory subunit of PKA) at 3p21, leading to a high PRKACA/PRKAR2A ratio at the mRNA and protein levels. **Conclusion:** We have characterized a subgroup of *BAP1*-driven HCC with fibrolamellar-like features and a dysregulation of the PKA pathway, which could be at the root of the clinical and histological similarities between BAP1 tumors and *DNAJB1-PRKACA* FLCs.

Lay summary: Herein, we have defined a homogeneous subgroup of hepatocellular carcinomas in which the *BAP1* gene is inactivated. This leads to the development of cancers with features similar to those of fibrolamellar carcinoma. These tumors more frequently develop in females without chronic liver disease or cirrhosis. The presence of PKA activation and T cell infiltrates suggest that these tumors could be treated with PKA inhibitors or immunomodulators.

© 2019 Published by Elsevier B.V. on behalf of European Association for the Study of the Liver.

Introduction

Fibrolamellar carcinoma (FLC) is a rare subtype of hepatocellular carcinoma (HCC) mostly diagnosed in adolescents and young adults. It was originally defined by specific histological features of both the tumor cells and their stroma, with the presence of abundant fibrosis arranged in a lamellar fashion around deeply eosinophilic large neoplastic hepatocytes, frequent central scar and calcifications. FLCs define a specific subgroup of HCC since they have peculiar clinical features compared to classical HCC, such as a young age at onset between 10 to 35 years old, a balanced sex ratio, an absence of underlying liver disease or risk factors and a better prognosis, with 80% survival at 5-years after resection. Biologically, FLCs show a high number of mitochondria and progenitor features, suggesting that the tumor cells

^{*} Senior, corresponding author. https://doi.org/10.1016/j.jhep.2019.12.006





Keywords: Liver cancer; Fibrolamellar carcinoma; BAP1; PRKACA; HCC; Immunotherapy; Genomics.

Received 6 September 2019; received in revised form 4 December 2019; accepted 5 December 2019; available online 18 December 2019

^{*} Corresponding author. Address: Centre de recherche des Cordeliers, Functional genomics of solid tumors, 15 rue de l'école de médecine, 75006 Paris, France. Tel.: +33 6 01 07 78 75.

E-mail address: jessica.zucman-rossi@inserm.fr (J. Zucman-Rossi).

[†] Co-first authors, contributed equally.

JOURNAL OF HEPATOLOGY

are blocked at a specific stage of differentiation with hepatocellular (HEPAR1), biliary (CK7) and CD68 co-expressed markers.^{1,5} In 2014, Honeyman and colleagues discovered a specific 400 kb chromosome deletion at chromosome 19 in FLC leading to a recurrent chimeric DNAJB1-PRKACA gene fusion.⁶ DNAJB1 encodes HSP40, a member of the heat shock protein family, while PRKACA codes for the cAMP-dependent protein kinase (PKA) catalytic subunit alpha; the chimeric gene results in PRKACA catalytic domain overexpression and subsequent PKA activation. In addition, rare FLC without DNAJB1-PRKACA fusion were identified in patients with Carney disease due to PRKAR1A germline mutations that also led to PKA activation and a similar phenotype.7 In contrast, PKA activation is only rarely identified in HCC (<1% GNAS mutations) or in cholangiocarcinoma (around 6% of GNAS mutations and rare fusions of PRKACA, PRKACB and PRKAR1B).8.

Frequently, FLC diagnosis can be difficult and tumors with histological features of both HCC and FLC have been described as mixed-FLC/HCC. In comparison with FLC, mixed-FLC/HCC patients were older, all above 35 years, and had a poor prognosis. Moreover, transcriptomic analyses showed a different profile of expression in the mixed-FLC/HCC and a lack of DNAJB1-PRKACA fusion. 13,14 Therefore, mixed-FLC/HCC should be better defined in the phenotypic/molecular diversity of liver tumors, in particular to identify similarities and differences with FLC of the young and other HCC subtypes. 12

In this study, to identify specific molecular driver(s) of the mixed-FLC/HCC subgroup of tumors, we performed an integrated genomic analysis using RNA sequencing (RNAseq) and wholegenome- or whole-exome sequencing (WGS/WES) of 151 liver tumors classified as HCC, FLC and mixed-FLC/HCC by pathological review.

Material and methods

Patients and tumors

We assembled a series of 151 patients (LICA-FR cohort) enriched with 15 FLC, 10 mixed-FLC/HCC cases and including 126 HCC controls; ^{8,15} genomic data (WGS or WES and RNAseq) and data from pathological review were available for all cases (see below). The study was approved by the local Ethics Committee (CCPPRB Paris Saint-Louis IRB00003835), and informed consent was obtained in accordance with French legislation for all patients. Tumor and corresponding non-tumor samples were frozen at -80°C after tumor resection and all tumor samples were primary tumors except 8 samples collected at relapse; clinical features are summarized in Table 1. For validation, we used 345 tumors (339 HCC, 4 FLC, 2 mixed-FLC/HCC) from the TCGA (The Cancer Genome Atlas) cohort, ¹⁶ whose clinical features are also described in Table 1.

Pathological review

Multiple slides of the same tumor were reviewed by at least 2 liver pathologists for several histological criteria previously described 11,17,18 including: tumor differentiation (WHO grade and Edmonson grade), vascular invasion (microscopic), tumor architecture (macrotrabecular, microtrabecular, pseudoglandular), abundant fibrous stroma (>20%), steatosis, histological patterns (scirrhous, macrotrabecular massive), lymphocytic inflammation (>20%), tumor invasion (biliary tract, perineural) and clear cell presence. HCC containing at least 1 area with FLC-like features were annotated as mixed-FLC/HCC as previously described 11

(Fig. S1). For the TCGA cohort, histological features were reviewed by at least 2 liver pathologists from the virtual slides available online via cBioPortal (http://www.cbioportal.org/). Tertiary lymphoid structures were annotated on hemateineosin-safran slides as in^{19,20} for a subset of the LICA-FR cohort (55 tumors) and all tumors from the TCGA cohort.

Genomic sequencing

A total of 151 tumors and their corresponding non-tumor tissues were sequenced by WES (n = 115 including 43 new cases) or WGS (n = 36 including 3 new cases) as previously described.^{8,21,22} For samples without WGS, targeted analysis of *TERT* promoter was performed with Sanger (n = 100) and/or miSeq (n = 38) sequencing as previously described.⁸ while *BAP1* was re-sequenced with miSeq technology in 24 samples (the list of primer sequences is provided in Table S1). Copy number analysis was performed as previously described²² and manually corrected with the help of the GAP tool.²³

RNAseq and transcriptomic analyses

mRNAs were extracted from 151 tumor (including 64 new cases) and 3 non-tumor tissues and sequenced using Illumina TruSeq or Illumina TruSeq Stranded mRNA kit, libraries were sequenced by IntegraGen (Evry, France) on an Illumina HiSeq 2,000 or 4,000 paired-end 75 bp or 100 bp reads as previously described.²⁴ Fastq files were aligned to the reference human genome GRCh38 using TopHat2.²⁵ Reads mapping to multiple locations were removed and we used HTSeq²⁶ to obtain the number of reads associated with each gene in the Gencode v27 database, restricting reads to protein-coding genes, pseudogenes, antisense and lincRNAs (n = 58,288). We used the Bioconductor DESeq2 package²⁷ to import raw HTSeq counts for each sample into R statistical software and applied variance stabilizing transformation to the raw count matrix to obtain an expression matrix without variance-mean dependence (vst matrix). FPKM scores (number of fragments per kilobase of exon model and millions of mapped reads) were calculated by normalizing the count matrix for the library size and the coding length of each gene. We used the area under the ROC curve (AUC) to identify and remove 2,404 genes with a significant batch effect (AUC >0.95 between one sequencing project and others). Unsupervised hierarchical clustering was done using Cosine distance and Ward method on most 5,000 differentially expressed genes from the vst matrix as previously described.2

Tumors were classified in the G1-G6 classification as previously described for the LICA-FR cohort²⁸ and the TCGA cohort.²⁹ We used the Bioconductor *limma* package³⁰ to test for differential gene expression between 2 groups of RNAseq samples of interest. All genes expressed in at least 5 samples (FPKM>0) were considered for the differential expression analysis. We applied a q-value threshold of ≤0.05 to define differentially expressed genes. We used an in-house adaptation of the gene-set enrichment analysis (GSEA) method³¹ to identify gene sets from the MSigDB (v. 6.0) database overrepresented among up- and downregulated genes. Single sample GSEA scores were calculated as gene-set variation analysis (GSVA) enrichment scores, using the GSVA package.³²

The relative abundance of immune and stromal cell infiltration within tumors was assessed through microenvironment cell population (MCP) scores computed with the MCP-counter method³³ adapted to RNAseq data (exp matrix) after filtering

Research Article

Hepatic and Biliary Cancer

Table 1. Clinical, histological and molecular features of tumors stratified by molecular alterations.

		LICA-	FR				TCGA	a		
	Non-BAP1/ fusPRKACA tumors (n = 118)	BAP1 tu (n = 1		fusPRKACA mors (n =		Non-BAP1/ fusPRKACA tumors (n = 323)	BAP1 tur (n = 1		fusPRKA tumors (n	100000000000000000000000000000000000000
	n/N (%)	n/N(%)	p	n/N (%)	p	n/N (%)	n/N(%)	p	n/N (%)	р
Histological Diagnosis										
HCC	116/118 (98)	10/18 (56)	***###	0/15 (0)	##	323/323 (100)	16/16 (100)	###	0/6 (0)	##
FLC	0/118 (0)	2/18 (11)	*###	13/15 (87)	##	0/323 (0)	0/16(0)	##	4/6 (67)	#
mixed-FLC/HCC	2/118 (2)	6/18 (33)	***	2/15 (13)		0/323 (0)	0/16(0)		2/6 (33)	##
Age at sampling (years)	64 (18-90)	51 (27-73)	**###	26 (17-36)	##	61 (20-90)	61 (44-77)	###	22 (17-35)	111
Female gender	23/118 (19)	12/18 (67)	***	9/15 (60)	#	92/323 (28)	12/16 (75)	***	3/6 (50)	
Alcohol intake	47/116 (41)	5/16 (31)		0/12 (0)	#	107/304 (35)	3/14 (21)		1/4 (25)	
Hepatitis B	39/118 (33)	1/17 (6)	*	0/12 (0)	İ	102/304 (34)	2/14 (14)		0/4(0)	
Hepatitis C	15/116 (13)	0/15 (0)		0/12 (0)		47/304 (15)	1/14(7)		0/4(0)	
Without etiology	14/118 (12)	8/16 (50)	***##	12/12 (100)	##	67/300 (22)	7/13 (54)		3/4 (75)	1
Non-tumor liver histology***!	±±*±									
F0-F1	52/118 (44)	16/17 (94)		15/15 (100)		92/192 (48)	9/12 (75)		5/5 (100)	
F2-F3	36/118 (31)	1/17 (6)		0/15 (0)		29/192 (15)	2/12 (17)		0/5 (0)	
F4	30/118 (25)	0/17(0)		0/15(0)		71/192 (37)	1/12 (8)		0/5 (0)	
Abundant fibrous stroma	32/115 (28)	13/18 (72)	***#	15/15 (100)	丗	36/323 (11)	6/16 (38)	**	4/6 (67)	#
Tumor steatosis	19/100 (19)	10/15 (67)	***##	2/13 (15)	111	105/323 (33)	12/16 (75)	***#	1/6 (17)	
Biliary Tract Invasion	2/104 (2)	5/16 (31)	***	1/13 (8)		7/323 (2)	2/16 (13)		0/6 (0)	
Perineural invasion	0/104 (0)	2/15 (13)	*	2/13 (15)	‡	0/323 (0)	1/16 (6)	*	1/6 (17)	‡
Macrotrabecular massive	13/114 (11)	0/13 (0)		0/15 (0)		62/323 (19)	1/16 (6)		0/6 (0)	
Scirrhous pattern	9/117 (8)	3/18 (17)		0/13 (0)		5/319 (2)	0/16(0)		0/6 (0)	
Lymphocytic inflammation	23/110 (21)	11/15 (73)	***##	1/12 (8)		70/323 (22)	8/16 (50)		2/6 (33)	
Boyault transcriptomic class			***##		#			***		
Ğ1	13/118 (11)	14/18 (78)		3/15 (20)	3.0	41/292 (14)	10/16 (63)		1/6 (17)	
G2	17/118 (14)	1/18 (6)		0/15 (0)		46/292 (16)	1/16 (6)		0/6 (0)	
G3	28/118 (24)	1/18 (6)		3/15 (20)		29/292 (10)	0/16 (0)		1/6 (17)	
G4	22/118 (19)	2/18 (11)		9/15 (60)		83/292 (28)	3/16 (19)		3/6 (50)	
G5	21/118 (18)	0/18 (0)		0/15 (0)		17/292 (6)	0/16 (0)		0/6 (0)	
G6	17/118 (14)	0/18 (0)		0/15 (0)		76/292 (26)	2/16 (13)		1/6 (17)	
BAP1 altered	0/118 (0)	18/18 (100)	***###	0/15 (0)		0/323 (0)	16/16 (100)	***###	0/6 (0)	
CTNNB1 mutated	41/118 (35)	1/18 (6)	*	1/15 (7)	‡	92/323 (28)	1/16 (6)		0/6 (0)	
TP53 mutated	47/118 (40)	2/18 (11)	*	0/15 (0)	#	107/323 (33)	3/16 (19)		0/6 (0)	
TERT altered	63/116 (54)	0/17 (0)	***	2/14 (14)	#	89/169 (53)	0/8 (0)	**	2/4 (50)	
DNAIB1-PRKACA fusion	0/118 (0)	0/18 (0)	###	15/15 (100)	##	0/323 (0)	0/16 (0)	###	6/6 (100)	丗

FLC, fibrolamellar carcinoma; HCC, hepatocellular carcinoma.

Wilcoxon test, trend γ^2 test, γ^2 test and Fisher exact test were used respectively for continuous, ordinal, categorical and binary data.

*BAP1 vs. non-BAP1/fusPRKACA; *BAP1 vs. fusPRKACA; ‡fusPRKACA vs. non-BAP1/fusPRKACA. ###, ***, $\ddagger p < 0.001$; ##, **, $\ddagger p < 0.001$. *For the TCGA series, only 1 or 2 slides were available for histological review.

out genes expressed in hepatocytes (the detailed list of genes used for each population is available in Fig. S2).

Immunoblotting

Proteins were extracted from frozen tissues samples using modified Laemmli lysis buffer (50 mM Tris pH = 6.8, 2% SDS, 5% glycerol, 2 mM DTT, 2.5 mM EDTA/EGTA) supplemented with 2x phosphatase and protease inhibitor cocktail (#78444, Thermo Fisher Scientific, Waltham, MA, USA), 2 mM Na₃VO₄ (#P0758S, BioLabs, Ipswich, MA, USA) and 10 mM NaF (#674141, Sigma Aldrich, St. Louis, MO, USA), homogenized by Qiagen TissueLyser II and boiled for 10 min. Protein concentration was measured with the BCA assay kit (Pierce Biotechnology, Rockford, IL, USA). Equal amounts of protein were deposed on polyacrylamide gel (Bio-Rad, Hercules, CA, USA), separated by electrophoresis, transferred on 0.2 µm nitrocellulose membrane (Bio-Rad) and incubated at 4°C with the following primary antibodies: anti-BAP1 (sc-28383 c4, Santa Cruz Biotechnologies, Dallas, TX, USA), anti-PKA-Cα (ab76238, Abcam, Cambridge, UK) and antiPKA-R2 (ab32514, Abcam, Cambridge, UK) at 1:10,000 dilution. Anti-mouse (#7076, Cell Signaling) or anti-rabbit (#7074, Cell Signaling) IgG horseradish peroxidase (HRP) linked secondary antibodies were used at 1:2,000 dilution. Proteins were detected using SuperSignal West Pico Plus kit (#34580, Thermo Fisher Scientific) and the signal was captured by the ChemiDoc XRS system. Quantification was done by measuring the intensity of each band using Image Lab software (Bio-Rad) and normalized by the Ponceau whole lane charge evaluated with Image] software (National Institute of Health, Bethesda, MD, USA).

Immunohistochemistry

Immunohistochemistry was performed on formalin-fixed paraffin-embedded tumor tissues with the Leica Bond automated stainer. The percentage of EpCAM positive tumor cells was assessed in 52 tumors from the LICA-FR series stained with an EpCAM monoclonal antibody (Dako, Santa Clara, California, Clone Ber-Ep4, dilution 1/50). Quantitative scores of infiltration by T cells and B cells were assessed in 41 tumors with antibodies

JOURNAL OF HEPATOLOGY

against CD3 (Dako, Clone F7.2.38, dilution 1/50) and CD20 (Dako, Clone L26, Dilution 1/500) respectively, with a separate estimation of positive cells within the tumor stroma and within the tumor parenchyma.

Statistical analysis

For statistical analysis of gene expression data, R version 3.3.2 (R Development Core Team, R: A language and environment for statistical computing. R Foundation for Statistical Computing, Vienna, http://www.R-project.org) and Bioconductor version 3.4 were used. Wilcoxon, Fisher or χ^2 statistical tests were applied with respect to the type of variable. Survival analysis was performed in patients treated by R0 liver resection (n = 112) as previously described including 5 patients with FLC without good quality RNAseq data available. We assessed overall survival defined by the interval between surgery and death (whatever the cause), and survival curves were represented using the Kaplan-Meier method compared with the Log-Rank test. Univariate analysis was performed using the Cox model. A p value <0.05 was considered significant.

Data availability

The sequencing data of the LICA-FR cohort reported in this paper have been deposited to the EGA (European Genome-phenome Archive) database (RNAseq accession [EGAS00001002879], [EGAS00001001284] and [EGAS00001003837]; WES accessions [EGAS00001000217], [EGAS00001001002], [EGAS00001003063], [EGAS00001000679] and [EGAS00001003837]; WGS accessions [EGAS00001002408], [EGAS00001000706], [EGAS00001002888] and [EGAS00001003837]), through the ICGC (International Cancer Genome Consortium) data access committee. The sequencing data from the TCGA cohort were retrieved from http://www.cbioportal.org/.

Results

FLC and mixed-FLC/HCC cluster into 2 distinct transcriptomic subgroups of tumors

We performed RNA sequencing of 151 liver tumor samples which included 126 HCC, 15 FLC and 10 mixed-FLC/HCC, defined by pathological review (Fig. S1) and with clinical features described in Table 1. Out of 15 FLC, 13 clustered together with 2 mixed-FLC/HCC in a robust subgroup of 15 tumors (Fig. 1). Interestingly, all 15 patients in this cluster were young (age min = 17 years; max = 36 years, mean = 26 years) and all the tumors harbored the DNAJB1-PRKACA fusion (Fig. 1). Six out of the 8 remaining mixed-FLC/HCC clustered in a second group of tumors also including 2 FLC and 9 HCC (Fig. 1). This cluster of 17 tumors highly enriched

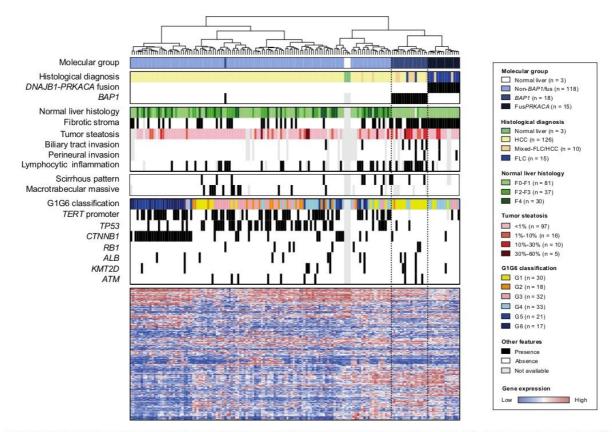


Fig. 1. FLC cluster together and are divided between BAP1-driven and DNAJB1-PRKACA-driven tumors. Hierarchical clustering based on the expression of the 5,000 genes with the higher variability in RNAseq analysis of 151 liver tumors and 3 non-tumor-liver samples. The top heatmaps show clinical, histological and molecular annotation of the samples, while the lower heatmap shows the expression pattern of the 5,000 genes. FLC, fibrolamellar carcinoma; RNAseq, RNA sequencing. (This figure appears in color on the web.)

Table 2. Detailed BAP1 alterations in the 18 patients from the LICA-FR series.

Case #	Gender	Age	Histological Diagnosis	Etiology / background	Non-tumor liver	BAP1 genomic alteration (GRCh37, chr3)	BAP1 protein change	BAP1 copy number variation
#794Ta	M	73	HCC	Hemochromatosis	F0-F1	52443600del	E31fs	Focal del
#1010T	F	53	HCC	Alcohol	FO-F1	52436869_52436870delinsAA	K637*	Focal del
#3894T	M	56	HCC	Alcohol	F0-F1	52443876C>A	E7*	Focal del
#3907T	M	39	HCC	Alcohol	FO-F1	52441270del	A167fs	Focal del
#2135T	F	57	HCC	Alcohol / HBV / NASH	F0-F1	52441301del + 52436304T>G	N157fs + *730C	
#2211T	F	37	HCC	Chronical intrahepatic obstructive cholestasis	F0-F1	52439814_52439830del	VLEANR295fs ^b	Focal del
#228T	M	48	HCC	Without etiology	F0-F1	52440294_52440295insTT	Q253fs	Focal del
#1182T	F	51	HCC	Without etiology	F0-F1	52442618_52442627del	PA42fs (splice)	large del
#800T	M	73	HCC	Without etiology	F2-F3	52441229del	F181fs	Chr3p del
#141T	F	67	HCC	Without etiology	F0-F1	52441252T>C	Y173C	Focal del
#412T	F	51	FLC	n.a.				Homozygous del
#411T	F	65	FLC	Alcohol	FO-F1			Homozygous del
#3919T	F	54	mixed-FLC/HCC	n.a.	F0-F1	Inversion (3;3)	Frameshift fusion	Focal del
#4211T	F	40	mixed-FLC/HCC	Without etiology	FO-F1	Translocation t(2;3)	Frameshift fusion	Chr3p del
#026T	F	38	mixed-FLC/HCC	Without etiology	F0-F1	52439136del	P370fs ^b	Focal del
#255T	F	39	mixed-FLC/HCC	Without etiology	F0-F1	52441473T>C + 52443758G>A	K127E + G13G (splice)	Focal del
#187T	M	27	mixed-FLC/HCC	Without etiology	F0-F1	52441991_52441992del	K120fs ^b	Focal del
#906T	F	50	mixed-FLC/HCC	NASH	FO-F1	52443580del	K38fs	Focal del

F0-F1: no fibrosis; F2-F3: mild fibrosis; F4: cirrhosis.

FLC, fibrolamellar carcinoma; HCC, hepatocellular carcinoma; NASH, non-alcoholic steatohepatitis; n.a., not available.

in mixed-FLC/HCC was located in proximity to the FLC cluster, but patients were older (age min = 27 years; max = 73 years, mean = 51 years) including the 2 FLC that developed at 51 years and 65 years. Interestingly all 17 of these tumors lacked the *DNAJB1-PRKACA* fusion but showed alterations in the *BAP1* gene. Only 1 HCC mutated for *BAP1* (#794T), without FLC features, was outside this FLC/HCC cluster. Finally, only 2 mixed-FLC/HCC, not mutated for *BAP1* nor harboring *DNAJB1-PRKACA* fusion, were distributed outside the 2 clusters (Fig. 1).

In agreement with the tumor suppressor function of BAP1 in various tumor types, ^{16,34–37} BAP1 alterations were predicted to inactivate the gene either by somatic mutations (9 frameshift, 2 nonsense, 1 splice site, 2 missense and 1 nonstop), by gene fusion in 2 cases (DAG1-BAP1 in #3919T and a complex event leading to both BAP1-LINCO1460 and RAB3GAP1-BAP1 fusions in #4211T, see Fig. S3), or by homozygous deletion in 2 tumors (Table 2). In all tumors, BAP1 alterations were biallelic with 2 mutations in 1 case (#2211T) or a deletion of the second allele of BAP1 (Table 2).

Since no FLC carrying the *DNAJB1-PRKACA* fusion showed *BAP1* alterations, we define 3 distinct groups of tumors: altered for *BAP1* (BAP1 tumors), with *DNAJB1-PRKACA* fusion (fusPRKACA tumors) or without either alterations (non-BAP1/fusPRKACA tumors), as represented in Fig. 1 (Molecular group annotation).

BAP1 altered hepatocellular carcinomas show distinct clinical and histological features

In our cohort (LICA-FR), patients with BAP1 tumors (n = 18) were younger (median 51 years) than patients with non-BAP1/fusPRKACA tumors (n = 118, median 64 years, p = 0.006) but older than patients with fusPRKACA tumors (n = 15, median 26 years, p = 3.3e-6, Fig. 2A). Compared to non-BAP1/fusPRKACA tumors, BAP1 tumors were more frequent in females (67% vs. 19%, p = 9.7e-5), in non-fibrotic liver (F0-F1), and in patients without known etiologies of HCC (50% vs. 12%, p = 0.0008, Fig. 2C-E and Table 1). Patients with BAP1 tumors had similar overall survival as those with non-BAP1/fusPRKACA HCC, whereas patients with fusPRKACA HCC had a better prognosis

(*p* = 0.02 in log-rank test, Fig. 2B). All of these clinical relations, except younger age, were also found in the TCGA cohort that included 16 BAP1 tumors and 6 fusPRKACA tumors out of 345 HCC (Fig. 2A-E and Table 1). Of note, a 67-year-old female patient in TCGA harbored both a *DNAJB1-PRKACA* fusion and a *BAP1* mutation in the tumor and was excluded from the statistical analysis.

BAP1 tumors were enriched in mixed-FLC/HCC (6 out of 18), characterized by an abundant fibrous stroma (72%), intratumor steatosis (67%), biliary tract invasion (31%), perineural invasion (13%), and a high lymphocytic infiltration (73%) (Fig. 1 & 2F-J, Table 1). Tertiary lymphoid structures were frequently identified in BAP1 tumors (70%) ranging from simple aggregate up to secondary follicles harboring a clear germinal center as previously described in HCC²⁰ (Fig. 2K). The MCP-counter method³³ applied to RNAseq data showed a high component of the microenvironment in BAP1 tumors, enriched in T and B lymphocytes, endothelial cells and myeloid dendritic cells when compared with non-BAP1/fusPRKACA tumors (Fig. 2L, Fig. S2). In accordance with these results, CD3 immunohistochemistry revealed a higher infiltration of T cells in the stroma of BAP1 tumors compared to non-BAP1/fusPRKACA tumors (Fig. 2M,N). Infiltrated CD20+ B cells were also observed within BAP1 tumors but in levels comparable to non-BAP1/fusPRKACA HCC (Fig. 20 and Fig. S2). In the TCGA cohort, we confirmed that BAP1 tumors were highly fibrous, steatotic, enriched in perineural invasion and with frequent lymphocytic infiltration organized in tertiary lymphoid structures (Fig. 2F-K and Table 1).

BAP1 tumors demonstrate a specific genomic profile with frequent *PRKACA* gain and *PRKAR2A* deletion

Analysis of the profile of gene mutations and chromosome alterations in BAP1 tumors showed a significant exclusion from alterations in the 3 most frequent drivers of HCC, namely *TERT* promoter, *CTNNB1* and *TP53*²² (Fig. 1 and Table 1). This exclusion was confirmed in the TCGA cohort and also observed in *DNAJB1-PRKACA* fusion tumors (Fig. 1 and Table 1). In contrast, BAP1

^aOf note, patient #794T was found outside the cluster of 17 BAP1 altered tumors (Fig. 1) but was later included in the group of BAP1 tumors for further analysis. ^b3 mutations were not detected in the first analysis of whole exome sequencing data but were later identified in target sequencing of BAP1 with a higher depth.

JOURNAL OF HEPATOLOGY

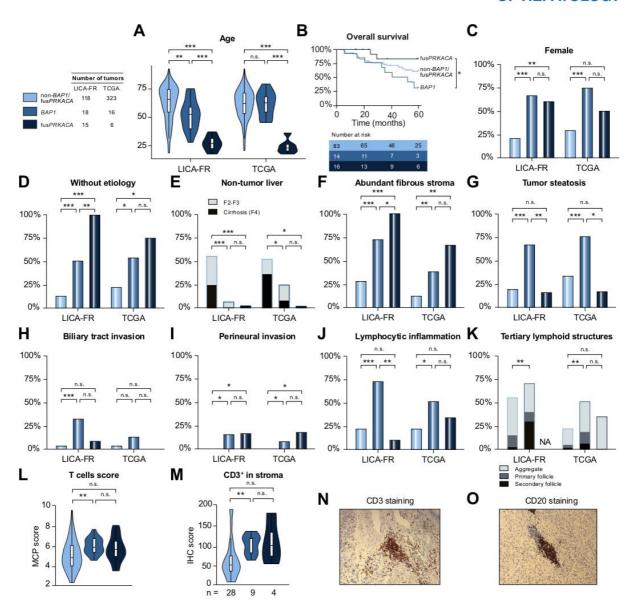


Fig. 2. Clinical and histological features of BAP1, fusPRKACA and non-BAP1/fusPRKACA tumors. (A) Distribution of age at surgery. (B) Kaplan-Meier plot showing the overall survival in the LICA-FR series. (C-E) Repartition of female gender (C), absence of liver disease etiology (D) and non-tumor liver histology (F2-F3: mild fibrosis; F4: cirrhosis) (E). (F-K) Histological review of abundant fibrous stroma (F), tumor steatosis (G), biliary tract invasion (H), perineural invasion (I), lymphocytic inflammation (J) and tertiary lymphoid structures (K). (L) T cell score calculated with the MCP-counter method applied to RNAseq data of the LICA-FR series. (M) Quantification of T cell abundance in tumor stroma with immunohistochemistry in a subset of tumors from the LICA-FR series. (N, O) Representative images of CD3 (N) and CD20 (O) staining in BAP1 tumors (#411T and #412T respectively), showing the aggregation of T and B cells within aggregate type tertiary lymphoid structures. Wilcoxon test, trend χ² test, Fisher exact test and Log-rank test were used respectively for continuous (A, L), ordinal (C, K), binary (B, D, F-J) and survival data (E): ****p <0.001, **p <0.05. MCP, microenvironment cell population; RNAseq, RNA sequencing. (This figure appears in color on the web.)

tumors were slightly enriched in *RB1*, *KMT2D*, *ATM* and *ALB* mutations (n = 3 for each gene, Fig. 1) but these associations did not reach significance.

In order to find alternative driver events associated with *BAP1* alterations in HCC, we compared the frequency of copy number alterations between the 3 molecular groups of tumors. In 15 out

of the 18 BAP1 tumors (83%) we identified a specific recurrent chromosome gain at the 19p13 locus centered on the *PRKACA* gene found in only 6% of the non-BAP1/fusPRKACA tumors (p = 3e-12) and in none of the fusPRKACA tumors (Fig. 3A-B). In addition, deletions at chromosome 3p21 identified in the BAP1 tumors encompassed both *BAP1* and *PRKAR2A* (coding for

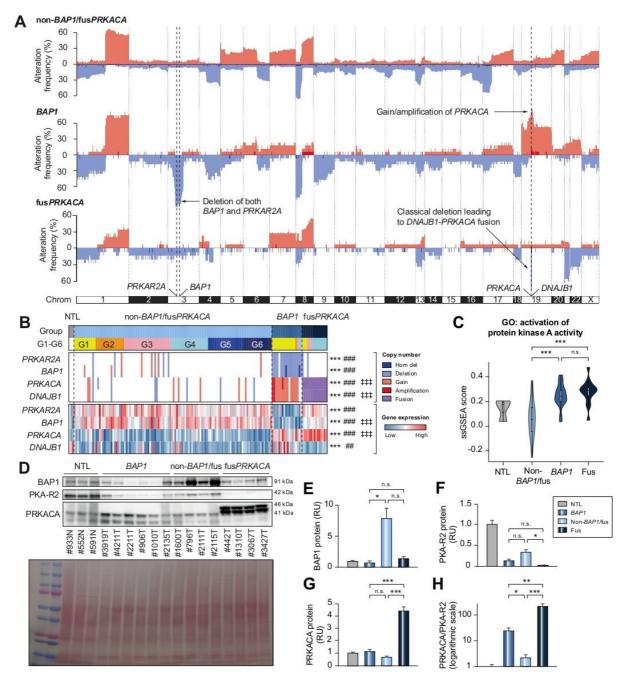


Fig. 3. Alternative copy number alterations activate the PKA pathway in BAP1 tumors. (A) Frequency of copy number alterations in the 3 molecular groups of HCC. (B) Heatmap representation of copy number alterations and relative gene expression for PRKAR2A, BAP1, PRKACA and DNAJB1 assessed by RNAseq. Statistical comparisons with exact Fisher test (copy number alterations) and Wilcoxon test (gene expression): "BAP1 vs. non-BAP1/fusPRKACA, #BAP1 vs. fusPRKACA, son-BAP1/fusPRKACA, (C) Comparison of single sample GSEA scores for the gene set GO: Activation of PKA activity between the 3 molecular groups of tumors. (D) Western-blot of BAP1, PKA-R2 and PRKACA in normal liver samples (NTL, n = 3) and in different liver tumors: BAP1 (n = 6), non-BAP1/fusPRKACA (n = 4), fusPRKACA (n = 4). In fusPRKACA tumors, the higher mass of the bands stained by the PRKACA antibody corresponds to the already described DNAJB1-PRKACA chimeric protein. Bottom image represents Ponceau coloration. (E-H) Quantification of protein expression of BAP1 (E), PKA-R2 (F), PRKACA (G) and of relative PKA activation measured by the ratio between PRKACA and PKA-R2 (H), compared with Wilcoxon test. ***, ###, $\frac{11}{12}$ p <0.001; **, ## p <0.01; *p <0.05. GO, gene ontology; GSEA, gene-set enrichment analysis; HCC, hepatocellular carcinoma; NTL, non-tumor liver; RNAseq, RNA sequencing. (This figure appears in color on the web.)

JOURNAL OF HEPATOLOGY

PKA-R2a, a negative regulatory subunit of the cAMP-dependent protein kinase PKA) genes distant by 3.5 Mb (94% vs. 4% in non-BAP1/fusPRKACA tumors, p = 2e-16, Fig. 3A-B and Fig. S4). In agreement with these findings, RNAseq data showed significantly lower PRKAR2A and higher PRKACA gene expression in BAP1 tumors compared to non-BAP1/fusPRKACA tumors and these results were confirmed at the protein level (Fig. 3B,D-F). A significantly increased ratio of PRKACA to PKA-R2 proteins, reflecting PKA activity, was monitored in both BAP1 and fusPR-KACA groups of tumors compared to non-BAP1/fusPRKACA HCC (Fig. 3H). Accordingly, PKA activity assessed by single sample GSEA was increased in both BAP1 and fusPRKACA tumors (Fig. 3C). These results suggest that like FLC with DNAJB1-PRKACA fusion, the PKA pathway is activated in BAP1 tumors but via an alternative mechanism associated with PRKACA chromosome gains and PRKAR2A deletions (Fig. S4).

BAP1 and fusPRKACA tumors share common proliferation and differentiation programs, distinct from other hepatocellular tumors

At the transcriptomic level, 78% of the BAP1 tumors were classified in the G1 subgroup of HCC, known to be associated with progenitor features, 17,28 compared to only 11% of the non-BAP1/fusPRKACA tumors (p=9.5e-9) and 20% of the fusPRKACA FLC and these results were confirmed in TCGA (63% vs. 14%, p=7.0e-5, Table 1). Single sample GSEA revealed that BAP1 and fusPR-KACA tumors were highly enriched for stem cell and neuronal features, vasculature development, extracellular matrix and epithelial-mesenchymal transition compared to non-BAP1/fusPRKACA HCC (Fig. 4A). FusPRKACA tumors appeared to be less proliferative than non-BAP1/fusPRKACA tumors, as illustrated by lower levels of cell cycle genes such as *CCNB1*, *PCNA* or *BIRC5*, while the tendency toward lower proliferation in BAP1 tumors did not reach significance (Fig. 4B).

Interestingly, expression of the 3 TGF- β ligands was increased in both BAP1 and fusPRKACA tumors (Fig. 4B), together with an enrichment in the signature of TGF- β signaling in fibroblasts (Plasari TGFb1 Targets 10hr Up, Fig. 4A). In contrast, a signature of TGF- β activation in hepatocytes defined by Coulouarn *et al.* ³⁸ was not retrieved in BAP1 nor fusPRKACA tumors, suggesting that activation of the TGF- β pathway in fibroblasts but not in tumor hepatocellular cells could be at the root of the fibrotic phenotype in both groups of tumors.

In accordance with the enrichment in stem cell features detected by GSEA, BAP1 and fusPRKACA tumors shared high expression of hepatic stem cell genes such as EPCAM, VIM or THY1 (CD90) (Fig. 4B). Immunohistochemistry performed on a subset of tumors confirmed the higher percentage of EpCAMpositive progenitor cells within both BAP1 tumors and fusPR-KACA tumors while this staining was absent in most non-BAP1/ fusPRKACA tumors (Fig. 4C, D). Furthermore, we also monitored high expression of markers of the common hepato-pancreatic progenitor^{39,40} such as PDX1 or SOX17 (Fig. 4B), 2 markers which have previously been detected by immunohistochemistry in most FLC samples.5 Among the differentiation markers, we observed a significant decrease of hepatocyte-specific genes ALB, PROX1 or HNF4A and a significant increase of cholangiocytespecific gene KRT7 in fusPRKACA compared to BAP1 or non-BAP1/fusPRKACA tumors (Fig. S5). Also, several markers of pancreatic lineage were overexpressed in BAP1 and/or fusPR-KACA tumors, but at various levels in the 2 groups of tumors. For instance, among the pancreatic markers, high expression of PDX1, PAX6, PAK3, and MNX1 was identified in BAP1 and fusPR-KACA tumors while NEUROG3 (NGN3), INSM1 (IA-1), PTF1A, TRIM50, GP2 and TGIF2 overexpression was restricted to BAP1 tumors and only fusPRKACA tumors overexpressed the pancreatic/neuroendocrine gene PCSK1 (Fig. 4B and Fig. S5). Other neuroendocrine genes such as CALCA, NTS, DNER or SSTR5 were overexpressed with different patterns in the 2 groups of tumors (Fig. S5). Moreover, we observed a high expression of genes coding for proteins involved in neural infiltration and guidance, such as neuron guide molecules (NGF, NTF3, BDNF) and their binding receptors expressed on neurons (TrkA-C (NTRK1-3) and p75NTR (NFGR), Fig. S5), possibly accounting for the enrichment in perineural invasion in both BAP1 and fusPRKACA tumors (Fig. 21). In line with a possible neural infiltration, other neuron expressed receptors such as UNC5A-D were found significantly overexpressed in BAP1 or fusPRKACA tumors (Fig. S5).

Lastly, the higher expression of the hepato-pancreatic progenitor marker PDX1 and the lack of expression of pancreatic-committed progenitor markers such as IA-1 or PTF1A in fusPR-KACA compared to BAP1 tumors, suggest a hepato-pancreatic progenitor-like program in fusPRKACA tumors and a more pancreatic-engaged program in BAP1 tumors (Fig. 4B and Fig. 5).

Discussion

In this study, we showed that BAP1 alterations delineate a specific subgroup of HCC with common clinical, histological and molecular features (Fig. 5A). BAP1 is a deubiquitinating enzyme active in both the cytosol, where it controls the stability of different proteins, and in the nucleus, where it targets H2A histones as part of the polycomb group repressive deubiquitinase complex, which is involved in development and stem cell pluripotency. 41,42 BAP1 is described as a tumor suppressor since it is lost in different tumors including cholangiocarcinoma (around 25%) and HCC (around 5%).16,34-37 However BAP1 was recently shown to also have an anti-apoptotic role in the liver, 42 which could explain our observation of an increased expression of BAP1 in HCC compared to normal liver (Fig. 3B,D-E). Here, we found that the BAP1 tumors include most of the mixed-FLC/HCC tumors and show several clinical and histological similarities with the classical FLC together with a common PKA pathway activation.

Fibrolamellar features in liver tumors are already known to be related to PKA activation through 3 different mechanisms: (i) the *DNAJB1-PRKACA* fusion in FLC,⁶ (ii) inactivating mutations in *PRKAR1A* in rare FLC developed in Carney complex patients⁷ and (iii) activating mutations in *GNAS* (leading to production of cAMP and subsequent activation of PKA) identified in rare hepatocellular adenomas characterized by fibrolamellar-like patterns.⁴³ Here, we discovered a fourth mechanism of PKA activation in BAP1 tumors resulting from recurrent gains of *PRKACA* and deletions of *PRKAR2A*, encoding respectively a catalytic subunit and an inhibitory regulatory subunit of PKA, with consequences at the mRNA and protein levels (Fig. 3 and Fig. S4).

An important characteristic of the *DNAJB1-PRKACA* and BAP1 tumors is their age distribution starting with FLC in the second and third decade, then BAP1 HCC occurring before non-BAP1/fusPRKACA HCC (Fig. 5A). This gradient could be related to the cell of origin of the malignant transformation since FLC has been proposed to originate from the biliary tree stem cell,⁵ a recently discovered hepato-pancreatic progenitor,^{39,40} in agreement with

Research Article

Hepatic and Biliary Cancer

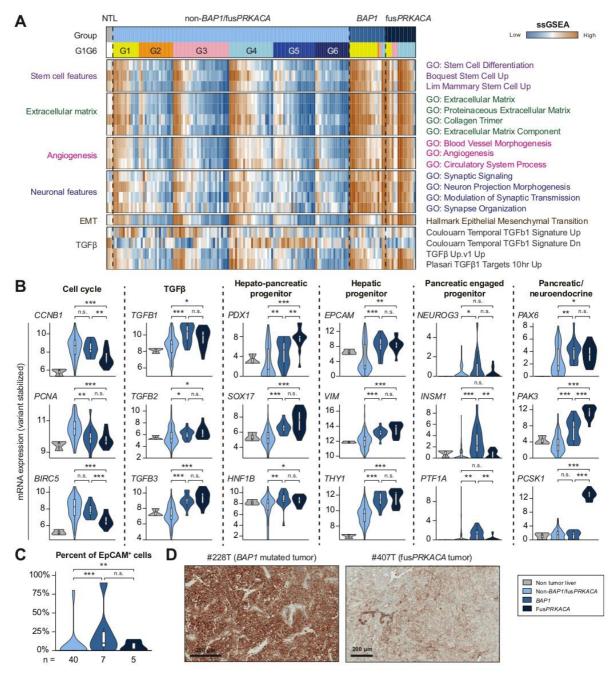


Fig. 4. Transcriptomic characterization of BAP1 and fusPRKACA tumors. (A) Heatmap of single sample GSEA for 3 normal liver samples and the different molecular groups of liver tumors ordered by G1-G6 classes. (B) RNAseq expression of representative cell cycle genes, TGFβ ligands as well as representative markers of the different progenitors found in the hepato-pancreatic lineage and of pancreatic / neuroendocrine markers. (C) Immunohistochemistry reveals a higher percentage of EpCAM positive tumor cells in both BAP1 and fusPRKACA tumors. (D) Representative images of EpCAM staining show the lighter staining in fusPRKACA tumors compared to BAP1 tumors. Wilcoxon test: ****p <0.001, **p <0.01, **p <0.05. GSEA, gene-set enrichment analysis. (This figure appears in color on the web.)

the hepato-pancreatic progenitor phenotype we identified in both fusPRKACA and BAP1 tumors (Fig. 5B). BAP1 loss may promote a dedifferentiation towards a progenitor phenotype since BAP1 silencing in the Huh7 HCC cell line induces an

increase in stemness marker expression, e.g. EPCAM or PROM1.⁴⁴ Similarly, CRISPR-based loss of BAP1 in human liver organoids increases the expression of progenitor markers while reducing markers of liver function and ultimately epithelial homeostasis,

JOURNAL OF HEPATOLOGY

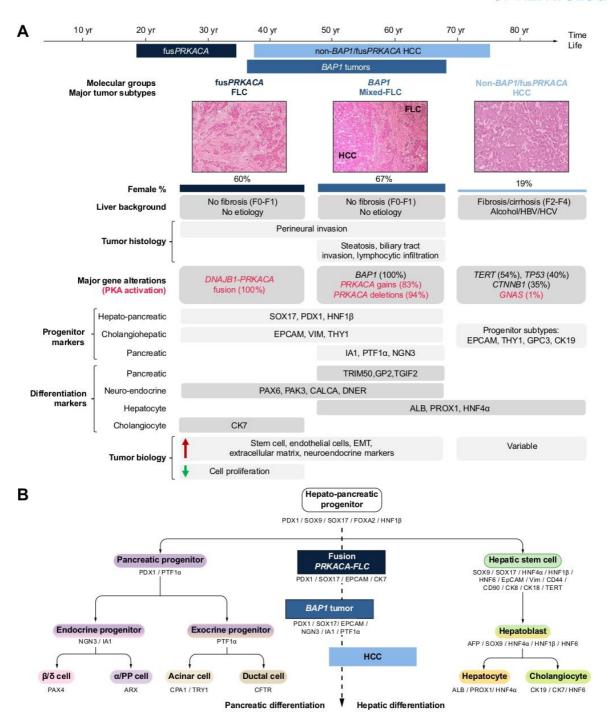


Fig. 5. Summarized characteristics of fusPRKACA and BAP1 tumors compared to non-BAP1/fusPRKACA HCC and relation to the common hepato-pancreatic lineage. (A) A recap of the most significant results in terms of histological, clinical and molecular features was represented. Age was represented from the 1st to 9th deciles. (B) Schematic differentiation program from the common hepato-pancreatic progenitor, adapted from Lanzoni *et al.*⁴⁰ FusPRKACA FLC are thought to be directly derived from hepato-pancreatic progenitors found in the young liver while BAP1 tumors have a more pancreatic-engaged program. FLC, fibrolamellar carcinoma; HCC, hepatocellular carcinoma. (This figure appears in color on the web.)

Research Article

Hepatic and Biliary Cancer

possibly via a direct regulation of transcription by BAP1 through its known role in the polycomb deubiquitinase complex. ⁴² In the TCGA cohort, the unique patient with HCC harboring both *DNAJB1-PRKACA* fusion and *BAP1* inactivation was old (67 years old), suggesting that the progenitor phenotype induced by BAP1 loss could be required for the oncogenic effect of PKA activation in an old liver. This is in line with our observation of a cooccurrence of BAP1 inactivation and PKA activation through copy number alterations. Remarkably, 2 independent teams recently reported the presence of *DNAJB1-PRKACA* fusions in rare pancreatic and biliary neoplasms, thus reinforcing the link between the oncogenic activation of PKA and the hepatopancreatic progenitor lineage, while challenging the exclusivity between FLC and the *DNAJB1-PRKACA* fusion. ^{45,46}

Of note, HCC usually lacks lymph node involvement or perineural invasion, commonly found in other epithelial tumors such as pancreatic adenocarcinomas^{47,48} or cholangiocarcinoma.^{49,50} Conversely, there is a high rate of lymph node metastasis in FLC (up to 70%)⁵¹ and here we identified an enrichment of perineural invasion in BAP1 and fusPRKACA tumors across the 2 series (Table 1). This enrichment could be a consequence of the overexpression of genes encoding neuron guide molecules (*NGF*, *NTF3*, *BDNF*) that allow the recruitment and growth of neurons expressing axonal guidance receptors (TrkA-C, p75NTR, UNC5A-D, see Fig. S5).

Strikingly, BAP1 tumors are never mutated in the *TERT* promoter (in both LICA-FR and TCGA cohort) while this alteration is found in 30–60% of HCC.^{16,52} This could also be a consequence of the progenitor state of the tumor cells associated with BAP1 loss, since *in vitro* experiments suggest that *BAP1* overexpression can repress *TERT* transcription⁵³ and progenitors cells are supposed to maintain their telomeres throughout replication without requiring mutations. This would also explain the exclusion between *DNAJB1-PRKACA* fusion and *TERT* alteration, following the hypothesis that the cell of origin of FLC is a progenitor.⁵

While it has been suggested that endocrine/pancreatic features were specific of FLC and not found in mixed-FLC/HCC, ¹³ here we show that both fusPRKACA and BAP1 tumors express high levels of neuroendocrine and pancreatic markers but with different patterns (Fig. S5). These different profiles of expression could reflect different stages of differentiation along the hepatopancreatic lineage in the 2 groups of tumors, as a consequence of their different cell of origin, as discussed above (Fig. 5B). Moreover, an association between neuroendocrine features and abundant fibrous stroma has already been described. ⁵⁴

Interestingly, BAP1 mutations are recurrently identified in several tumor types including uveal or cutaneous melanoma, mesothelioma, renal cell carcinoma, mesothelioma and lung cancers.55 In 2013, a pan-cancer study defined a typical morphology of BAP1-mutated cells as "rounded or polygonal cell shape with abundant amphophilic or eosinophilic cytoplasm". Interestingly, these features are also retrieved in FLC1,4 as well as in BAP1 liver tumors (in both FLC and HCC components). This, along with the abundant fibrous stroma, hinders the distinction between BAP1 and fusPRKACA tumors based solely on histology in our cohort of tumors and in other reports. 13,57 These observations argue for the use of molecular characterization to distinguish BAP1 tumors not only from the fusPRKACA FLC but also from scirrhous HCC, another type of highly fibrous liver tumor usually not mutated in BAP1 (Fig. 1 and Table 1). However, it is worth noting that the detection of BAP1 mutations is

challenging due to the high level of stromal contamination: in our series, 3 out of the 15 *BAP1* mutations were not found at first in the analysis of whole exome data, but were later detected in target sequencing of *BAP1* with a higher depth.

From a clinical perspective, our observations of similarities between fusPRKACA and BAP1 tumors may be in favor of developing common therapeutic strategies. Indeed, the overactivation of PKA in both groups of tumors argues that potential future treatments targeting PKA, if successful in FLC, could be repositioned to also combat BAP1 tumors. From a therapeutic perspective, the 2 groups of tumors could benefit from antiangiogenic drugs such as sorafenib58 due to their common enrichment in markers of angiogenesis and endothelial cells (Fig. 4A and Fig. S2). Of note, a link between BAP1 alterations and angiogenesis was also recently described in uveal melanoma.51 Finally, as BAP1 HCC are highly infiltrated by lymphocytes (Fig. 2J), a feature also described in BAP1-mutated peritoneal mesothelioma,60 they can be considered as good candidates for immunotherapy. Of note, despite this higher lymphocytic infiltration, we did not monitor a difference in the tumor mutational burden of BAP1 tumors compared to non-BAP1/fusPRKACA tumors, while both groups of tumors had more mutations than fusPRKACA tumors (Fig. S2B).

In conclusion, we characterized a new molecular subgroup of HCC, driven by *BAP1* loss of function and PKA activation in the context of hepato-pancreatic progenitor de-differentiation, associated with a specific pathological subtype of tumors, including abundant fibrous stroma, steatosis, lymphocyte infiltration, perineural and biliary tract invasion, which develop mainly in female patients without cirrhosis or chronic liver disease.

Abbreviations

AUC, area under the ROC curve; *BAP1*, *BRCA1*-associated protein 1; FLC, fibrolamellar carcinoma; GO, gene ontology; GSEA, geneset enrichment analysis; HCC, hepatocellular carcinoma; MCP, microenvironment cell populations; NASH, non-alcoholic steatohepatitis; NTL, non-tumor liver; PKA, cAMP-dependent protein kinase; RNAseq, RNA-sequencing; WES, whole-exome sequencing; WGS, whole-genome sequencing.

Financial support

This work was supported by Institut National du Cancer (INCa) with the International Cancer Genome Consortium (ICGC LICA-FR project), INSERM with the « Cancer et Environnement » (plan Cancer), MUTHEC projects (INCa), and the HTE consortium, HetCoLi (plan Cancer). The group is supported by the Ligue Nationale contre le Cancer (Equipe Labellisée), Labex Oncolmmunology (investissement d'avenir), Coup d'Elan de la Fondation Bettencourt-Shueller, the SIRIC CARPEM, FRM prix Rosen, Ligue contre le cancer comité de Paris (prix René et André Duquesne) and Fondation Mérieux.

Conflict of interest

The authors declare no conflicts of interest that pertain to this work.

Please refer to the accompanying ICMJE disclosure forms for further details.

Authors' contributions

Study concept and design: JZR, TZH, AN. Acquisition of data: JZR, TZH, AN, BG, SC, BN, GC, QB, LM, GM, JYC, JFB, GA, JCN, PBS, MZ,

JOURNAL OF HEPATOLOGY

AB, VP, JC, SI. Analysis and data interpretation: TZH, AN, SC, QB, LM, JZR. Manuscript writing: JZR, TZH, AN and all. Obtained funding: JZR.

Acknowledgments

We warmly thank the team UMR-1138 for all the advice and support in particular Sandra Rebouissou and Eric Letouzé for helpful scientific discussions, Eric Trepo for the help in bioinformatics, Camille Péneau and Jie Yang for experimental help. A special thanks to all the clinician, surgeon, pathologist, hepatologist and oncologist who contributed to the tissue collection and clinical annotations within the GENTHEP network. T.Z.H. was supported by a fellowship from Cancéropole lle de France and Fondation d'Entreprise Bristol-Myers Squibb pour la Recherche en Immuno-Oncologie, SC was funded by CARPEM and the Labex Oncolmmunology, AN was funded by the Labex Oncolmmunology, QB and LM were funded by a FRM and MRESI fellowships.

Supplementary data

Supplementary data to this article can be found online at https://doi.org/10.1016/j.jhep.2019.12.006.

References

Author names in bold designate shared co-first authorship

- Craig JR, Peters RL, Edmondson HA, Omata M. Fibrolamellar carcinoma of the liver: a tumor of adolescents and young adults with distinctive clinico-pathologic features. Cancer 1980;46:372–379.
- [2] Edmondson HA. Differential diagnosis of tumors and tumor-like lesions of liver in infancy and childhood. AMA J Dis Child 1956;91:168–186.
- [3] Kassahun WT. Contemporary management of fibrolamellar hepatocellular carcinoma: diagnosis, treatment, outcome, prognostic factors, and recent developments. World J Surg Oncol 2016;14:151.
- [4] Lin C-C, Yang H-M. Fibrolamellar carcinoma: a concise review. Arch Pathol Lab Med 2018;142:1141–1145.
- [5] Oikawa T, Wauthier E, Dinh TA, Selitsky SR, Reyna-Neyra A, Carpino G, et al. Model of fibrolamellar hepatocellular carcinomas reveals striking enrichment in cancer stem cells. Nat Commun 2015;6:8070.
- [6] Honeyman JN, Simon EP, Robine N, Chiaroni-Clarke R, Darcy DG, Lim IIP, et al. Detection of a recurrent DNAJB1-PRKACA chimeric transcript in fibrolamellar hepatocellular carcinoma. Science 2014;343:1010–1014.
- [7] Graham RP, Lackner C, Terracciano L, González-Cantú Y, Maleszewski JJ, Greipp PT, et al. Fibrolamellar carcinoma in the Camey complex: PRKAR1A loss instead of the classic DNAJB1-PRKACA fusion. Hepatology 2018;68: 1441–1447.
- [8] Nault J-C, Martin Y, Caruso S, Hirsch TZ, Bayard Q, Calderaro J, et al. Clinical impact of genomic diversity from early to advanced hepatocellular carcinoma. Hepatology 2020;71(1):164–182.
- [9] Nakamura H, Arai Y, Totoki Y, Shirota T, Elzawahry A, Kato M, et al. Genomic spectra of biliary tract cancer. Nat Genet 2015;47:1003–1010.
- [10] Malouf G, Falissard B, Azoulay D, Callea F, Ferrell LD, Goodman ZD, et al. Is histological diagnosis of primary liver carcinomas with fibrous stroma reproducible among experts? J Clin Pathol 2009;62:519–524.
- [11] Malouf GG, Brugières L, Le Deley MC, Faivre S, Fabre M, Paradis V, et al. Pure and mixed fibrolamellar hepatocellular carcinomas differ in natural history and prognosis after complete surgical resection. Cancer 2012;118: 4981–4990.
- [12] Calderaro J, Ziol M, Paradis V, Zucman-Rossi J. Molecular and histological correlations in liver cancer. J Hepatol 2019;71:616–630.
- [13] Malouf GG, Job S, Paradis V, Fabre M, Brugières L, Saintigny P, et al. Transcriptional profiling of pure fibrolamellar hepatocellular carcinoma reveals an endocrine signature. Hepatology 2014;59:2228–2237.
- [14] Malouf GG, Tahara T, Paradis V, Fabre M, Guettier C, Yamazaki J, et al. Methylome sequencing for fibrolamellar hepatocellular carcinoma depicts distinctive features. Epigenetics 2015;10:872–881.
- [15] Nault JC, De Reyniès A, Villanueva A, Calderaro J, Rebouissou S, Couchy G, et al. A hepatocellular carcinoma 5-gene score associated with survival of patients after liver resection. Gastroenterology 2013;145:176–187.

- [16] Ally A, Balasundaram M, Carlsen R, Chuah E, Clarke A, Dhalla N, et al. Comprehensive and integrative genomic characterization of hepatocellular carcinoma. Cell 2017;169:1327–1341.e23.
- [17] Calderaro J, Couchy G, Imbeaud S, Amaddeo G, Letouzé E, Blanc J-F, et al. Histological subtypes of hepatocellular carcinoma are related to gene mutations and molecular tumour classification. J Hepatol 2017;67:727– 738.
- [18] Ziol M, Poté N, Amaddeo G, Laurent A, Nault J-C, Oberti F, et al. Macro-trabecular-massive hepatocellular carcinoma: a distinctive histological subtype with clinical relevance. Hepatology 2018;68:103–112.
- [19] Murakami J, Shimizu Y, Kashii Y, Kato T, Minemura M, Okada K, et al. Functional B-cell response in intrahepatic lymphoid follicles in chronic hepatitis C. Hepatology 1999;30:143–150.
- [20] Calderaro J, Petitprez F, Becht E, Laurent A, Hirsch TZ, Rousseau B, et al. Intra-tumoral tertiary lymphoid structures are associated with a low risk of early recurrence of hepatocellular carcinoma. J Hepatol 2019;70: 58–65.
- [21] Guichard C, Amaddeo G, Imbeaud S, Ladeiro Y, Pelletier L, Maad IB, et al. Integrated analysis of somatic mutations and focal copy-number changes identifies key genes and pathways in hepatocellular carcinoma. Nat Genet 2012;44:694–698.
- [22] Schulze K, Imbeaud S, Letouzé E, Alexandrov LB, Calderaro J, Rebouissou S, et al. Exome sequencing of hepatocellular carcinomas identifies new mutational signatures and potential therapeutic targets. Nat Genet 2015;47:505–511.
- [23] Popova T, Manié E, Stoppa-Lyonnet D, Rigaill G, Barillot E, Stern MH. Genome Alteration Print (GAP): a tool to visualize and mine complex cancer genomic profiles obtained by SNP arrays. Genome Biol 2009;10:R128.
- [24] Bayard Q, Meunier L, Peneau C, Renault V, Shinde J, Nault J-C, et al. Cyclin A2/E1 activation defines a hepatocellular carcinoma subclass with a rearrangement signature of replication stress. Nat Commun 2018;9:5235.
- [25] Kim D, Pertea G, Trapnell C, Pimentel H, Kelley R, Salzberg SL. TopHat2: accurate alignment of transcriptomes in the presence of insertions, deletions and gene fusions. Genome Biol 2013;14:R36.
- letions and gene fusions. Genome Biol 2013;14:R36.

 [26] Anders S, Pyl PT, Huber W. HTSeq-a Python framework to work with high-throughput sequencing data. Bioinformatics 2015;31:166–169.
- [27] Love MI, Huber W, Anders S. Moderated estimation of fold change and dispersion for RNA-seq data with DESeq2. Genome Biol 2014;15:550.
- [28] Boyault S, Rickman DS, De Reyniès A, Balabaud C, Rebouissou S, Jeannot E, et al. Transcriptome classification of HCC is related to gene alterations and to new therapeutic targets. Hepatology 2007;45:42–52.
- alterations and to new therapeutic targets. Hepatology 2007;45:42–52. [29] Calderaro J, Meunier L, Nguyen CT, Boubaya M, Caruso S, Luciani A, et al. ESM1 as a marker of macrotrabecular-massive hepatocellular carcinoma. Clin Cancer Res 2019;25(19):5859–5865.
- [30] Ritchie ME, Phipson B, Wu D, Hu Y, Law CW, Shi W, et al. limma powers differential expression analyses for RNA-sequencing and microarray studies. Nucleic Acids Res 2015;43:e47.
- [31] Subramanian A, Tamayo P, Mootha VK, Mukherjee S, Ebert BL, Gillette MA, et al. Gene set enrichment analysis: a knowledge-based approach for interpreting genome-wide expression profiles. Proc Natl Acad Sci U S A 2005;102:15545–15550.
- Hänzelmann S, Castelo R, Guinney J. GSVA: gene set variation analysis for microarray and RNA-seq data. BMC Bioinformatics 2013;14:7.
 Becht E, Giraldo NA, Lacroix L, Buttard B, Elarouci N, Petitprez F, et al.
- [33] Becht E, Giraldo NA, Lacroix L, Buttard B, Elarouci N, Petitprez F, et al. Estimating the population abundance of tissue-infiltrating immune and stromal cell populations using gene expression. Genome Biol 2016;17:218.
- [34] Harbour JW, Onken MD, Roberson EDO, Duan S, Cao L, Worley LA, et al. Frequent mutation of BAP1 in metastasizing uveal melanomas. Science 2010;330:1410–1413.
- [35] Bott M, Brevet M, Taylor BS, Shimizu S, Ito T, Wang L, et al. The nuclear deubiquitinase BAP1 is commonly inactivated by somatic mutations and 3p21.1 losses in malignant pleural mesothelioma. Nat Genet 2011;43: 668–672.
- [36] Peña-Llopis S, Vega-Rubín-de-Celis S, Liao A, Leng N, Pavía-Jiménez A, Wang S, et al. BAP1 loss defines a new class of renal cell carcinoma. Nat Genet 2012;44:751–759.
- [37] Jiao Y, Pawlik TM, Anders RA, Selaru FM, Streppel MM, Lucas DJ, et al. Exome sequencing identifies frequent inactivating mutations in BAP1, ARID1A and PBRM1 in intrahepatic cholangiocarcinomas. Nat Genet 2013;45:1470–1473.
- [38] Coulouarn C, Factor VM, Thorgeirsson SS. Transforming growth factor-β gene expression signature in mouse hepatocytes predicts clinical outcome in human cancer. Hepatology 2008;47:2059–2067.

Research Article

Hepatic and Biliary Cancer

- [39] Cardinale V, Wang Y, Carpino G, Cui C-B, Gatto M, Rossi M, et al. Multi-potent stem/progenitor cells in human biliary tree give rise to hepatocytes, cholangiocytes, and pancreatic islets. Hepatology 2011;54: 2159–2172.
- [40] Lanzoni G, Cardinale V, Carpino G. The hepatic, biliary, and pancreatic network of stem/progenitor cell niches in humans: a new reference frame for disease and regeneration. Hepatology 2016:64:277–286.
- for disease and regeneration. Hepatology 2016;64:277–286.

 [41] Scheuermann JC, de Ayala Alonso AG, Oktaba K, Ly-Hartig N, McGinty RK, Fraterman S, et al. Histone H2A deubiquitinase activity of the Polycomb repressive complex PR-DUB. Nature 2010;465: 243–247.
- [42] Artegiani B, van Voorthuijsen L, Lindeboom RGH, Seinstra D, Heo I, Tapia P, et al. Probing the tumor suppressor function of BAP1 in CRISPRengineered human liver organoids. Cell Stem Cell 2019;24(6): 927–943.e6.
- [43] Nault JC, Fabre M, Couchy G, Pilati C, Jeannot E, Tran Van Nhieu J, et al. GNAS-activating mutations define a rare subgroup of inflammatory liver tumors characterized by STAT3 activation. J Hepatol 2012;56: 184–191.
- [44] Woo HG, Choi J-H, Yoon S, Jee BA, Cho EJ, Lee J-H, et al. Integrative analysis of genomic and epigenomic regulation of the transcriptome in liver cancer. Nat Commun 2017;8:839.
- [45] Vyas M, Hechtman JF, Zhang Y, Benayed R, Yavas A, Askan G, et al. DNAJB1-PRKACA fusions occur in oncocytic pancreatic and biliary neoplasms and are not specific for fibrolamellar hepatocellular carcinoma. Mod Pathol 2019. https://doi.org/10.1038/s41379-019-0398-2 [Epub ahead of print].
- [46] Singhi AD, Wood LD, Parks E, Torbenson MS, Felsenstein M, Hruban RH, et al. Recurrent rearrangements in PRKACA and PRKACB in intraductal oncocytic papillary neoplasms of the pancreas and bile duct. Gastroenterology 2020;158(3):573–582.e2.
- [47] Liu B, Lu K-Y. Neural invasion in pancreatic carcinoma. Hepatobiliary Pancreat Dis Int 2002;1:469–476.
- [48] Winter JM, Cameron JL, Campbell KA, Arnold MA, Chang DC, Coleman J, et al. 1423 pancreaticoduodenectomies for pancreatic cancer: a singleinstitution experience. J Gastrointest Surg 2006;10:1199–1210. discussion 1210-1.

- [49] Bhuiya MR, Nimura Y, Kamiya J, Kondo S, Fukata S, Hayakawa N, et al. Clinicopathologic studies on perineural invasion of bile duct carcinoma. Ann Surg 1992;215:344–349.
- [50] Pichlmayr R, Weimann A, Klempnauer J, Oldhafer KJ, Maschek H, Tusch G, et al. Surgical treatment in proximal bile duct cancer. A single-center experience. Ann Surg 1996;224:628–638.
- [51] Yamashita S, Vauthey J-N, Kaseb AO, Aloia TA, Conrad C, Hassan MM, et al. Prognosis of fibrolamellar carcinoma compared to non-cirrhotic conventional hepatocellular carcinoma. J Gastrointest Surg 2016;20:1725–1731.
- [52] Nault J-C, Ningarhari M, Rebouissou S, Zucman-Rossi J. The role of telomeres and telomerase in cirrhosis and liver cancer. Nat Rev Gastroenterol Hepatol 2019;8:294–296.
- [53] Linne H, Yasaei H, Marriott A, Harvey A, Mokbel K, Newbold R, et al. Functional role of SETD2, BAP1, PARP-3 and PBRM1 candidate genes on the regulation of hTERT gene expression. Oncotarget 2017;8:61890– 61900.
- [54] Laskaratos F-M, Rombouts K, Caplin M, Toumpanakis C, Thirlwell C, Mandair D. Neuroendocrine tumors and fibrosis: an unsolved mystery? Cancer 2017;123:4770–4790.
- [55] Masoomian B, Shields JA, Shields CL. Overview of BAP1 cancer predisposition syndrome and the relationship to uveal melanoma. J Curr Ophthalmol 2018;30:102–109.
- [56] Murali R, Wiesner T, Scolyer RA. Tumours associated with BAP1 mutations. Pathology 2013;45:116–126.
- [57] Griffith OL, Griffith M, Krysiak K, Magrini V, Ramu A, Skidmore ZL, et al. A genomic case study of mixed fibrolamellar hepatocellular carcinoma. Ann Oncol 2016;27:1148–1154.
- [58] Wilhelm SM, Adnane L, Newell P, Villanueva A, Llovet JM, Lynch M. Preclinical overview of sorafenib, a multikinase inhibitor that targets both Raf and VEGF and PDGF receptor tyrosine kinase signaling. Mol Cancer Ther 2008;7:3129–3140.
- [59] Brouwer NJ, Gezgin G, Wierenga APA, Bronkhorst IHG, Marinkovic M, Luyten GPM, et al. Tumour angiogenesis in uveal melanoma is related to genetic evolution. Cancers (Basel) 2019;11:1–12.
- [60] Shrestha R, Nabavi N, Lin Y-Y, Mo F, Anderson S, Volik S, et al. BAP1 haploinsufficiency predicts a distinct immunogenic class of malignant peritoneal mesothelioma. Genome Med 2019;11:8.

BAP1 mutations define a homogenous subgroup of hepatocellular carcinoma with fibrolamellar-like features and activated PKA

Théo Z Hirsch, Ana Negulescu, Barkha Gupta, Stefano Caruso, Bénédicte Noblet, Gabrielle Couchy, Quentin Bayard, Léa Meunier, Guillaume Morcrette, Jean-Yves Scoazec, Jean-Frédéric Blanc, Giuliana Amaddeo, Jean-Charles Nault, Paulette Bioulac-Sage, Marianne Ziol, Aurélie Beaufrère, Valérie Paradis, Julien Calderaro, Sandrine Imbeaud, Jessica Zucman-Rossi

Table of contents

Fig. S1	2
Fig. S2	3
Fig. S3	5
Fig. S4	6
Fig. S5	7
Table S1	8

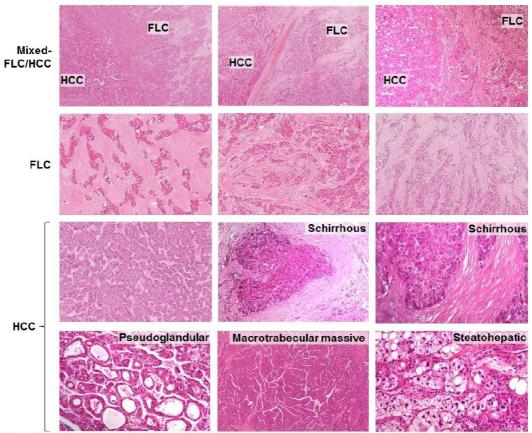


Fig. S1. Representative hematein-eosin-safran staining of different HCC subtypes

Mixed-FLC/HCC are defined as HCC containing at least one area with FLC features. Examples of distinct histological HCC subtypes (scirrhous, macrotrabecular massive, steatohepatic) as well as pseudoglandular pattern are shown.

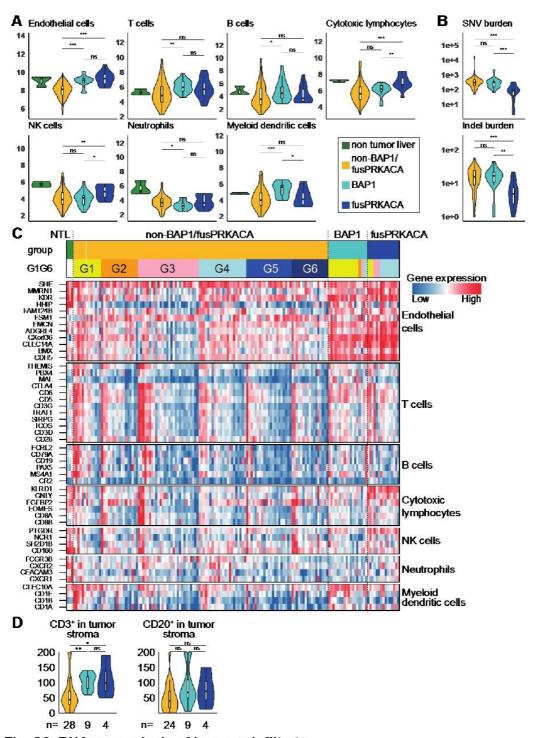


Fig. S2. RNAseq analysis of immune infiltrate

(A) Different immune scores calculated with the Microenvironment Cell Populations-counter method applied to RNAseq data. (B) Comparison of the tumor mutational burden (based on the number of mutations in whole-exome-sequencing with a variant allele frequency above 10%) split between single nucleotide variants (SNV, top) and

small insertions and deletions (indel, bottom). (C) Detailed expression of immune related genes used for determining Microenvironment Cell Populations scores in all samples of the LICA-FR cohort, ordered by molecular group, G1-G6 and CD45 expression. (D) Quantification of CD3 $^{+}$ T cells and CD20 $^{+}$ B cells abundance in tumor stroma. Wilcoxon test: ***p-val < 0.001, **p-val < 0.01, *p-val < 0.05.

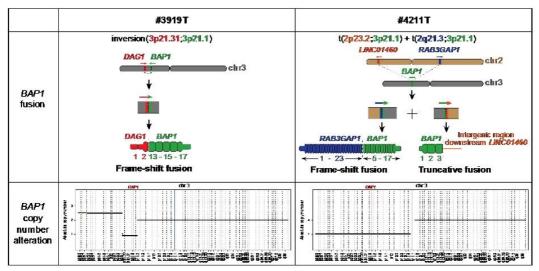


Fig. S3. Biallelic inactivation of *BAP1* through gene fusion and copy number alteration in 2 patients

In tumor #3919T, an unbalanced inversion between locus 3p21.31 and 3p21.1 gave rise to a frameshift fusion between *DAG1* and *BAP1* (top panel), while the second *BAP1* allele was lost in a focal deletion (lower panel). In tumor #4211T, a complex event implicating chromosome 2 and 3 led to two translocations, t(2p23.2;3p21.1) and t(2q21.3;3p21.1), with two subsequent gene fusions: a truncative fusion between *BAP1* and the intergenic region downstream to *LINC01460* and a frameshift fusion between *RBA3GAP1* and *BAP1*. The other *BAP1* allele was lost together with the whole 3p arm (lower panel).

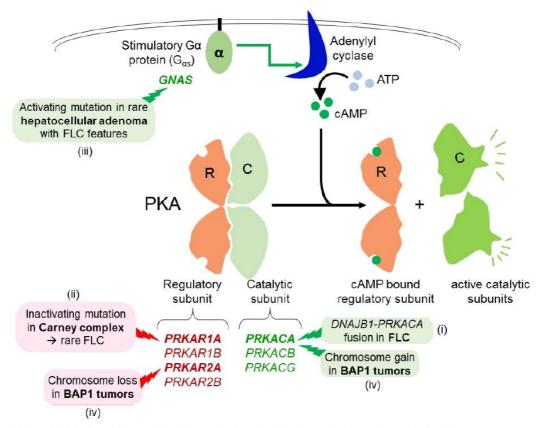


Fig. S4. Different mechanism of PKA activation in hepatocellular tumors

PKA (cAMP-dependent protein kinase) is composed of regulatory subunits (encoded by genes PRKAR1A/B and PRKAR2A/B) which normally repress the catalytic subunits (encoded by PRKACA/B/C). When cAMP bounds to the regulatory subunits, the catalytic subunits become active. Alpha subunits of stimulatory G-protein ($G_{\alpha s}$, encoded by GNAS) activates the adenylyl cyclase, leading to production of cAMP and subsequent activation of PKA. Over-activation of PKA in liver tumors is associated with fibrolamellar features in 4 settings: (i) the DNAJB1-PRKACA fusion in FLC, (ii) inactivating mutations in PRKAR1A in rare FLC developed in Carney complex patients, (iii) activating mutations in GNAS in rare hepatocellular adenomas characterized by fibrolamellar-like patterns and (iv) recurrent gains of PRKACA and deletions of PRKAR2A in BAP1 tumors.

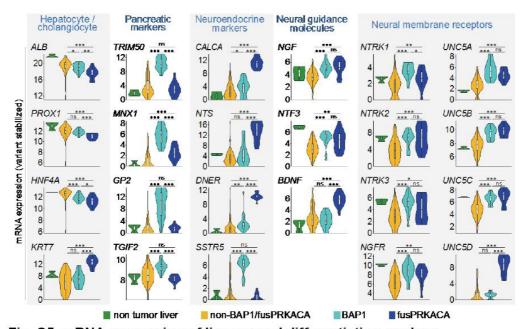


Fig. S5. mRNA expression of lineage and differentiation markers mRNA expression of markers of hepatocytes, cholangiocytes (*KRT7*), pancreas, neuroendocrine markers, neural guidance molecules and receptors located on the membrane of the neurons assessed by RNAseq in normal liver (n=3), non-BAP1/fusPRKACA (n=118), BAP1 (n=18) and fusPRKACA (n=15) tumors. Wilcoxon test: ***p-val < 0.001, **p-val < 0.01, *p-val < 0.05.

Table S1. Primers used for BAP1 sequencing in miSeq technology.

Table S1. Primers	sused	for BAP1 sequencing in miSe	q technology.
Amplicon name	Exon	Forward primer sequence w/o adapter	Reverse primer sequence w/o adapter
BAP1_Ex01_Amp01x1	exon01	CCATCCGGCCTCCCCAG	GCCGTCGCGCCTTGG
BAP1_Ex01_Amp01x2	exon01	AGGGAGAAAAGGCTCTTACCGA	GTTGTCTGTGTGGGACTGAG
BAP1_Ex01_Amp02x1	exon01	CCCGACCCTCCCCTTC	CTCAGTCCCACACACAGACAAC
BAP1_Ex01_Amp02x2	exon01	CTCAGTCCCACACACAGACAAC	CCCCTCTTCCCTTCGCCC
BAP1_Ex01_Amp03x1	exon01	GGGCGAAGGGAGGAC	CGCCCAGCACTTCCCG
BAP1_Ex01_Amp03x2	exon01	ACCTGCGCCCAGCACT	GCGCTCGAAGGCGAAC
BAP1_Ex02_Amp01x1	exon02	TGAGGAAAGGAAAGCAGTAGGGA	GCTGGGGAGGCCGGAT
BAP1_Ex02_Amp01x2	exon02	GGTCGTAGATCTCCTCCACTTG	CCCACCCAGGCCTCTTCA
BAP1_Ex02_Amp02x2	exon02	ATGAATAAGGGCTGGCTGGAG	CGATGAGGAAAGGAAAGCAGTA
BAP1_Ex03_Amp01x1	exon03	TAGGGTTCCTGGCACTGTCTTC	CTTTTCTCCCTGCCGGACC
BAP1_Ex03_Amp01x2	exon03	GCGGGCACTCAGAGAGCAA	GTCAAGGGGGTGCAAGTGG
BAP1_Ex03_Amp02x2	exon03	CAGCACTCTGGGTGTAAGGGG	AGCCTTTTCTCCCTGCCGG
BAP1_Ex04_Amp01x1	exon04	CCCTCCAAACAAAGCACAGAGT	TCTTCTCCCCTTTGGCTGATCT
BAP1_Ex04_Amp01x2	exon04	CTTGGTGGATGATACGTCCGTG	TACCCACTGGATATCTGAGGACA
BAP1_Ex04_Amp02x2	exon04	CCTGGTGGGCAAAGAACATGTT	CGCAGTGCAAAGGATTAATGGG
BAP1 Ex05 Amp01x1	exon05	GCTGTGAGCCAGGATGAAGG	CTTGCAGTGAGGGGTGCTG
BAP1_Ex05_Amp01x2	exon05	ACAATCATTTGAAAAAGAAACAGCCT	GTGCTCCTGAACTGCAGCAG
BAP1 Ex05 Amp02x2	exon05	GCTGAAACCCTTGGTGAAGTCC	TGCTCTGGATCCCCATTCTTGA
BAP1 Ex06 Amp01x1	exon06	AGGTGGCGTGGCTCGG	CCTCCAGGCTGCTCTCTGAAG
BAP1 Ex06 Amp01x2	exon06	CATGGTCCGCACTGCACTAAG	CAATGCCCCGGAGTTGGC
BAP1 Ex06 Amp02x2	exon06	CCTACTCCCACCCCACATCAG	TGCTCTCTGAAGCTTTGCCTTC
BAP1 Ex07 Amp01x1	exon07	CTAGGAGGTAGGCAGAGACACC	TTGGGCCCTGACTCTGTTTTTC
BAP1 Ex07 Amp01x2	exon07	GTGAAACCCCAGCCAGAGC	CCACTTTGTCAGCTATGTGCCT
BAP1 Ex07 Amp02x2	exon07	TGGTCAATGGGGTAGACCTTCA	TAATAGCCATGCCAGGTGTGTG
BAP1 Ex08 Amp01x1	exon08	CACCTGGATACTCTCTGTCCCT	CTGGCTCAACTGCTCTTCTCTG
BAP1 Ex08 Amp01x2	exon08	TGAGAACCCATGATCTAAGCCTGA	GACGAGGAGTGGACAGACAAGG
BAP1 Ex08 Amp02x2	exon08	CCAGAGAGTAGAACAGGGCAGG	CTGGCTCAACTGCTCTTCTCTG
BAP1 Ex09 Amp01x1	exon09	AATGCAGGGAGGGTTGGGC	CTGCTCTCACGGCTGCG
BAP1 Ex09 Amp01x2	exon09	GTGGTTAGCTGAAGCCCAGATC	GCAGGATCAAGTATGAGGCCAG
BAP1 Ex09 Amp02x2	exon09	CTGCTGCAGAGCCTCTAGTACT	CTGCCAGGATATCTGCCTCAAC
BAP1 Ex10 Amp01x1	exon10	CTCTGAGGTCCACAAGAGGTCC	TTTCTCCTCTGAGCCCTGGATT
BAP1 Ex10 Amp01x2	exon10	CTCTCCCTCTACCTTCTGACGG	TCCAAGTCAGCCAGCAACAAG
BAP1_Ex10_Amp02x2	exon10	CCTGTGTGGTTGCCCTCAGA	TTTAAGGTAGAAGCCCGGGTCT
BAP1 Ex11 Amp01x1	exon11	AGTAGAGAATCCTGCAAGGGTG	TGGAGATCCTACTGGAGGTCCT
BAP1 Ex11 Amp01x2	exon11	ATCAGGCAGAGGAACCTAGCAA	GCTAGTGGTGAAGCCTCCAGG
BAP1_Ex11_Amp02x2	exon11	GATTGTCTAGAAAGGCCGGCAG	CTTCTCTGGGAAGTGCTGGTTC
BAP1_Ex12_Amp01x1	exon12	ATGGGATCCGAAGCACCTAGAA	GCAGCACTTGTTTGTAACTGCC
BAP1 Ex12 Amp01x2	exon12	CAGCCCCATCATGCCAGC	ACCCCAGCAGTACTCAGATGAT
BAP1_Ex12_Amp02x2	exon12	CCTAAGGGCAGAGTTGGTGTTC	TCTCTGGCTGTGAGTGTCTAGG
BAP1 Ex13 Amp01x1	exon13	CAAGTGGCCAGTGAGCCAG	CAATGAGAGTACAGACACGGCC
BAP1 Ex13 Amp01x2	exon13	GGAACCCTTCCCACCCTCTG	CCCACATCTCCAAGGTGCTTTT
			L

BAP1 Ex13 Amp02x1	exon13	GAAAGCACTGCCGATCTCAGAG	CCGTTCCCTTGCTTCACATCTT
BAP1 Ex13 Amp02x2	exon13	TGTAGCGTATGCAGTCAACACG	GCTGAGAAGCTCAAAGAGTCCC
BAP1 Ex13 Amp03x2	exon13	GGACAGAGGAATTGAGAGGTCCT	AGCATGGCTAGTTCAAGTTGCT
BAP1_Ex14_Amp01x1	exon14	GGCCTTACCCTCTGCCAGG	GTGTCCTGCACTCTGATGATTT
BAP1_Ex14_Amp01x2	exon14	CCACCCAACCCAGAAAGTCTTC	CAGCCCAGTGGAGAAGGAGG
BAP1_Ex14_Amp02x2	exon14	GTGAGTATTTCTCCCCACTCAAGG	CACTGGCCACTTGGTGCAC
BAP1_Ex15_Amp01x1	exon15	CGGGAGAGGCCAGATCAGG	TTTGTTGCTGGCCCGCC
BAP1_Ex15_Amp01x2	exon15	ACTCATCGTAGTTGTGGGTCCT	GTGGAGGCTGAGATTGCAAACT
BAP1_Ex15_Amp02x2	exon15	GCAACTGGAGAAATCACCCACC	CTGCTCATCCTTGCCTCTAGCT
BAP1_Ex16_Amp01x1	exon16	CAAGGTCTGCTCAAGCCTCAG	TTTCTCCAGTTGCCTGATCTGG
BAP1_Ex16_Amp01x2	exon16	CCTCAGGCCAGGAGCTGAG	AGGACCCACAACTACGATGAGT
BAP1_Ex16_Amp02x2	exon16	GGGCATTCCAGTTAAGACAGCA	TTTCTCCAGTTGCCTGATCTGG
BAP1_Ex17_Amp01x1	exon17	AGCCTCCATATCTCAGGCCAG	GACCTGATGCCAAGGGGTAATG
BAP1_Ex17_Amp01x2	exon17	ATTCCAAGGATCTCTGGCCCAA	AGCAGGCCCCTTTATCTGTACA
BAP1_Ex17_Amp02x1	exon17	CCATGGGGCTGTGTTGGG	CTCTGTCCAGCCCCTCAGTATT
BAP1_Ex17_Amp02x2	exon17	CTAGAGGGGTCAAGCTGTGCTC	AGCTCTTCCTGCTACTCCAGTT
BAP1_Ex17_Amp03x1	exon17	CCTATAAGCAACCCTGTCTCTGC	CCAGTGGGGTTGGGGTGA
BAP1_Ex17_Amp03x2	exon17	GCTCCAACGGGTTGTCTTGATC	GCTGTTCAAGACTGCTCTCCAT
BAP1_Ex17_Amp04x1	exon17	ACAAGGAAGACAGTTCACAGGC	GTCCTTGTATCATGCCACGGTC
BAP1_Ex17_Amp04x2	exon17	GGACAGAGACCTAGAGCCCAAT	TGTAAGGAAGCCAGGTCTTCTCT
BAP1_Ex17_Amp05x1	exon17	CTGGTGGCTGGGGCTAGAG	GAGGTACTGCAGCTTCCTCCA
BAP1_Ex17_Amp05x2	exon17	CTACTCCCAACCCAGCCCAG	TCTATTTTTCTGGGCTCCAACC
BAP1_Ex17_Amp06x1	exon17	AATATATTCTGCTGCCCAGGC	CTGCAGCCCACTCTTGCC
BAP1_Ex17_Amp06x2	exon17	CAGGACAGCTCCTAGGAGAGAA	CTGGGAATGGGAGGAACCAGG
BAP1_Ex17_Amp07x1	exon17	GGACTCTCCAGCTGGGACTATT	TCAAGGGTCTCTACCTCTTCGC
BAP1_Ex17_Amp07x2	exon17	GATGCTGCCTCCTGAGCACTAT	GTCAGCATCGGCCGGC
BAP1_Ex17_Amp08x2	exon17	TCAGGGCCAGCAGTCCTC	CTGAGGGCCGTGTCCTTCAG

Adapter sequences were as follow: Forward: CTACACGACGCTCTTCCGATCT Reverse: CTCCACCGATAAATATTAGCCCGT